UNCLASSIFIED

AD NUMBER

AD821123

NEW LIMITATION CHANGE

TO

Approved for public release, distribution unlimited

FROM

Distribution authorized to DoD only; Administrative/Operational Use; AUG 1967. Other requests shall be referred to US Army Aviation Test Activity, Edwards AFB, CA.

AUTHORITY

usaavscom ltr, 12 Nov 1973

THIS PAGE IS UNCLASSIFIED

AD821123

RTD&E PROJECT NO. F1F131201D161
USATECOM PROJECT NO. 4-5-1220-01
USAAVNTA PROJECT NO. 62-72

PART 2 OF 2 PARTS

ENGINEERING FLIGHT RESEARCH EVALUATION OF THE XV-5A LIFT-FAN AIRCRAFT

PART 2 - PERFORMANCE

FINAL REPORT

BY

KENNETH R. FERRELL
PROJECT ENGINEER

WILLIAM L. WELTER
MAJOR, U.S. ARMY, TC
PROJECT PILOT

AUGUST 1967

U.S. ARMY AVIATION TEST ACTIVITY
EDWARDS AFB, CALIFORNIA

Best Available Copy

DDC Availability Notice

U. S. military agencies may obtain copies of this report directly from DDC. Other qualified users shall request through Commanding General, Hq, U. S. Army Materiel Command (USAMC), ATTN: AMCRD-D, Washington, D. C. 20315.

Reproduction Limitations

Reproduction of this document in whole or in part is prohibited except with permission obtained through Commanding General, Hq, USAMC, ATTN: AMCRD-D, Washington, D. C. 20315. DDC is authorized to produce the document for United States Government purposes.

Disposition Instructions

Destroy this report when it is no longer needed. Do not return it to the originator.

Disclaimer

The findings in this report are not to be construed as an official Department of the Army position, unless so designated by other authorized documents issued and approved by the Department of the Army.

Trade Names

The use of trade names in this report does not constitute an official endorsement or approval of the use of the commercial hardware and software.

This document may be further distributed by any holder only with specific prior approval obtained through Commanding General, Hq, USAMC, ATTN: AMCRD-D, Washington, D. C. 20315.

RTD&E PROJECT NO. F1F131201D161
USATECOM PROJECT NO.4-5-1220-01
USAAVNTA PROJECT NO. 62-72

PART 2 OF 2 PARTS

ENGINEERING FLIGHT RESEARCH EVALUATION OF THE XV-5A LIFT-FAN AIRCRAFT

PART 2 - PERFORMANCE

FINAL REPORT

BY

KENNETH R. FERRELL
PROJECT ENGINEER

WILLIAM L. WELTER
MAJOR, US ARMY, TC
PROJECT PILOT

AUGUST 1967

U. S. ARMY AVIATION TEST ACTIVITY
EDWARDS AIR FORCE BASE, CALIFORNIA

ABSTRACT..... vi

FOREWORD..... vii

SECTION 1. GENERAL..... 1

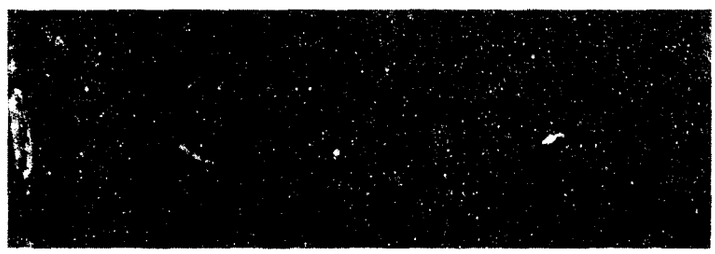

SECTION 2. DETAILS OF TEST..... 25

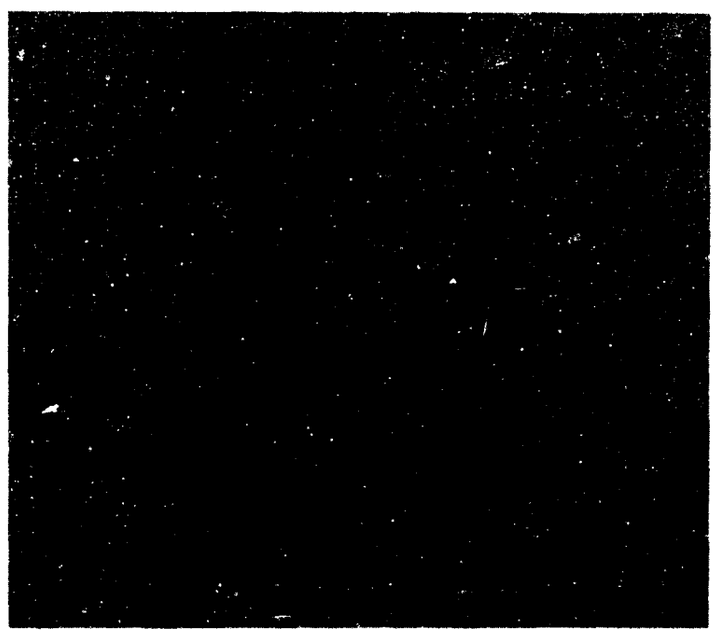

SECTION 3. APPENDICES..... 78

SECTION 4. DISTRIBUTION LIST..... 379

ABSTRACT

An engineering flight research evaluation of the XV-5A aircraft was conducted to obtain performance criteria applicable to future Army developmental aircraft using the lift-fan concept. The flight evaluation was conducted at Edwards Air Force Base, California, by the U. S. Army Aviation Test Activity, under the technical cognizance of the U. S. Army Aviation Materiel Laboratories. The testing consisted of 18.1 productive flight hours and was conducted from 22 July through 15 November 1965. The performance capability was sufficient to allow an evaluation of the overall concept/installation. The hovering power required was less than that necessary at conversion. With the proper flight profile, however, a conversion could be accomplished at any gross weight for which a vertical takeoff was possible. The jet-mode performance was poor compared with the performance of current fixed-wing jet aircraft. Since there were no mission requirements or performance guarantees, the recommendations concerned general rather than specific improvements in performance capabilities.

FOREWORD

1. AUTHORITY

Letter, AMSTE-BG, Hq, U.S. Army Test and Evaluation Command (USATECOM), 12 March 1965, subject: "Test Directive for Military Potential Test of the Lift-Fan Propulsion System Concept Installed in the XV-5A Aircraft, USATECOM Project Task No. 4-5-1220-01."

2. REPORT PUBLICATION

The results of the Engineering Flight Research Evaluation of the XV-5A Lift-Fan Aircraft are published in two parts. Part 1, consisting of the Stability and Control evaluation, was presented in Final Report published in August 1966. Part 2, consisting of the Performance evaluation, is presented in this Final Report.

3. REFERENCES

A list of references is contained in Section 3, Appendix VIII.

PHOTO 1

XV-5A IN FAN MODE CONFIGURATION

PHOTO 2

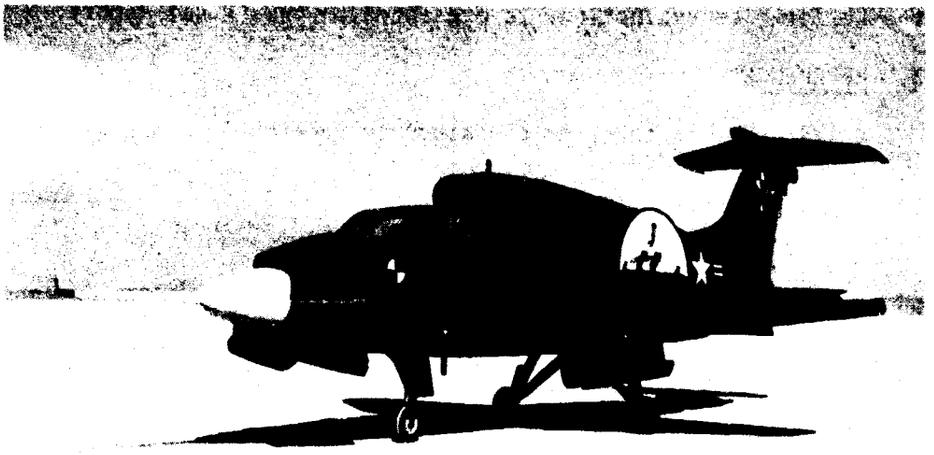

SECTION 1. GENERAL

1.1 OBJECTIVE

To evaluate the lift-fan concept of VTOL Propulsion and to conduct research in the V/STOL field to obtain design criteria for application to future Army developmental VTOL aircraft.

This objective was not satisfied in all details due to limited test time available because of the loss of one of the two test aircraft during the initial testing phase.

1.2 RESPONSIBILITIES

The U.S. Army Aviation Materiel Laboratories (USAAVLABS) had technical control and cognizance of the overall program and provided an on-site Program Manager's Representative.

The U.S. Army Aviation Test Activity (USAAVNTA) had responsibility for conduct of the test program as outlined in paragraph 1.1. This included preparation and coordination of the plan of test with USAAVLABS , coordination of test execution, and preparation of required test reports.

USAAVLABS negotiated a contract that required the commercial contractor to furnish support (maintenance, logistics, and facilities) for the test program (reference b).

1.3 DESCRIPTION OF MATERIEL

The XV-5A (former military designation VZ-11) is a mid-wing, tri-fan, turbojet-powered research aircraft. The total aircraft assembly has a maximum gross weight of 12,500 pounds. The crew stations consist of a single cockpit with side-by-side seating for a pilot and an observer. In the conventional takeoff and landing (CTOL) flight mode, thrust is supplied by two J-85-5B turbojet engines. In the vertical takeoff and landing (VTOL) and short takeoff and landing (STOL) flight modes, engine thrust is diverted to drive two wing fans designated as the X353-5B system and a single nose-mounted pitch-control fan designated as the X376 system.

The XV-5A aircraft has two basic primary flight control systems: the fan control system and the conventional control system.

Except for the lift control (collective stick) of the fan system, both control systems are operated from common cockpit controls and linkage to common junctures within the fuselage. From these control junctures the linkage is branched off as required to serve either fan or conventional system functions. The conventional surfaces (elevator, rudder, and ailerons) are operable at all times; the fan controls are electromechanically made ineffective during transition to conventional flight.

A detailed description of the XV-5A aircraft systems is presented in appendix III.

1.4 BACKGROUND

USAAVLABS was assigned the overall program responsibility for a lift-fan research program divided into two phases: Phase I (reference a), consisting of design, fabrication, and 50 hours of flight testing of two XV-5A aircraft by the contractor; and Phase II (references b, c, and d), consisting of 100 hours of flight testing by the U.S. Government.

Specific objectives of Phase I were to determine and evaluate the flight characteristics of the lift-fan in the hover and transition regimes and to evaluate the compatibility of the lift-fan propulsion system with a high subsonic speed aircraft configuration. This phase was completed on 26 January 1965, and the two XV-5A aircraft were delivered to the Army on 28 January 1965.

A Test Directive defining objectives and responsibilities for Phase II was issued by USATECOM 12 March 1965. The responsibilities for this flight research program for USAAVLABS and USAAVNTA were as stated in paragraph 1.2 and appendix VIII. A test plan (reference f) was submitted by USAAVNTA for coordination by USAAVLABS in December 1964.

The performance flight research testing consisted of 18.1 productive flight hours and was conducted at Edwards Air Force Base, California, from 22 July 1965 through 15 November 1965.

USAAVNTA submitted "Letter Report of Preliminary Pilot Qualitative Evaluation of the XV-5A Research Aircraft" (reference g) to USAAVLABS on 28 October 1965. Part I of the Engineering Flight Research Evaluation of the XV-5A Lift-Fan Aircraft, consisting of the Stability and Control evaluation (reference h) was published in August 1966.

Throughout these tests the aircraft was flown under conditions other than those contained in the design specification

(reference k). For example, increased weight, changed louver schedule, and various other conditions.

1.5 FINDINGS

1.5.1 FAN-MODE PERFORMANCE

The general fan-mode performance findings for each area tested are presented in the following paragraphs and a detailed discussion of fan-mode performance test results is presented in paragraph 2.1.

1.5.1.1 Hover

The non-dimensional hovering coefficient data were consistent and did not exhibit excessive scatter. The free-flight hovering performance was in good agreement with that calculated

PHOTO 3- XV-5A LIFT FAN AT HOVER

from the vertical-thrust-stand data. The thrust changes with engine speed and wing-fan speed were 460 pounds and 262.5 pounds respectively for each percent revolutions-per-minute (RPM) change. At a T/W = 1, the sea-level standard-day out-of-ground effect (OGE) hovering capability was 12,800 pounds. The hovering performance was limited by engine power available for all conditions. Performance was decreased approximately 400 pounds for each increase of 1,000 feet of altitude and 100 pounds for each degree Centigrade (C) higher temperature. Results from the thrust stand and hover performance tests indicated a slight positive ground effect. The in-ground-effect (IGE) hovering data were obtained at a non-stabilized condition due to the adverse aircraft disturbances exhibited by the test aircraft at wheel heights of 10 feet and below (paragraph 2.1.1.4). A complete discussion of this characteristic is found in reference h.

1.5.1.2 Takeoff

For a rolling takeoff technique, inadequate louver actuation rate,(reference h)at low speeds limited the minimum climbout airspeed at 45 knots true airspeed (KTAS). The minimum distance required to clear a 50-foot obstacle with this technique was 1550 feet at a thrust-to-weight ratio (T/W) of approximately 1.15. The 45-degree aft vector angle limited the horizontal thrust and the amount of collective stagger that could be used during the acceleration. With the hovering acceleration technique (described in reference h), the minimum distance over a 50-foot obstacle was 1300 feet for a T/W of approximately 1.15 and an airspeed of 60 KTAS. Application of longitudinal stick to control the pitch attitude reduced the pitch-fan noseup moment and the total wing-fan thrust available during the acceleration. For both techniques, obtaining the maximum performance required a high degree of pilot effort. The rolling takeoff technique required excessive pilot attention to maintain the proper louver angle-airspeed relationship. Undesirable flight conditions resulted when the proper louver angle-airspeed relationship was not maintained. This characteristic is fully described in reference h, paragraphs 2.1.2.3 and 2.1.2.4.

1.5.1.3 Vertical Climb

The maximum vertical rate of climb of 2400 feet per minute (fpm) was reached at a T/W of 1.174. The fan effectivity was decreasing above this value. A rapid application of engine power or collective caused no apparent performance loss or unusual control requirements. (paragraph 2.1.3.4)

1.5.1.4 Forward Climb

The non-dimensional coefficients developed were adequate to correct and standardize the data. At low airspeeds a zero angle of attack provided better climb performance, and at airspeeds above 79 KTAS a negative angle of attack provided the higher rate of climb. A gross weight increase of 1000 pounds resulted in a rate of climb decrease of 480 fpm. The hot-day, high-altitude performance was limited by the engine power available, while the performance for other conditions was limited by the vector angle and fan speed. For all conditions, the rate of climb decreased with higher climb airspeeds.

1.5.1.5 Level Flight

The non-dimensional coefficients accurately described the level flight performance characteristics. The power required was essentially a constant from zero to 12 KTAS and above this speed the drag rise with airspeed was quite rapid. The power required was decreased approximately 8.5 percent as the landing gear was retracted. The engine power and wing-fan speed required increased with altitude and temperature. An increasingly positive angle of attack caused a greater fan speed and engine power required. Reference h described in detail the various flying quality characteristics observed during fan-mode level flight. The maximum level flight airspeed was approximately 104 KTAS at sea-level standard conditions, with the landing gear down, a gross weight of 10,000 pounds, and a zero angle of attack. The maximum airspeed decreased to approximately 77 KTAS at an altitude of 6000 feet. For similar conditions on a hot day, the maximum airspeed was limited by the power available to approximately 86 KTAS at sea level. The maximum specific range was limited by the maximum airspeed that could be attained. The maximum specific range obtained was at an altitude of 2500 feet and was 0.0183 nautical air miles per pound of fuel (NAMPP). Retracting the landing gear increased the specific range approximately 11 percent. The specific range performance was lowered by any change from the zero angle-of-attack condition. (paragraph 2.1.5.4)

1.5.1.6 Vertical Descent

The maximum fan-mode rate of descent was limited by a deterioration of directional control. The maximum rate attained was 485 fpm at a T/W of .935, full engine power, and a collective stick position of 30-percent full up. This rate of descent could be stopped and a stabilized hover achieved without application of maximum thrust available. (paragraph 2.1.6.4)

1.5.1.7 Angle-of-Attack Calibration

The test data showed an excessive amount of scatter and the position error was negative for all indicated angle-of-attack values from -5 degrees to +9 degrees. The position error was linear and varied from -0.5 to -4.5 degrees for the indicated angle-of-attack range of -5 to +9 degrees. The position error could not be correlated as a function of wing-fan cross-flow ratio. The flight test data did not agree precisely with data previously obtained by the contractors during wind tunnel tests. (paragraph 2.1.7.3)

1.5.1.8 Airspeed Calibration

The nose-boom (low-speed) airspeed system showed a constant negative position error of 3 knots throughout the airspeed range. There was no change in the position error as the angle of attack was varied from -2 degrees to +5 degrees. (paragraph 2.1.8.4)

1.5.2 JET MODE PERFORMANCE

The limited tests conducted during this evaluation showed the XV-5A drag characteristics to be considerably higher than for similar jet aircraft. Overheating of the right-wing-fan area constituted a level-flight airspeed limitation of 374 knots. (paragraph 2.2.1.4)

1.5.3 PROPULSION SYSTEM PERFORMANCE

The propulsion system tests defined the performance of the standard and modified engines and quantitatively defined the engine power, thrust, fuel flow, and operating conditions. The inlet losses due to inlet instrumentation were established and the results of effective nozzle-area changes were determined. The data from the various tests were used for comparison and data validation purposes. The horizontal thrust-stand data were also used to determine the jet-mode thrust, while the vertical thrust-stand results determined the lift capability and were useful in the hovering performance calculations. The accuracy and magnitude of the engine inlet pressure and temperature instrumentation were marginal for determining the inlet pressure recovery and distortion characteristics. The wing-fan instrumentation did not define the fan operating conditions and there was no external environment instrumentation available. The inlet performance data were inconclusive in many areas and the analysis effort was not sufficient to analyze completely the data available. General findings for each area tested are presented in the following paragraphs and a detailed discussion of test results is presented in paragraph 2.3.

1.5.3.1 Engine Calibration

With the inlet rakes installed for engine Serial Number (S/N) 875, the thrust and power were decreased approximately 200 pounds and 250 horsepower (HP) by the engine stall modification. The engine comparison showed that S/N 875 had higher thrust, power, fuel flow, and exhaust gas temperature (EGT) than engine S/N 876. The diverter valve leakage flow was .047 pounds/second at an engine speed of 100-percent RPM and EGT trim of 700 degrees C. The percentage of leakage loss decreased from 1.52 to 1.08 as engine speed was increased from 70-to 100-percent RPM. Changing the EGT trim from 660 degrees C to 700 degrees C resulted in a 920-HP power increase and 265-pounds greater thrust.

Moving the curved diverter door to a position of 2 inches of over-travel resulted in an EGT increase of 126 degrees C. (paragraph 2.3.1.4)

1.5.3.2 Ground Tests

The ground test data showed the engine installation loss to be 6.15 percent for the left engine and 4.0 percent for the right engine. The fan scroll trim and EGT trim required during these tests were primarily accomplished through a trial process and several runs were often required. The data from these tests were required to accomplish the empirical power determination method. (paragraph 2.3.2.4)

1.5.3.3 Horizontal Thrust Stand

The total horizontal thrust recorded during the jet-mode dual engine runs was 5725 pounds. The sum of the two single-engine runs produced 120 pounds less thrust than the dual engine runs. During fan-mode with the collective vector at 45 degrees, the corrected horizontal thrust was 7520 pounds for engine speeds of 100-percent RPM. (paragraph 2.3.3.4)

1.5.3.4 Vertical Thrust Stand

1.5.3.4.1 Engine Speed and Power

1.5.3.4.1.1 Pitch Fan

The maximum pitch-fan speed was obtained at an engine speed of 104-percent RPM. At 105-percent pitch-fan RPM the vertical thrust was 1000 pounds for a pitch-fan door position of 78.5 degrees. The ground proximity did not exhibit an influence on the

pitch-fan speed or thrust. The pitching moment increased directly as the product of the pitch-fan thrust change times the moment arm. (paragraph 2.3.4.4.1.1)

1.5.3.4.1.2 Wing Fan

The maximum corrected wing-fan speed obtainable was 97-percent RPM with a corrected engine speed of 103-percent RPM. Wing-fan speed characteristics were not changed by ground proximity. The wing-fan thrust varied directly as the fan speed squared. The maximum corrected thrust obtained during the test was 13,000 pounds at an H/D of 1 and an engine speed of 103-percent RPM. The thrust data showed a decrease of 300 pounds for each unit higher H/D above the ground. (paragraph 2.3.4.4.1.2)

1.5.3.4.2 Collective Stagger

1.5.3.4.2.1 Pitch Fan

The wing-fan stagger angle change and pitch-fan door position programming did not influence the pitch-fan speed characteristics. The programming reduced the thrust by 260 pounds. (paragraph 2.3.4.4.2.1)

1.5.3.4.2.2 Wing Fan

The wing-fan speed increased 2 percent with a collective stagger increase of 20 degrees. The thrust change accompanying this change was 3150 pounds. The stagger effectiveness decreased from 0.945 at a stagger angle of 17 degrees to 0.62 at a stagger angle of 36 degrees. The pitching moment change from the wing fans due to a change from maximum stagger angle to minimum stagger angle was 7250 foot-pounds nosedown. (paragraph 2.3.4.4.2.2)

1.5.3.4.3 Pitch-Fan Door

1.5.3.4.3.1 Pitch-Fan

The pitch-fan speed was not influenced by changes in pitch-fan door variations. The pitch-fan thrust was changed by 2310 pounds by a full deflection change. Increasing the height above the ground from an H/D = 1 to an H/D = 3 decreased the thrust by 180 pounds. The total change in pitching moment was 19,000 foot-pounds for a full door deflection. (paragraph 2.3.4.4.3.1)

1.5.3.4.3.2 Wing Fan

The small change in wing-fan thrust with variation in pitch-fan door position did not cause any measurable change in pitching moments. (paragraph 2.3.4.4.3.2)

1.5.3.4.4 Collective Vector

1.5.3.4.4.1 Pitch Fan

The pitch-fan speed was unchanged by collective vector angle changes. The pitch-fan door programming with vector angle reduced the thrust by 710 pounds and increased the nosedown moment by 13,500 feet. (paragraph 2.3.4.4.4.1)

1.5.3.4.4.2 Wing Fan

There was essentially no fan speed change as a result of collective vector angle changes. The vertical thrust was decreased approximately 75 pounds for each degree of aft vector angle. Zero horizontal thrust occurred at a vector angle of 7.5 degrees aft. The wing fan provided 13,900 foot-pounds of noseup pitching moment change as vector angle was moved from 9 degrees forward to 36 degrees aft. The pitching moment change decreased with increased fan height above the ground. (paragraph 2.3.4.4.4.2)

1.5.3.4.5 Differential Stagger

1.5.3.4.5.1 Pitch Fan

The pitch fan speed was not changed by differential stagger angle changes. The pitch fan door programming caused a thrust increase of 100 pounds and noseup moment change of 1200 foot-pounds. (paragraph 2.3.4.4.5.1)

1.5.3.4.5.2 Wing Fan

A maximum differential stagger caused a wing-fan speed increase of 6.7-percent RPM. The change in thrust was only 90 pounds at a collective stagger angle of 25 degrees and increased with lower angles to 875 pounds at 17 degrees stagger angle. At the maximum stagger angle, the rolling moment change was 7000 foot-pounds and was decreased 65 percent as the stagger angle was decreased to 15.6 degrees. (paragraph 2.3.4.4.5.2)

1.5.3.4.6 Differential Vector

1.5.3.4.6.1 Pitch Fan

The wing-fan speed increased 3-percent RPM as the differential vector angle was varied 20 degrees, and the thrust was decreased approximately 360 pounds. The tests did not provide data as a function of stagger angle or ground proximity. The yawing moment was 430 foot-pounds/degree of differential vector angle at a stagger angle of 17 degrees and decreased to 297 foot-pounds/degree at a stagger angle of 25 degrees. (paragraph 2.3.4.4.6.2)

1.5.3.4.7 Thrust Spoiler

The maximum thrust spoiled at the full spoiler deflection was 1610 pounds at 100-percent engine RPM and the residual unspoiled thrust at flight-idle was 240 pounds. (paragraph 2.3.4.4.7)

1.5.3.5 Inlet

1.5.3.5.1 Engine Calibration

The maximum inlet pressure ratio (P_{T2}/P_a) loss as a result of the stall modification was 1.1 percent for the two engines calibrated. One engine was not affected by the installation of the inlet flight rakes while the other engine showed a 3.2-percent loss of inlet pressure ratio. There was no inlet temperature rise evident during the calibration. (paragraph 2.3.5.4)

1.5.3.5.2 Horizontal Thrust Stand

The inlet total pressure recovery loss was 3 percent for an engine speed change of 50-percent RPM. The right and left inlet performance were similar and were not changed by single-engine operation. (paragraph 2.3.5.4.2)

1.5.3.5.3 Hover

The inlet recovery changed from 0.989 to 0.998 as the hovering wheel height was increased from 2 to 10 feet. There was no change in the inlet distortion characteristics as a function of wheel height. The left inlet distortion was 0.04 and the right inlet distortion was 0.06. The recovery and distortion characteristics were the same for all collective stagger angles.

The engine inlet temperature rise was 6 degrees F for OGE (wheel height greater than 10 feet). The rise was approximately 20 degrees F for a wheel height of less than 5 feet. The engine

inlet temperature conditions were essentially the same for both a stabilized hover and a vertical takeoff. Wing-fan hot-gas reingestion caused a 2-percent corrected speed reduction as the hovering height was reduced from 5 to 2 feet. (paragraph 2.3.5.4.3)

1.5.3.5.4 Takeoff and Vertical Climb

The maximum engine inlet temperature rise during a vertical takeoff was approximately 40 degrees F. The value decreased during the climbout and was 20 degrees F at a wheel height of 10 feet. The temperature level was slightly higher than that recorded during a stabilized hover at a comparable wheel height. The right inlet temperature was approximately 10 degrees F higher than for the left inlet at all test conditions. (paragraph 2.3.5.4.4)

1.5.3.5.5 Fan-Mode Level Flight

The engine inlet pressure recovery performance was 0.993 at hover and improved with increased airspeed. The total pressure distortion also decreased with higher airspeeds. The right inlet performance was better than the left inlet performance. There was no significant change in the inlet performance for angle-of-attack changes of ± 4 degrees or for sideslip variations of 10 degrees.

The engine inlet temperature rise decreased linearly from 6 degrees F at a hover to zero degrees F at 60 knots calibrated airspeed (KCAS) and was the same for both inlets. There was no change at airspeeds above 60 KCAS. (paragraph 2.3.5.4.5)

1.5.3.5.6 Jet-Mode Level Flight

The jet-mode engine inlet performance was not determined during the tests. The contractor test data showed an inlet temperature ratio change of 0.992 to 1.032 for an airspeed variation from 120 to 320 KCAS. (paragraph 2.3.5.4.6)

1.5.3.5.7 Vertical Descent and Landing

The engine inlet temperature rise was approximately 6 degrees F during OGE flight and increased during the landing approach to a value of 40 degrees F at touchdown. The data were not sufficient to determine the effects due to surface wing conditions and pilot techniques. As discussed in reference h, three unsatisfactory characteristics were noted during vertical takeoff and landing (VTOL) operations in close proximity to the ground (from zero wheel height to 10-foot wheel height). Aircraft disturbances, engine reingestion, and degradation of lateral control power characteristics were all observed within the specific wheel-height region. (paragraph 2.3.5.4.7) (appendix VIII paragraph h)

1.5.3.5.8 Sideward and Rearward Flight

1.5.3.5.8.1 Sideward Flight

A sideward speed change resulted in an engine inlet recovery factor change of 1 percent. The downwind inlet (inlet away from the direction of translation) recovery was improved while the upwind inlet suffered a loss. The characteristics were similar for both right and left inlets. The left inlet showed a large distortion increase during left sideward flight and a small distortion increase during right translation. The right inlet distortion was symmetrical with respect to translational direction. Test data were not available to determine the fan inlet conditions. (paragraph 2.3.5.4.8.1) (appendix VIII paragraph h)

1.5.3.5.8.2 Rearward Flight

Increased rearward translational speed caused a slight decrease in the engine inlet recovery performance and an increase in inlet distortion. The right inlet performance was superior to the left inlet performance. There were no data obtained to determine the fan inlet conditions. (paragraph 2.3.5.4.8.2) (appendix VIII paragraph h)

1.5.3.6 Engine Flight

The engine data recorded during all flight regimes, other than during in-ground-effect, were essentially the same as that found during the engine calibration. There was no difference in characteristics during jet-mode and fan-mode operation. At engine speeds below 90-percent RPM, there were small differences between the flight test data and the engine calibration.

The instantaneous power method was superior to the other methods and data obtained with this method were used to calculate the power available. The power available varied with the inlet performance as well as the ambient conditions. The power available was presented for zero inlet losses and the appropriate correction curves were included. (paragraph 2.3.6.4)

The J-85-5B operating characteristics (starting, stopping, compressor stall tendencies, etc.) observed during this evaluation were excellent except for high operating temperatures noted during low-speed flight in fan-powered configuration. During the course of the flight evaluation, the maximum EGT limitation was raised from 680 degrees C to 700 degrees C to permit 10-minute high-speed fan-powered flights to be conducted. During conventional flight, engine accelerations from flight-idle to maximum power required approxi-

mately 5 seconds with no over-temping tendencies noted. An allied problem caused by J-85-5B heat dissipation was noted during conventional flight. The right wing-fan cavity area reached its over-temp condition (120 degrees C) at approximately 96-percent J-85-5B RPM, thereby constituting a performance limitation. Additionally, the aircraft exhibited undesirable engine reingestion characteristics when in close proximity to the ground. (reference h)

1.6 CONCLUSIONS

The XV-5A lift-fan aircraft was suitable as a research vehicle. The aircraft limitations, low flight productivity, high maintenance, and limited test time available prevented accomplishing a complete evaluation throughout the available flight envelope. The testing conducted was sufficient to allow an evaluation of the overall concept. The limited test conditions prevented a complete determination of the altitude, gross weight, and temperature effects; however, the non-dimensional data should provide quite accurate data for altitudes of sea level to 6000 feet, gross weights of 9000 to 11,000 pounds, and ambient temperatures from -10 degrees F to + 35 degrees F. The wing-fan instrumentation was inadequate and the environmental inlet or exit conditions were not determined. The external fan exhaust velocity and temperature conditions were not measured and no correlations could be made with existing environmental data. General conclusions for the areas tested are presented in the following paragraphs. (paragraph 1.5)

1.6.1 FAN-MODE PERFORMANCE

1.6.1.1 Hovering

The non-dimensional coefficients developed provided an excellent means for correcting the data for aircraft configuration and to standard atmospheric conditions and allowing easy calculations of summary performance. The maximum fan performance during hover could not be obtained because of the limited power available. The performance was relatively insensitive to altitude but was very sensitive to increased ambient temperature conditions. The ground proximity effects could not be determined due to the adverse aircraft disturbances at wheel heights of 10 feet and below. (paragraph 1.5.1.1)

1.6.1.2 Takeoff

The hovering acceleration technique provided better takeoff performance than the rolling acceleration technique requiring a minimum distance of 1300 feet. The pilot technique was difficult and the 45-degree aft vector angle limited the horizontal thrust during the rolling acceleration. The vector angle operation and timing were difficult to accomplish. Based on these results the XV-5A should not be considered a short takeoff (STO) aircraft. (paragraph 1.5.1.2)

1.6.1.3 Vertical Climb

The maximum vertical rate of climb was limited by the engine power available. The maximum of 2400 fpm was higher than that obtained for any forward airspeed climb condition. The climb OGE was sufficiently rapid to prevent the establishment of a recirculation pattern or introduction of control requirements. A T/W of 1.05 provided a vertical climb rate of 300 fpm. (paragraph 1.5.1.3)

1.6.1.4 Forward Climb

The forward climb performance decreased as the climb airspeed was increased above zero. The non-dimensional coefficient data were adequate for calculating performance. Climb performance was limited by vector angle, power available, or wing-fan speed. Positive angles of attack at high forward speeds resulted in fan overspeed conditions, power reduction and performance loss. (paragraph 1.5.1.4)

1.6.1.5 Level Flight

The non-dimensional coefficients developed for the level flight should be used to calculate summary performance. The level flight power required was insensitive to airspeed changes from zero to 12 KTAS and above this speed the drag rise with airspeed was quite rapid. The engine power and wing-fan speed required increased with altitude and temperature. Drag and power required were significantly reduced by retracting the landing gear. The maximum airspeed capability was limited by wing-fan speed for all conditions. Positive angles of attack resulted in a high engine power and wing-fan speed required. In addition, high airspeeds and positive angles of attack tended to cause a higher wing-fan speed than would exist for a similar power and zero airspeed condition. The range performance was severely limited by wing-fan speed, vector angle, and power available, which prevented achieving the maximum specific range. (paragraph 1.5.1.5)

1.6.1.6 Vertical Descent

The deteriorating directional control with vertical rate of descent limited the maximum to 485 fpm. (paragraph 1.5.1.6)

1.6.1.7 Angle-of-Attack Calibration

The test data were of generally poor quality and were not of sufficient magnitude to define precisely the angle-of-attack position error. There was no indication that the position error was a function of wing-fan cross-flow ratio as predicted by the contractor data. Independent of cross-flow considerations, the results showed the same trend as the full-scale wind-tunnel tests but the position error was 1.5 degrees less negative. (paragraph 1.5.1.7)

1.6.1.8 Airspeed Calibration

The nose-boom (low-speed) airspeed system provided the angle-of-attack position error correction. The position error was not sensitive to airspeed, angle of attack, or fan speed changes. (paragraph 1.5.1.8)

1.6.2 JET-MODE PERFORMANCE

The drag characteristics were considerably higher than those of similar jet aircraft. The overheating of the right-wing fan area constituted a performance limitation. (paragraph 1.5.2)

1.6.3 PROPULSION SYSTEM PERFORMANCE

The engine contractor's flight test facility was satisfactory for the engine calibrations. The engine calibration data allowed for a precise quantitative determination of the power required by the lift fans and the maximum performance available from the aircraft. The engine inlet instrumentation installation was marginal and the profile data are not conclusive. The engine operation was sensitive to the diverter valve condition, with the wing-fan performance being influenced by any discrepancy. The diverter valve also showed a leakage flow which introduced a performance loss. For some undetermined reason, there were variations in the thrust data from the engine calibrations, horizontal thrust stand, and vertical thrust stand. The vertical thrust stand tests were very productive and provided a great deal of useful information. The thrust stand design was such that the hot gas environment caused the force and moment sensors to assume large changes during the course of the tests.

Care was necessary to apply the proper correction procedures to obtain valid data. The lack of external instrumentation prevented determining the quantitative nature of the external fan environment during the tests. General conclusions for each area tested are presented in the following paragraphs. (paragraph 1.5.3)

1.6.3.1 Engine Calibration

The engine calibration data were sufficient to allow calculation of engine power and thrust and quantitatively defined the engine operational characteristics. The inlet rake installation did not introduce an engine loss; however, the engine stall modification introduced a loss of approximately 2-percent thrust and horsepower. The diverter valve leakage flow was 1.08 percent of the total engine mass flow at 100-percent engine speed. Decreasing the engine nozzle area resulted in a higher EGT and greater engine power. The engine operation was sensitive to the position of the diverter valve curved door (paragraph 1.5.3.1)

1.6.3.2 Ground Tests

The ground test data showed an average engine installation loss of approximately 5 percent with the left engine loss being slightly higher than that for the right engine. The data were satisfactory for the empirical power calculation method. The EGT and fan trim scroll procedures were unreliable and excessively time consuming. (paragraph 1.5.3.2)

1.6.3.3 Horizontal Thrust Stand

The installed engine thrust was 10 percent higher than that obtained during the engine calibrations. The single-engine operation showed a thrust loss of 1 percent compared with the engine values during a dual-engine operation. The horizontal thrust was increased approximately 31 percent by converting to fan-mode operation and moving the collective vector angle to 45 degrees aft. (paragraph 1.5.3.3)

1.6.3.4 Vertical Thrust Stand

1.6.3.4.1 Engine Speed and Power

The maximum engine speed of 106-percent RPM resulted in a pitch-fan thrust of 1200 pounds and a speed of 106-percent RPM. For a similar engine condition the wing-fan thrust was 13,000 pounds and the speed was 98.5-percent RPM. The wing-fan thrust varied directly as the fan speed squared. The wing-fan

thrust was sensitive to the ground proximity and was decreased 300 pounds for each unit higher H/D. (paragraph 1.5.3.4.1)

1.6.3.4.2 Collective Stagger

The pitch-fan performance was not a function of collective stagger angle. The wing-fan speed increased 2 percent and the thrust decreased 3150 pounds as the stagger angle was increased by 20 degrees. The pitch-fan door programming with stagger input was insufficient and an additional 4.6 degrees of door motion would be required to balance the wing-fan pitching amounts introduced as the stagger angle was moved through the maximum range available. (paragraph 1.5.3.4.2)

1.6.3.4.3 Pitch-Fan Door

The pitch-fan speed was not influenced by pitch-fan door movement or ground proximity. The pitch-fan door was a strong pitch control with a full door deflection resulting in a pitching moment change of 19,000 foot-pounds. The total aircraft thrust was also changed by 2310 pounds with this door motion. The wing-fan characteristics were not significantly changed as a function of pitch-fan door position. (paragraph 1.5.3.4.3)

1.6.3.4.4 Collective Vector

The pitch-fan door programming with a collective vector angle variation of 25 degrees changed the vertical thrust by 100 pounds and the pitching moment by 13,500 foot-pounds. The wing-fan speed was unchanged by collective vector angle changes. Zero horizontal thrust occurred at a vector angle of 7.5 degrees aft and the vertical thrust change was 75 pounds per degree of vector angle change. The total horizontal thrust recorded at the maximum aft vector was approximately 10 percent less than that obtained during the horizontal thrust stand tests. The wing-fan pitching moments were essentially balanced by the pitch-fan door programming. (paragraph 1.5.3.4.4)

1.6.3.4.5 Differential Stagger

The pitch-fan door programming with differential stagger angle introduced very small pitching moment, thrust, and pitch-fan speed changes. The wing-fan speed, rolling moment, and thrust were sensitive to the collective stagger angle. The maximum rolling moment available was decreased by 65 percent as the collective stagger angle was changed from 25 to 17 degrees. The vertical lift loss for a maximum differential stagger input was 875 pounds at a collective stagger angle of 17 degrees. (paragraph 1.5.3.4.5)

1.6.3.4.6 Differential Vector

The pitch-fan characteristics were not influenced by differential vector angle changes. A differential vector angle caused a slight wing-fan speed increase and a small vertical thrust loss. The maximum yaw control available was poor at a collective stagger angle of 17 degrees and further decreased with greater stagger values. (paragraph 1.5.3.4.6)

1.6.3.4.7 Thrust Spoilers

With the thrust spoilers fully extended, the residual unspoiled thrust at the engine flight-idle was high and required excessive braking to maintain a safe taxi speed. When brakes were not applied, a taxi speed of approximately 40 knots resulted. (paragraph 1.5.3.4.7)

1.6.3.5 Inlet

1.6.3.5.1 Engine Calibration

A small engine inlet pressure ratio loss was introduced by the stall modification. The effect of the inlet flight rakes was not conclusive from the test data obtained and the variation in the two engines cannot be accounted for. The engine inlet temperature was not sensitive to engine speed. (paragraph 1.5.3.5.1)

1.6.3.5.2 Horizontal Thrust Stand

The engine static inlet loss was not excessive. The inlet was not sensitive to single-engine operation and there was no apparent effect visible in the test data. (paragraph 1.5.3.5.2)

1.6.3.5.3 Hover

The engine inlet recovery performance improved 1.0 percent as the hovering height was increased from IGE to OGE. The inlet distortion was characteristically higher for the right inlet and there was no influence by changes in wheel height above the ground. Inlet performance was not changed by variation of collective stagger angle.

Engine inlet temperature showed some hot-gas reingestion for an OGE hover and a significant rise as the hovering height was decreased. The recirculation pattern and reingestion level were established very rapidly and, as a result, the transient takeoff data were essentially the same as the steady-state hovering data. The increased inlet temperature changed

the corrected engine power, wing-fan speed, and resultant vertical thrust.

The inlet performance testing was not of sufficient magnitude to evaluate the effects of surface wind variation or fan control positions. (paragraph 1.5.3.5.3)

1.6.3.5.4 Takeoff and Vertical Climb

The inlet temperature rise reached a maximum value just prior to liftoff. Immediately after the liftoff, the temperature decreased rapidly because of the increasing height above the ground and the free-stream inflow velocity. The rate of decrease in the inlet temperature was evidenced by the increasing thrust available and climb rate during the takeoff and climb. The temperature rise during these transient conditions was slightly higher than that recorded during the stabilized hover condition and was probably caused by the higher T/W being utilized. (paragraph 1.5.3.5.4)

1.6.3.5.5 Fan-Mode Level Flight

The engine inlet recovery performance was sensitive to airspeed and improved with increased velocity from a hover. The performance was not influenced by the angle of attack or sideslip ranges tested.

The engine inlet temperature rise was greatest at a hover and decreased to zero for all airspeeds above 60 KCAS. (paragraph 1.5.3.5.5)

1.6.3.5.6 Jet-Mode Level Flight

Jet-mode inlet performance test data were not obtained during this program and the contractor data were used as necessary in the performance calculations. These contractor data showed no unusual characteristics such as split-duct separation or high-speed canopy turbulence. (paragraph 1.5.3.5.6)

1.6.3.5.7 Vertical Descent and Landing

The engine inlet characteristics during descent and landing were the same as those for comparable conditions during takeoff, climb, and hover. The upward free-stream velocity did not carry the hot gases into the upper fuselage area. Ground proximity caused an increasing inlet temperature as the ground was approached; this indicated the hot gas environment was established quickly and was not minimized by the downward

aircraft velocity. The influences of surface winds and fan control positions during the maneuver were not determined. Three unsatisfactory characteristics were noted during VTOL operations in close proximity to the ground (zero-foot to 10-foot wheel heights). Aircraft disturbances, engine reingestion and degradation of lateral control power characteristics were all observed within the specified wheel height region. (paragraph 1.5.3.5.7) (appendix VIII paragraph h)

1.6.3.5.8 Sideward and Rearward Flight

1.6.3.5.8.1 Sideward Flight

The engine inlet was not significantly affected by sideward velocities up to 30 knots. The engine inlet distortion results were not the same and the cause for the variation in the left inlet data is not known. (paragraph 1.5.3.5.8.1)

1.6.3.5.8.2 Rearward Flight

The engine inlet performance was not sensitive to rearward velocities from hover to 20 knots. (paragraph 1.5.3.5.8.2)

1.6.3.6 Engine Flight Performance

The engine installation did not introduce detrimental effects and the engine performance was essentially the same as during the engine calibrations. The engine performance was not sensitive to changes in flight-mode or configuration. (paragraph 1.5.3.6)

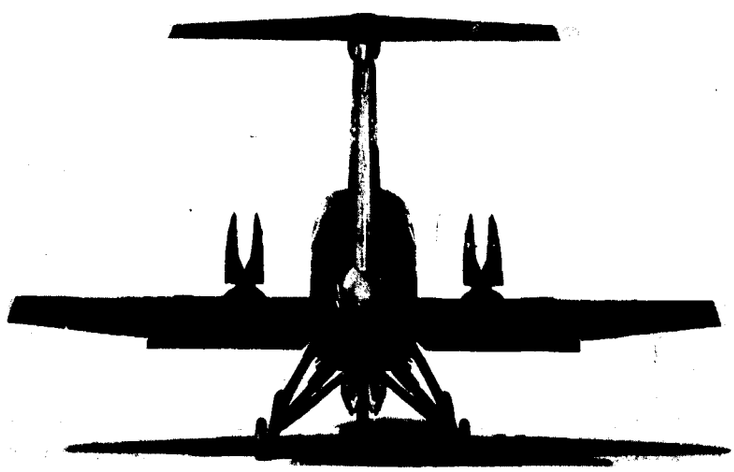

PHOTO 4 - XV-5A FAN-MODE REAR VIEW

1.7 RECOMMENDATIONS

1.7.1 FAN-MODE PERFORMANCE

It is recommended that work be accomplished toward improving fan-mode performance for future V/STOL designs. Additional testing should be conducted to establish further the validity of extrapolating the non-dimensional test data, to evaluate the entire envelope available, and to determine the maximum performance available. Testing should also be conducted with the instrumentation necessary to define the fan operating environment and to measure the fan exhaust conditions. Detailed recommendations for the areas evaluated are presented in the following paragraphs.

1.7.1.1 Hover

a. Investigate methods of maintaining wing-fan speed for all conditions. (paragraph 1.6.1.1)

b. Investigate methods to reduce performance losses associated with increased temperature. (paragraph 1.6.1.1)

c. Investigate requirements for obtaining IGE performance flight test data. (paragraph 1.6.1.1)

d. Conduct additional testing to measure the external fan pressure, velocity, and temperature environment. (paragraph 1.6)

1.7.1.2 Takeoff

a. Establish that the XV-5A should not be considered to be a STO aircraft in its present configuration. (paragraph 1.6.1.2)

b. Investigate methods of increasing the horizontal acceleration during the ground roll to improve short takeoff capability. (paragraph 1.6.1.2)

c. Investigate the effect of a faster vector rate on short takeoff performance capability. (paragraph 1.6.1.2)

1.7.1.3 Vertical Climb

Investigate methods of maintaining wing-fan speed during vertical climbs to improve climb capability. (paragraph 1.6.1.3)

1.7.1.4 Forward Climb

a. Investigate increased aft vector angle capability to determine climb performance. (paragraph 1.6.1.4)

b. Investigate capability of obtaining maximum fan speed at hot-day and/or high-altitude conditions. (paragraph 1.6.1.4)

1.7.1.5 Level Flight

a. Investigate areas of possible drag reduction. (paragraph 1.6.1.5)

b. Provide a means for increasing the horizontal thrust in the fan-mode configuration.

c. Investigate methods of improving hot-day and high-altitude performance. (paragraph 1.6.1.5)

d. Investigate the feasibility of improved fan designs with a greater overspeed capability. (paragraph 1.6.1.5)

1.7.1.6 Vertical Descent

Investigate methods of increasing the vertical rate of descent capability through improvements in handling qualities. (paragraph 1.6.1.6)

1.7.2 JET-MODE PERFORMANCE

Advance diverter valve and fan cavity sealing technology to reduce leakage and subsequent fan cavity overheating. (paragraph 1.6.2)

1.7.3 PROPULSION SYSTEM PERFORMANCE

1.7.3.1 Engine Calibration

Investigate methods of improving diverter valve curved door position actuation and repeatability. (paragraph 1.6.3.1)

1.7.3.2 Ground Tests

Replace trial methods for trimming the nozzle area and wing-fan scrolls with a more exact method to reduce the time and effort required for adjustment after maintenance. (paragraph 1.6.3.2)

1.7.3.3 Vertical Thrust Stand Performance

Conduct additional tests to determine the effect of ground proximity and interactions of the fan controls. (paragraph 1.6.3.3)

1.7.3.4 Inlet

1.7.3.4.1 Engine Calibrations

Determine the engine performance effects associated with flight test inlet rake installations. (paragraph 1.6.3.5.1)

▲ PHOTO 5 · XV-5A IN JET-MODE CONFIGURATION · PHOTO 6 ▼

SECTION 2. DETAILS OF TEST

2.0 INTRODUCTION

The engineering flight research performance evaluation of the XV-5A aircraft was conducted to achieve the objectives specified in paragraph 1.1. The results are presented in this report. The program was conducted by USAAVNTA at Edwards Air Force Base, California. The productive test time totaled 18.1 hours and the flying was accomplished from 22 July 1965 through 15 November 1965. The results of the stability and control evaluation were presented in Part 1, which was published in August 1966 (reference h).

The test program was conducted within the flight envelope presented to the Army by the contractor and in many instances did not encompass the entire envelope available. During the evaluation, any necessary envelope expansion and/or procedural improvements were conducted by the contractor to meet specified Army objectives. All quantitative performance tests were conducted under the direction of the on-site U.S. Army test team.

The U.S. Army test team on site consisted of USAAVLABS Contracting Officer's representative (COR), USAAVNTA Test Director, flight test engineers, and engineering test pilot. The contractor provided logistics, maintenance, instrumentation, and engineering support. A detailed description of the organizational structure and responsibilities is presented in Appendix VIII.

Tests were conducted in smooth air so that turbulence factors would not influence the power required, thrust, and operational characteristics of the lift-fan propulsion system. The average aircraft gross weight used during the tests was 10,000 pounds and the center of gravity (C.G.) was maintained near 241.0 inches (mid).

The test instrumentation was supplied, calibrated, installed, and maintained by the contractor.

The test data were reduced and corrected to standard atmosphere, configuration, and performance conditions through the combined use of USAAVNTA data analysis technicians and contractor computer facilities.

2.1 FAN-MODE PERFORMANCE

The fan mode performance was limited by the test time available and the performance capabilities of the aircraft. The testing was limited to one C.G., one gross weight, and an essentially constant 2500-foot altitude. Only a limited amount of wing-fan instrumentation was available. No adequate external pressure or temperature instrumentation was available. The test conditions chosen throughout were those considered necessary for evaluation of the overall concept. In many cases these conditions were not sufficient to define the precise performance.

The aircraft fan-mode performance was accomplished by stabilizing the aircraft at the desired flight condition prior to recording the test data. The flight techniques used during the fan-mode tests were generally the same as those used during conventional helicopter tests. When necessary, special test techniques were developed to evaluate fully the unique characteristics of the aircraft and the lift-fan propulsion system. The fan-mode performance as discussed in paragraph 2.1 is relative to the aircraft performance while in the fan-mode configuration. This aircraft performance is described in terms of both engine and wing-fan parameters. This method of presentation permits application of design criteria to either engines or fans and calculating the resultant performance from the non-dimensional and summary data. The propulsion system performance, independent of the aircraft performance is presented in detail in paragraph 2.3.

2.1.1 HOVER

2.1.1.1 Objective

The objectives of these tests were to evaluate the lift-fan control and propulsion system characteristics and to determine the hovering capabilities available.

2.1.1.2 Method

The hovering performance was evaluated by using the free-flight hovering technique. The aircraft was stabilized vertically at the desired wheel height by varying the engine power and/or the collective stagger angle. Longitudinal, lateral, and directional control were used as required to balance the forces and moments contributed by the fan control system as well as those contributed by external sources. The aircraft was stabilized for a sufficient time to allow the development of steady-state conditions with respect to propulsion system operation, atmospheric

environment, aircraft position, and attitude. The aircraft height above the ground was recorded photographically by a visual theodolite. The airborne instrumentation was used to record the engine and aircraft parameters. Atmospheric conditions were recorded by a weather station adjacent to the test site.

2.1.1.3 Test Results

The test results are presented graphically in figures 1 through 9, appendix I.

2.1.1.4 Analysis

The non-dimensional power and weight coefficients produced data that were consistent and showed a minimum amount of scatter for all the test flights. The curves used to correct the coefficient data are presented in figures 3 and 4. The stagger angle and thrust coefficient data obtained from the vertical thrust stand tests (paragraph 2.3.4) were slightly different from those obtained during the free-flight hovering tests. The hovering data were used in the correction procedures since they were actual hovering performance.

The thrust from the hovering tests in general agreed with that obtained during the vertical thrust stand tests. This agreement was particularly good for functions of wing-fan speed, engine speed, and power. The wing-fan-speed-versus-engine-speed relationship was not precisely the same for data of both tests although there was no discrepancy in the wing-fan speed and engine-power characteristics.

The total thrust change was 262.5 pounds for each percent of RPM change in wing-fan speed. The variation was essentially linear and the characteristics were the same for both maximum and 50-percent stagger angles. The stagger effectiveness in the area of 50- to 100-percent stagger angles was 287.5 pounds of thrust per degree of angle change. The total thrust change with engine speed was 540 pounds for each percent of RPM change.

The summary hovering performance showed a sea-level standard-day OGE maximum hovering capability of 12,800 pounds. The hovering performance was limited by power available rather than by wing fan speed for all altitude and temperature conditions summarized. For a constant temperature, the hovering performance was decreased approximately 400 pounds for each 1000 feet of increased altitude. The performance deterioration was approximately 100 pounds for each degree F of increased

temperature at a constant altitude. The temperature and altitude variations were essentially linear with no unusual or critical conditions apparent.

The effect of ground proximity could not be accurately established with the data obtained during this evaluation. A stationary hover at a minimum wheel height of 2 feet was possible; however, large thrust variations which required large, rapid, collective stick inputs to maintain the hover condition were present. These transient control and height conditions prevented correcting the data to constant conditions and presenting them in the non-dimensional form.

The IGE hovering data were obtained at non-stabilized conditions due to the adverse aircraft disturbances exhibited at wheel heights of 10 feet and below. A complete discussion of this characterictistic is presented in reference h.

2.1.2 TAKEOFF

2.1.2.1 Objective

The objectives of these tests were to evaluate the capability of the lift-fan propulsion system to provide an overload takeoff capability and to determine the optimum technique for maximum performance.

2.1.2.2 Method

The fan mode takeoff performance was evaluated by conducting maximum performance takeoffs using two different techniques (ground roll and hovering acceleration). The engine power was at the maximum available while the collective stick was at the maximum allowable for the takeoff technique being used. Each takeoff was accomplished at a different airspeed to determine the optimum airspeed and flight path for minimum distance required to clear a 50-foot obstacle. For safety considerations, the test gross weight for each takeoff was adjusted to provide a thrust to weight ratio (T/W) available of not less than 1.15. Angle-of-attack variations were investigated during the climbout portion of the takeoff. A Fairchild Flight Analyzer was used to record photographically the flight path, horizontal distance, vertical distance, and time. The airborne instrumentation recorded flight conditions and aircraft and engine parameters. Static atmospheric conditions were recorded by a weather station adjacent to the test site.

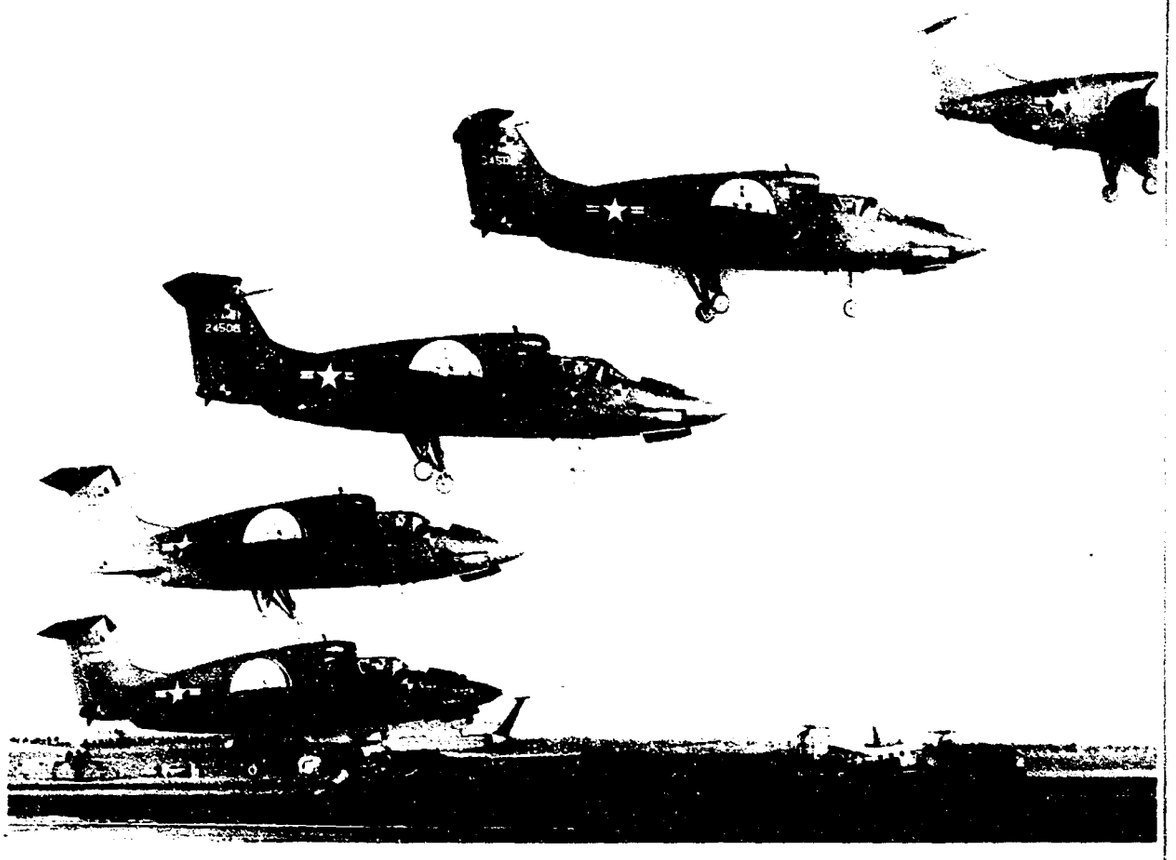

PHOTO 7 XV-5A PERFORMING A VERTICAL TAKEOFF AND ACCELERATION.

2.1.2.3 Test Results

Test results are presented graphically in figures 10 through 13, appendix I.

2.1.2.4 Analysis

2.1.2.4.1 Ground Roll

Flying qualities were significantly influenced by the climbout airspeed and variations in the technique. This discussion is presented in reference h. For the ground roll technique there was no short takeoff and landing (STOL) capability for a T/W available of 1.15. The minimum distance over a 50-foot obstacle

was 1530 feet at a true airspeed of 79 knots. At higher airspeeds, the distance increased rapidly although there was an improvement in the flying qualities. As climbout airspeed was decreased below 60 knots true airspeed (KTAS), there was a significant deterioration in both takeoff performance and flying qualities.

The horizontal accelerating force was provided by the aft collective vector angle of the exit louvers. To obtain the low-speed climbout, the vector had to be rotated early during the acceleration run. This decreased the forward thrust component and horizontal acceleration and increased the distance required to reach the liftoff speed. For the high liftoff speeds, the accelerating force was at a maximum for a greater length of time but the increased power required with airspeed reduced the excess thrust available and thus increased the distance. Based on the power required curve illustrated in figure 2, appendix I, an overload takeoff capability (T/W>1) exists at a gross weight of 12,800 pounds for sea-level standard-day conditions; however, it was anticipated that the takeoff distance would considerably exceed the commonly accepted STOL value of 500 feet.

The rolling takeoff technique used was limited by the collective setting that could be used and still have the aircraft remain on the ground during the acceleration. Excessive collective caused the vertical lift component to be greater than the aircraft weight and limited the available engine thrust that could be used. Figures 155 and 170 illustrate the vertical lift and vector angle relationships. To realize fully the maximum STOL capability, the configuration must be modified to provide a greater horizontal thrust component during the acceleration and to overcome the high drag during climbout. This may be accomplished by a partial conversion capability or a greater vector angle capability. Consideration of the louver vector effectiveness would indicate that considerable losses could occur at vector angles above 45 degrees (figure 172, appendix I). A faster vector rate would allow the pilot to move more quickly the vector angle from the aft position to that required for the liftoff and to adjust to the proper value during the climbout.

The liftoff was affected by rotating the vector forward until sufficient vertical lift was available for the aircraft to become airborne. This was difficult to accomplish precisely and in some cases a considerable mismatch between airspeed and vector angle resulted. This mismatch had to be corrected immediately after liftoff. Failure to accomplish the correction would result in the loss of performance and, in the case of a large deviation, could cause a hazardous flight condition. A vector angle which was forward for the rotating air-

speed being used resulted in an insufficient horizontal thrust and a decreasing airspeed during climbout. This situation occurred when the vector angle was rotated too far forward or during a vectoring overshoot. The vertical force was excessive and the horizontal force was not great enough to overcome the aircraft drag components. When the vector angle was too far aft for the airspeed, the vertical lift was not sufficient for the climbout and the aircraft had to accelerate until there was a decrease in the power required and an excess thrust was available for the climbout. During this acceleration the aircraft might have descended and struck the ground. This particular condition could be caused by using pitch-fan control to rotate the aircraft for liftoff rather than using the vector angle and the accompanying vertical thrust to accomplish the liftoff.

2.1.2.4.2 Hovering Acceleration

The level acceleration distance was linear with airspeed and for a given airspeed above 60 KTAS was greater than that for the rolling acceleration technique. With a T/W of 1.15 available, the distance required to clear an obstacle was 1300 feet at an airspeed of 60 KTAS. The overall flying qualities were better than during a rolling takeoff although there was a characteristic deterioration at airspeeds from 40 to 60 knots (reference h).

The collective stick position was lower during the hovering acceleration and the effective T/W was approximately 1.06. The thrust vector was moved aft both by collective vector control and by the aircraft nosedown attitude. The hovering power-required curve (figure 2) shows that there is no large change in power required from wheel heights of 15 to 50 feet and that for all practical purposes, when a 15-foot hover height is available, a vertical climbout over a 50-foot obstacle is also possible. As such, this technique had very little usefullness other than avoidance of the critical engine loss area when a ground roll could not be accomplished.

2.1.3 VERTICAL CLIMB

2.1.3.1 Objective

The objective of these tests was to determine the minimum T/W for takeoff, maximum vertical takeoff gross weight capability, and vertical climb capability as a function of excess thrust.

2.1.3.2 Method

The takeoff was initiated from a condition of full engine power and collective at the maximum allowable without the aircraft becoming airborne. The liftoff was then accomplished by rapidly applying the maximum collective stick. Longitudinal, lateral, and directional controls were used as required to maintain a vertical flight path. The climb was continued until the acceleration had reached a maximum value. Gross weight was changed on each takeoff to obtain various values of T/W. The flight path, vertical height, and time were photographically recorded by a Fairchild Flight Analyzer. Airborne instrumentation was used to record aircraft and propulsion system parameters. The ambient atmospheric conditions were recorded by a weather station located adjacent to the test site.

2.1.3.3 Test Results

The test results are presented graphically in figures 14 through 26.

2.1.3.4 Analysis

The vertical acceleration was reached approximately 5 seconds after the start of collective application. The vertical acceleration decreased gradually and reached a zero value 10 to 16 seconds after attaining the maximum value. The rate-of-climb characteristics were more well defined than the acceleration characteristics with a gradual increase to the maximum value. In both cases the data were erratic at the start of the climb. This was caused by poor data correlation and inaccuracy of the Fairchild Flight Analyzer as well as small variation in the pilot technique.

The T/W data show the aircraft was extremely sensitive to very small values of excess thrust. Vertical rate of climb increased from 23 fps at a T/W of 1.066 to 39.8 fps at a T/W of 1.172. The fan effectivity was decreased above this value. A T/W of 1.05 produced a vertical velocity of 17 fps. These T/W performance data are based on the static thrust available at the existing power and fan speed available. Any environmental factors influencing the performance were included in the net performance values.

The calculated non-dimensional climb coefficient data from the individual climbs correlate well with the thrust stand and the hovering performance data. In this presentation, the hovering performance data are plotted as a zero rate-of-climb condition.

The vertical climb performance is summarized in figures A, B, and C. The climb performance capability was limited by power available rather than by fan speed at all altitudes for standard-day conditions. The performance deteriorated more rapidly with altitude at the maximum power available than at the limit fan speed. For hot-day conditions, the variation with altitude was similar for both fan speed and engine limits. Performance variation with gross weight was similar for both fan and engine limits at all atmospheric conditions. A 1000-pound increase in gross weight decreased the vertical rate of climb approximately 700 fpm.

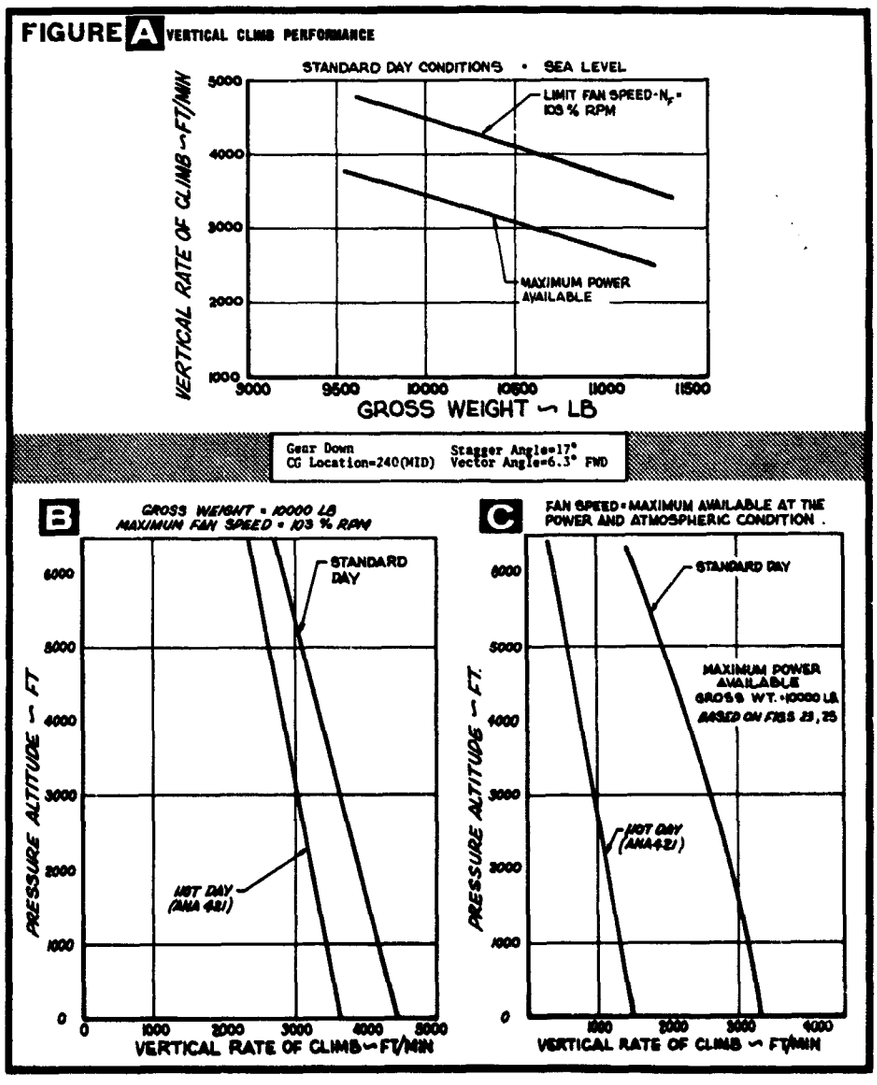

2.1.4 FORWARD CLIMB

2.1.4.1 Objective

The objective of these tests was to determine the forward climb capability, best climb speed schedule, and technique required to obtain the maximum performance.

2.1.4.2 Method

The forward climb tests were conducted at essentially one gross weight, one C.G., and one average altitude. Each climb was conducted at a different airspeed to provide the best climb speed data. The collective stick position was full up and the engine power was at the maximum available for the test conditions. The angle of attack was varied during the tests to establish the associated drag and performance changes. Each climb was conducted through a 1000-foot altitude increment with the aircraft in a stabilized condition. All the test data were recorded by the airborne instrumentation during the stabilized portion of the climb.

2.1.4.3 Test Results

Test results are presented graphically in figures 27 through 50.

2.1.4.4 Analysis

The non-dimensional data presented in figures 27 through 31 utilize level flight as well as climb data. In this presentation the stabilized level flight data have a zero equivalent drag coefficient while the climb data have a negative equivalent drag coefficient (excess thrust). The test data were not complete and it was necessary to extrapolate the faired curves to provide an adequate representation of the performance capability.

The effect of angle of attack on the climb performance is summarized in Figure D. For airspeeds between 80 and 100 knots, the climb performance was better at negative angles of attack for a fan speed limit of 103-percent RPM. As the airspeed was decreased below 79 KTAS the zero angle-of-attack condition provided higher rates of climb.

At a zero angle of attack the climb performance was limited by the maximum aft vector angle at the sea-level standard-day condition. The vector angle imposed a limit only at air-

FIGURE D FORWARD CLIMB PERFORMANCE

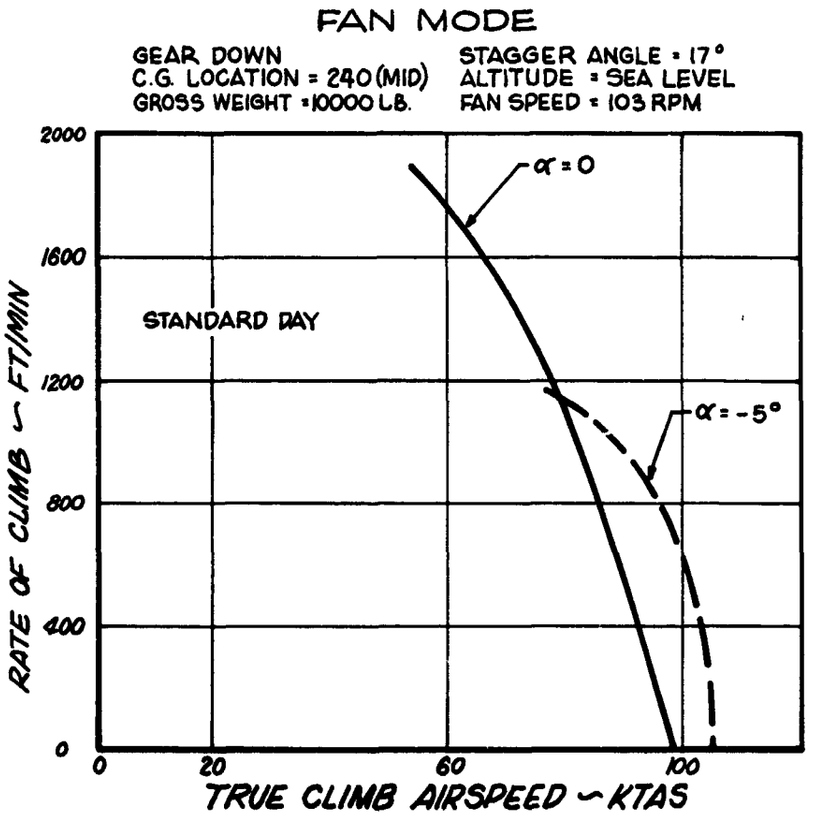

speeds above 89 KTAS for an altitude of 2500 feet and did not impose a limit at higher altitudes.

The hot-day performance was not limited by the vector angle available.

At 10,000-pound gross weight, standard-day, zero angle-of-attack conditions, the performance was limited by power available at an altitude of 6000 feet. Hot-day performance was limited by power available in all cases.

For standard-day conditions and a gross weight of 10,000 pounds, the climb performance was limited by the maximum allowable fan speed prior to being power-limited for altitudes of sea level and 2500 feet. The maximum fan speed was not a limiting factor for hot-day conditions. At a gross weight of 11,000 pounds, climb performance was wing-fan speed-limited for only the sea-level altitude.

The gross weight effect on the climb performance is presented in figure E. At an airspeed of 60 knots an increase of 1000 pounds gross weight decreased the rate of climb 470 fpm. The gross weight effect was essentially constant over the range of airspeed shown.

FIGURE E FORWARD CLIMB PERFORMANCE

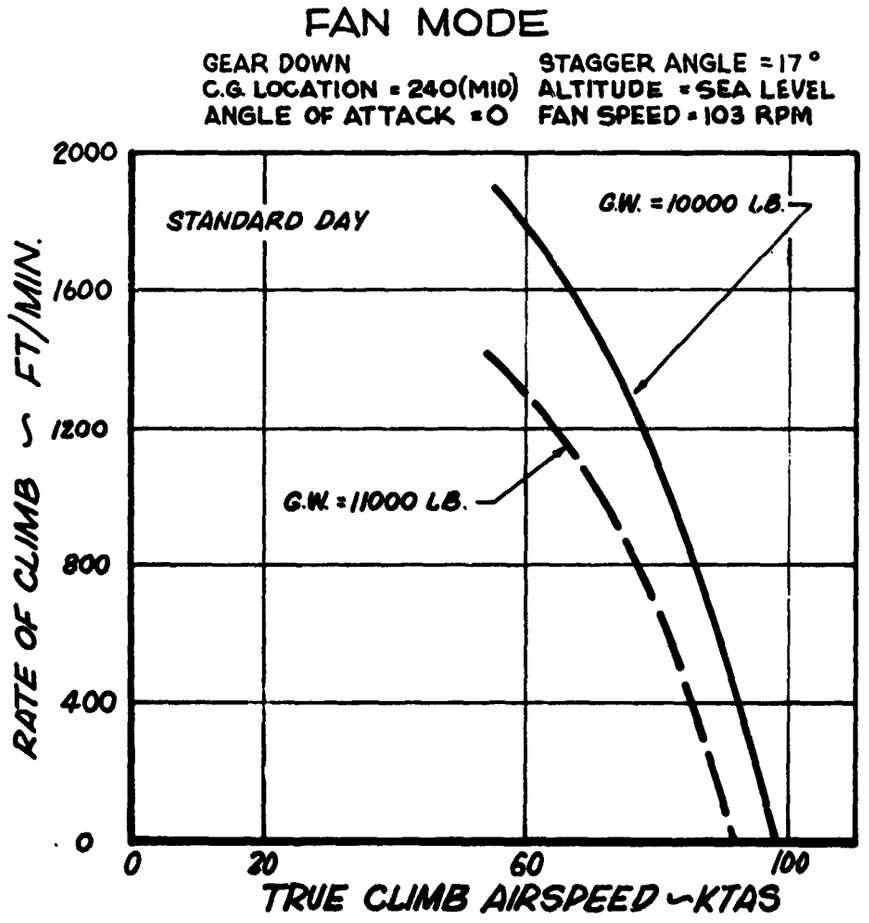

The performance variation with temperature is shown in figure F. The effect was least at low airspeeds and increased with higher airspeeds. Standard-day performance was changed slightly more by airspeed than was the hot-day performance.

FIGURE F FORWARD CLIMB PERFORMANCE

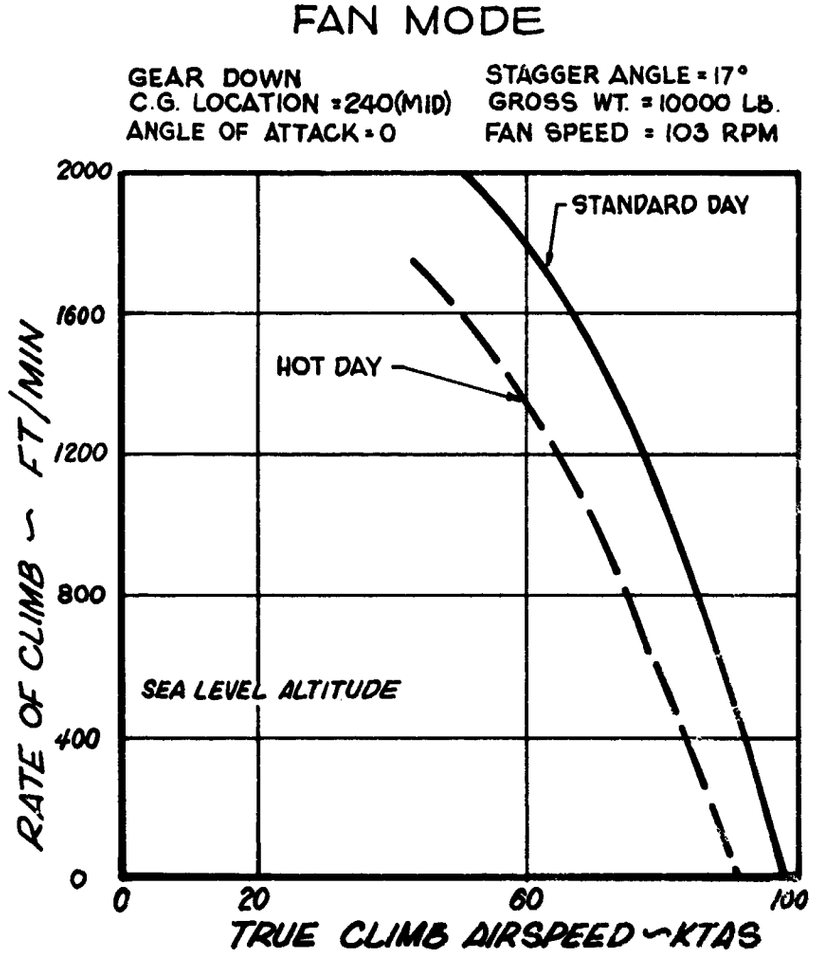

Fan performance variation with altitude is presented in figure G. At an airspeed of 60 KTAS increasing the altitude from sea level to 6000 feet resulted in the rate of climb being changed from 1760 to 820 fpm. Altitude performance variation with power could not be accomplished because the test conditions were such that the necessary extrapolation was excessive.

FIGURE G FORWARD CLIMB PERFORMANCE

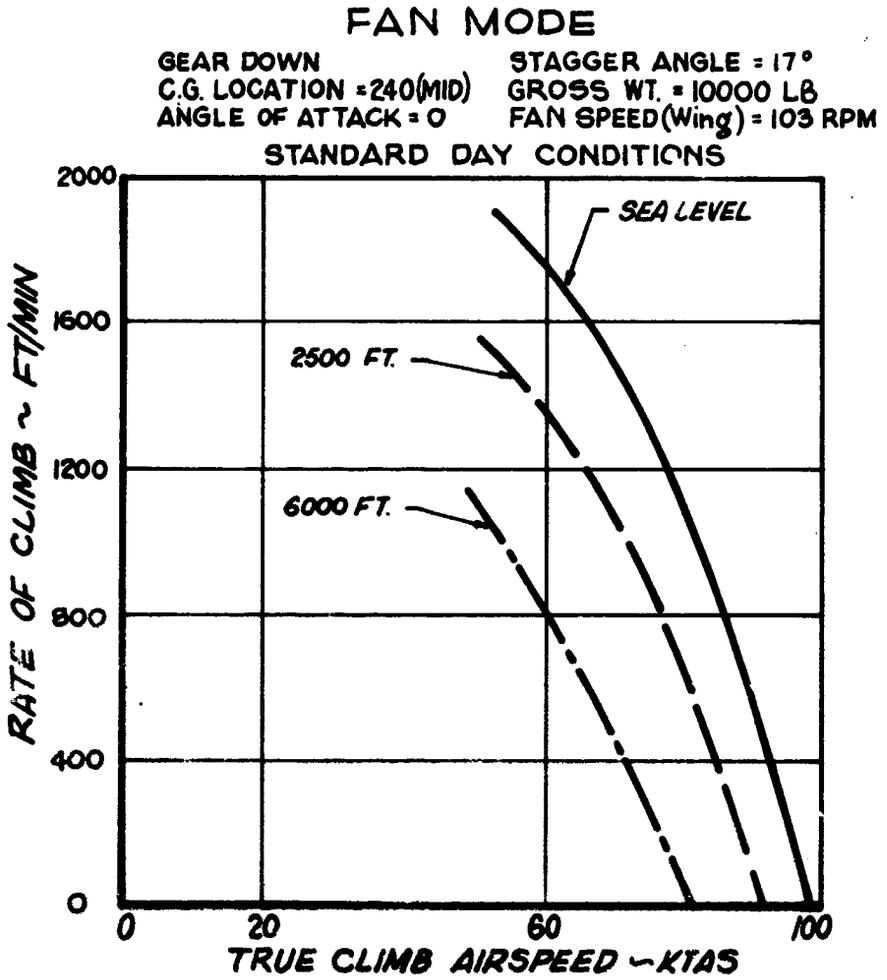

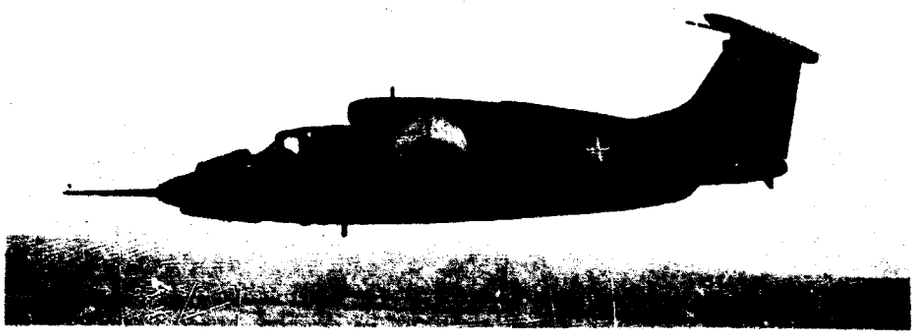

PHOTO 8 - XV-5A PREPARING TO CONVERT TO CONVENTIONAL JET FLIGHT

TABLE 1 SUMMARIZES THE CLIMB PERFORMANCE AND THE LIMITING FACTORS.

FORWARD CLIMB PERFORMANCE SUMMARY

Figure No.	Gross Weight lb	Altitude ft	Angle of Attack deg	Limiting Factor
32	10,000	SL Std	0	β_V
33	10,000	2500 Std	0	β_V @ a/s > 89 KTAS, N_F @ a/s < 89 KTAS
34	10,000	6000 Std	0	$HP_{available}$
35	10,000	SL Hot Day	0	$HP_{available}$
36	10,000	SL Std	-5	β_V @ a/s > 81 KTAS, N_F @ a/s < 81 KTAS
37	10,000	2500 Std	-5	$HP_{available}$ @ a/s > 80 KTAS, N_F @ a/s > 80 KTAS and < 93 KTAS, β_V @ a/s > 93 KTAS
38	10,000	6000 Std	-5	$HP_{available}$
39	10,000	SL Hot Day	-5	$HP_{available}$
40	10,000	2500 Hot Day	0	$HP_{available}$
41	10,000	2500 Hot Day	-5	$HP_{available}$
42	10,000	6000 Hot Day	-5	$HP_{available}$
43	11,000	SL Std	0	N_F
44	11,000	2500 Std	0	$HP_{available}$
45	11,000	6000 Std	0	$HP_{available}$
46	11,000	SL Std	-5	N_F @ a/s < 92 KTAS, β_V @ a/s > 92 KTAS
47	11,000	2500 Std	-5	$HP_{available}$ @ a/s < 75 KTAS, N_F @ a/s > 75 KTAS

2.1.5 LEVEL FLIGHT

2.1.5.1 Objective

The objective of these tests were to determine the power required and to evaluate the engine and fan characteristics throughout the flight envelope.

2.1.5.2 Method

The aircraft was stabilized for each specified test condition with the collective full up and engine power as required. The tests were conducted from 30 knots indicated airspeed (KIAS) to the maximum speed available for both positive and negative angles of attack. The C.G. was maintained near mid (station 240 inches) during each flight by management of fuel. The limited performance available restricted the average gross weight to approximately 10,000 pounds and the density altitude to a maximum of approximately 5000 feet. The tests were conducted in non-turbulent air to eliminate any effects from external disturbances. For each test condition, the aircraft was maintained stabilized for a sufficient time to allow development of steady-state fan and engine conditions. The test data were recorded entirely by the airborne instrumentation system.

2.1.5.3 Test Results

Test results are presented graphically in figures 51 through 70, appendix I.

2.1.5.4 Analysis

2.1.5.4.1 Non-dimensional Performance

The non-dimensional level flight performance is presented in figures 51, 52, 67, and 69. The data presented have been carefully screened to insure that only true stabilized flight is included, i.e., $c^{s}_{d_e}$ = zero. The angle-of-attack data have been corrected by use of the calibration curve presented in figure 72, and are discussed in paragraph 2.1.7. Examination of the data points presented shows that the angle-of-attack variation during the test program was from 5 degrees nosedown to 2.5 degrees noseup. This range was considerably less than the maximum angle-of-attack range available within the flight envelope and was not large enough to define precisely the performance effects of this parameter. The data were not sufficiently distributed through the thrust coefficient range available and the angle of attack was not controlled closely enough to provide data at constant angle-of-attack values. As a result, in some cases, it was necessary to fair the lines where sufficient data were not available to define the curve accurately.

Due to the variation in the angle-of-attack data, it was necessary to obtain empirical correction factors from the test data to correct the individual points to the desired constant angle-of-attack values. The correction factors obtained were then used to correct the data to constant values and determine the proper fairings at these values. These fairings were then transferred to the test points on the composite nondimensional performance plots.

2.1.5.4.2 Engine Power Required

In forward level flight, the minimum power required characteristically occurred at a true airspeed of approximately 10 knots. This minimum power required was essentially the same as that required for the hover condition. The speeds for minimum power required for various altitudes, gross weights, and temperatures are illustrated in figures 55 through 58. Above the minimum-power airspeed, the power required increased gradually until the maximum power available was reached.

The change in power required with the landing gear up and down is shown in figure 54. The power required was significantly reduced with the landing gear retracted and this reduction was equivalent to a 38-knot airspeed increase at a horsepower of 8000. The difference in power required for the two configurations increased at higher power levels and with greater airspeeds.

The engine power required became greater with higher altitudes as shown in figures 55 through 58. There was no significant change as a result of increased ambient temperatures (Air Force-Navy Aeronautical Bulletin (ANA) 421 hot day). This increase in power required, in addition to the decrease in power available, resulted in a significant loss of maximum airspeed as altitude was increased. The maximum airspeed capability as limited by engine power available is summarized in figures II and I, page 42.

An increase of 1000 pounds in gross weight resulted in a power-required increase of 1100 horsepower at 10 KTAS and 1170 horsepower at 80 KTAS. The shape of the curve at 11,000 pounds was somewhat different from that of the 10,000-pound curve. The induced drag effect was smaller at 11,000 pounds and the decrease in power required with forward speed was less evident. The momentum drag change was more significant at the higher power setting and this resulted in a greater separation of the curves at the 80-knot condition.

2.1.5.4.3 Wing-Fan Speed Required

The fan-speed required characteristics were of the same general nature as the power-required characteristics at a zero angle

of attack. The landing-gear-up configuration reduced the required wing-fan speed 3.7-percent RPM at 80 KTAS and at the limit fan speed of 103 percent RPM. This reduced drag resulted in an airspeed differential of approximately 23 KTAS.

FIGURE H MAXIMUM AIRSPEED

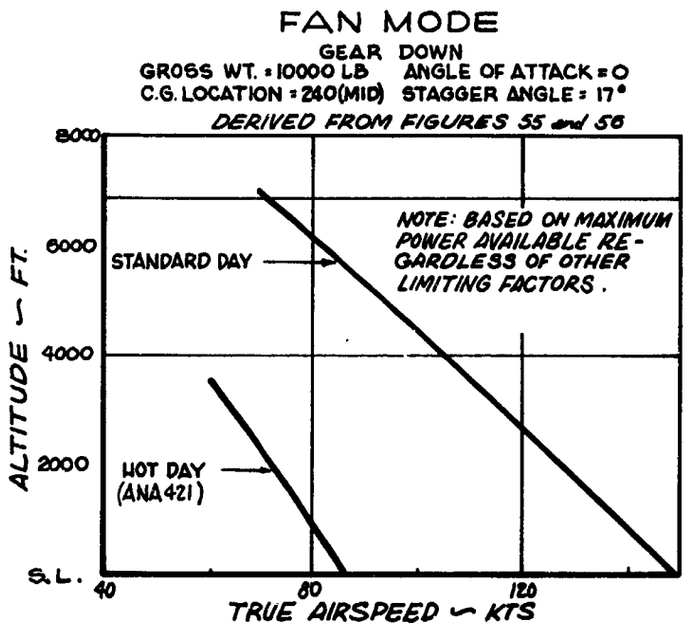

FIGURE I HORSEPOWER REQUIRED

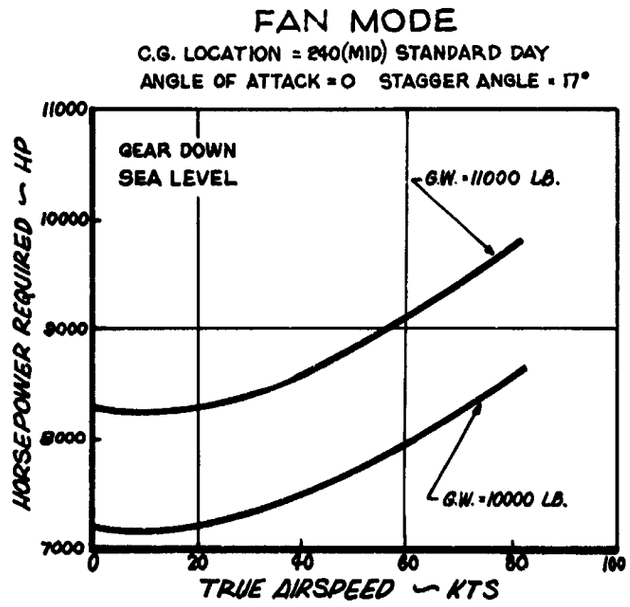

Fan speed required increased with increased altitude and temperature as shown in figures 55 through 58. This variation was essentially linear with altitude and the increased temperature introduced no significant detrimental effects. The speed capability was decreased approximately 23 KTAS by a 6000-foot increase in altitude and there was no speed loss with a temperature change from standard to hot day (ANA 421). The maximum wing-fan-speed limited speed capability is presented in figures J and K.

A gross weight increase of 1000 pounds increased the fan speed required by 4-percent RPM at 10 KTAS and by 3.5-percent RPM at 80 KTAS.

FIGURE J MAXIMUM AIRSPEED

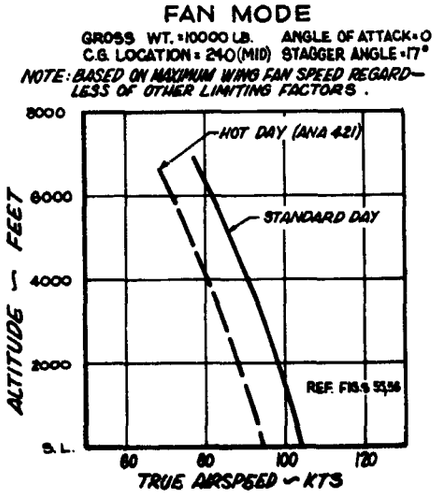

FIGURE K WING FAN SPEED REQUIRED

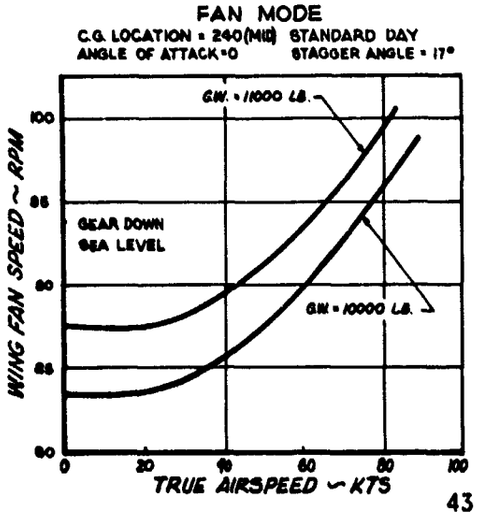

2.1.5.4.4 Angle of Attack

The engine power and wing-fan speed required were both significantly changed by variations in the angle of attack as illustrated in figure 53. For the angle-of-attack range of ± 2.5 degrees, the power required was greatest at 2.5 degrees and smallest at -2.5 degrees with zero being an intermediate value. At airspeeds above 50 KTAS, the power required for 2.5 degrees increased rapidly and tended to diverge from the power required at zero and -2.5-degrees. At a negative angle of 5 degrees, there appeared to be a change in the curve characteristics. For this condition, the curve appeared to intersect the zero angle-of-attack curve at 50 KTAS with lower power required at speeds less than 50 KTAS and with greater power required at any speeds higher than 50 KTAS.

The wing-fan speed required as a function of angle of attack was more clearly defined than was the power required. The change in fan speed required is shown in figures L and M. As can be seen, approximately 2-percent RPM was required to increase the angle of attack from -5 to 2.5 degrees. The fan speed differential increased somewhat with higher airspeeds but the characteristics were essentially linear with no significant discontinuities.

FIGURE L WING FAN SPEED REQUIRED

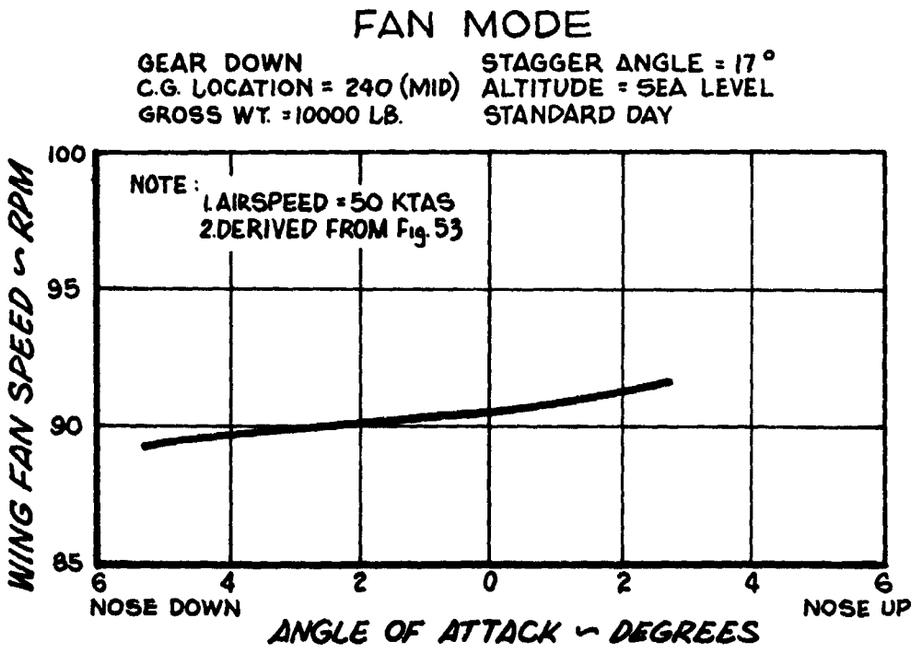

FIGURE M WING FAN SPEED CHARACTERISTICS

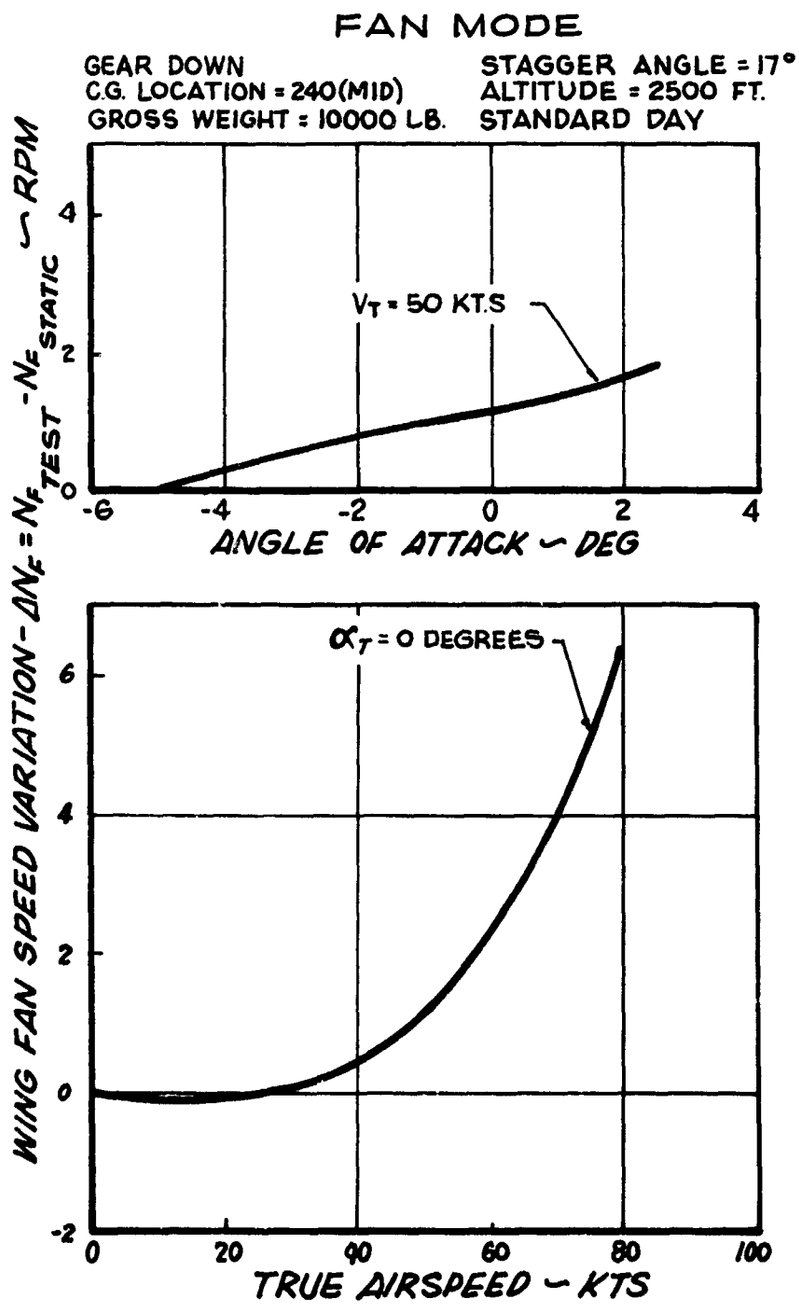

2.1.5.4.5 Endurance Performance

The specific endurance performance is shown in figures 59 through 61. The airspeed for maximum endurance was 10 KTAS at sea-level standard-day conditions and at all gross weights from 10,000 to 11,000 pounds. At altitudes of 2500 and 6000 feet, the airspeed increased to approximately 11 KTAS. The airspeed increased with gross weight and was 12.7 KTAS at 2500 feet and 11,000 pounds. The airspeed for best endurance was not changed as ambient temperature was increased from standard to hot-day conditions (ANA 421). The best endurance airspeed increased with angle of attack with a change from 10 to 13.7 KTAS as the angle of attack was increased from -2.5 to 2.5 degrees.

The maximum specific endurance increased with higher altitude. The specific endurance at 10,000 pounds was .01430 at sea level and became .01458 at 6000 feet. This altitude effect tended to be more pronounced at a higher gross weight of 11,000 pounds. The endurance performance decreased significantly with increased temperature as a result of the higher power required at these ambient conditions. At an altitude of 2500 feet, a temperature increase of 24 degrees F reduced the specific endurance from .01436 to .01381. The increased power required with higher positive angles of attack also decreased the specific endurance slightly. The change was more apparent for a change from zero to 2.5 degrees than for a change from zero to -2.5 degrees.

2.1.5.4.6 Range Performance

The specific range performance is presented in figures 62 through 66. The airspeed for maximum range performance could not be reached prior to encountering fan-speed, power-available, or vector-angle limits. At sea level, the speed was limited to 84.5 KTAS by maximum vector angles for a zero angle of attack. For a similiar condition, at 2500 feet, the limiting factor was also the vector angle available and the maximum airspeed was 87.5 KTAS. The best range speed was 81 KTAS at 6000 feet and the limit was imposed by both power available and maximum fan speed. For a hot-day 2500-foot condition, the aircraft was power-limited to an airspeed of 68 KTAS. The airspeed for best range varied with the angle of attack.

The specific range performance improved slightly with increased altitude with the change being more significant at higher airspeeds. The specific range performance available and the limiting factors are summarized in table 2.

TABLE 2

SPECIFIC RANGE PERFORMANCE SUMMARY

Altitude ft	Airspeed kt	Nautical Air Miles Per Pound of Fuel NAMPP	Limiting Factor
SL	84.5	.0176	βV_{max}
SL	104.0	.0208	$N_{F_{max}}$
2500	87.5	.0183	βV_{max}
2500	95.5	.0197	$N_{F_{max}}$
2500	137.0	.0258	Hp_{avail}
6000	81.5	.0176	$N_{F_{max}}$
6000	81.5	.0176	Hp_{avail}
6000	93.5	.0196	βV_{max}

The range performance was best at a zero angle of attack and was decreased by either positive or negative angle-of-attack values. As was previously noted, the vector angle available limited the airspeed prior to reaching the best range speed. The range performance was greatly improved by retracting the landing gear and reducing the power required. In both conditions, the maximum vector angles was the limiting factor, with the specific range available being .0192 for the landing-gear-down configuration and .0217 for the landing-gear-up configuration.

2.1.6 VERTICAL DESCENT

2.1.6.1 Objective

The objectives of these tests were to determine the fan and engine performance during vertical descent and to establish the T/W as a function of descent rate.

2.1.6.2 Method

The descents were conducted with the engine power at the maximum and the collective stick as required to maintain the rate of descent. Each descent was initiated from a stabilized hover approximately 700 feet above the ground. The collective was lowered until the rate of descent was the maximum allowable as determined by the pilot. The collective was then used to stabilize and maintain the descent rate at this maximum value. Longitudinal, lateral, and directional controls were used as necessary to maintain a vertical flight path. Verbal inputs from ground observers were also used by the pilot to control the flight path. As the aircraft neared the ground, the collective stick was used to slow the rate of descent and enter a hover. Each descent was conducted at a different gross weight to provide a variation in the T/W data. The descents were graphically recorded by a Fairchild Flight Analyzer to provide flight-path, rate-of-descent, and height information. Propulsion system and aircraft parameters were recorded by the airborne instrumentation while ambient atmospheric conditions were recorded by a weather station near the test site.

2.1.6.3 Test Results

Test results are presented graphically in figure 71, appendix I.

2.1.6.4 Analysis

The rate-of-descent variation was essentially linear with the steady-state T/W being used. The rate of descent of 485 fpm at a T/W of 0.935 was the highest allowable based on increasing difficulties in maintaining directional control during the descent. This deterioration of flying qualities prevented testing at further reduced values of T/W and/or higher rates of descent. The tests did not include maximum performance relative to rapidly stopping the rate of descent or accomplishing vertical landings. For the test conditions specified in figure 71, the maximum T/W available was approximately 1.14. For all the descents, it was possible to stop the rate of descent and enter an OGE hover condition without utilizing the maximum T/W available. The engine and inlet performance characteristics during vertical descents are discussed in detail in paragraph 2.3.

2.1.7 ANGLE-OF-ATTACK CALIBRATION

2.1.7.1 Objective

The objective of the angle-of-attack calibration was to establish the magnitude of the angle-of-attack position error as a function of wing-fan cross-flow ratio, aircraft attitude, and airspeed.

2.1.7.2 Method

The angle-of-attack calibration was accomplished by flying the aircraft in level flight at various airspeeds and angles of attack. The airspeed range was from 30 knots to the maximum available level flight speed while the angle of attack was varied from -2 degrees to +5 degrees. Two different techniques were used to accomplish the calibration. The first technique was a by-product of the level flight performance, stability and control tests. In this case, all the data were obtained from the airborne instrumentation. The second technique utilized a Fairchild Flight Analyzer to establish the flight path, airspeed, and angle of attack. Aircraft propulsion system, and atmospheric parameters were recorded by the airborne instrumentation.

2.1.7.3 Test Results

Test results are presented graphically in figure 72, appendix I.

2.1.7.4 Analysis

The angle-of-attack position error could not be identified as a function of cross-flow ratio and indicated angle of attack as predicted by the full-scale wind-tunnel results. The position error appeared to be a constant with airspeed and a variable for the indicated angle-of-attack range evaluated during the tests.

The induced flow through the fans resulted in a large upflow at the angle-of-attack sensor as evidenced by the positive position error correction. This local angle of attack was considerably different from the free airstream true angle of attack. The correction became more positive with a greater positive angle of attack. The variation of position error was linear from -0.4 degrees at a -5-degree indicated angle of attack to -4.0 degrees at a +8-degree indicated angle of attack. The trend of the flight test variation of the position error was essentially the same as the wind tunnel data; however, the magnitude of the correction was approximately 1.5 degrees less positive.

2.1.8 AIRSPEED CALIBRATION

2.1.8.1 Objective

The objective of the airspeed calibration was to determine the position error of the low-airspeed (nose-boom) system during fan-mode flight.

2.1.8.2 Method

The airspeed calibration of the low-airspeed system was accomplished by flying formation with a calibrated pacer helicopter. The system was calibrated over an indicated airspeed range of 30 to 85 knots and for angles of attack of -2, zero, and 5 degrees. The tests were conducted at an average gross weight of 10,000 pounds, a C.G. of 240 inches (mid), and an altitude of 5800 feet.

2.1.8.3 Test Results

Test results are presented graphically in figure 73, appendix I.

2.1.8.4 Analysis

The nose-boom (low-airspeed) system indicated low for all airspeeds between 30 and 85 knots. The correction was linear throughout with a constant value of 3 knots. There was no clearly defined variation in the position error at the angles of attack tested. There was, however, an indication that a variation would occur at greater angles of attack both positive and negative. The test data showed that the greatest position errors were encountered at a zero angle of attack and the magnitude tended to become slightly smaller at both -2 and +5 degrees. The total variation for all three angles of attack was approximately 3 knots. There was no apparent change in the angle-of-attack effect as a function of airspeed.

2.2 JET-MODE PERFORMANCE

The jet-mode performance testing was assigned a lower priority than the fan-mode and the propulsion system performance testing. Due to this low priority, the jet-mode testing was primarily accomplished when fan-mode operation could not be conducted because of adverse weather conditions for fan operation, instrumentation discrepancies, or fan-system maintenance problems. The jet-mode testing was limited to level flight performance and airspeed calibration for the cruise and pre-conversion configurations. One test flight was a split-mode configuration (fan doors open and diverter valves in jet-mode position) to evaluate the capabilities in the event of

a malfunction during a conversion. Additional performance test data were previously obtained during contractor tests and are presented in references i and j.

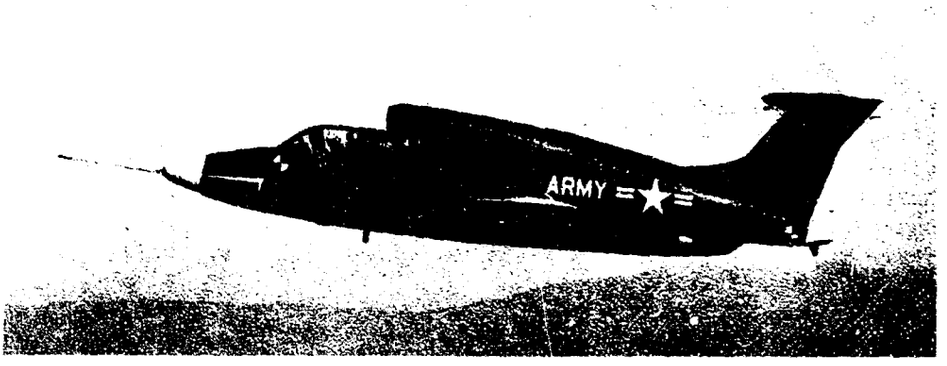

PHOTO 9 - XV-5A IN JET-MODE CONFIGURATION

2.2.1 LEVEL FLIGHT

2.2.1.1 Objective

The objective of these tests was to determine the power and thrust required, drag and lift capabilities, endurance, and range performance for the jet-mode configuration.

2.2.1.2 Method

The cruise configuration performance was evaluated by accomplishing speed-power polars using a constant weight/pressure ratio (w/δ) technique. The standard gross weight was 10,500 pounds and the test altitudes were 5000, 10,000, and 15,000 feet. The tests were conducted prior to the installation of either the inlet pressure instrumentation or the calibrated engines. The pre-conversion testing was accomplished on several flights with the data being recorded prior to conversion for fan-mode tests. As a result, the data were essentially at a constant pressure altitude for all gross weights tested. The fan-doors-open test was a special configuration with the system modified to allow opening of the fan doors without activating the remainder of the conversion system. In all the tests, the minimum airspeed was limited to the onset of stall buffet to prevent an inadvertent stall while the maximum speed limit was to Mach = .7 or the maximum power available. The atmospheric and aircraft test parameters were recorded by the airborne instrumentation.

2.2.1.3 Test Results

Test results are presented graphically in figures 74 through 85, appendix I.

2.2.1.4 Analysis

The jet-mode cruise configuration performance characteristics are similar to those of conventional jet aircraft. A detailed discussion of jet-mode handling characteristics is contained in reference h. The T-38A aircraft was selected for drag characteristics comparison with those of the XV-5A due to the nearly common power plant, size and weight. This comparison appears in figure MM. As expected the XV-5A exhibited high drag characteristics.

FIGURE MM COMPARATIVE DRAG CHARACTERISTICS

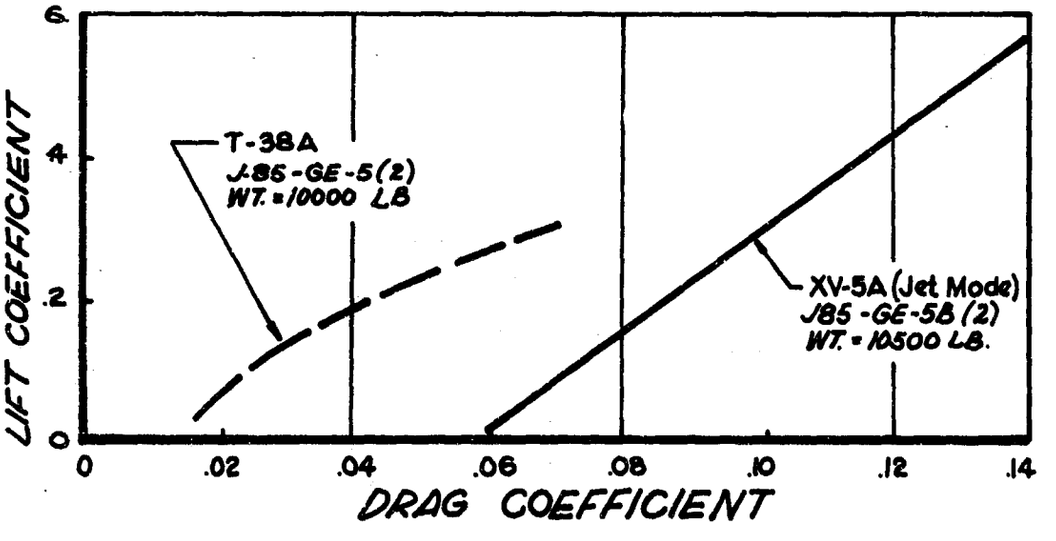

During these tests maximum velocity (V_{max}) was limited to 374 KTAS due to the overheating of the right-wing-fan area. This characteristic, resulting in a performance limitation, should be corrected in future aircraft designs incorporating the fan-in-wing concept.

2.2.2 AIRSPEED CALIBRATION

2.2.2.1 Objective

The objective of the jet-mode airspeed calibration was to determine the position error and operating characteristics of wing-boom (high-airspeed) and the nose-boom (low-airspeed) systems.

2.2.2.2 Method

The airspeed calibration was accomplished by flying formation with a calibrated pacer aircraft. Both systems were calibrated in clean, power-approach (P.A.), and pre-conversion (PC) configurations. The tests were conducted OGE at an altitude ranging from 5000 to 15,000 feet, an average gross weight of 10,500 pounds, and a mid C.G. (240.5 inches).

2.2.2.3 Test Results

Test results are presented graphically in figures 86 and 87, appendix I.

2.2.2.4 Analysis

The nose-boom (low-airpseed) system position error was nonlinear for all configurations and varied in magnitude from a minimum of -4.5 knots to a maximum of +9.0 knots. For the cruise configuration, the position error varied from a value of -4.5 knots at 103 KIAS to +4.5 knots at 135 KIAS. In the pre-conversion configuration with gear up or down, the position error varied from -3 knots at 95 KIAS to +9 knots at 143 KIAS. The position error in power-approach configuration was positive and had a value of +3 knots at 103 KIAS and varied to +8.5 knots at 123 KIAS.

The wing-boom (high-airspeed) system position error was nonlinear and was the same for all configurations. The position error varied from -7 knots at 110 KIAS to +0.3 knots at 175 KIAS. The position error then decreased from +0.3 knots at 175 KIAS to -1.5 knots at 250 KIAS and remained the same up to an airspeed of 293 KIAS.

2.3 PROPULSION SYSTEM PERFORMANCE

The propulsion system encompasses the engines, ducting, diverter valves, pitch fan and doors, wing fans and exit louvers. The system evaluation provided the data necessary to correlate the aircraft performance in terms of the test parameters of engine and wing-fan speed. The engine/fan relationships presented here are

valid for only the XV-5A geometry and may not be the same for another installation. The basic fan uninstalled data were not available for comparison with the installed performance data. The test instrumentation on the fans was not adequate to define the wing-fan pressure and temperature environment as a function of the flight conditions. The IGE testing was not of sufficient magnitude to determine the reingestion and recirculation patterns for various wind conditions and takeoff techniques. There was no instrumentation available to evaluate the external pressure, velocity, and temperature characteristics relative to the aircraft.

2.3.1 ENGINE CALIBRATION

2.3.1.1 Objective

The objectives of the engine calibrations were to determine the uninstalled power and thrust available from the standard and modified J-85-5B engines and to evaluate the engine characteristics such as fuel flow, temperature ratios, pressure ratios, bleed valve operation, diverter valve leakage, and effects of variation of engine exhaust gas temperature trim.

2.3.1.2 Method

The calibration was conducted with the engines mounted in the engine contractor's test facility. The following calibrations were accomplished:

Calibration Bleed Valve Rigging/Inlet Configuration	Engine Configuration	Exhaust Gas Temperature Trim
Nominal/Calibrated	Standard	680°C
Nominal/Calibrated	Modified	680°C
Nominal/Flight Rakes	Modified	680°C
Nominal/Flight Rakes	Modified	660°C
Nominal/Flight Rakes	Modified	700°C

The calibrated inlet was a special, highly instrumented bellmouth attached to the engine inlet. The flight rakes were modified from a previous T-38 aircraft installation. The standard engine calibrated was the "as shipped" engine while the modified engine calibrated was one which incorporated the stall modifications.

The calibrations were conducted with engines equipped with individual aircraft diverter valves and a standard XV-5A tailpipe. The tests were run with the bleed valves set both above and below the stall modification bleed valve schedule (nominal rigging schedule).

One calibration run was made with a nominal bleed valve schedule, an EGT trim of 680 degrees C, flight rakes, and the curved diverter valve door set at three different positions.

The calibration technique was to vary engine speed incrementally from flight-idle to maximum power. The data were then recorded at each stabilized point.

2.3.1.3 Test Results

Test results are presented graphically in figures 88 through 121, appendix I.

2.3.1.4 Analysis

2.3.1.4.1 Inlet Configuration

The bellmouth calibration is shown in figure 88, appendix I. At an inlet pressure ratio (P_{T_2}/P_{S_2}) of 1.16, the measured airflow was 2.49 percent less than the calculated airflow based on no losses. There were no engine losses introduced as a result of the inlet rake installation. The engine performance with the calibrated inlet is compared with the ideal values in figures 90 through 93, appendix I, and summarized in table 3.

TABLE 3

ENGINE PERFORMANCE COMPARISON

Engine Speed % RPM	Corrected Inlet Airflow Ideal/Measured lb/sec	Engine Serial Number	Engine Configuration	Engine Thrust Ideal/Measured lb
100	44.7/43.4	875	standard	--
100	44.7/43.4	876	standard	--
100	--	875	modified	2740/2630
100	--	876	modified	2580/2520

2.3.1.4.2 Engine Comparison

The two test engines S/N 875 and 876 were reasonably well matched. A comparison of the two engines is presented in table 4.

TABLE 4

ENGINE CALIBRATION COMPARISON

	Engine Serial Number 875	Engine Serial Number 876
Engine Speed - % RPM	100	100
Interstage Bleed Airflow - lb/sec	.055	.058
Engine Configuration	mod.	mod.
Inlet Configuration	calib.	calib.
Inlet Airflow - lb/sec	43.5	42.5
Turbine Discharge Airflow - lb/sec	43.2	42.0
Corrected Fuel Flow - lb/hr	2615	2520
Corrected Customer Bleed - lb/sec	.128	.125
Corrected Exhaust Gas Temperature - °R	1655	1660
Corrected Engine Thrust - lb	2630	2530
Corrected Engine Power - HP	5050	4750

The engine S/N 875 produced more power and thrust and had higher fuel-flow and exhaust gas temperature (EGT) than engine S/N 876. The operating characteristics were similar for both engines.

The engine modification decreased the overall engine performance with the change being greater for engine S/N 876 than for 875. The change in performance due to the modification at engine speed of 100 percent is summarized in table 5.

2.3.1.4.3 Diverter Valve Leakage and Exhaust Gas Temperature Trim

The diverter valve leakage increased directly with the differential pressure across the valve and inversely with the gas leakage temperature. The leakage flow increased nonlinearly with the engine speed. The leakage flow increased from 0.29 to 0.47 pounds/second at an engine speed of 100-percent RPM as the EGT trim was increased from 660 to 700 degrees C. The percentage of gas flow loss through leakage was higher at a 700-degree C EGT trim than at a 660-degree C EGT trim; however, the variation trend with engine speed was opposite. At 700 degrees C, the loss was 1.52 percent at an engine speed of 70 percent and decreased to 1.08 percent at 100-percent RPM. For the 660-degree C condition, the loss increased from .44 to .7 percent over a similar engine speed.

TABLE 5

ENGINE MODIFICATION PERFORMANCE

Engine Serial Number	Corrected Exhaust Gas Temperature Δ°R	Corrected Fuel Flow Δlb/hr	Corrected Engine Thrust Δlb	Corrected Engine Power ΔHP
875	75	200	295	250
876	60	185	250	450

The EGT trim setting did not change the inlet pressure ratio characteristics of either engine. For engine S/N 875, the corrected fuel flow increased 165 pounds/hour as EGT trim was increased from 680 to 700 degrees C and decreased 35 pounds/hour with a change from 680 to 660 degrees C. The fuel-flow change for engine S/N 876 was slightly less and the characteristics were similar. The engine S/N 876 power and thrust characteristics were much more sensitive to EGT trim than those of engine S/N 875. Changing the EGT trim from 660 to 700 degrees C resulted in a power increase of 930 horsepower and a thrust increase of 265 pounds for engine S/N 876. For a similar change the values for engine S/N 875 were 400 horsepower and 125 pounds.

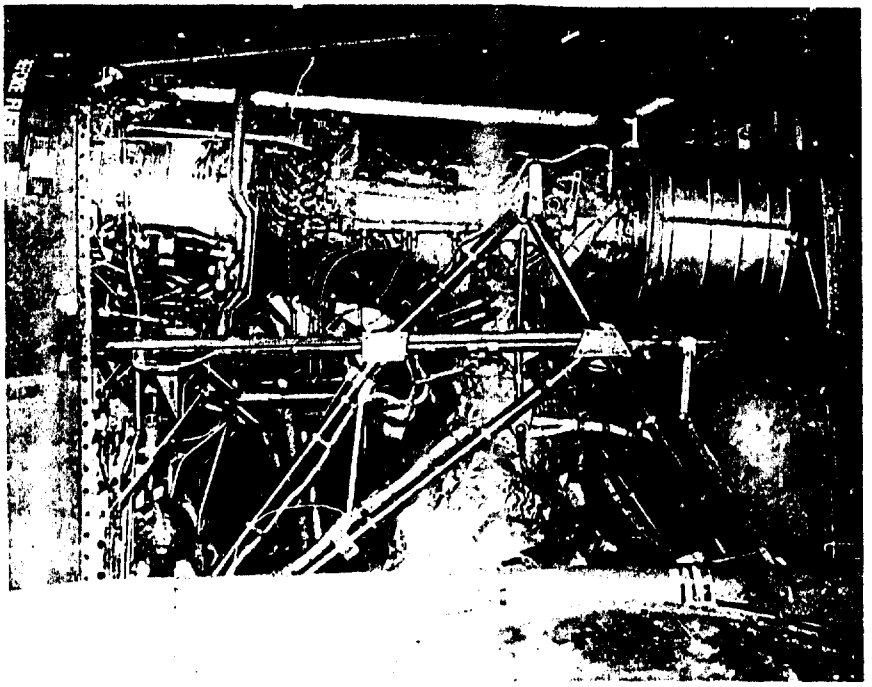

PHOTO 10 - LEFT HAND DIVERTER VALVE INSTALLED

2.3.1.4.4 Bleed Valve Rigging

The bleed valve riggings evaluated are presented in figure 110. The inlet airflow was unchanged by a low bleed valve position (BVP); however, a high rigging decreased the airflow by 1.9 percent at an engine speed of 98-percent RPM. Fuel flow, turbine gas flow, and turbine discharge pressure were decreased by a high BVP rigging. The EGT was essentially the same for all riggings at engine speeds above 97-percent RPM. The corrected horsepower and thrust were decreased 11 percent and 9.8 percent respectively for a BVP change from low to high at an engine speed of 98-percent RPM.

2.3.1.4.5 Curved Diverter Door Position

The EGT was very sensitive to the curved diverter door position. Overtravel reduced the EGT while undertravel increased the EGT. The variation is illustrated in figure N. Any misalignment greater than 1 inch of undertravel resulted in a significant increase in the EGT.

FIGURE N

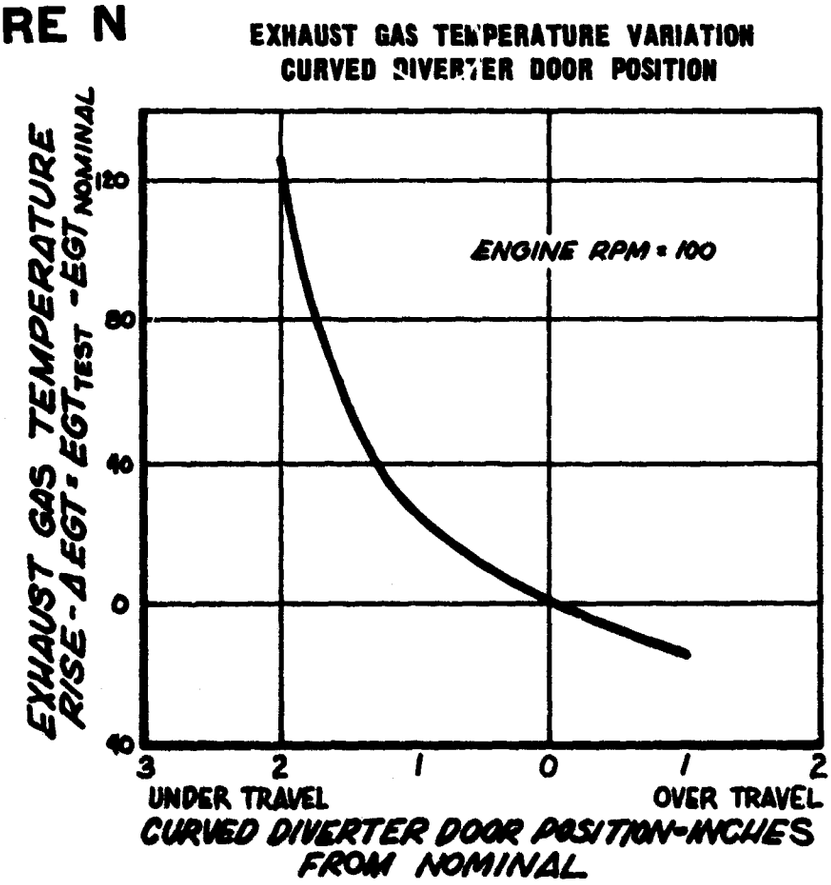

2.3.2 GROUND TESTS

2.3.2.1 Objective

The objectives of these tests were to establish the installed engine/fan power and speed relationship during zero airspeed conditions, provide data for comparison with the uninstalled performance, and provide correlating parameters for the empirical power determination method.

2.3.2.2 Method

The ground tests were accomplished with the aircraft secured to the ramp. Engine speed was incrementally varied from flight-idle to maximum available with data being recorded at each stabilized point. The aircraft, engine, and fan parameters were recorded by the aircraft instrumentation and the ground-support engine analyzer equipment. Ambient atmospheric conditions were recorded by an adjacent weather station. Following the dual-engine runs the tests were repeated for single-engine operation. The engine analyzer was also used to monitor engine performance in real time and to control the test conditions.

2.3.2.3 Test Results

Test results are presented graphically in figures 122 through 126, appendix I.

2.3.2.4 Analysis

2.3.2.4.1 Curved Diverter Door Position

Variation of one curved diverter door did not influence one wing fan and the pitch fan. The other wing fan showed an increase in speed as the position moved either direction from normal. These characteristics are illustrated in figure 0.

2.3.2.4.2 Installed Static Performance

The engine-installed static performance for the ground tiedown tests was compared with the engine calibration performance in figures 103, 104, 125, and 126, appendix I. The power loss was 310 horsepower (6.15 percent) for the left engine, S/N 875, and 190 horsepower (4 percent) for the right engine, S/N 876.

FIGURE 0 ▶

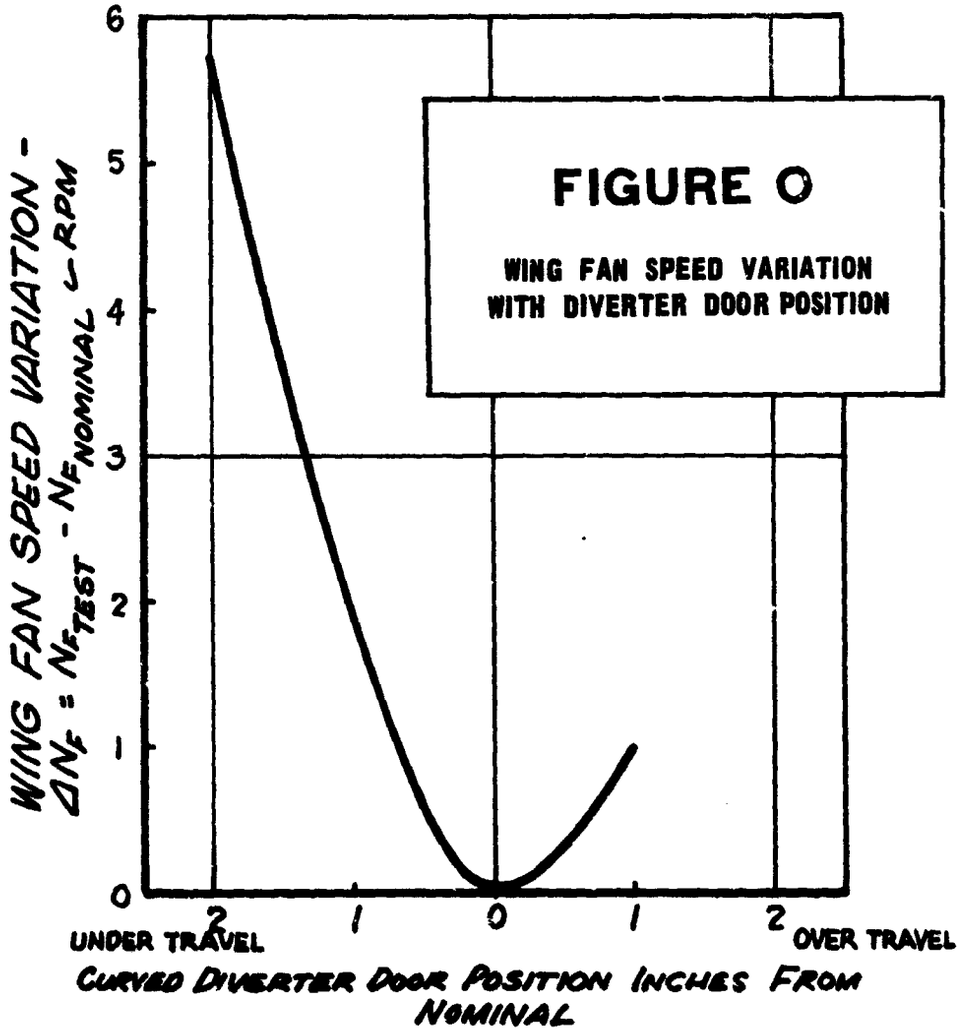

FIGURE O

WING FAN SPEED VARIATION WITH DIVERTER DOOR POSITION

2.3.3 HORIZONTAL THRUST STAND

2.3.3.1 Objective

The objectives of the horizontal thrust stand test were to determine the installed static thrust and engine inlet performance and to provide installed engine performance data for comparison with data obtained during the engine calibrations.

2.3.3.2 Method

The aircraft was positioned on the horizontal thrust stand in the jet-mode configuration. The thrust stand instrumentation was corrected to a zero force condition with the engines off prior to starting the test. The engines were incrementally stabilized through-

out the entire range available from idle to full power. The initial tests were for the dual-engine configuration. Each engine was then run individually to establish any interference effects that might degrade thrust or engine inlet performance as a result of single-engine operation. The horizontal thrust was also determined with the wing-fan exit louvers set at the most aft (45-degree) position. The propulsion system and aircraft parameters were recorded by the aircraft instrumentation. At the conclusion of the tests an "engine off" tare reading was obtained to determine any change that occurred in the thrust stand instrumentation during the tests. Static ambient atmospheric conditions were recorded by an adjacent weather station.

2.3.3.3 Test Results

Test results are presented graphically in figures 127 through 138, appendix I.

2.3.3.4 Analysis

2.3.3.4.1 Jet-Mode Configuration

The total corrected engine thrust in the jet-mode configuration was 5725 pounds at a corrected engine speed of 100-percent RPM. The thrust value was 590 pounds greater than the sum of the two single-engine thrusts recorded during the engine calibrations. The fuel flow was also higher by 625 pounds/hour with the left engine (S/N 875) fuel flow being 320 pounds/hour greater than the right engine (S/N 876) fuel flow. The EGT was also 20 degrees C higher for the left engine. The bleed valve schedules were the same for both engines and were higher than for the rigged schedule.

During single-engine operation the thrust recorded was the same for both left and right engines. The fuel flow and EGT were also the same for both engines. The sum of the two single-engine thrust values was 5600 pounds and the total fuel flow was 5760 pounds/hour at 100-percent RPM engine speed. The left-engine operation was somewhat irregular in that data from previous engine calibrations, ground runs and dual-engine thrust-stand tests showed that at 100-percent RPM the left-engine thrust and fuel flow were usually higher than for the right engine. This would suggest that the thrust loss of 125 pounds was attributed to an installation loss during a left-engine operation. The single engine bleed valve operation was not the same as for dual-engine operation.

2.3.3.4.2 Fan-Mode Configuration

With the vector angle 45 degrees aft and a corrected engine speed of 98-percent RPM, the total corrected horizontal thrust

was 7520 pounds. The total fuel flow was 5835 pounds/hours, with the fuel flow of the left engine being 115 pounds/hour higher than that of the right engine. The EGT of the left engine was also 5 degrees C higher than that of the right engine and the bleed valve positions were not the same for the two engines.

2.3.4 VERTICAL THRUST STAND

2.3.4.1 Objective

The objective of these tests was to establish the performance characteristics of the engines, fans, and fan controls comprising the fan-in-wing propulsion system.

2.3.4.2 Method

The aircraft was rigidly mounted on the vertical thrust stand which was adjusted to the desired wheel height. Prior to the start of each test, the forces and moments were balanced when possible and data were recorded to show the existing bias values. Each test was conducted by incrementally varying only one parameter while holding all others constant. The tests conducted and the parameters controlled during each test are presented in the following table:

Controlled Variable	Constants
N_G, HP	β_S, $\Delta\beta_s$, β_V, $\Delta\beta_V$, δ_{PFD}, H/D
β_S	HP, N_G, $\Delta\beta_S$, β_V, $\Delta\beta_V$, δ_{PFD}, H/D
δ_{PFD}	HP, N_G, β_S, $\Delta\beta_S$, β_V, $\Delta\beta_V$, δ_{PFD} H/D
β_V	HP, N_G, β_S, $\Delta\beta_S$, $\Delta\beta_V$, δ_{PFD}, H/D
$\Delta\beta_S$	HP, N_G, β_S, β_V, $\Delta\beta_V$, δ_{PFD}, H/D
$\Delta\beta_V$	HP, N_G, β_S, $\Delta\beta_S$, β_V, δ_{PFD}, H/D
δ_{T_s}	N_G, HP, β_S, δ_{PFD}, β_V, $\Delta\beta_s$, $\Delta\beta_V$

During these tests, the ambient atmospheric conditions were recorded by a weather station adjacent to the test site. The recorded weather data included wind velocity and direction, ambient air temperature and pressure, and information necessary for correlation of the thrust stand and aircraft recorded data.

Following the completion of the tests, the thrust stand was calibrated by applying a suitable range of forces and moments to all the appropriate existing instrumentation installed on the thrust stand.

2.3.4.3 Test Results

Test results are presented graphically in figures 139 through 180, appendix I.

2.3.4.4 Analysis

2.3.4.4.1 Engine Power and Speed Tests

2.3.4.4.1.1 Pitch-Fan Performance

2.3.4.4.1.1.1 Pitch-Fan Speed

The pitch-fan speed increased with an engine-power and engine-speed increase. This increase was essentially linear up to 98-percent engine speed (8000 $HP_{5.1}$) where the efficiency appeared to decrease and additional power resulted in a smaller incremental fan-speed increase. This efficiency characteristics appeared in both the engine-speed and engine-power data. The maximum pitch-fan speed of 106.5-percent corrected RPM was obtained at an engine speed of 106-percent corrected RPM. The pitch-fan speed characteristics were not affected by changes in fan height above the ground.

2.3.4.4.1.1.2 Pitch-Fan Thrust

The pitch fan was relatively ineffective as a thrust producer at speeds below 90-percent RPM. At higher speeds, the effectivity increased rapidly and was essentially linear to 105-percent RPM. At this speed, the thrust was approximately 1000 pounds noseup for a pitch-fan door position of 78.5 degrees. There was no tendency for the thrust effectiveness to deteriorate at a high power setting as was evident in the fan-speed characteristics data. The thrust performance with respect to H/D was inconclusive, and it was not possible to confirm the nature of the ground-effect characteristics as a result of ground proximity.

2.3.4.4.1.1.3 Pitching Moment

The pitching moments increased in a noseup direction as the result of the increased pitch fan thrust at greater engine speeds. The value of the pitching moment change can be obtained from the product of the increased thrust and the moment arm.

2.3.4.4.1.2 Wing-Fan Performance

2.3.4.4.1.2.1 Wing-Fan Speed

The wing-fan speed increased with engine speed and power. In both cases, the increases were essentially linear from 60-

to 90-percent RPM although the shapes of the speed and power curves were somewhat different. The reason for this dissimilarity was not determined. At engine speeds above 100-percent RPM, the tip turbine efficiency apparently decreased and this caused the fan speed to increase more slowly with additional power. The maximum engine speed of 104-percent RPM resulted in a wing-fan speed of 98.5-percent RPM. Wing-fan speed characteristics were dependent entirely upon the power input and were not influenced by the ground proximity.

2.3.4.4.1.2.2 Wing-Fan Thrust

Wing-fan thrust increased linearly with engine power through the area from flight-idle to 100-percent power. Above this power level, the previously discussed loss in turbine efficiency resulted in a decrease in thrust performance relative to engine speed or power. As was previously the case with the pitch fan, the thrust characteristics data were somewhat dissimilar for engine power and speed parameters. The wing-fan thrust varied directly as the square of the wing-fan speed. The maximum thrust obtained during the tests was 13,000 pounds at an H/D of 1, a fan speed of 97.4-percent RPM, and an engine speed of 103-percent corrected RPM. The wing-fan thrust characteristics showed no indication of an efficiency loss of a maximum possible blade loading at the highest power available for the test conditions.

The test data indicated a positive ground effect for fan heights of 15 feet or less ($H/D > 3$). The thrust increased approximately 300 pounds for each fan diameter closer to the ground. This increase in performance was the net gain above what losses in power were being suffered due to hot gas reingestion of both the engines and fans. There were no special provisions made to change or alleviate any reingestion.

2.3.4.4.2 Collective Stagger Tests

2.3.4.4.2.1 Pitch-Fan Performance

2.3.4.4.2.1.1 Pitch-Fan Speed

There was no significant change in pitch-fan speed as the wing-fan stagger angle was changed. The data indicated that there was a tendency for the speed to decrease as the stagger angle was varied from 15.6 to 36.2 degrees. This change caused the fan speed to be lowered by approximately 1-percent RPM. As the stagger was further increased to the maximum stagger value, the fan speed increased and was similar to the minimum stagger value. The pitch-fan door was programmed to close automatically 4 degrees with the

stagger increase from 15.6 to 36.2 degrees. The purpose of this door position change was to balance the change in pitching moments from the wing fans as a result of the increased collective stagger angle. The programmed door position change was not responsible for the variation in the pitch-fan speed characteristics. The test data did not include ground proximity information.

2.3.4.4.2.1.2 Pitch-Fan Thrust

The variation in pitch-fan thrust due to the fan speed change was approximately 15 pounds. The pitch-fan door motion from 78.6 to 74.3 degrees, however, reduced the pitch-fan thrust by 260 pounds. The tests were conducted at only one value of H/D.

2.3.4.4.2.1.3 Pitching Moment

The pitching moment change from fan speed change was not significant. The programmed pitch-fan door motion increased the nose-down moment by 3350 foot-pounds. The test data were for an H/D of 3 (OGE).

2.3.4.4.2.2 Wing-Fan Performance

2.3.4.4.2.2.1 Wing-Fan Speed

Wing-fan speed increased as the stagger angle was increased. The characterisitcs were essentially the same for both wing fans although there was a 1-percent RPM trim speed difference caused by the fan riggings. Changing the stagger angle from 10 to 30 degrees resulted in a 2-percent RPM speed increase. Ground proximity was not investigated during the stagger tests.

2.3.4.4.2.2.2 Wing-Fan Thrust

The wing-fan thrust was decreased by 3150 pounds as the collective stagger angle increased from 15.6 to 36.2 degrees. The total thrust from the wing fans plus the pitch fan was decreased from 10,700 to 7300 pounds by increasing the wing fan collective stagger angle (β_s) from the minimum to maximum angle (15.6 degrees to 36.2 degrees). This change included the thrust contribution from the pitch-fan door programming.

The wing-fan stagger effectiveness is presented as the ratio of the thrust at a given β_s divided by the thrust at a minimum β_s (15.6 degrees) and at a wing-fan speed of 100-percent RPM. This method of presentation accounts for the fan-speed change with the β_s and the thrust spoiled by the exit louvers. Thus, the maximum thrust effectivenessthat could be obtained with this fan propulsion system

was 0.938 due to the residual minimum β_s of 15.6 degrees. At the maximum β_s of 36.2 degrees, the stagger effectiveness as 0.62. Ground proximity effects were not investigated during the tests.

2.3.4.4.2.2.3 Pitching-Moment

As the wing fan collective stagger angle (β_s) was increased from minimum to maximum, the total resulting pitching moment was reduced from 6200 to 2300 foot-pounds nosedown. This total moment change included the contribution of the pitch-fan door which was 2500 foot-pounds nosedown during the β_s increase. The pitching-moment change from the wing fan was opposite the pitch-fan input and was 7250 foot-pounds nosedown. An additional 4.6 degrees of pitch-fan door programming would be required to balance the pitching moment over the total range of β_s variation available. Fan-height-above-the-ground contributions to the pitching moment variations with stagger angle were not determined during these tests.

2.3.4.4.3 Pitch-Fan Door Tests

2.3.4.4.3.1 Pitch-Fan Performance

2.3.4.4.3.1.1 Pitch-Fan Speed

The pitch-fan speed characteristics were not influenced by a movement of the pitch-fan door throughout the maximum travel available.

2.3.4.4.3.1.2 Pitch-Fan Thrust

The pitch-fan thrust varied from a negative value of 670 pounds at a fan-door position of 43.5 degrees to a positive value of 1640 pounds at the fully opened fan-door position of 108 degrees. The thrust variation was essentially linear from 64 degrees to 85 degrees. At the extremes of the door travel, there was a marked decrease in the efficiency and as a result a smaller change in thrust per degree of door motion. Pitch-fan lift was decreased approximately 60 pounds by increasing the fan height from H/D = 2 to H/D = 3.

Pitch-fan effectiveness is presented as pitch-fan thrust divided by the pitch-fan lift at 100-percent RPM pitch-fan door fully opened, and standard-day conditions. The maximum effectiveness value attained during the test was 0.97 at the fully-open pitch-fan door position of 108 degrees. When reduced to the effectiveness parameters, the effect of ground proximity was not evident.

2.3.4.4.3.1.3 Pitching Moment

The total change in pitching moment was from 26,500 foot-pounds nosedown at a door position of 43 degrees to 7500 foot-pounds nosedown at a door fully-open position of 108 degrees. The pitching-moment characteristics were similar to the previously discusssed thrust characteristics. Based on thrust change with ground proximity, the pitch-door trim requirement would be different but the moment variation with door-position change would be the same.

2.3.4.4.3.2 **Wing-Fan Performance**

2.3.4.4.3.2.1 Wing-Fan Speed

The wing-fan speed characteristics were not influenced by changes in the pitch-fan door position.

2.3.4.4.3.2.2 Wing-Fan Thrust

There was an increase of 360 pounds in the total lift of the wing fans for a full pitch-fan door deflection. The reason for this unexpected change is not known.

2.3.4.4.3.2.3 Pitching Moment

The small change in wing-fan thrust did not cause any measurable change in the pitching moments.

2.3.4.4.4 Collective Vector Angle Tests

2.3.4.4.4.1 **Pitch-Fan Performance**

2.3.4.4.4.1.1 Pitch-Fan Speed

The pitch-fan door position was programmed to close with an aft vector motion. As previously discussed, this change in door position had no influence on the pitch-fan speed.

2.3.4.4.4.1.2 Pitch-Fan Thrust

The pitch-fan door motion was from 65 degrees at a vector angle of 10 degrees forward to 44 degrees at a vector angle of 40 degrees aft. This door motion reduced the pitch-fan thrust by 710 pounds.

2.3.4.4.4.1.3 Pitching-Moment

The change in pitch-fan thrust due to the pitch-fan door programming resulted in a change in the pitching moment from 12,500 foot-pounds nosedown to 26,500 foot-pounds nosedown. These considerations for full vector angle travel at zero airspeed are not necessarily those that will exist during flight in which aerodynamic factors become significant.

2.3.4.4.4.2 Wing-Fan Performance

2.3.4.4.4.2.1 Wing-Fan Speed

An aft motion of the louvers resulted in an automatic programming of the wing fan collective stagger angle (β_S). This programming was from 16.5 degrees β_S at a wing fan collective vector angle of 10 degrees forward to zero degrees β_S at the maximum aft β_V position. This programming had a different characteristic for each collective stagger setting. The independent effect of decreased β_S would be to decrease the wing-fan speed. During the OGE vector tests (H/D = 3), the fan-speed characteristics appeared to be symmetrical about the zero β_V position with a tendency for a small fan-speed increase either direction from trim. The effect was not as apparent at β_S = 25 degrees position as at the β_S= 17 degrees position. For the H/D = 1 tests, the results were unusual in that a fan-speed decrease existed from β_V= 10 degrees forward to β_V= 8 degrees aft. The unusual shape of the curve may be caused by variations in the pitch fan inlet total temperature ratio ($_{20}$) due to increased hot gas reingestion at the closer ground proximity.

2.3.4.4.4.2.2 Wing-Fan Thrust

The wing-fan vertical thrust was decreased approximately 75 pounds for each degree of aft vector angle. The total vertical thrust change including the pitch-fan door contribution was from 11,000 pounds at β_V= 9 degrees forward to 9760 pounds at β_V= 7 degrees aft.

The horizontal force was forward 400 pounds at 10 degrees of forward vector angle and became zero for a vector angle of 7.3 degrees forward. The horizontal thrust then increased with aft vector angle to a maximum of 6800 pounds at a vector angle of 40 degrees aft. The horizontal thrust appeared to be greater for a stagger angle of 25 degrees of collective stagger than for β_S= 17 degrees.

The wing-fan vector effectiveness is expressed as the ratio of the horizontal force divided by wing-fan thrust at 100-

percent fan speed, minimum stagger angle, and standard-day conditions. The maximum effectiveness attained was 0.57 at maximum aft vector angle (β_v = 40 degrees).

2.3.4.4.4.2.3 Pitching Moment

Moving the vector aft resulted in a strong noseup pitching tendency. The resultant change on the total aircraft was 4100 foot-pounds noseup for a vector angle change from 10 degrees forward to 36 degrees aft. The pitch-fan door programming provided 9800 foot-pounds nosedown which was overcome by the wing fans. The total contributions from the wing fans was 13,900 foot-pounds noseup moment for a vector change from 9 degrees forward to 36 degrees aft.

The effective change in pitching moment with vector angle change was decreased as the H/D was increased from 1 to 3. At an H/D of 1, the noseup moment increased rapidly from 10 degrees forward to 20 degrees aft. From this point, there was a gradual decrease in the noseup contribution from the wing fan as the vector angle was further increased. At the H/D = 3 condition, the noseup contribution was much weaker and there was a reversal in the curve at a vector angle of 4 degrees aft. As was the case in the thrust characteristics, the stagger angle of 25 degrees was more effective than was the 17-degree stagger condition.

2.3.4.4.5 Differential Stagger Angle Tests

2.3.4.4.5.1 Pitch-Fan Performance

2.3.4.4.5.1.1 Pitch-Fan Speed

The pitch-fan door was programmed to open approximately 2.7 degrees as the differential stagger was varied through the full range. This pitch-fan door motion did not influence the pitch-fan speed characteristics during differential stagger inputs.

2.3.4.4.5.1.2 Pitch-Fan Thrust

The change in the pitch-fan thrust was a result of the pitch-fan door change since there was no speed change. The thrust was increased approximately 100 pounds by the pitch-fan door programming.

2.3.4.4.5.1.3 Pitching Moment

The nosedown pitching moment from the pitch fan was decreased by 1200 foot-pounds as a result of the thrust change caused by the pitch-fan door motion.

2.3.4.4.5.2 Wing-Fan Performance

2.3.4.4.5.2.1 Wing-Fan Speed

Wing-fan speed characteristics with differential stagger angle ($\Delta\beta_s$) were similar for both fans. As the $\Delta\beta_s$ was increased from the trim point to the maximum available, the wing-fan speed increased approximately 6.7 percent above the trim value.

2.3.4.4.5.2.2 Wing-Fan Thrust

The wing-fan thrust variation was from 10,145 pounds at zero $\Delta\beta_s$ to 9275 pounds at the maximum angle of 39 degrees for a collective stagger angle of 17 degrees. The effectiveness was essentially constant throughout the range of $\Delta\beta_s$ available. The thrust change with stagger differential change was very small at a collective stagger angle of 25 degrees. The change was 75 pounds for an input of 25 degrees. The thrust and $\Delta\beta_s$ characteristics were not established as a function of ground proximity.

2.3.4.4.5.2.3 Rolling Moment

The rolling moment was increased from zero to 7000 pounds by an increase of 15 degrees right $\Delta\beta_s$ at a collective stagger angle setting of 25 degrees. The rolling effectiveness of the $\Delta\beta_s$ increased with differential stagger angles to the right and decreased with differential stagger angles to the left. The rolling moment available at the fixed power condition was decreased approximately 65 percent as the collective stagger angle was decreased to 15 degrees.

2.3.4.4.6 Differential Vector Angle Tests

2.3.4.4.6.1 Pitch-Fan Performance

2.3.4.4.6.1.1 Pitch-Fan Speed

The pitch-fan speed was not changed by wing-fan differential vector angles.

2.3.4.4.6.1.2 Pitch-Fan Thrust

The pitch-fan thrust was independent of wing-fan differential vector angles.

2.3.4.4.6.1.3 Pitching Moment

Differential vector-angle changes did not change the pitching moment contributions from the pitch fan.

2.3.4.4.6.2 Wing-Fan Performance

2.3.4.4.6.2.1 Wing-Fan Speed

The wing-fan speed increased as the vector angle was increased from the trim position. The increase was approximately 3-percent RPM for a deflection of 20 degrees. The test data indicated some discrepancy between fans and some dissymmetry at the different collective stagger angles. Insufficient data were available to define individual fan characteristics or ground proximity effects.

2.3.4.4.6.2.2 Wing-Fan Thrust

The vertical thrust decreased 540 pounds as the differential vector was increased by 30 degrees. The effectiveness was the same for both right and left wing fans. The influences of ground proximity and of variation with collective stagger were not established during the tests.

2.3.4.4.6.2.3 Yawing Moment

The yawing moment variation with differential vector angle was linear throughout the range available. At a collective stagger angle of 17 degrees, the effectivity was 430 foot-pounds of yawing moment per degree of differential vector angle. Decreasing the stagger angle to 25 degrees did not change the characteristics but reduced the effectivity to 297 foot-pounds/degree of differential vector angle change. These values were for an H/D = 3 condition.

2.3.4.4.7 Thrust Spoiler Tests

2.3.4.4.7.1 Thrust Spoiler Performance

The thrust spoiler provided essentially no change in horizontal thrust for the first 25 percent of deflection. Above 20-percent deflection, the thrust spoiler was essentially linear with spoiler deflection. The maximum thrust spoiler was 1640 pounds at full deflection, a H/D = 1, and an engine speed of 100-percent RPM. For the flight-idle condition, the residual unspoiled thrust was 400 pounds with the spoiler closed and was 240 pounds at the fully-opened spoiler condition.

2.3.4.4.7.2 Thrust Spoiler Effectiveness

The thrust spoiler effectiveness is presented as the ratio of horizontal thrust divided by the thrust available with the spoilers closed. The effectivity was essentially linear at spoiler

angles above 30-percent open. Effectiveness was the same for 100-percent and idle power as well as for fan heights above the ground of one and two diameters.

2.3.5 INLET PERFORMANCE

2.3.5.1 Objective

The objective of these tests were to determine the engine inlet temperature and pressure characteristics and to evaluate the effects of installation and flight condition on the inlet performance.

2.3.5.2 Method

The inlet performance tests were conducted simultaneously with the engine calibrations, thrust stand tests, and flight tests. The inlet temperatures and pressures were sensed by inlet probes and manifold rakes and were recorded by the aircraft instrumentation. Instantaneous pressure data as well as averaged data were recorded. Ambient atmospheric conditions were recorded by the adjacent ground weather station.

2.3.5.3 Test Results

Test results are presented graphically in figures 181 through 225, appendix I.

2.3.5.4 Analysis

2.3.5.4.1 Engine Calibration

The relative performance of the individual calibrations and various configurations is illustrated in figure 181. The inlet pressure ratio P_{T2}/P_a was greatest for the standard engine equipped with the calibrated bellmouth inlet. The ratio increased by 0.115 for an engine speed increase of 40 to 100-percent RPM. The engine S/N 875 showed no change in pressure ratio after the modification; however, engine S/N 876 showed a pressure ratio loss of 0.011 at an engine speed of 100-percent RPM. The total loss with the installation of the flight rakes was 0.032. The engine inlets and rakes were well matched with essentially the same inlet pressure ratios for the flight configuration of modified engine, flight rakes, and 680 EGT trim. There was no inlet temperature rise evident during the engine calibration.

2.3.5.4.2 Horizontal Thrust Stand

The horizontal thrust stand inlet data are shown in figure 182. Above engine speeds of 50-percent RPM there was a

pressure recovery loss. The pressure recovery was 0.97 at an engine speed of 100-percent RPM. The characteristics were the same for both right and left inlets and there was no change as a result of single-engine operation.

2.3.5.4.3 Hover

2.3.5.4.3.1 Inlet Recovery and Distortion

The inlet pressure recovery improved approximately 1 percent from 0.989 to 0.0998 as the hovering wheel height was increased from 2 to 10 feet. The left engine exhibited better pressure recovery characteristics than the right engine. The inlet distortion was not affected significantly by the change in height above the ground. The left engine distortion was greater than that of the right engine with the values being approximately 0.04 and 0.06 respectively.

The inlet recovery and distortion characteristics with variation of collective stick position showed very little change from 40-to 100-percent full-up collective. The trend was for the right inlet recovery to decrease slightly with higher collective while the left inlet increased in a similar manner. The inlet distortion improved slightly for both inlets as the collective was changed from 40- to 100-percent full-up.

2.3.5.4.3.2 Inlet Temperature Rise and Reingestion

The engine inlet temperature rise was 6 degrees Fahrenheit (F) at an OGE wheel height (H/D = 3) and increased rapidly with decreased height as illustrated in figure 188. This stabilized hovering data compared well with the transient takeoff and climb data. This indicated that the recirculation pattern and the temperature reingestion level were very rapidly established. A time history of the inlet conditions during stabilized IGE hover is presented in figure 240. The effect of the increased inlet temperature was evident in the corrected engine and fan-speed data. The corrected wing-fan speed decreased approximately 0.5-percent RPM as height was decreased from 5 to 4 feet. A similar loss was present for a change from 4 to 5 feet, the magnitude of the speed loss became greater at lower wheel heights. The total wing-fan speed loss was 2-percent RPM for a hovering height change from 5 to 2 feet. The corrected engine speed was slightly less sensitive to reingestion than the wing-fan speed at heights above 3 feet; however, at lower heights this trend was reversed.

2.3.5.4.4 Takeoff and Vertical Climb

The inlet temperature rise during takeoff and vertical

climb is shown in figures 183 through 192. The maximum inlet temperature rise prior to and immediately after the liftoff was normally on the order of 40 degrees F. The precise liftoff time was difficult to determine; however, the calculated time agreed well with the recorded takeoff time. For normal takeoffs, the reingestion levels decreased approximately 20 degrees within 4 seconds after the liftoff. During maximum-performance takeoffs, the temperature decrease with time was more rapid because of the greater vertical acceleration and the higher wheel height attained per unit time. With this type of takeoff, a 20 degree F inlet temperature drop occurred within approximately 2 seconds from liftoff. In both cases, the wheel height was approximately 10 to 15 feet. During the OGE stabilized climb, there was no reingestion and the recorded engine inlet temperature was the same as ambient temperature. For all conditions tested, the right-engine inlet temperature was approximately 10 degrees F higher than the left-engine inlet temperature, although the characteristics were otherwise the same.

2.3.5.4.5 Fan-Mode Level Flight

2.3.5.4.5.1 Inlet Pressure Recovery and Distortion

For low-speed forward flight the inlet recovery was 0.993 at airspeeds slightly above a hover and improved with increased airspeed. The inlet distortion also decreased with the higher airspeed. The right-engine inlet recovery performance was superior to that of the left-engine inlet. There was little variation in the pressure recovery as a function of angle of attack for a range from -4.5 to +4 degrees. The distortion tended to increase slightly as the angle of attack became more positive. An angle of sideslip change of 10 degrees left or right introduced no significant change in the inlet recovery performance. The inlet distortion was increased slightly as the sideslip angle increased either direction from zero.

2.3.5.4.5.2 Inlet Temperature Rise and Reingestion

For symmetrical OGE level flight, the engine inlet temperature rise decreased linearly from 6 degrees F at a hover to zero at 60 KCAS. There was no temperature rise as airspeed was further increased above 60 KCAS. The characteristics were the same for both engine inlets.

2.3.5.4.6 Jet-Mode Level Flight

The engine inlet pressure instrumentation was not available during the tests and it was necessary to calculate the pressure recovery based on previous contractor tests and wind tunnel data.

These calculated data are presented in figure 224. The inlet temperature ratio increased from 0.992 to 1.031 for an airspeed change of 120 to 320 KCAS.

2.3.5.4.7 Vertical Descent and Landing

The inlet temperature rise characteristics during steady-state vertical descents were the same as those encountered during fan-mode level flight. As the aircraft entered ground effect, the inlet temperature rise was approximately 40 degrees C during the last 2 seconds prior to touchdown and the general characteristics were the same as those encountered in comparable areas during take-off and hovering. There were not sufficient data available to determine the effect of a surface wind or control positions during the touchdown and landing.

2.3.5.4.8 Sideward and Rearward Flight

2.3.5.4.8.1 Sideward Flight

During sideward flight the inlet recovery factor changed approximately 1 percent with a sideward speed change of 30 KTAS. The change was slightly greater for the left inlet than for the right inlet. This characteristic was such that the downwind inlet (inlet away from the direction of translation) recovery was improved while the upwind inlet suffered a recovery loss. This characteristic was present during both left and right sideward translations. The pressure distortion for the right inlet was symmetrical with a small increase being present for motion in either direction. The left inlet had a large distortion increase during left sideward translation and a small distortion decrease during right sideward translation.

2.3.5.4.8.2 Rearward Flight

Increased rearward translational speed resulted in a smaller inlet recovery factor. The right inlet performance was better than that for the left inlet. The inlet distortion also increased with rearward speed and was greatest for the left inlet.

2.3.6 ENGINE FLIGHT

2.3.6.1 Objective

The objectives of these tests were to determine the engine performance characteristics during the various flight regimes, to determine the effects of installation and inlet losses on power available, and to obtain a comparison of the various engine conditions encountered during this test program.

2.3.6.2 Method

The engine flight data were obtained by recording all engine parameters during the hovering, takeoff and vertical climb, forward climb, level flight, and vertical descent tests. The engine and operating parameters were recorded by the pulse code modulator (PCM) while the ground site atmospheric conditions were recorded by an adjacent weather station. Static engine performance data were obtained from the engine calibrations, ground tests, and thrust-stand tests.

2.3.6.3 Test Results

Test results are presented graphically in figures 226 through 239, appendix I.

2.3.6.4 Analysis

2.3.6.4.1 Engine Flight Performance

The engine characteristics were the same for all ground tests and flight regimes other than IGE operations. Also, there was no difference between engine characteristics for jet-mode and fan-mode configurations. For both engines, the power and speed characteristics during flight were essentially the same as those recorded during the engine calibrations. The fuel-flow and thrust characteristics were the same as for the engine calibration for speeds above 90-percent RPM. At lower speeds, the characteristics were slightly different from those of the calibration data.

The power calculated by the various methods showed very good agreement particularly at engine speeds above 95-percent RPM. The empirical method tended to indicate high power at low engine speeds with the difference becoming greater as the speed was decreased. In general, the instantaneous power method showed a lower power developed and agreed more closely with the engine calibration data. Since the validity of the time averaged pressure data was questionable, the instantaneous power method was used to calculate the power developed and power available for the performance evaluation.

The engine performance having IGE operation is a transient condition and is not shown on the engine characteristics curves. The effect on power or thrust can be obtained from the standardized curves for any desired inlet temperature. The variation in corrected engine as a result of reingestion can be seen in the time history of the IGE hovering shown in figure 240, appendix I.

2.3.6.4.2 Power Available

The summary power available shown in figure 226 is for a zero inlet loss condition and does not represent any actual operating condition. These curves in addition to the inlet curves however, were used to calculate the power available and the maximum performance shown in the various sections of the report. This method of presentation was chosen since it was not realistic to present the power available for all the pertinent flight regimes and operating conditions.

SECTION 3. APPENDICES

APPENDIX I
TEST DATA

I.	Test Data	79
II.	Definitions, Symbols and Abbreviations	327
III.	General Aircraft Information	339
IV.	Flight and Operation Limits	355
V.	Test Instrumentation	366
VI.	Weight and Balance	372
VII.	Detailed Description of Test Responsibilities	373
VIII.	References	377
SECTION 4.	Distribution List	379

FIGURE NO. 1

SUMMARY HOVERING PERFORMANCE

XV-5A USA 62-4505

OUT OF GROUND EFFECT

NOTES:

1. BASED ON POWER AVAILABLE FROM FIGURE NO. 17A APPENDIX V.
2. BASED ON INLET TEMPERATURE FROM FIGURE NO. 18C APPENDIX I.
3. BASED ON INLET PRESSURE FROM FIGURE NO. 18E APPENDIX I.
4. GROSS WEIGHT OBTAINED FROM FIGURE NO. 2 APPENDIX I.
5. RUNS INDICATE LESS THAN 2 HOVERS.
6. C.G. - 7 MAC NO TRIMMER ALLOWANCE

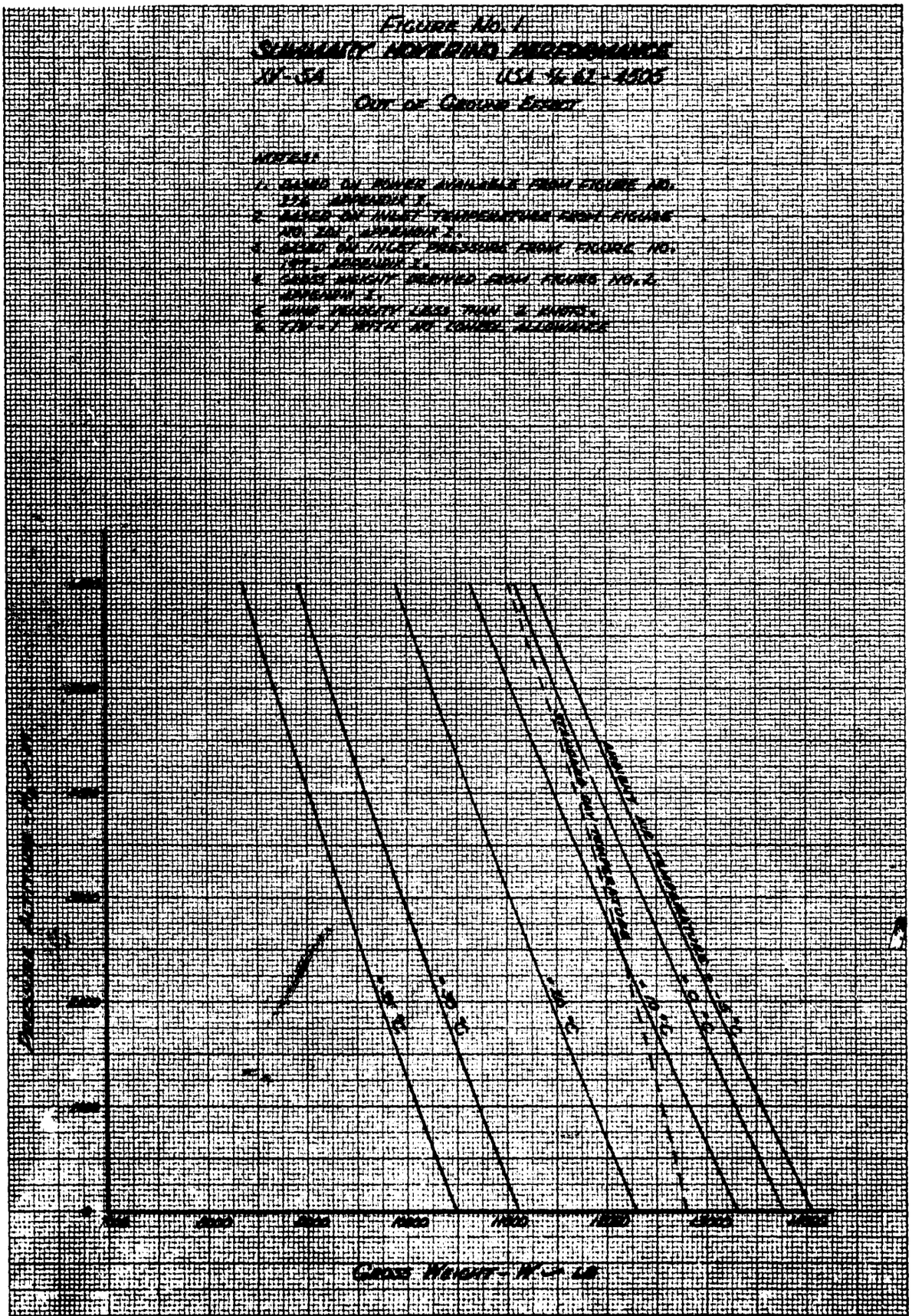

FIGURE No. 2

NON-DIMENSIONAL HOVERING PERFORMANCE

XV-5A

LASA No 62-1505

FREE FLIGHT TECHNIQUE
OUT OF GROUND EFFECT

SYM	ALT.	DENSITY ALT-h_σ-FT.	REL. GAGE ALT-W-LB
○	SEA LEVEL	31120	9000
⊙		32320	8940
◇		10810	10970
◆		2300	10,930
△		1000	10,430
▲		4100	9400
□		2350	10,330
■		3432	9840
⊕		31,30	10,030

NOTES:
CORRECTED TO COLLECTIVE STAGGER AND VECTOR OF R_2 = 17 DEG. AND R_1 = 5.7 DEG. ACT.

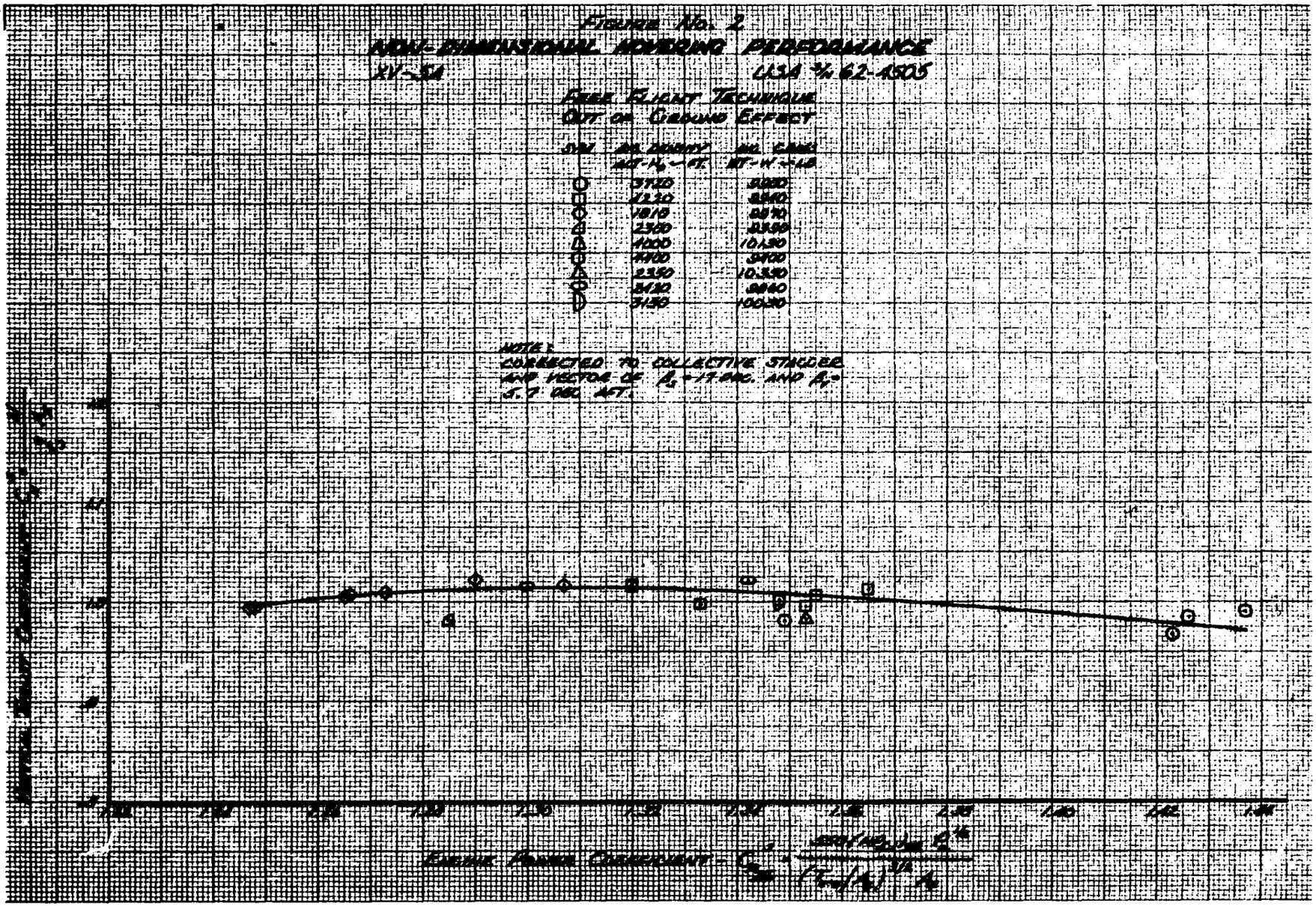

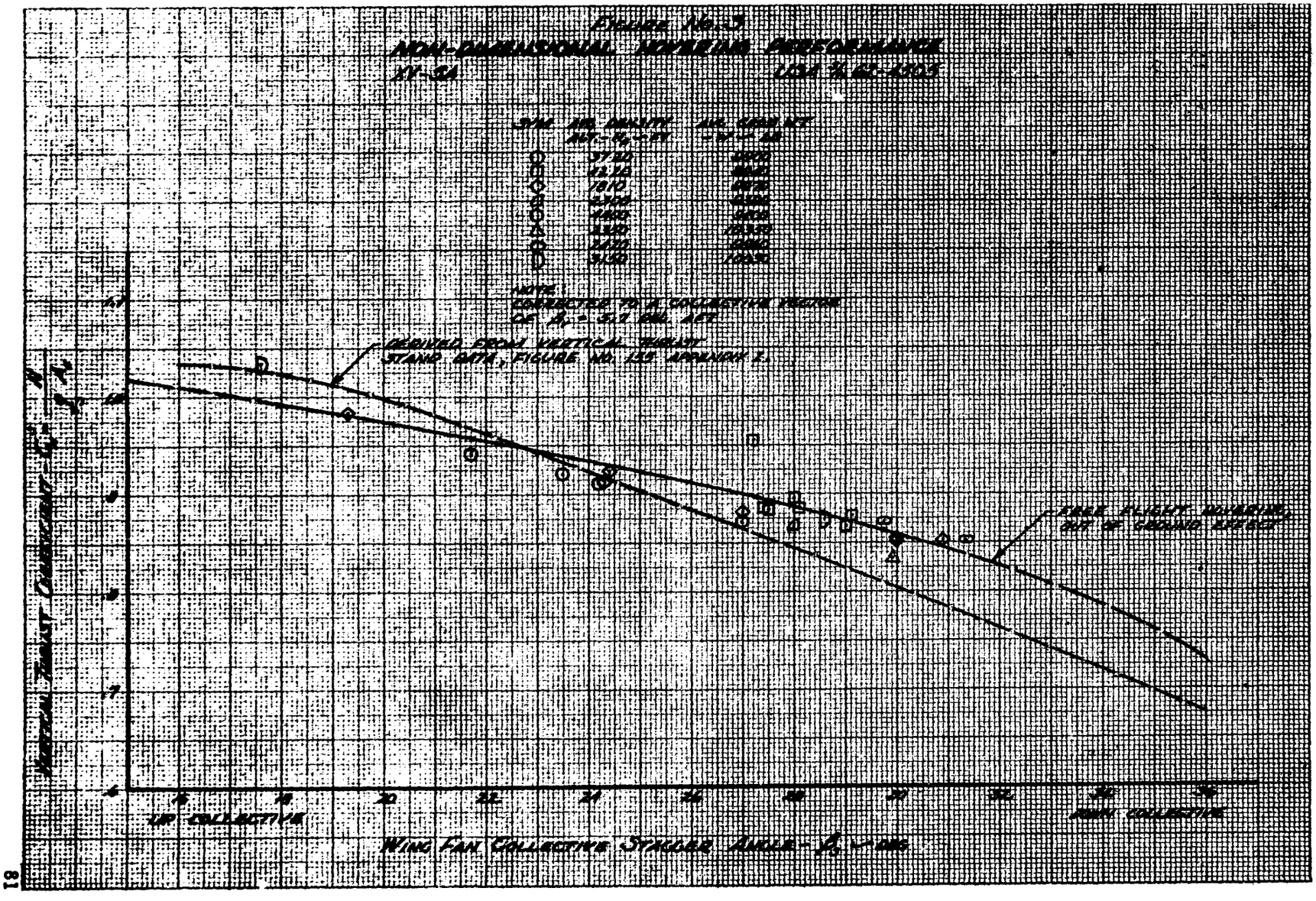
FIGURE No. 3
NON-DIMENSIONAL HOVERING PERFORMANCE
XV-3A
WING FAN COLLECTIVE STAGGER ANGLE - i_w = -4.5°
WING FAN COLLECTIVE
TAIL ROTOR COLLECTIVE
TAKE FLIGHT WITH AIR OUT OF GROUND EFFECT
DERIVED FROM VERTICAL FLIGHT STAND DATA, FIGURE NO. 15 APPENDIX I.
NOTE:
CORRECTED TO A COLLECTIVE FACTOR OF k_c = 5.7 BEL. 4.5°

FIGURE NO. 4

NON-DIMENSIONAL HOVERING PERFORMANCE

XV-5A

LSA # 62-4505

FREE FLIGHT TECHNIQUE

OUT OF GROUND EFFECT

SYM	ALT - FT	AIR CODE WT - LB
◇	3720	11000
◇	1220	11000
◇	1010	11000
◇	2480	9500
◇	4440	9400
◇	2450	10350
◇	3240	9960
◇	3450	10030

NOTE:
CORRECTED TO COLLECTIVE STAGGER
β_c = 14° DEG.

VERTICAL THRUST COEFFICIENT - $C_T = \frac{T}{\rho A_r}$

1.6
1.2
.8
.4
0

-10 AWD -8 -6 -4 -2 0 2 4 6 8 10 AFT

WING FAN COLLECTIVE VECTOR ANGLE - β_c — DEG

FIGURE NO. 5

HOVERING PERFORMANCE

XV-3A USA No. 62-4503

OUT-OF-GROUND EFFECT ($\mu/\Omega R > .4$)

SYM	REF. ALT. $-h_p$ — FT	AMB. TEMP. T_a — °C	AVG. MAST STRG. ANG. $\Delta\beta_s$ — DEG	AVG. PITCH FAN AP. ANG. $\delta_{M.R.}$ — DEG	AVG. M_t — ANG.	AVG. $\Delta\beta_s$ — DEG.
○□	15,500	27.8	4.03	86.3	7.83 FWD	−.93
▽	15,500	28.4	3.97	84.5	6.43 FWD	−1.25
△	15,500	2.7	4.93	74.9	2.50 AFT	−4.77

NOTES:

1. OPEN SYMBOLS DENOTE A_s = 17 DEG
2. CLOSED SYMBOLS DENOTE A_s = 25 DEG
3. WING CONFIGURATION

SYM	REL-V_w — KTS	AVG. DEG. FLAP ANGLE
○□	0	◇
▽	4	35.0
△	8.5	●

4. LANDING GEAR DOWN

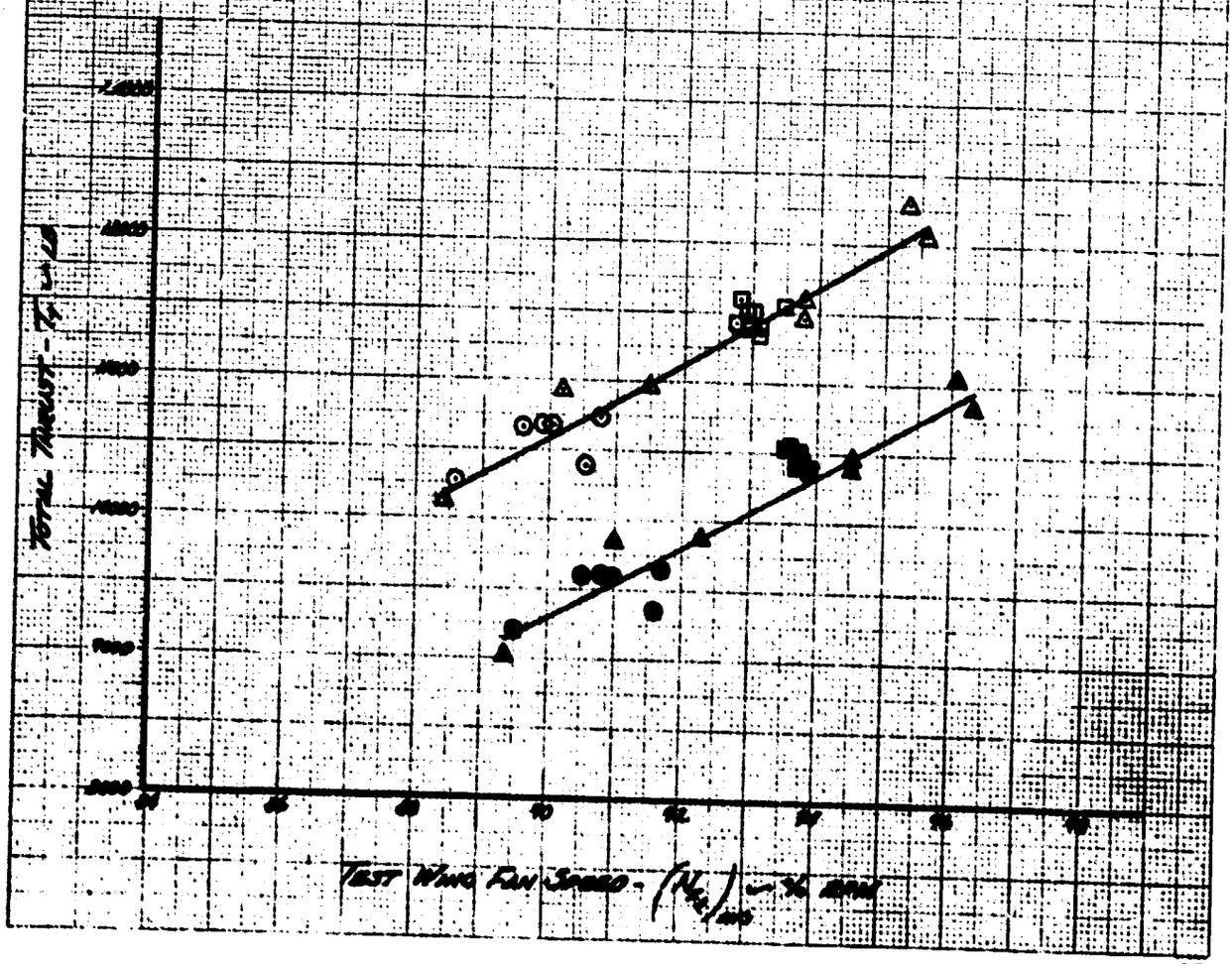

FIGURE NO. 6

HOVERING PERFORMANCE

XV-3A (154 FT-62-4305

OUT OF GROUND EFFECT ($\mu/\lambda_t \geq 0$)

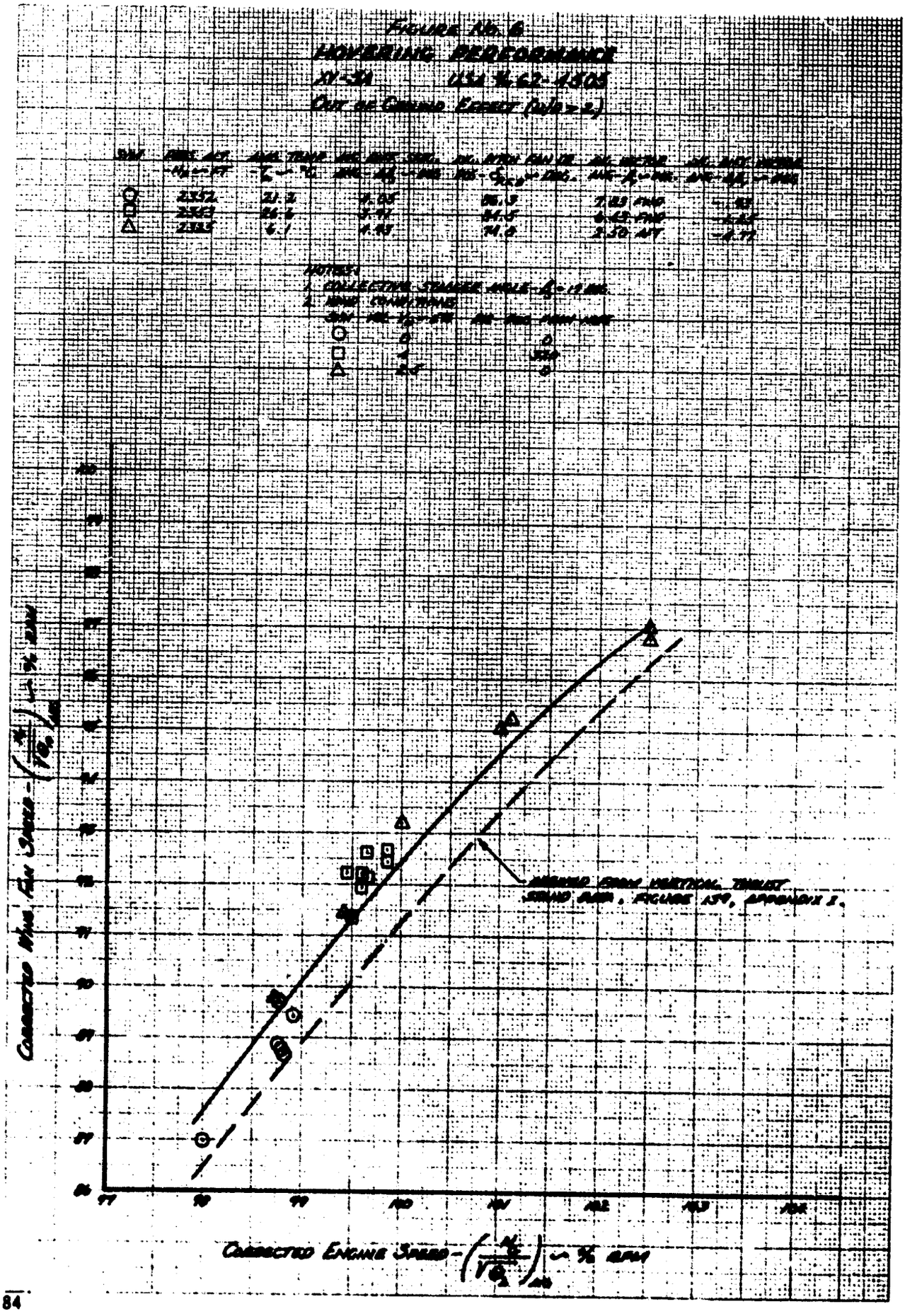

FIGURE No. 7

HOVERING PERFORMANCE

XV-3A USA # 62-4505

OUT OF GROUND EFFECT (H/D = 2.)

SYM	REF. ALT. H_p - FT	AMB. TEMP. - °C	ROT. SYS. ANG. α_R - DEG	ATTCH. PLN. OF R_{ref} - DEG	ANG. INCIDENCE ANG. i_1 - DEG	VTOL ANG. INCIDENCE ANG. i_2 - DEG.
○	4500	21.2	1.05	84.3	7.85 FWD	-.82
□	5000	24.4	2.91	84.2	4.45 FWD	-1.38
△	5500	8.1	1.43	84.8	2.50 AFT	-1.77

NOTES:

1. OPEN SYMBOLS DENOTE A_1 = 17 DEG
2. CLOSED SYMBOLS DENOTE A_1 = 25 DEG
3. WING CONTROLS

SYM	INC. VEL. V_w - KTS	ANG. INC. FROM HORZ
○	0	0
□	4	350
△	2.5	0

4. LANDING GEAR DOWN

CURVES DERIVED FROM FIGURES NO. 141 AND 155, APPENDIX E.

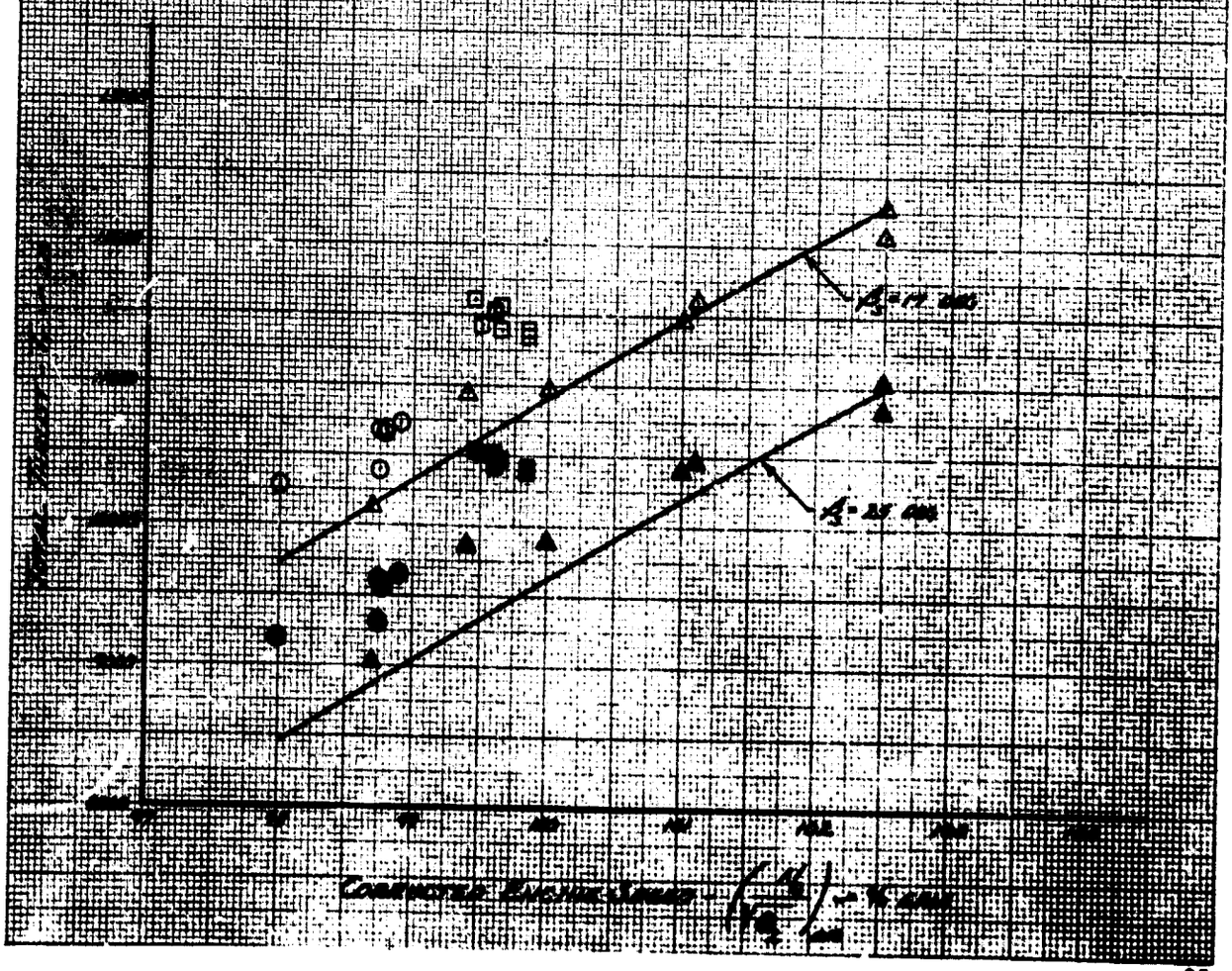

COMPUTED ENGINE SPEED - $\left(\frac{N}{\sqrt{\theta}}\right)$ - % RPM

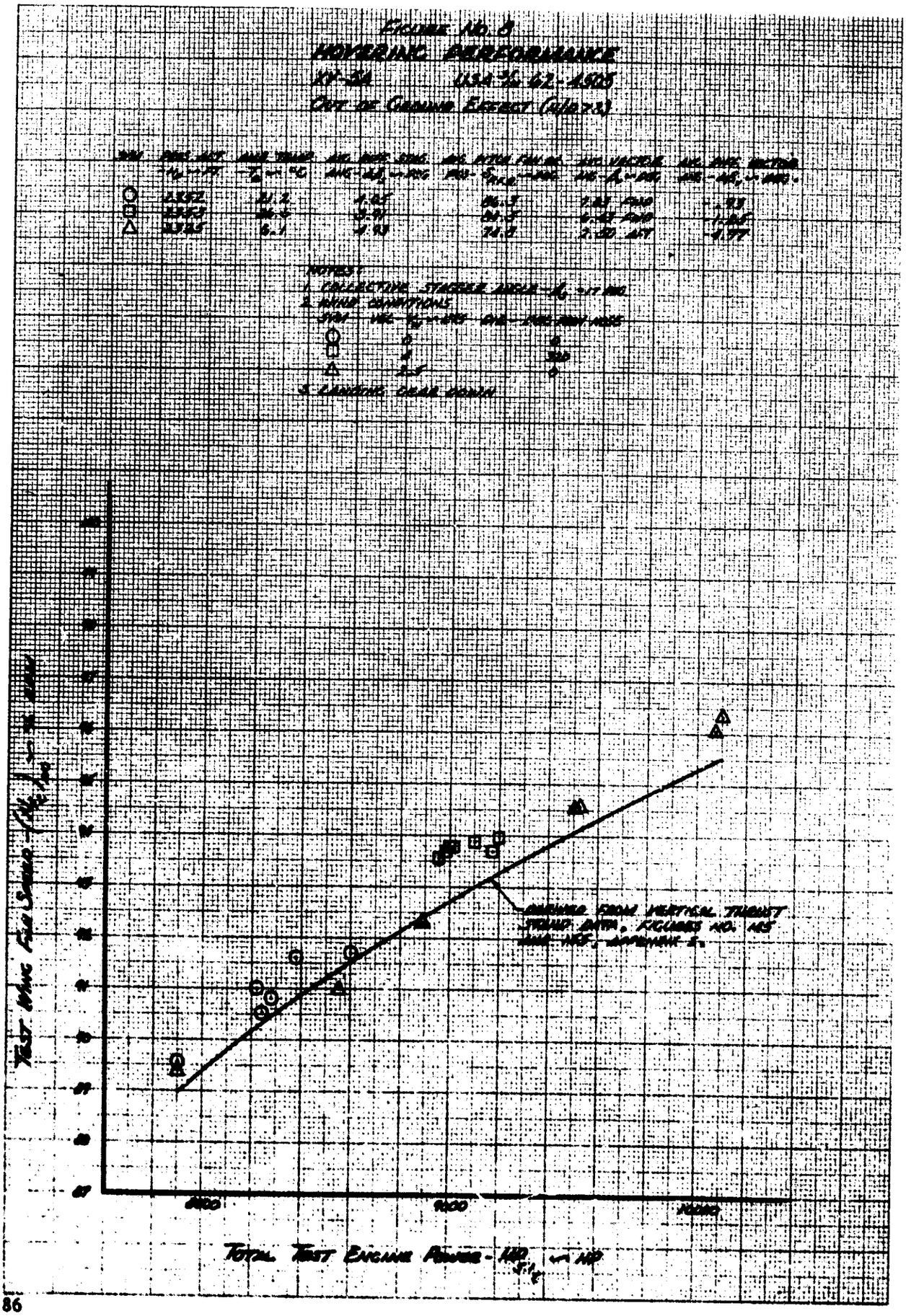
FIGURE NO. 8
HOVERING PERFORMANCE
XV-3A USA 62-4205
OUT OF GROUND EFFECT (Alt 0 FT)
NOTES:
1 COLLECTIVE STAGGER ANGLE
2 RADIO COMPARISONS
3 LANDING GEAR DOWN
DERIVED FROM VERTICAL THRUST STAND DATA, FIGURES NO. 165
TOTAL TEST ENGINE POWER - HP

FIGURE No. 9

HOVERING PERFORMANCE

XV-5A USA No. 62-4505

OUT OF GROUND EFFECT ($\mu/\Omega R \geq 2$)

SYM	BASIC ALT. H_{PA} - FT	AMB. TEMP. T_A - °C	ANG. DISP. STAB. ANG - $\Delta\beta_s$ - DEG.	ANG. PITCH FAN AX. POS - δ_{FCA} - DEG.	ANG. VECTOR ANG - Δ_j - DEG.	ANG. VANE VECTOR ANG - $\Delta\beta_v$ - DEG.
○	2,332	21.2	1.85	86.3	7.83 FWD	- .93
□	2,833	26.6	3.91	84.5	6.43 FWD	-1.25
△	2,328	6.1	1.93	91.9	2.50 AFT	-1.77

NOTES:

1. OPEN SYMBOLS DENOTE Δ_j = 17 DEG.
2. SOLID SYMBOLS DENOTE Δ_j = 25 DEG.
3. WIND CONDITIONS

SYM	VEL - V_w - KTS	DIR - DEG. FROM NOSE
	0	0
	4	320
	2.5	0

4. LANDING GEAR DOWN.

CURVES DERIVED FROM FIGURES NO. 147 AND 155, APPENDIX I.

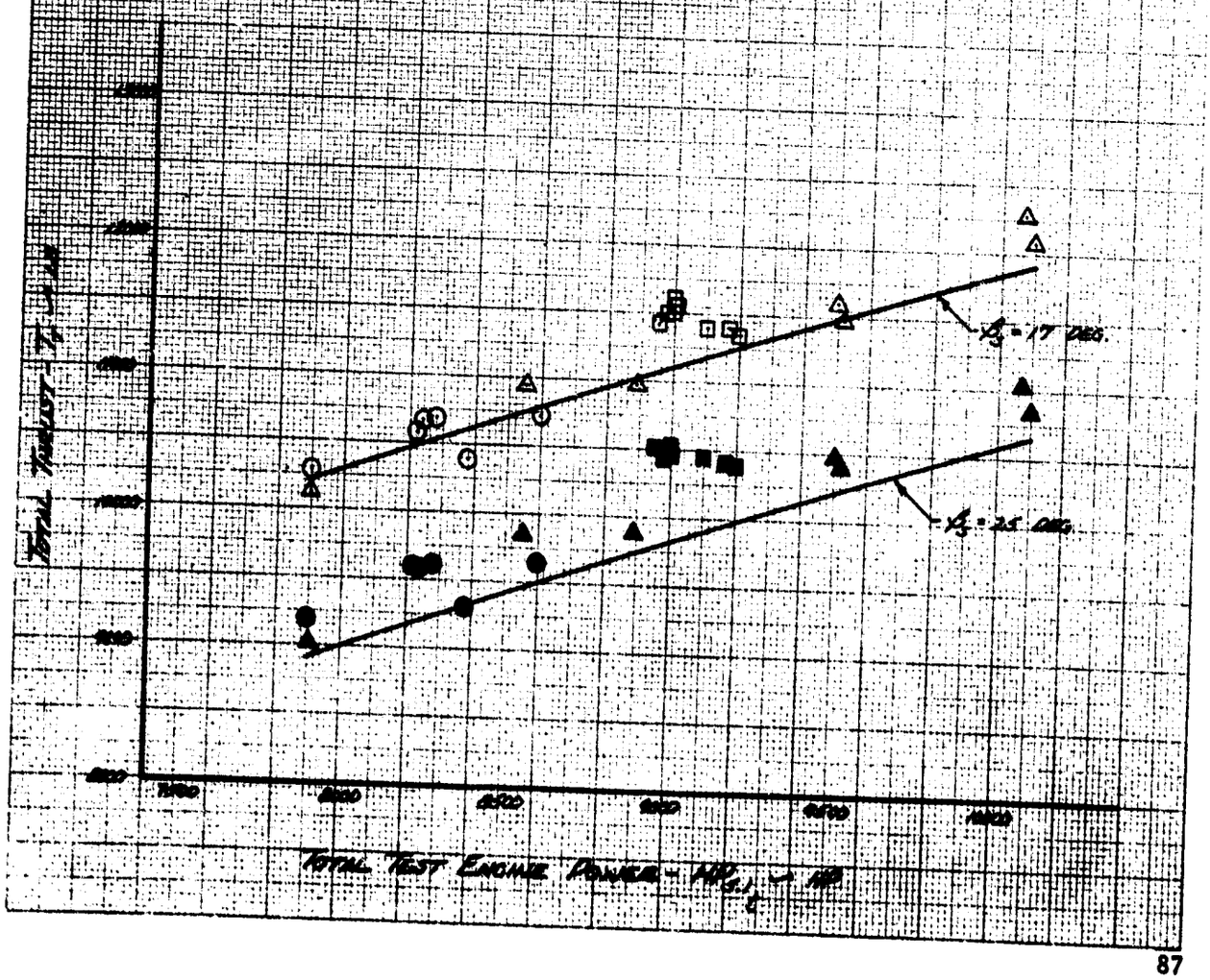

FIGURE NO. 10

FAN MODE TAKE-OFF PERFORMANCE

XV-5A USA TM 62-4505

TECHNIQUE: GROUND ACCELERATION

PRESSURE ALTITUDE - H_p = SL TO 2,100
AVERAGE GROSS WEIGHT - W = 18 TO 19,000
DRY CONCRETE RUNWAY
CORRECTED TO ZERO WIND CONDITIONS

NO LANDING GEAR RETRACTION
FAN MODE CONFIGURATION
ENGINE POWER - NP_{21} = 10000

TAKE-OFF TECHNIQUE AS SHOWN IN FIGURE NO. 12, APPENDIX 2.

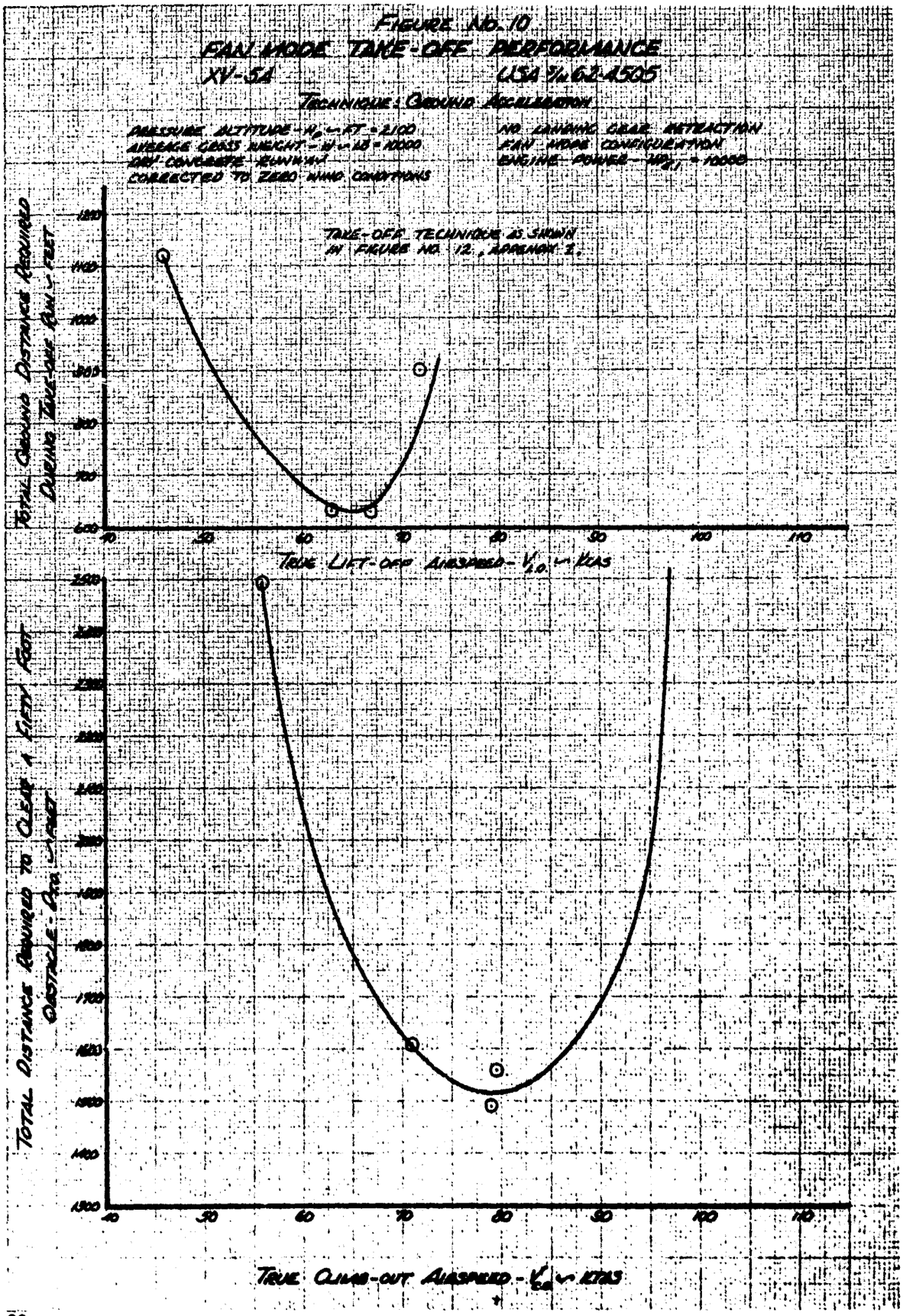

FIGURE NO. 11

FAN MODE TAKE-OFF PERFORMANCE

XV-5A

USA 62-4505

TECHNIQUE: LEVEL ACCELERATION FROM A 15 FOOT HOVER

ASSUMED ALTITUDE - H_A = SEA LEVEL

AVERAGE GROSS WEIGHT - W = 13,000 LB

CORRECTED TO ZERO WIND CONDITIONS

NO LANDING GEAR RETRACTION

FAN MODE CONFIGURATION

ENGINE POWER - WP_{SL} = MP = 100%

NOTE 1

TAKE-OFF TECHNIQUE AS SHOWN IN FIGURE NO. 13, APPENDIX I.

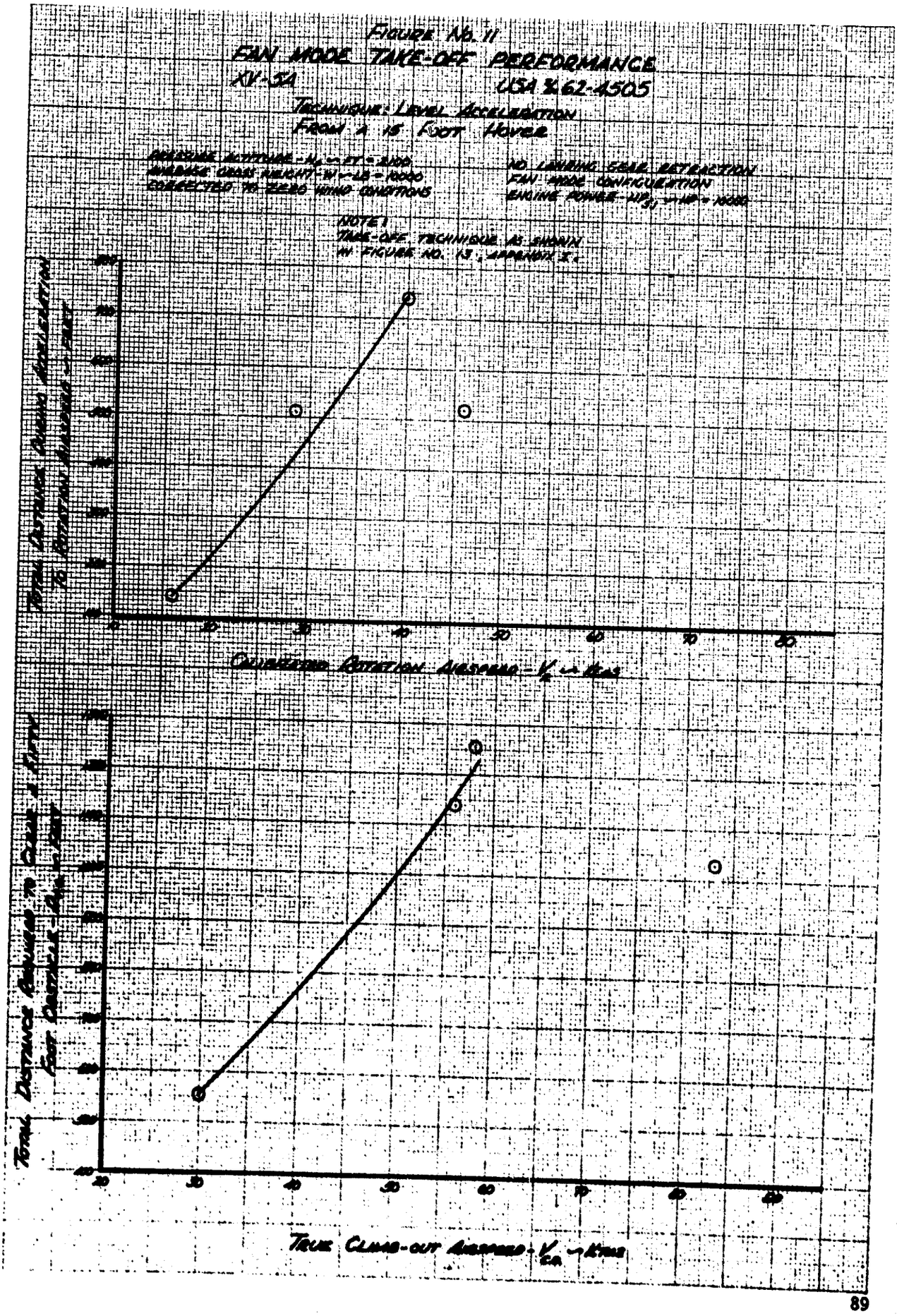

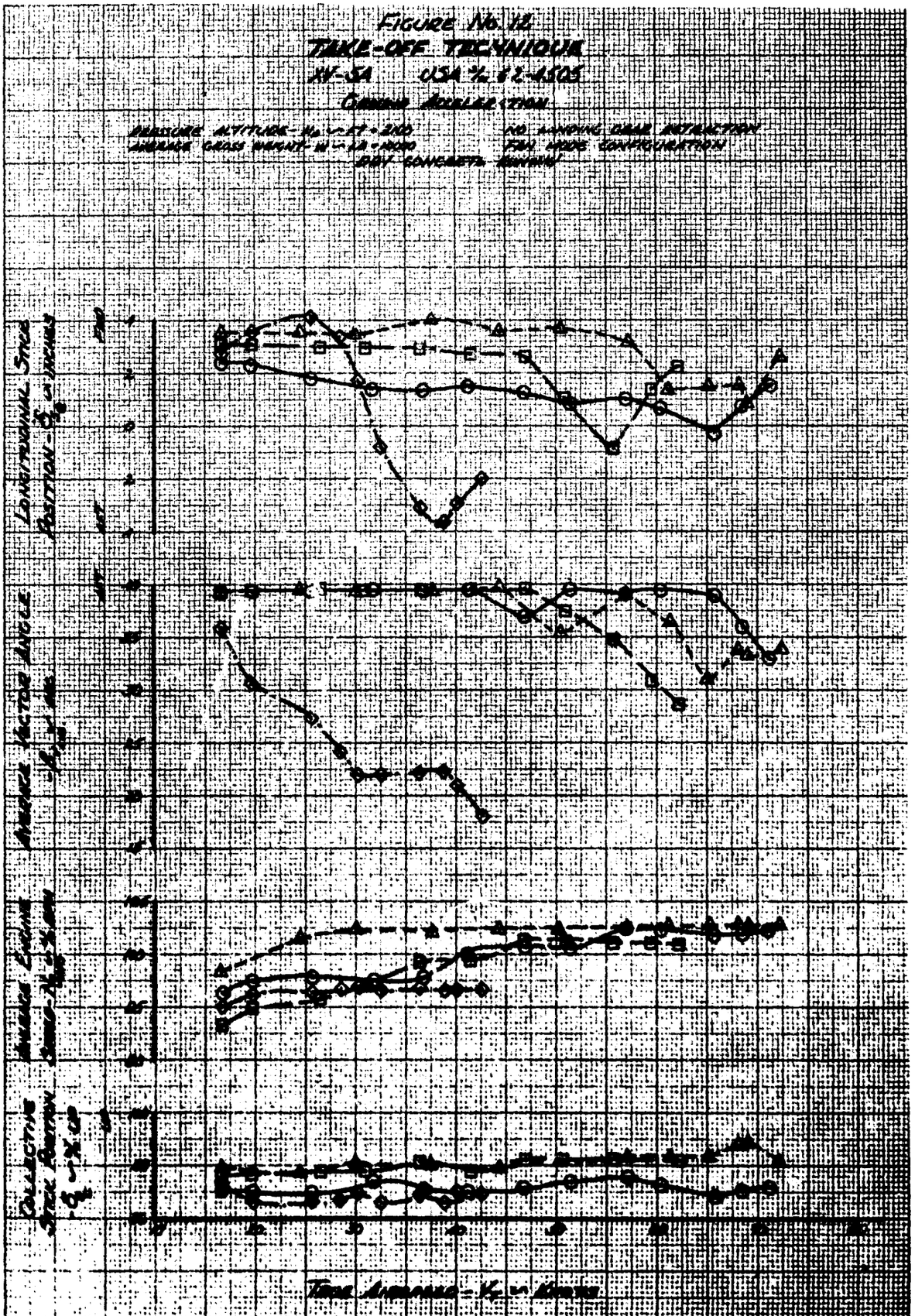
Figure No. 12
TAKE-OFF TECHNIQUE
XV-5A USA No. 62-4505
Gross Acceleration
Pressure Altitude - H_p = -47 - 200
Ambient Gross Weight - W = 23 - 4000
Duty Concrete Runway
400 Landing Gear Retraction
Full Droop Configuration
Longitudinal Stick Position - δ_e - Inches
Pitch Angle - θ - Deg.
Angle of Attack - α - Deg.
Collective Stick Position - δ_{coll} - Inches
Time Increments - K - Knots

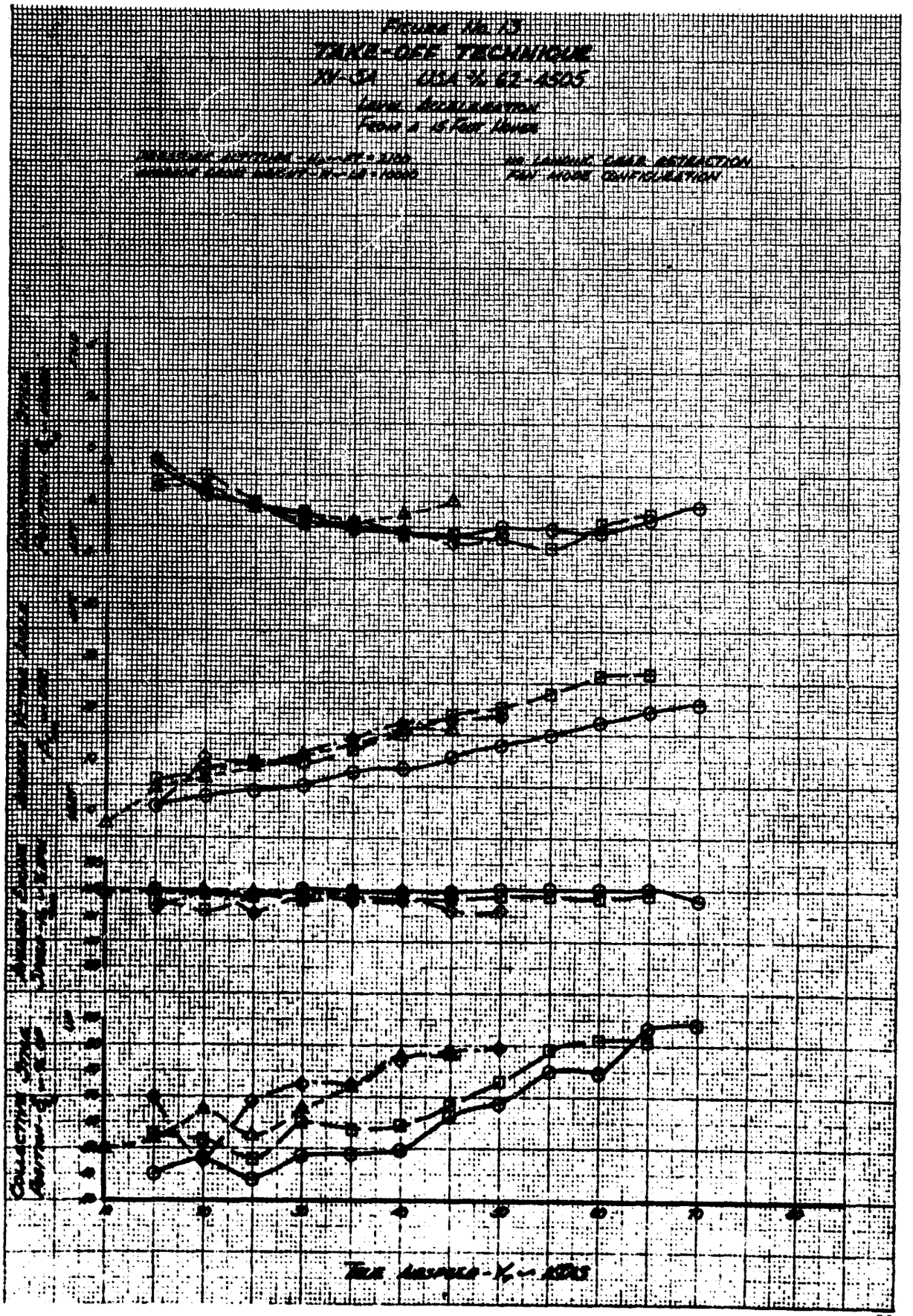
FIGURE NO. 13
TAKE-OFF TECHNIQUE
N-24 USA X 62-4525
LEVEL ACCELERATION
FROM 0 TO 500 KNOTS
INCREASE ALTITUDE 40 FEET PER 1000
INCREASE CLIMB ANGLE 2° AT 10 KNOTS
NO CLIMBING CLIMB ATTRACTION
FOR MORE CONFIGURATION
Time Elapsed - Minutes
True Airspeed - Knots

FIGURE NO. 14

VERTICAL CLIMB PERFORMANCE

XV-3A CL34 X 62-4525

CAL MARK

SYM	CLIMB AT -V = KIAS	ALT = MSL	TRUE T_a °C	ABS PRESS P_a - IN	WING TAIL N_x - KTS	WING CROSSTRK - KTS FROM WEST
◇	97/0	3800	21.6	9763	2.4	0
○	70/98	7852	12.3	9558	0	0
△	70/96	7826	12.2	9542	1.5	0
□	70/93	7862	12.4	9570	1.5	0
▽	70/90	7878	12.2	9534	2.2	0

NOTES:

1. TRUEST AVAILABLE WINDS AT THE STARTING TURNOUT AT THE TEST ALTITUDE FROM PILOTS REPORTS AND RADIOSONDE.
2. VECTORIAL VELOCITY VALUES OBTAINED BY CROSS FIGURE NO. 16 SYMBOLS.

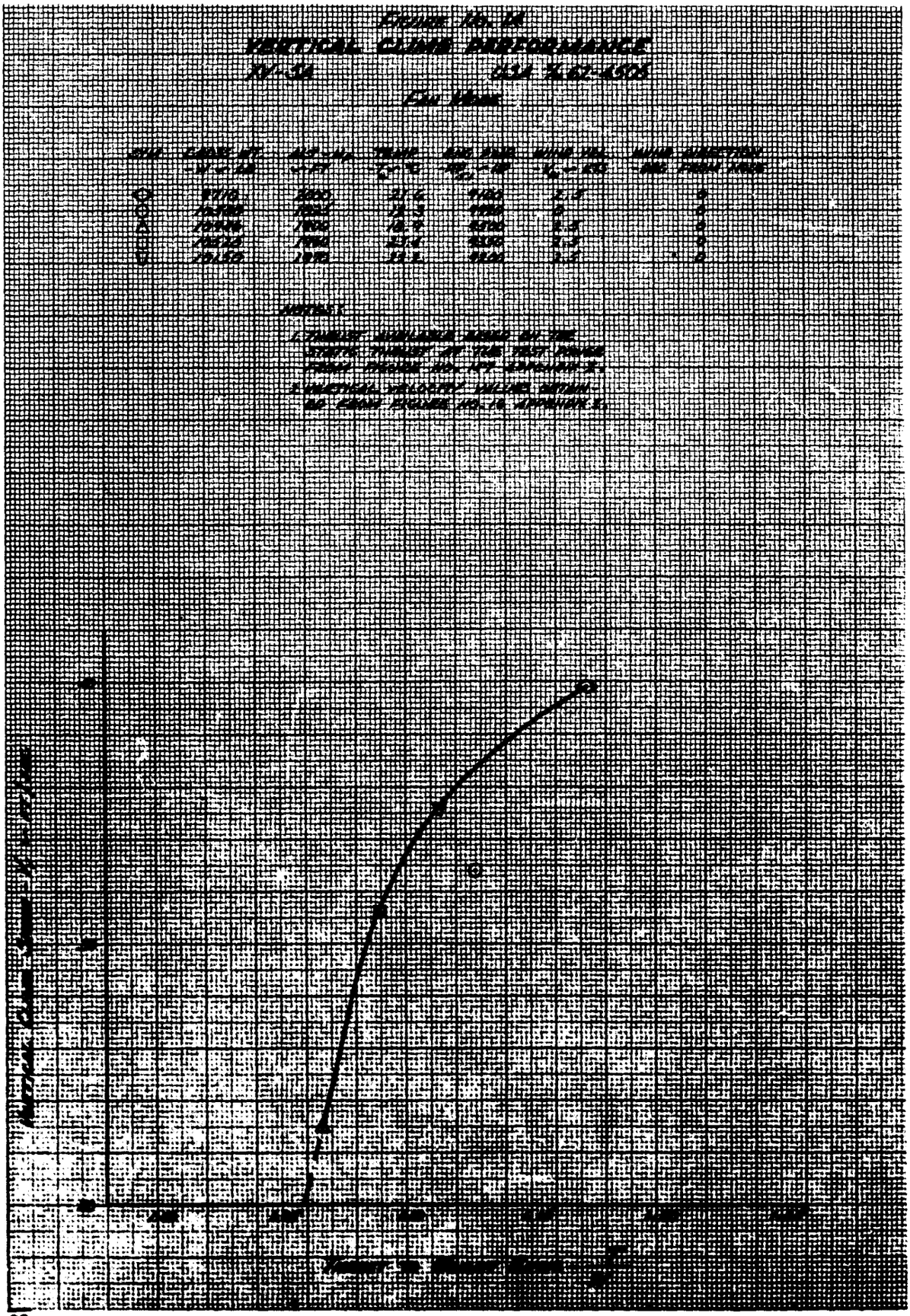

FIGURE NO. 65

VERTICAL CLIMB PERFORMANCE

XV-5A USA S/N 62-4505

FULL AFTER

SYM	GROSS WT. W_g LB	ALT. - H_p FT	TEMP. T_a °C	BAR. PRES. P_{amb} IN HG	WIND VEL. V_w KTS	WIND DIRECTION (MAG. FROM)
○	17140	2000	21.4	9400	2.5	0
□	16750	2000	18.3	9250	0	0
△	16946	1900	18.9	9300	2.5	0
◇	16833	1960	23.1	9350	2.3	0
▽	16750	1900	23.2	9200	2.5	0

NOTES:

1. THRUST BASED ON STATIC THRUST AVAILABLE AT THE TEST POWER FROM FIGURE NO. 147, APPENDIX I.
2. VERTICAL ACCELERATION VALUES OBTAINED FROM FIGURE NO. 17 APPENDIX I.

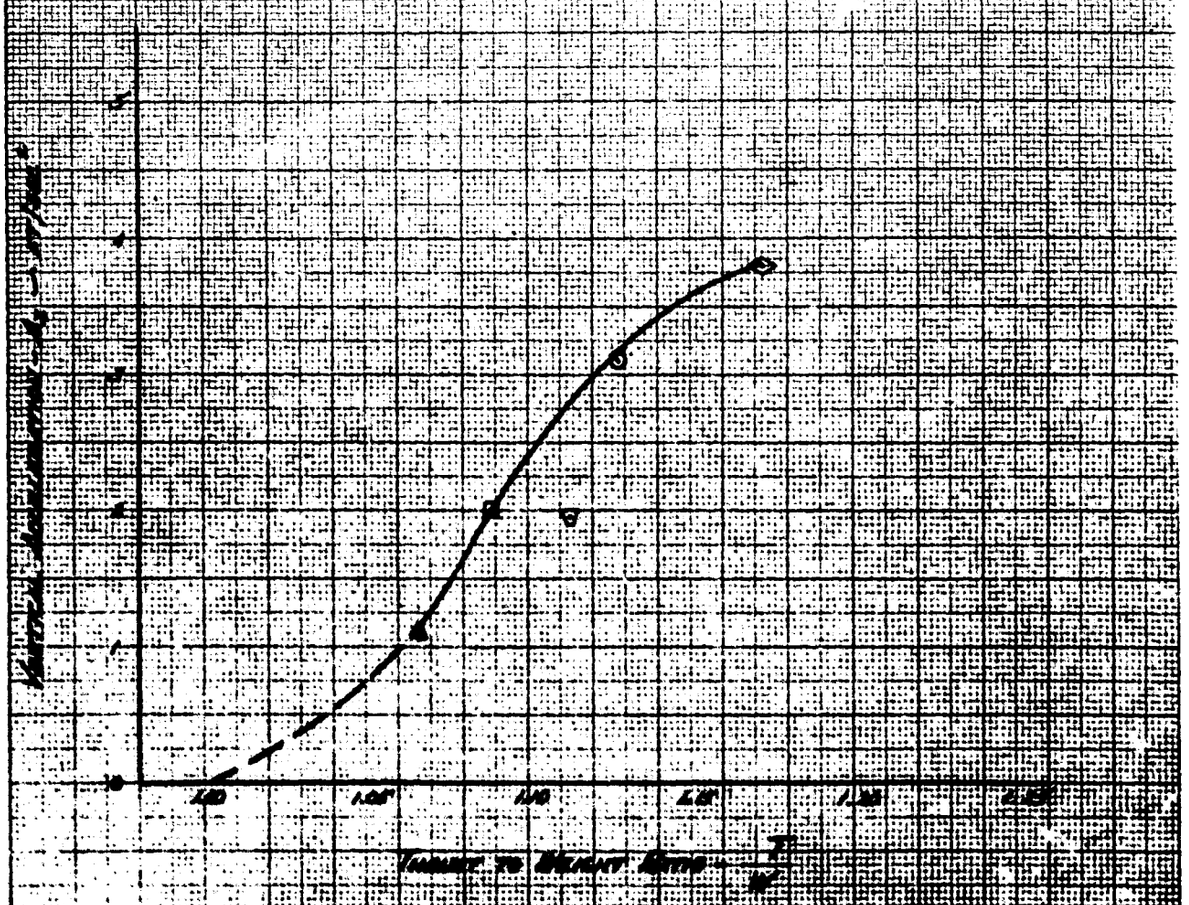

THRUST TO WEIGHT RATIO = $\frac{T}{W}$

FIGURE NO. 16

VERTICAL CLIMB PERFORMANCE

XV-5A USA # 62-4505

FAN MODE

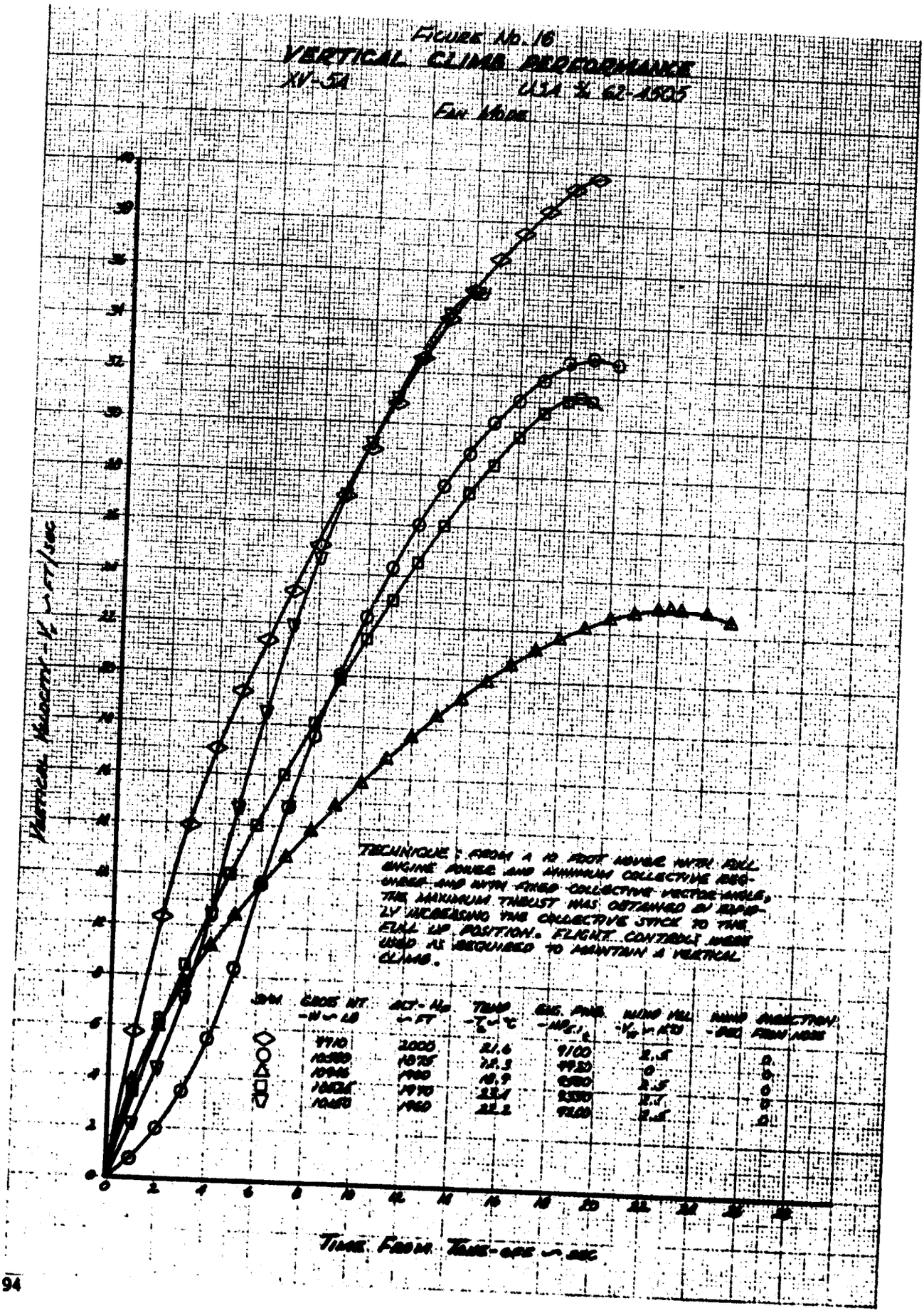

SYM	GROSS WT. -W- LB	ACT.- H_p - FT	TEMP $-T_a-$ °C	EXC. PWR. $-HP_{E.I.}-$	HOVER HGT $-Y_{ag}$- ACTU	HOVER DRIFT - SEC	HOVER DIRECTION FROM NOSE
◇	9710	2000	21.6	9100	2.5		0
○	10,580	1975	15.3	9950	0		0
◇	10,845	1960	18.9	9850	2.5		0
○	11,025	1970	23.4	9350	2.5		0
□	10,450	1960	22.2	9400	2.5		0

FIGURE No. 17

VERTICAL CLIMB PERFORMANCE

XV-5A USA S/N 62-4505

FAN MODE

SYM	GROSS WT. -W ∽ LB	ALT. -H_p ∽ FT	TEMP -T_a ∽ °C	ENG. PWR. -$HP_{S.L.}$	WIND VEL -V_W ∽ KTS	WIND DIRECTION -DEG. FROM NOSE
◇	9710	2000	21.6	9100	2.5	0
○	10530	1975	12.3	9920	0	0
△	10946	1900	16.9	9500	2.5	0
□	10525	1970	23.4	9350	2.5	0
▽	10150	1960	22.2	9200	2.5	0

TECHNIQUE

FROM A 10 FOOT HOVER WITH FULL ENGINE SPEED, MINIMUM COLLECTIVE STICK REQUIRED AND FIXED COLLECTIVE VECTOR ANGLE, THE MAXIMUM THRUST WAS OBTAINED BY RAPIDLY INCREASING THE COLLECTIVE STICK TO THE FULL UP POSITION. FLIGHT CONTROLS WERE USED AS REQUIRED TO MAINTAIN A VERTICAL CLIMB.

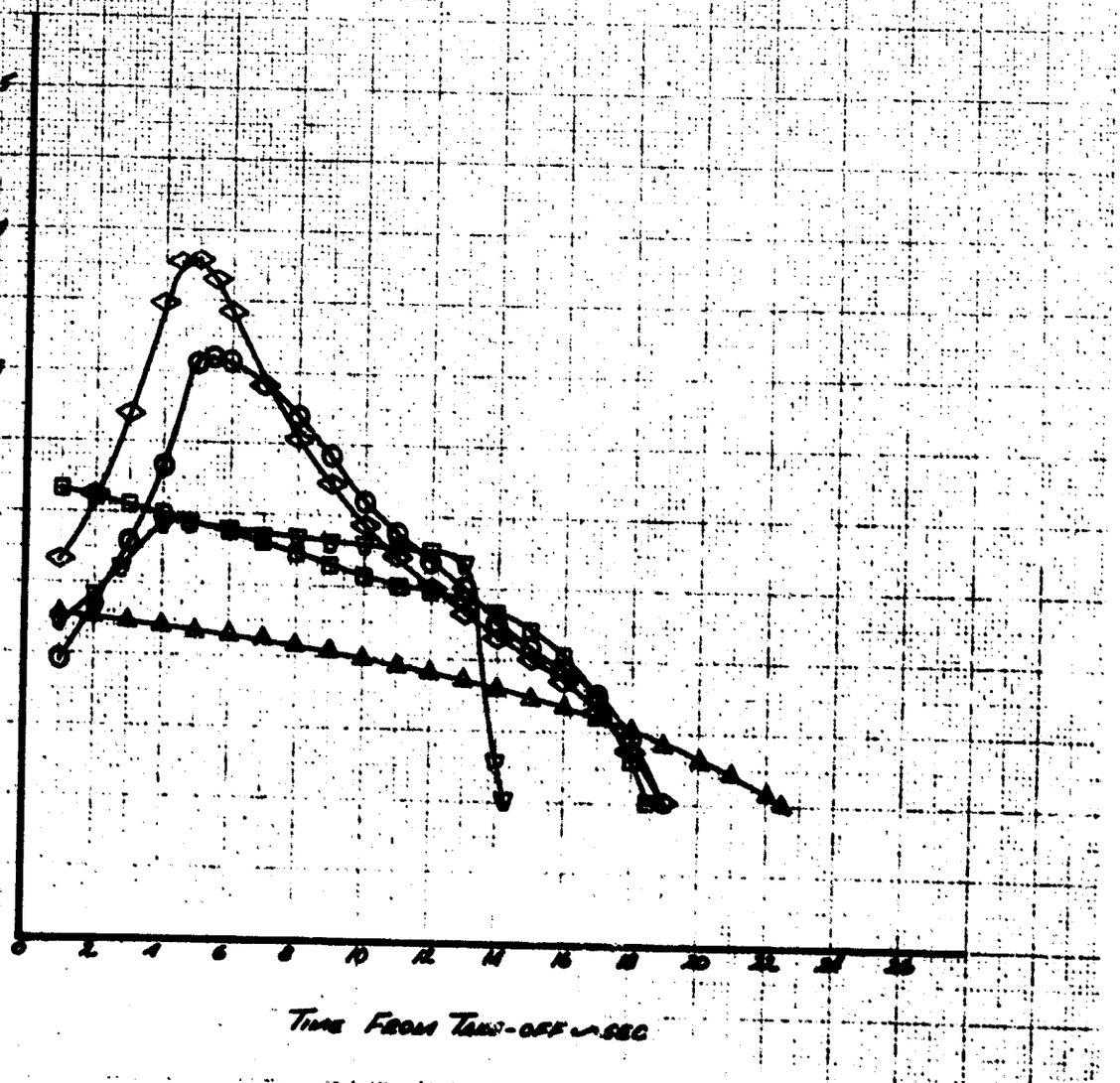

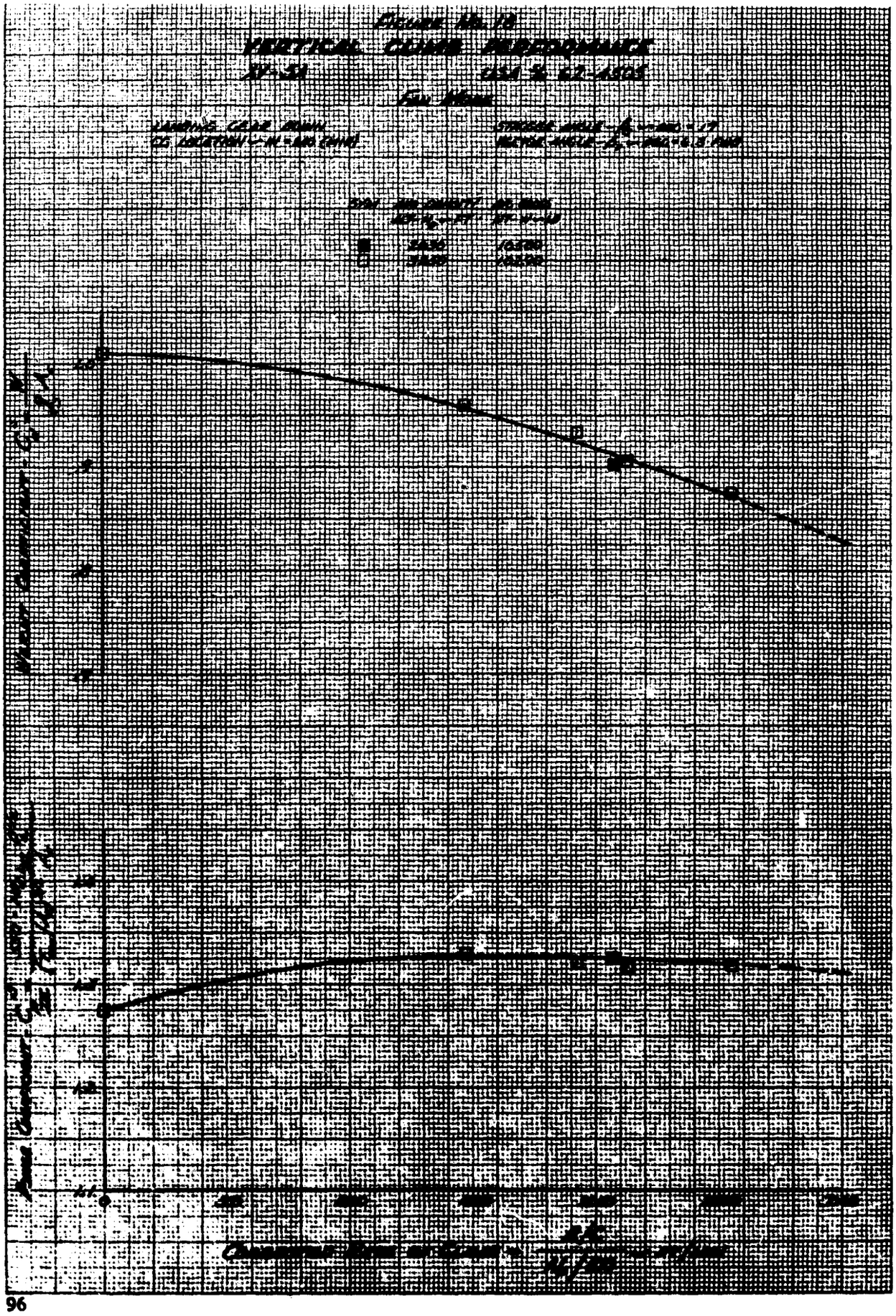
VERTICAL GUST ENVELOPE

FIGURE No. 10

VERTICAL CLIMB PERFORMANCE

XV-3A

CL34 & 62-4005

FAN MODE

ENGINE CLAD DOWN
CG LOCATION - IN = 240 (AFT)
GROSS WEIGHT - W = 42,000 LBS

STAGGER ANGLE - β_s = 90° - ϕ = 17°
VECTOR ANGLE - β_v = ARC TAN 6.5 / 600
HOT AIR SIMULATOR GAGE 432

CURVES RECEIVED FROM FIGURE NO. 12, APPENDIX I.

VERTICAL RATE OF CLIMB - $(W_c)_{max}$ - FT/MIN

3000
2000
1000
500
0

90 92 94 96 98 100 102 104

WING FAN SPEED - $(N_f)_{max}$ - % RPM

UNIT FAN SPEED

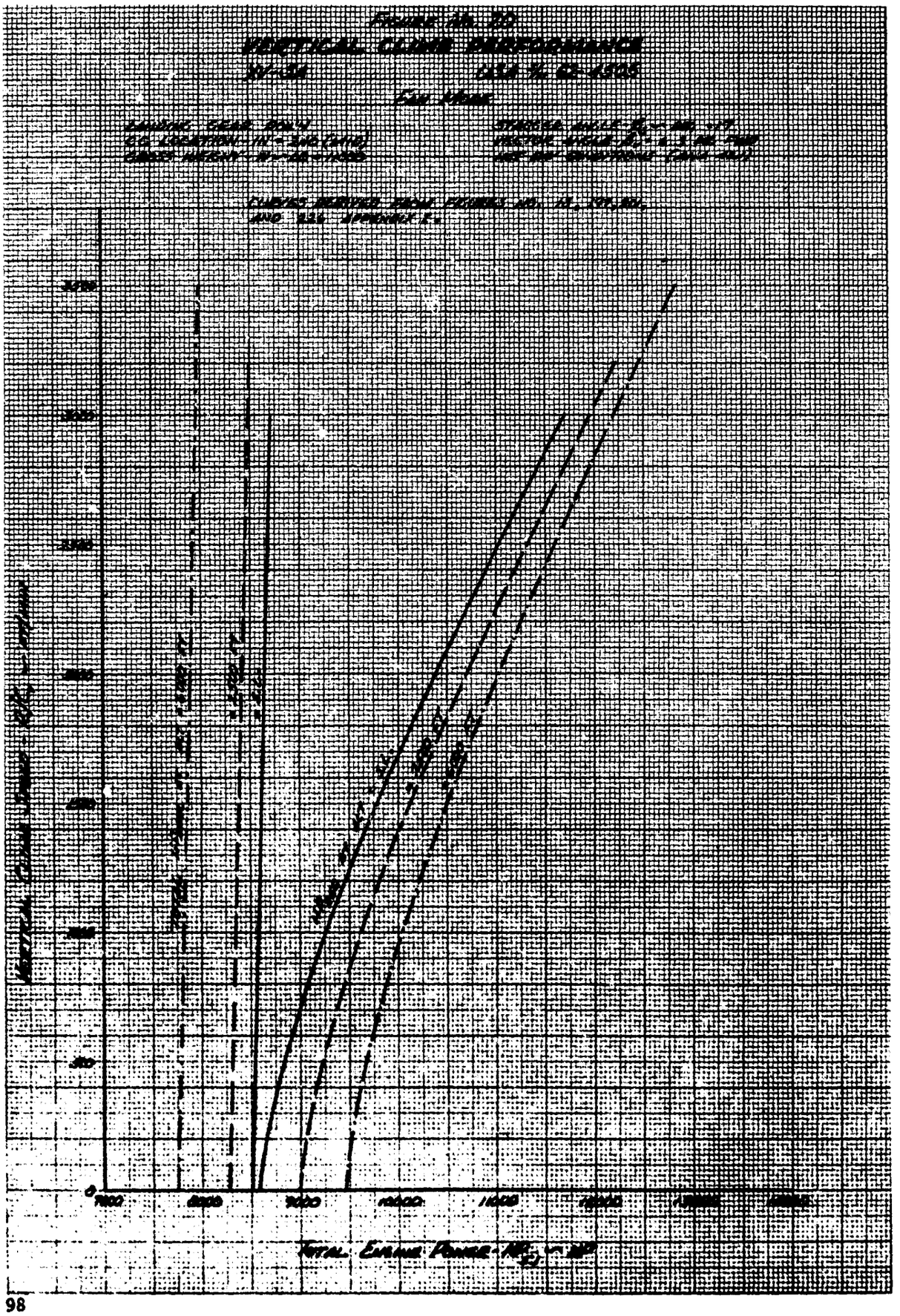
FIGURE No. 20
VERTICAL CLIMB PERFORMANCE
XF-84
Sea Level
ENGINE GEAR RATIO
CG LOCATION
GROSS WEIGHT
STANDARD DAY
ENGINE SPEED
PROPER SPEED
USE OF EMERGENCY POWER LIMIT
CURVES DERIVED FROM FIGURES
AND USE OF SYMBOLS
Rate of Climb - Feet per Minute
Total Engine Power

FIGURE No. 21

VERTICAL CLIMB PERFORMANCE

XV-5A

USA N. 62-4505

ESU MODE

ENGINE GEAR BOX
CG LOCATION - IN = 240 (AFT)
GROSS WEIGHT - 6 - 28 - 1000

STAGGER ANGLE - β_1 = ONE = 15°
VECTOR ANGLE - β_1 = TWO = 6.3 DEG
STANDARD DAY CONDITIONS

CURVES MODIFIED FROM FIGURES NO. 184, 185, 186, AND 226, APPENDIX I.

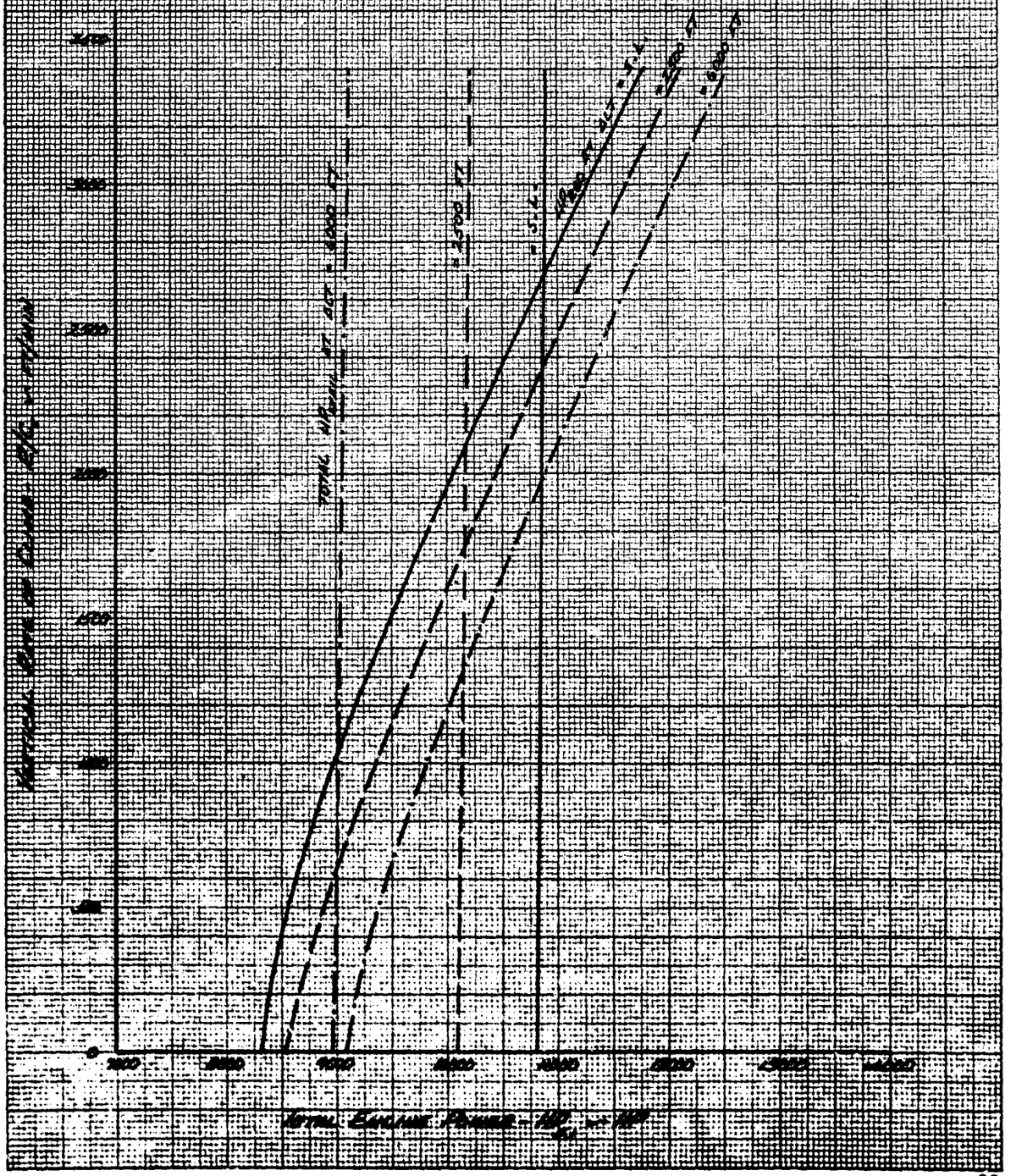

FIGURE No. 22

VERTICAL CLIMB PERFORMANCE

XV-5A USA # 62-4505

FAN MODE

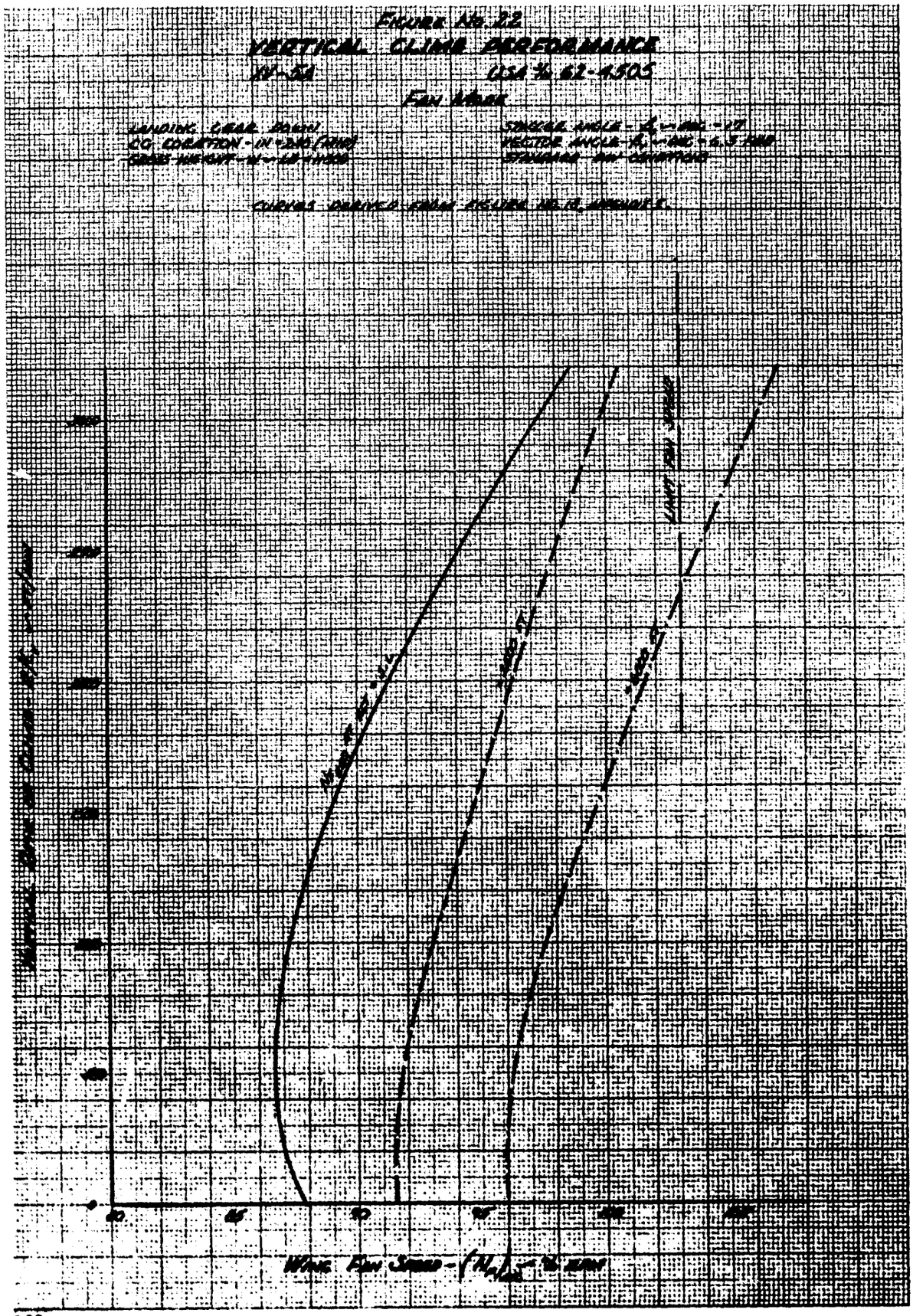

FIGURE NO 25

VERTICAL CLIMB PERFORMANCE

XV-5A USA # 62-4508

FAN MODE

LANDING GEAR DOWN
C.G. LOCATION - IN = 240 (MID)
GROSS WEIGHT - W = LB = 10000

STAGGER ANGLE - β_1 = DEG = 17
VECTOR ANGLE - β_2 = DEG = 2.3 MAX
ACT. DAY CONDITIONS (SEA LEV)

CURVES DERIVED FROM FIGURES NO. 10, 197, 201 AND 226, APPENDIX I.

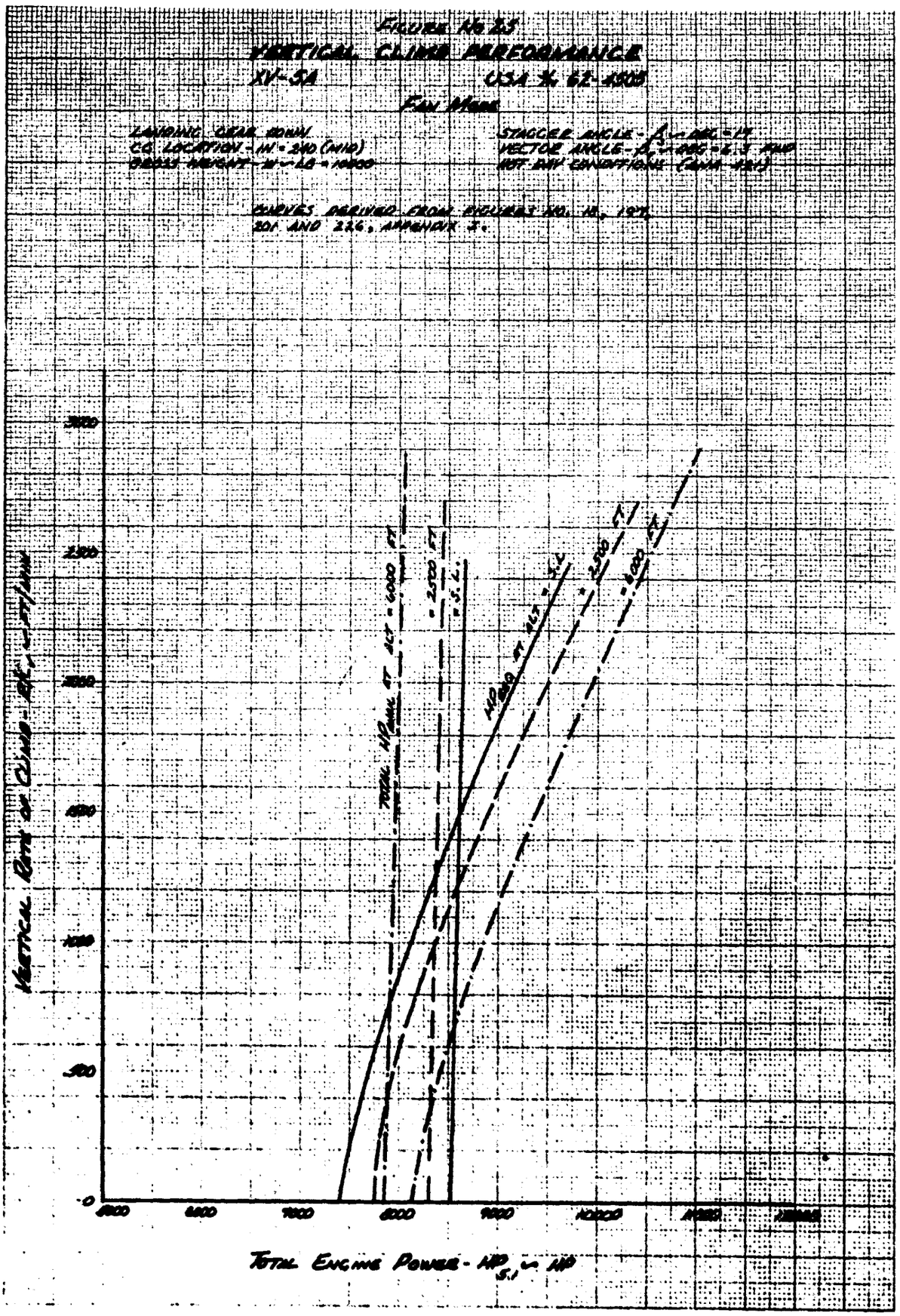

FIGURE NO. 24

VERTICAL CLIMB PERFORMANCE

XV-3A

CLIMB % 62-4525

Gw Maint

LANDING GEAR DOWN
CG LOCATION - IN - 240 (MAX)
CARB INTAKE - NORMAL

STANDARD ATMOS - SL - 59F - 29.92
VECTOR MOTOR 2 - 28V - 0 A - 0 RPM
PROP ANTI-ICE/DE-ICE - OFF

CLIMBS RECORDED FROM FIGURE 10-14, APPENDIX II.

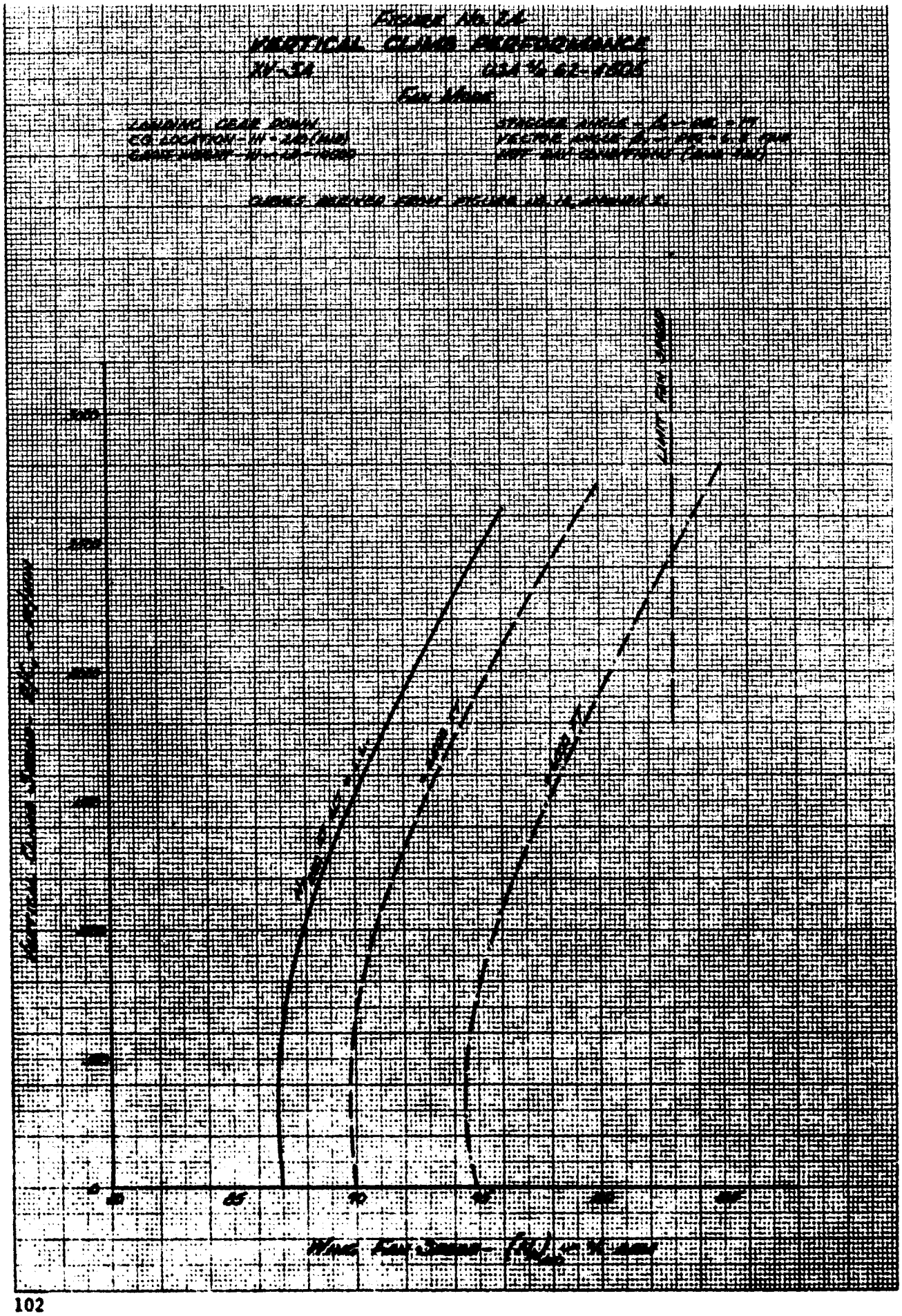

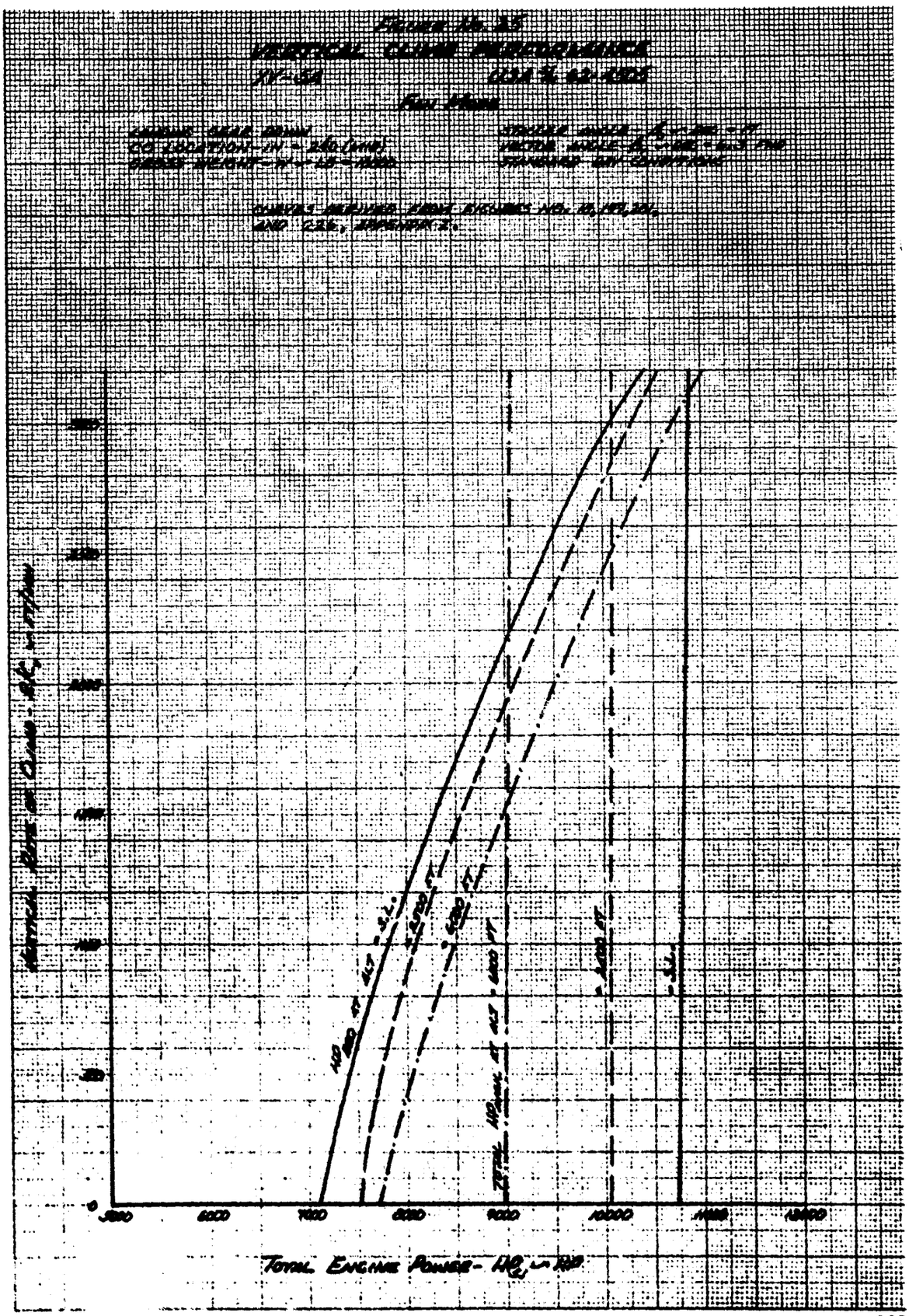
Total Engine Power - HP

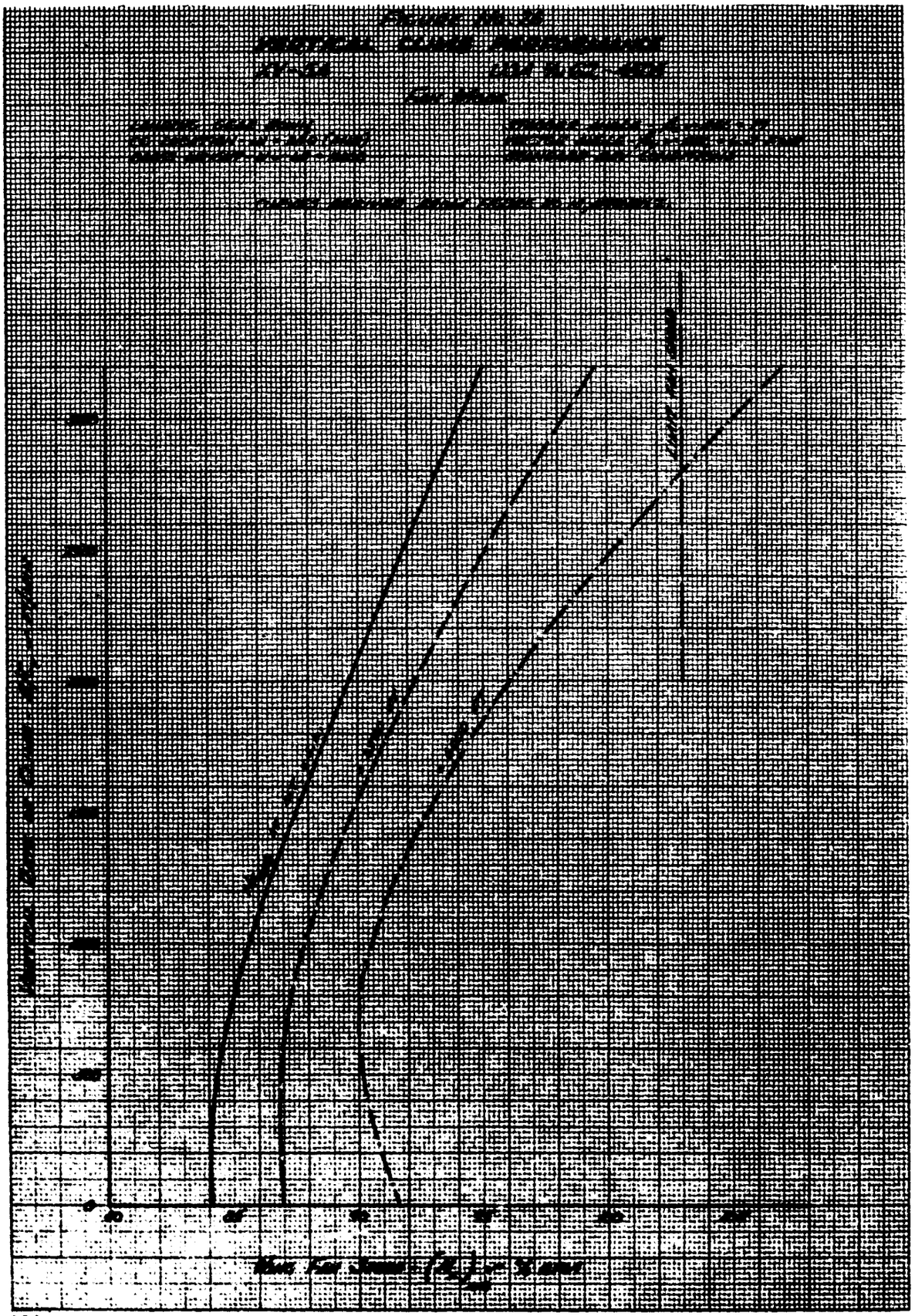

FIGURE NO. 27

FORWARD CLIMB PERFORMANCE

XF-51 (43-6 62-4005

Sea Level

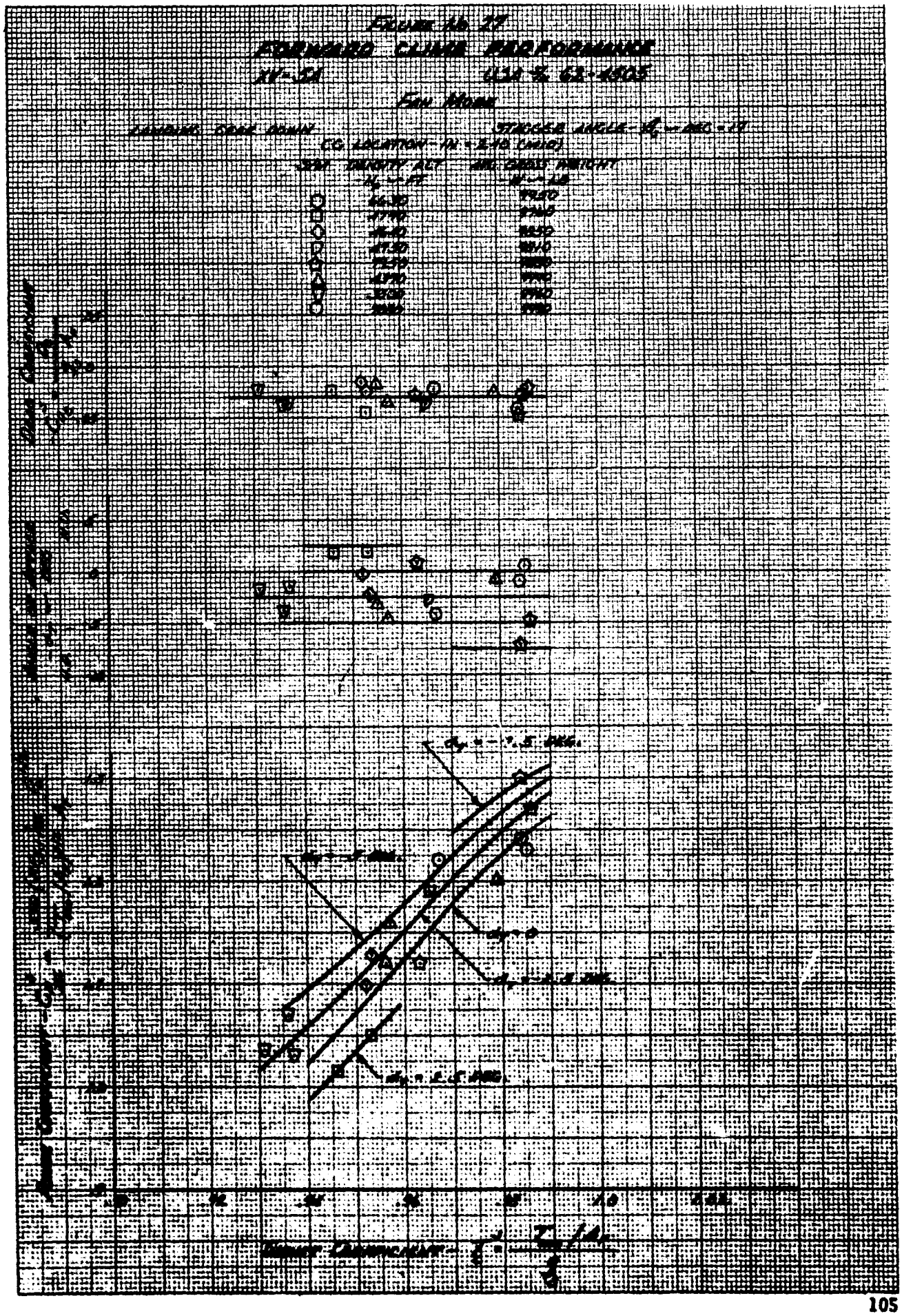

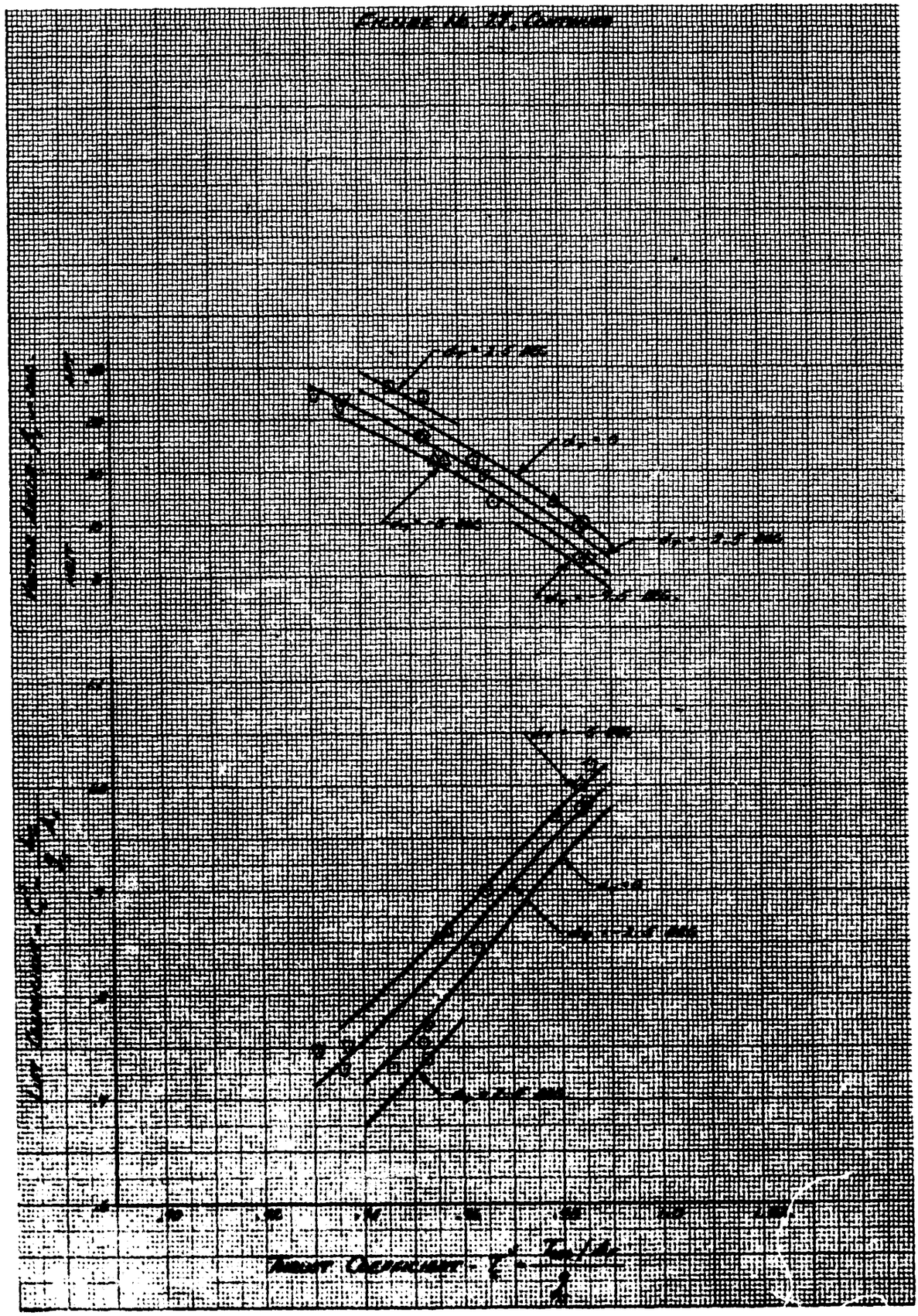

FIGURE 46. 27, CONTINUED

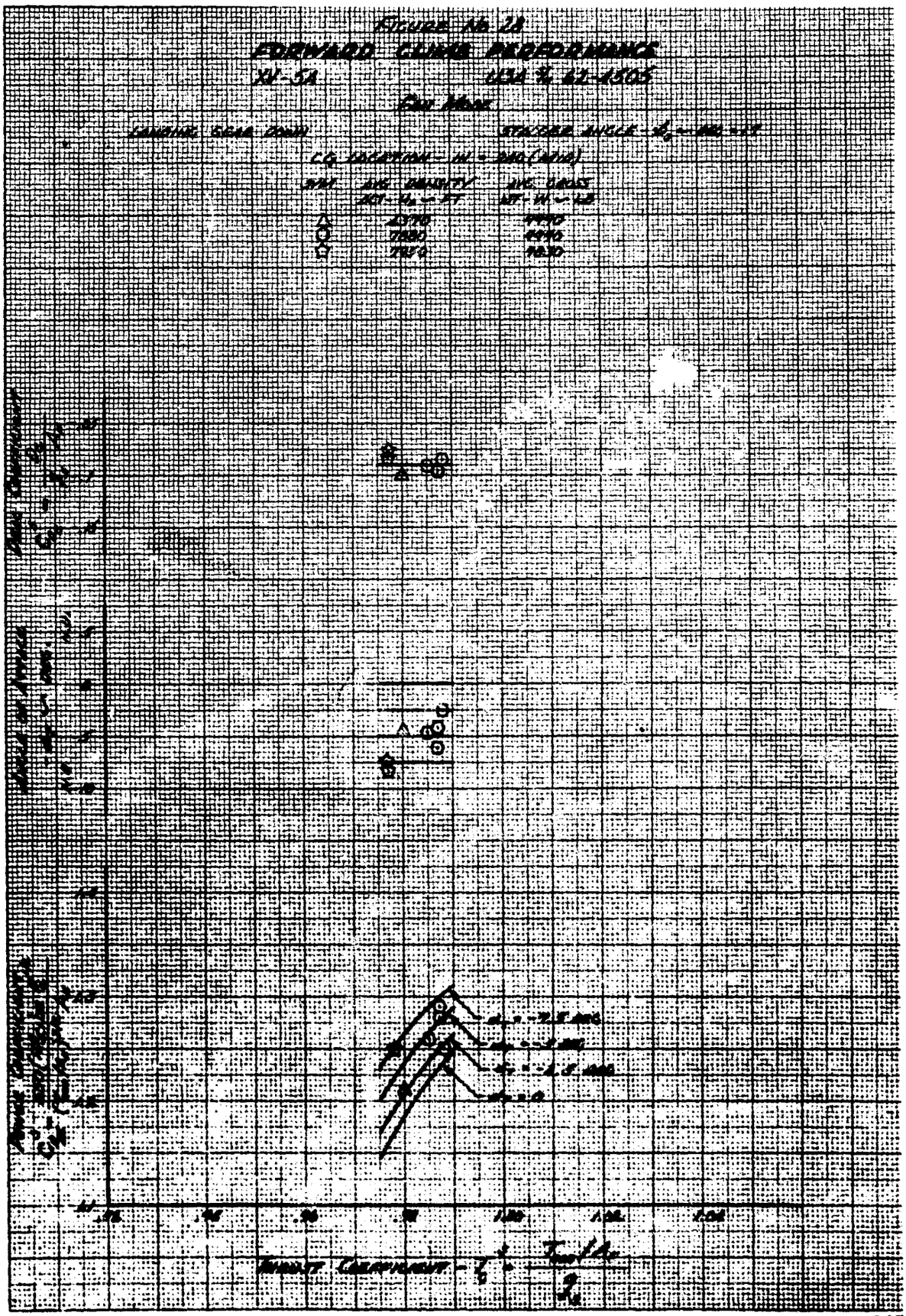
FIGURE A6-23
FORWARD CENTER PERFORMANCE
XV-5A
LANDING GEAR DOWN
STRUCTURE ANGLE
CG LOCATION
WING
TAIL
ANGLE OF ATTACK
ANGLE OF ATTACK
WEIGHT COEFFICIENT

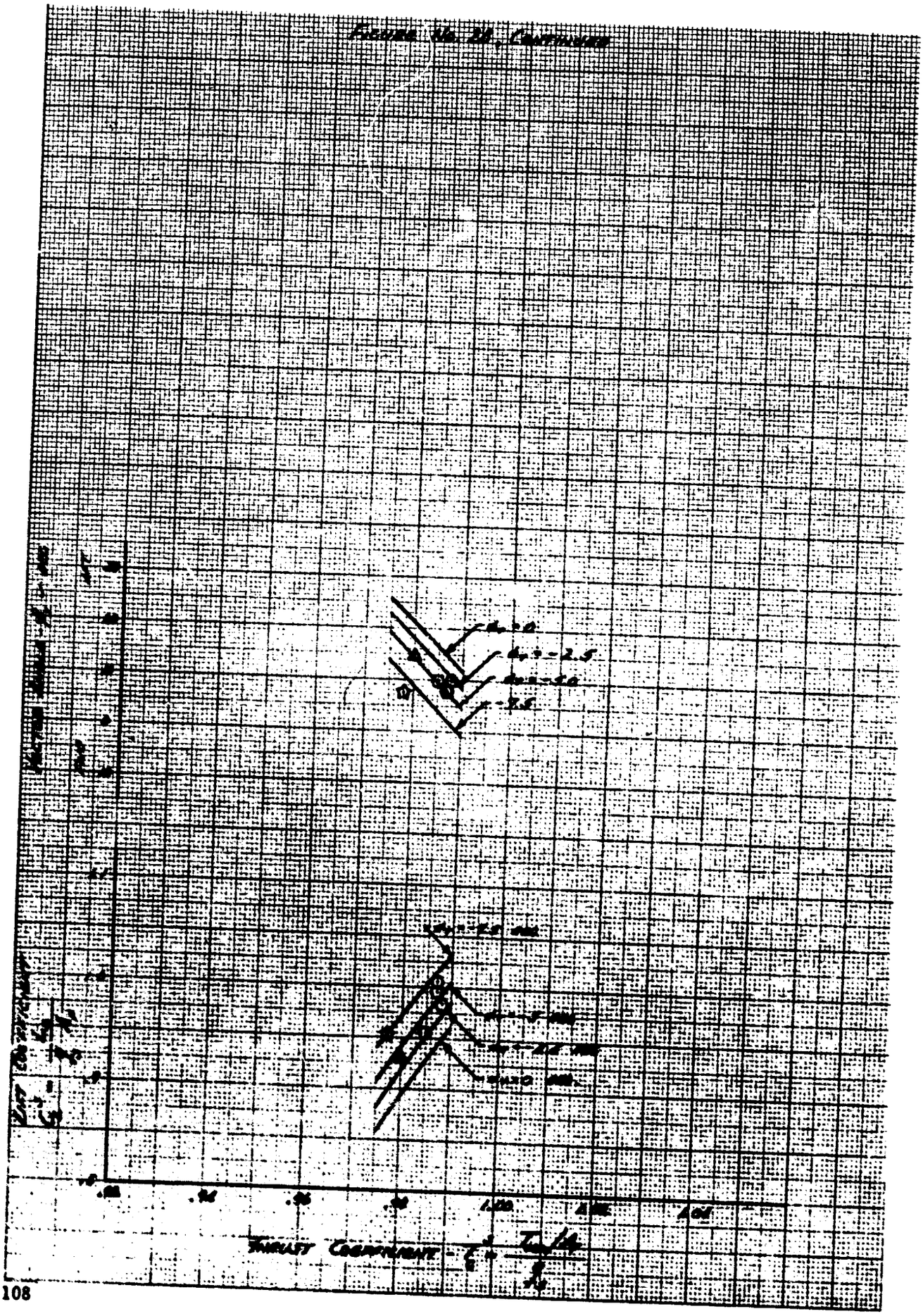
FIGURE No. 28, CONTINUED
THRUST COEFFICIENT

FIGURE NO. 29

FORWARD CLIMB PERFORMANCE

XV-5A

USA 7-62-C505

FAN MODE

LANDING GEAR DOWN
CG LOCATION - N = 240 (MAC)

STABILIZER ANGLE - i_t = 7 DEG = 17
ANGLE OF ATTACK - α_s = 0 DEG = 5°

CURVES DERIVED FROM FIGURES NO. 27 AND 28, APPENDIX I.

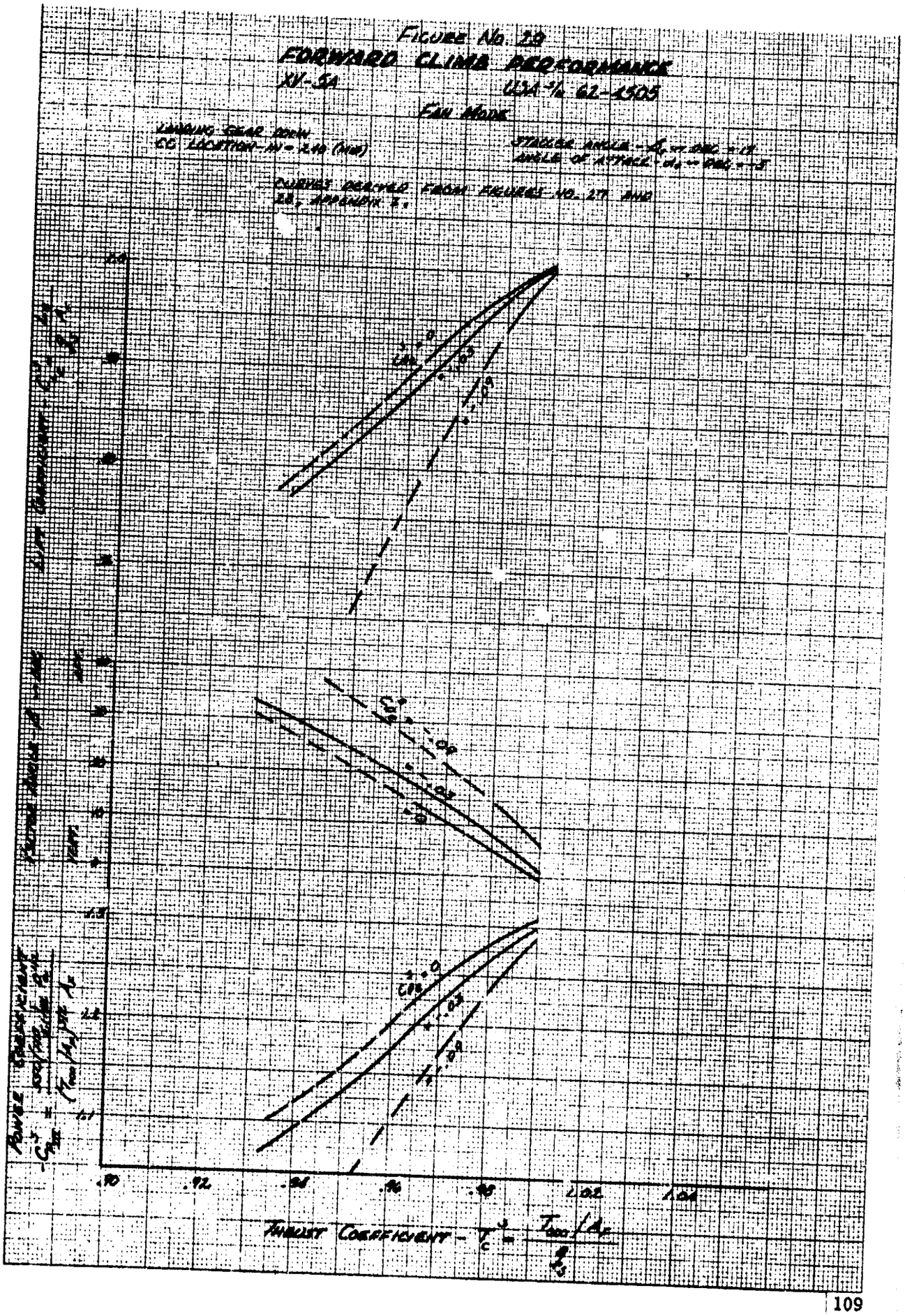

FIGURE No. 30

FORWARD CLIMB PERFORMANCE

XF-85A

USAF No. 46-523

Full Flaps

LANDING GEAR DOWN
CG LOCATION - M = 2.20 (Aug)

STABILIZER ANGLE - i_t = -2.5° - -1°
ANGLE OF ATTACK - α = 10° - 8°

CURVES ARRANGED FROM FIGURES NO. 27 AND 28, APPENDIX I.

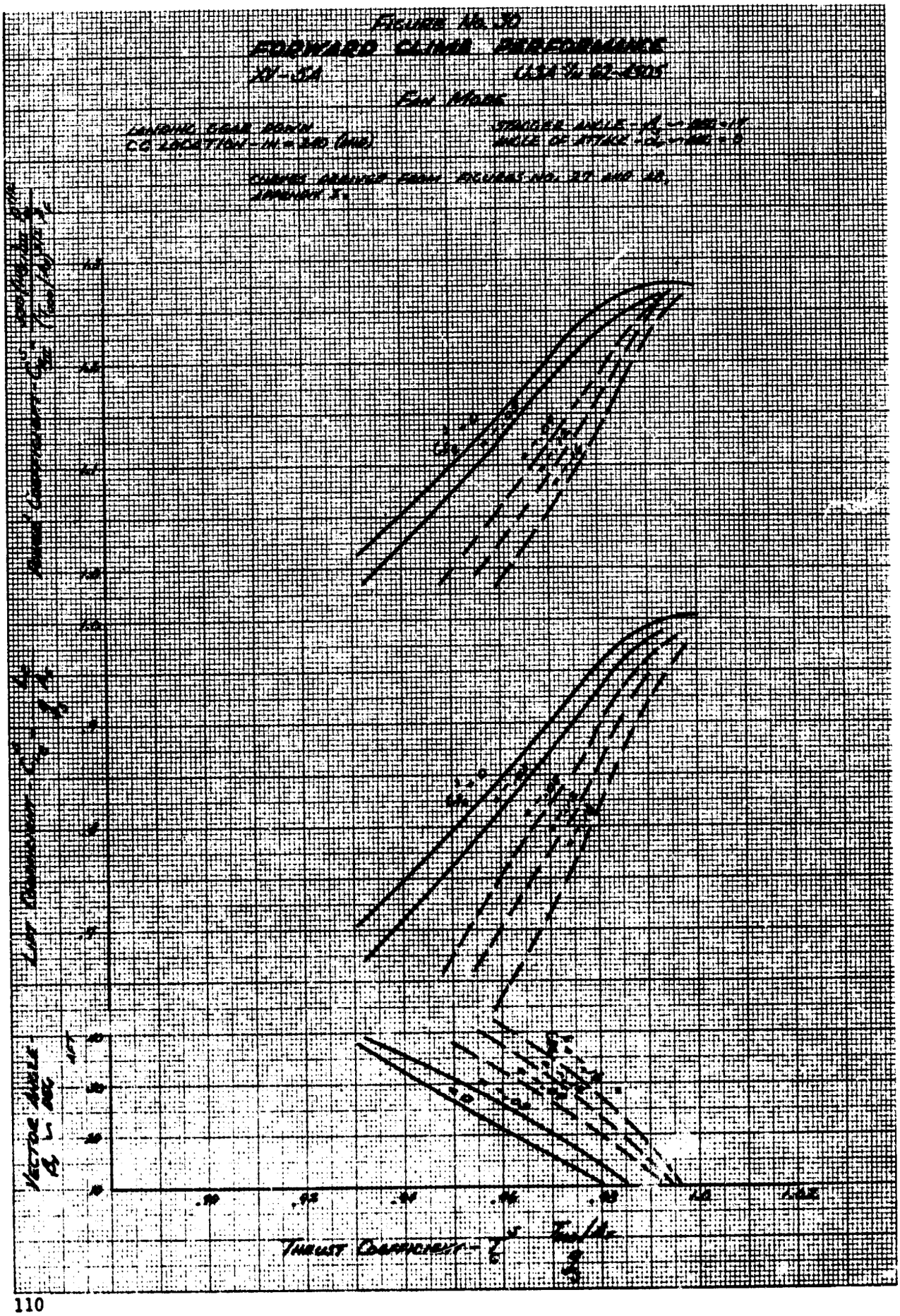

Figure No. 51

FORWARD CLIMB PERFORMANCE

XV-5A USA No. 62-4505

Fan Mode

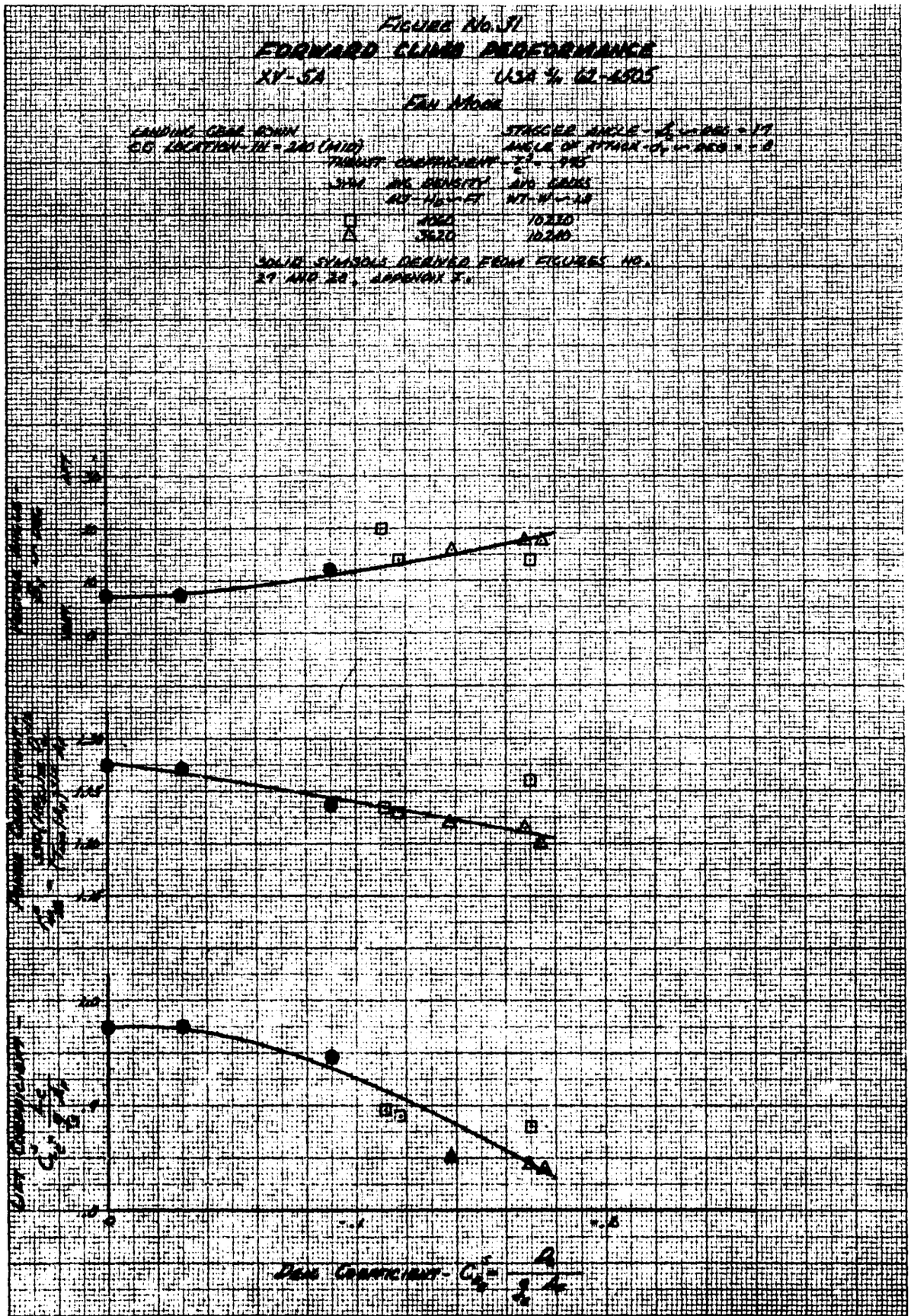

FIGURE No. 32

FORWARD CLIMB PERFORMANCE

XV-5A

CCSA No. 62-4925

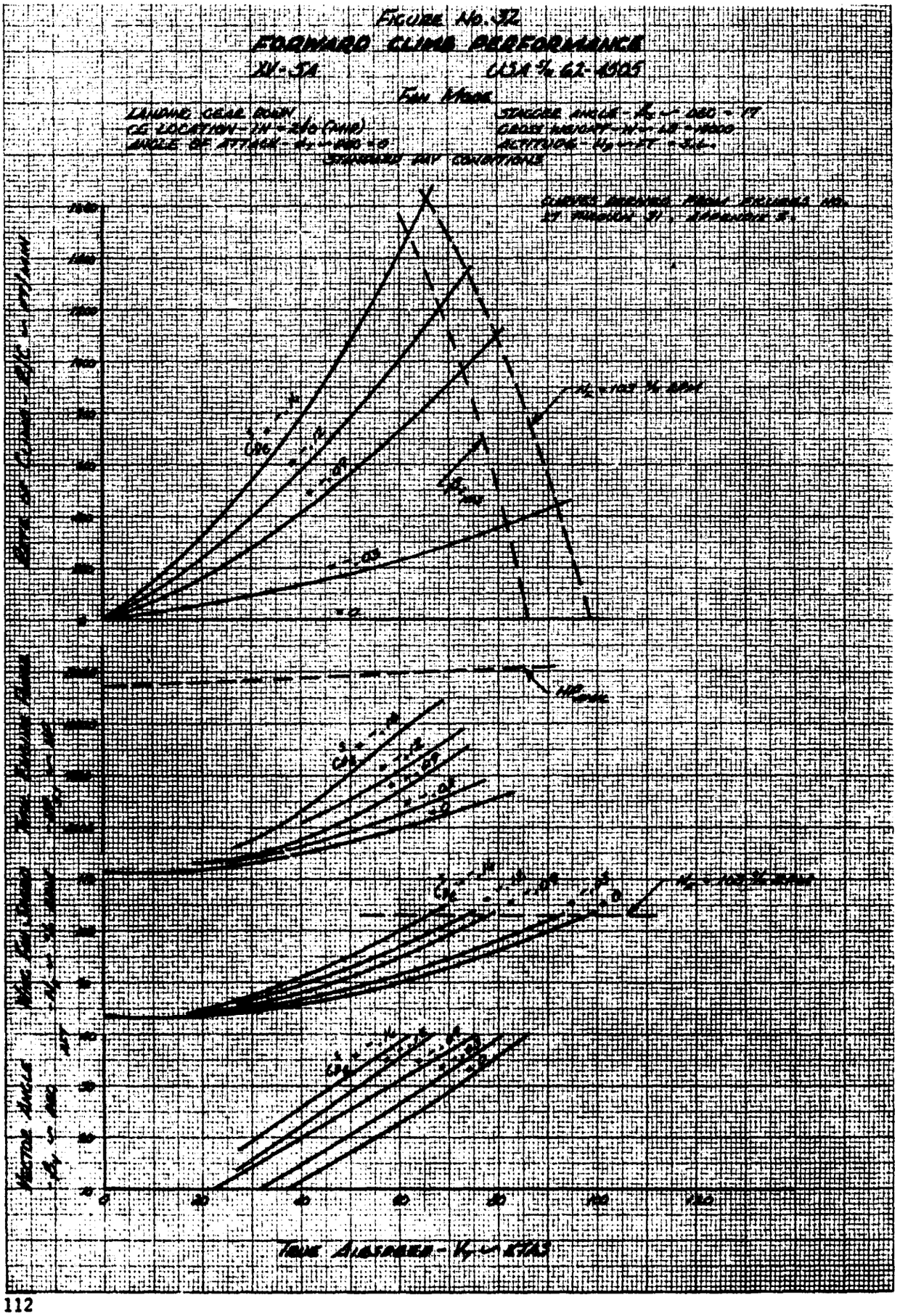

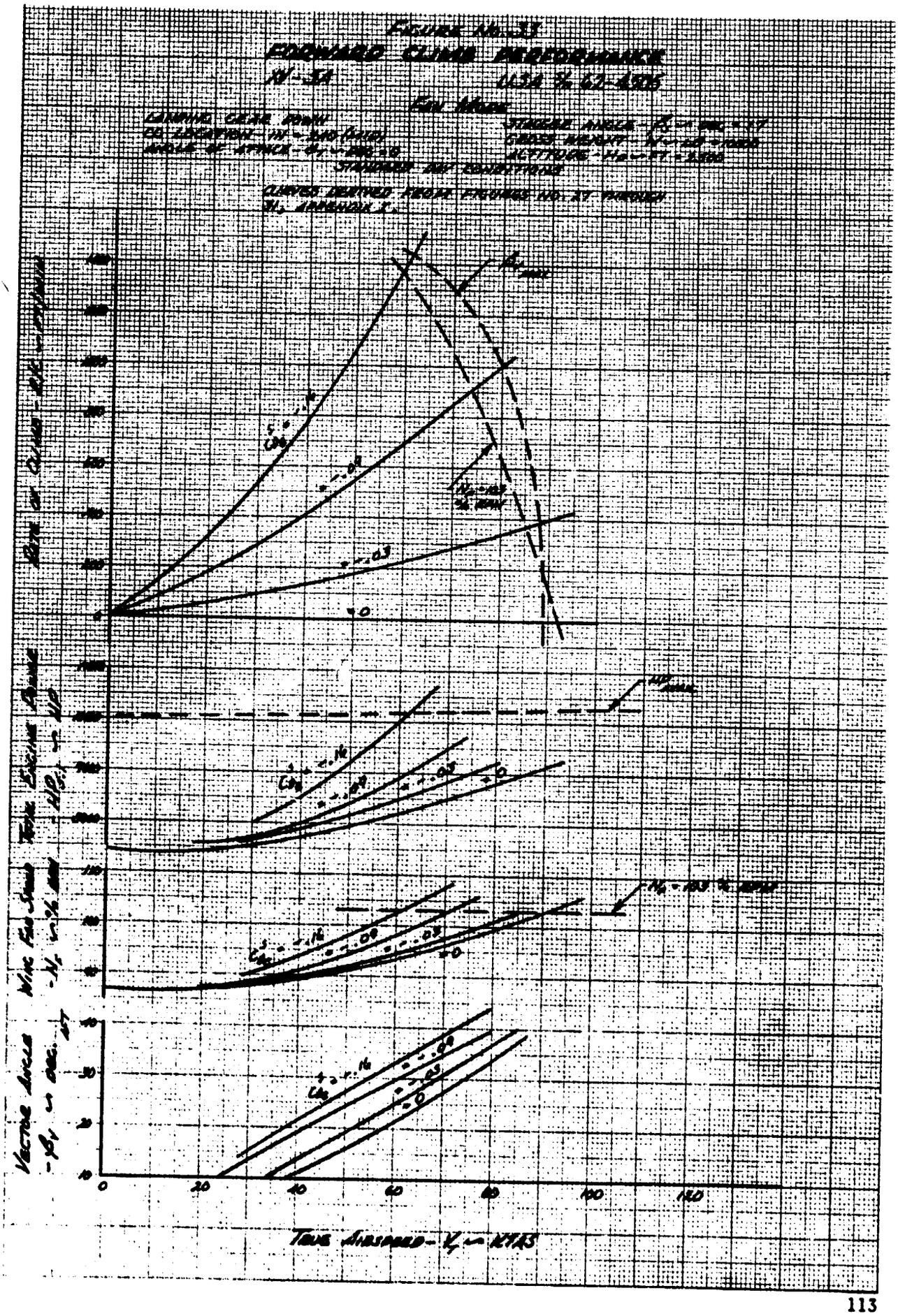
FIGURE A6.3.1
EDGEWISE CLIMB PERFORMANCE
M=.34
CASE % 62-4505
FAN MODE
CAMMING GEARS POWER
CG LOCATION - in. = 240 (Level)
ANGLE OF ATTACK - α_f = 240 -10
STANDARD DAY CONDITIONS
CURVES DERIVED FROM FIGURES NO. 27 THROUGH
31, APPENDIX I.
STAGGER ANGLE - β_s = 240 - 27
GROSS WEIGHT - W_g = 24 - 24000
ALTITUDE - H_p = 27 - 27000
$H_{p_{max}}$
$H_{p_{max}}$ = 100 % RPM
C_{H_p} = .16
.09
.03
0
$H_{p_{max}}$
C_{H_p} = .16
.09
.03
0
H_p = 100 % RPM
C_{H_p} = .16
.09
.03
0
C_{H_p} = .16
.09
.03
0
Rate of Climb - R/C - Feet/Min
Vertical Angle - γ_f - Deg.
0
20
40
60
80
100
120
True Airspeed - V_t - KTAS

FIGURE 46.34

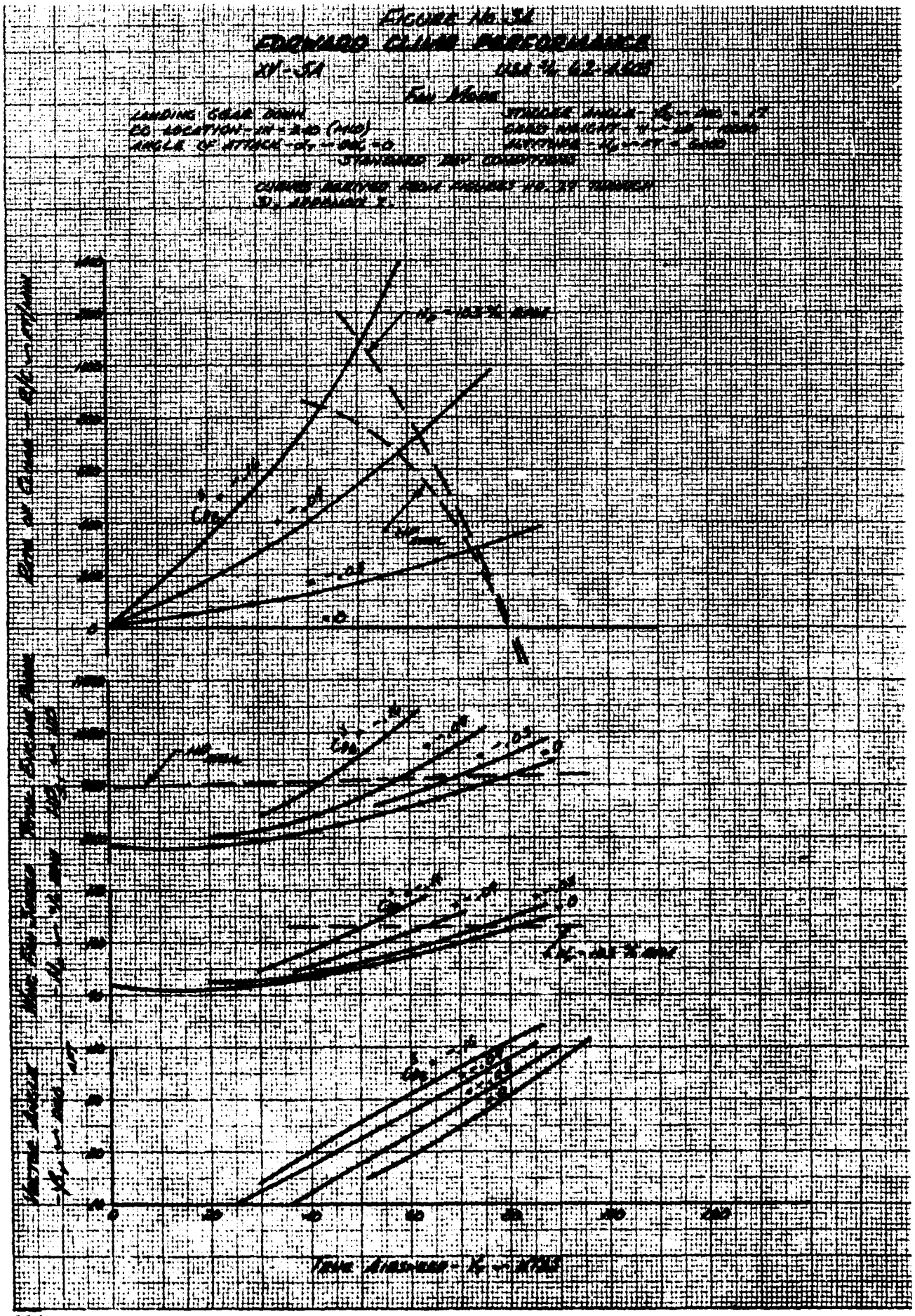
ELEVATOR CLIMB PERFORMANCE
XF-T1
CLEAN
FULL POWER
LANDING GEAR DOWN
CG LOCATION - sta = 240 (MAC)
ANGLE OF ATTACK - α = MAC
STANDARD DAY CONDITIONS
CURVES ADJUSTED FROM FLIGHT AT 30 000 FEET
(3) ALTITUDE, FT.
RATE OF CLIMB - FPM
TRUE AIRSPEED - KT

FIGURE NO. 35

FORWARD CLIMB PERFORMANCE

XV-5A CASA-No. 62-4505

FAN MODE

LANDING GEAR DOWN
CG LOCATION - $\bar{N}$ = 240 (FWD)
ANGLE OF ATTACK - α_f = DEG. 8

STAGGER ANGLE - β_s = DEG. 17
GROSS WEIGHT - W = LB = 10000
ALTITUDE - H_p = FT. = S.L.

HOT DAY CONDITIONS (CASE 2E)

CURVES DERIVED FROM FIGURES NO. 27 THROUGH 31, APPENDIX I.

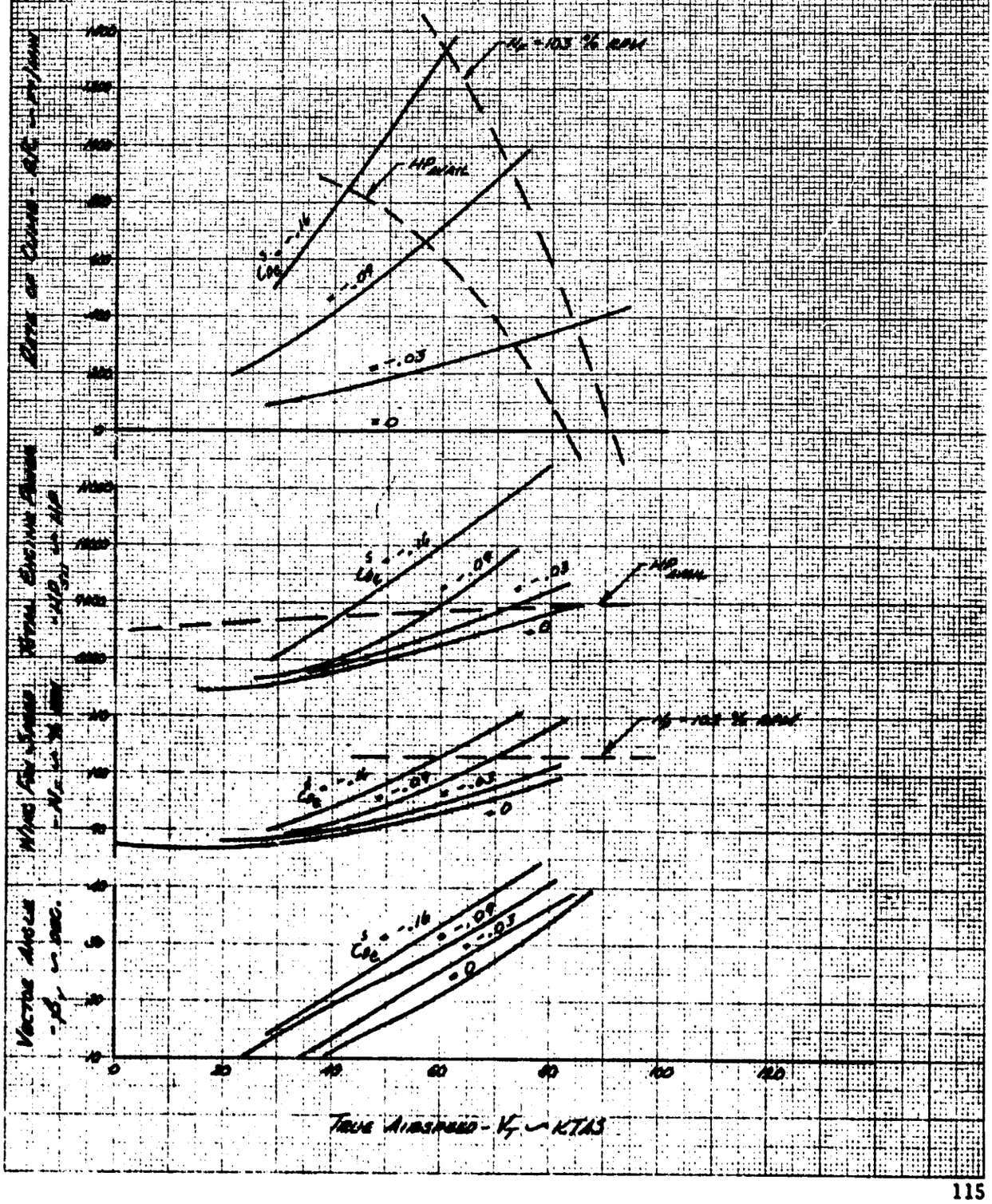

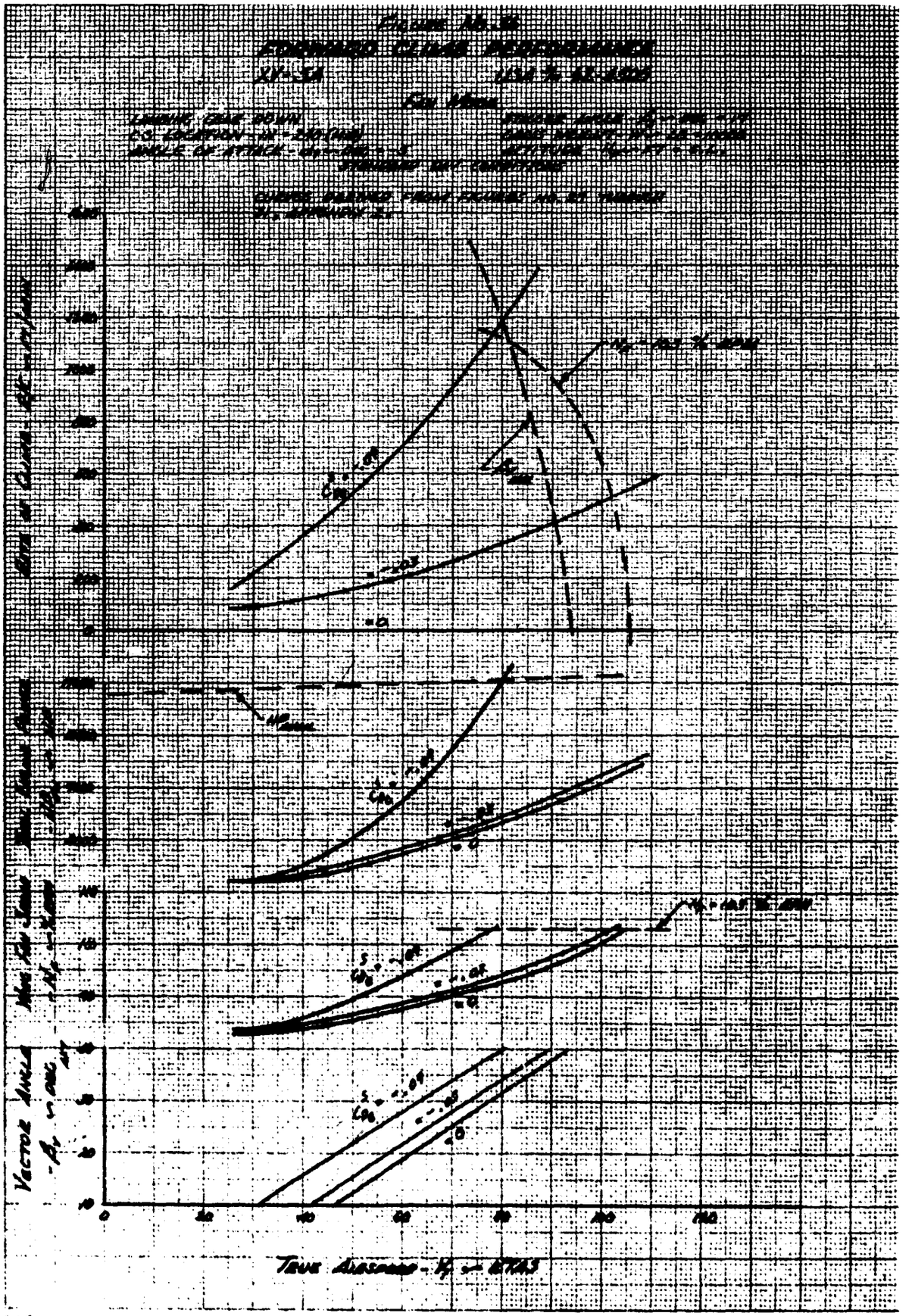

FIGURE No. 37

FORWARD CLIMB PERFORMANCE

XV-5A USA S/N 62-4505

FAN MODE

LANDING GEAR DOWN
CG LOCATION
ANGLE OF ATTACK - α ~ DEG = -3

STAGGER ANGLE - β_s ~ DEG = 17
GROSS WEIGHT - W ~ LB = 10000
ALTITUDE - Hp ~ FT = 2300

STANDARD DAY CONDITIONS

CURVES DERIVED FROM FIGURES NO. 27 THROUGH 34, APPENDIX I

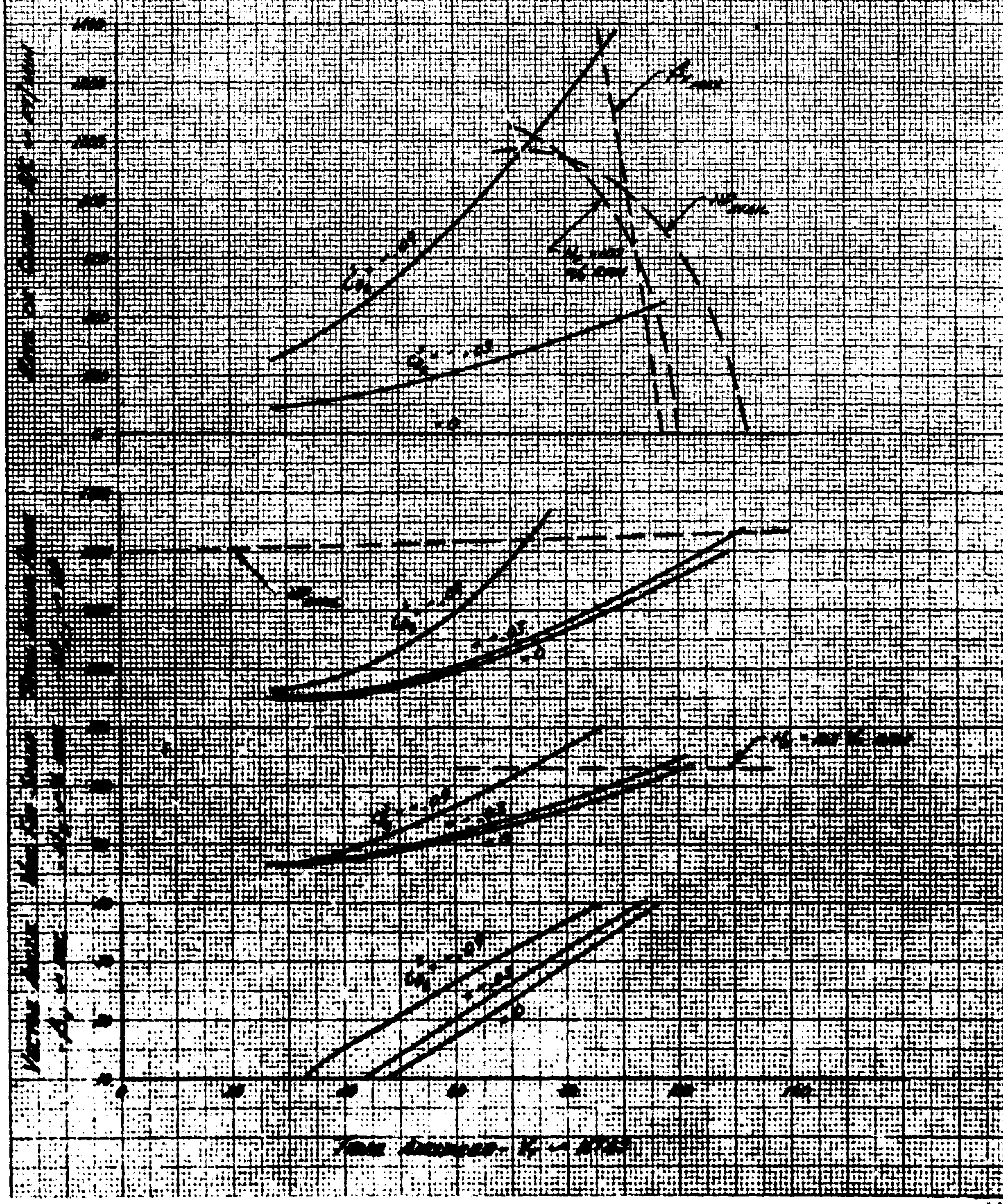

FIGURE No. 38

FORWARD CLIMB PERFORMANCE

XV-5A

USA No. 62-4503

Fan Mode

LANDING GEAR DOWN
CG LOCATION - N_{CG} = 240 (AVG)
ANGLE OF ATTACK - α_f or α_{DES} = -5
STAGGER ANGLE - β_S = -- AVG = 17
GROSS WEIGHT - W = -- LB = 14000
ALTITUDE - H_p = -- FT = 3000
STANDARD DAY CONDITIONS

CURVES RECEIVED FROM FIGURES NO. 27 THROUGH 31, APPENDIX II.

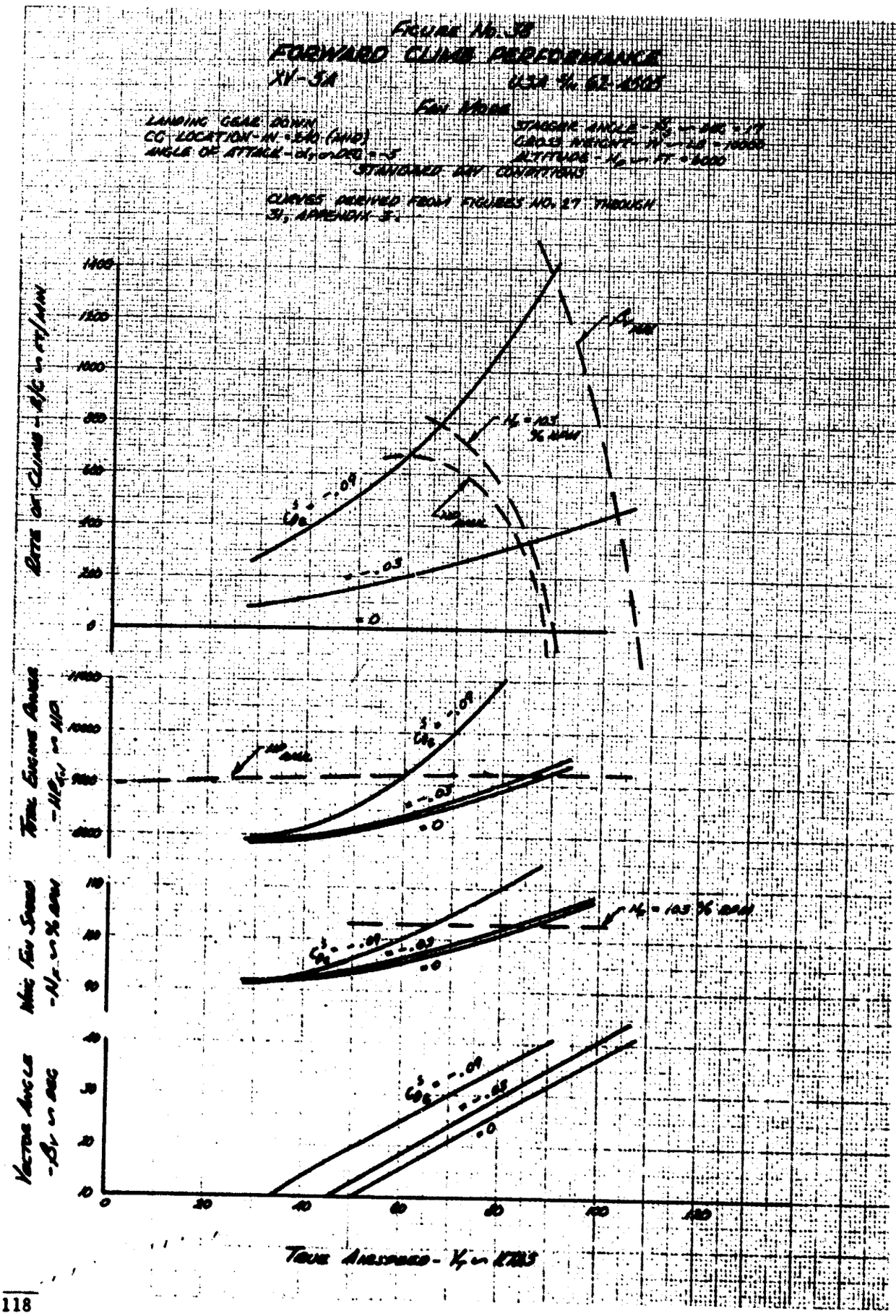

FIGURE No. 30

FORWARD CLIMB PERFORMANCE

XV-5A

CLSA % 62-4505

FLY NOOSE

LANDING GEAR DOWN
CG LOCATION - i_W = 240 (MAC)
ANGLE OF ATTACK - α_T = MED = -5
HOT DAY CONDITIONS (ARIA 1ST)

STAGGER ANGLE - i_T = DEC = 17
GROSS WEIGHT - W = LB = 14000
ALTITUDE - H_p = FT = S.L.

CURVES DERIVED FROM FIGURES NO. 27 THROUGH 31, APPENDIX I.

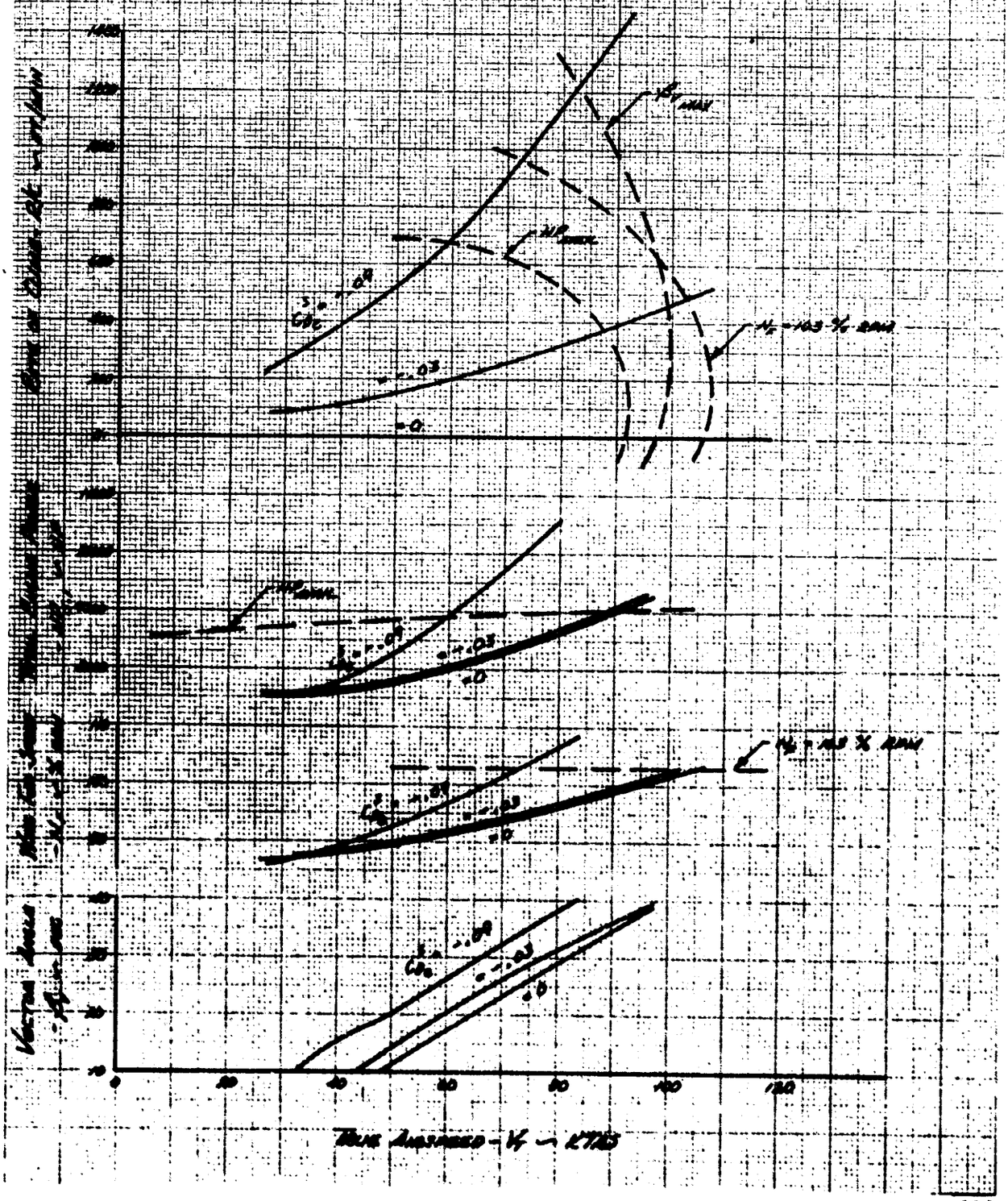

FIGURE No. 40

FORWARD CLIMB PERFORMANCE

XV-5A USA S/N 62-4505

FAN MODE

LANDING GEAR DOWN
C.G. LOCATION - IN = 240 (MID)
ANGLE OF ATTACK - α_T - DEG = -5
HOT DAY CONDITIONS (ANA 421)

STAGGER ANGLE - β_s - DEG = 17
GROSS WEIGHT - W - LB = 10000
ALTITUDE - H_D - FT = 2500

CURVES DERIVED FROM FIGURES NO. 27 THROUGH 31, APPENDIX I.

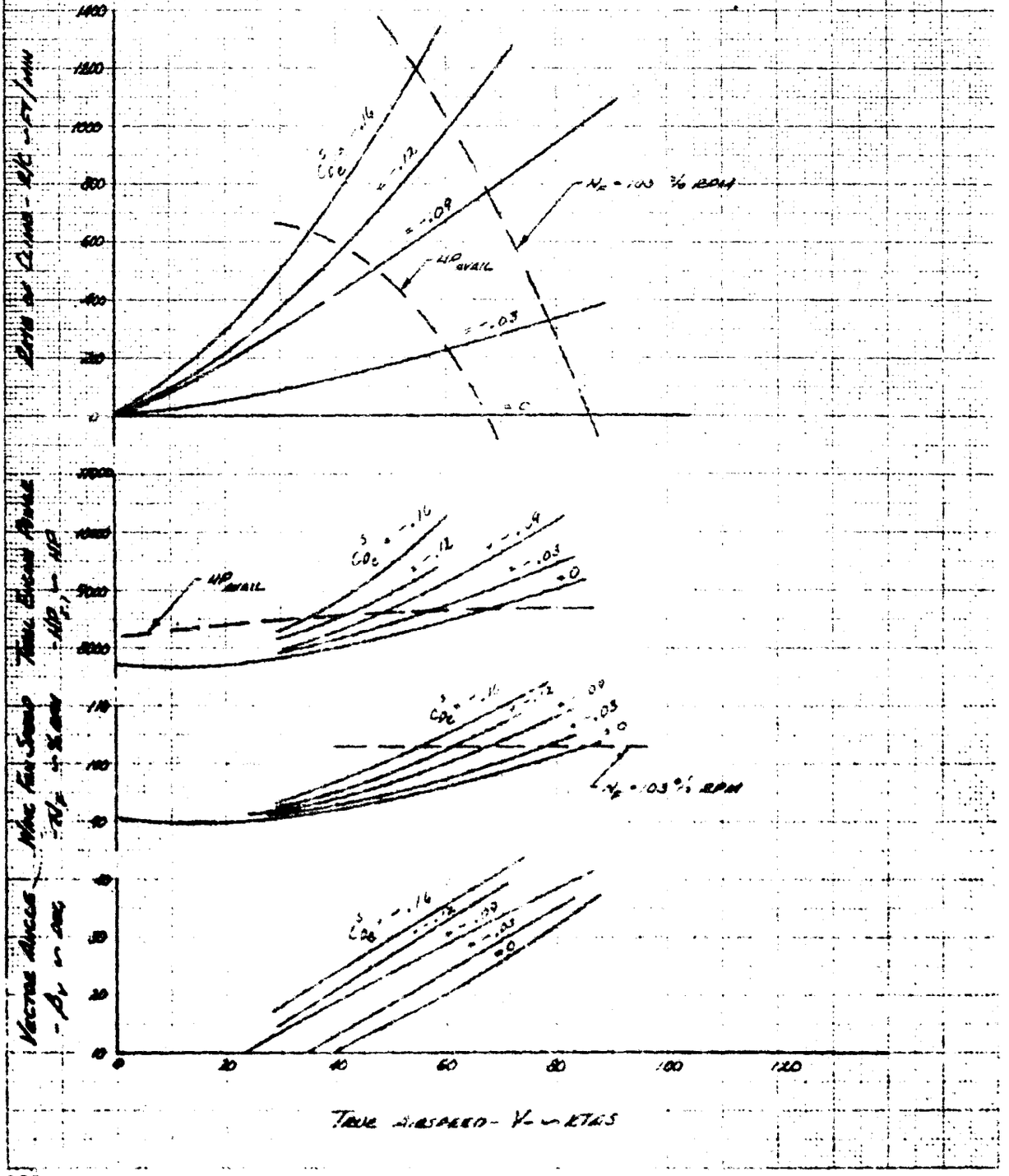

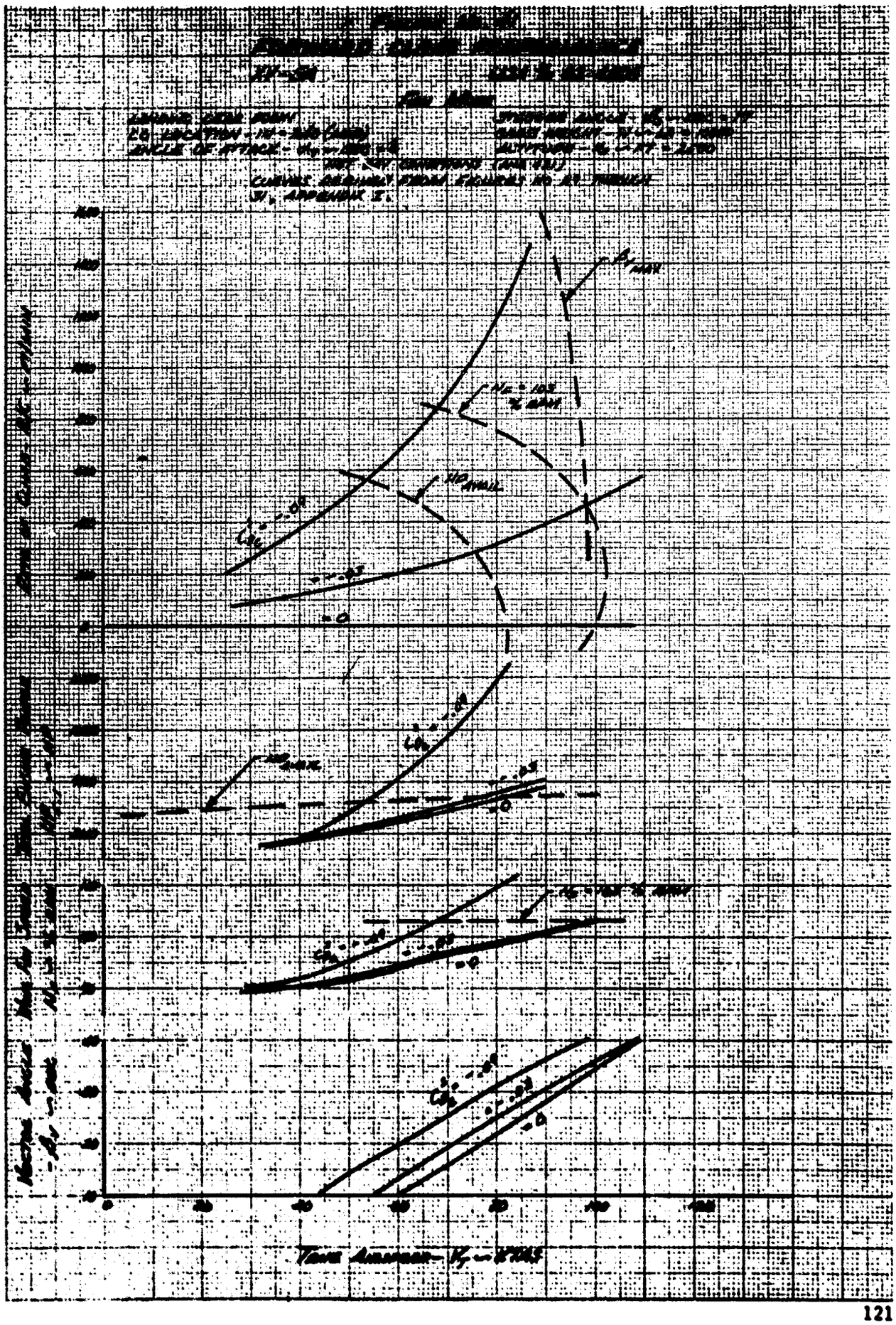

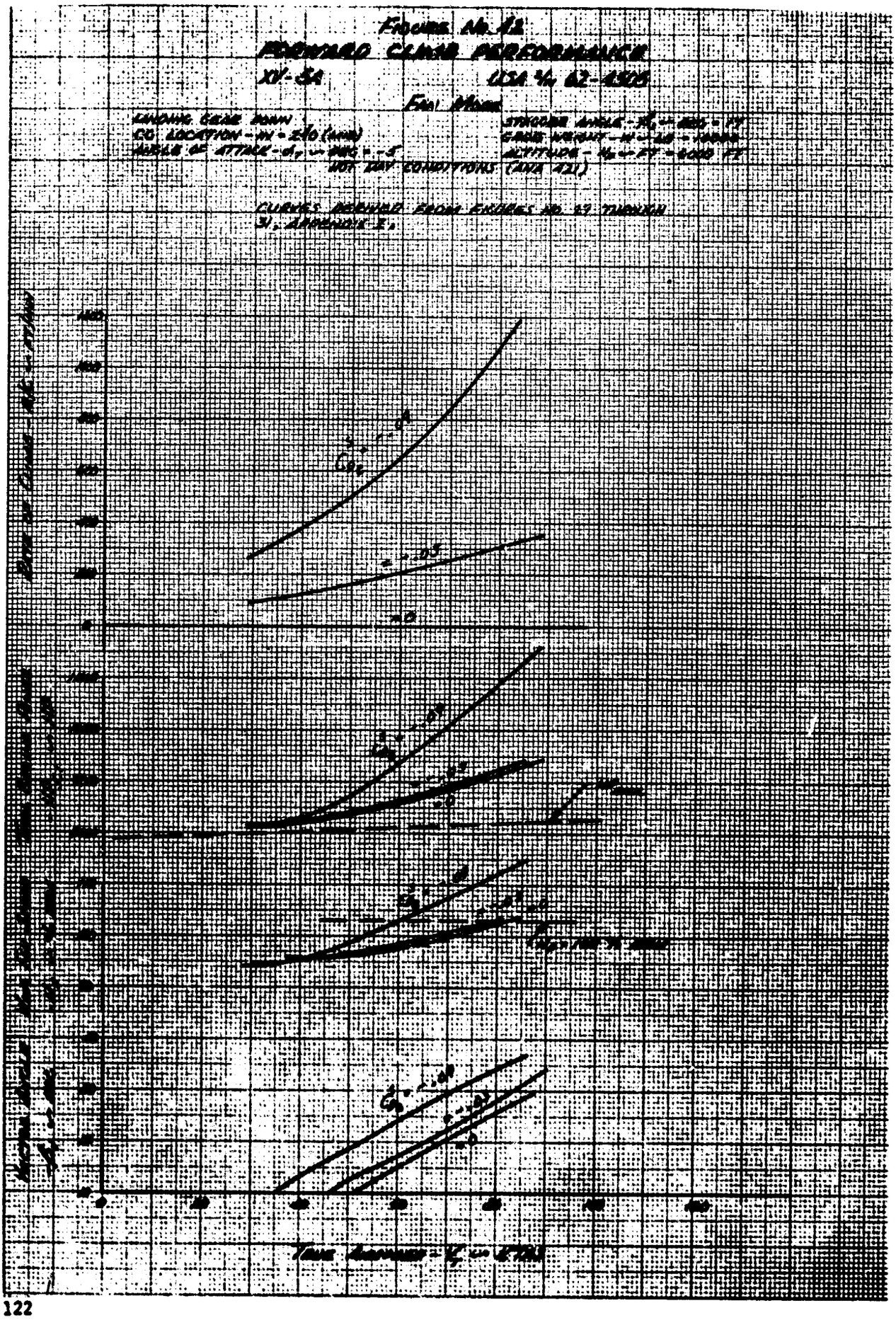
FIGURE NO. 42
FORWARD CLIMB PERFORMANCE
XV-3A
USA 4/4 62-4205
LANDING GEAR DOWN
CG LOCATION - WW - Z/0 (MAC)
ANGLE OF ATTACK - α_T = DEG = -5
HOT DAY CONDITIONS (CAA A21)
CURVES DERIVED FROM FIGURES NO. 39 THROUGH 41, APPENDIX II.

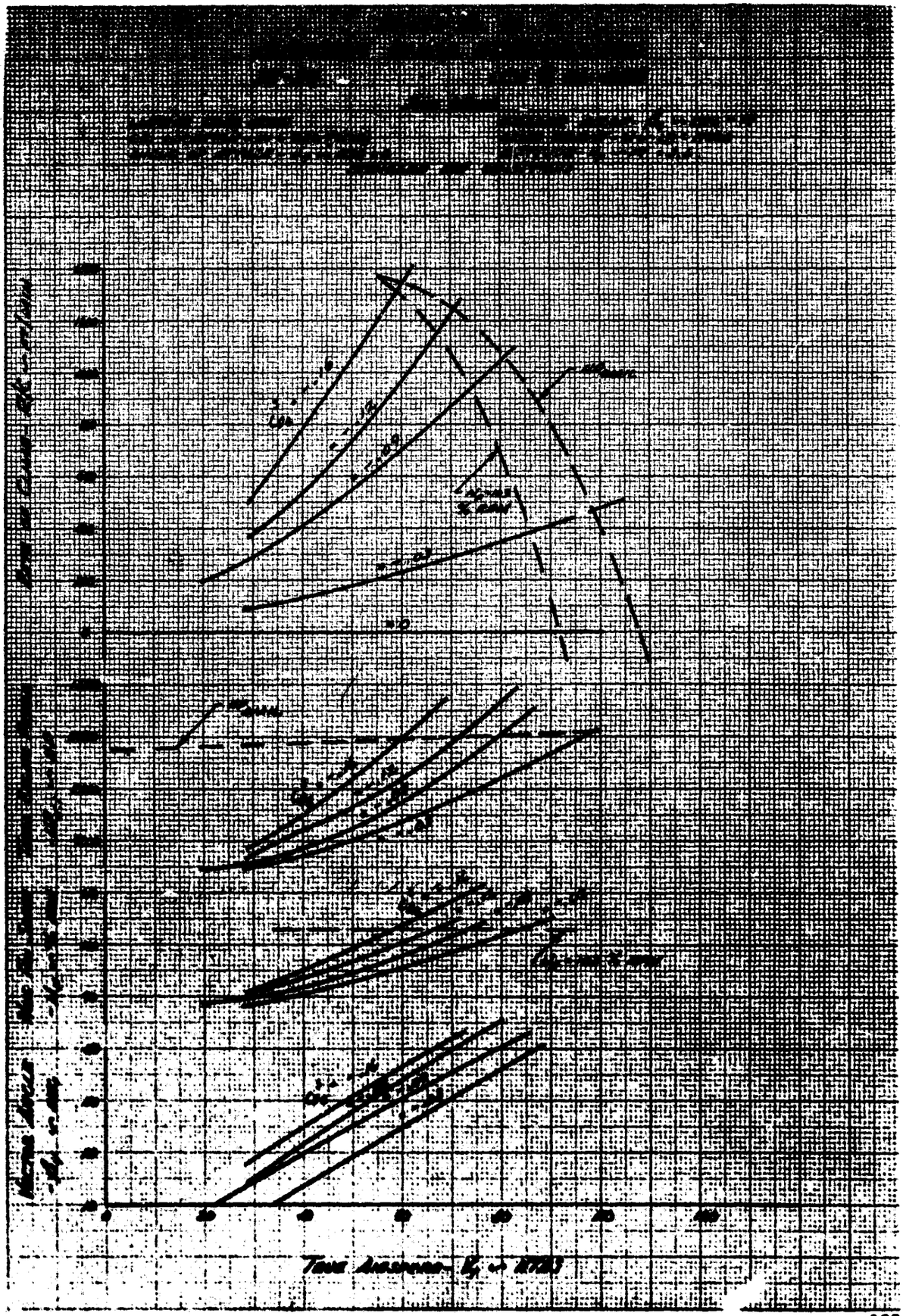

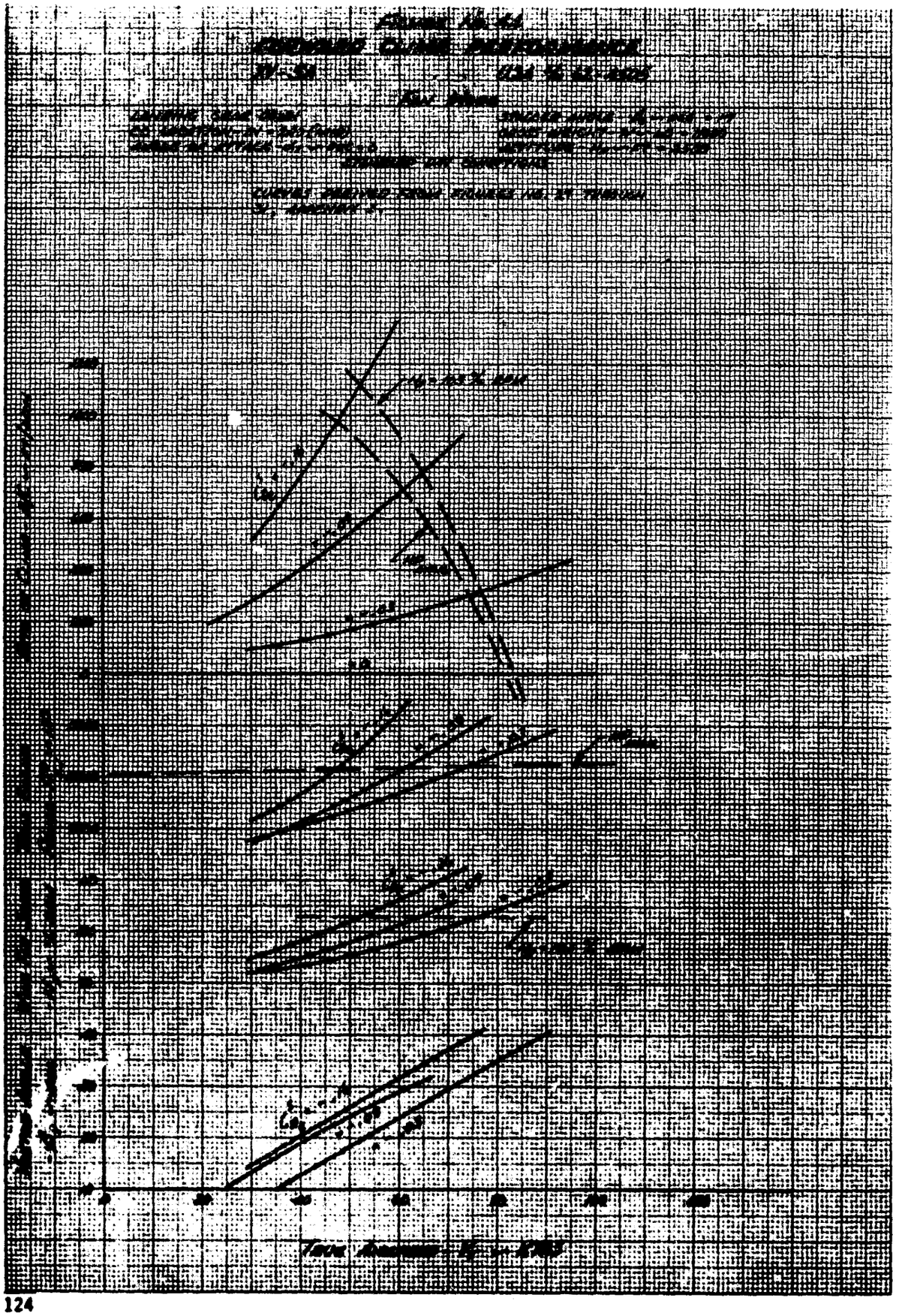

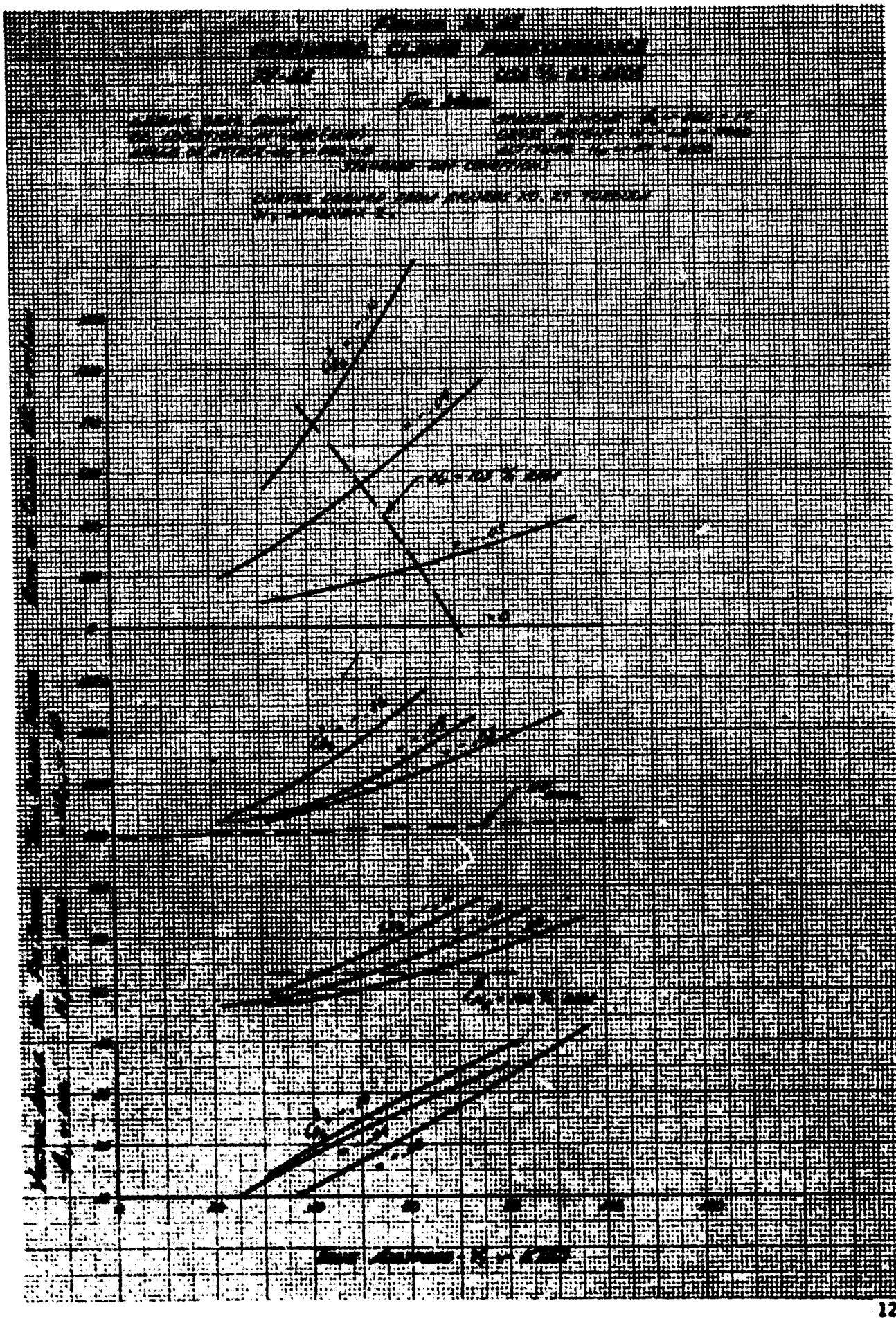

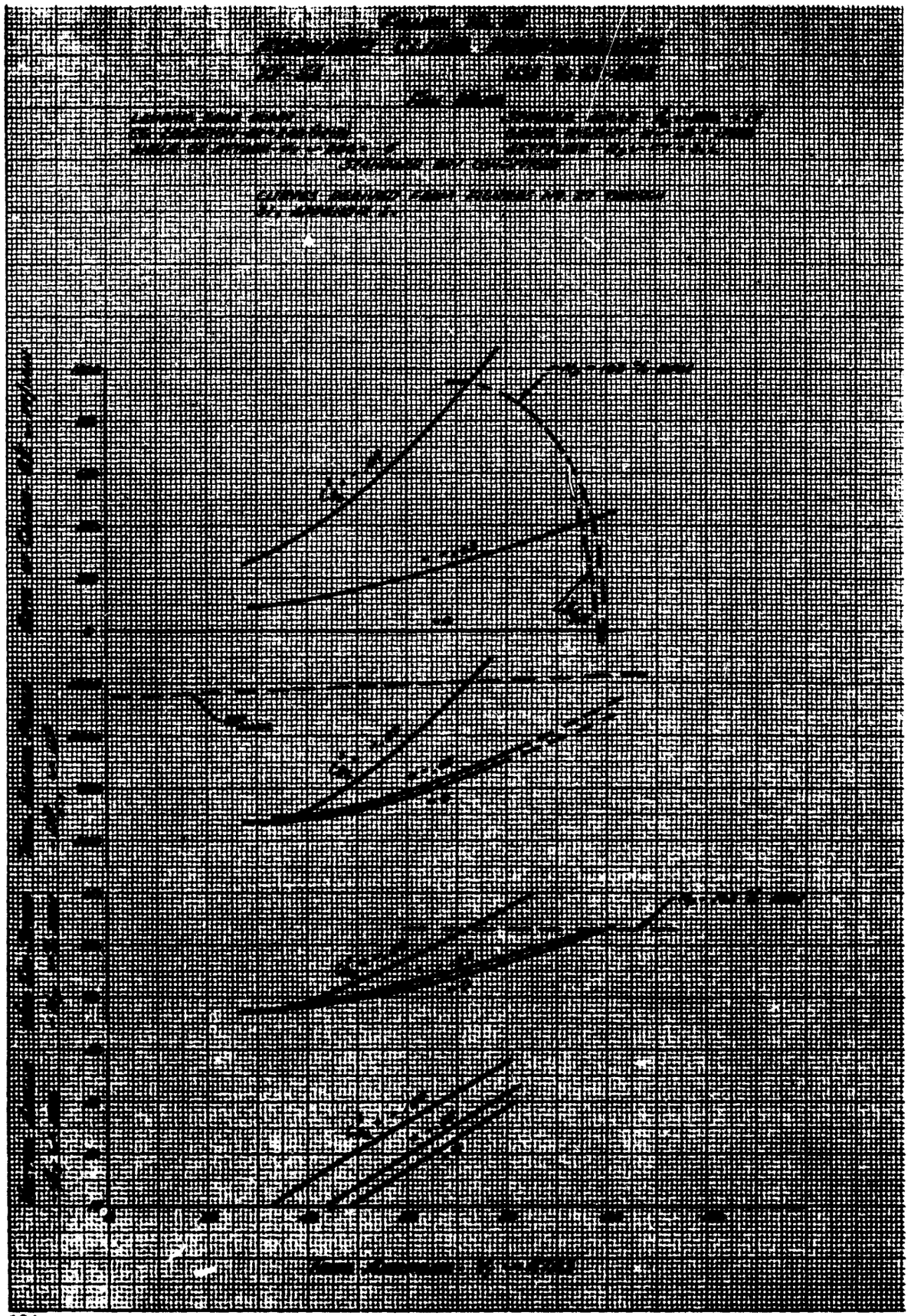

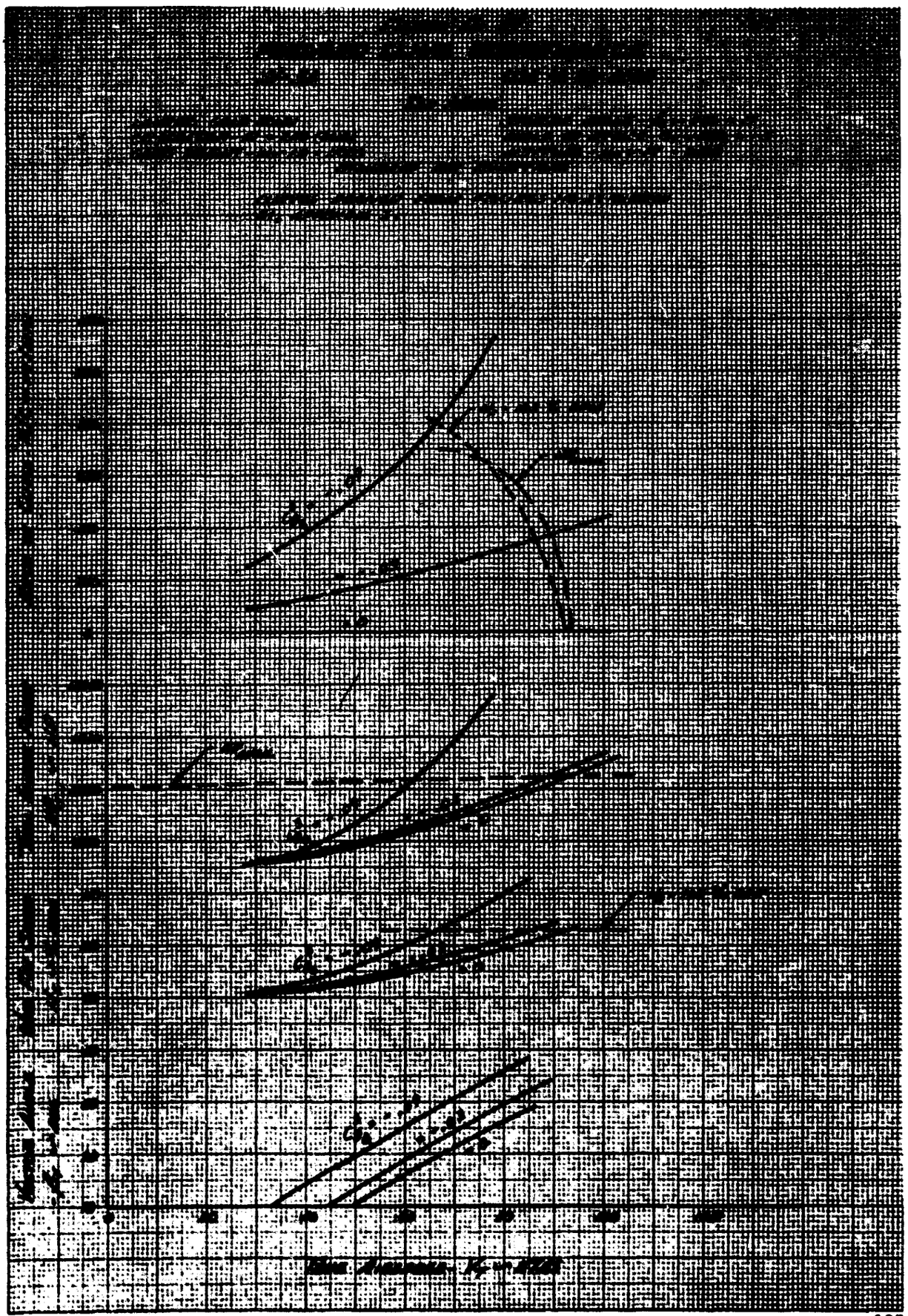

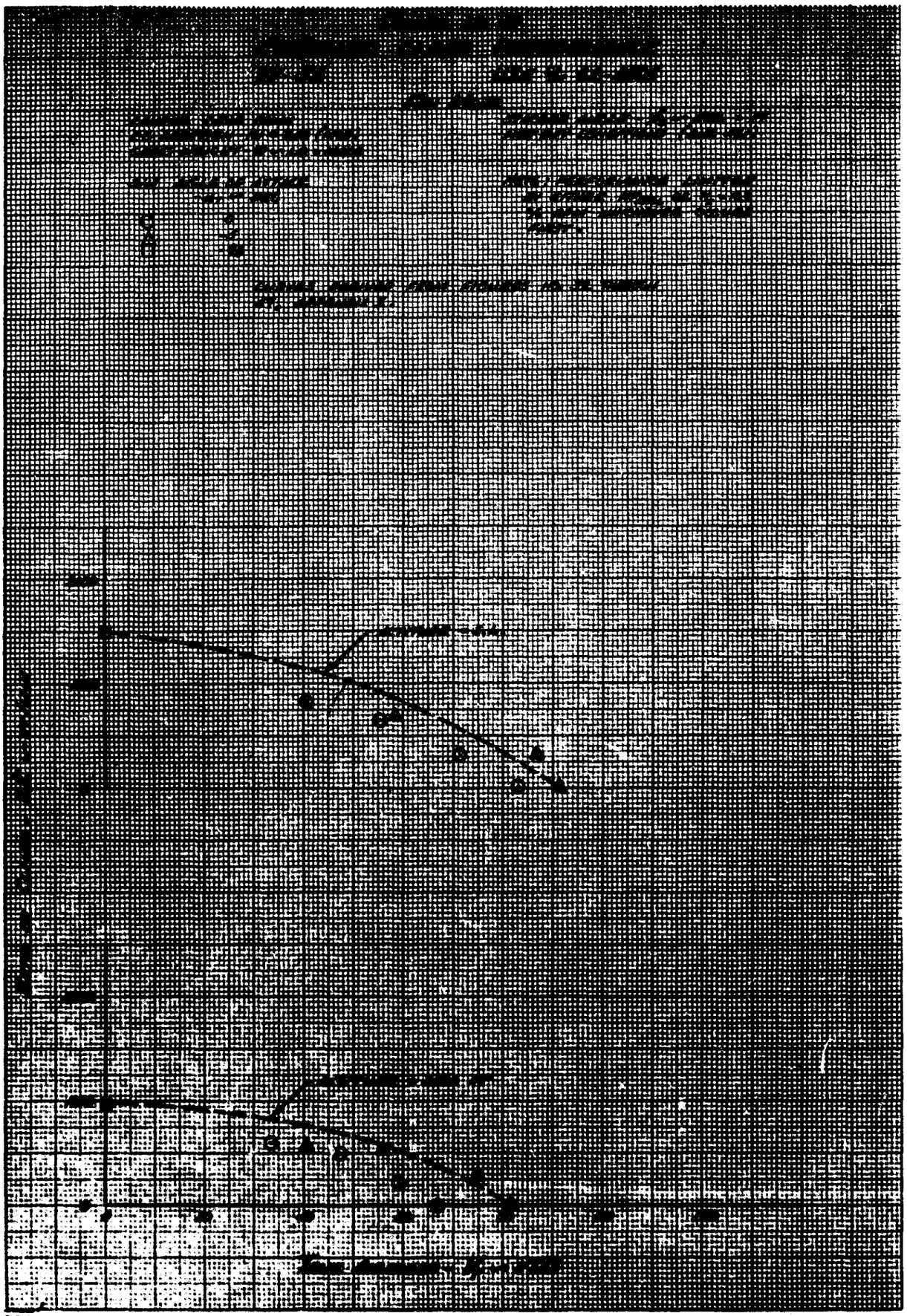

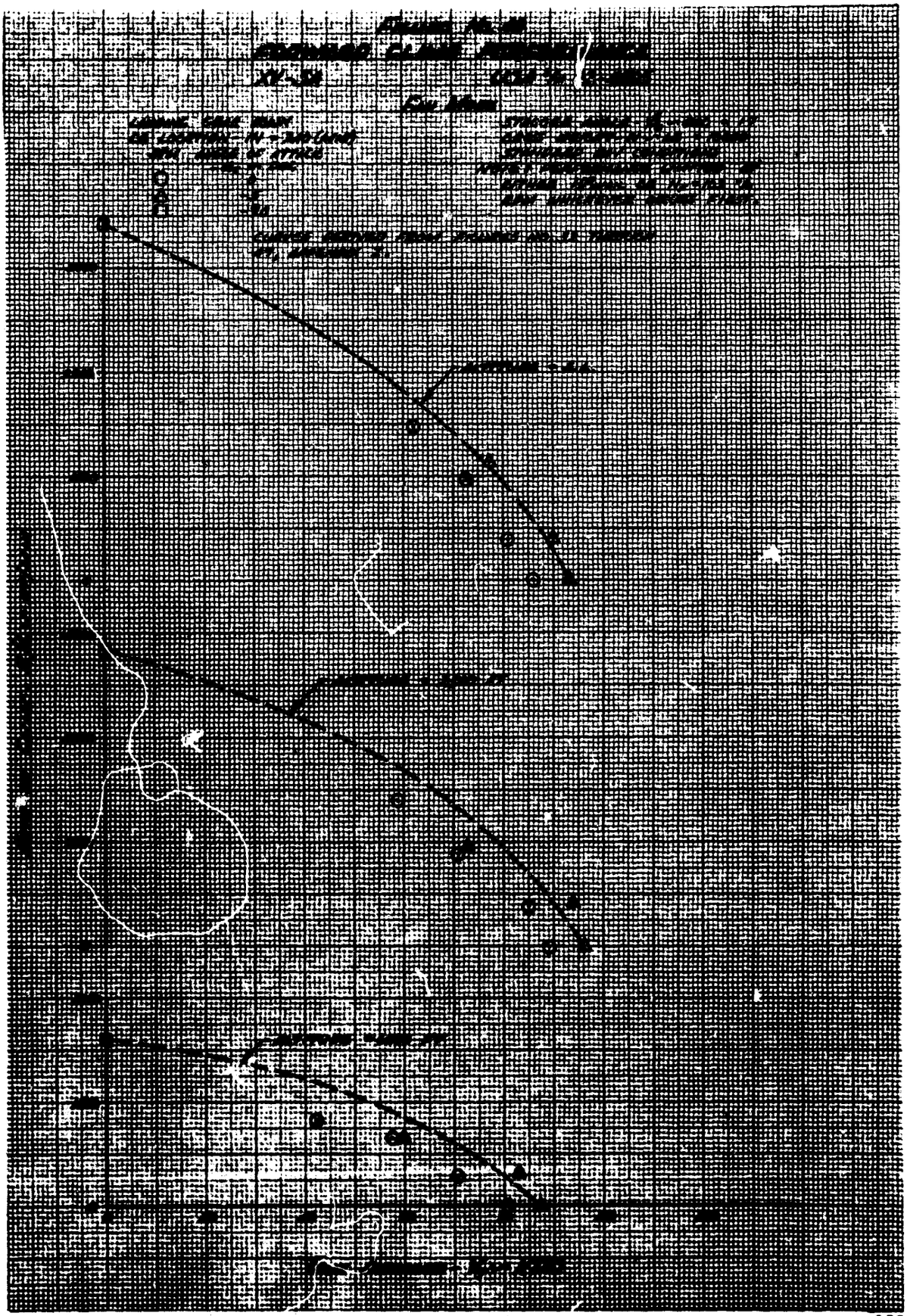

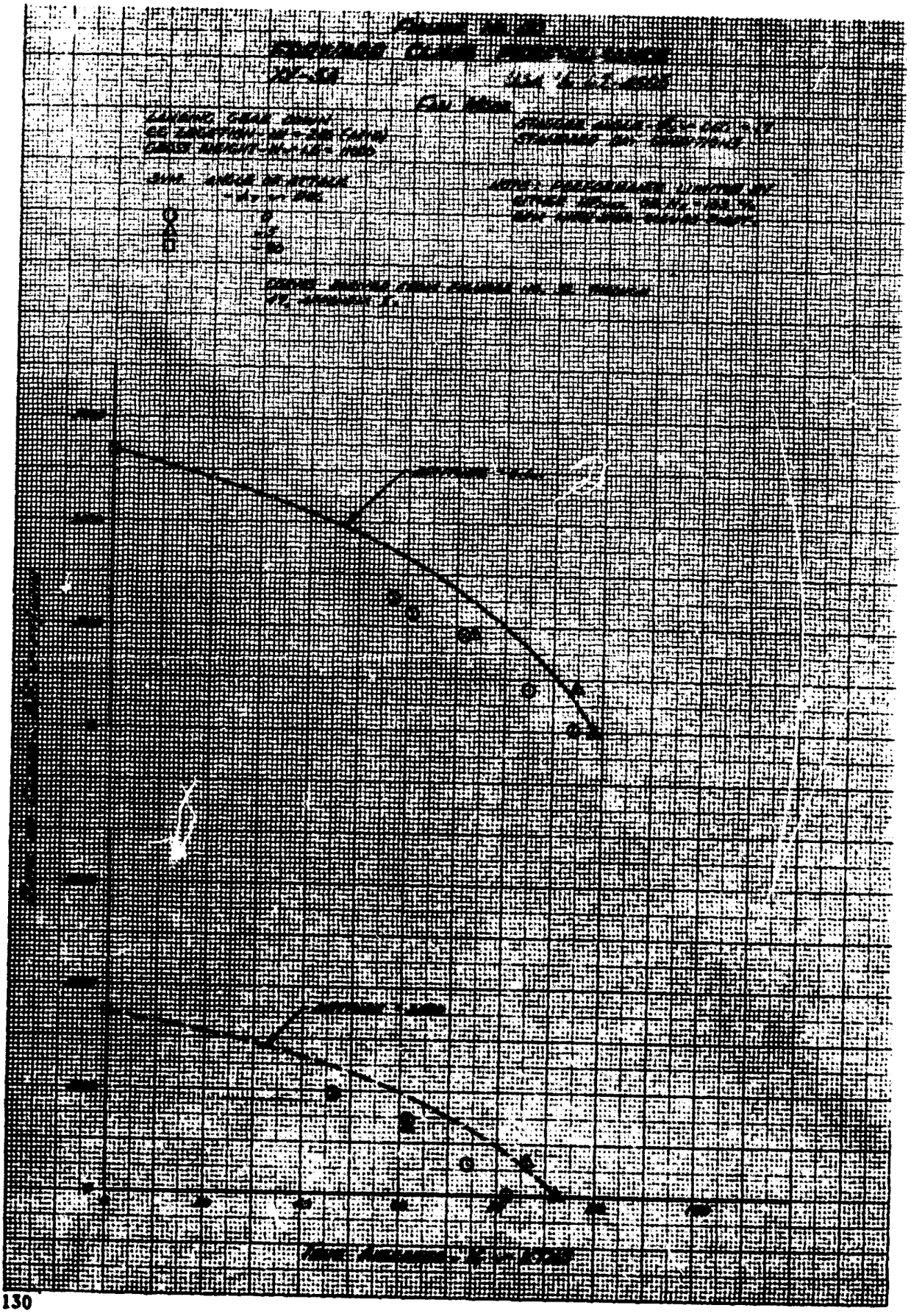

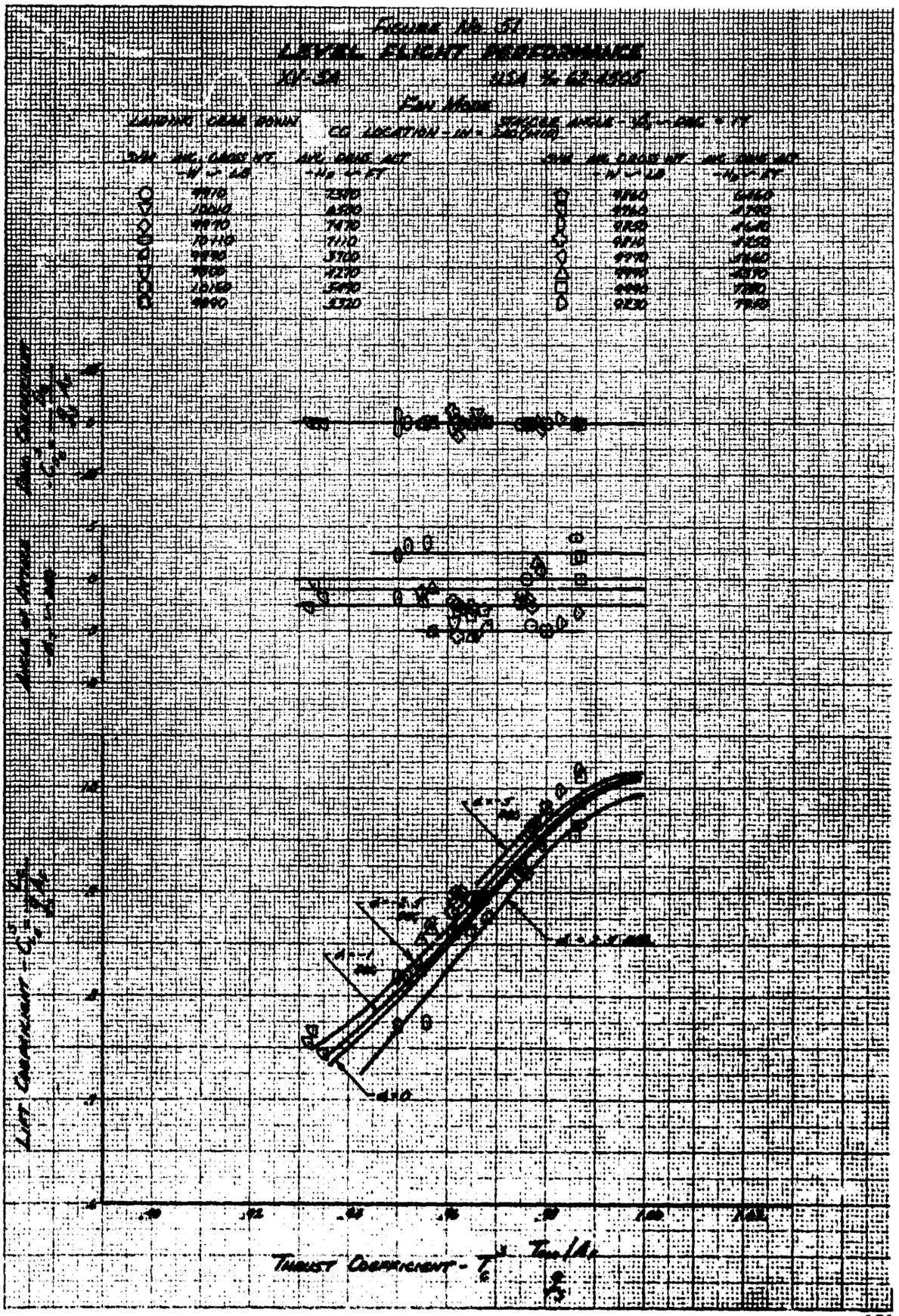
FIGURE No. 51
LEVEL FLIGHT PERFORMANCE
XF-92
Lift Coefficient - $C_L = \frac{L}{q_0 S}$
Thrust Coefficient - $T_C = \frac{T_{req'd}}{q_0 S}$

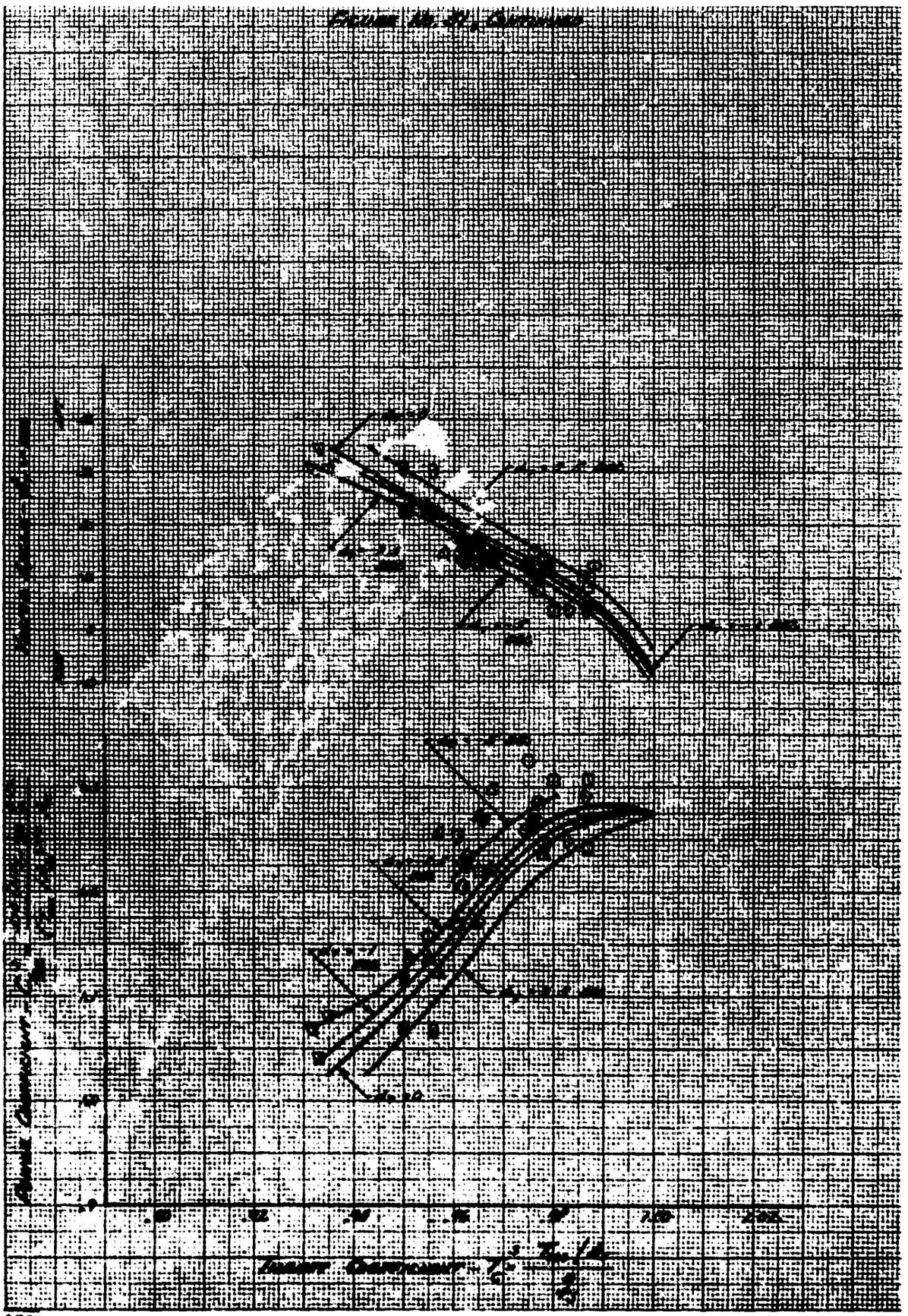

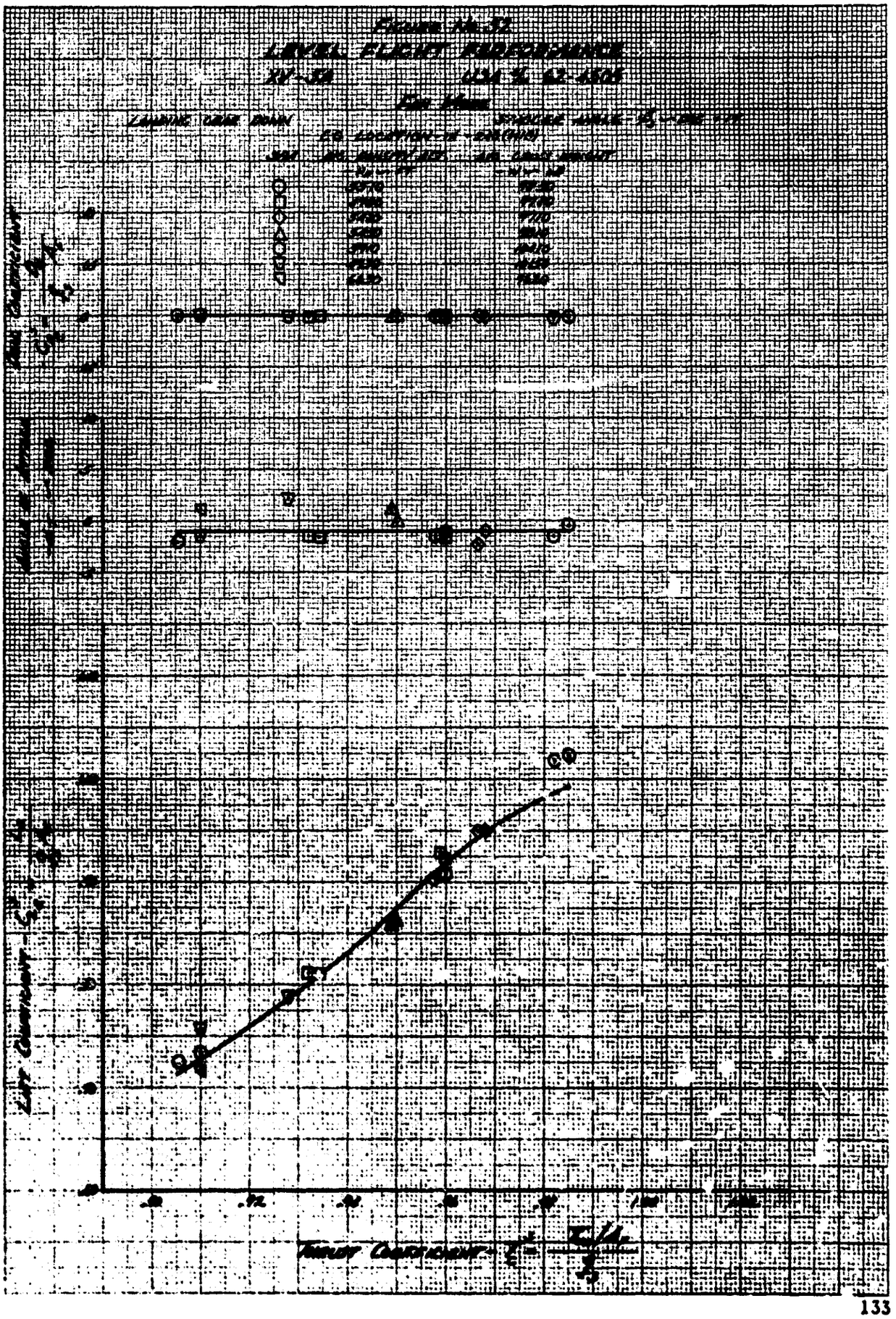

133

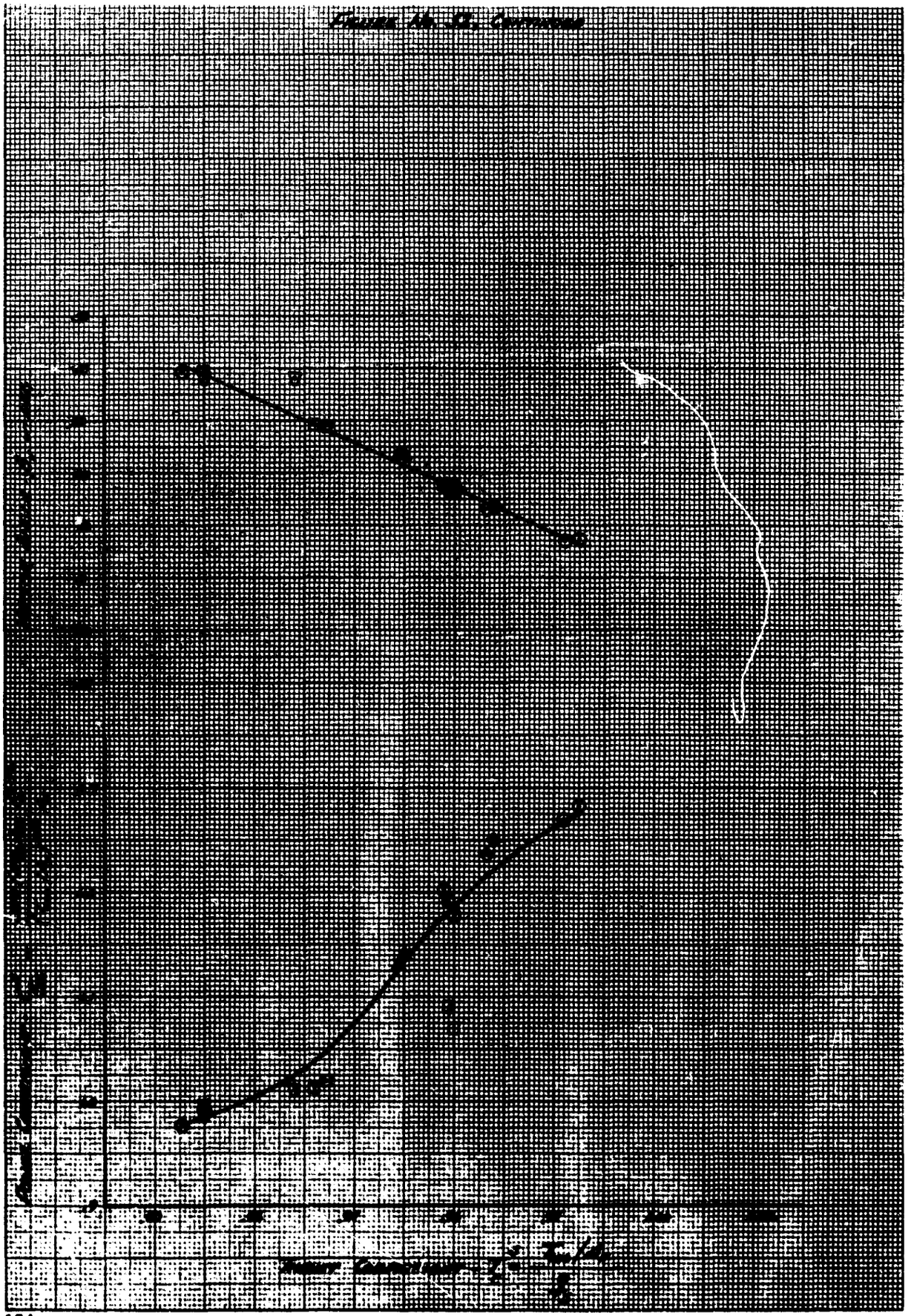

135

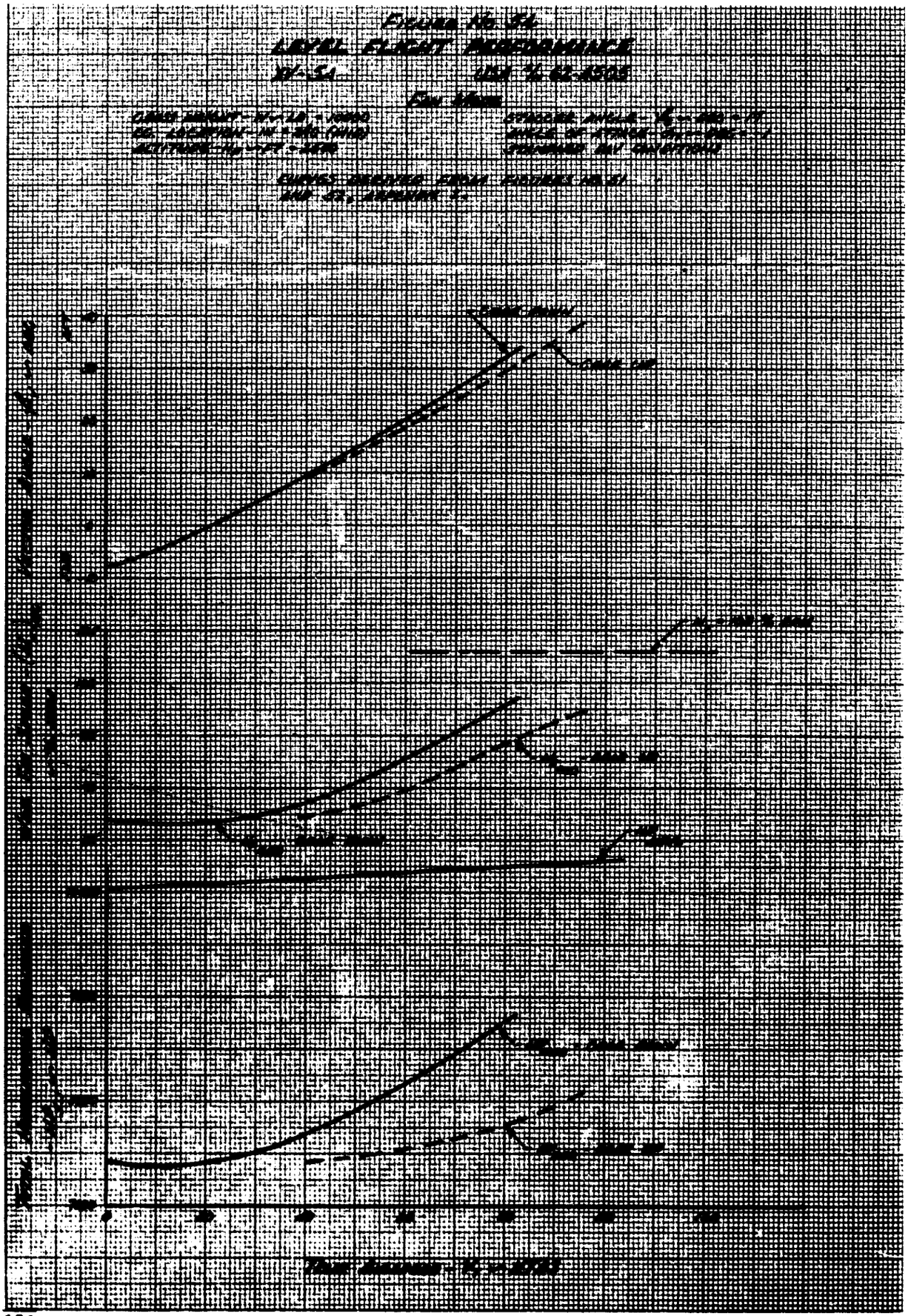

136

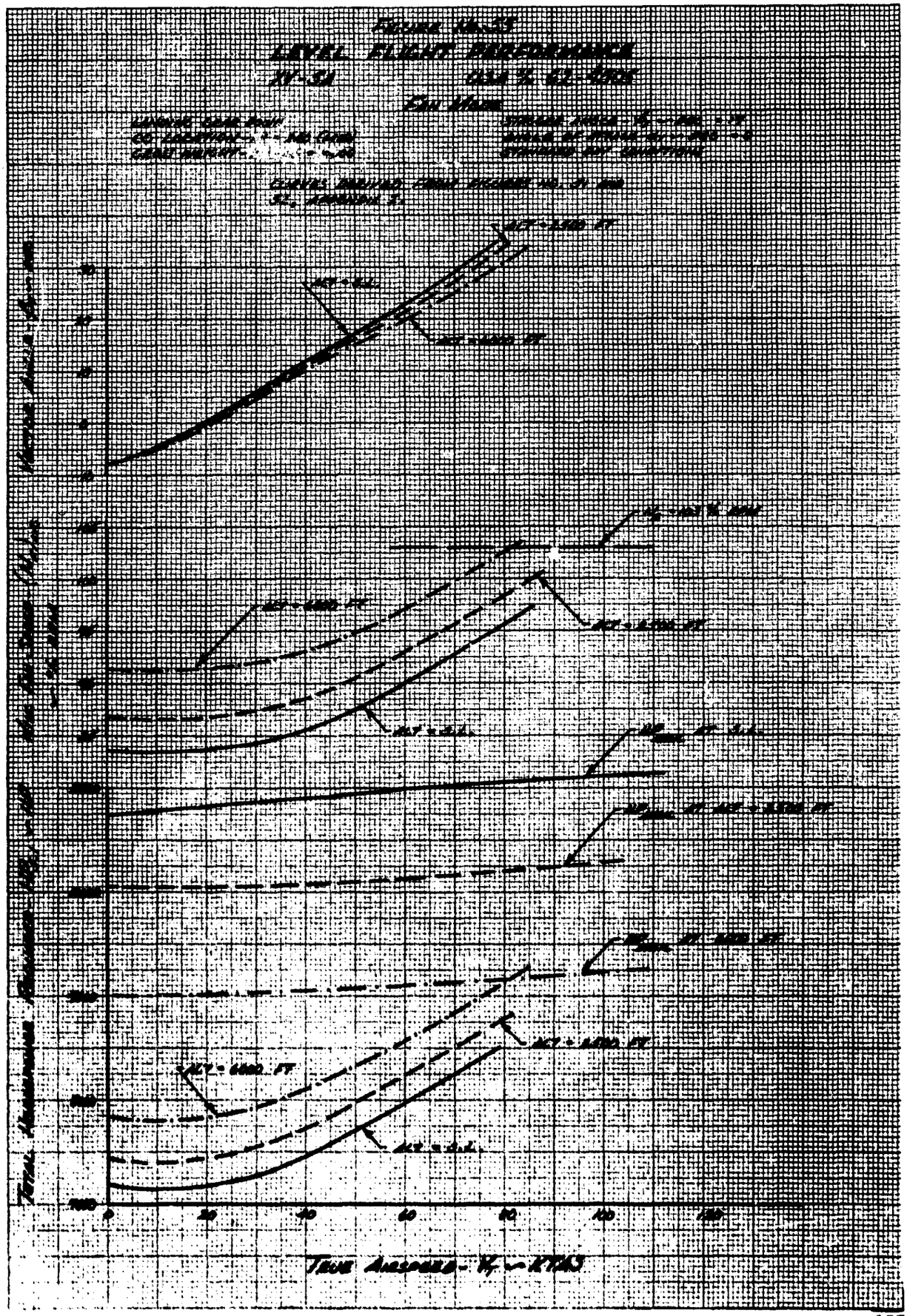
LEVEL FLIGHT PERFORMANCE
ALT = SEA LEVEL
ALT = 5000 FT
ALT = 10,000 FT
ALT = 15,000 FT
ALT = 20,000 FT
ALT = 25,000 FT
TRUE AIRSPEED - KNOTS

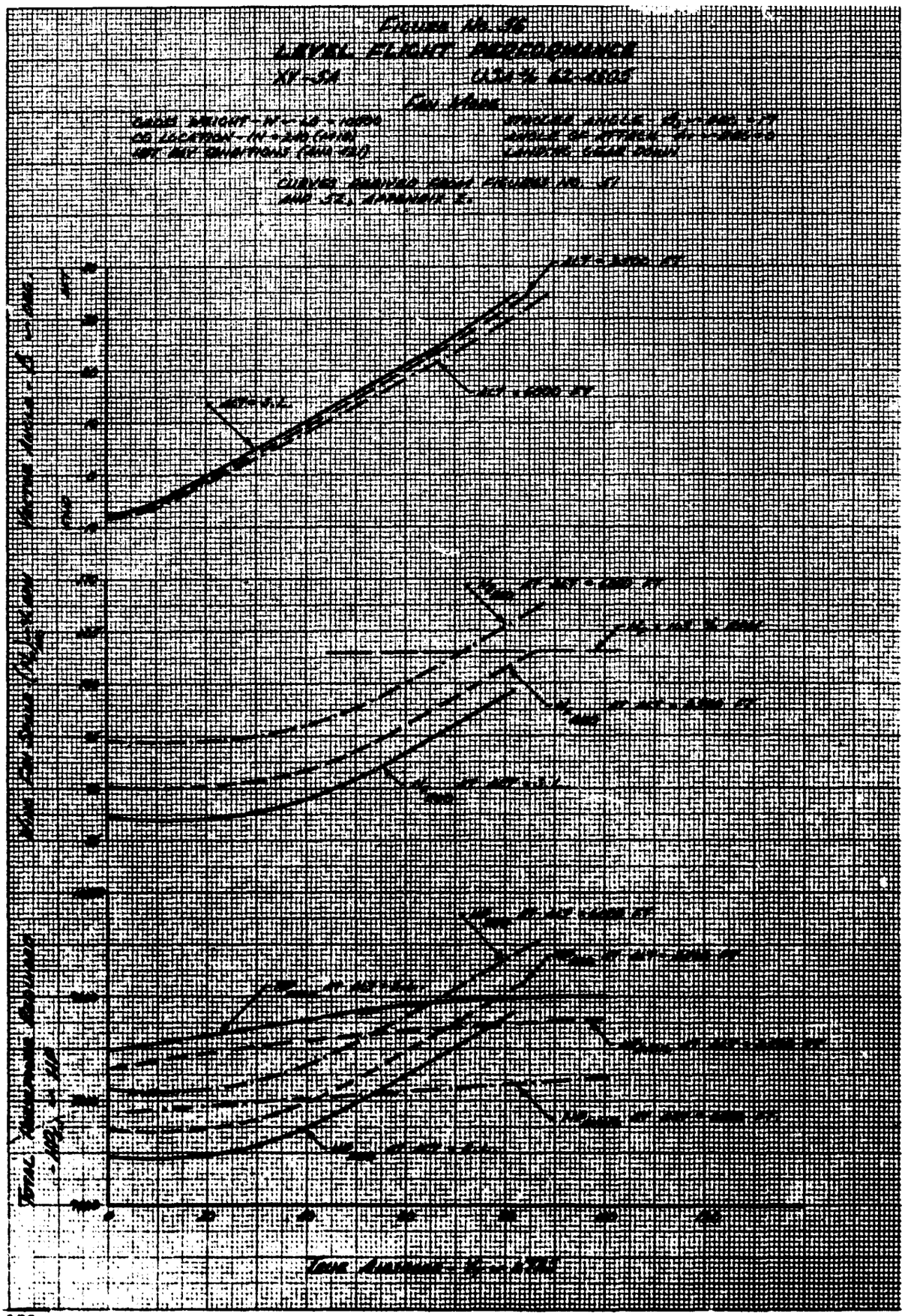

138

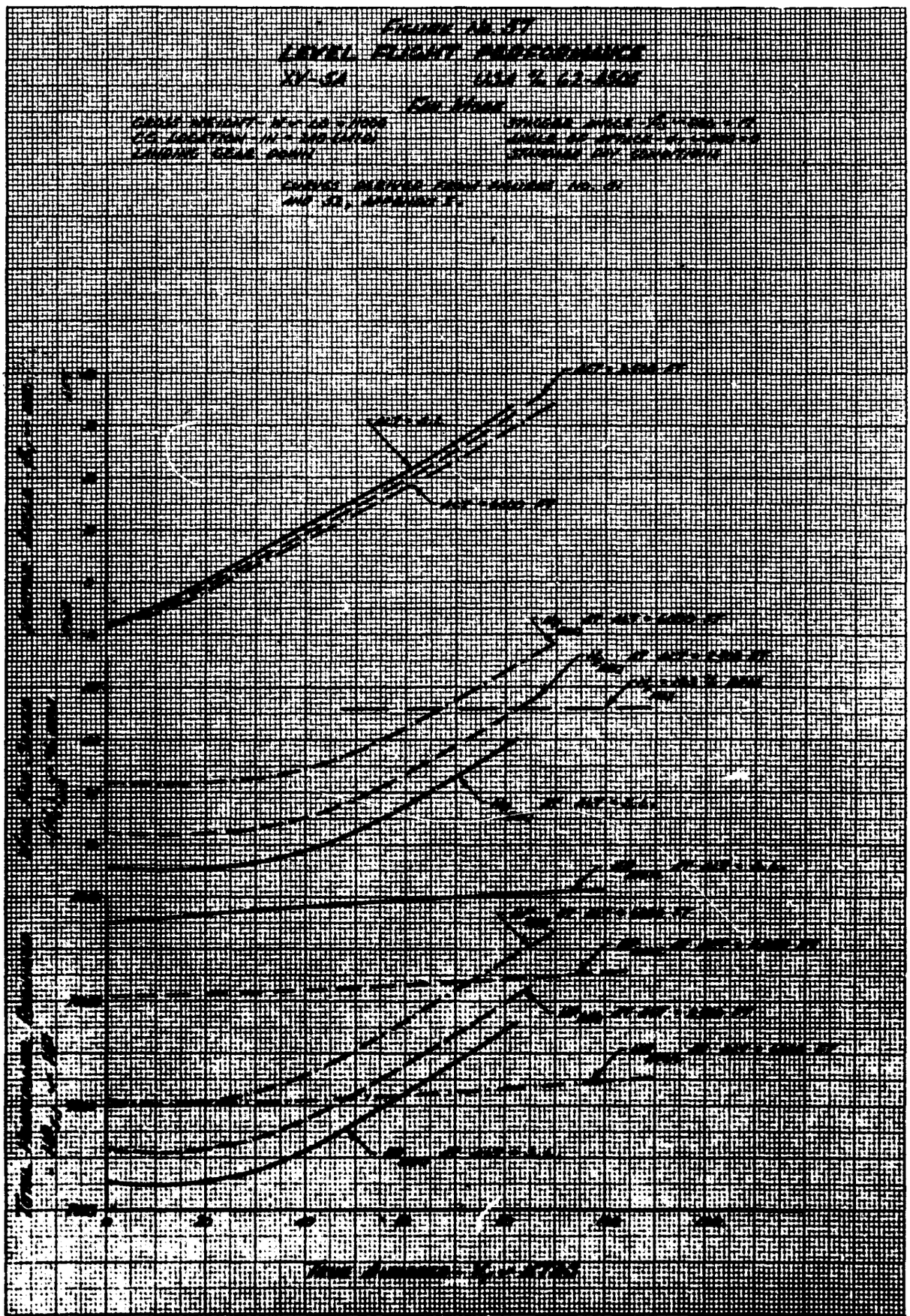

FIGURE 10.37
LEVEL FLIGHT PERFORMANCE
XV-5A USAF S/N 62-4505

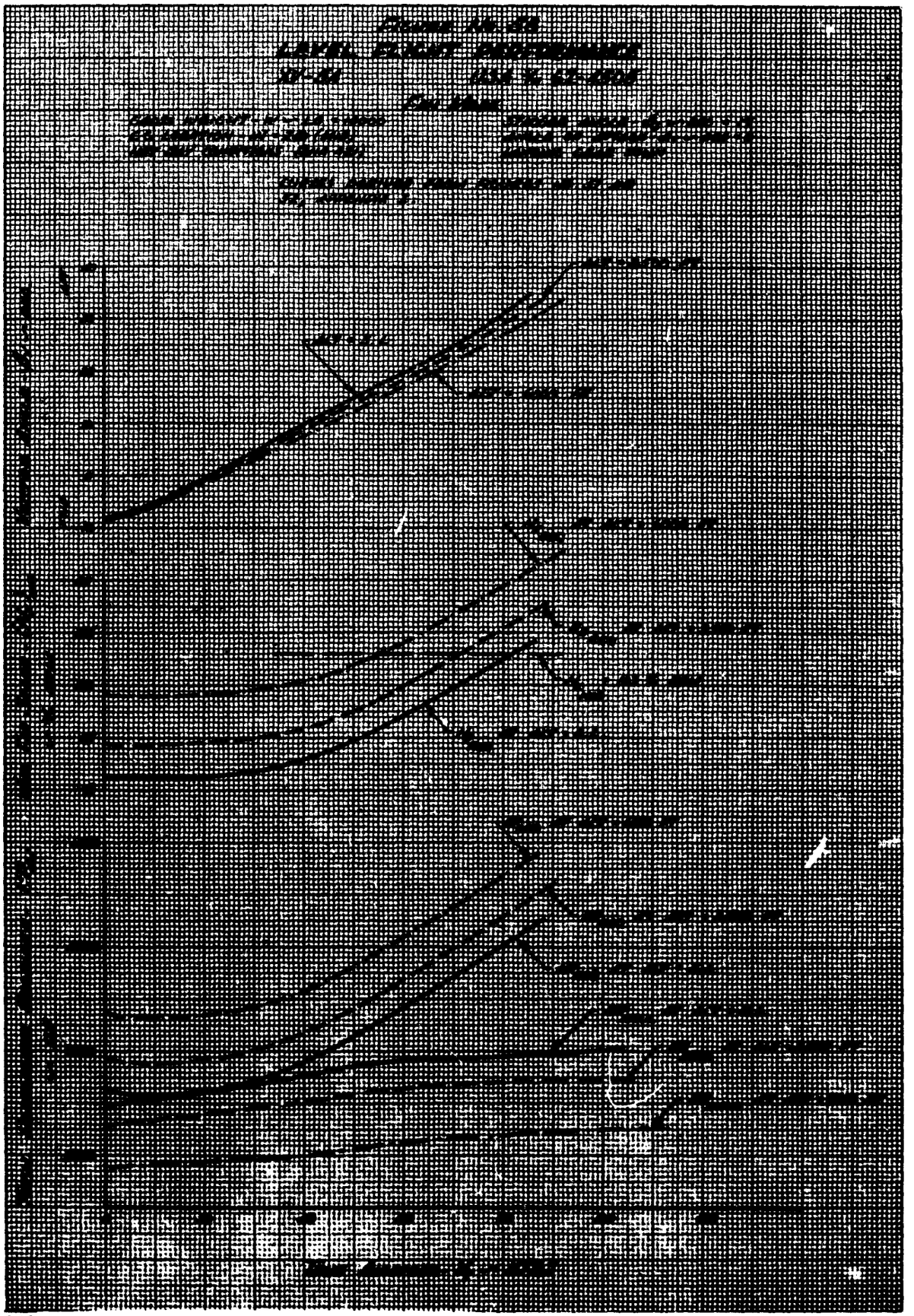

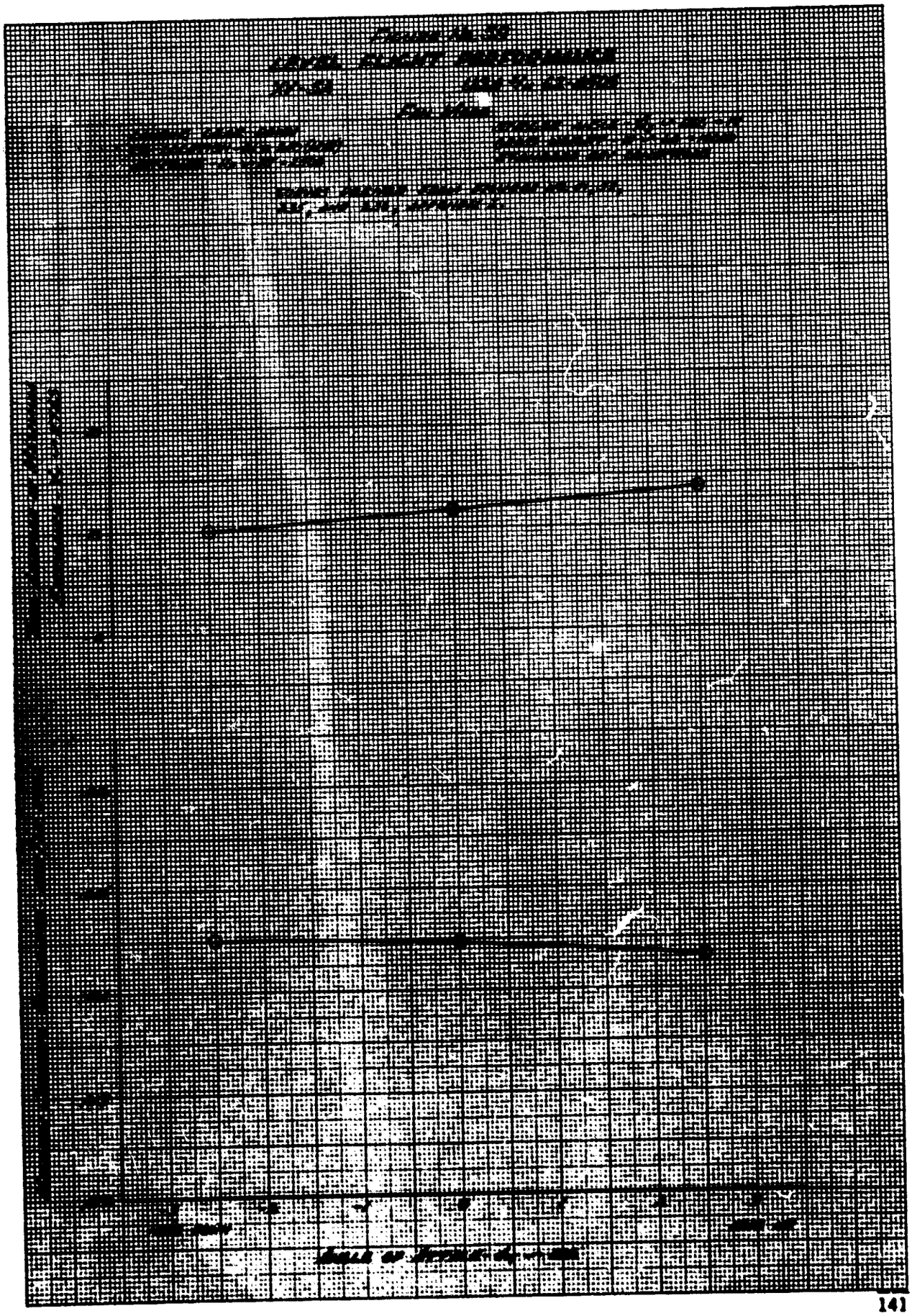

FIGURE No. 60

LEVEL FLIGHT PERFORMANCE

XF-5A USAF No. 62-4205

Sea Level

LANDING GEAR DOWN
CG LOCATIONS - W = 210,000
STANDARD DAY CONDITIONS

STAGGER ANGLE - i_B = 2.0° W.R.T. i_T
ANGLE OF ATTACK - α_T = 2.0° - 0

CURVES SHOWING CRUISE SETTINGS AT 85%, 75%, 65%, 55%, 50% AND 35%, MAXIMUM R.P.M.

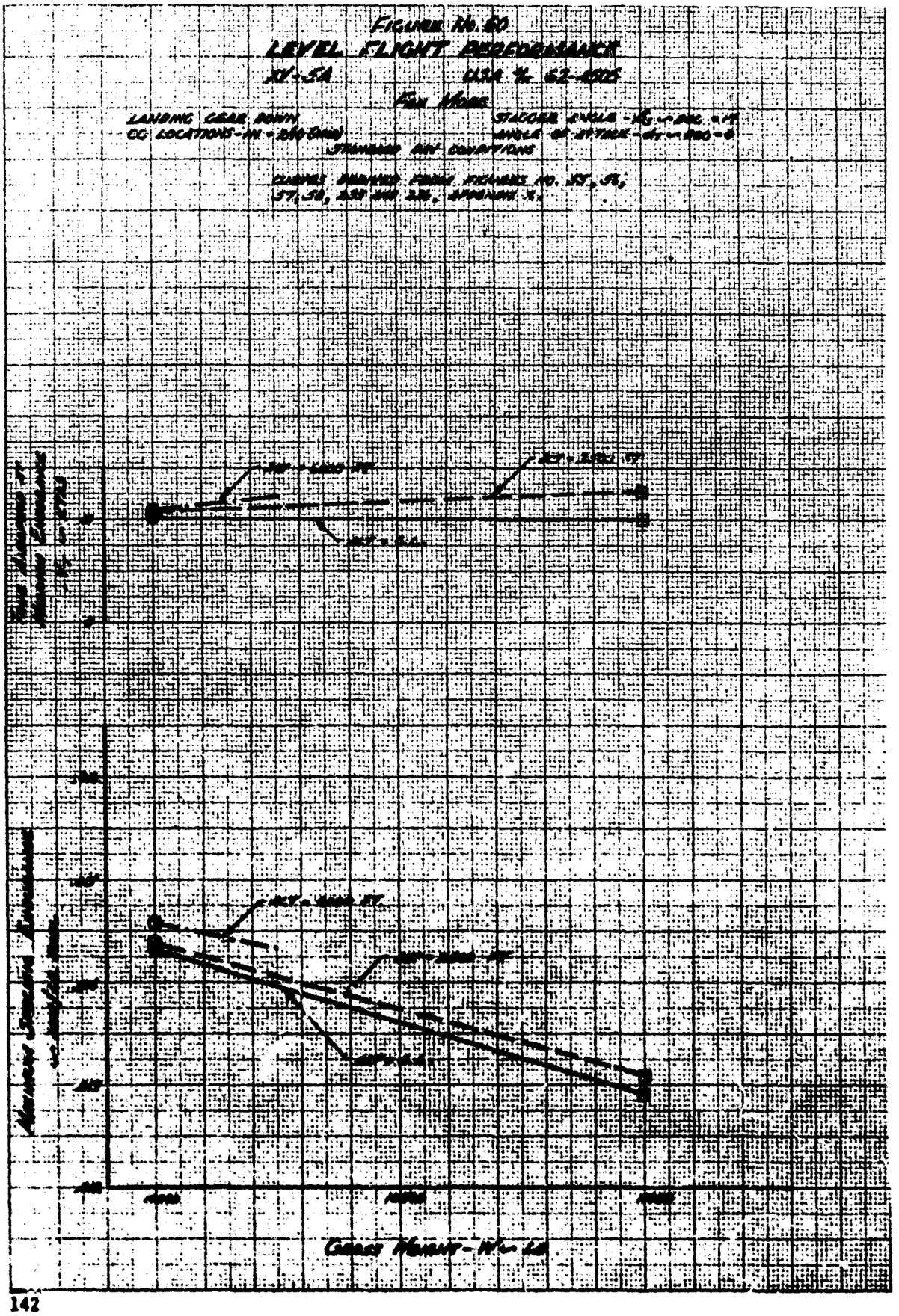

FIGURE 16.61

LEVEL FLIGHT PERFORMANCE

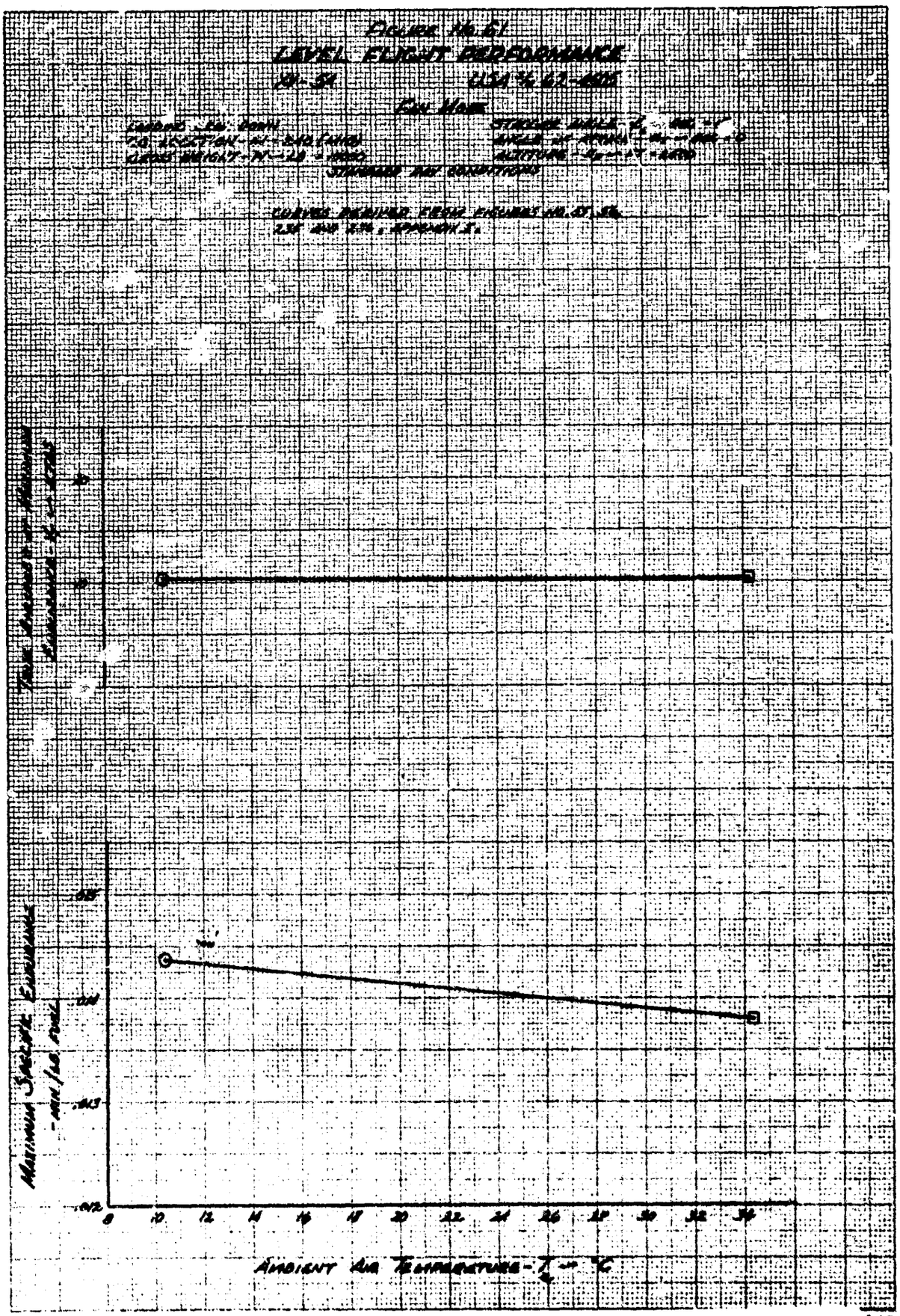

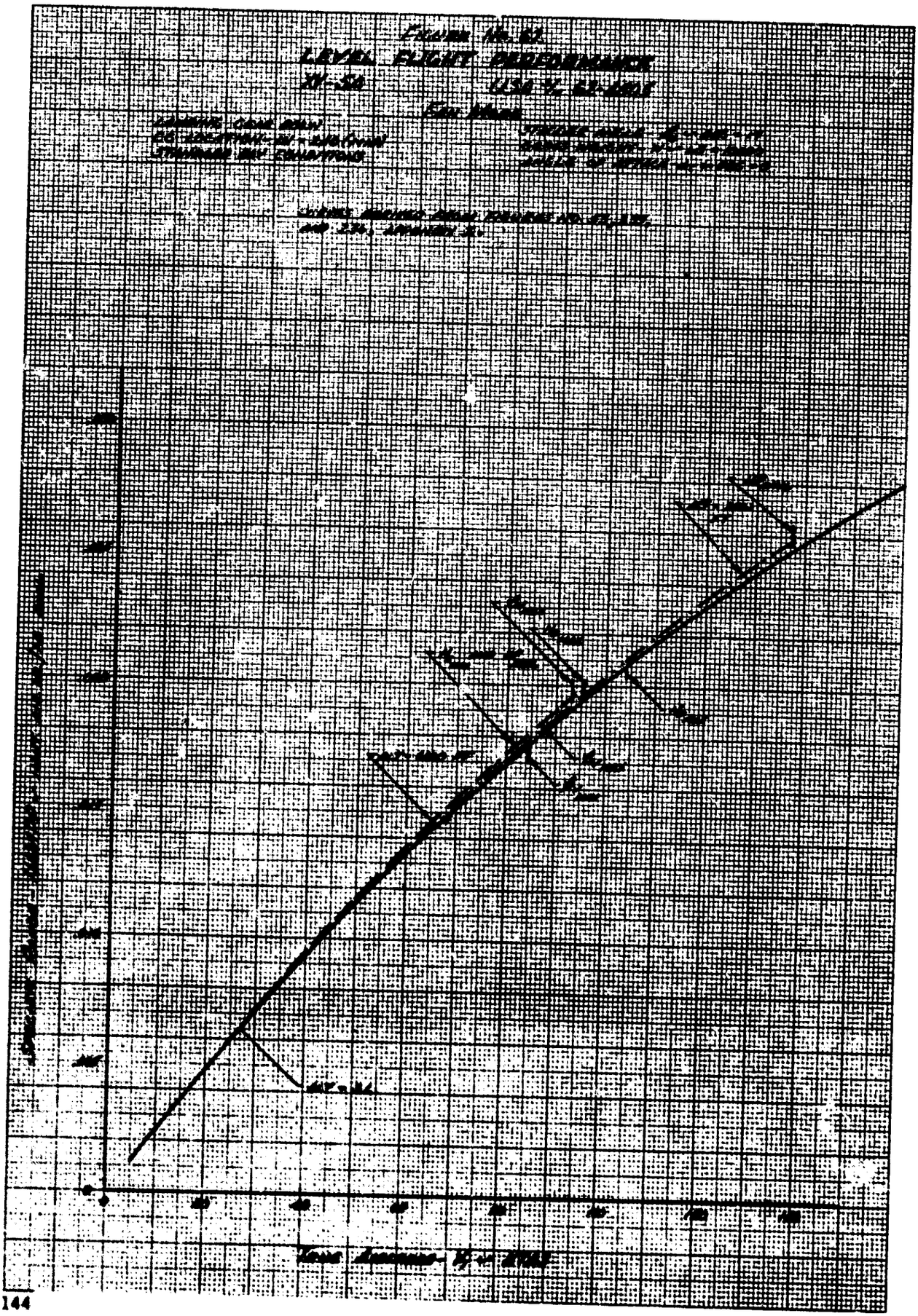

144

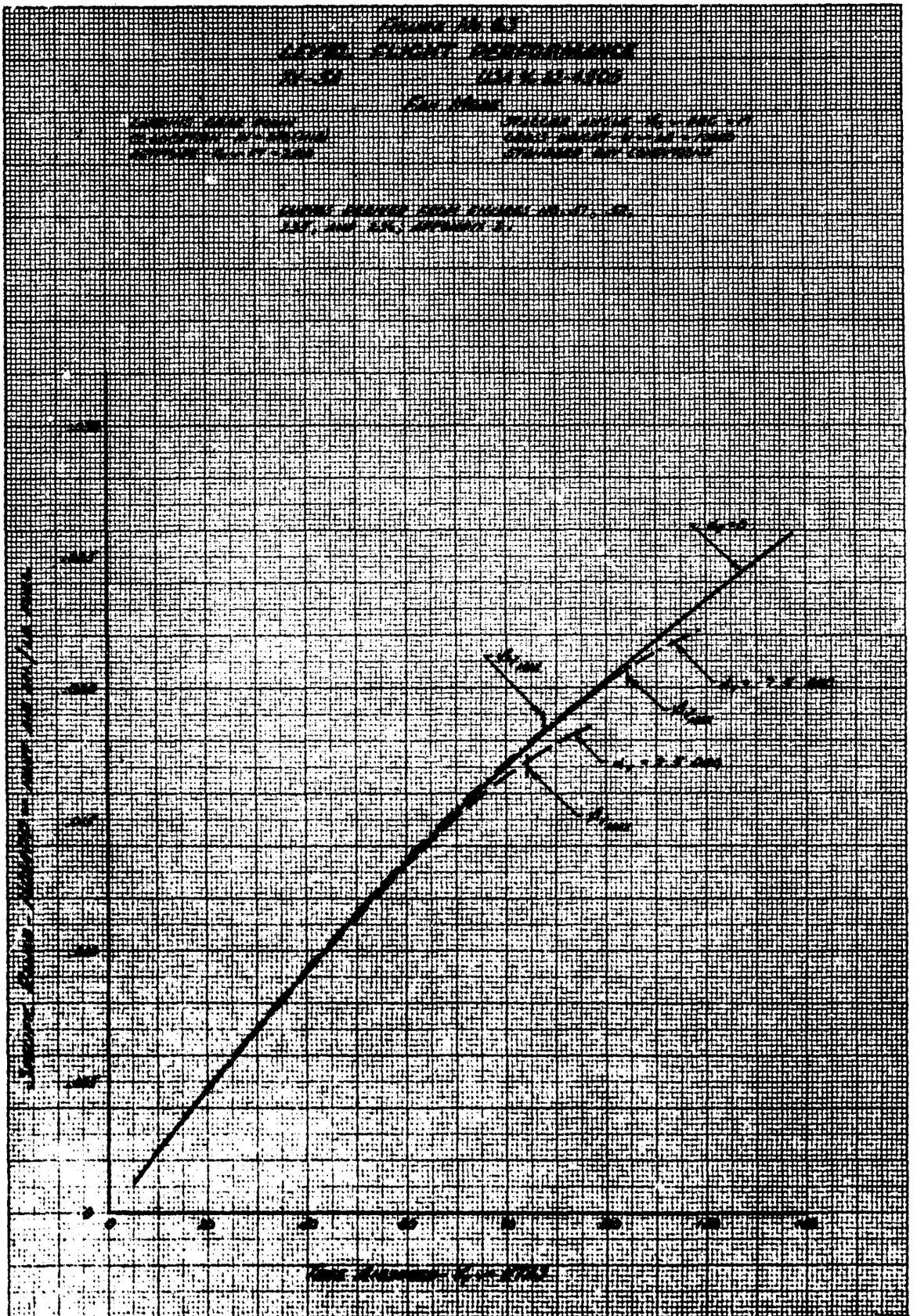

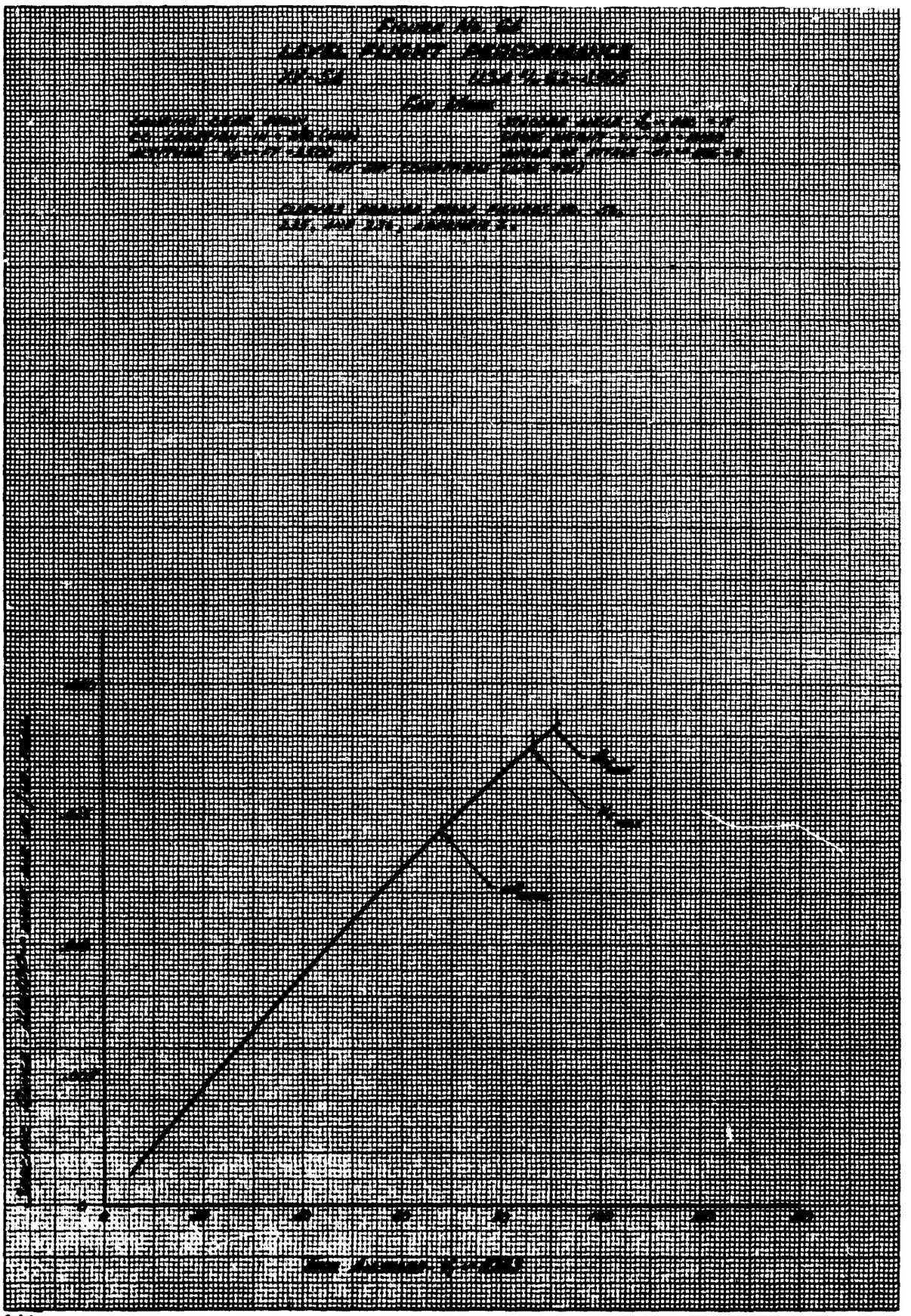

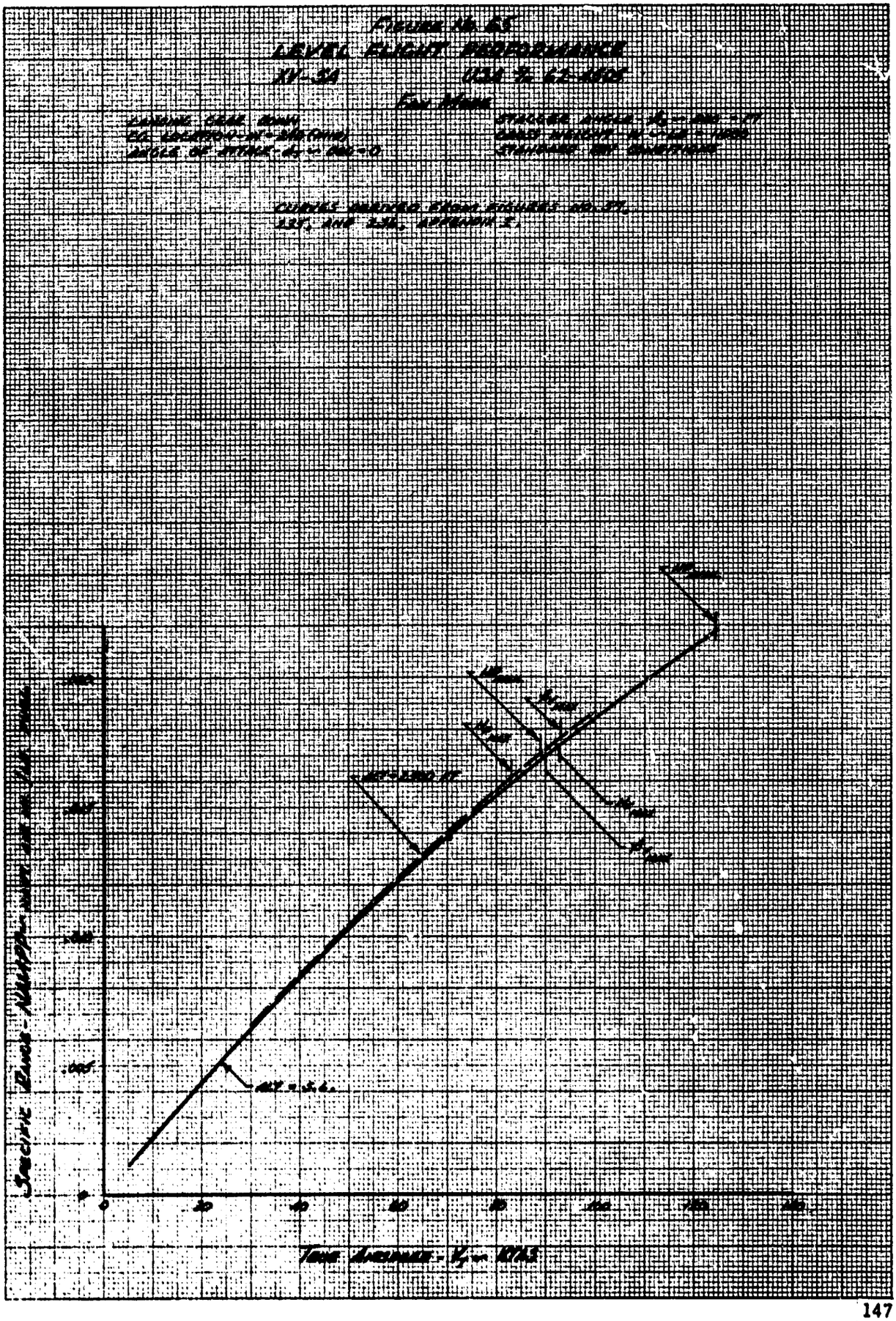
Specific Excess Power - P_s - ft/sec
Turn Anchored - V_T = 0.75

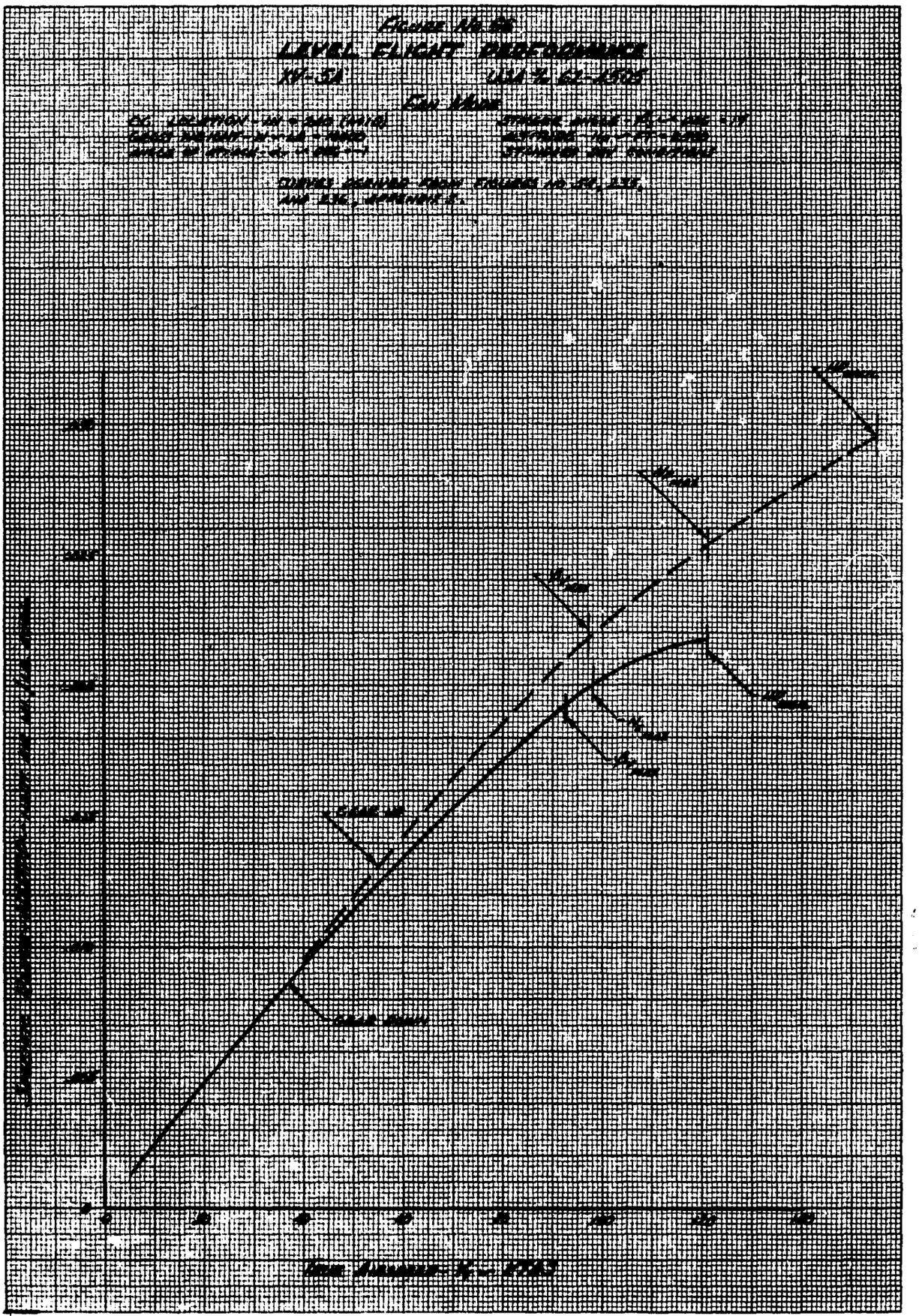

148

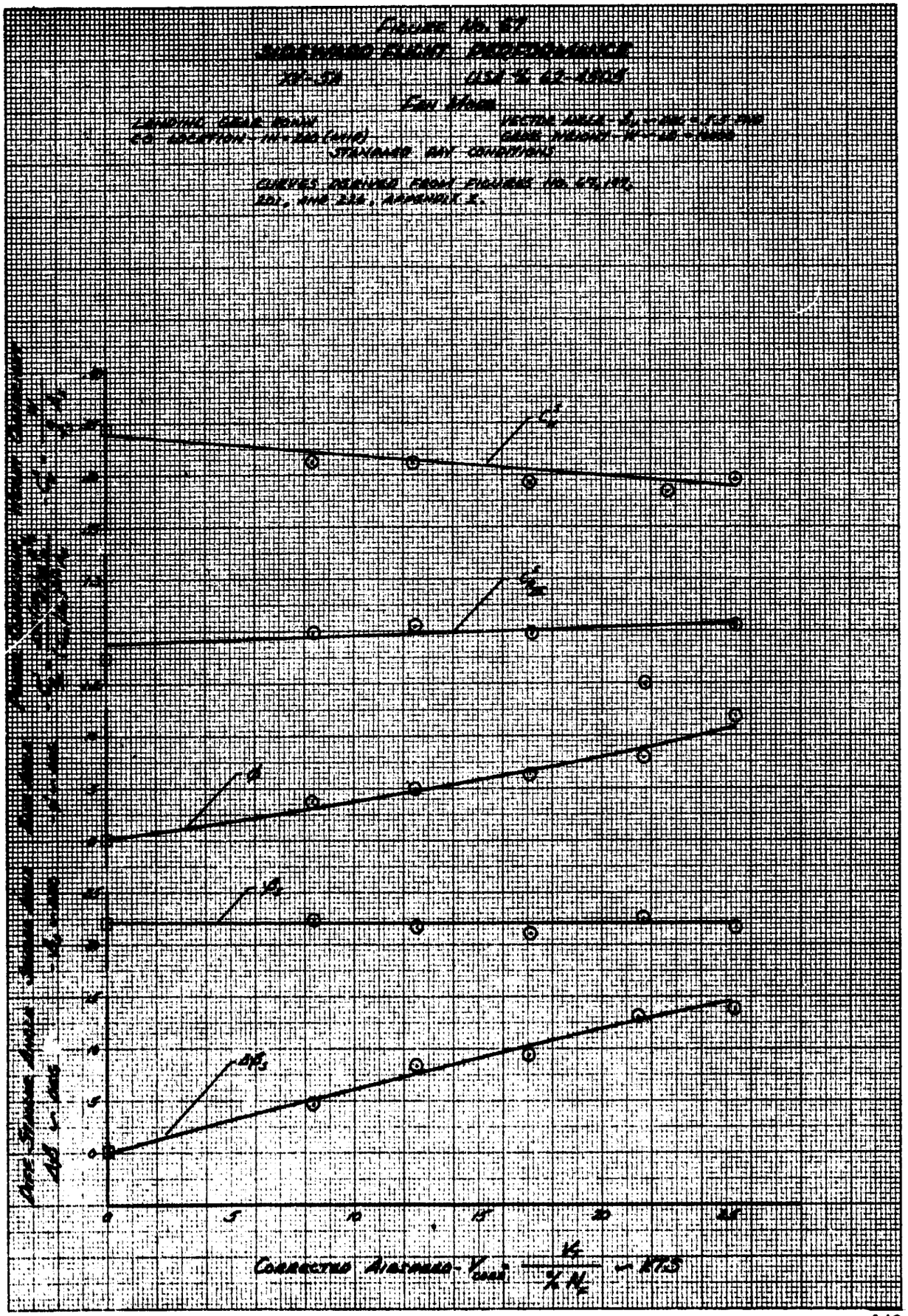
CONFIG. NO. 67
STANDARD FLIGHT PERFORMANCE
XF-92A
LEM No. 42-12004
FLAPS UP
LANDING GEAR DOWN
CG LOCATION - 14.2% (mid)
STANDARD DAY CONDITIONS
CURVES DERIVED FROM FIGURES NOS. 172, 173, 221, AND 222, APPENDIX X.
C_L
$C_{L_{max}}$
C_D
C_{D_i}
ΔC_{D_c}
$\Delta C_{D_{MACH}}$
$\Delta C_{D_{TRIM}}$
$\Delta C_{D_{FLAPS}}$
$\Delta C_{D_{GEAR}}$
$\Delta C_{D_{MISC}}$
$\Delta C_{D_{TOTAL}}$
$C_{D_{min}}$
$C_{D_{min}} + \Delta C_{D_{TOTAL}}$
$C_{D_{min}} + \Delta C_{D_{MACH}} + \Delta C_{D_{TRIM}} + \Delta C_{D_{FLAPS}} + \Delta C_{D_{GEAR}} + \Delta C_{D_{MISC}}$
0
5
10
15
20
25
Corrected Airspeed - V_{corr} $\frac{kt}{\sqrt{\sigma}}$ - KTAS

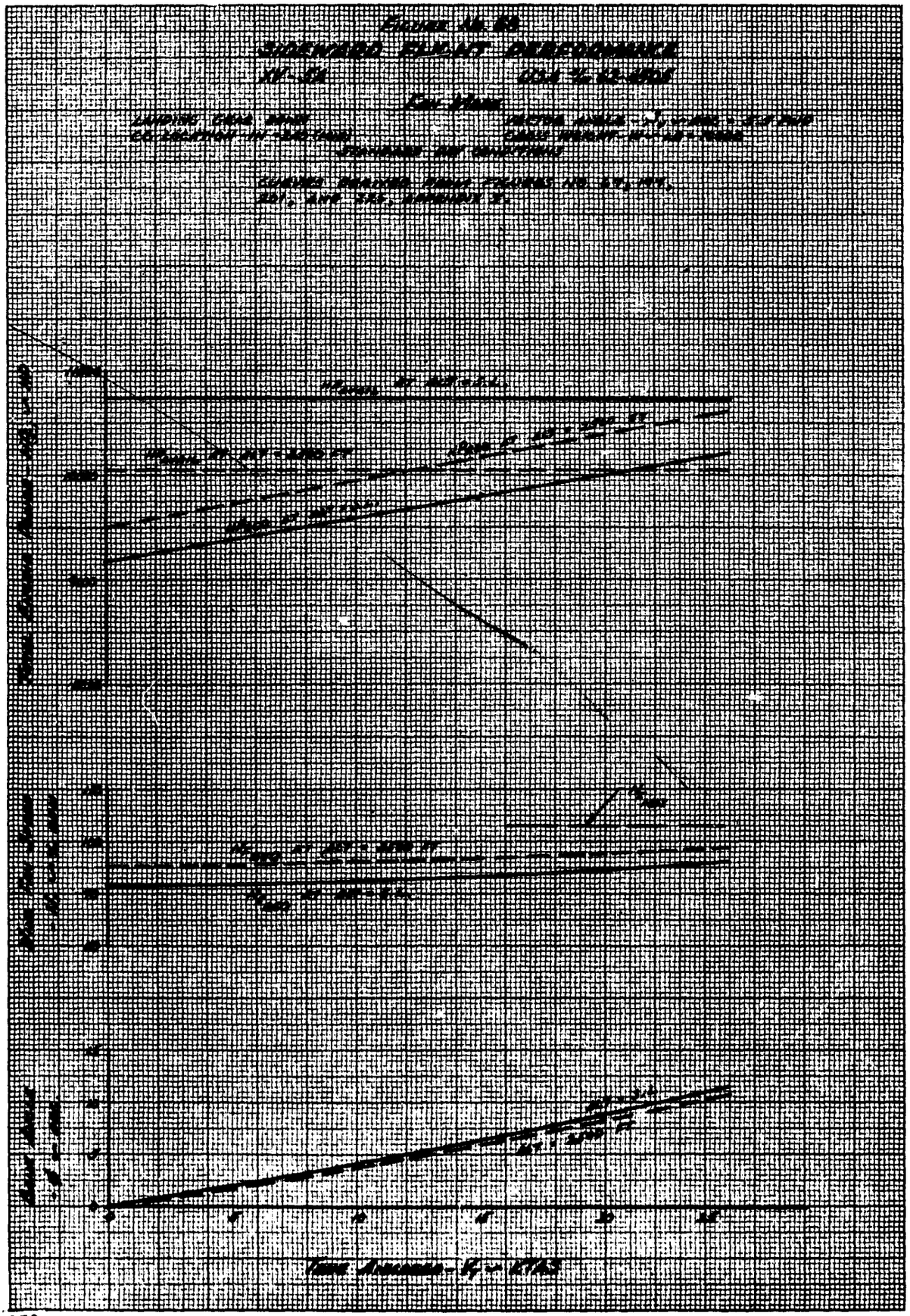

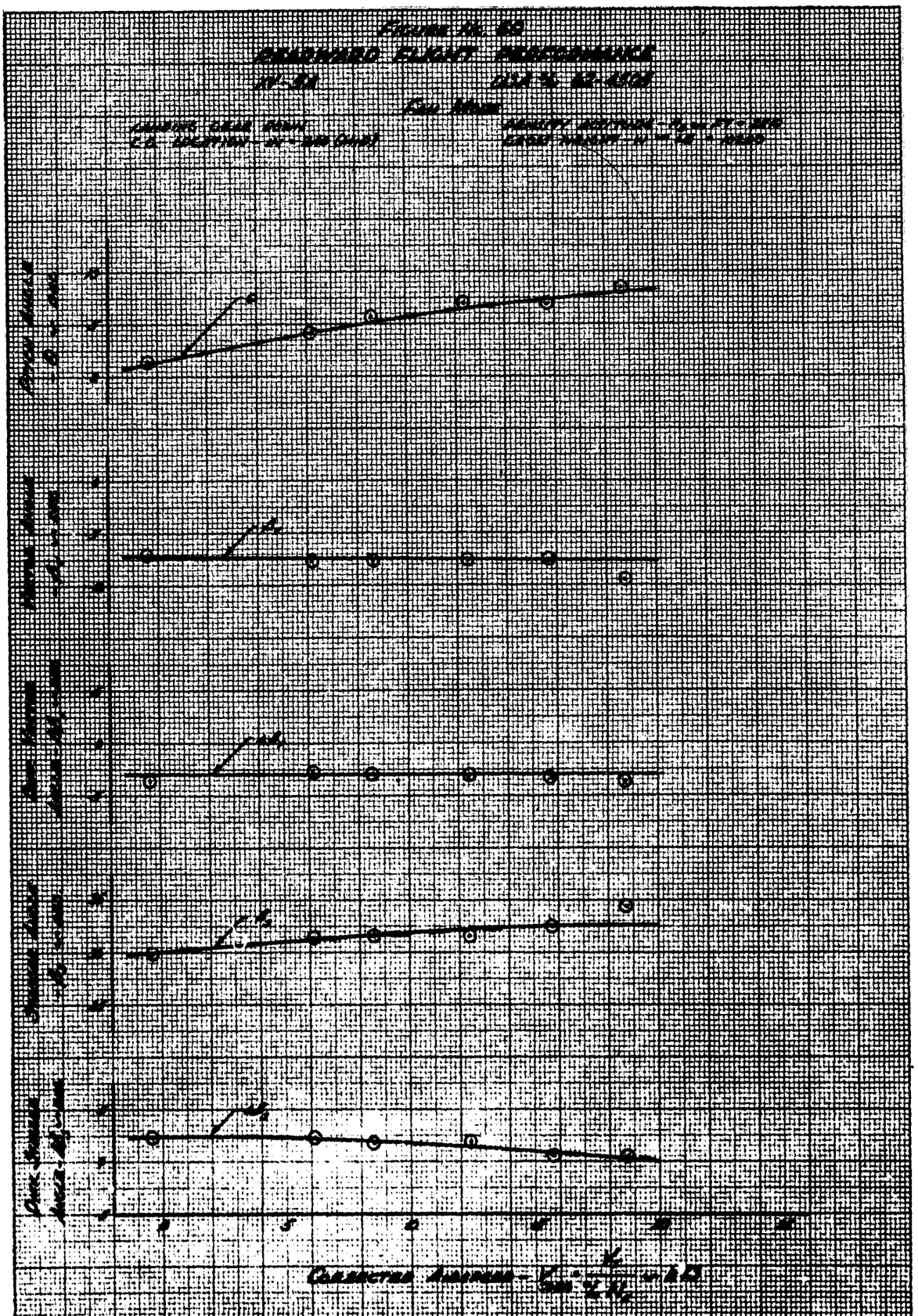

151

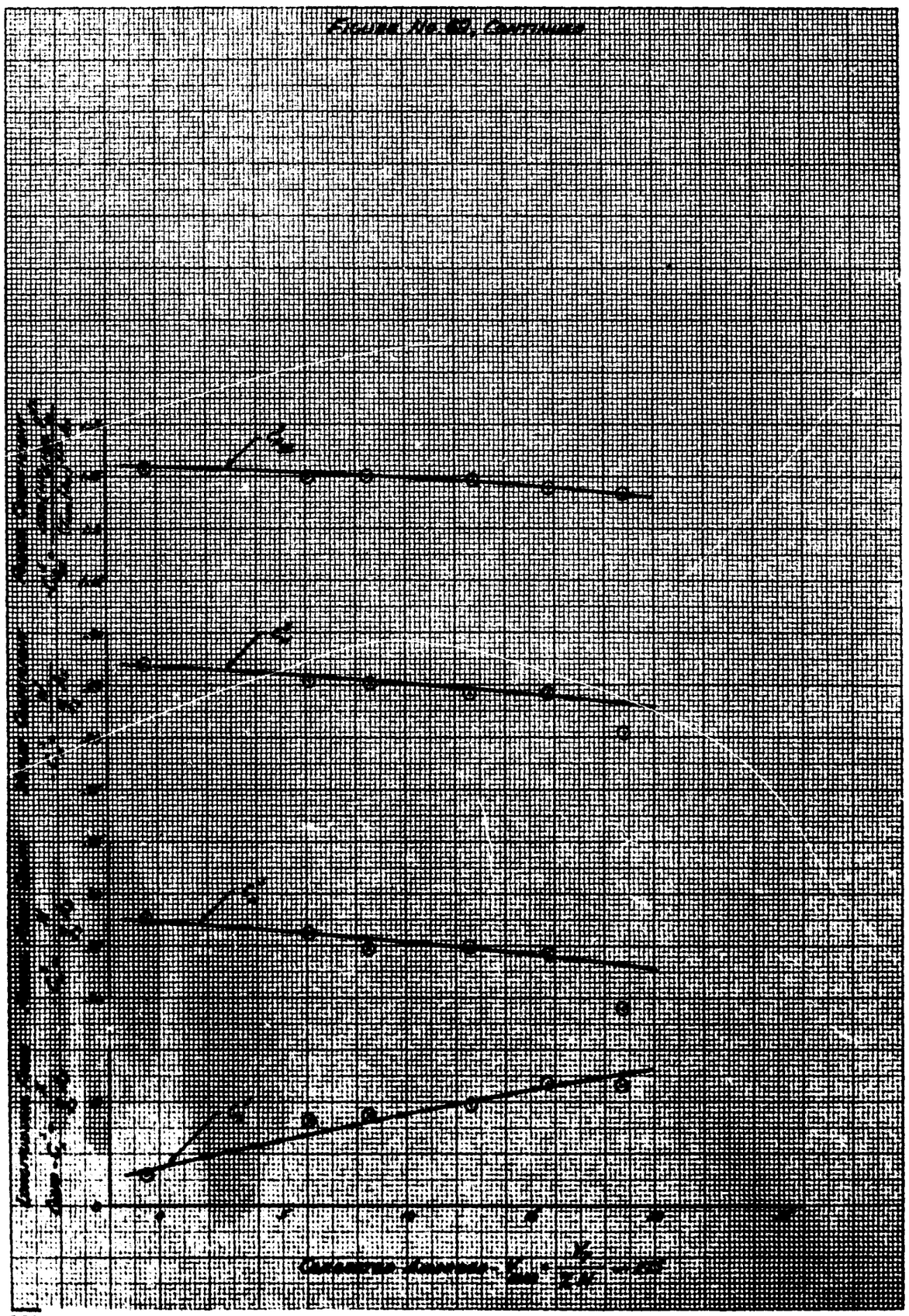

152

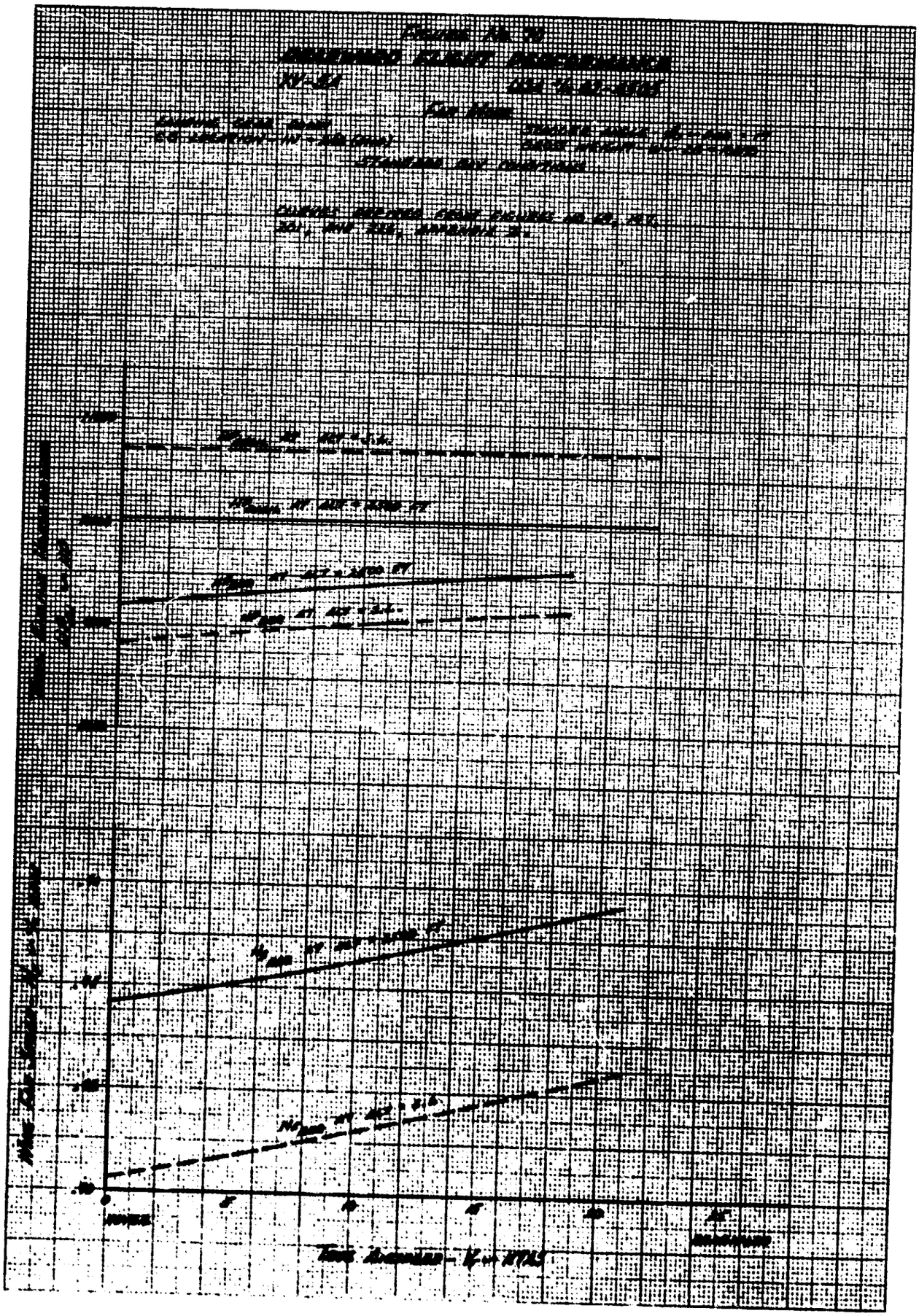

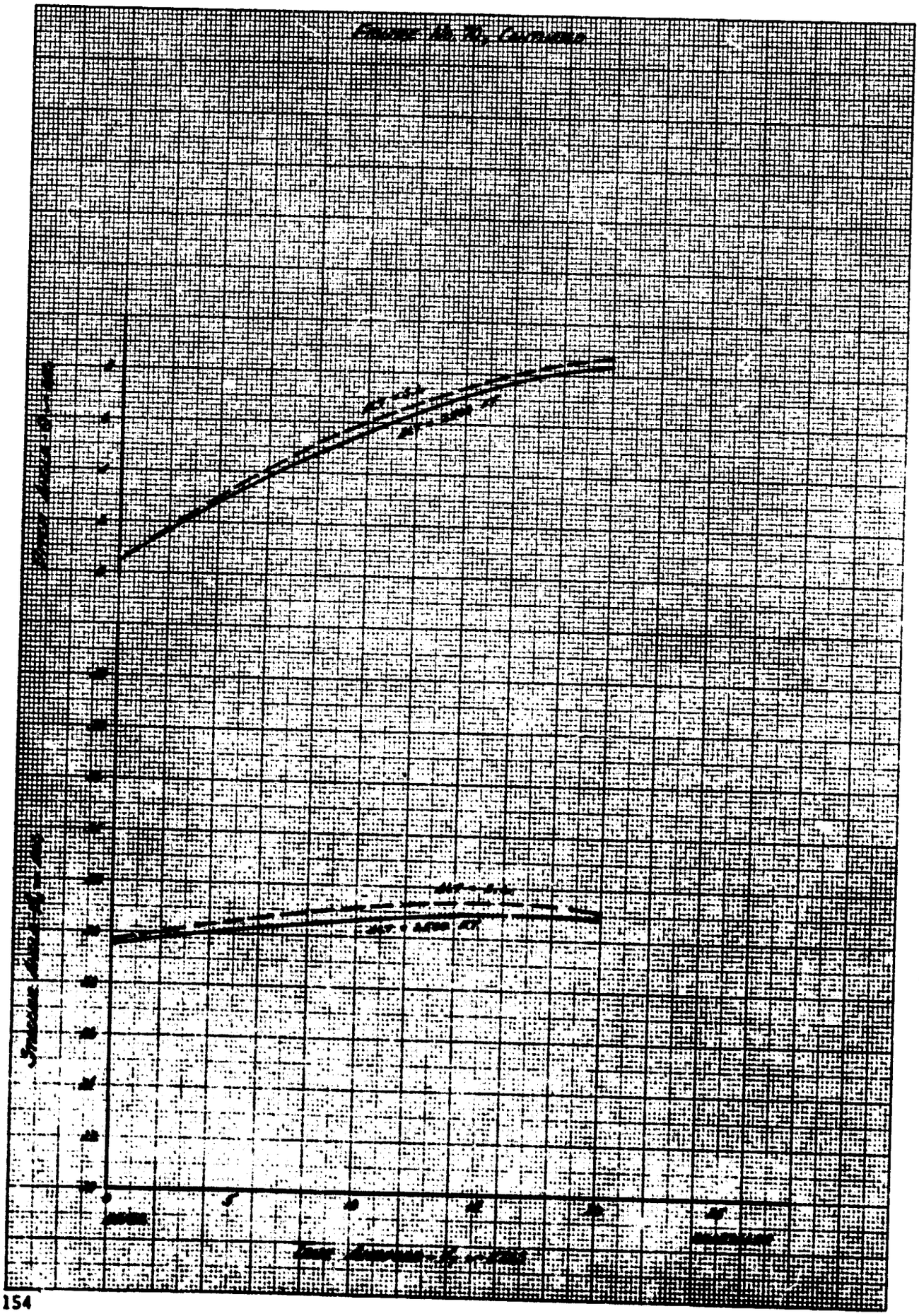

FIGURE No. 91

DESCENT PERFORMANCE

XV-5A USA No. 62-4505

Fan Mode

CODE	SPEED SET N_{fan} - RPM	ACTUATOR α_{fan} - DEG	FAN INLET $T_{t_{fan}}$ - °C	FAN EXIT $P_{t_{fan}}$ - PSIA	FLIGHT SEL. $P_{t_{fan}}/P_{t_{fan}}$ - PSID	FLIGHT CONDITION
○	10,000	30.0	21.4	19.70	2.5	9
□	10,000	15.0	15.9	19.40	2.5	9
△	9,600	14.0	13.3	19.00	2.5	9

NOTES:

1. THRUST BASED ON STATIC THRUST AVAILABLE AT THE TEST ANGLE FROM FIGURE NO. 92 ORDINATE T_{fan}.
2. DATA OF AIRCRAFT FALLING OBTAINED ABOUT FOLLOWING FLIGHT DIRECTOR.

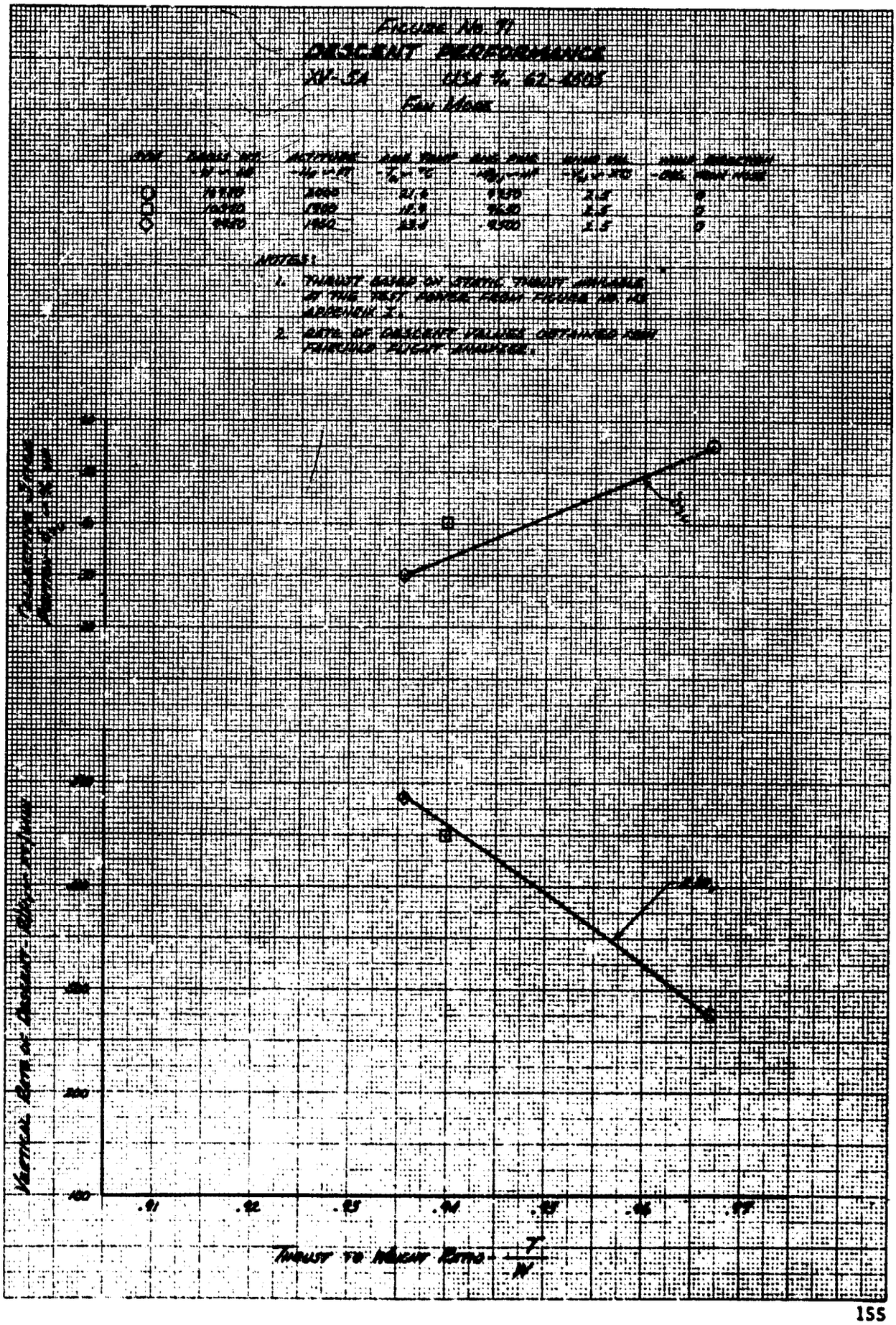

Figure No. 72

ANGLE OF ATTACK CALIBRATION

XV-5A USA #62-4505

SYM	CONFIGURATION	GROSS WT $-W_g$ - LB	ALTITUDE $-H_p$ - FT
○	FAN PROBE	10200	31100
△	JET WAKE PROBE	10300	31100

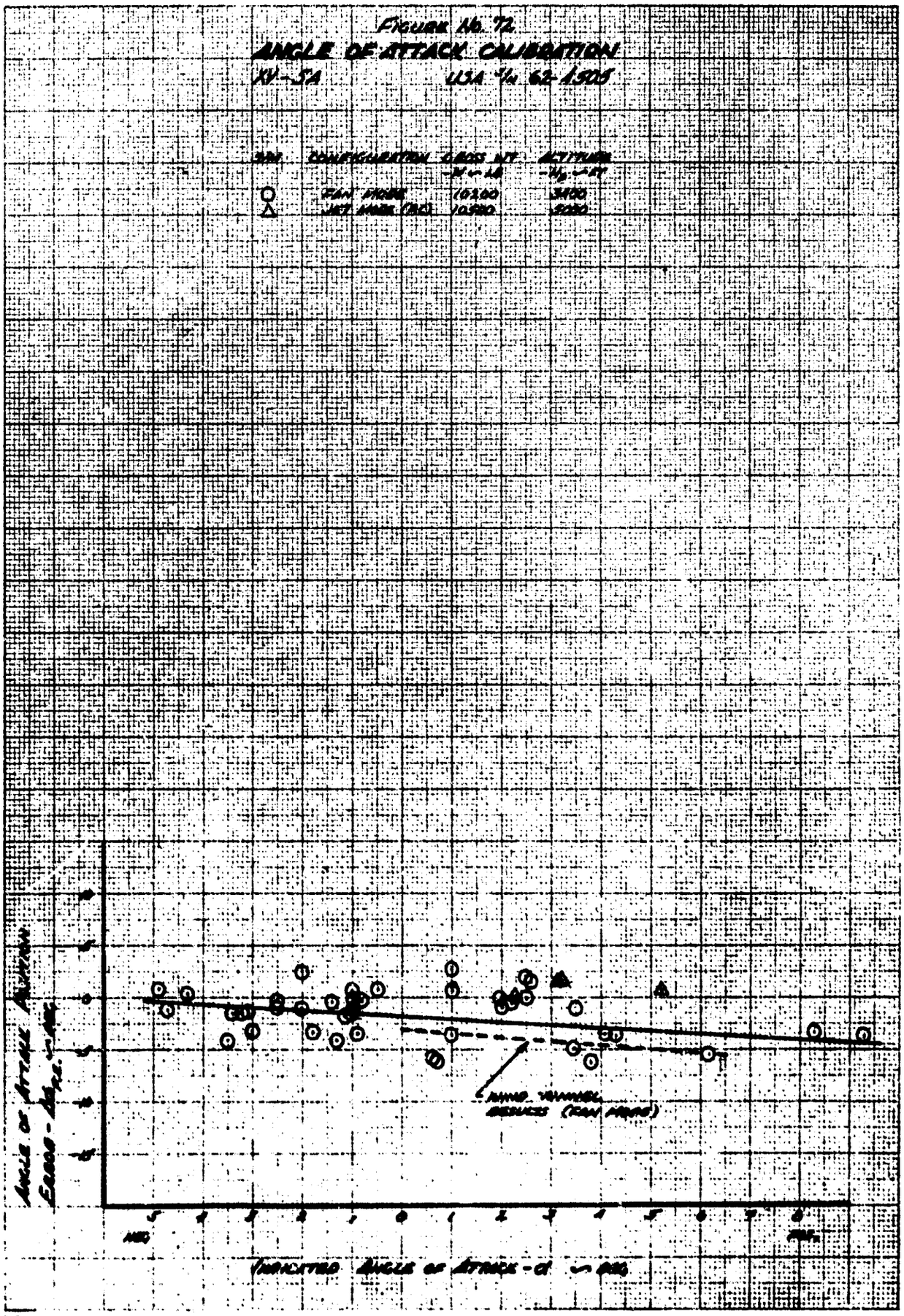

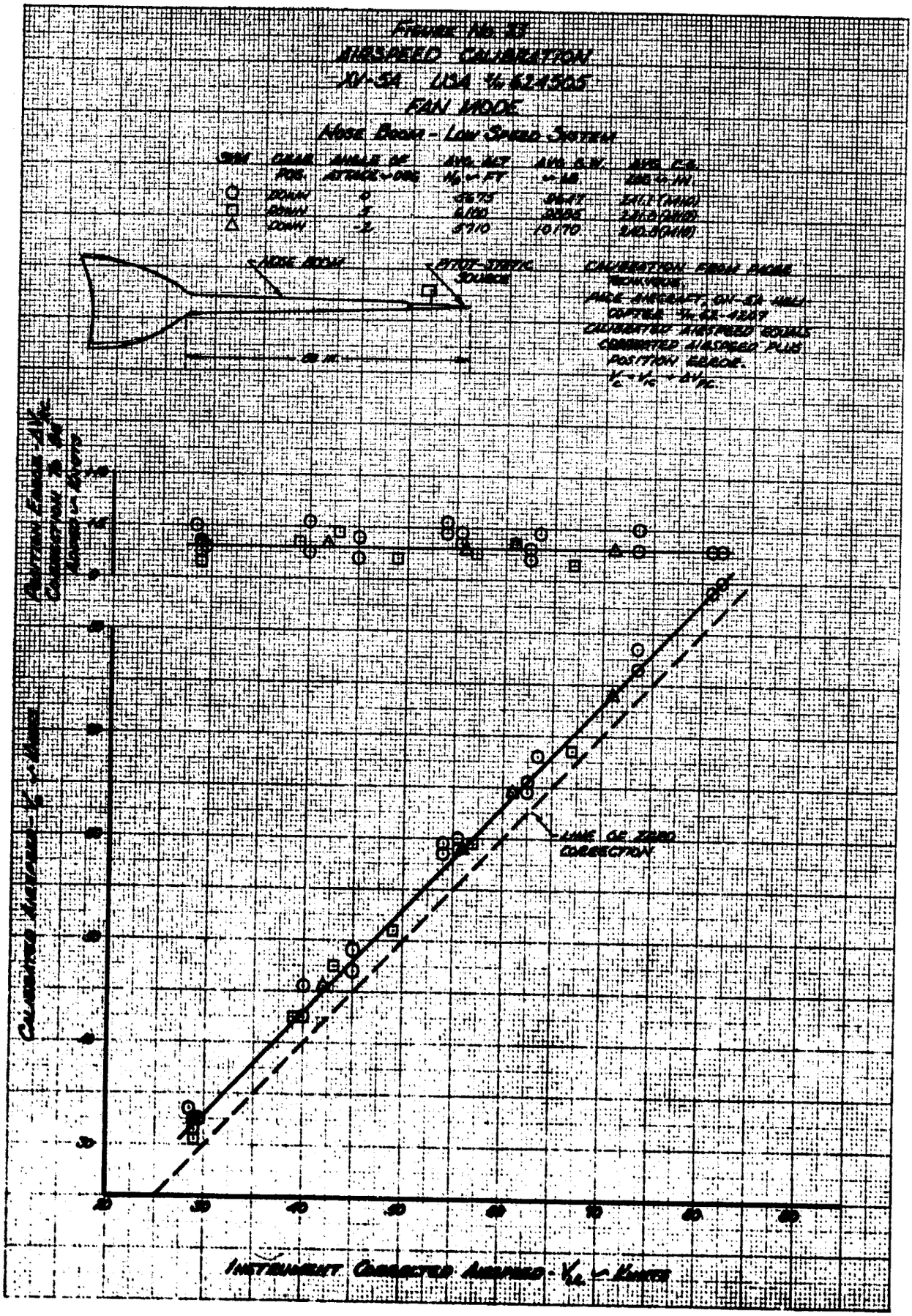
FIGURE NO. 37
AIRSPEED CALIBRATION
XV-3A 1134 ft 624505
FAN MODE
Nose Boom - Low Speed System
SYM
GEAR POS.
ANGLE OF ATTACK - DEG
AVG. ALT. Hp - FT
AVG. C.G. STA - IN
DOWN 0 3575 241.1 (AVG)
DOWN 3 4100 240.5 (AVG)
DOWN -2 3710 240.3 (AVG)
NOSE BOOM
PITOT-STATIC SOURCE
20 in
CALIBRATION FROM FLIGHT TEST DATA
FLIGHT CALIBRATION OF NOSE BOOM PITOT-STATIC SOURCE
CALIBRATED AIRSPEED EQUALS CORRECTED INDICATED PLUS POSITION ERROR.
$V_c = V_{ic} + \Delta V_{pc}$
CALIBRATED AIRSPEED - V_c - KNOTS
LINE OF ZERO CORRECTION
INSTRUMENT CORRECTED AIRSPEED - V_{ic} - KNOTS

158

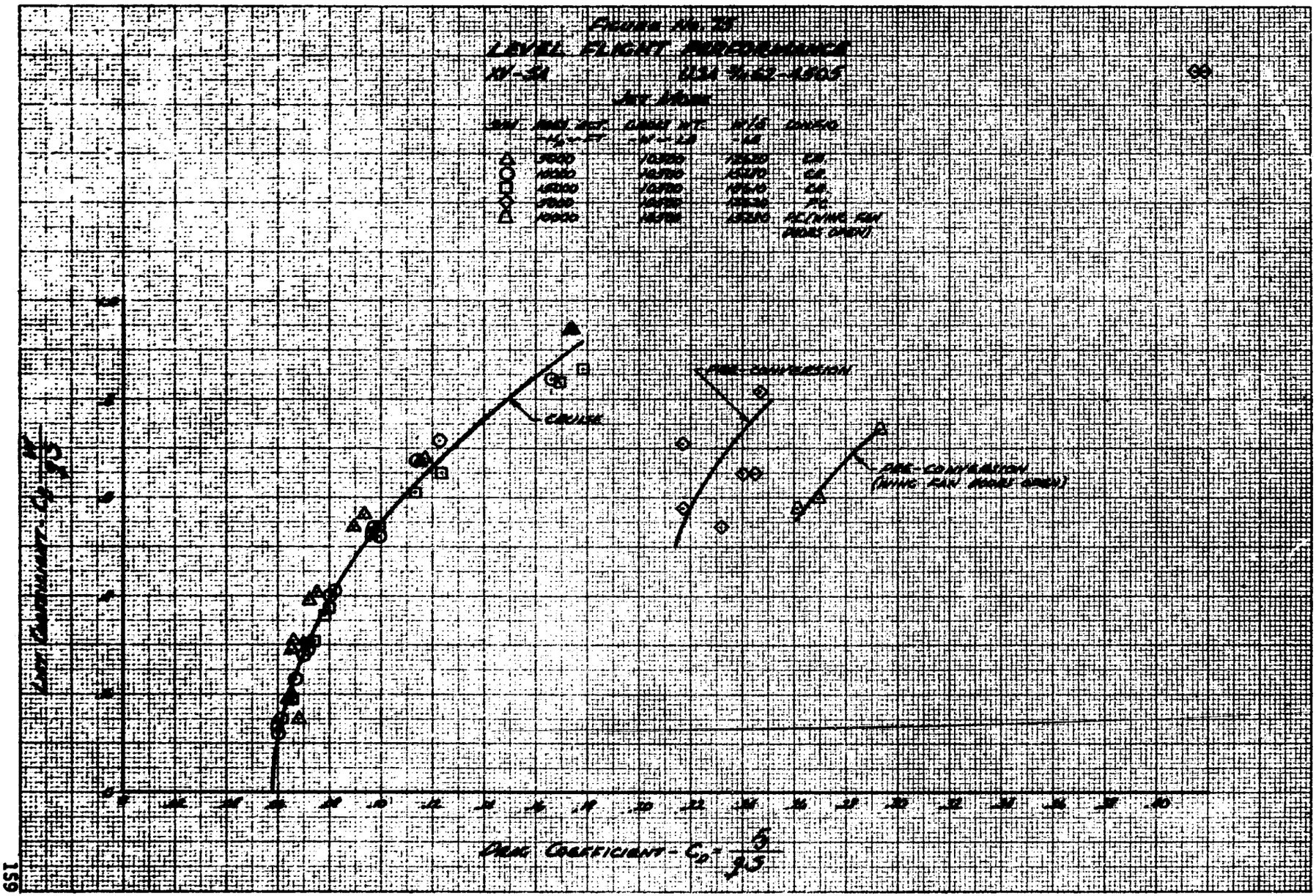
FIGURE NO. 28
LEVEL FLIGHT PERFORMANCE
XF-84
JET POWER
DRAG COEFFICIENT - $C_D = \frac{D}{qS}$
CALC.
FREE-CONVECTION
FREE-CONVECTION (WING RAM INLET CLOSED)

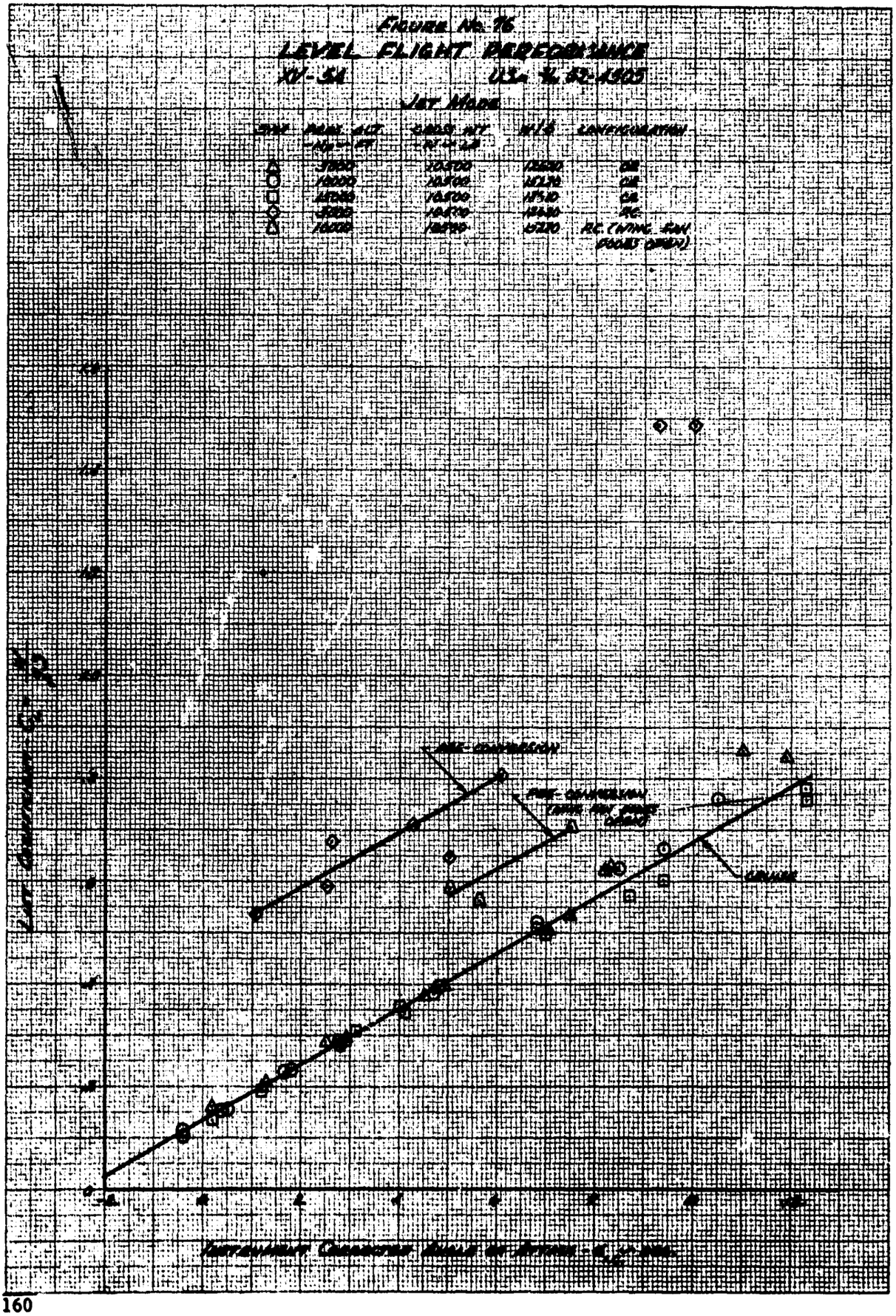
FIGURE No. 76
LEVEL FLIGHT PERFORMANCE
XV-5A
Jet Mode
SYMBOL
MACH NO.
ALT. -Hp- FT
GROSS WT. -W- LB
W/δ
CONFIGURATION
A
B
C
D
E
RC (WING FAN POWER OFF)
MIN. DRAG
MAX. RANGE
MAX. ENDURANCE
Instrument Character Height on Artwork - 1/8 in. min.

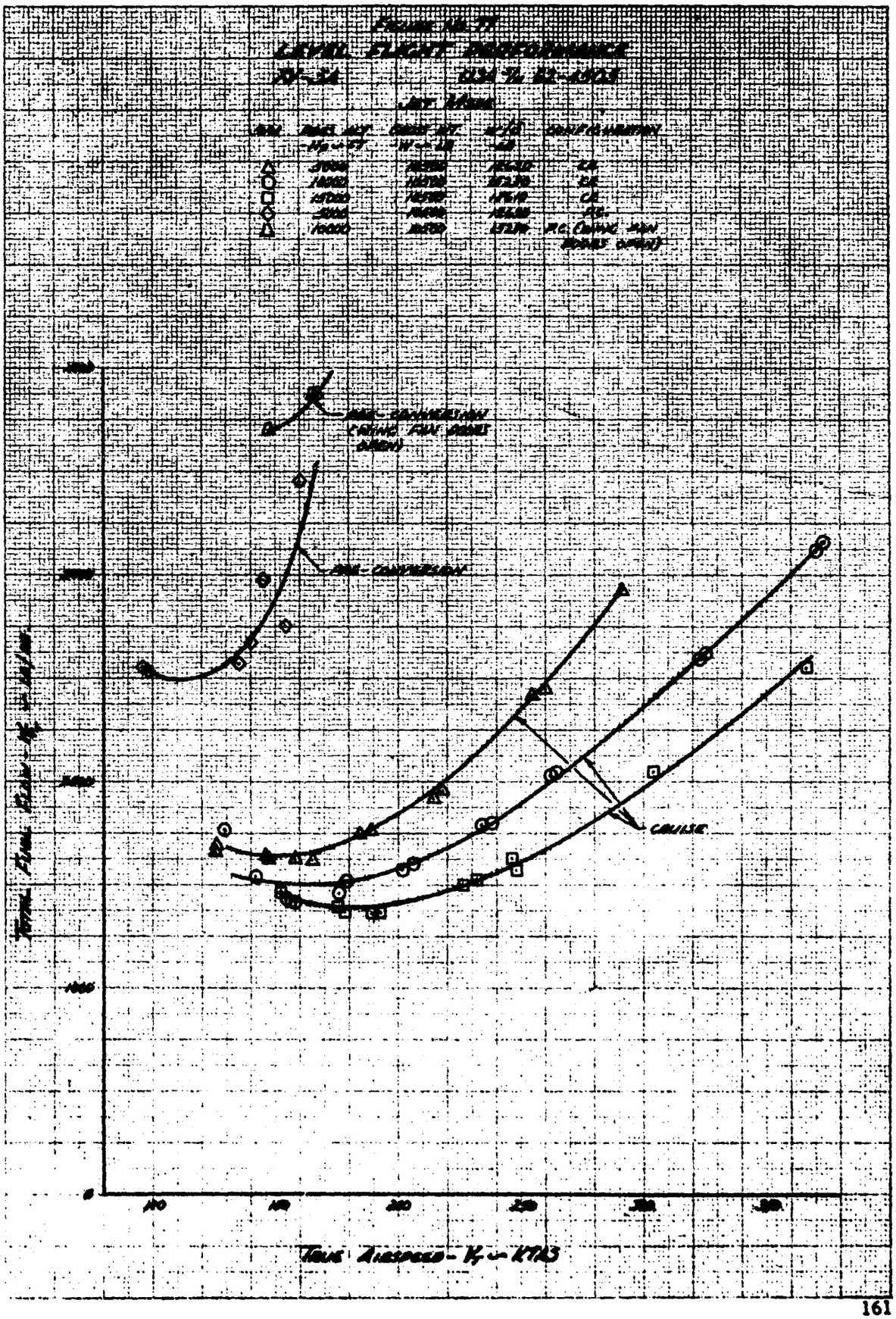
CRUISE

FIGURE No. 78

LEVEL FLIGHT PERFORMANCE

XF-84H USAF No. 52-1903

Sea Level

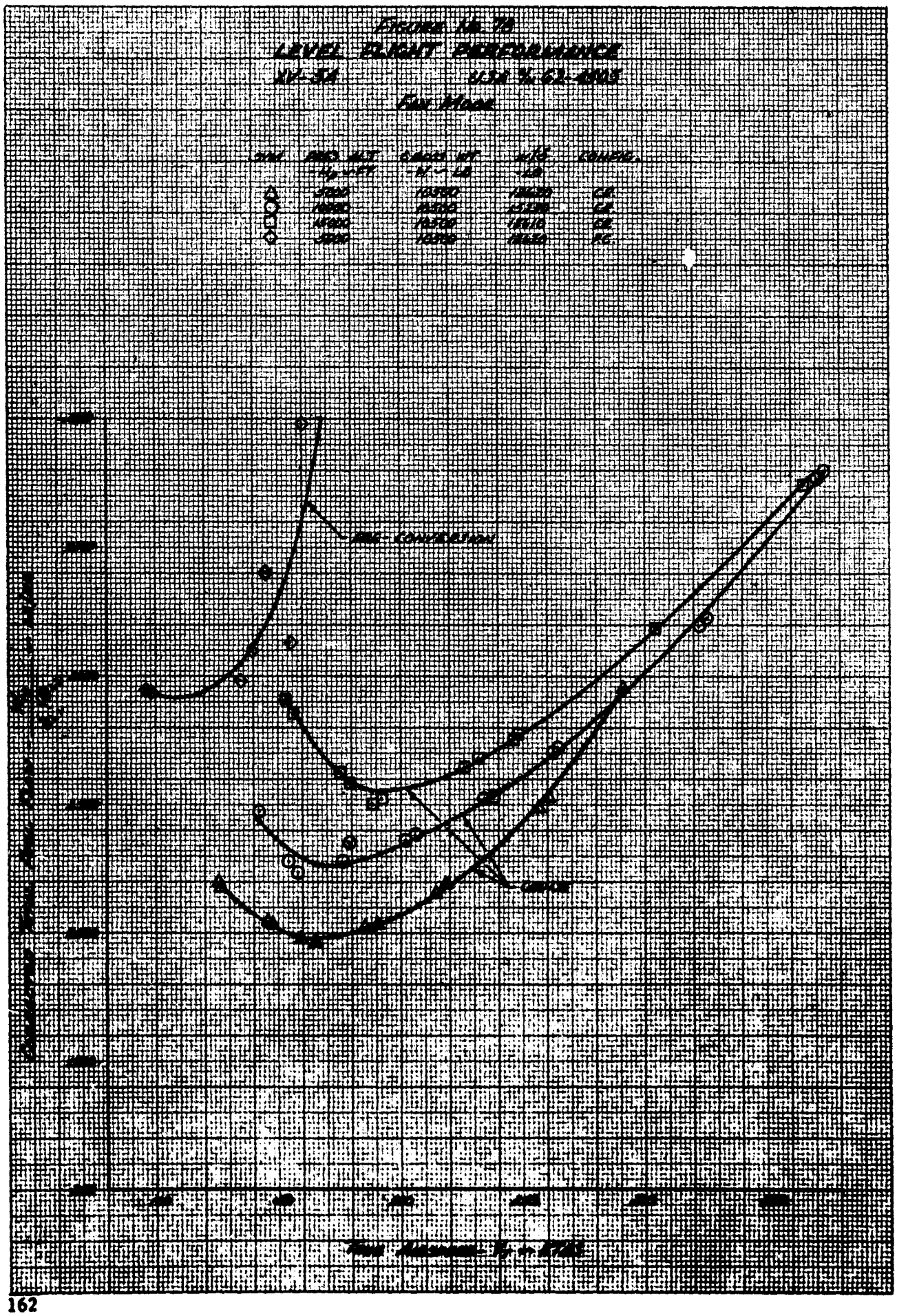

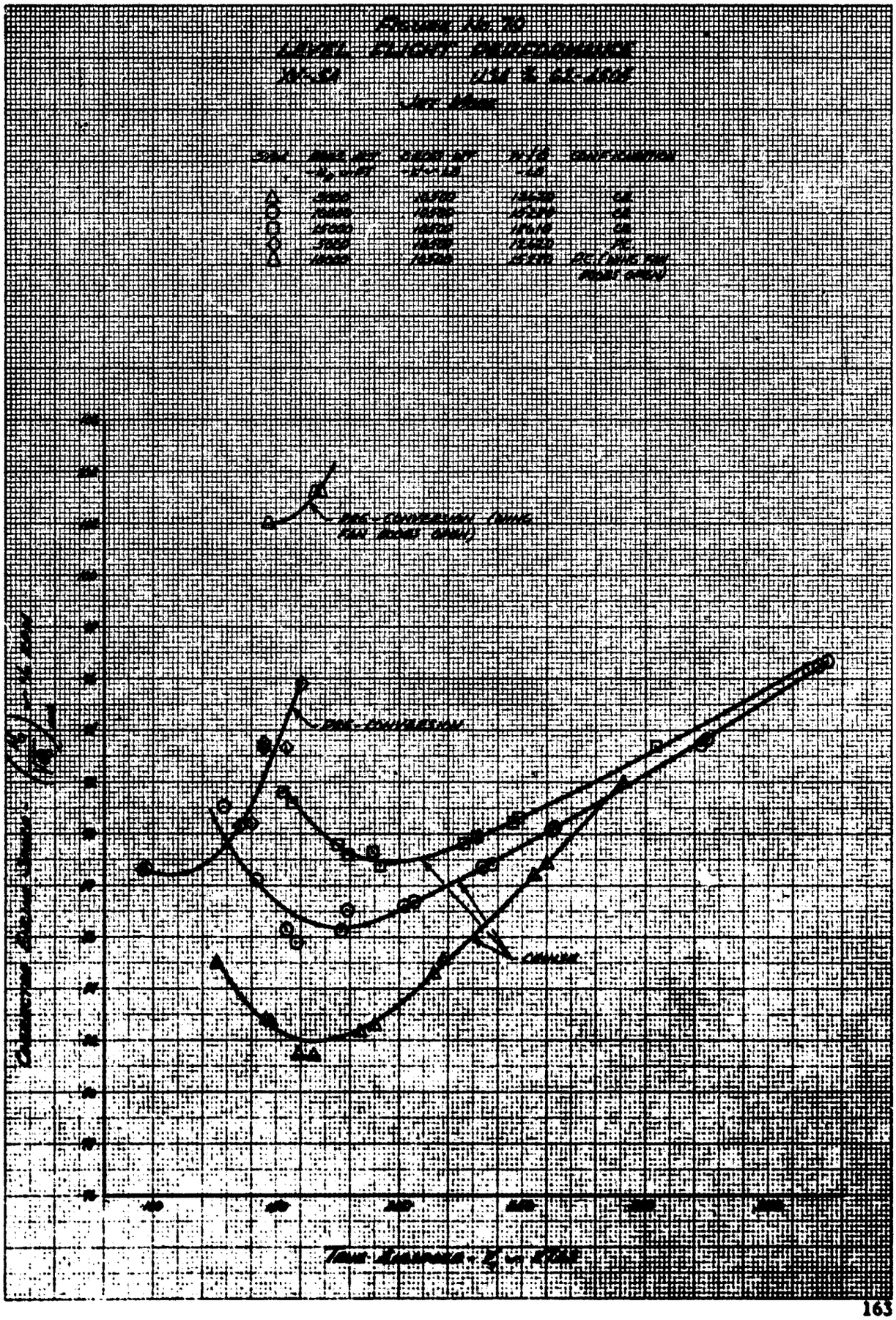

163

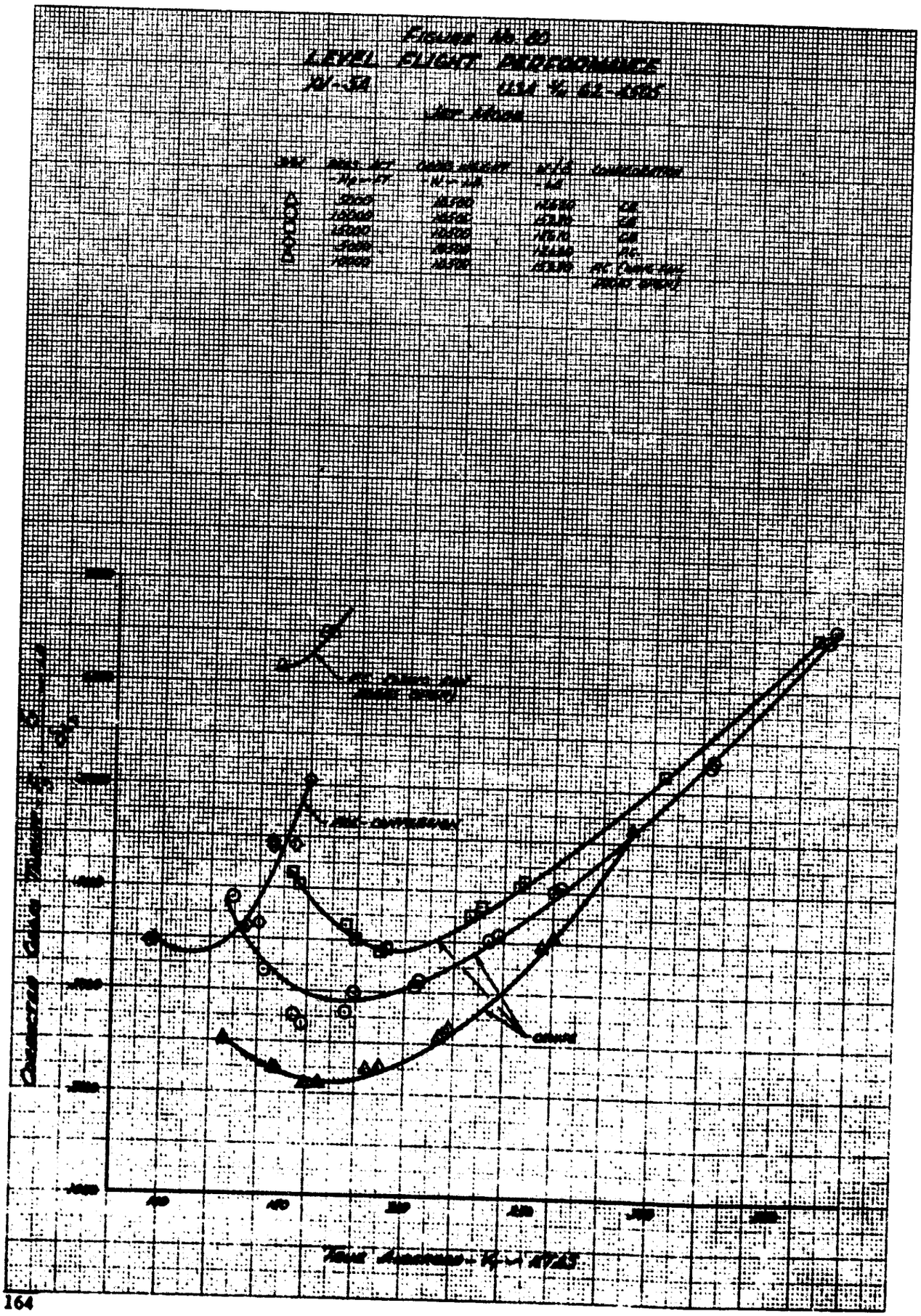
FIGURE 46.20
LEVEL FLIGHT PERFORMANCE
XV-3A
ARMY
ARMY
CONFIGURATION
CLEAN
CLEAN
CLEAN
CLEAN
CLEAN
CLEAN
PRE-CONVERSION
CRUISE

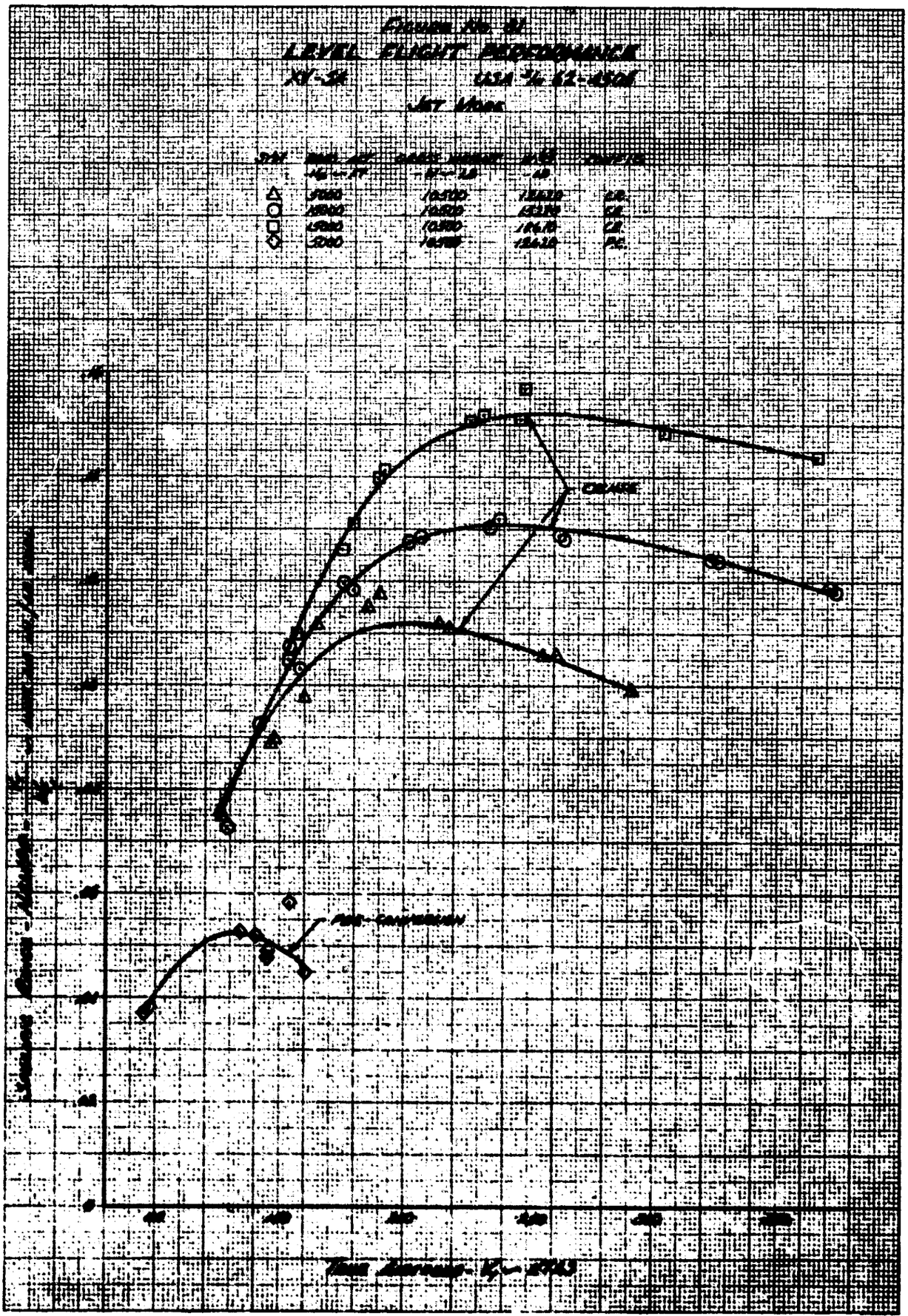
LEVEL FLIGHT PERFORMANCE
XF-5K
JET MODE
CRUISE
MAX. CONTINUOUS

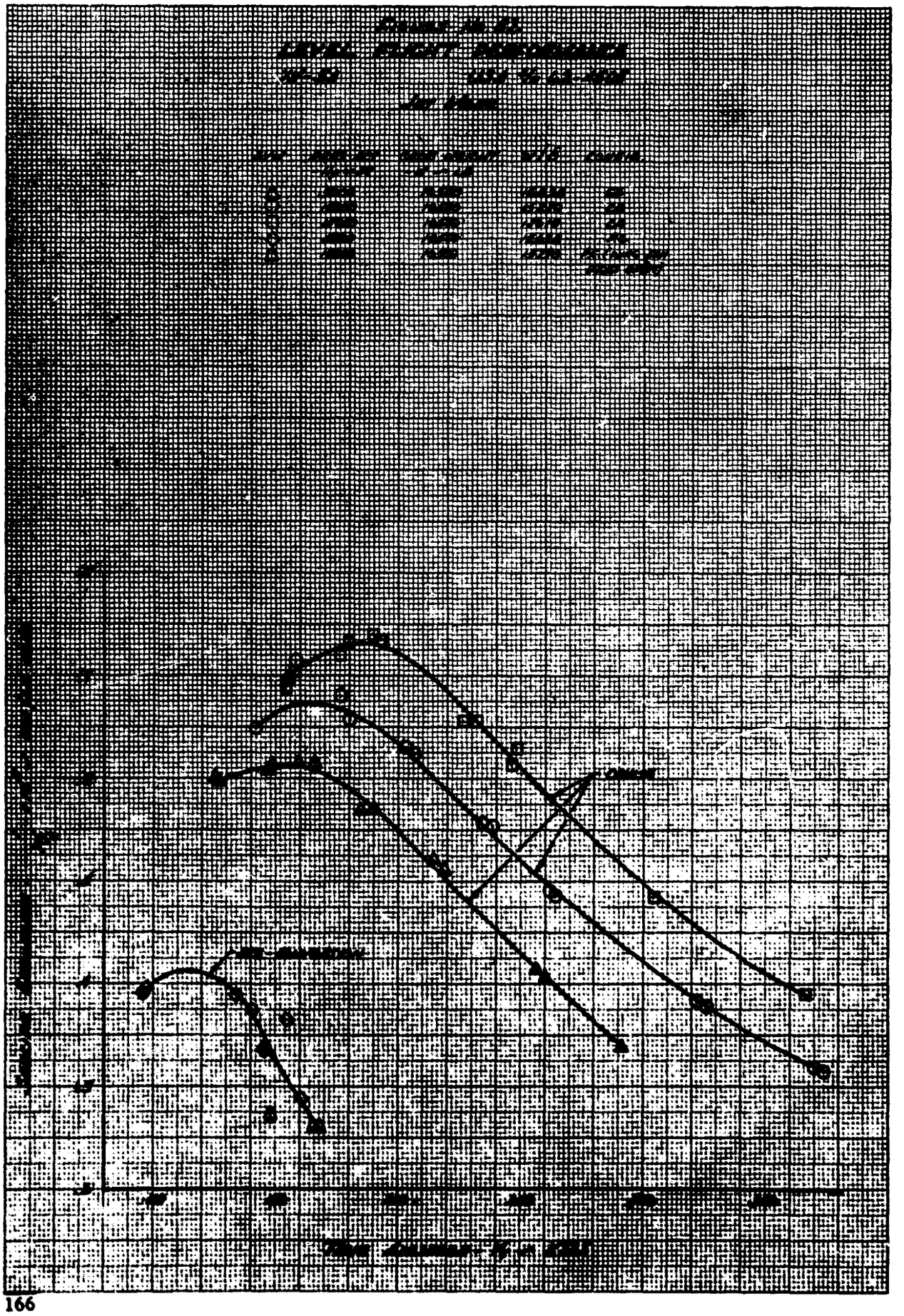

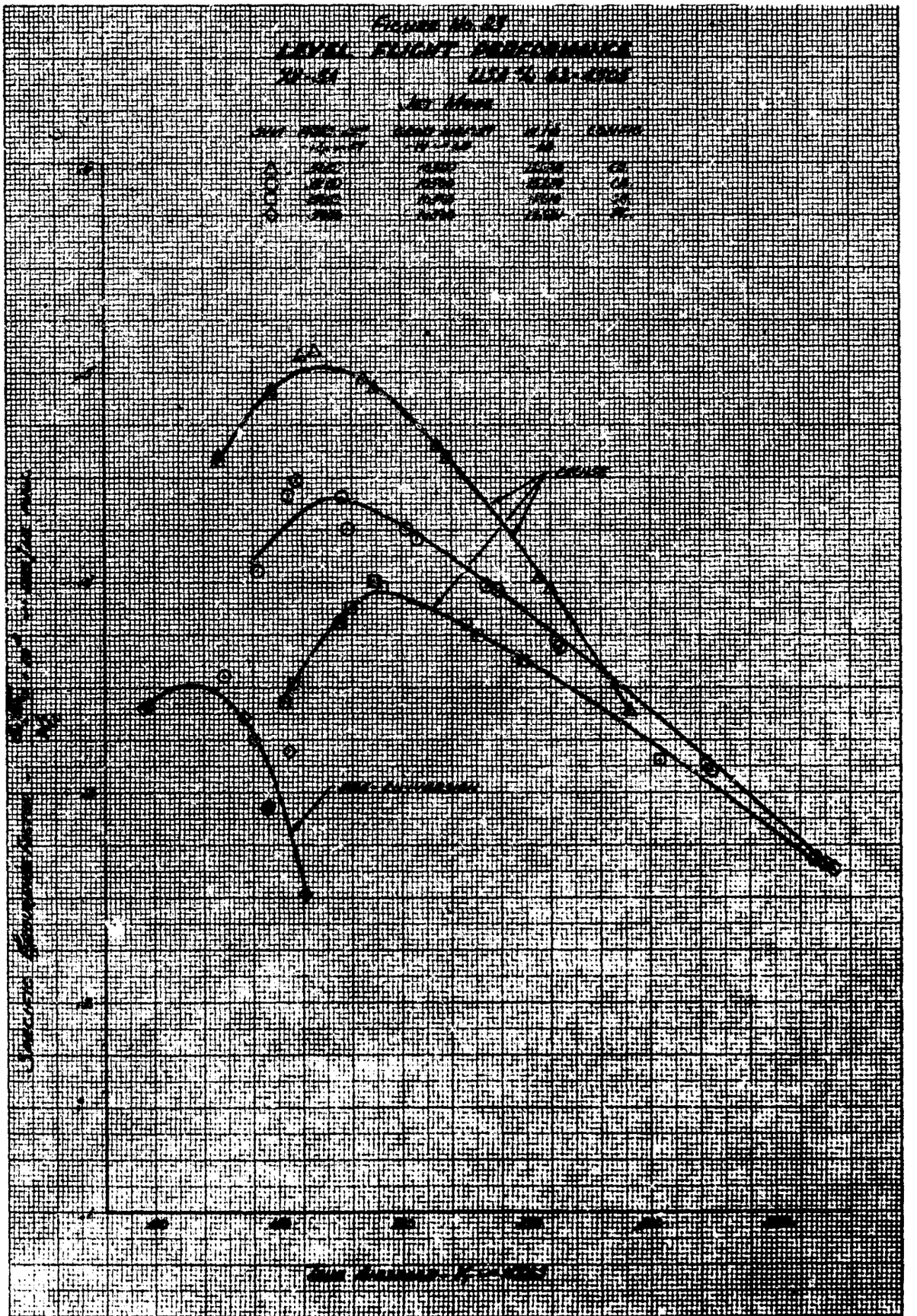

168

Figure 46-27
LEVEL FLIGHT PERFORMANCE
XF-84 USAF No. 47-1406

Corrected Gross Weight = $\frac{W}{\delta}\sqrt{\theta}$ in M

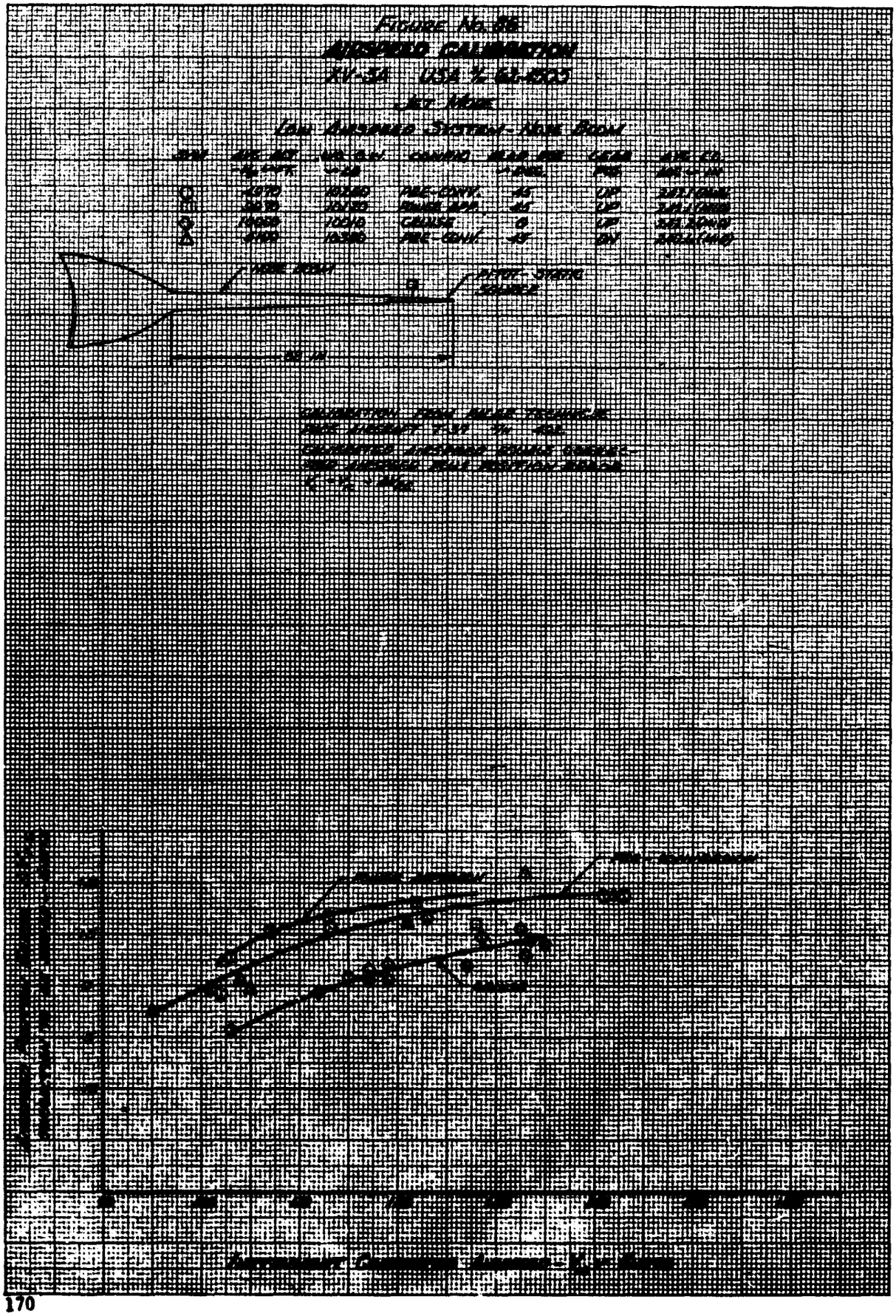
FIGURE No. 88
AIRSPEED CALIBRATION
XV-5A USA # 64-17105
JET MODE
LOW AIRSPEED SYSTEM - NOSE BOOM
NOSE BOOM
ALTERN. STATIC SOURCE
CALIBRATION FROM ALTER. PRESSURE TO FREE AIRSTREAM P(alt) vs. Mc
CALIBRATED AIRSPEED SQUARED (KNOTS)²
FREE AIRSTREAM MACH NUMBER - Mc
Instrument Calibration Airspeed - Kc - Knots

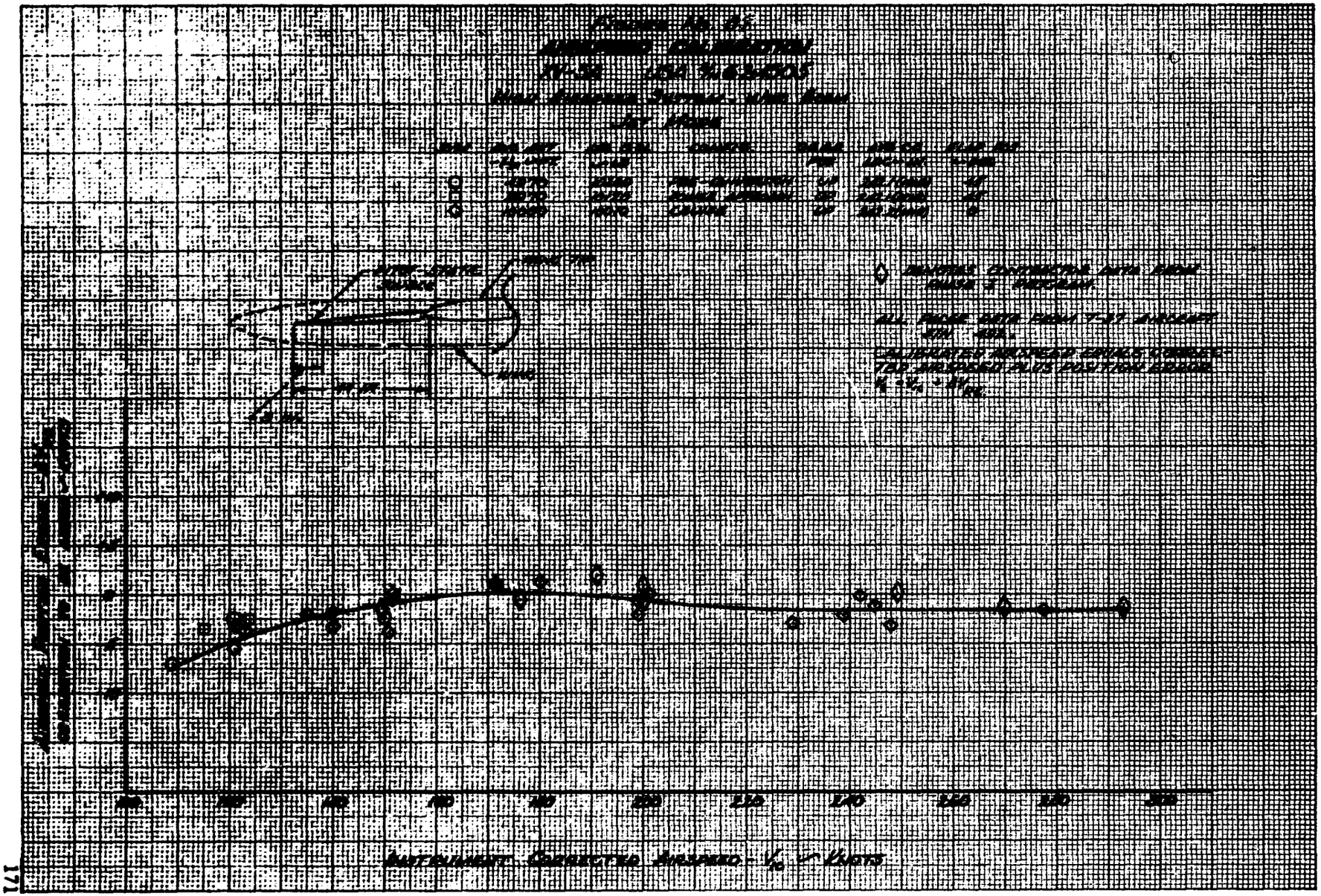
INSTRUMENT CORRECTED AIRSPEED - KNOTS

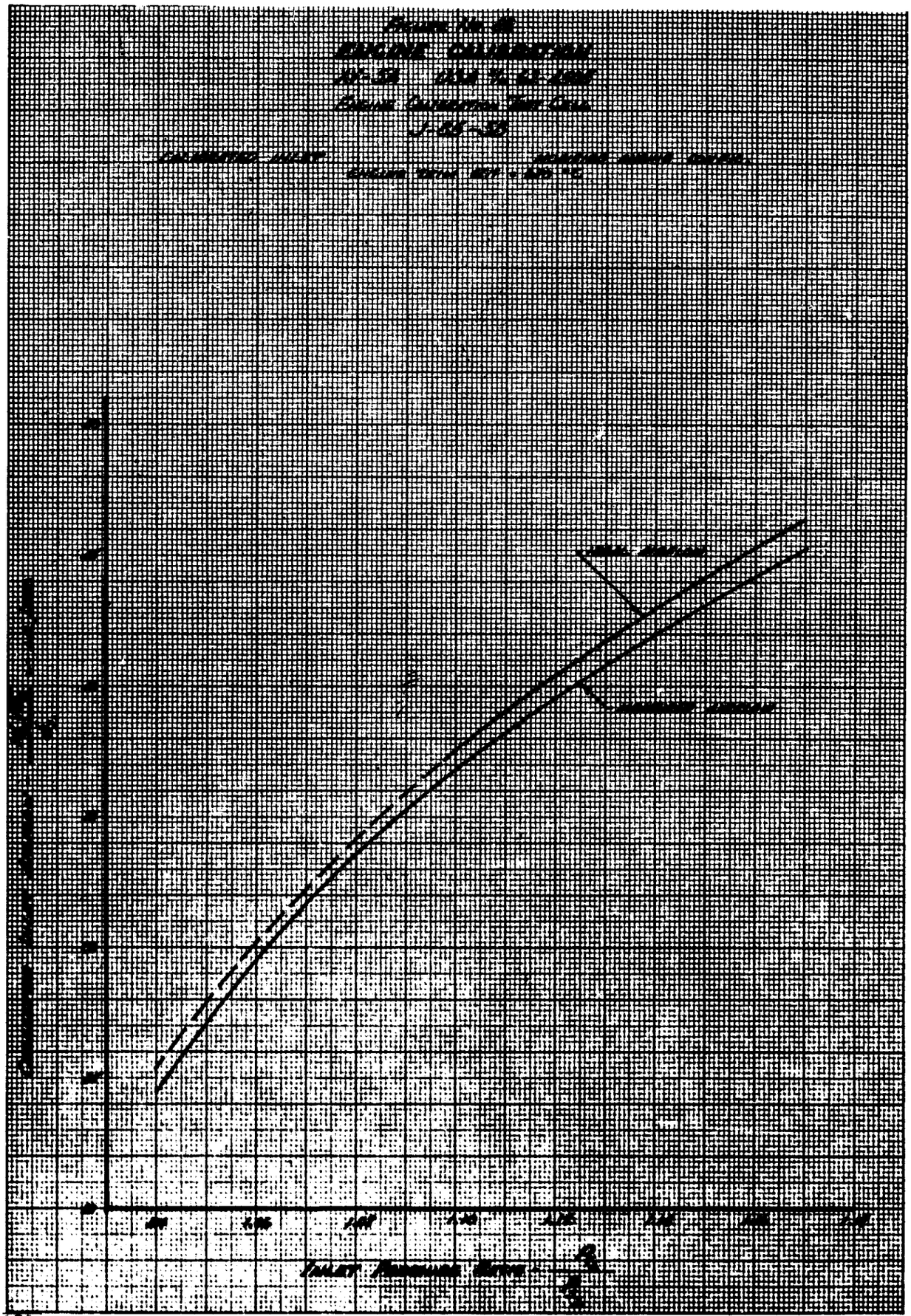

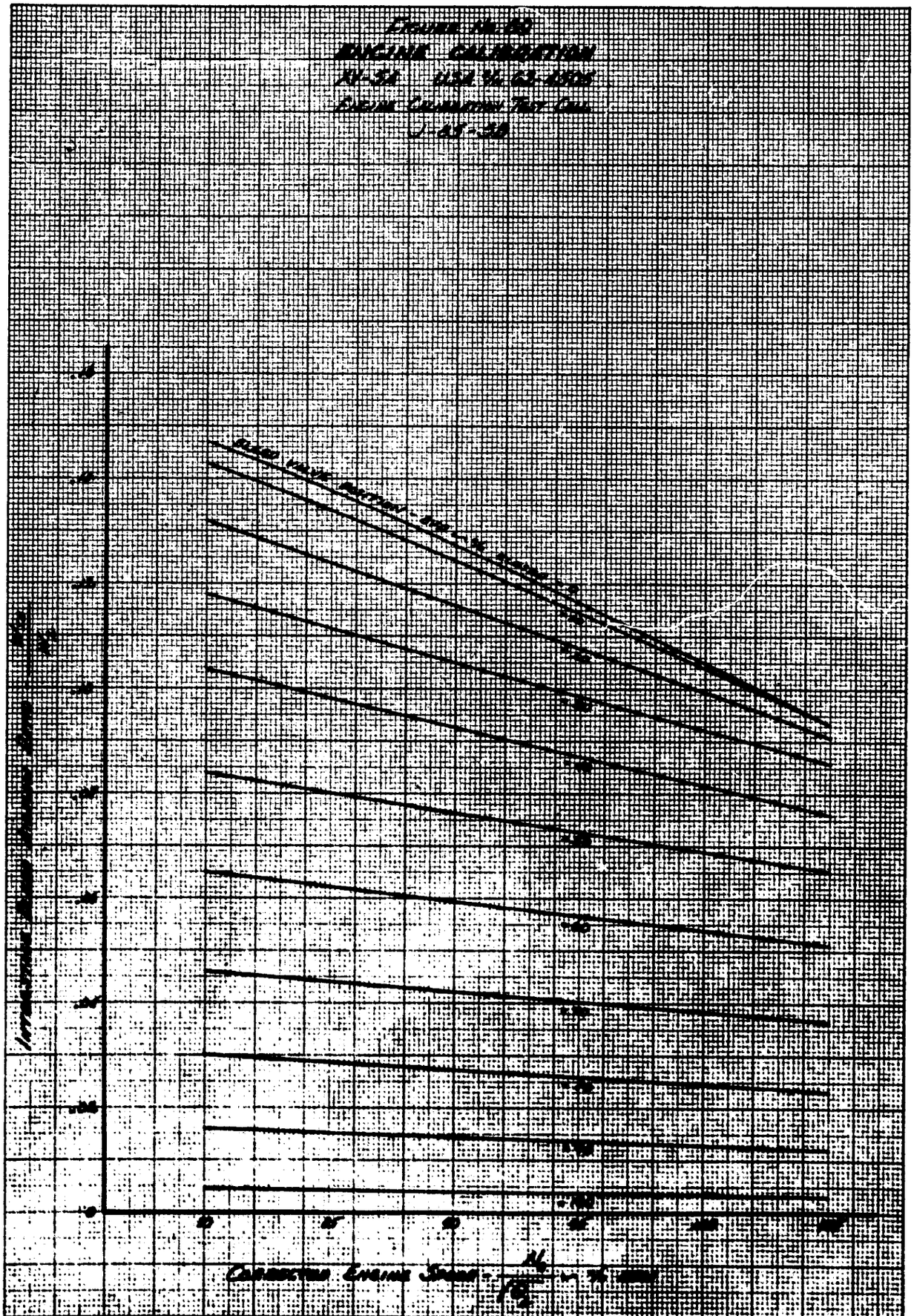

FIGURE No. 62
ENGINE CALIBRATION
XF-51 USAF No. 43-6506
ENGINE CALIBRATION TEST CELL
J-47-27

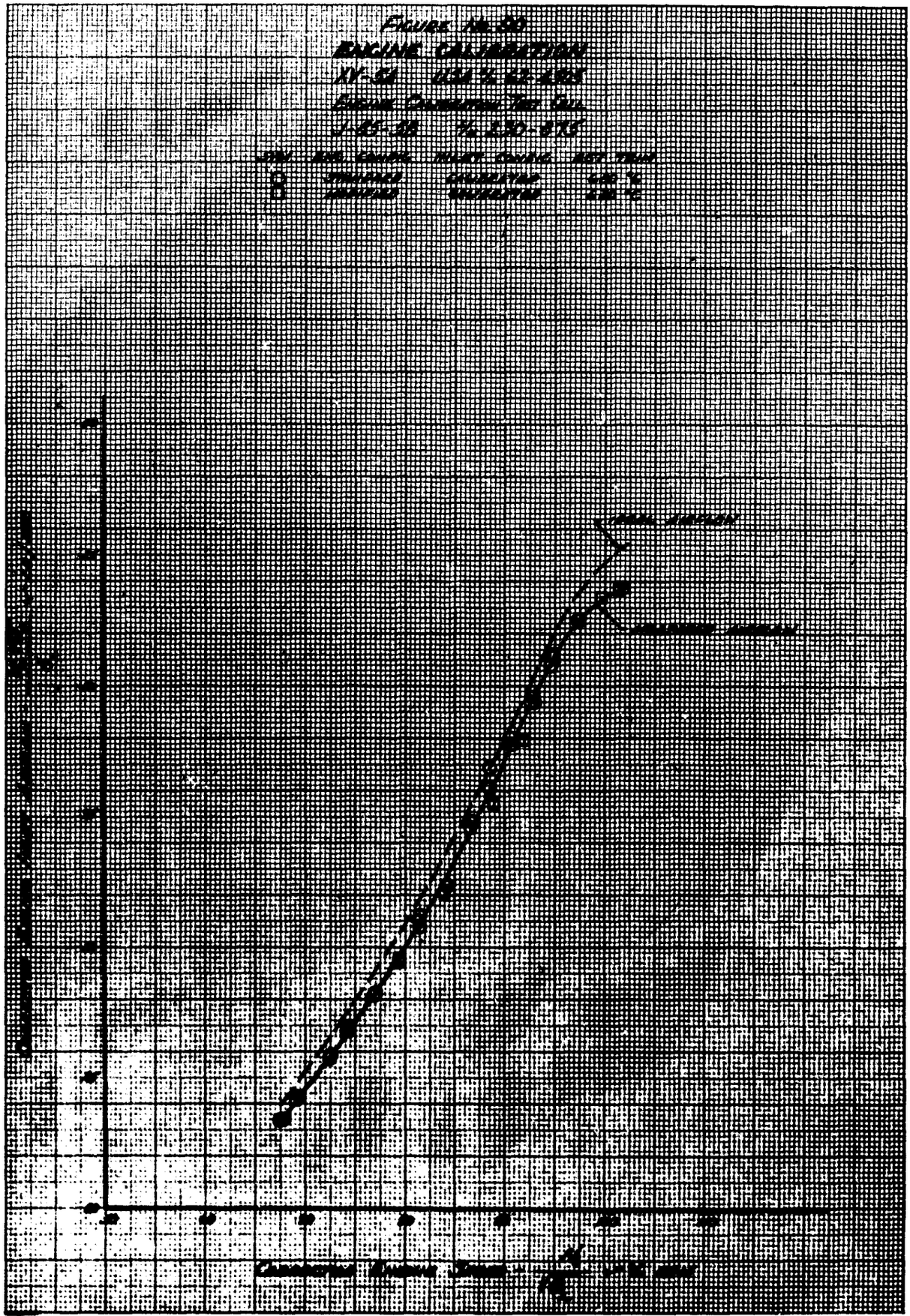

Figure No. 80
ENGINE CALIBRATION
XT-34 (534 & 42-43)
Engine Calibration Test Cell
J-65-B3 & L30-B75
Jan. 8th, 1945 Nozz. Orifice Area Test
8 Stainless Calibrated 448 in²
Jennings Variable 22 in²

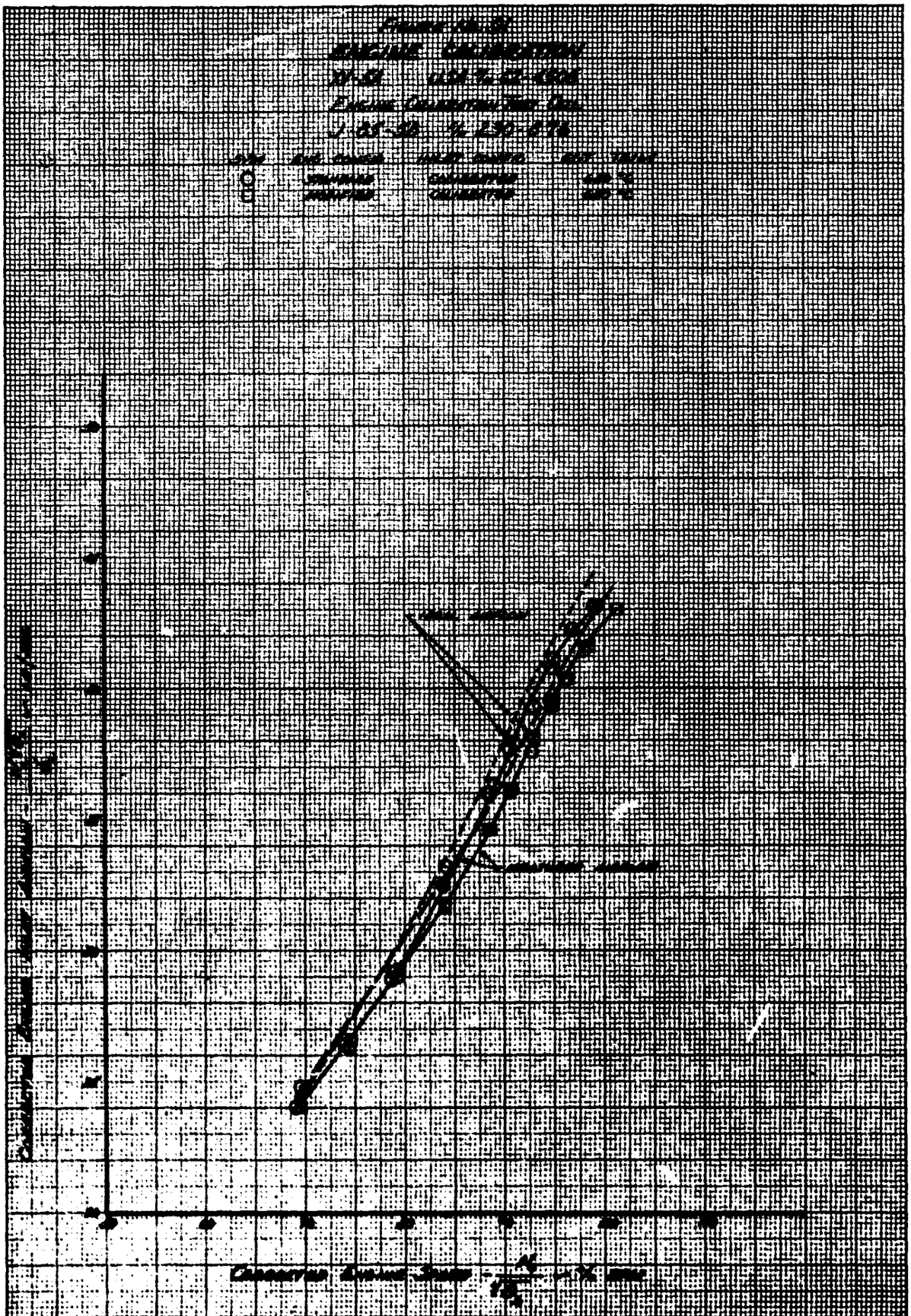

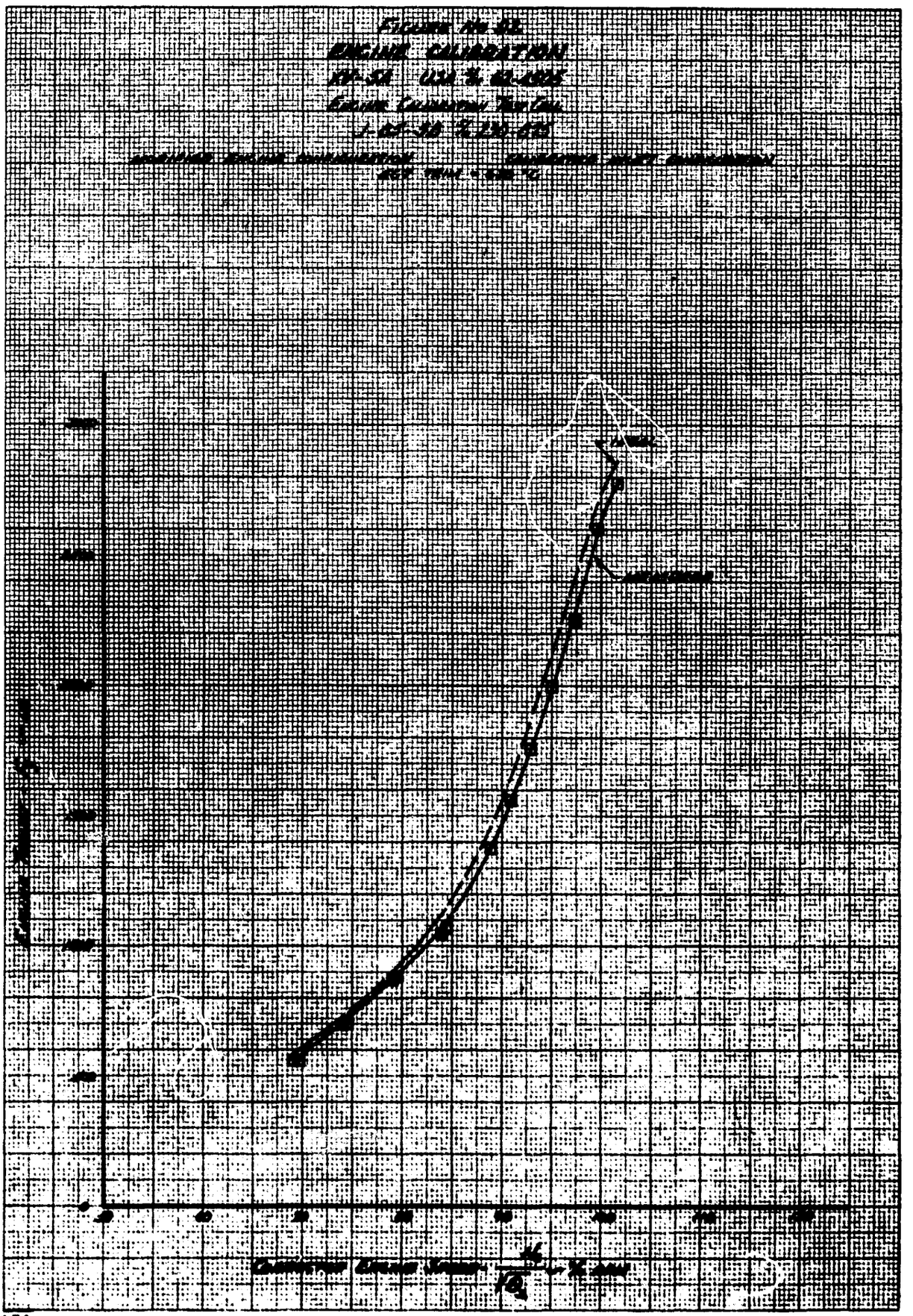

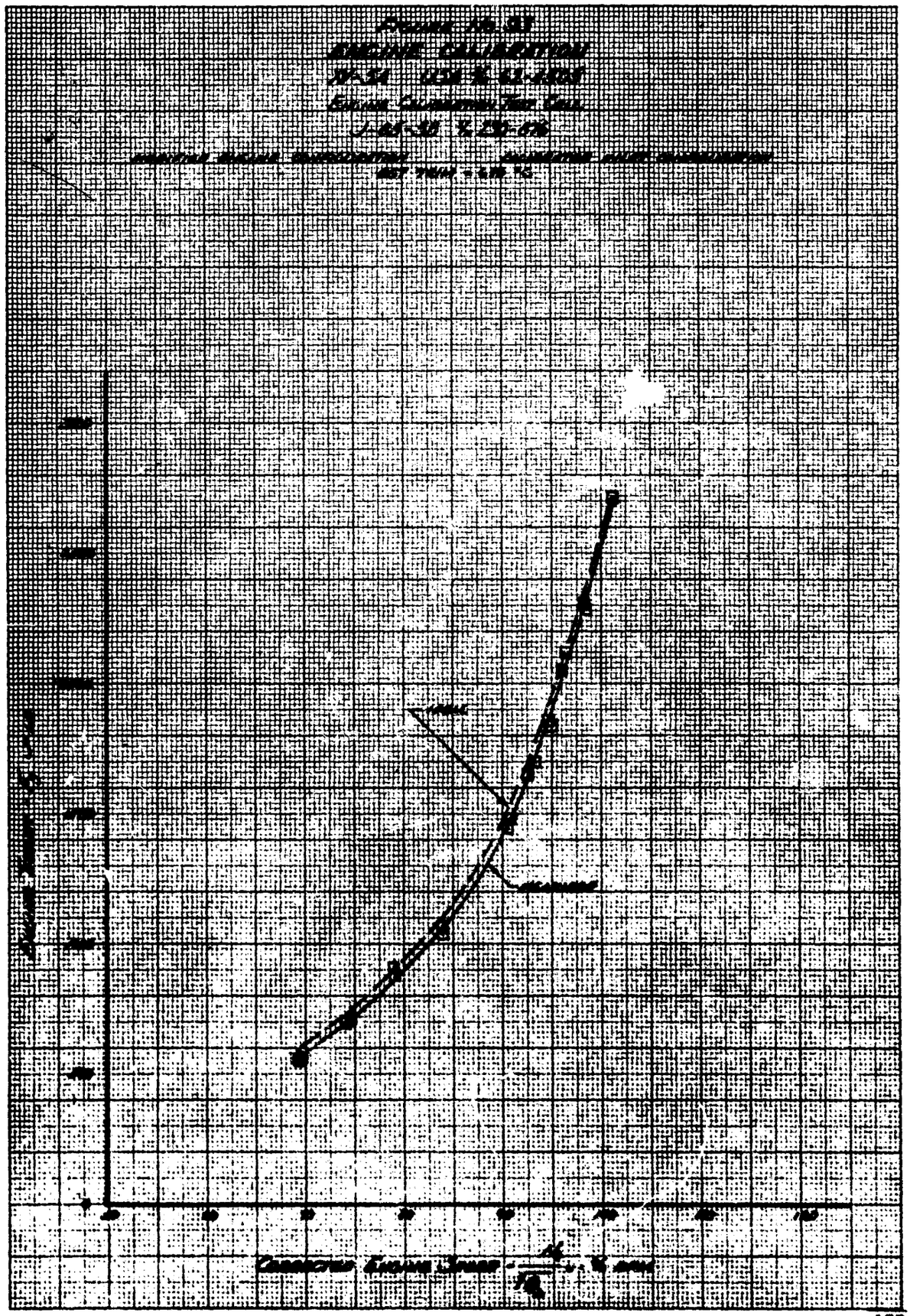

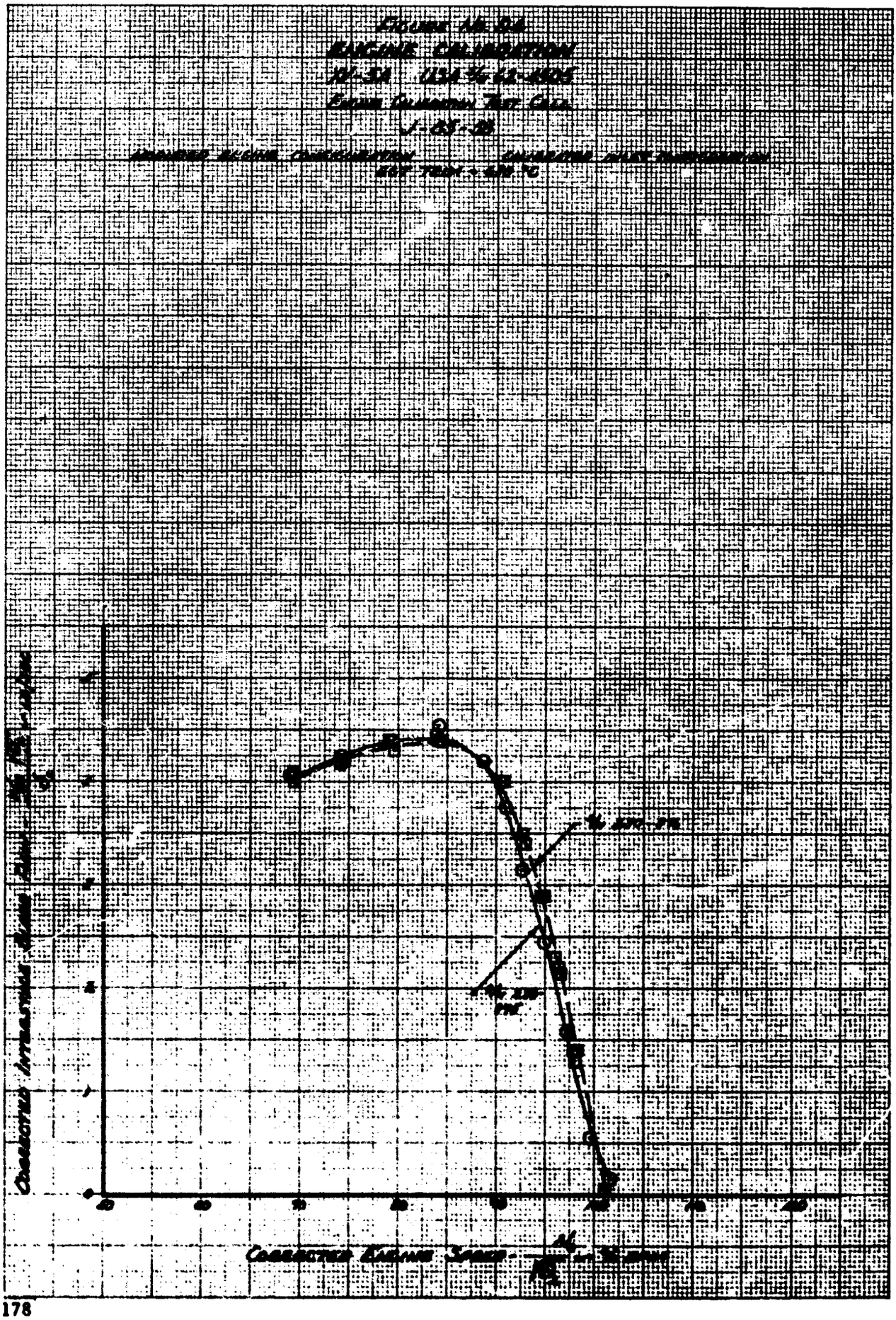
Engine Calibration
Corrected Airflow Index

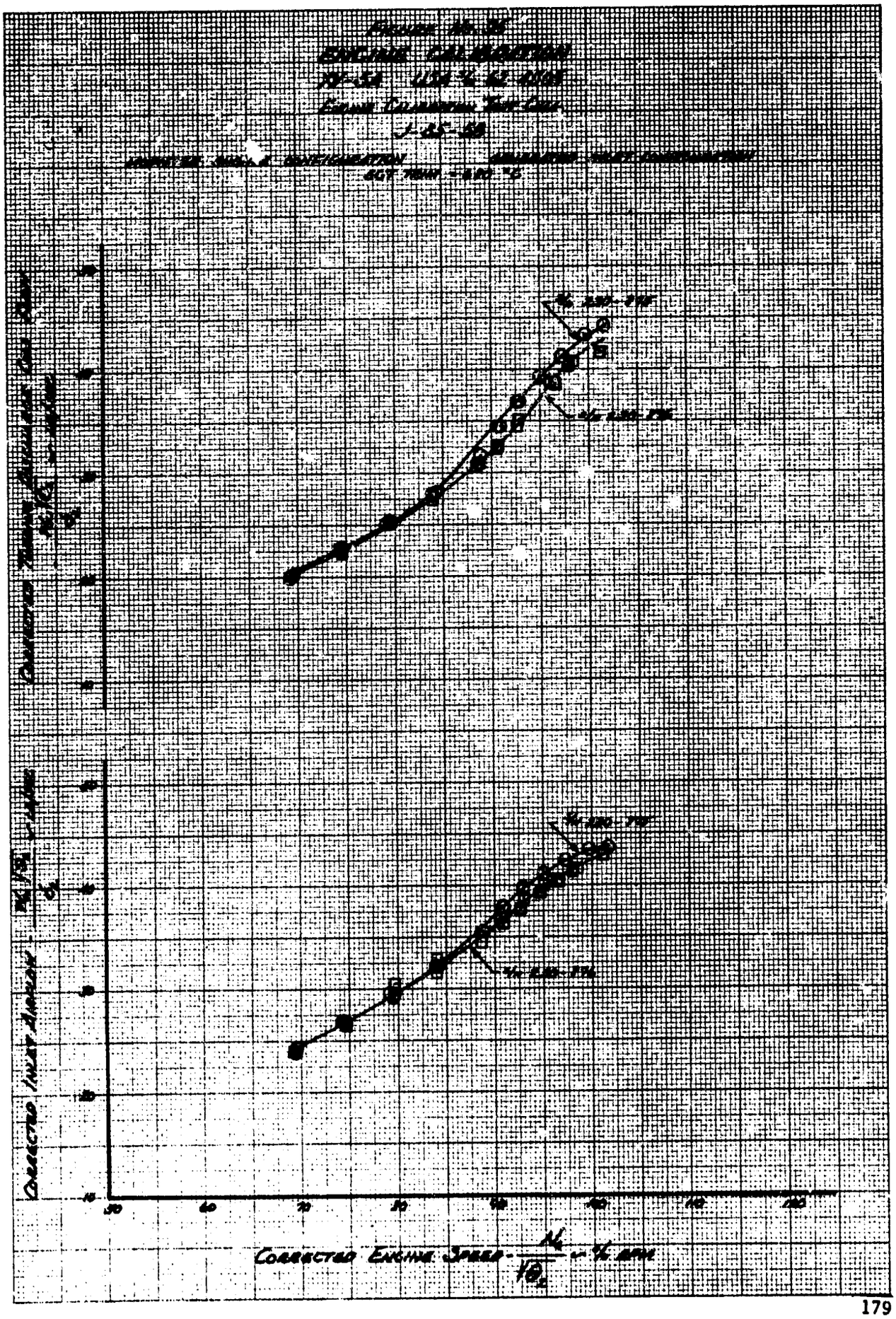
Corrected Inlet Airflow - W√θ2/δ2 - Lb/Sec
Corrected Engine Speed - N1/√θ2 - % RPM

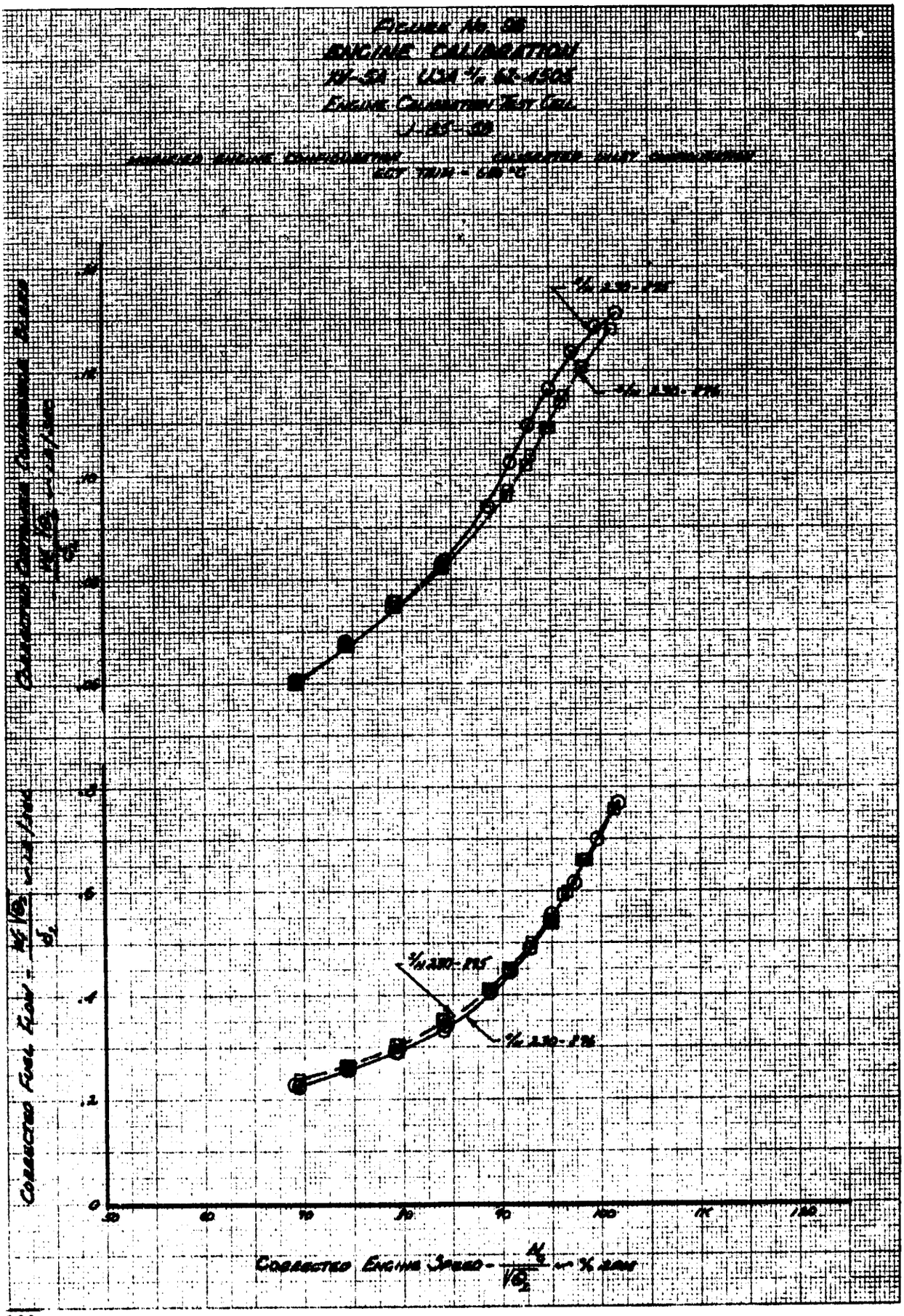
FIGURE No. 28
ENGINE CALIBRATION
Engine Calibration Test Cell
Corrected Engine Speed
Corrected Fuel Flow
0
.2
.4
.6
.8
1.0
1.2
1.4
1.6
1.8
2.0
20
40
60
80
100
120
140
160

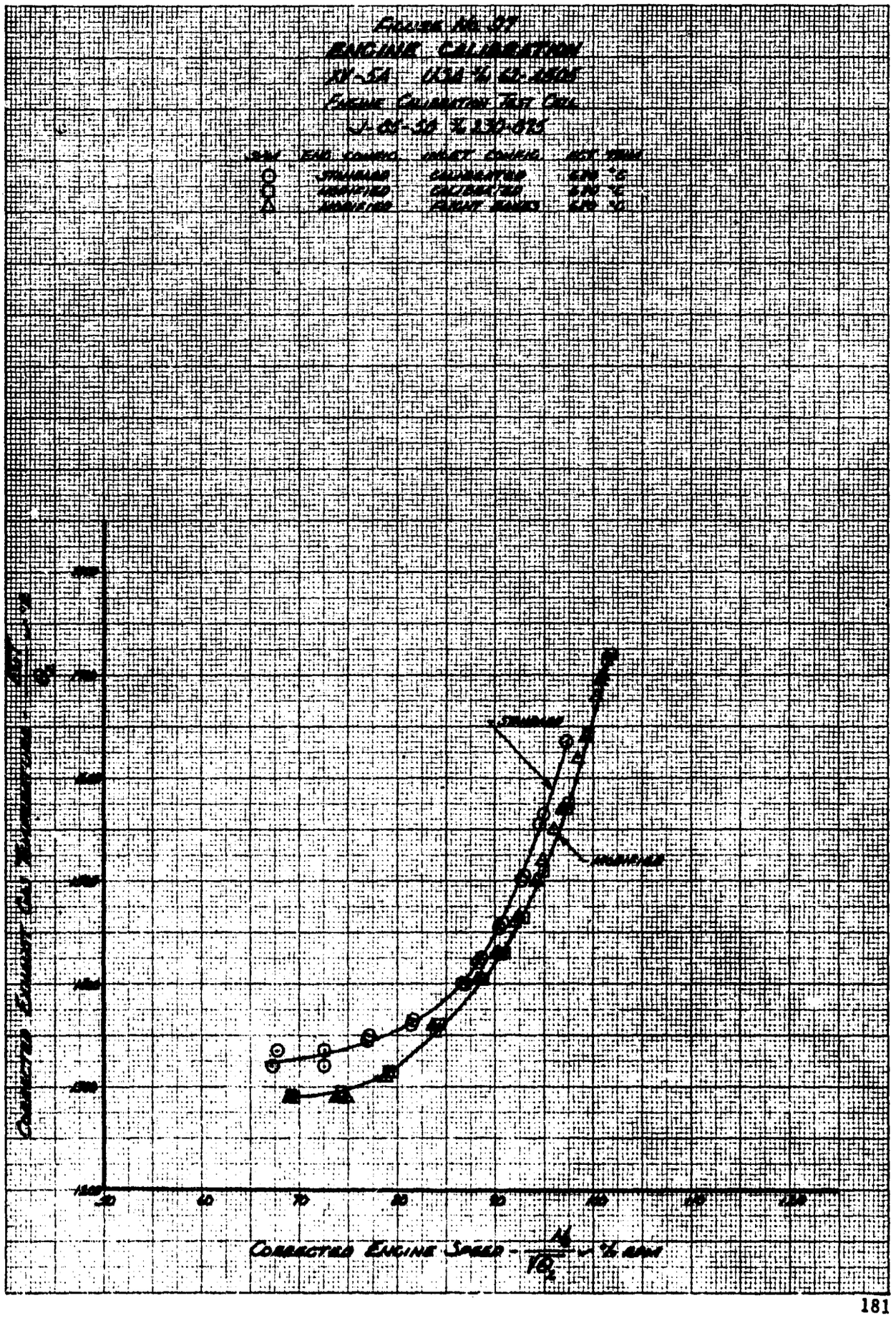
ENGINE CALIBRATION
Corrected Engine Speed - $\frac{N}{\sqrt{\theta}}$ - r.p.m.

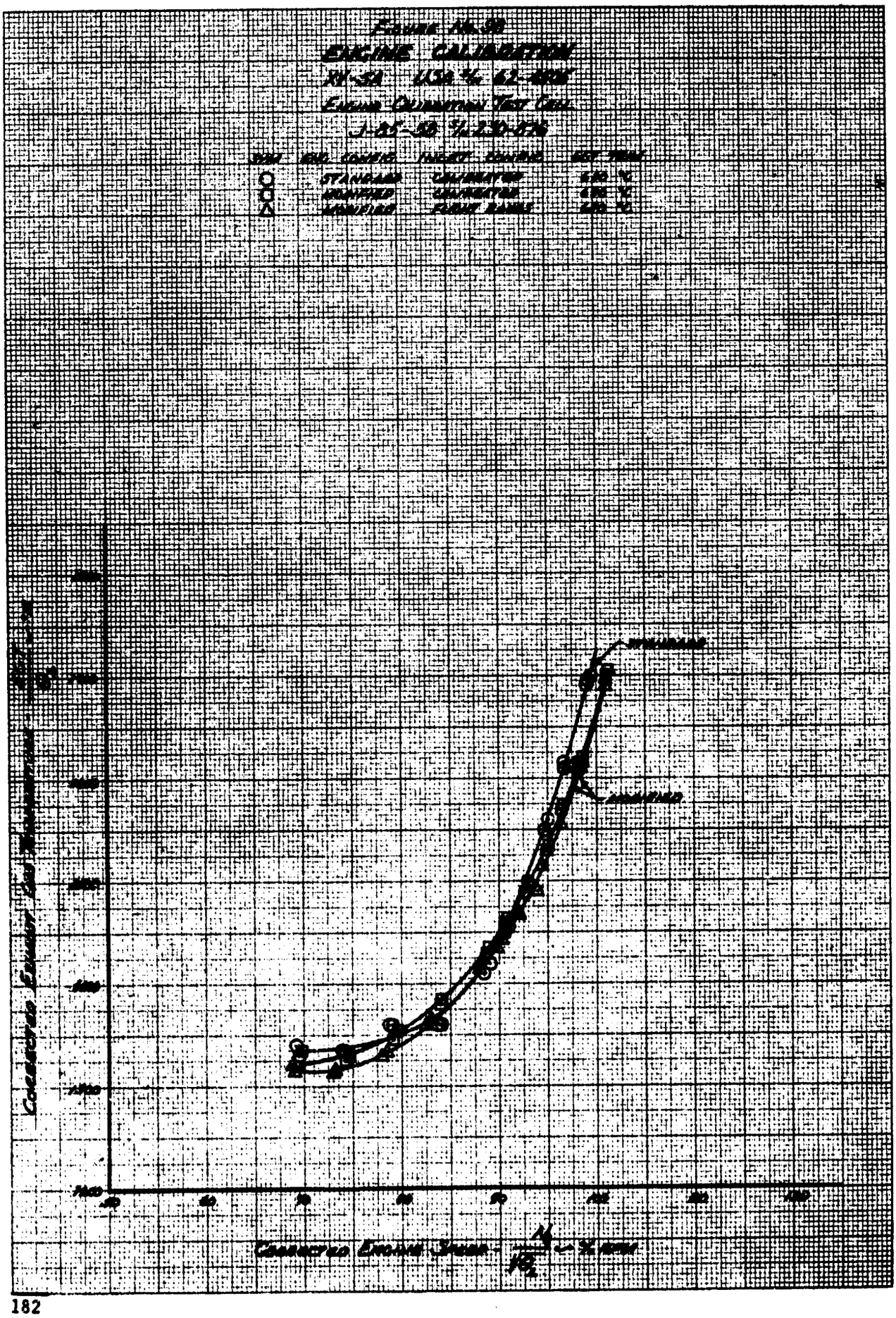
FIGURE No. 58
ENGINE CALIBRATION
XH-32 USN No. 62-4026
ENGINE CERTIFICATION TEST CELL
J-65-B7 No. 230-276
SYM. ENG. CONFIG. INLET CONFIG. DET. TEMP.
STANDARD CALIBRATED 610 °C
CALIBRATED CALIBRATED 610 °C
STANDARD FLIGHT RAKE 610 °C
STANDARD
CALIBRATED
Corrected Engine Fuel Flow
Corrected Engine Speed - N/√θ2 - % RPM

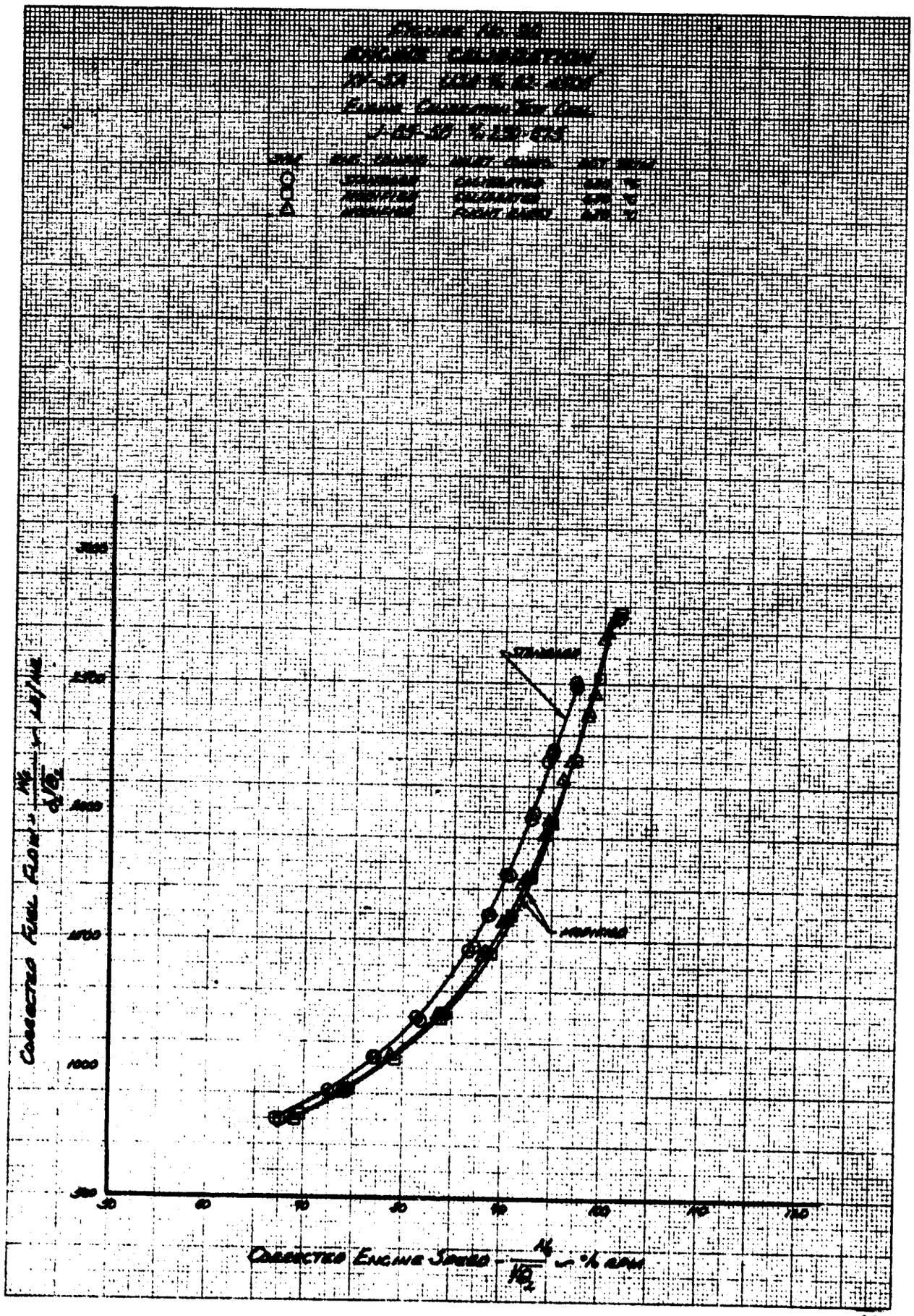
Corrected Fuel Flow - $\frac{W_f}{\delta\sqrt{\theta_2}}$ - Lb/Hr
Corrected Engine Speed - $\frac{N}{\sqrt{\theta_2}}$ - % rpm
Standard
Maximum

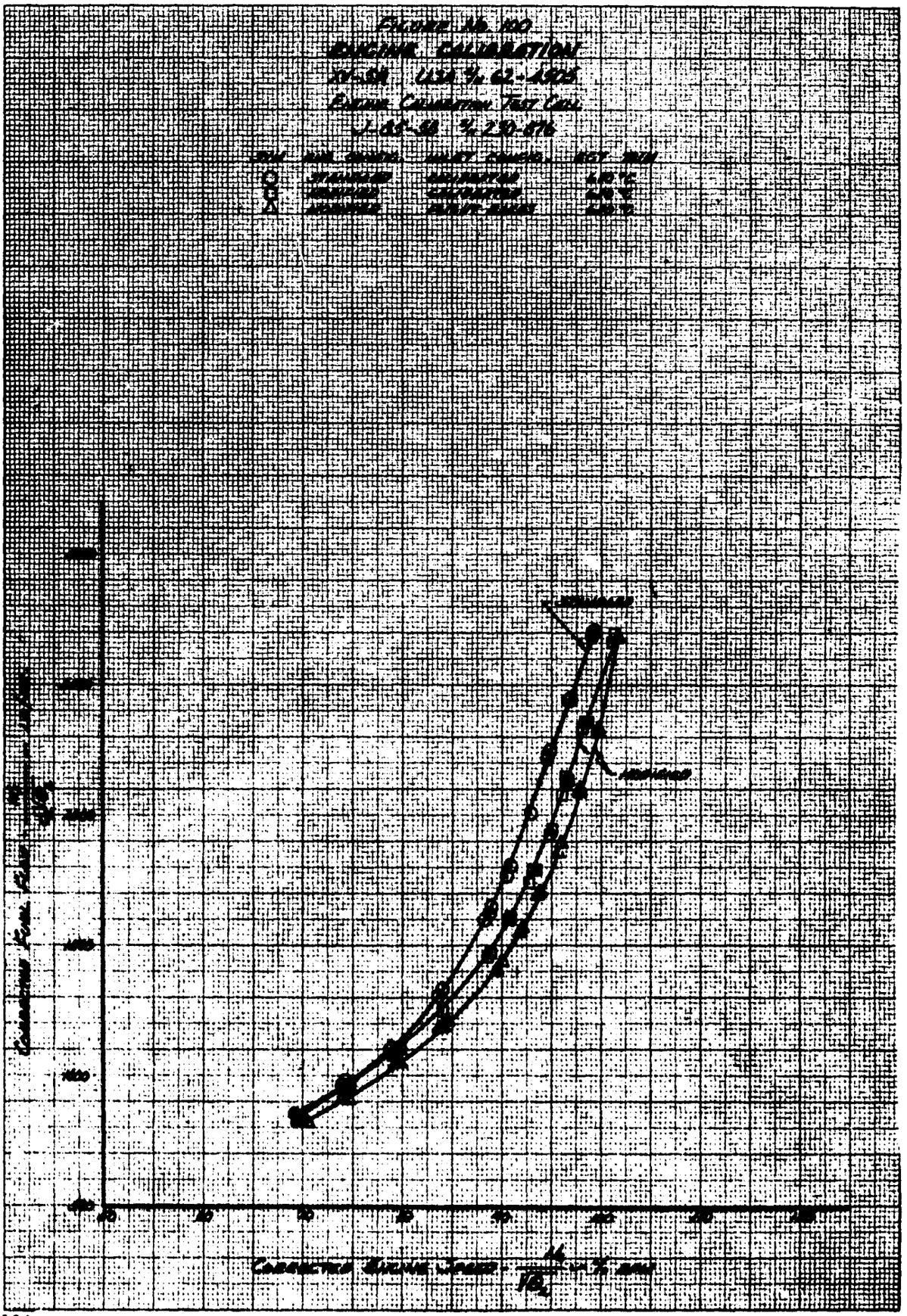
ENGINE CALIBRATION
Corrected Engine Speed, RPM
Corrected Engine Torque, Ft-Lbs

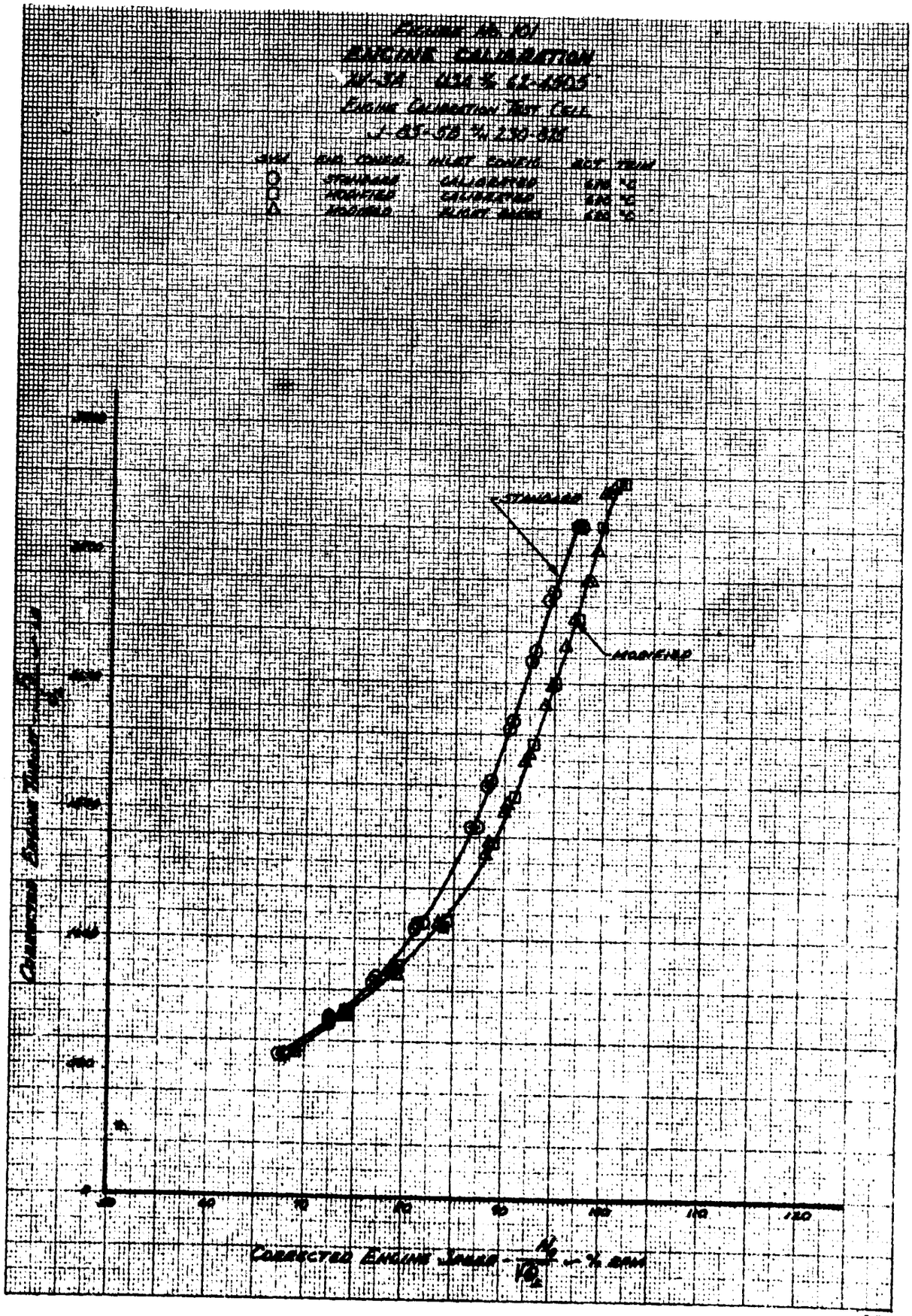
ENGINE CALIBRATION
Engine Calibration Test Cell
STANDARD
MODIFIED
Corrected Engine Speed - % RPM

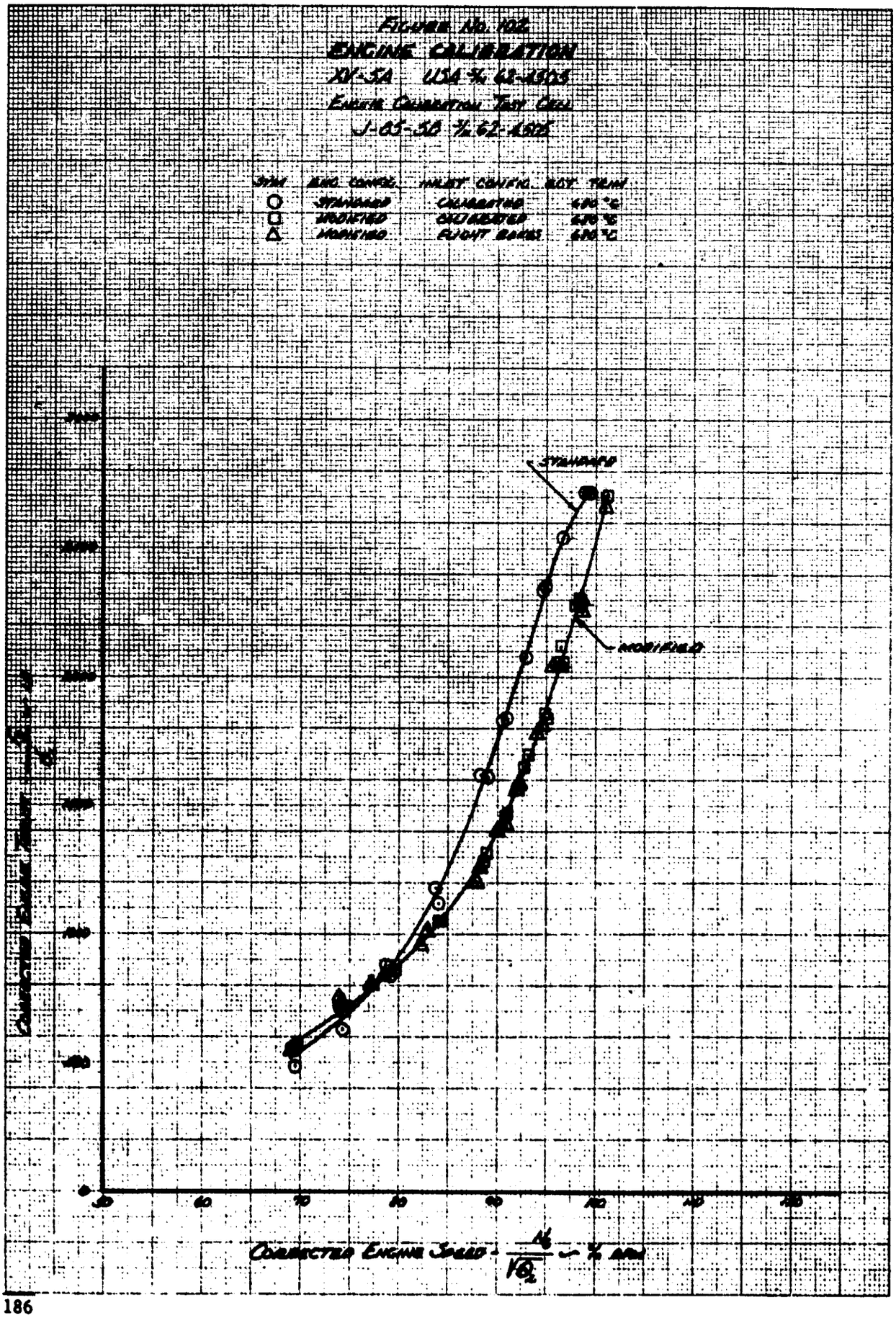
FIGURE NO. 102
ENGINE CALIBRATION
XF-5A USA No. 62-4205
ENGINE CALIBRATION TEST CELL
J-65-5D No. 62-4205
SYMBOL
BASIC CONFIG.
INLET CONFIG.
EXIT TEMP.
STANDARD
CALIBRATED
MODIFIED
CALIBRATED
MODIFIED
FLIGHT BOARD
STANDARD
MODIFIED
CORRECTED ENGINE SPEED - N/√θ2 - % RPM

FIGURE No. 103

ENGINE CALIBRATION

XV-5A USA S/N 62-4505

ENGINE CALIBRATION TEST CELL

J-85-5A S/N 130-810

SYM.	BAR. CONTR.	INLET CONFIG.	RUN	TRIM
○	STANDARD	UNCALIBRATED	430	°C
□	PERFECTED	CALIBRATED	430	°C
△	MODIFIED	FLIGHT BARS	430	°C

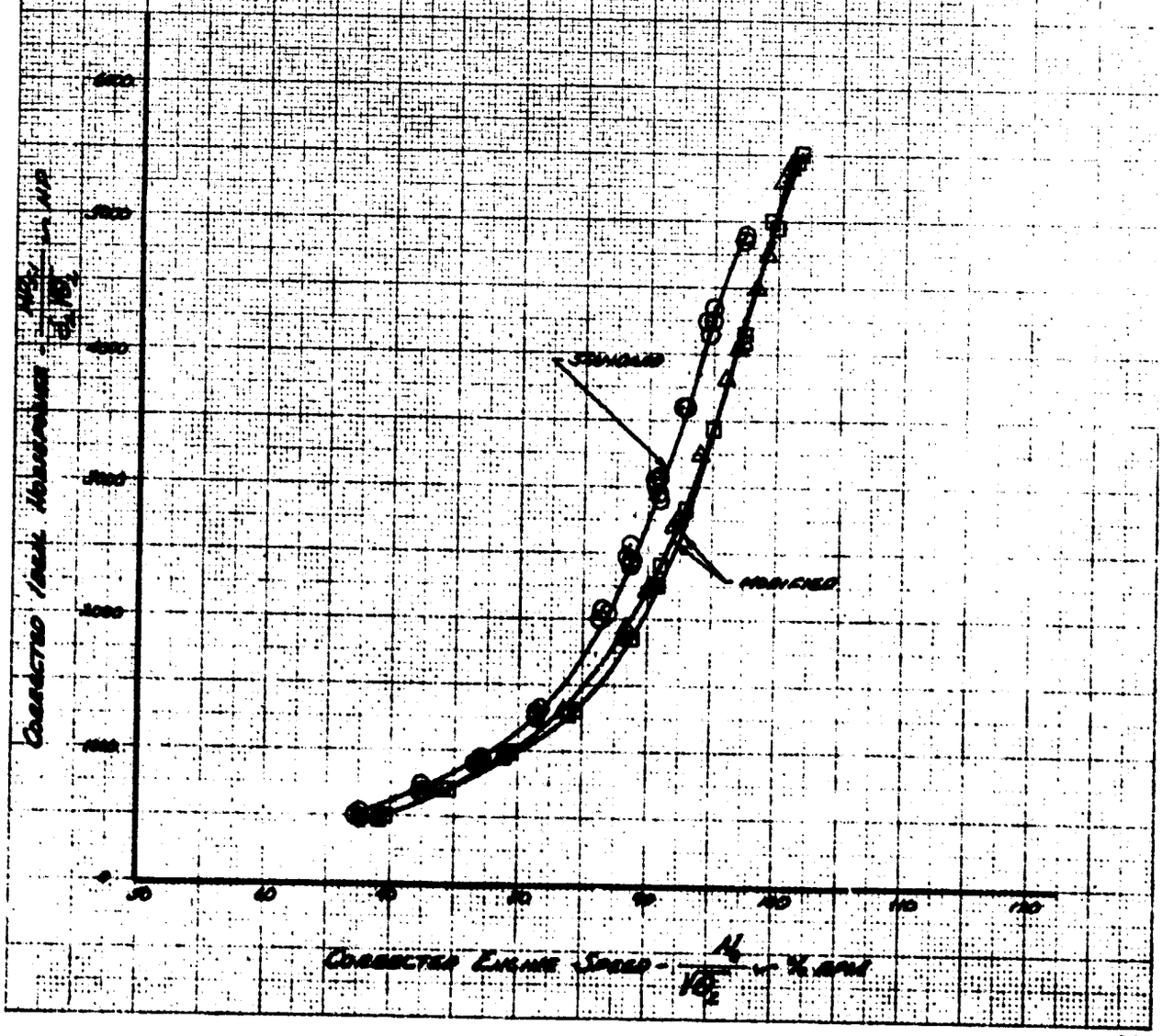

FIGURE NO. 104

ENGINE CALIBRATION

XV-5A USA S/N 62-4505

ENGINE CALIBRATION TEST CELL

J-85-5D S/N 230-076

SYM	EXH. CONFIG.	INLET CONFIG.	EGT TRIM
○	STANDARD	CALIBRATED	680 °C
□	MODIFIED	CALIBRATED	670 °C
△	MODIFIED	FLIGHT DOORS	670 °C

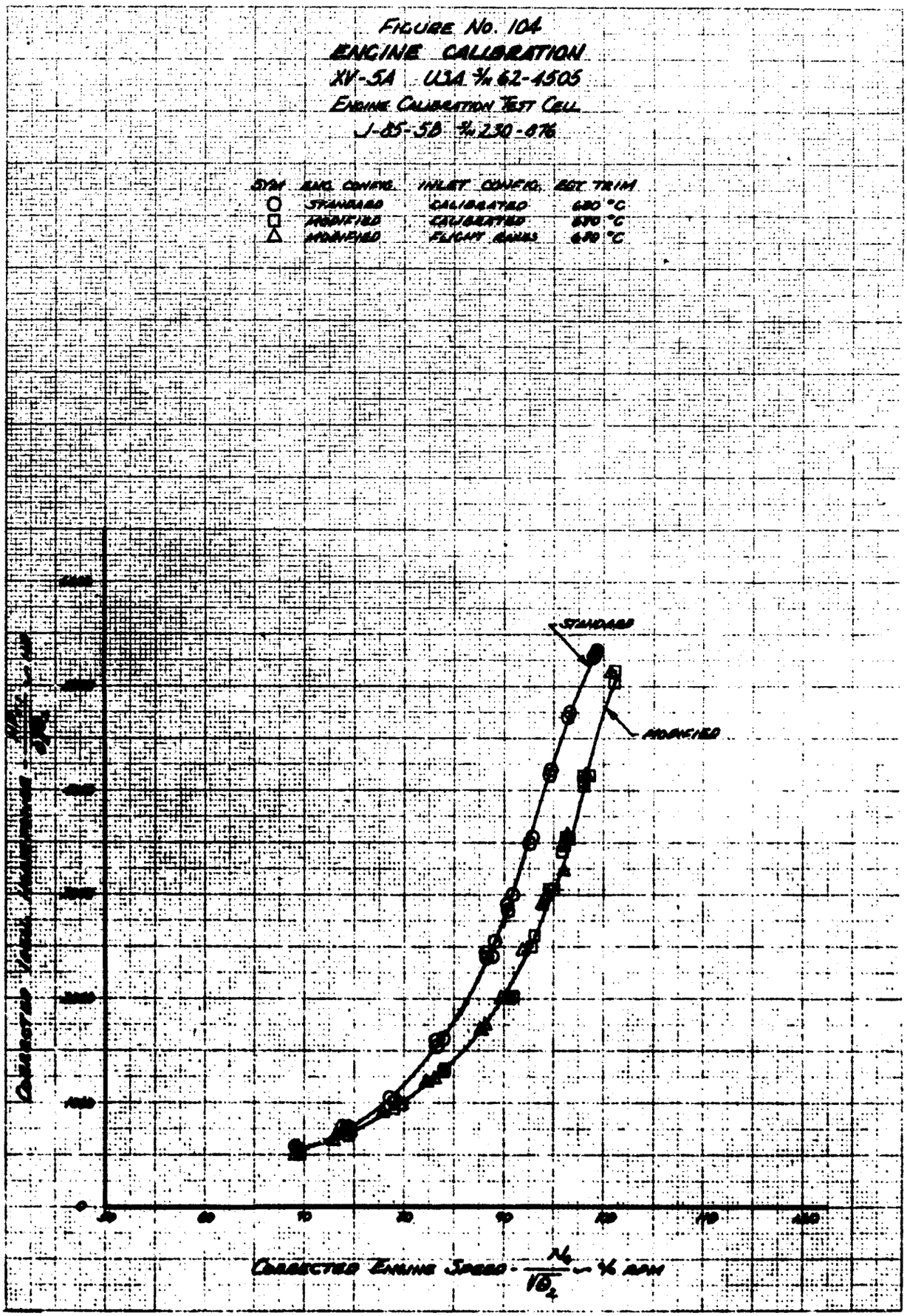

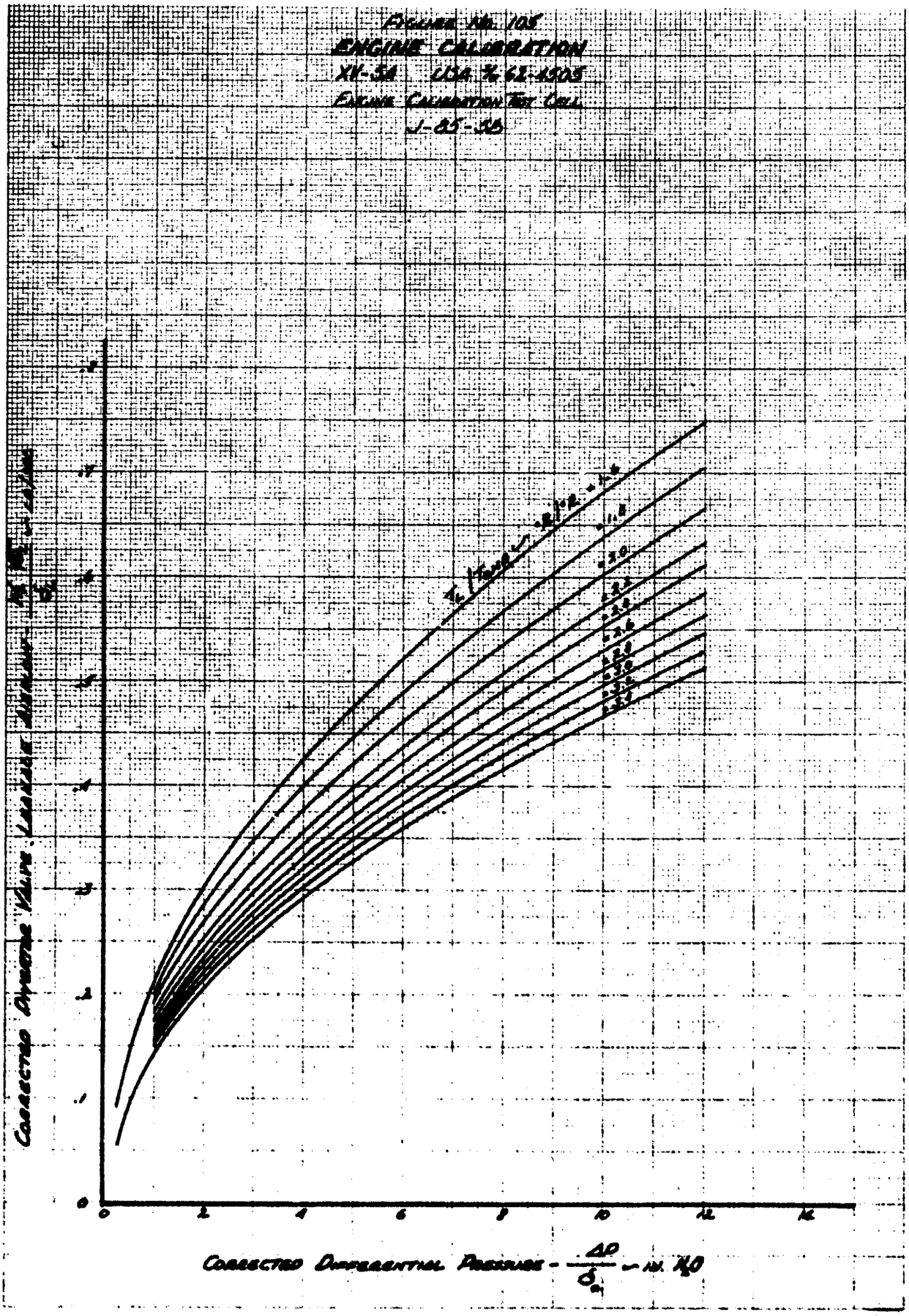
FIGURE NO. 105
ENGINE CALIBRATION
XH-34 LOT NO. 62-4905
ENGINE CALIBRATION TEST CELL
J-85-5B
CORRECTED DIFFERENTIAL PRESSURE - $\frac{\Delta P}{\delta_2}$ - IN. H2O
0
2
4
6
8
10
12

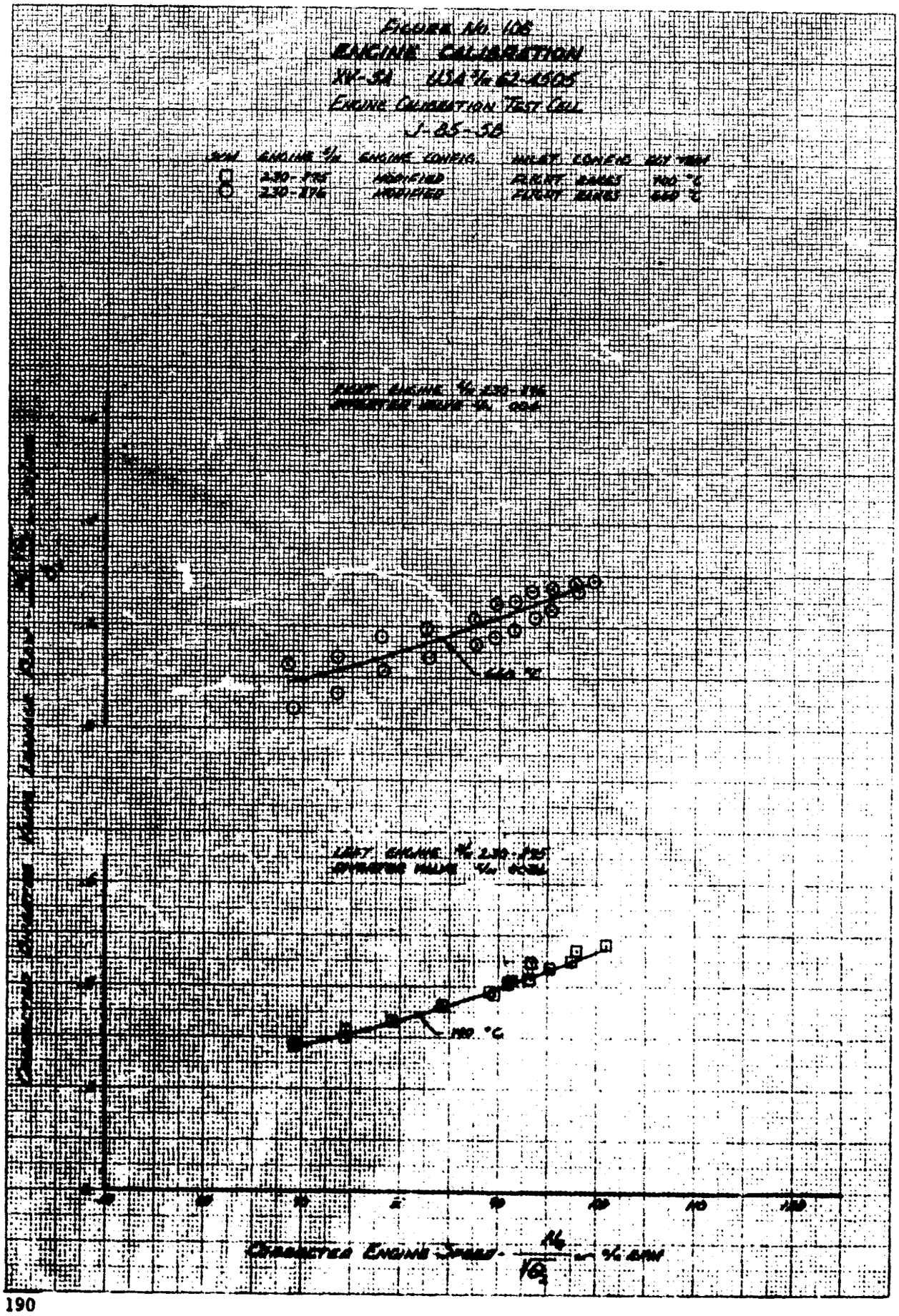
FIGURE NO. 106
ENGINE CALIBRATION
XH-3A USA No 62-4405
ENGINE CALIBRATION TEST CELL
J-35-3B
SYM. ENGINE No. ENGINE CONFIG. INLET CONFIG. JET TEMP
2.30-195 MODIFIED FLIGHT RAKES 760 °C
2.30-196 MODIFIED FLIGHT RAKES 650 °C
FLIGHT ENGINE No 230-196
APPROVED VALUE No. 0.04
LAST ENGINE No 230-195
APPROVED VALUE No. 0.04
760 °C
650 °C
CORRECTED ENGINE SPEED - N1/√θ2 - % RPM

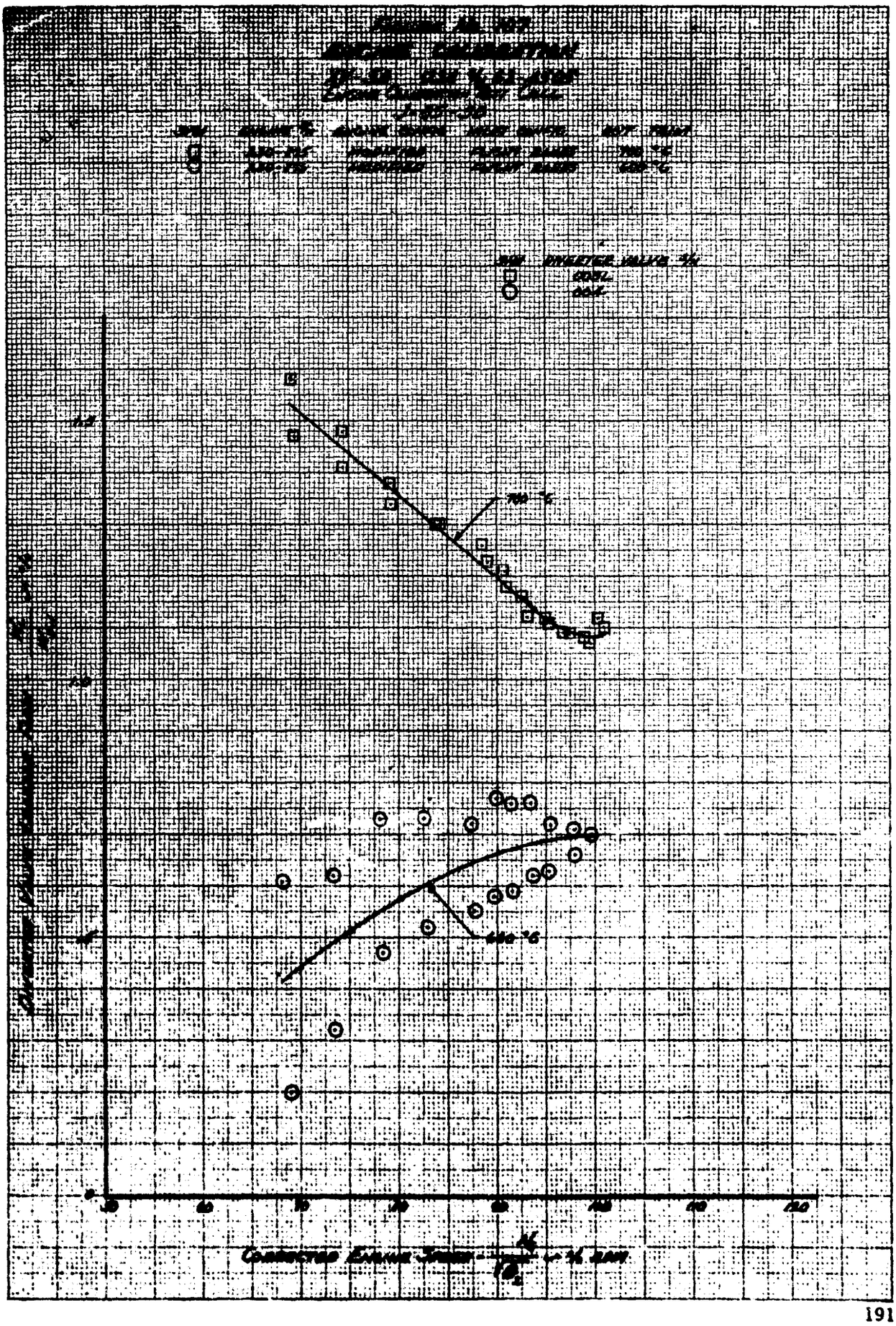

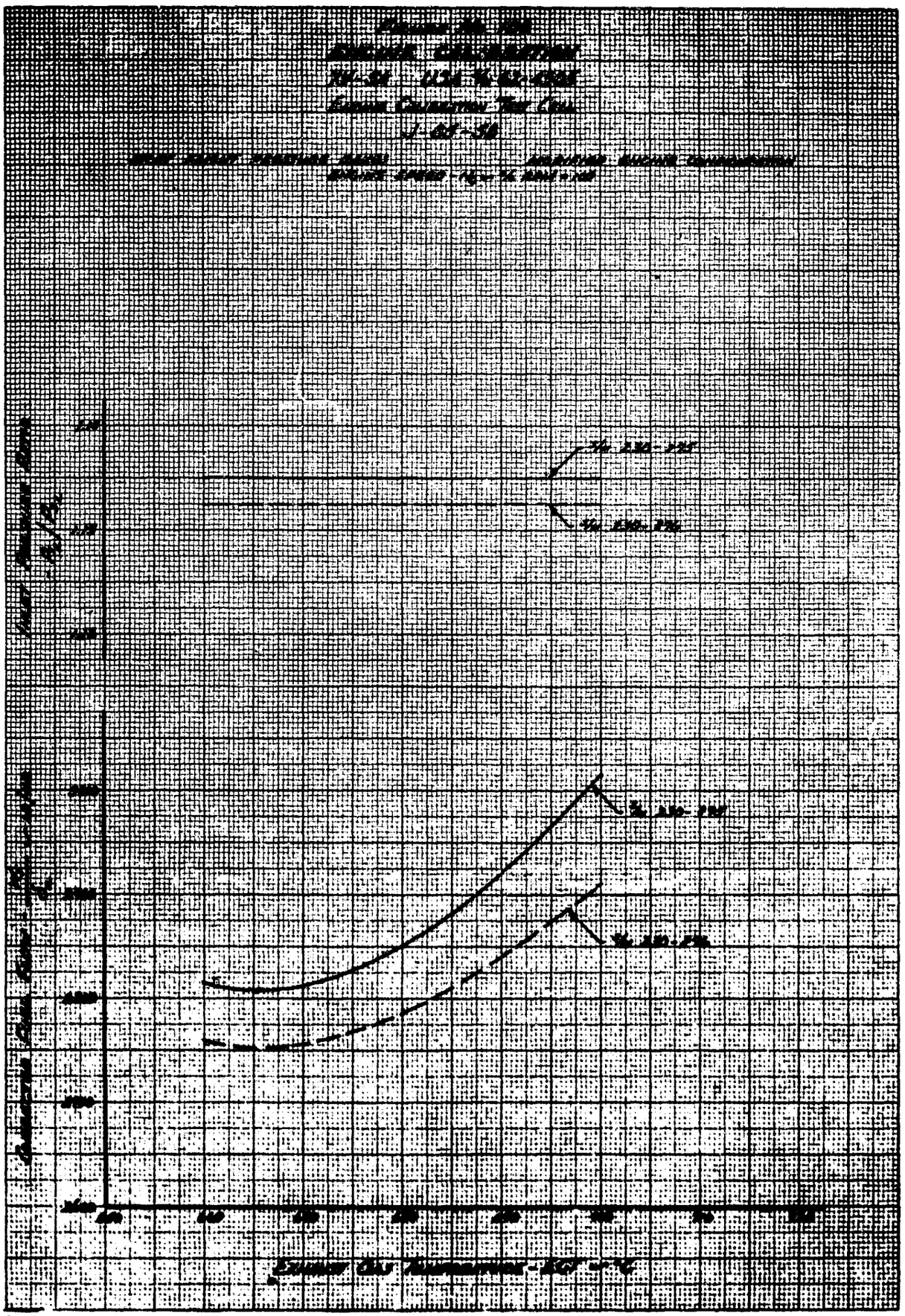

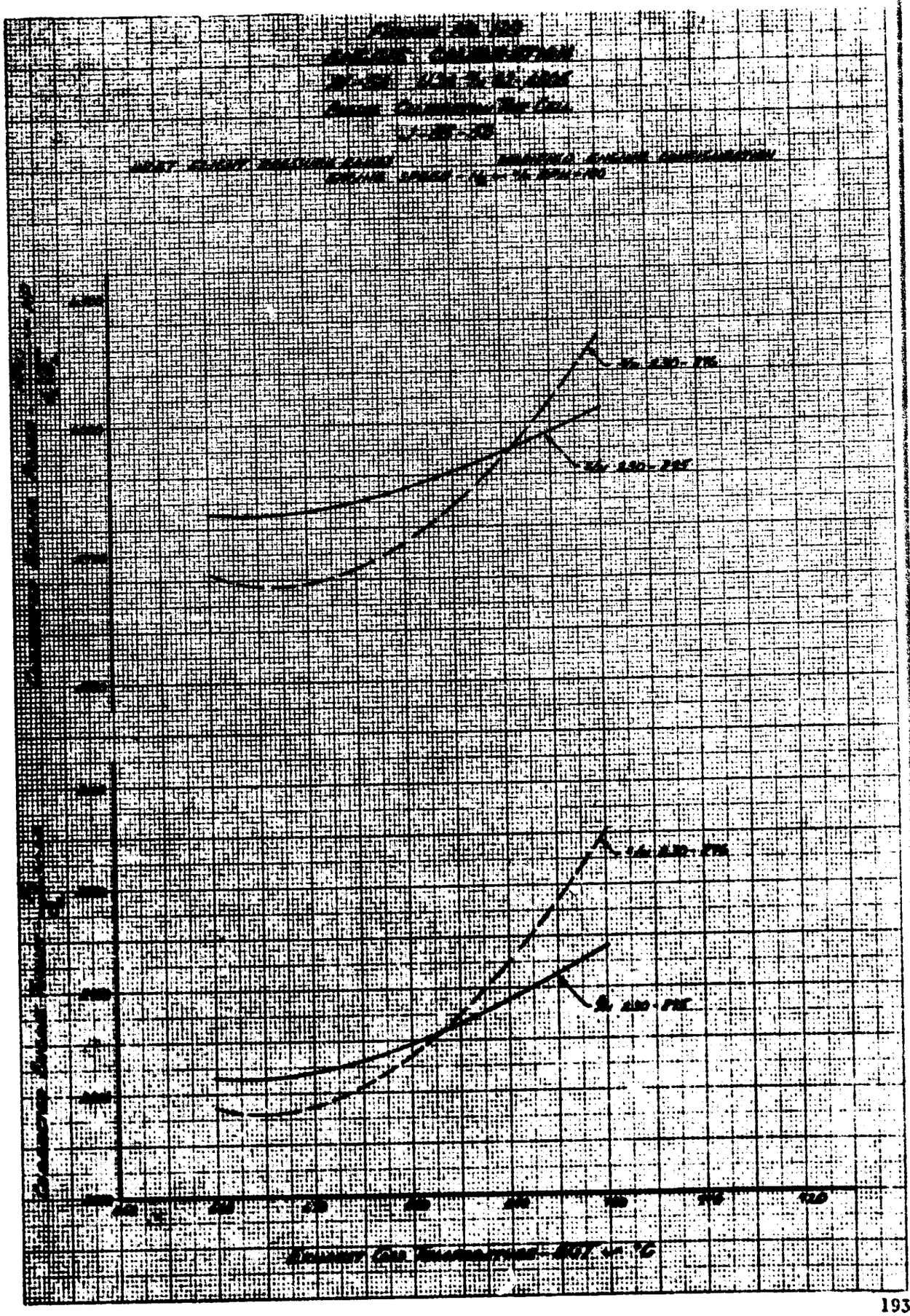

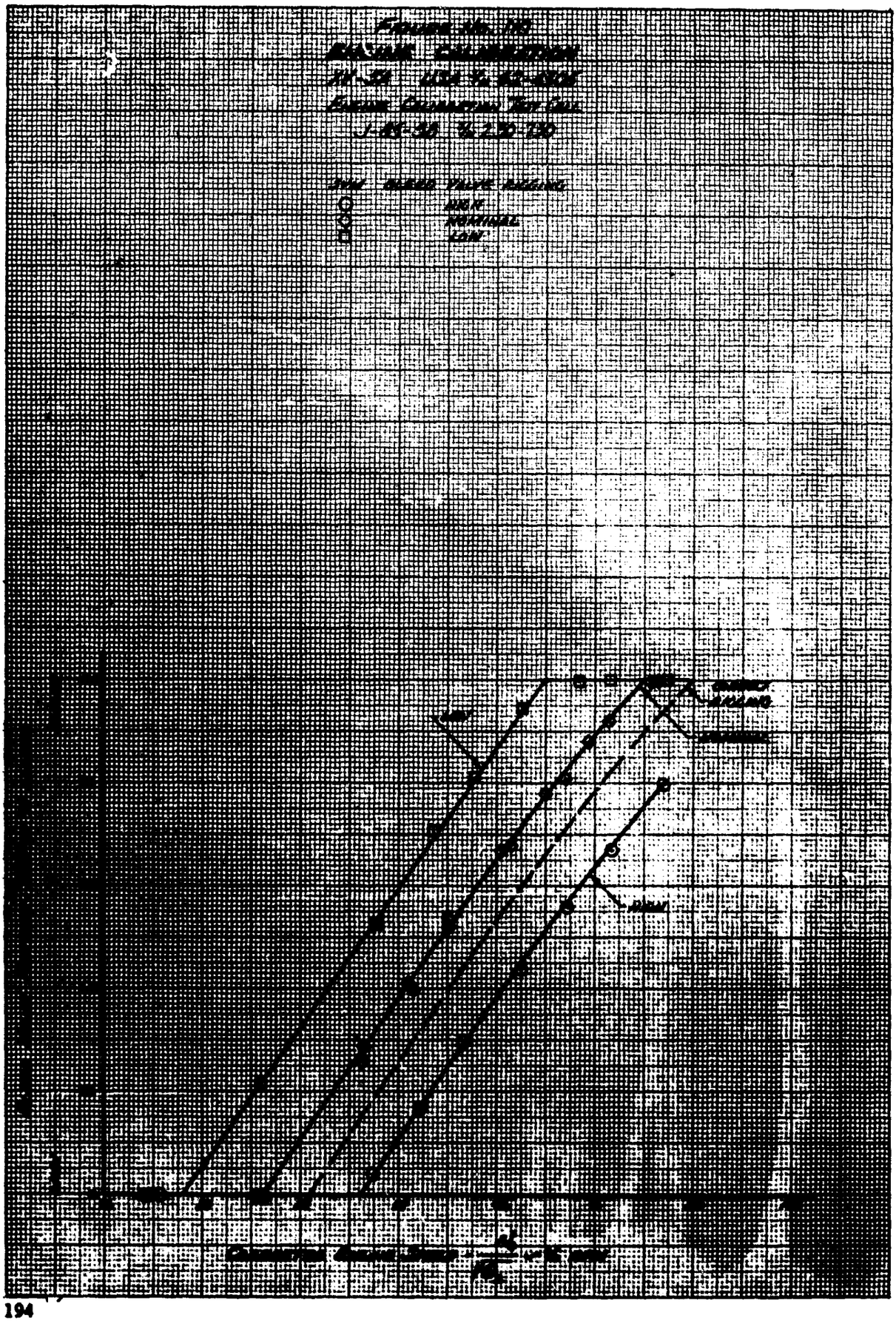

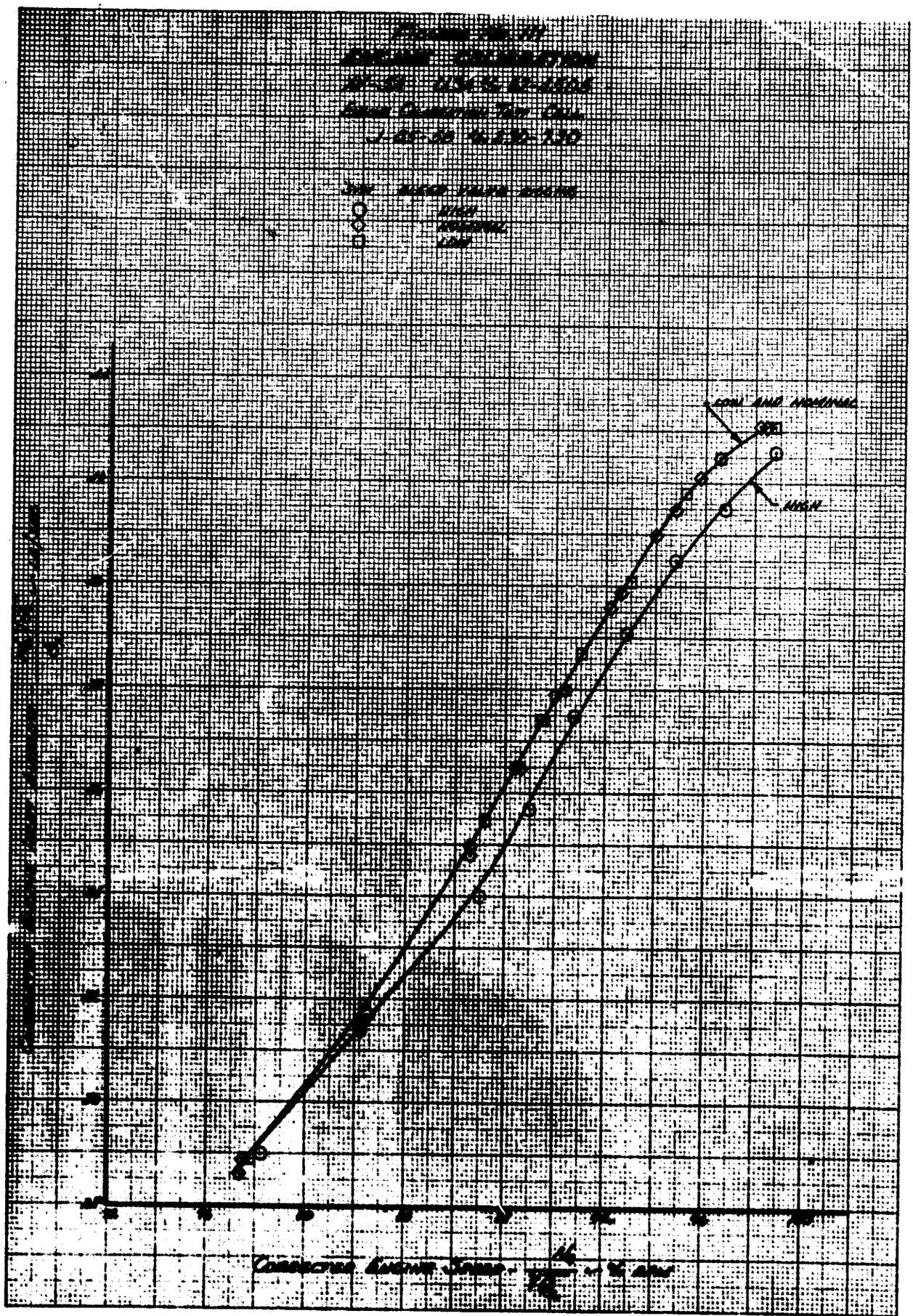
LOW AND MEDIUM
HIGH

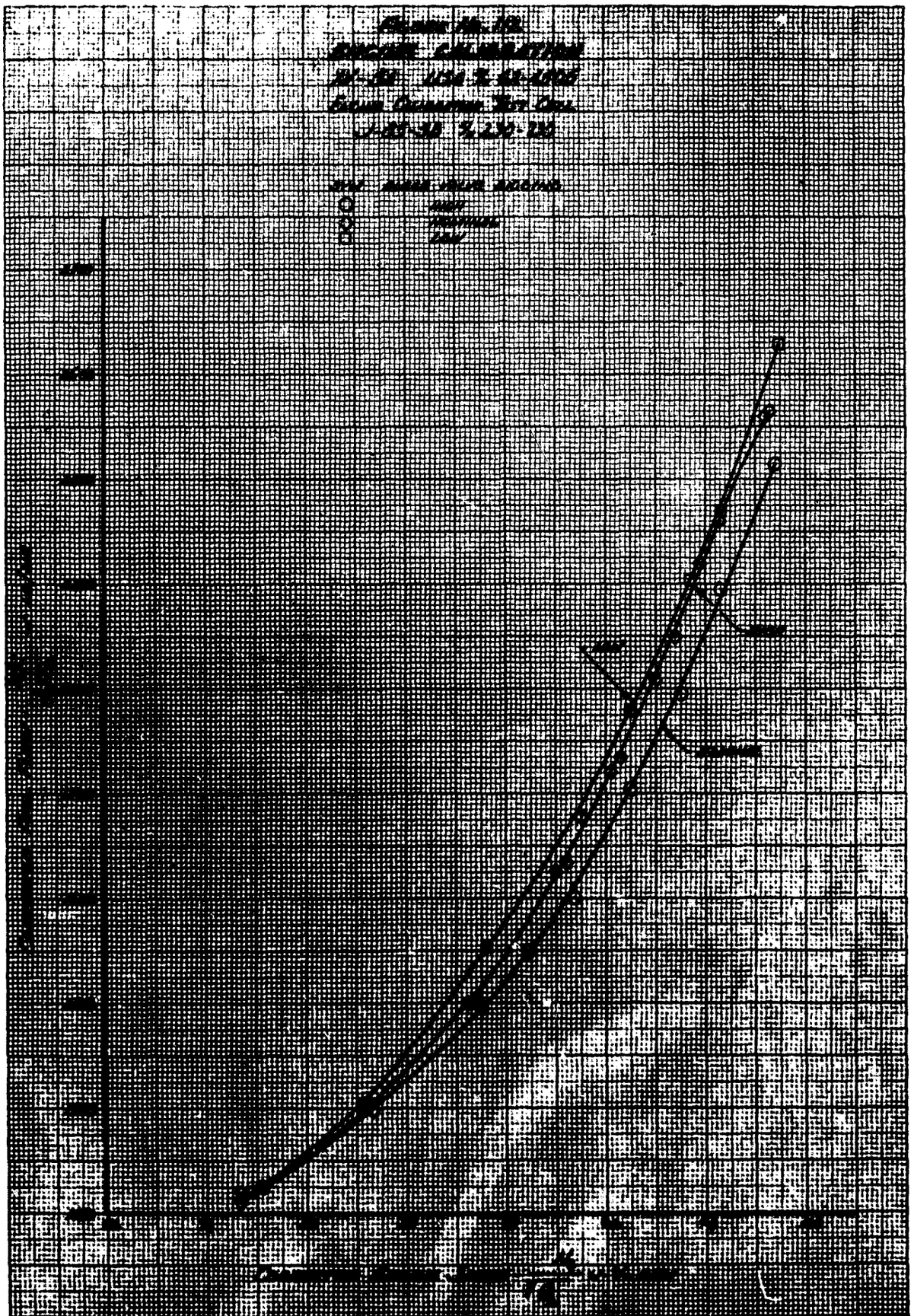

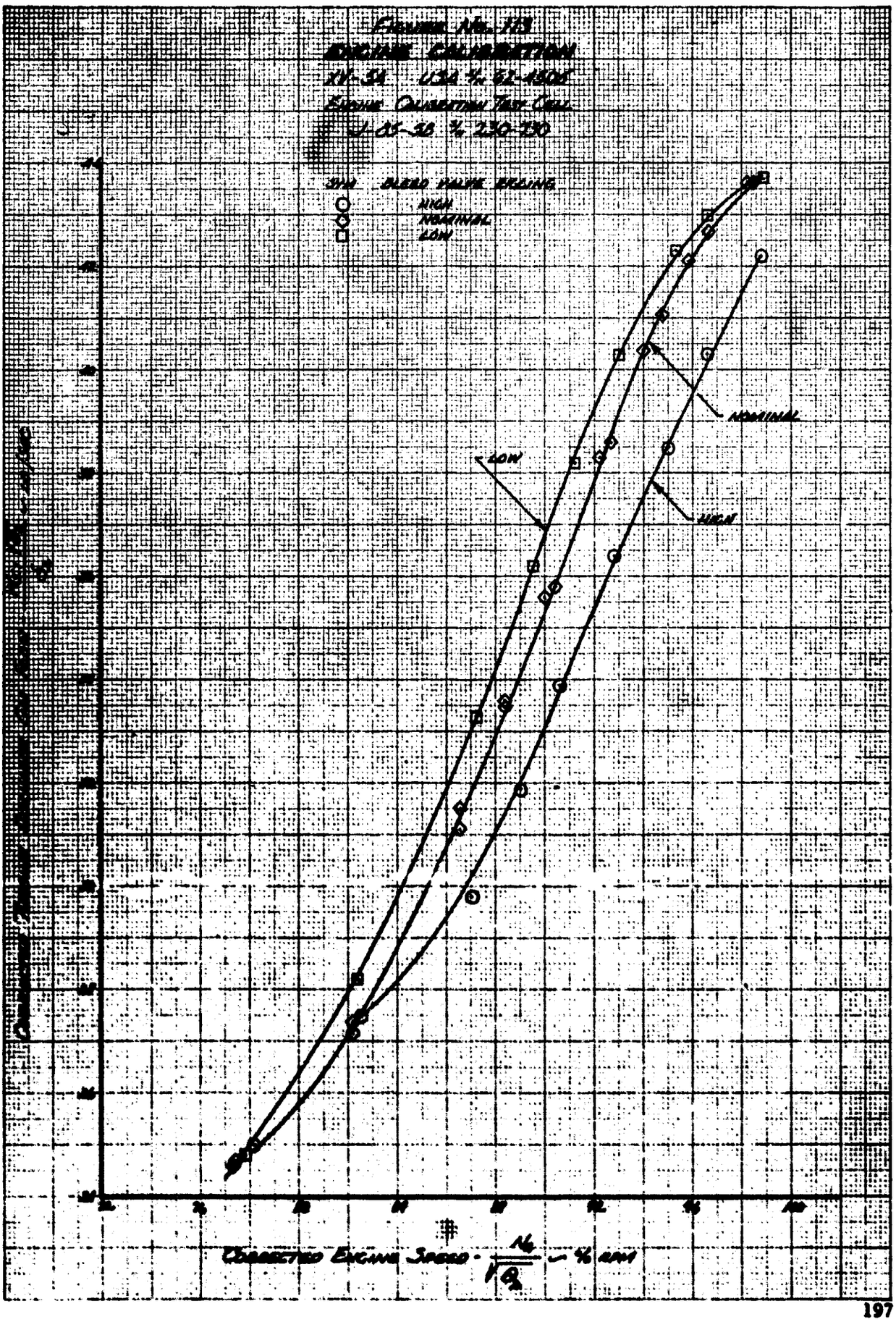
Figure No. 113
ENGINE CALIBRATION
XH-34 USA No. 52-1505
Engine Calibration Test Cell
J-35-35 & 230-230
BLEED VALVE RIGGING
HIGH
NOMINAL
LOW
NOMINAL
LOW
HIGH
Corrected Engine Speed - N/√θ2 - % RPM

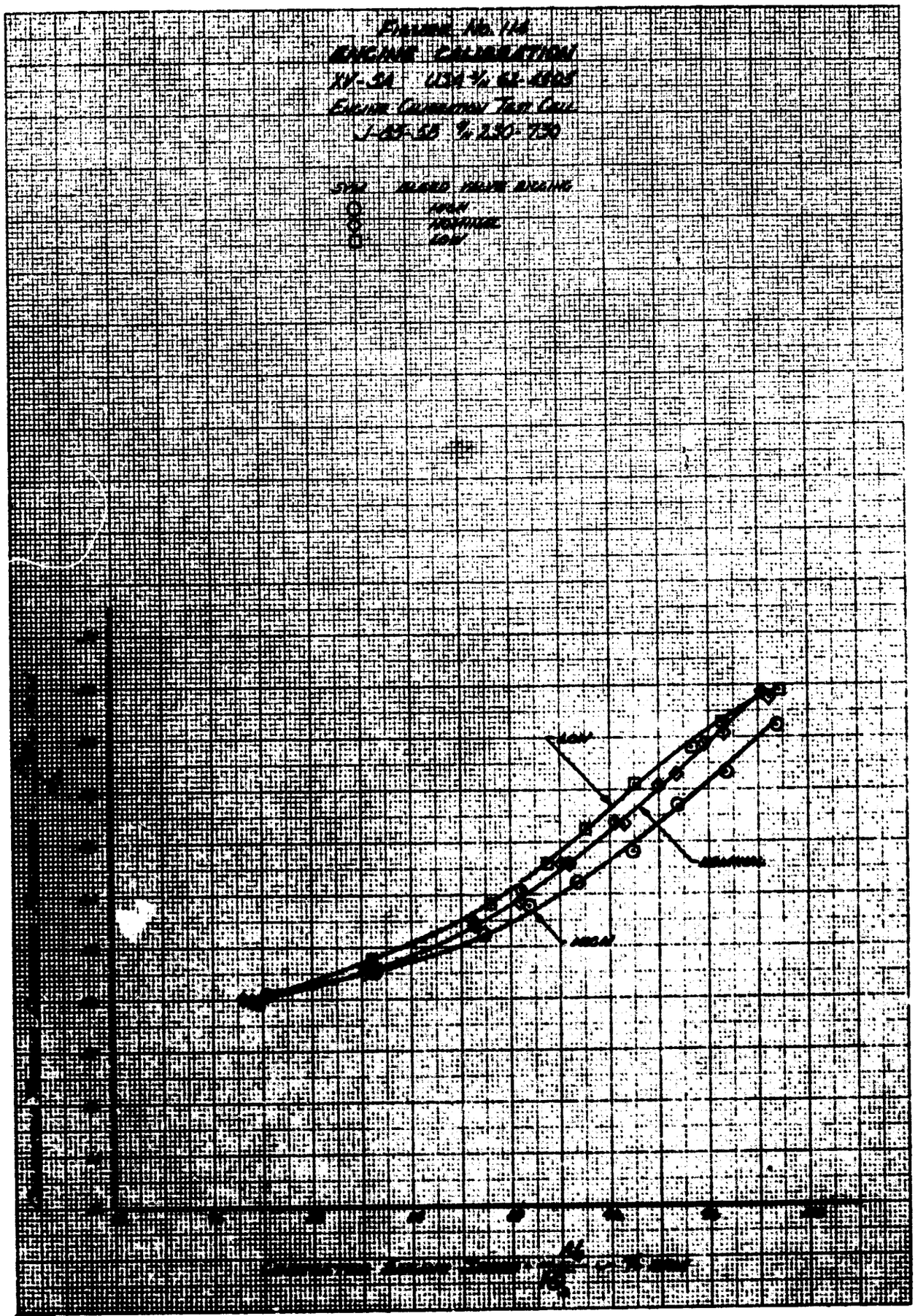
Engine No. 114
ENGINE CALIBRATION
XV-3A 1154 H.P. 42.4 PSI
Engine Calibration Test Cell
J-65-B-3 S.L.S. 750
STAB. BOARD VALVE RATING
MAX. PERMISSIBLE TEMP.
Intake
Exhaust
Metal

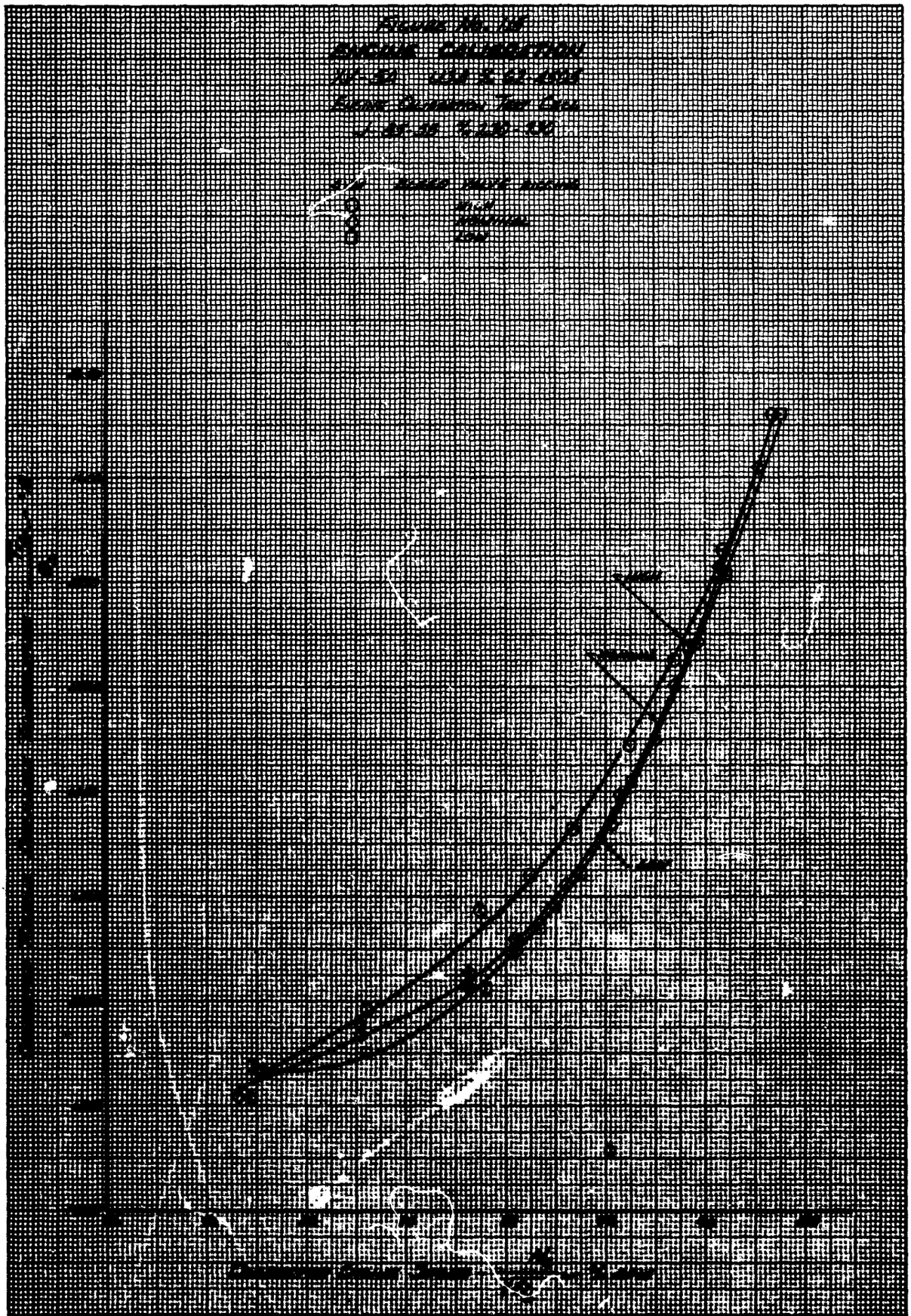

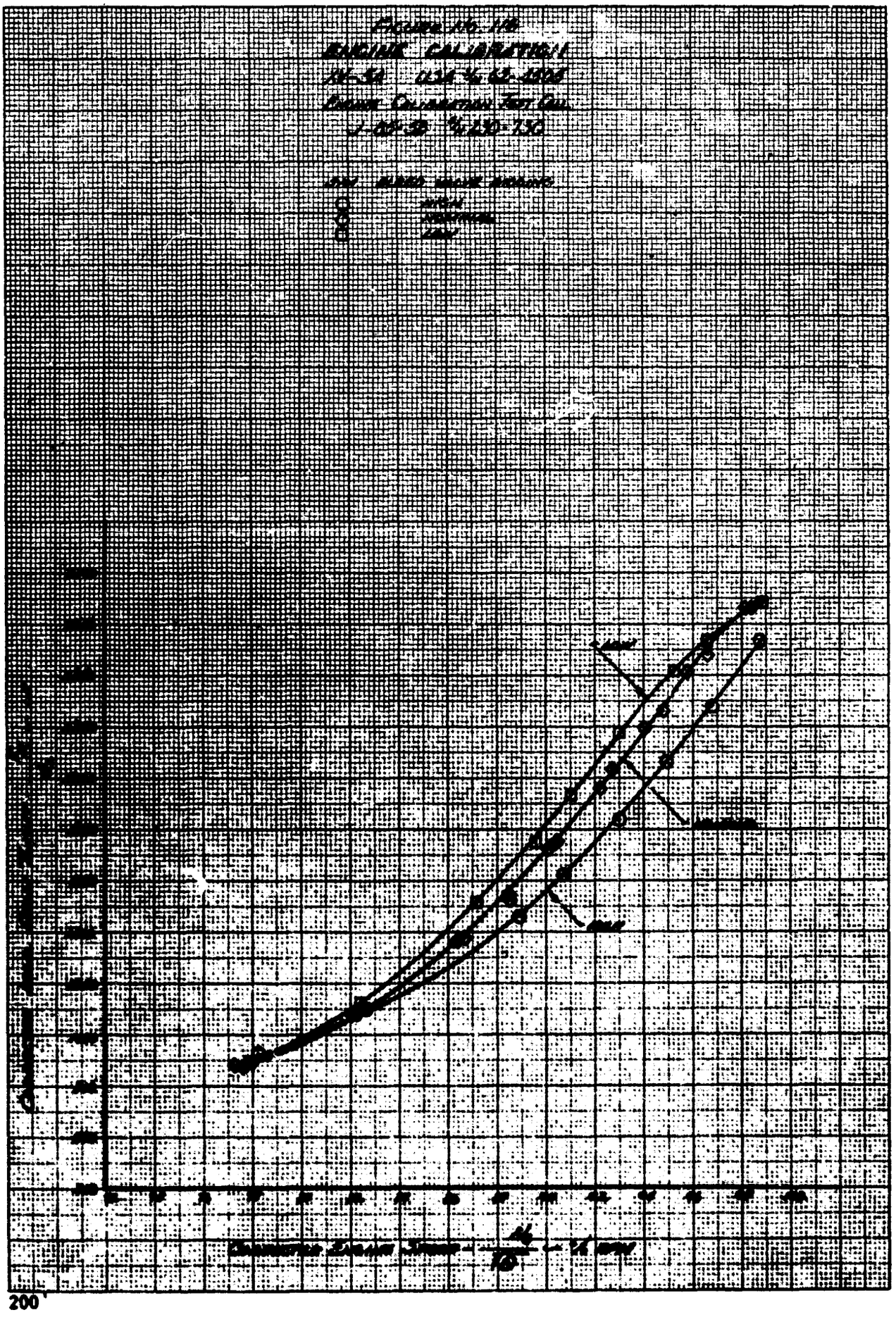

200

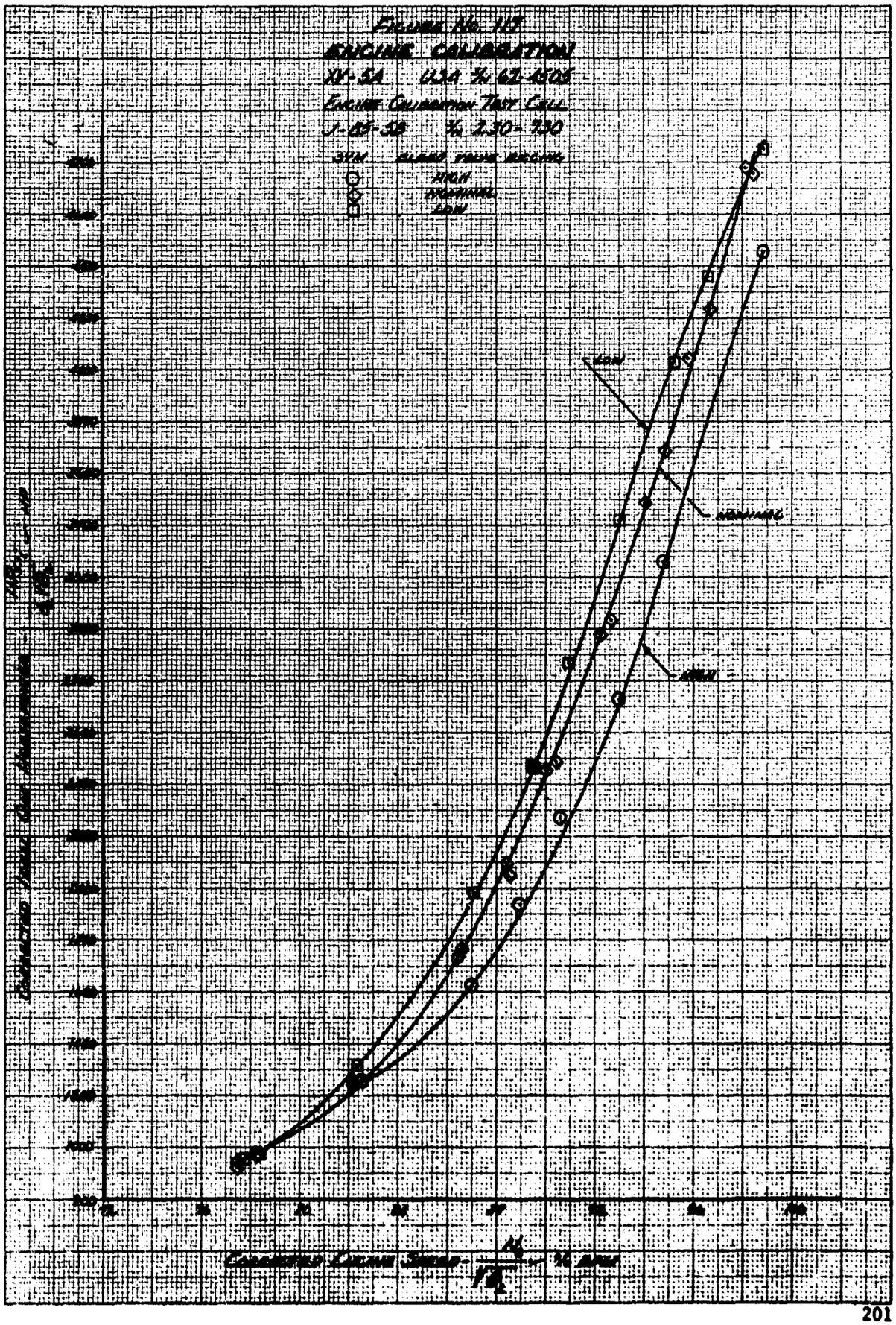
ENGINE NO. 107
ENGINE CALIBRATION
XV-5A USA # 62-4505
ENGINE CALIBRATION TEST CELL
J-85-5B # 2.30-230
SEAL CLOSED, VALVE MISSING
HIGH
NOMINAL
LOW
LOW
NOMINAL
HIGH
CORRECTED ENGINE SPEED - $\frac{N_2}{\sqrt{\theta_2}}$ - % RPM

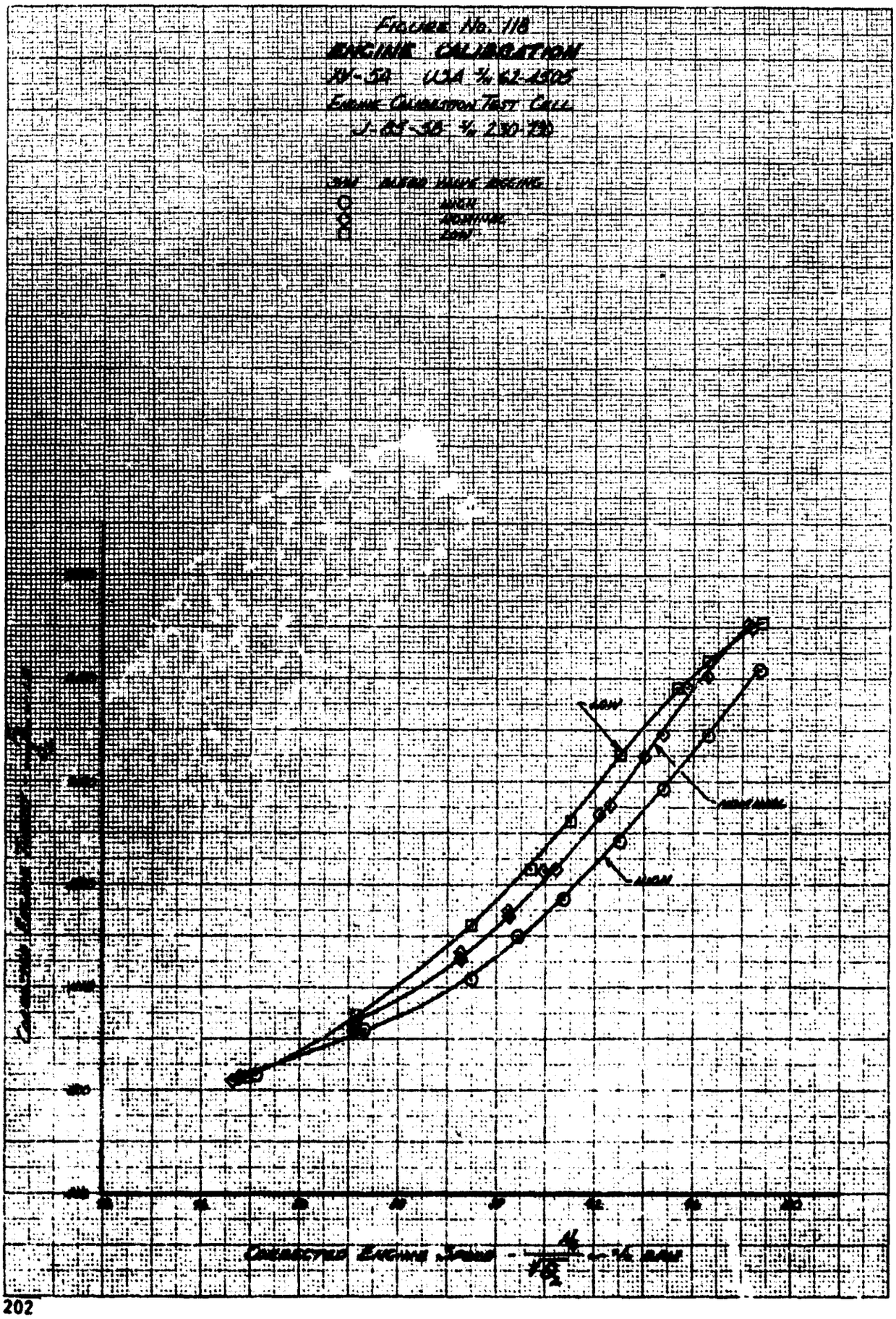
FIGURE No. 118
ENGINE CALIBRATION
XH-53 USA ⅞ 62-4205
ENGINE CALIBRATION TEST CELL
J-85-GE-5B ⅞ 230-230
Corrected Engine Speed - N/√θ2 - % RPM

FIGURE NO. 110

ENGINE CALIBRATION

XR-54 USA No. 62-4205

ENGINE CALIBRATION TEST CELL

J-57-29 3-30-70

CORRECTED ENGINE SPEED - $\frac{N_2}{\sqrt{\theta_2}}$ - % RPM

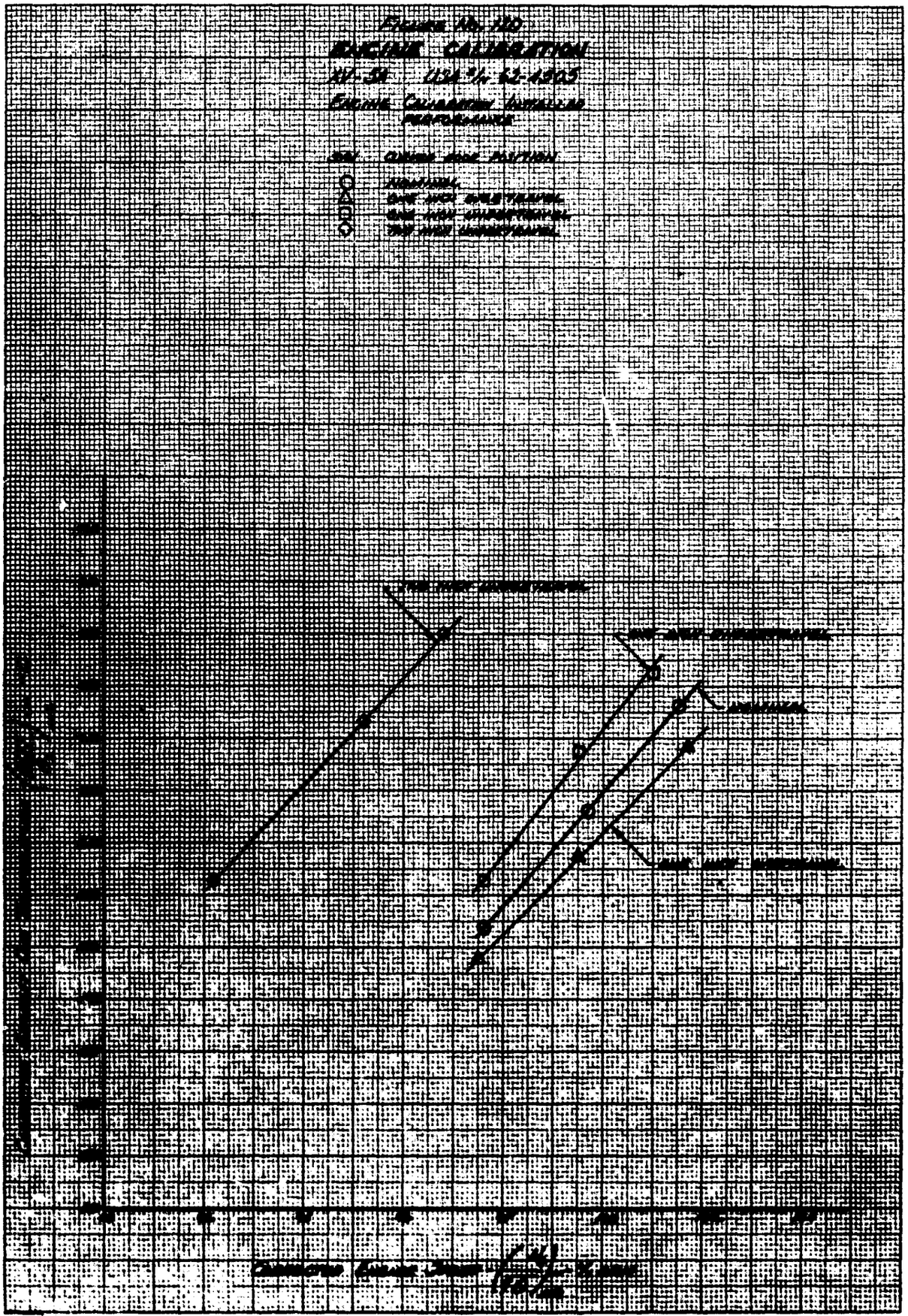

FIGURE NO. 121

ENGINE CALIBRATION

XK-31 (USA No. 62-4105)

ENGINE OPERATION TEST CELL

J-20-30

INLET FLUID PRESSURE RATIO — MEASURED ENGINE CALIBRATION

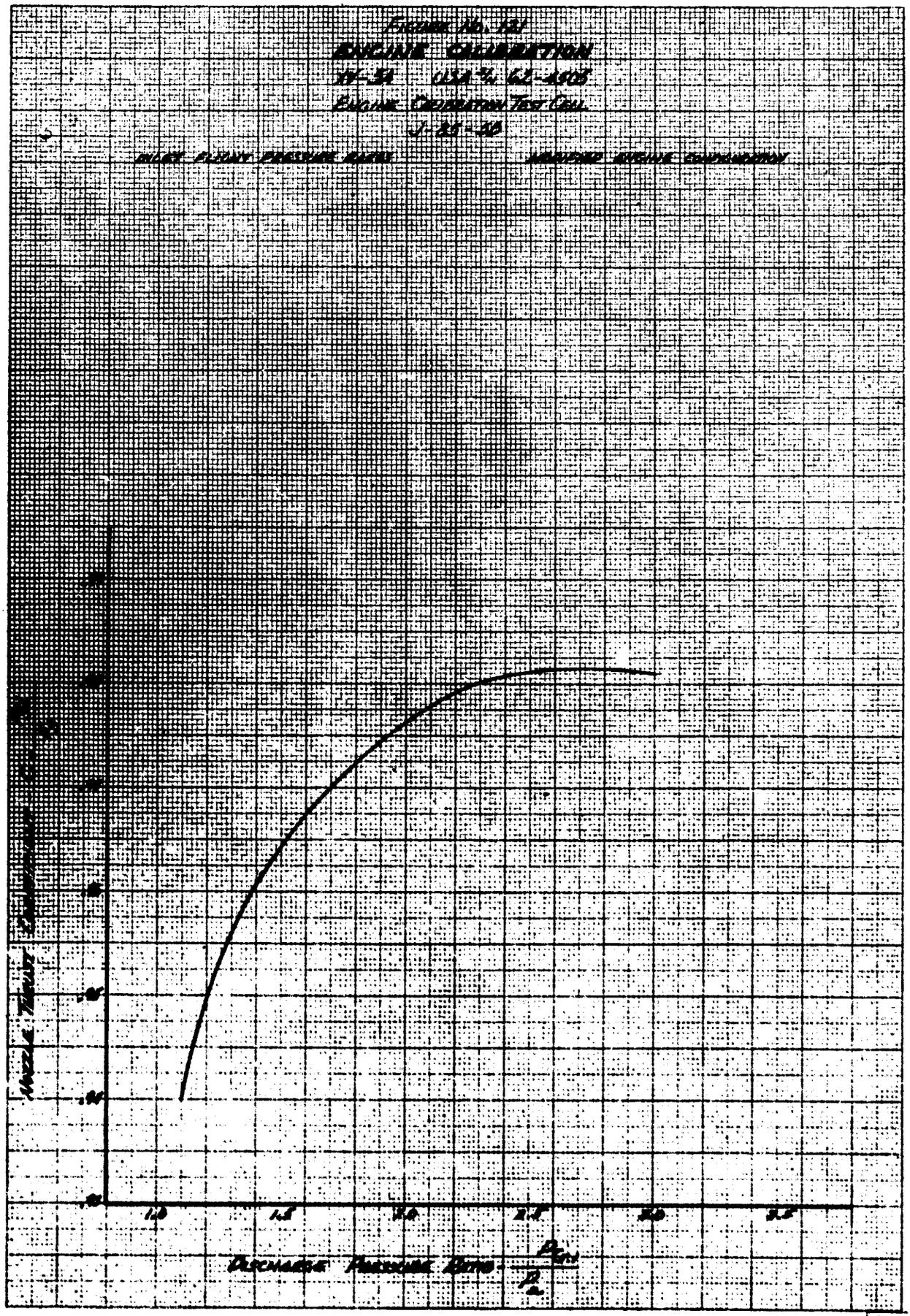

FIGURE NO. 122

ENGINE CHARACTERISTICS

XF-84 USA # 42-4505

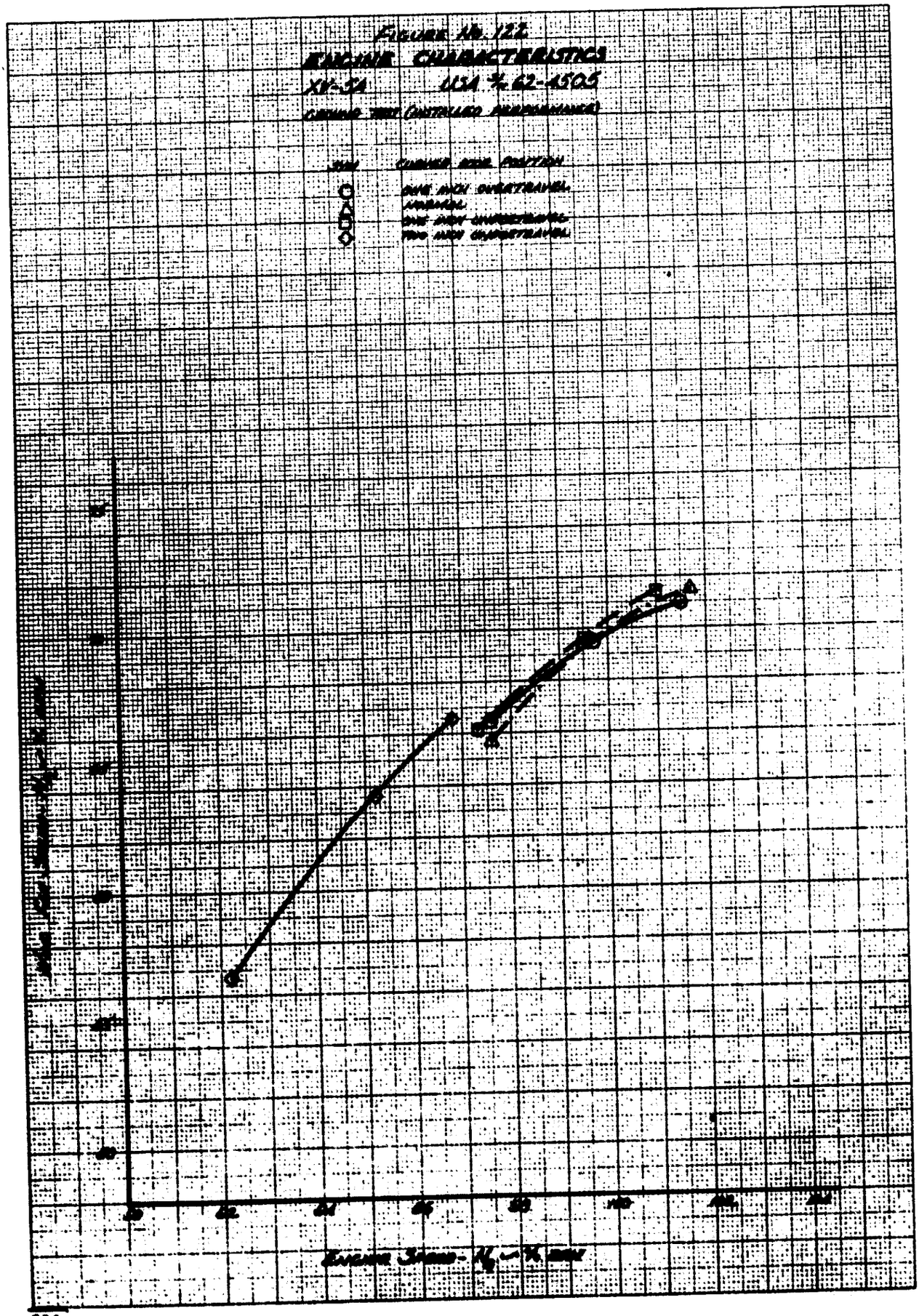

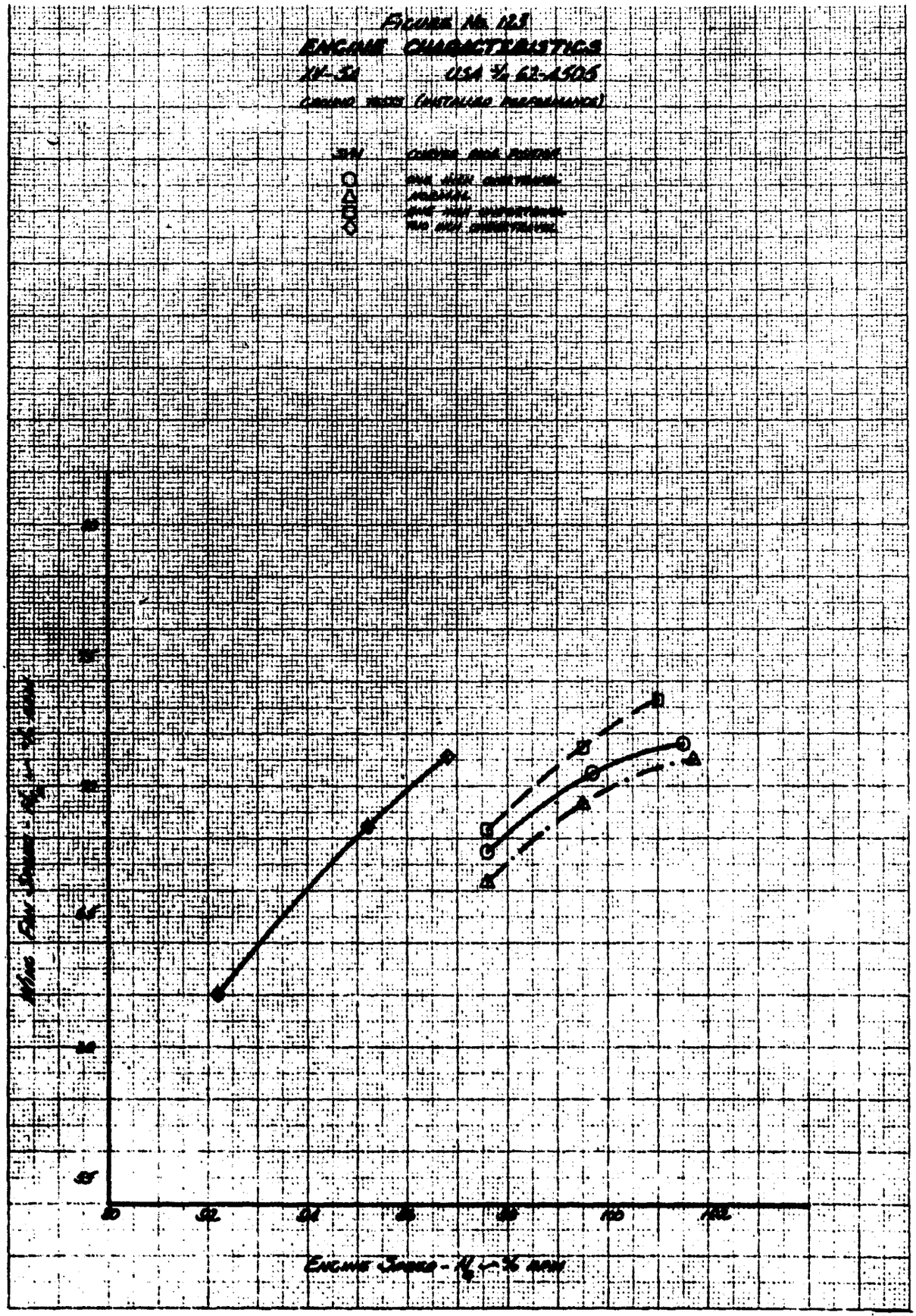
FIGURE No. 12.1
ENGINE CHARACTERISTICS
XR-34 USA ½ 62-4505
CARBURETOR (CONTROLLED PERFORMANCE)
CARB
Engine Speed - R.P.M. x 100

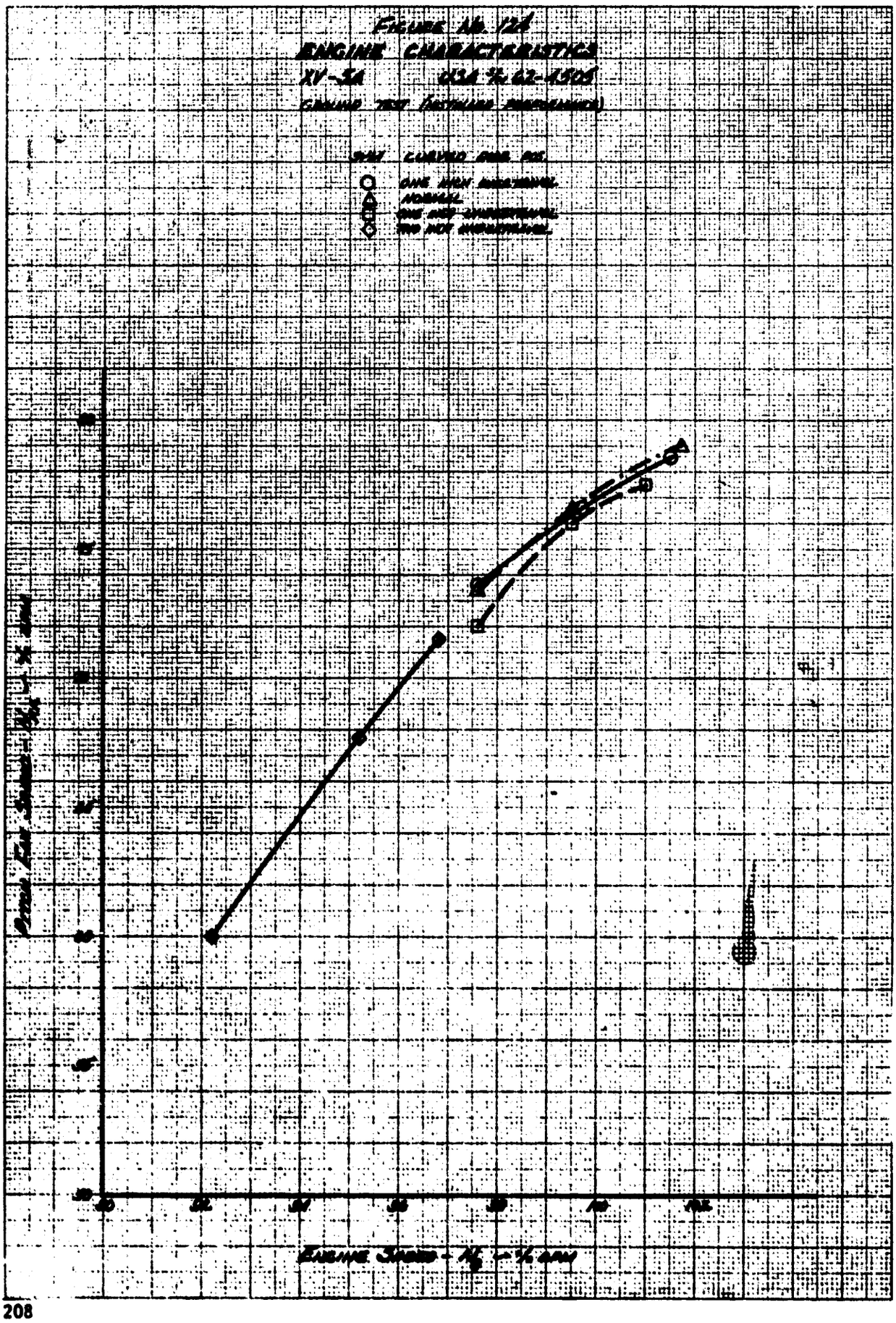
FIGURE AB. 124
ENGINE CHARACTERISTICS
XV-5A
CURVES NOT FACTORED (UNCORRECTED)
ONE HOUR MILITARY
NORMAL
ONE HOUR INTERMEDIATE
TWO HOUR INTERMEDIATE

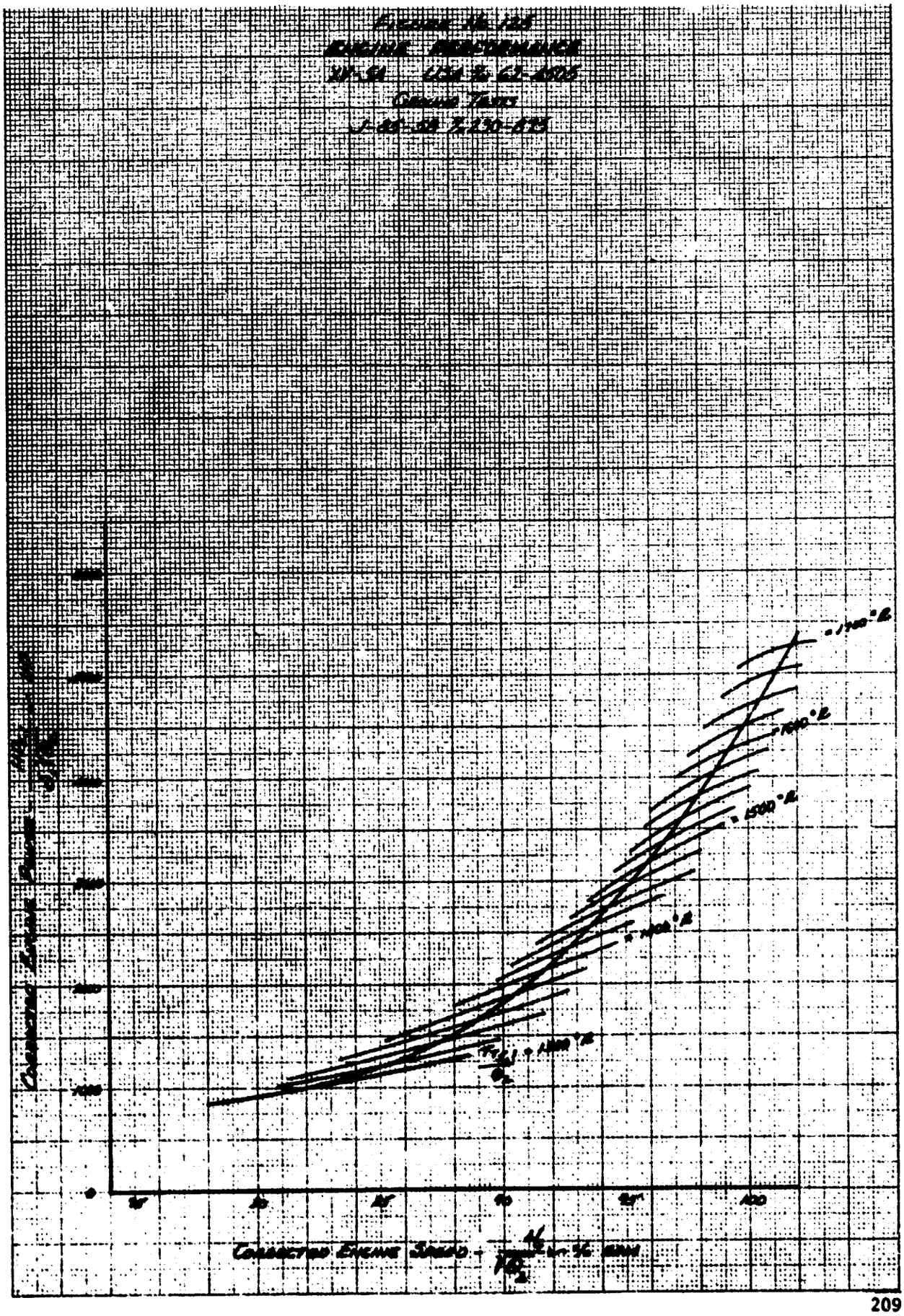
Aerojet No. 124
ENGINE PERFORMANCE
XLR-99 USA-3 62-4026
Ground Tests
L-60-28 X-230-625
1500°R
1540°R
1500°R
1400°R
1300°R
400
Corrected Engine Thrust, lb
Corrected Engine Speed, rpm

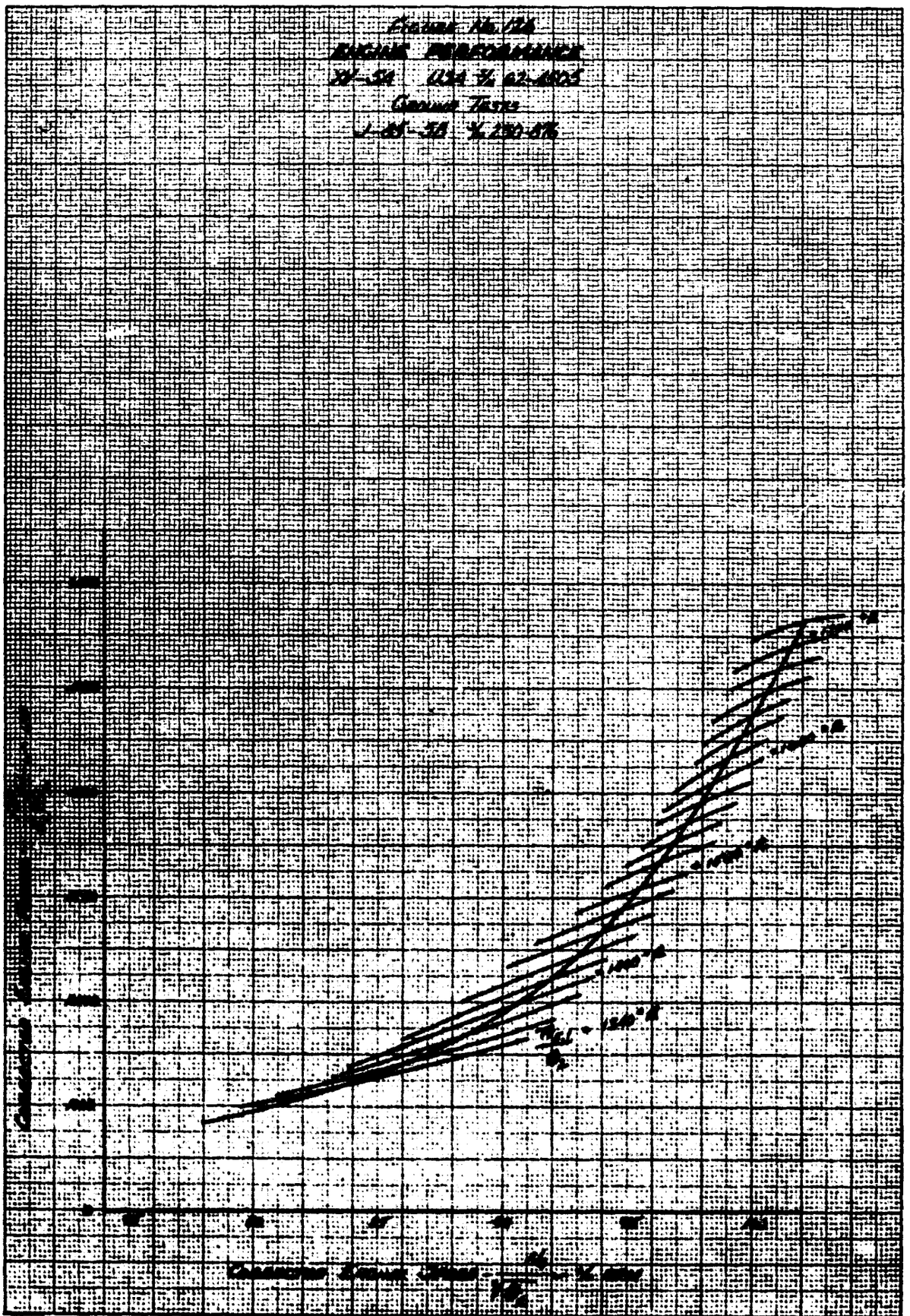

Figure No. 124
ENGINE PERFORMANCE
XF-84 (124 & 42-6025
Ground Tests
J-65-B1 & 130-B1

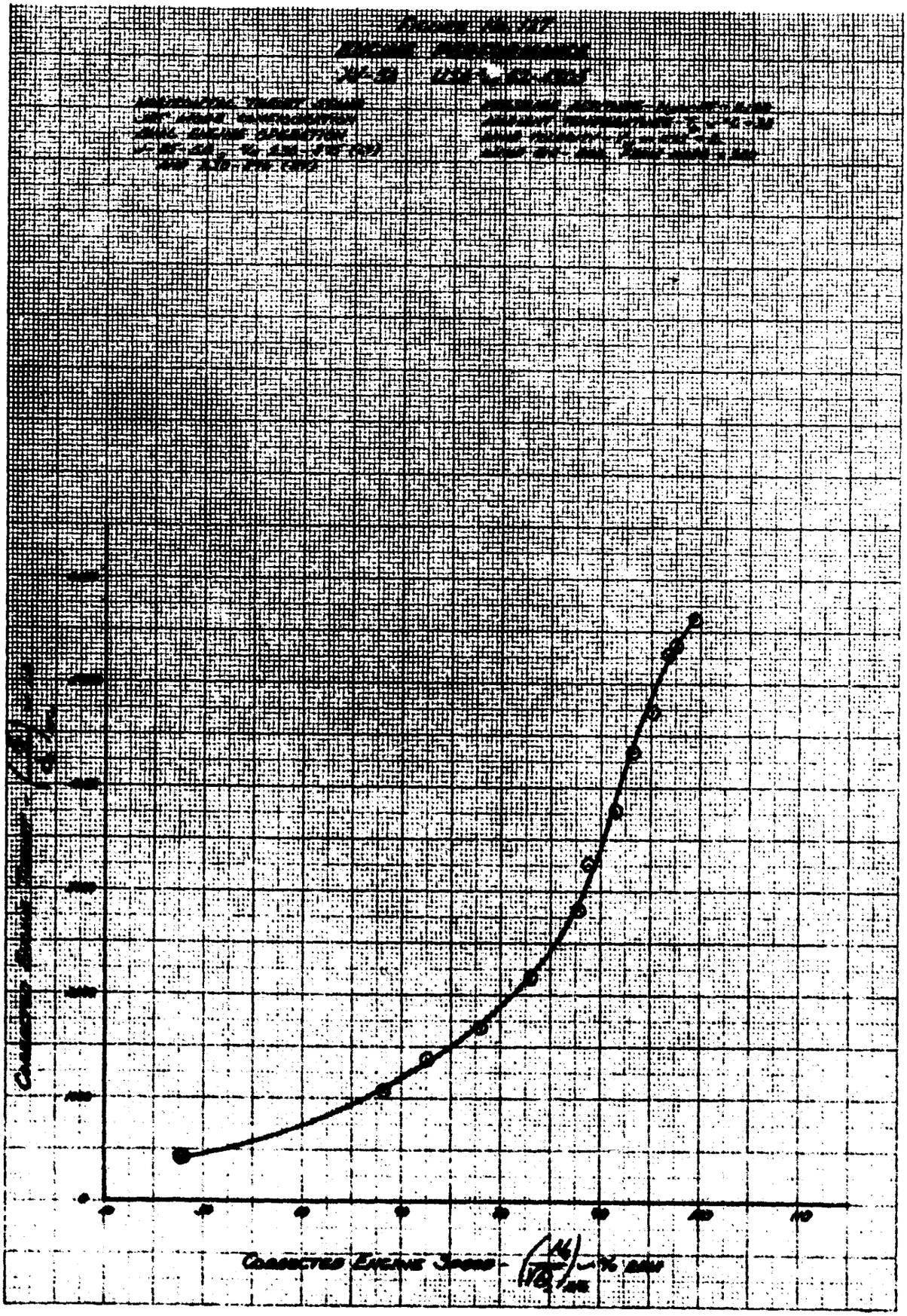

211

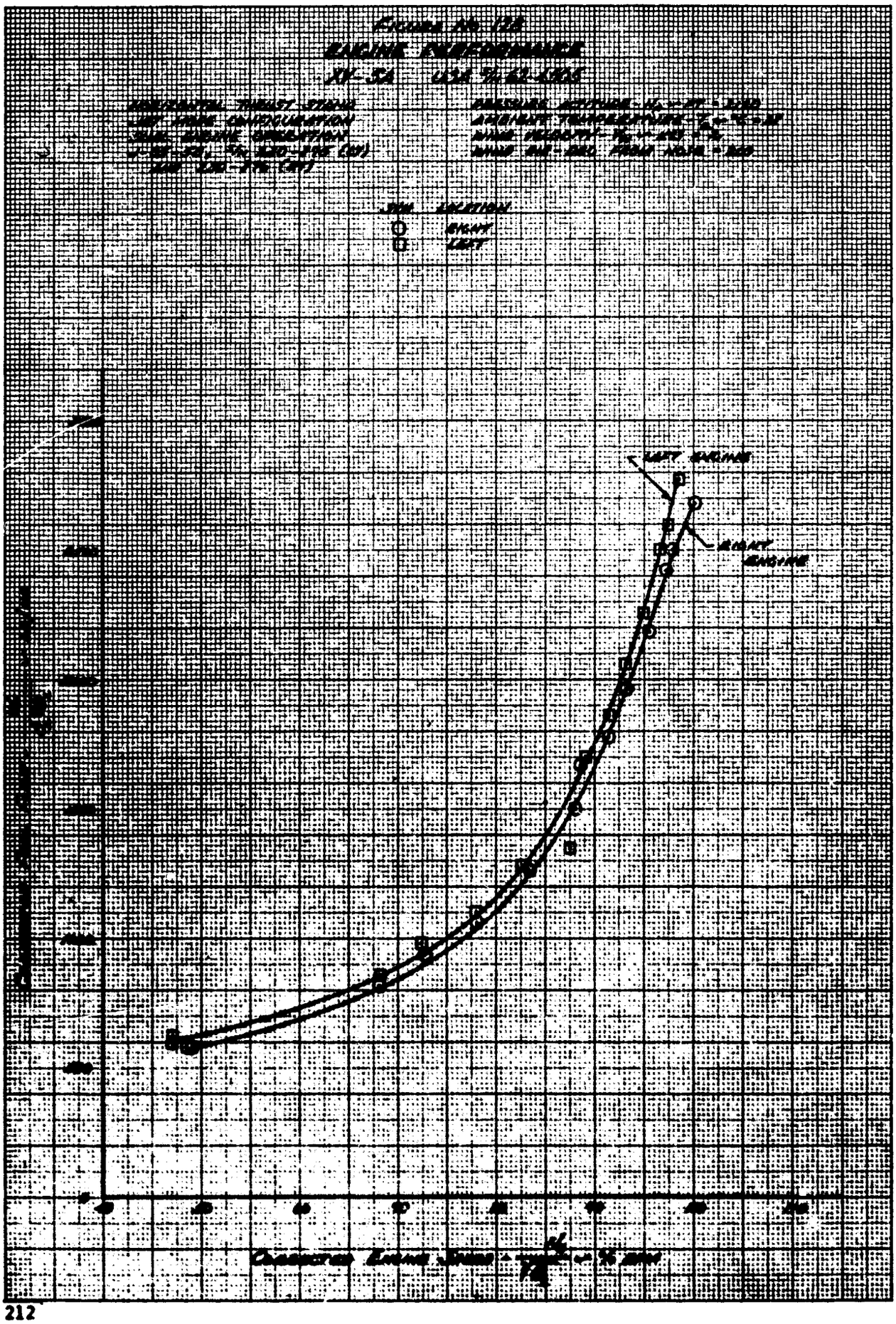
ENGINE PERFORMANCE
XIV-3A
RIGHT ENGINE
LEFT ENGINE

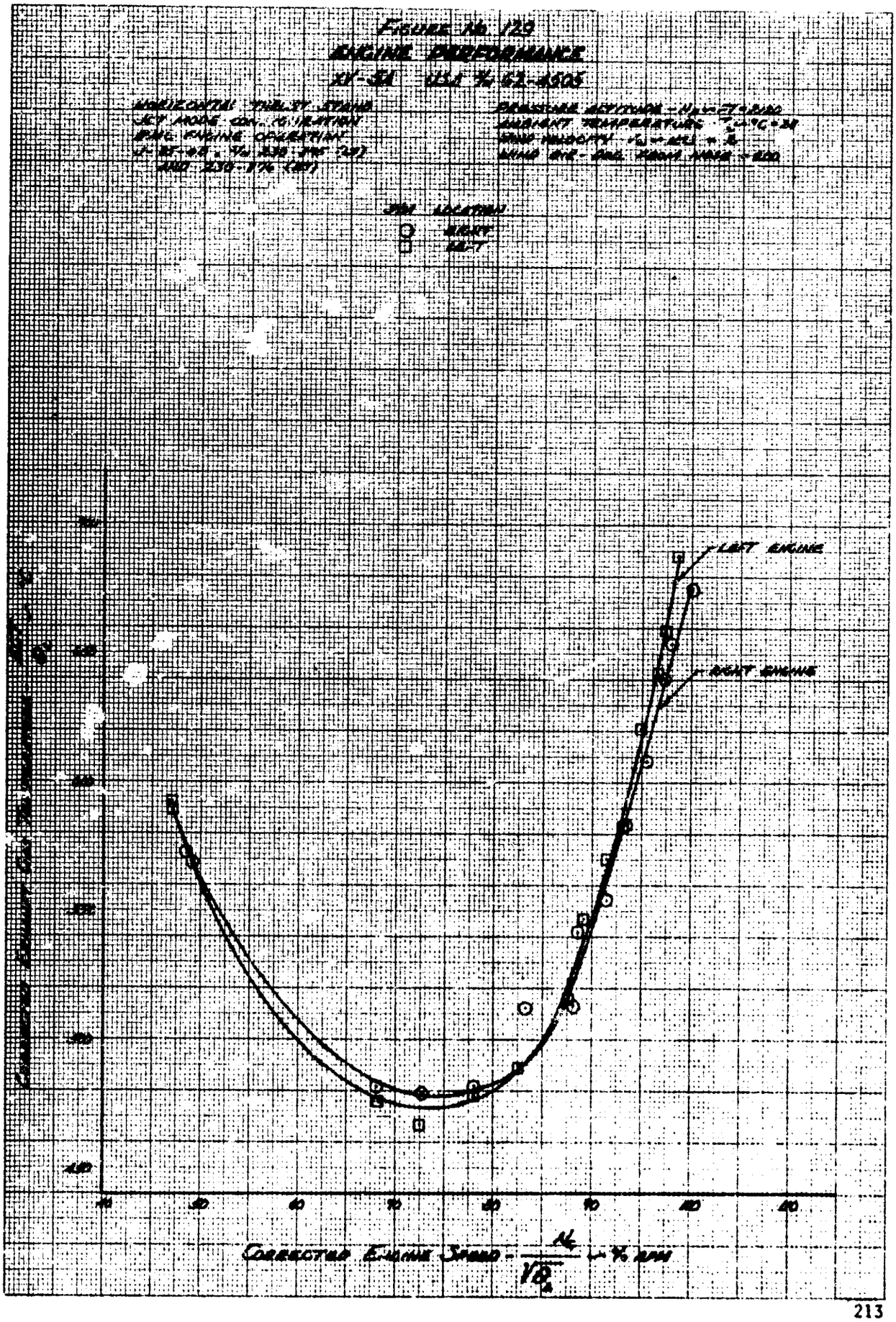
FIGURE NO. 129
ENGINE PERFORMANCE
XH-26 USAF No 52-6505
HORIZONTAL TAIL ST. STANDS
SET ANGLE CONFIGURATION
PWC ENGINE OPERATION
JET LOCATION
RIGHT
LEFT
LEFT ENGINE
RIGHT ENGINE
Corrected Engine Speed - $\frac{N_c}{\sqrt{\theta_a}}$ - % RPM

FIGURE No. 130

ENGINE PERFORMANCE

XV-5A USA # 62-4505

HORIZONTAL THRUST STAND
JET ENGINE CONFIGURATION
SEVERAL ENGINE OPERATION
J-85-5A, T_{t_2} 430 - 435 (LH)
AND 430 - 436 (RH)

PRESSURE ALTITUDE - H_p --FT = SEA
AMBIENT TEMPERATURE - T_a -- °C = 26
WIND VELOCITY - V_w --KTS = 2
WIND DIR - DEG. FROM NOSE = 200

SYM LOCATION
○ RIGHT
□ LEFT

CORRECT ENGINE

RIGHT AND LEFT ENGINES

CORRECTED AIRFLOW - LBS/SEC

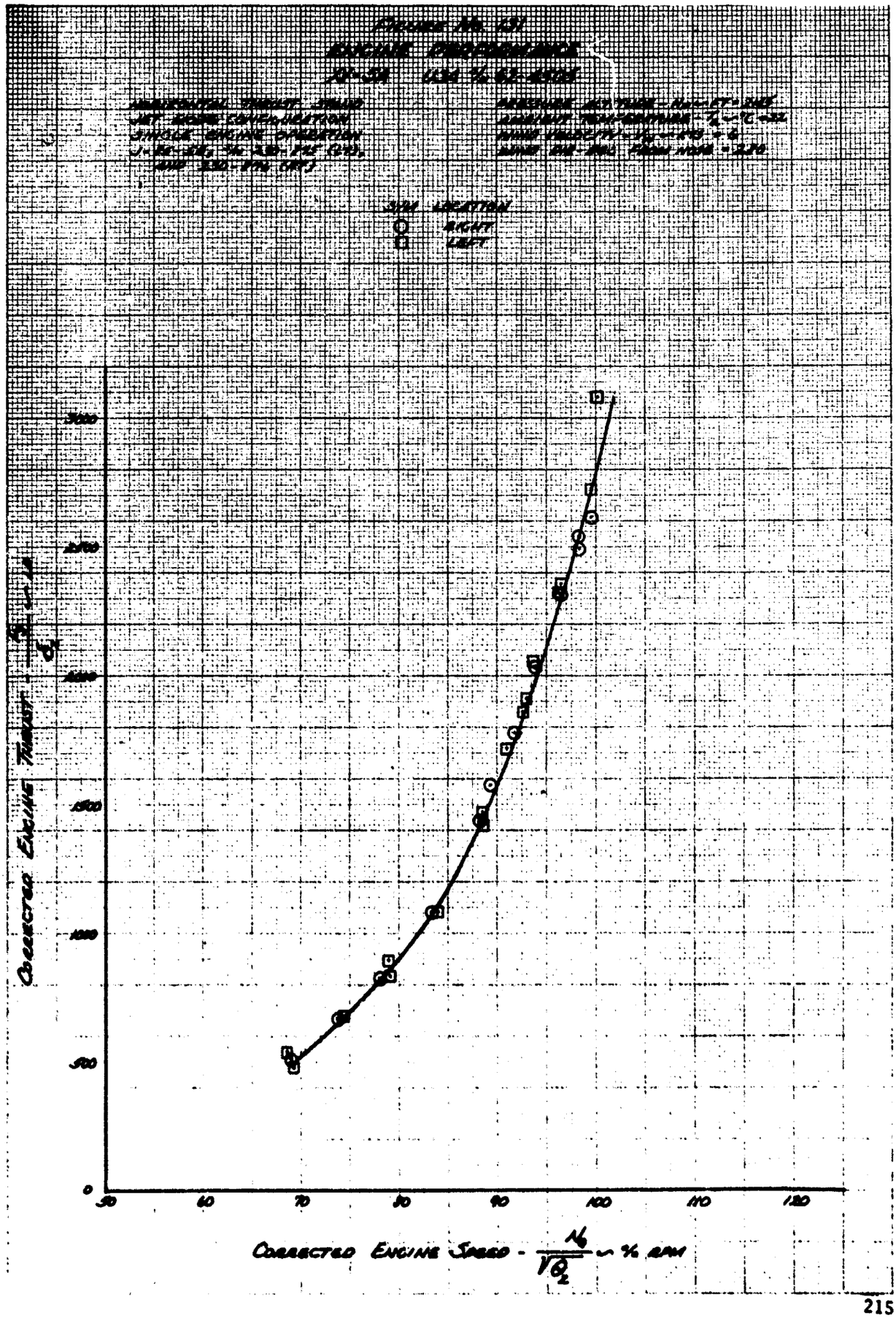
SYM LOCATION
RIGHT
LEFT
0
500
1000
1500
2000
2500
3000
50
60
70
80
90
100
110
120
Corrected Engine Thrust - $\frac{F_n}{\delta_2}$ ~ lb
Corrected Engine Speed - $\frac{N_1}{\sqrt{\theta_2}}$ ~ % RPM

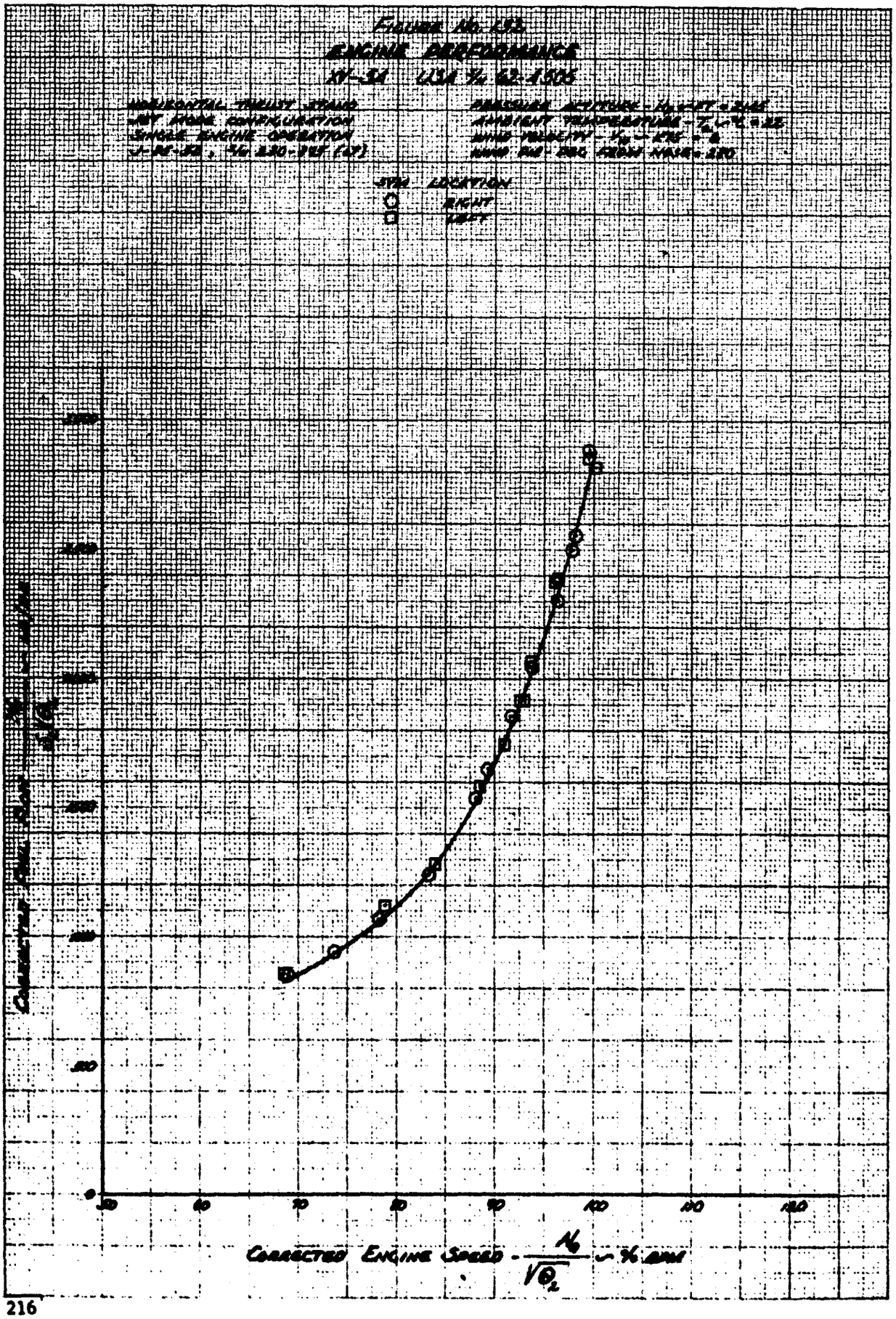
FIGURE NO. 132
ENGINE PERFORMANCE
XT-34 USA Ac 52-1905
HORIZONTAL TAILLIST STAND
JET ENGINE CONFIGURATION
SINGLE ENGINE OPERATION
J-34-34, MIL 650 JET FUEL
AMBIENT TEMPERATURE
STA LOCATION
RIGHT
LEFT
30
40
50
60
70
80
90
100
110
120
CORRECTED ENGINE SPEED - $\frac{N_2}{\sqrt{\theta_2}}$ - % RPM

FIGURE No. 133

ENGINE PERFORMANCE

XH-5A USA S/N 62-4905

HORIZONTAL THRUST STAND
JET MODE CONFIGURATION
SINGLE ENGINE OPERATION
J-85-5A's S/N 230-5715 (LT)
AND 230-5716 (RT)

PRESSURE ALTITUDE - H_{p_a} = FT = 2145
AMBIENT TEMPERATURE - T_a = °C = 22
WIND VELOCITY - V_w = KTS = 6
WIND DIR - RELATIVE FROM NOSE 280

SYM	LOCATION
○	RIGHT
□	LEFT

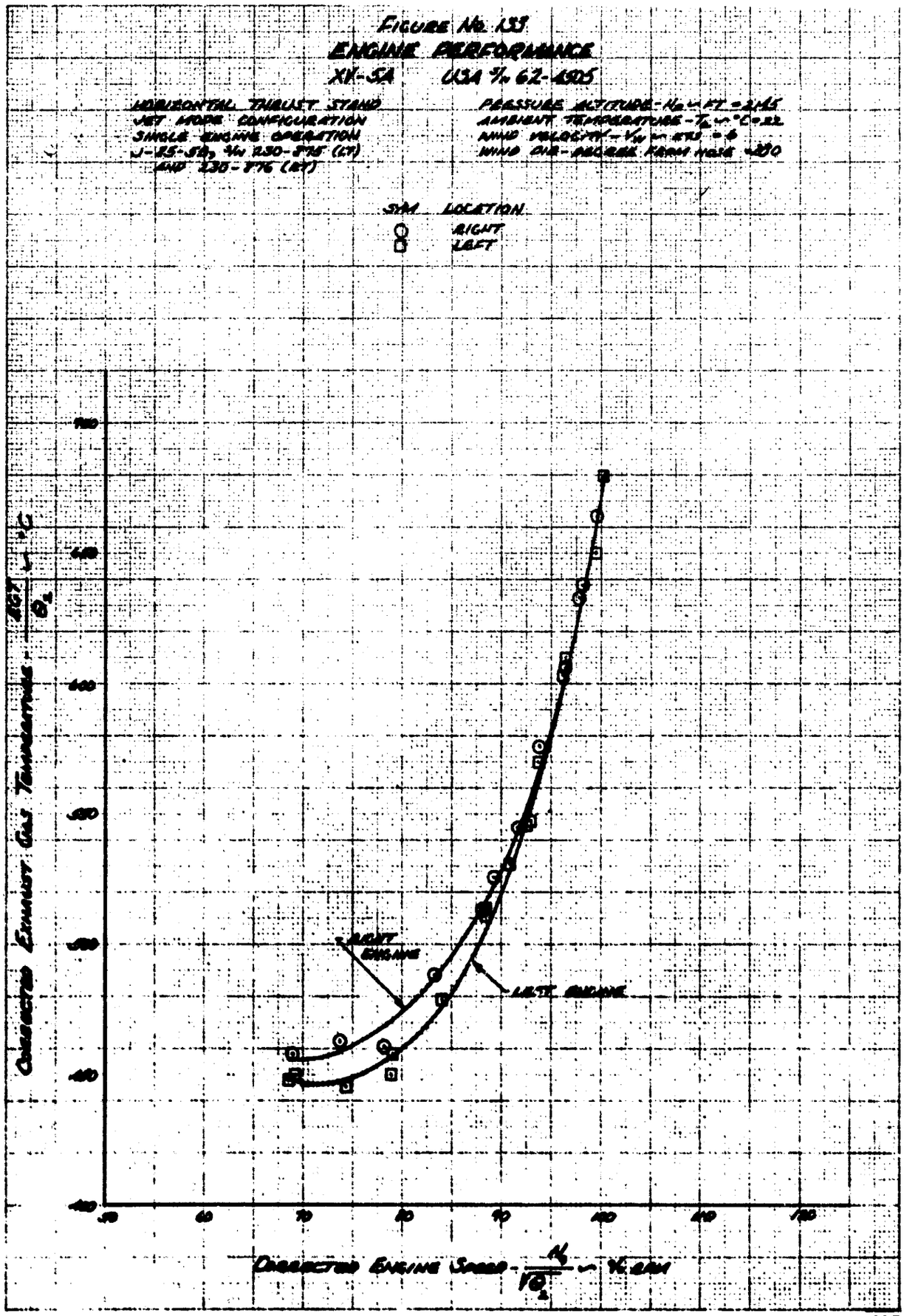

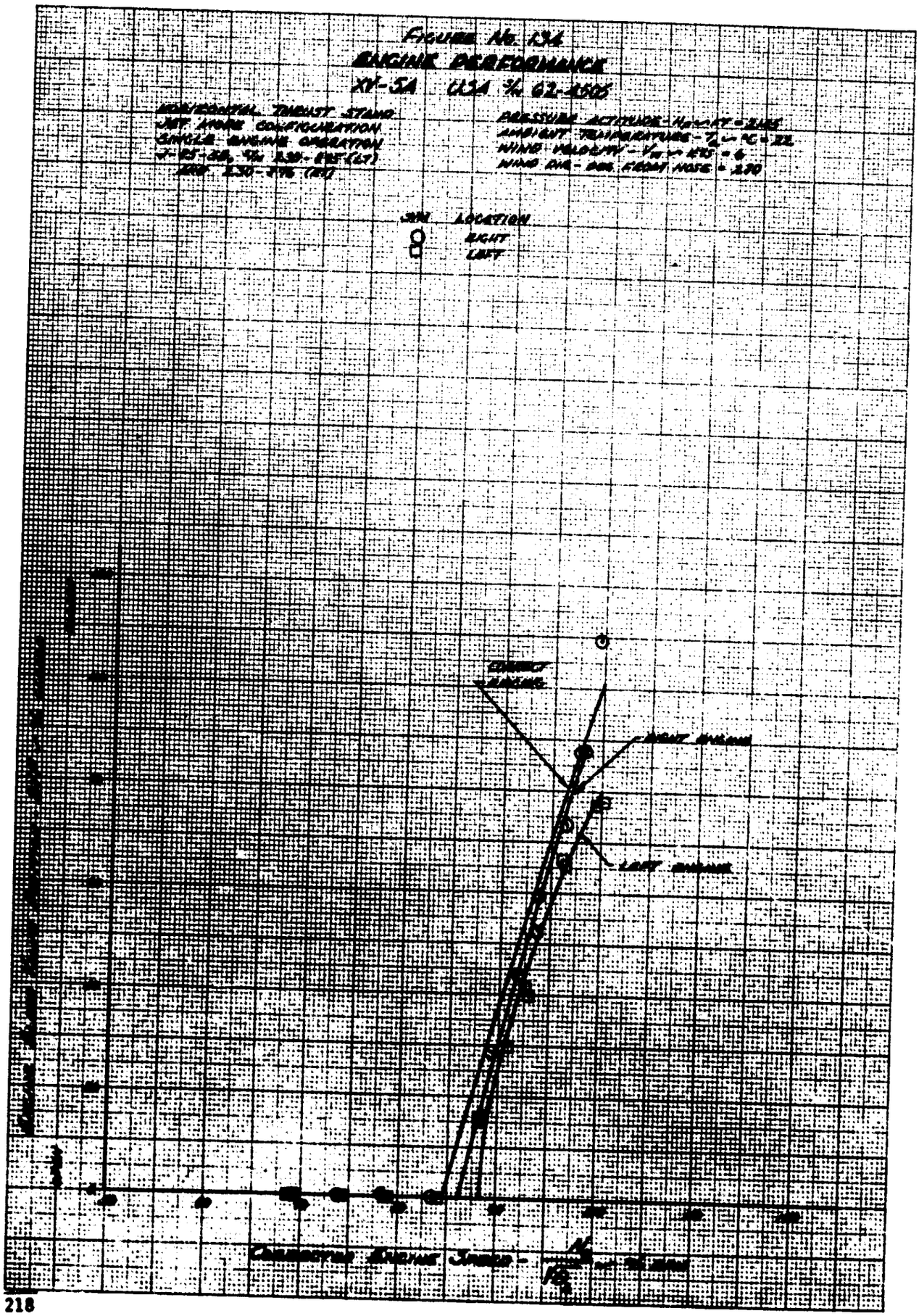
FIGURE No. 134
ENGINE PERFORMANCE
XV-5A CL5A % 62-4505
HOR/VERTICAL THRUST STAND
JET ENGINE CONFIGURATION
SINGLE ENGINE OPERATION
J-85-5A, % 330-885 (LT)
885 330-895 (RT)
PRESSURE ALTITUDE - H_p = AT = 2,465
AMBIENT TEMPERATURE - T_A = °C = 22
WIND VELOCITY - V_W = 4.15 = 6
WIND DIR - DEG. FROM NOSE = 330
JET LOCATION
RIGHT
LEFT
DIRECT RANGE
RIGHT ENGINE
LEFT ENGINE
CHAMPION ENGINE JUMBO -

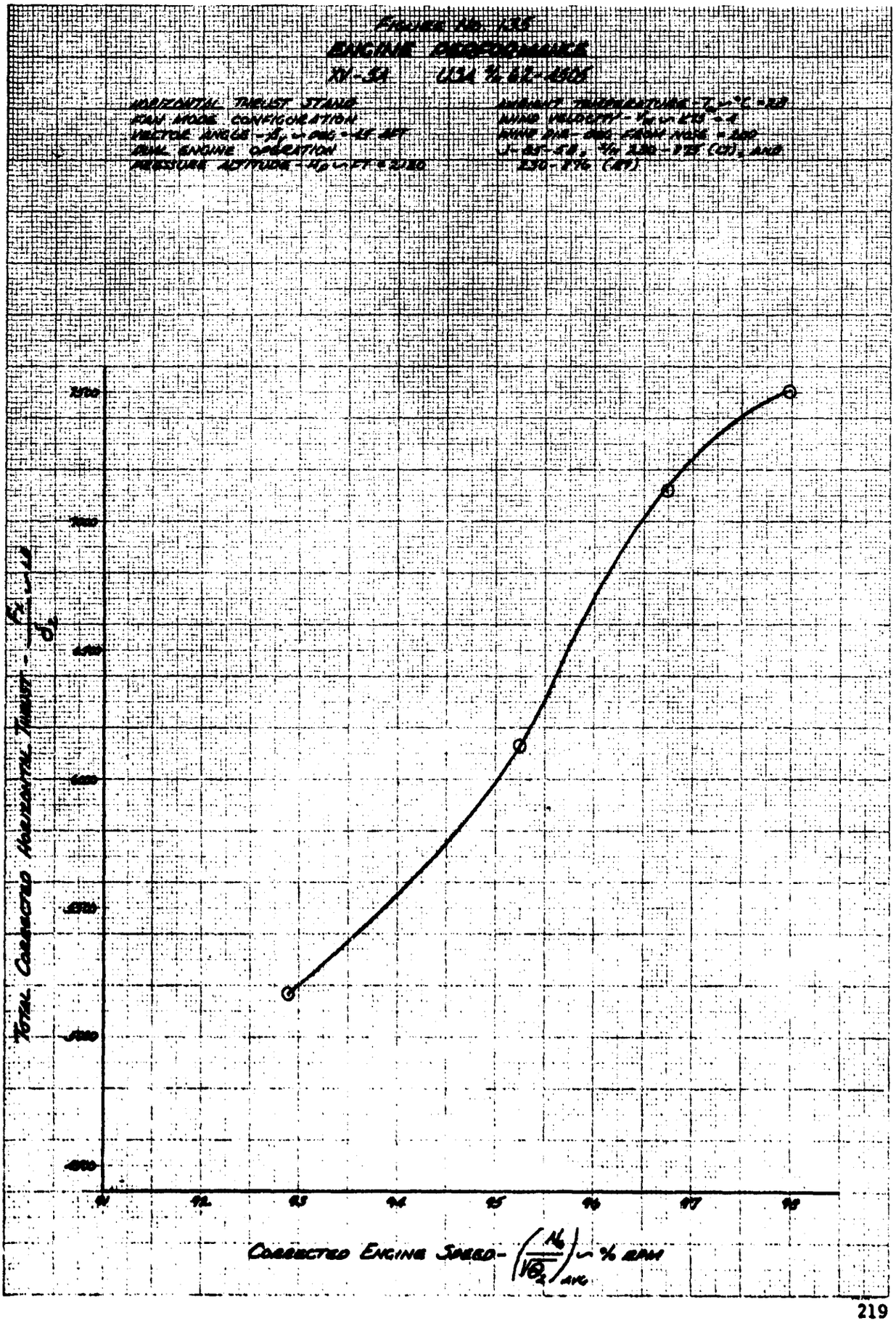
ENGINE NO. 1235
ENGINE PERFORMANCE
XV-3A USA 56-6706
HORIZONTAL TEST STAND
STAN MODE CONFIGURATION
INLET ANGLE - A_1 = ONE - 45° AFT
FINAL ENGINE CONDITION
PRESSURE ALTITUDE - H_p = FT = 2180
AMBIENT TEMPERATURE - T_a = °C = 23
RAMP DIA. - ONE STREAM MODE = 100
J - 85° - 91, % 2180 - 1785 (CD), AND
2170 - 1% (AT)
TOTAL CORRECTED HORIZONTAL THRUST - F_n - LB
CORRECTED ENGINE SPEED - $\left(\frac{N_1}{\sqrt{\theta_2}}\right)_{AVG}$ - % RPM

FIGURE No. 136

ENGINE PERFORMANCE

XT-34 USN TG 62-4004

HORIZONTAL THRUST STAND
RAM JAMME CONFIGURATION
INJECTOR ANGLE - β_{INJ} = DEG = 45 MT
REAL ENGINE OPERATION
PROPELLER ACTIVITY - H_p = FT = 7,150

AMBIENT TEMPERATURE - T_{amb} = °C = 15
WIND VELOCITY - V_{wind} = KTS = 0
WIND DIR. FROM RIGHT ABEAM = 000
W - 25 - 30, 5% ± 30 - 70% (CH_4) AMB
4% ± 30 - 70% (AIR)

SYM LOCATION
○ RIGHT
□ LEFT

LEFT ENGINE

RIGHT ENGINE

Corrected Air Flow - $W_a\sqrt{\theta_2}/\delta_2$ - lbs/sec

1600 1800 2000 2200 2400 2600 2800

92 93 94 95 96 97 98 99

Corrected Engine Speed - $N_2/\sqrt{\theta_2}$ - % RPM

FIGURE No. 137

ENGINE PERFORMANCE

XV-5A USA S/N 62-4504

HORIZONTAL THRUST STAND
FAN MODE CONFIGURATION
VECTOR ANGLE - δ_N = 90° = 45 AFT
DUAL ENGINE OPERATION
PRESSURE ALTITUDE - H_p = FT = 2150

AMBIENT TEMPERATURE - T_0 = °C = 28
WIND VELOCITY - V_w = KTS = 12
WIND DIR - DEG FROM NOSE = 300
J-85-5A ; S/N 430-872 (RH), AND
430-876 (LH)

SYM LOCATION
○ RIGHT
□ LEFT

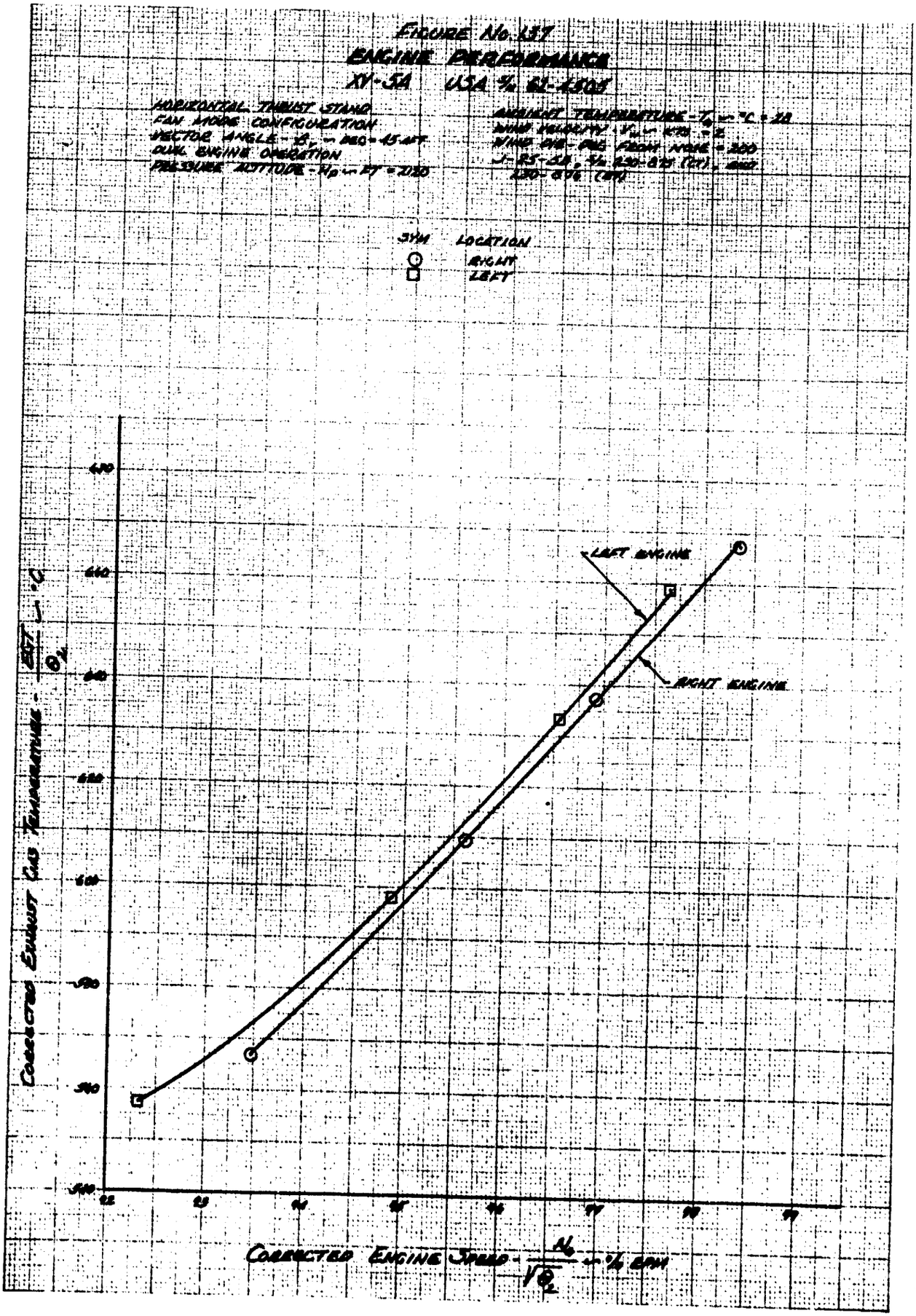

FIGURE NO. 138

ENGINE PERFORMANCE

XV-3A LL34 ⅞ 62-4205

EXPERIMENTAL TURBOJET STAND
TWIN NACELLE CONFIGURATION

VENTURI GAUGE - ΔH_v = INCH. = IN.
DUAL ENGINE OPERATION

SYM	RAM ALT. $-H_p$ = FT	RAM TEMP. T_A = °C	ENG. LOC.	ENGINE %	WING INL. $-V_W$ = KTS	WING INJECTION -INC. FROM NOSE
○	2120	34	RT.	230-276	4	200
	2120	34	LT.	230-225	4	200

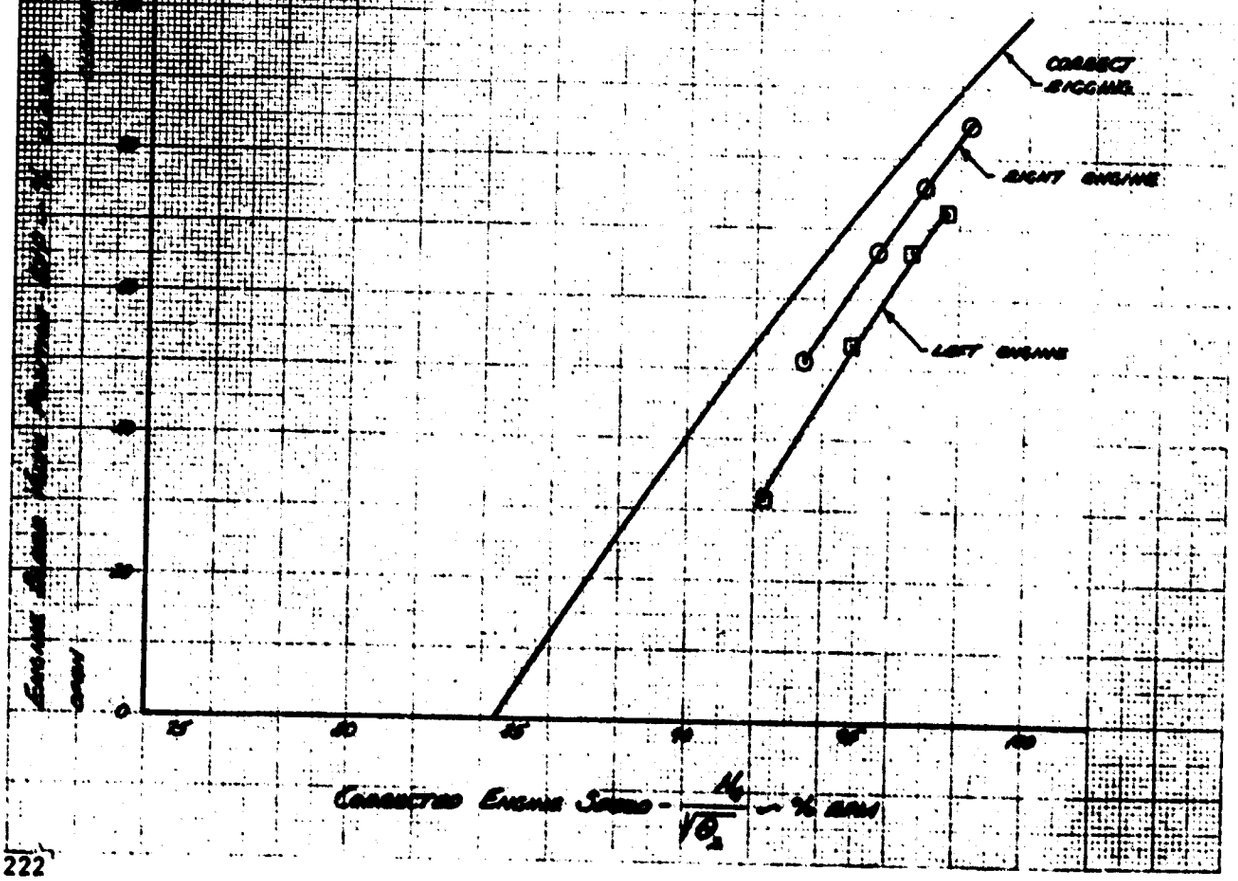

FIGURE No. 139

WING FAN SPEED VARIATION WITH ENGINE SPEED

XV-5A USA #1 62-1505

Vertical Thrust Stand

SYM	ABES. ALT $-H_p$ — FT	DENS. ALT $-H_\sigma$ — FT	VECTOR ANG. $-\beta_f$ — DEG.	FAN NT $-N/O$	PITCH FAN DR. POS $-\delta_{FAN}$ — DEG.	DIFF STAGGER ANG $-\Delta\beta_2$ — DEG.	DIFF VECTOR ANG $-\Delta\beta_f$ — DEG.
○	7845	1400	5.14 FWD	1	64.62	-.79	-4
□	1895	3570	4.65 FWD	2	78.3	-1.14	-5.5
△	1990	2150	5.7 FWD	3	78.7	-.74	-2.9

TECHNIQUE: COLLECTIVE, VECTOR, LONGITUDINAL, LATERAL, AND DIRECTIONAL CONTROLS HELD FIXED WHILE ENGINE SPEED WAS STABILIZED AT EACH POINT.

WIND CONDITIONS

SYM	VEL-V_w — KTS	DIR-DEG. FROM NOSE
○	2	130 L
□	3.5	125 R
△	2	35 R

COLLECTIVE STICK POSITION - δ_c — % UP = 100

LANDING GEAR DOWN.

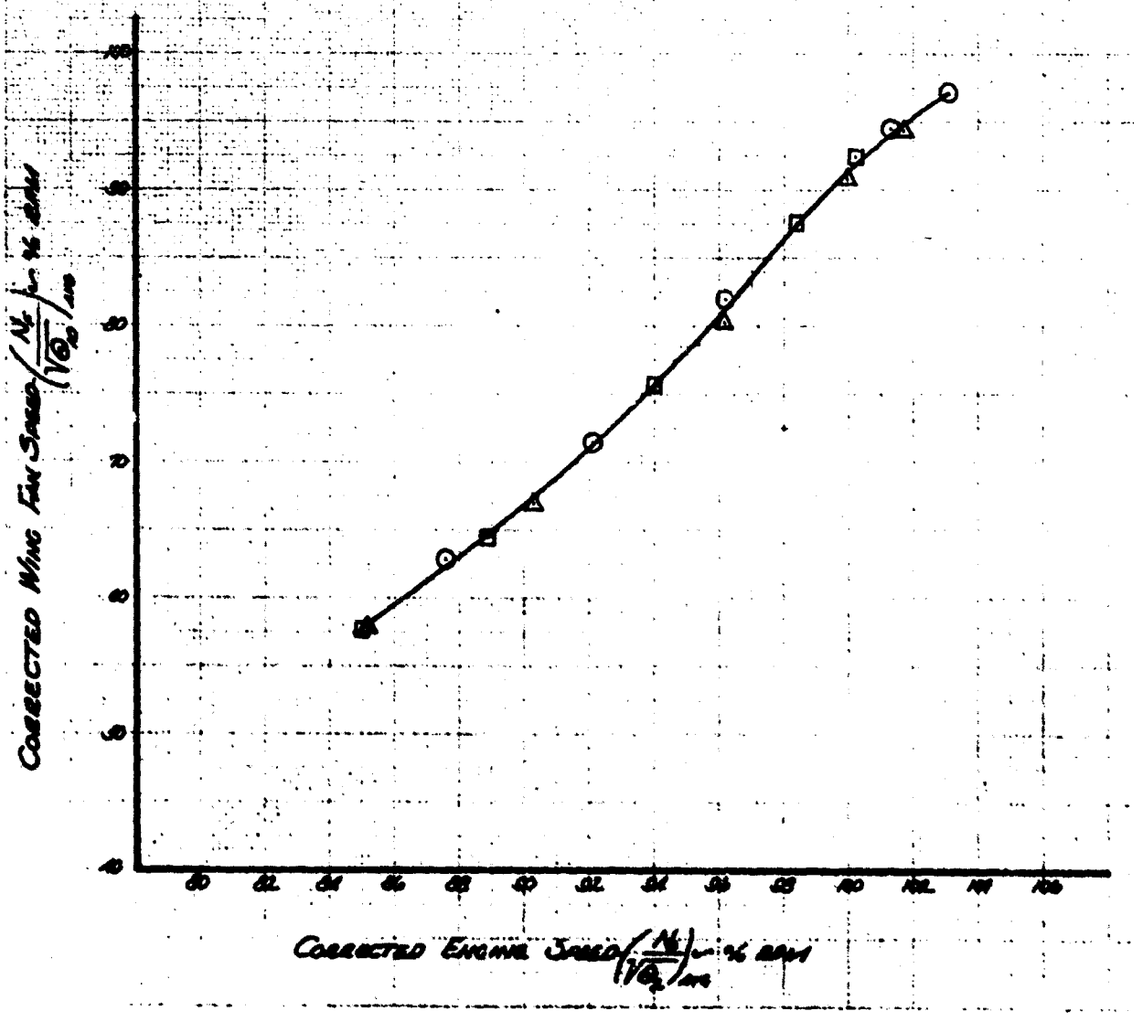

FIGURE NO. 110

PITCH FAN SPEED VARIATION WITH ENGINE SPEED

XV-5A USA S/N 62-4505

VERTICAL THRUST STAND

SYM	PRES. ALT. $-H_p$ — FT	DENS. ALT. $-H_D$ — FT	FAN HT. $-H/D$	VECTOR ANG. $-\delta_v$ — DEG	PITCH FAN DR. POS $-\delta_{FAN}$ — DEG	DIFF STAGGER ANG $-\Delta\beta_3$ — DEG	DIFF VECTOR ANG $-\Delta\delta_v$ — DEG
○	1845	1600	1	5.14 FWD	64.02	-.78	-1
□	1895	3570	2	4.65 FWD	77.3	-1.14	-5.5
△	1990	2450	3	5.7 FWD	79.7	-.74	-2.9

TECHNIQUE: COLLECTIVE, VECTOR, LONG-ITUDINAL, LATERAL, AND DIRECTIONAL CONTROLS HELD FIXED WHILE ENGINE SPEED WAS STABILIZED AT EACH POINT.

WIND CONDITIONS

SYM	VEL — V_w — KTS	DIR — DEG FROM NOSE
○	2	150 L
□	3.5	125 R
△	2	65 L

COLLECTIVE STICK POSITION — δ_c — % UP = 100

LANDING GEAR DOWN.

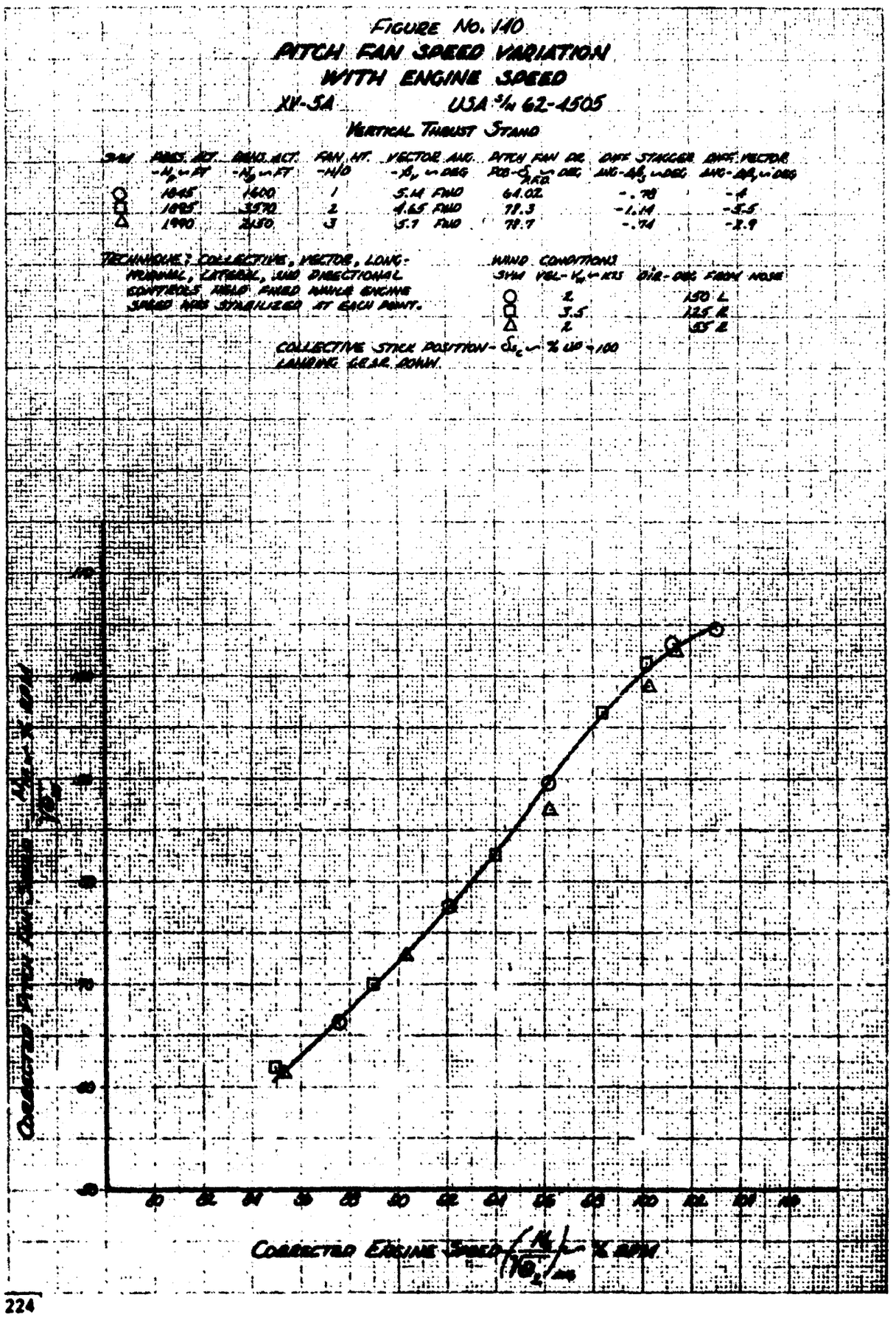

FIGURE NO. 141

THRUST VARIATION WITH ENGINE POWER

XV-5A

USA No. 62-4505

VERTICAL THRUST STAND

SYM	PRESS. ALT. $-H_p$ - FT	DENS. ALT. $-H_\sigma$ - FT	VECTOR ANG. $-\delta_V$ - DEG	RAM RT. -N/D	PITCH RAM ERR. δ_{RCS} - DEG	DIFF. STRAIGHT ANG - $\Delta\delta_s$ - DEG	DIFF. VECTOR ANG - $\Delta\delta_v$ - DEG
○	1925	7680	5.74 FWD	1	64.02	-.78	-1
□	1905	3570	4.65 FWD	2	79.3	-1.14	-5.5
△	1990	2150	5.17 FWD	3	82.7	-.74	-2.9

TECHNIQUE: COLLECTIVE, VECTOR, LONGITUDINAL, LATERAL, AND DIRECTIONAL CONTROLS HELD FIXED WHILE ENGINE SPEED WAS STABILIZED AT EACH POINT.

WIND CONDITIONS

SYM	VEL - V_w - KTS	DIR - DEG FROM NOSE
○	2	130 L
□	3.5	125 R
△	2	55 R

COLLECTIVE STICK POSITION - δ_c - % UP = 100

LANDING GEAR DOWN

CURVES DERIVED FROM FIGURES NO. 142 AND 143, APPENDIX I.

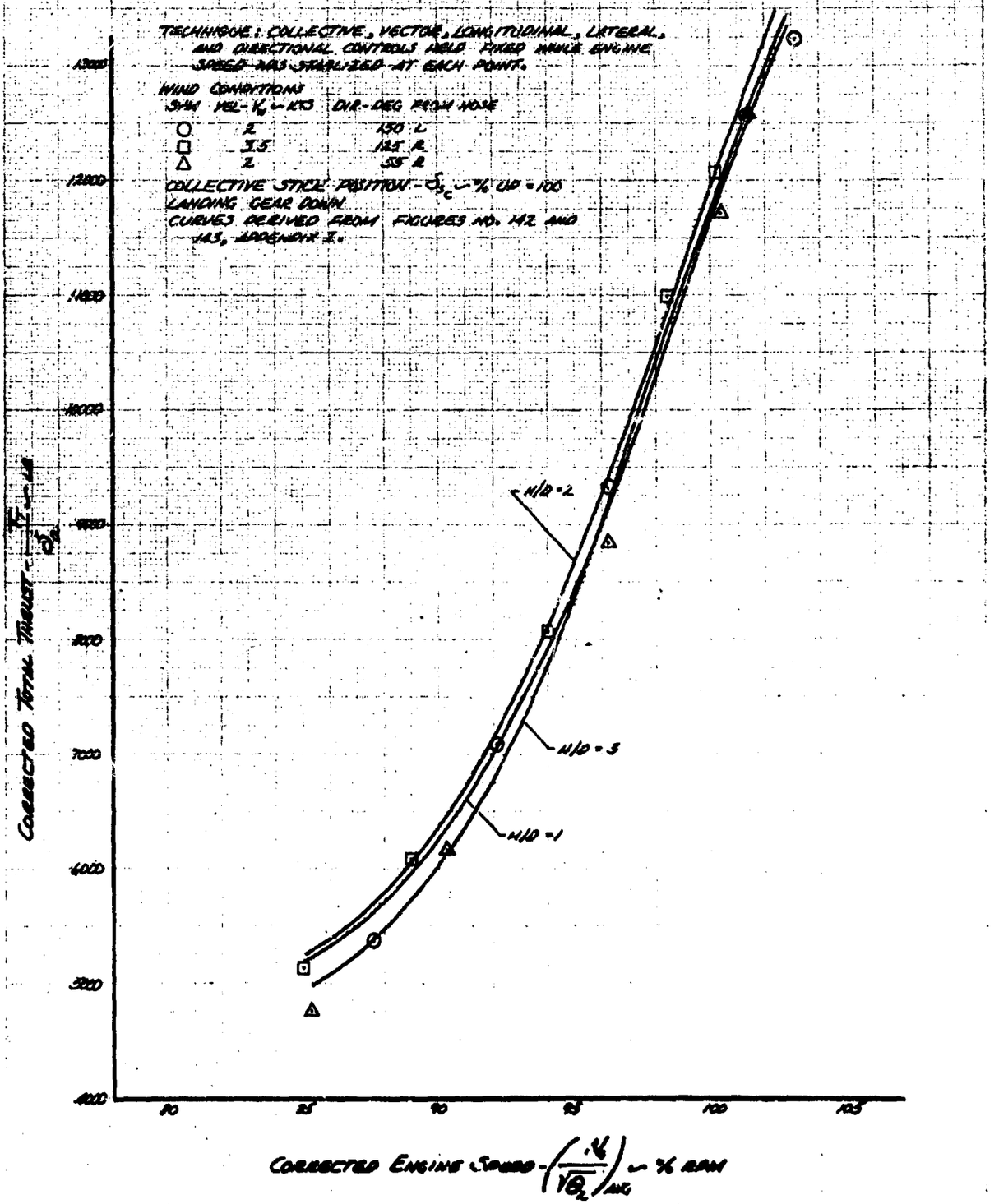

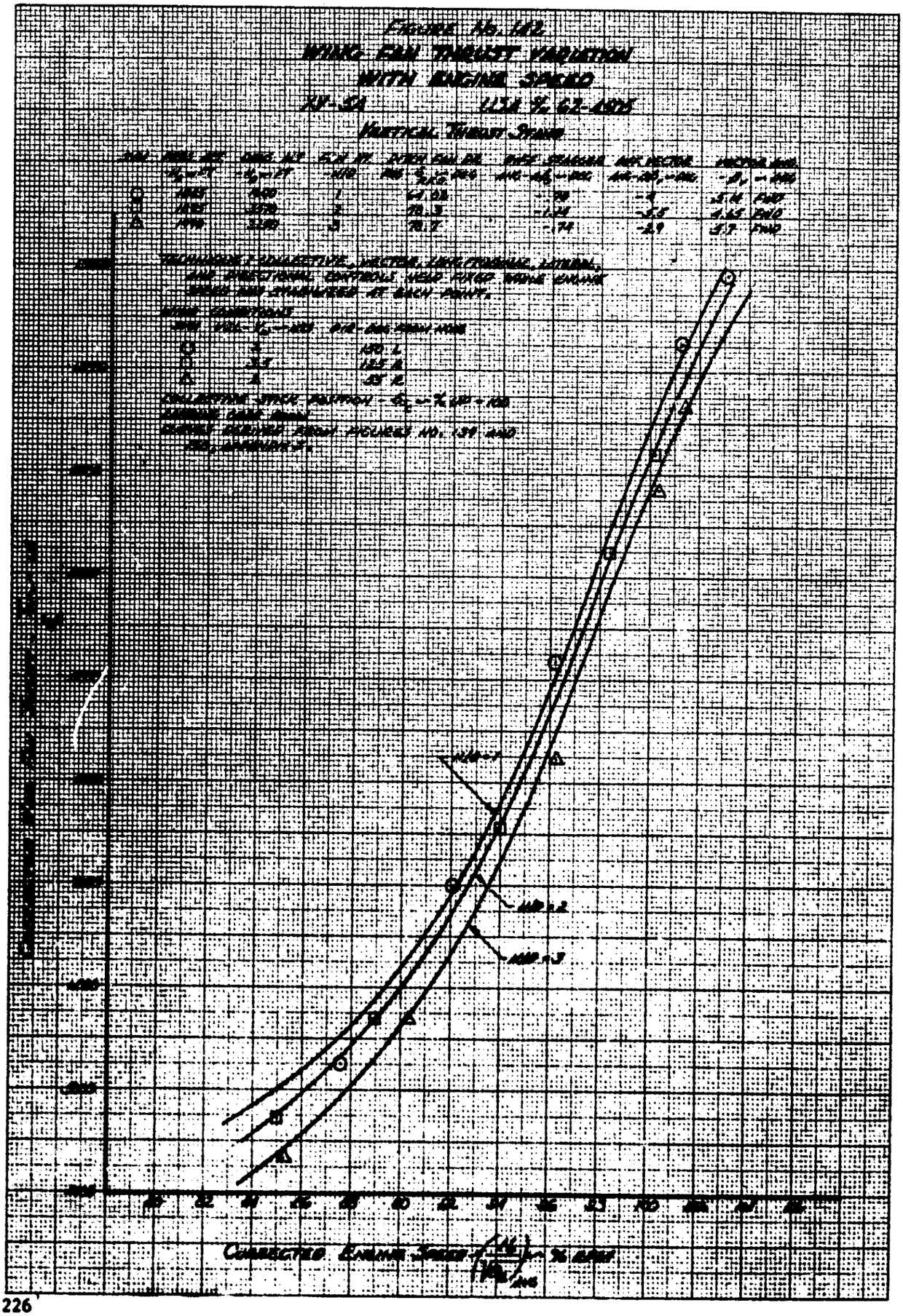
FIGURE NO. 142
WING FAN THRUST VARIATION
WITH ENGINE SPEED
XF-92A
VERTICAL THRUST STAND

FIGURE NO. 143

PITCH FAN THRUST VARIATION WITH ENGINE SPEED

XV-5A

Vertical Thrust Stand

STAB	ABSOL. ALT. $-H_p$ — FT	AMBIENT ALT. $-H_p$ — FT	AIRSPEED — KNOTS	ACTUAL GROSS WT. $-W_{ACT}$ — LBS	HOVER ATTITUDE $-\beta_p$ — DEG	AVG. ROLL TRIM — $\Delta\phi_T$ — DEG	AVG. STAGGER — $\Delta\phi_S$ — DEG
□	1095	3570	2	28.5	4.65 FWD	-5.5	-1.16
△	1990	2150	3	28.2	4.7 FWD	-2.9	-.74
○	1045	1400	1	27.02	3.24 FWD	-4	-.98

TECHNIQUE: COLLECTIVE, VECTOR, LONG. - ITUDINAL, LATERAL, AND DIRECTIONAL CONTROLS HELD FIXED WHILE ENGINE SPEED WAS STABILIZED AT EACH POINT.

AVIAR CONVENTIONS		
STAB	$\Delta\phi_C = -\phi_C$ — DEG	$\Delta\phi_T$ — DEG FROM NOSE
□	3.5	135 R
△	2	135 R
○	2	150 L

COLLECTIVE STICK POSITION - $-\phi_C$ — DEG = 4.100

LANDING GEAR DOWN

CURVES DERIVED FROM FIGURES NO. 140 AND 142, APPENDIX I.

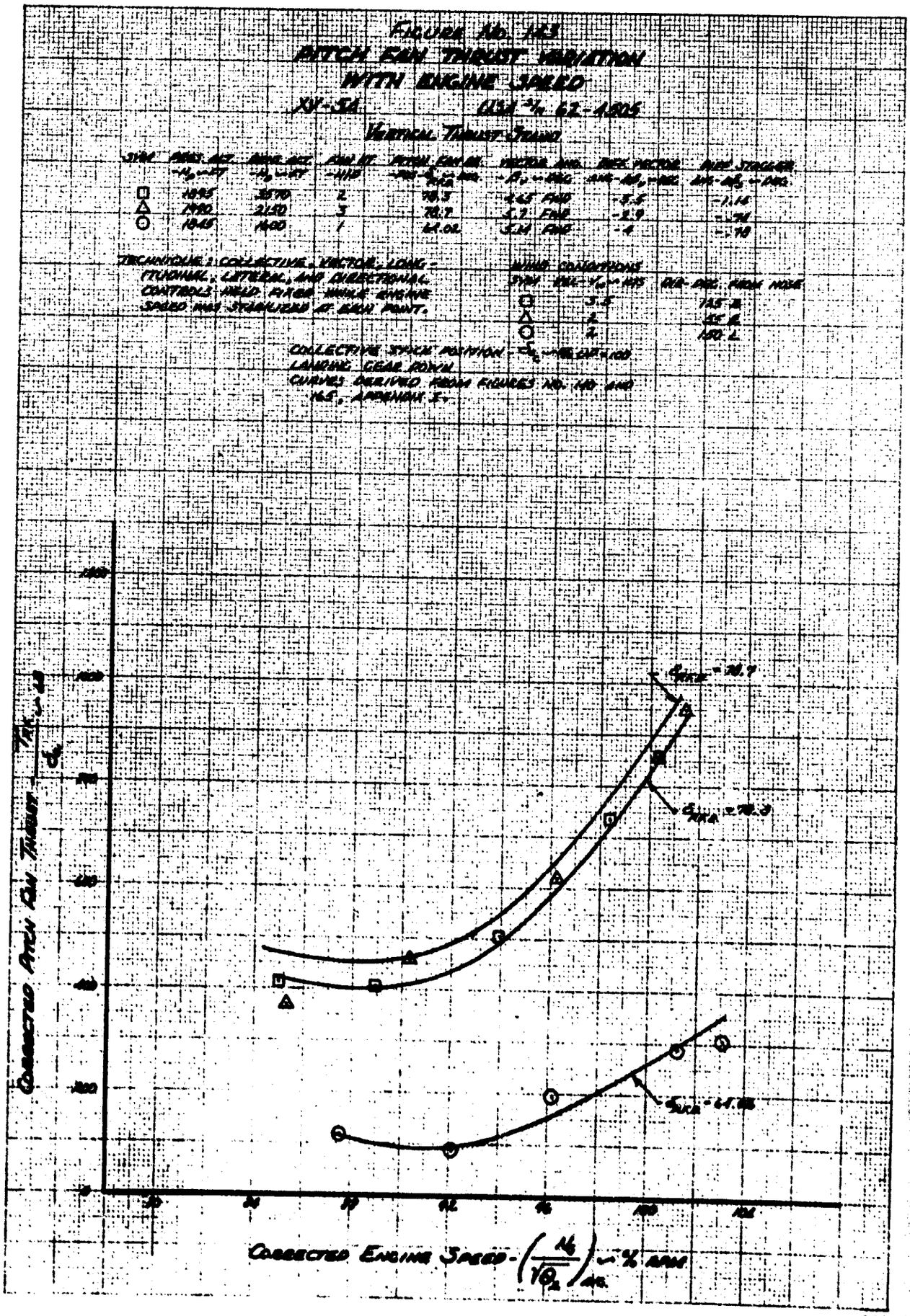

FIGURE No. 111

ENGINE POWER VARIATION WITH ENGINE SPEED

XV-5A USA 3/4 62-4505

VERTICAL THRUST STAND

SYM	PRESS. ALT. H_p – FT	AMB. ALT. H_a – FT	FAN HT. – H/D	PITOT FAN DIA. POS – $S_{H.P.}$ = DIA.	VECTOR ANG. – δ_V – DEG	CHOKE FACTOR ANC – A/A_c + PCT.	CHOKE STAGGER ANC – $\Delta\delta_c$ – DEG
□	1015	3570	2	78.3	11.65 FWD	-5.5	-1.14
△	1250	3450	5	78.5	5.7 FWD	-2.9	-.74
○	1845	1400	1	64.02	5.14 FWD	-4	-.79

TRUNNIONS: COLLECTIVE, VECTOR, LONGITUDINAL, LATERAL, AND DIRECTIONAL CONTROLS HELD FIXED WHILE ENGINE SPEED WAS STABILIZED AT EACH POINT.

COLLECTIVE STICK POSITION: δ_{C_c} – % TRAVEL = 100 FORWARD STICK DOWN

WIND CONDITIONS

SYM	VEL – V_w – KTS	DIR – DEG FROM NOSE
□	3.5	125 R
△	2	55 R
○	2	150 L

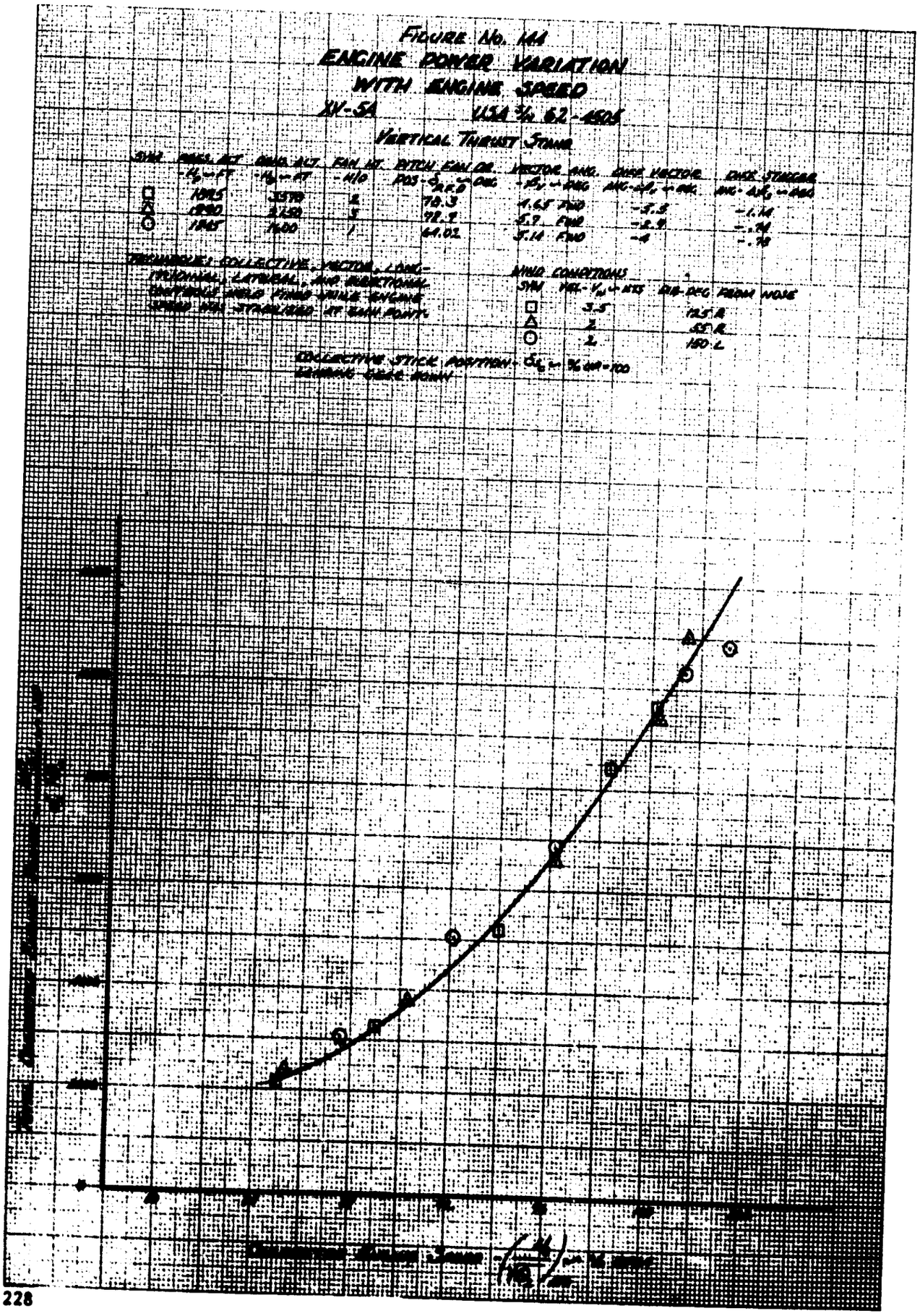

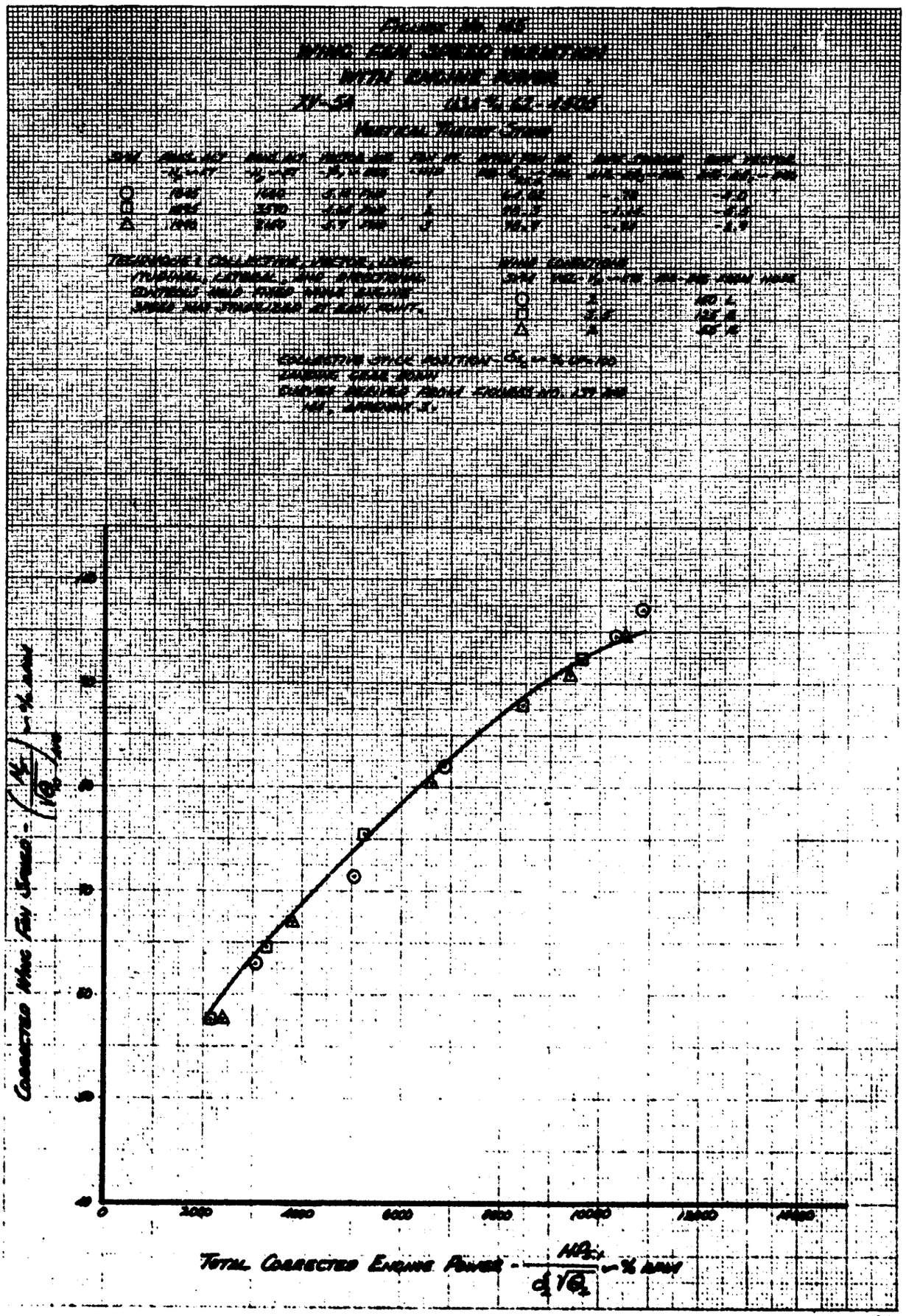
Total Corrected Engine Power - $\frac{NP_{2.1}}{\delta_1\sqrt{\theta_2}}$ - % Army

FIGURE NO. 146

PITCH FAN SPEED VARIATION WITH ENGINE POWER

XH-51A ULSA 61-4505

VERTICAL THRUST STAND

SYM	ENG. ALT. $-H_{e_1}$ — FT	AIRC. ALT. $-H_{a_1}$ — FT	VELOCITY AND $-V_a$ — KNOTS	FAN RPM $-N_f$	PITCH FAN DIA. $\frac{D_{f_{2-3}}}{2}$ — RAD	INLET STAGGER ANG. $-\beta_{f_1}$ — DEG	INLET VECTOR ANG. $-\beta_{f_2}$ — DEG
○	1625	1500	S.M. FWD	1	41.02	-.98	-4.0
□	2000	2000	4.5 KT FWD	3	39.3	1.14	-5.4
△	4000	3500	S.T. FWD	5	39.7	-.94	-2.9

TRIMMABLE COLLECTIVE, VECTOR, LONGITUDINAL, LATERAL, AND DIRECTIONAL CONTROLS HELD FIXED WHILE ENGINE SPEED WAS STABILIZED AT EACH POINT.

SYM	WIND VELOCITY — V_w — KTS	DIR — DEG FROM NOSE
○	2	130 L
□	5.5	135 R
△	2	35 R

COLLECTIVE STICK POSITION - δ_c — % OF TOTAL

LANDING GEAR DOWN

CURVE DERIVED FROM FIGURES NO. 130 AND APP. APPENDIX I.

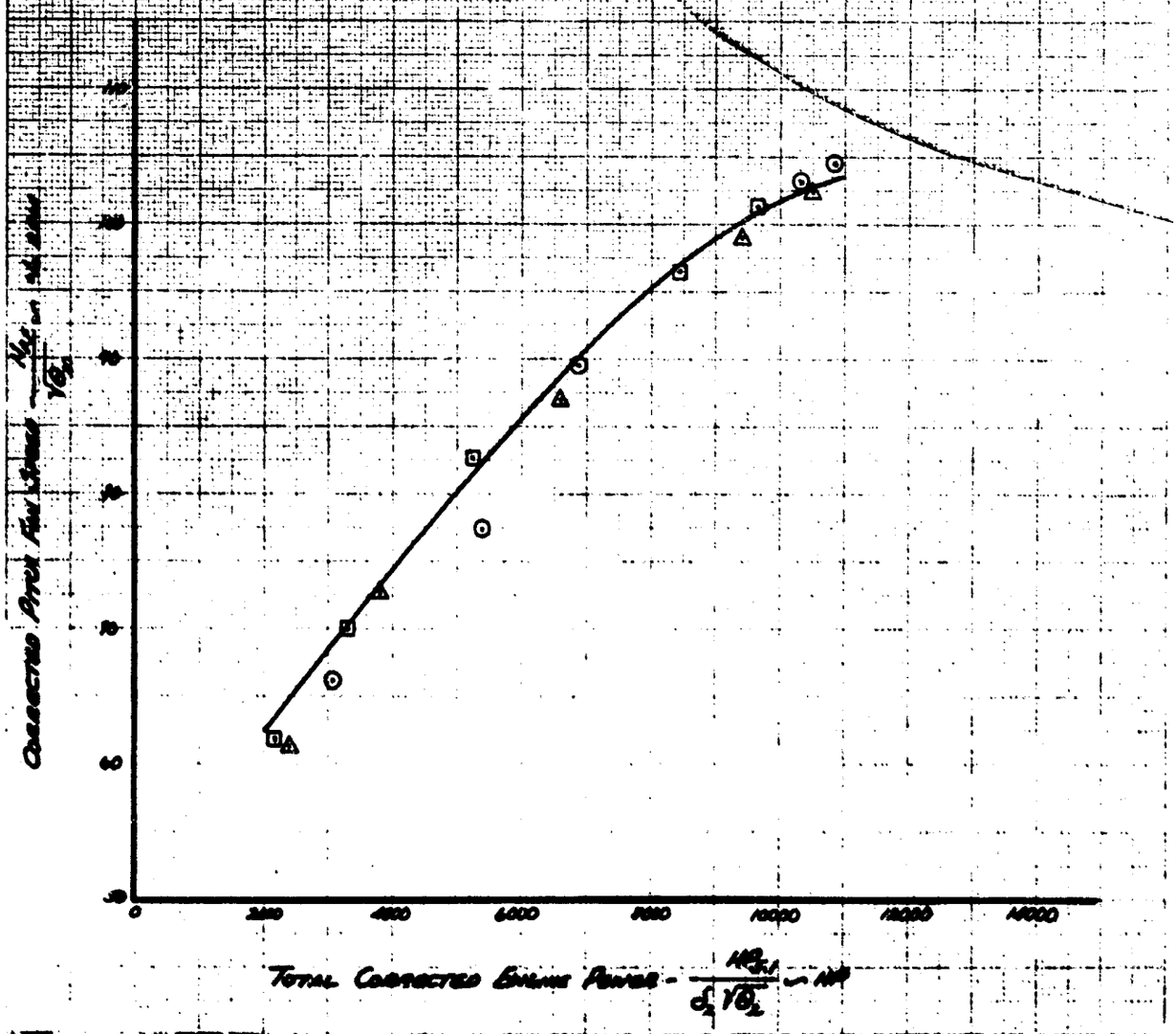

FIGURE No. 147

THRUST VARIATION WITH ENGINE POWER

XV-5A USA ¾ 62-1505

VERTICAL THRUST STAND

SYM	PRESS. ALT $-H_p$ — FT	DENS. ALT $-H_\sigma$ — FT	VECTOR ANG. $-\delta_{V_n}$ — DEG	FAN RT. $-n_{FD}$	PITCH FAN DIR. POS. $-\delta_{F_{1,2}}$ DEG.	DIFF. STAGGER ANG. $-\Delta\delta_y$ — DEG	DIFF. VECTOR ANG. $-\Delta\delta_{V_n}$ — DEG.
○	1845	1600	5.14 FWD	1	64.0 D	-.74	-4
□	1985	3670	4.65 FWD	2	78.3	-1.14	-5.5
△	1990	2450	5.7 FWD	3	75.9	-.74	-2.9

TECHNIQUE: COLLECTIVE, VECTOR, LONGITUDINAL, LATERAL, AND DIRECTIONAL CONTROLS HELD FIXED WHILE ENGINE SPEED WAS STABILIZED AT EACH POINT.

WIND CONDITIONS

SYM	VEL - V_w — MPH	DIR - DEG FROM NOSE
○	2	150 L
□	3.5	125 R
△	2	30 R

LANDING GEAR DOWN

COLLECTIVE STICK POSITION - δ_{C_n} — % UP = 100

CURVES DERIVED FROM FIGURES NO. 141 AND 142, APPENDIX I.

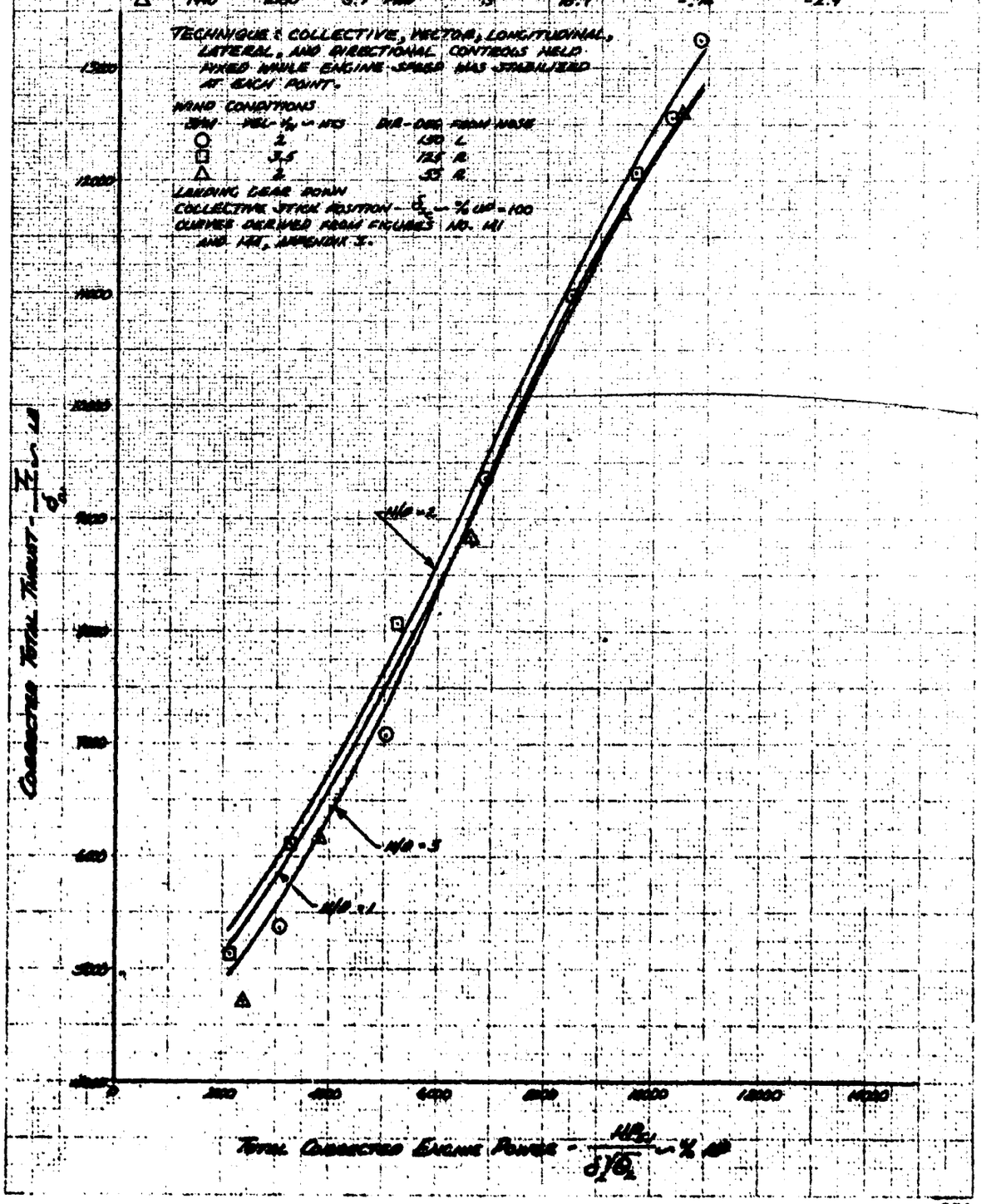

FIGURE NO. 148

WING FAN THRUST VARIATION WITH ENGINE POWER

XV-3A USA No. 62-1505

VERTICAL THRUST STAND

SYM	WING ACT. $-\delta_{f_L}$ — DEG	FLAP ACT. $-\delta_{f_R}$ — DEG	VECTOR ANG. $-\beta_v$ — DEG	FAN SYM. — H/D	ROTOR RPM OR Ω_{TIP}	DIFF. STABILIZER Δi_s — DEG	DIFF. VECTOR Δi_v — DEG
○	1845	1600	STK FWD	1	64.02	-.78	-4
□	1965	2070	-1.65 AFT	2	70.3	-1.14	-4.5
△	1990	2150	3.7 FWD	3	78.7	.78	-2.9

TECHNIQUE: COLLECTIVE, VECTOR, LONGITUDINAL, LATERAL, AND DIRECTIONAL CONTROLS HELD FIXED WHILE ENGINE SPEED WAS STABILIZED AT EACH POINT.

WING CONDITIONS

SYM	WING δ_{f_L} — DEG	δ_{f_R} — DEG	AVG. AREA NOSE
○	2		140 A
□	3.5		145 A
△	2		135 A

LANDING GEAR DOWN

COLLECTIVE STICK POSITION - δ_c — % UP = 100

CURVES DERIVED FROM FIGURES NO. 142 AND 143, APPENDIX B.

H/D = 1

H/D = 2

H/D = 3

CORRECTED WING FAN THRUST - $\frac{T_{FL}}{\delta_2}$ — LB

TOTAL CORRECTED ENGINE POWER - $\frac{HP_{SL}}{\delta_2\sqrt{\theta_2}}$ — HP

FIGURE No. 140

PITCH FAN THRUST VARIATION WITH ENGINE POWER

XV-5A USA S/N 62-4505

VERTICAL THRUST STAND

SYM	ABBS. ALT. $-H_p$ ~ FT	DENS. ALT. $-H_\sigma$ ~ FT	VECTOR ANG. $-\beta_v$ ~ DEG	FAN MT. -M/D	PITCH FAN DIR. POS. $-\delta_{RRD}$ ~ DEG	DUCT STAGGER ANG. $-\Delta\beta_d$ ~ DEG.	AUX VECTOR ANG. $-\Delta\beta_a$ ~ DEG.
○	1845	1600	5.14 FWD	1	64.02	-.78	-4
□	1895	3570	4.65 FWD	2	79.3	-1.14	-5.5
△	1990	2150	5.9 FWD	3	79.7	-.74	-2.9

TECHNIQUE: COLLECTIVE, VECTOR, LONGITUDINAL, LATERAL, AND DIRECTIONAL CONTROLS HELD FIXED WHILE ENGINE SPEED WAS STABILIZED AT EACH POINT.

HAND CONDITIONS

SYM	VEL - V_m ~ KTS	DIR - DEG. FROM NOSE
○	2	150 L
□	3.5	125 R
△	2	65 R

COLLECTIVE STICK POSITION - δ_{SC} ~ % UP = 100

LANDING GEAR DOWN

CURVES DERIVED FROM FIGURES NO. 144 AND 165, APPENDIX I.

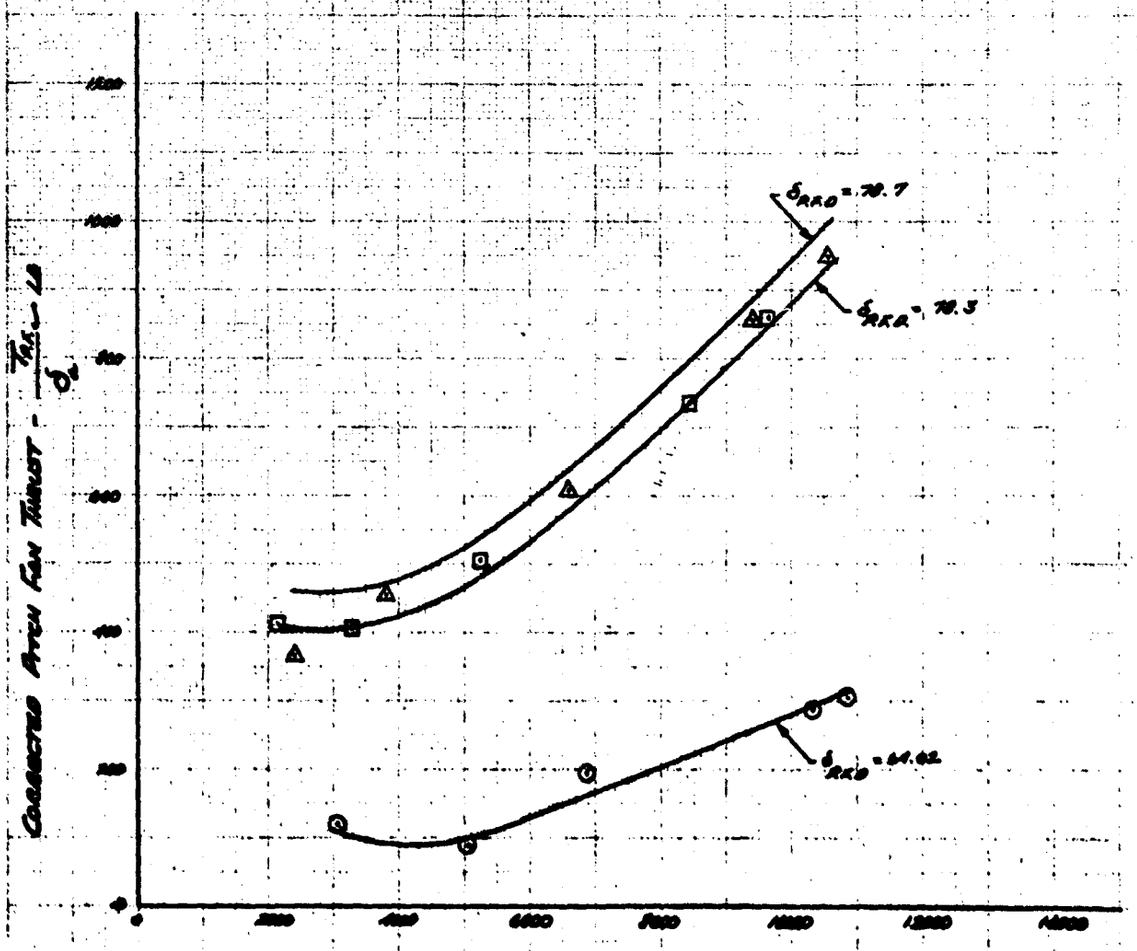

CORRECTED FAN THRUST - $\frac{T_{FAN}}{\delta_2}$ ~ LBS

TOTAL CORRECTED ENGINE POWER - $\frac{HP_{ENG}}{\delta_2\sqrt{\theta_2}}$ ~ HP

FIGURE No. 150

WING FAN THRUST VARIATION WITH FAN SPEED

XV-5A

USA ¾ 62-1505

VERTICAL THRUST STAND

SYM	PRES. ALT. $-H_p$ – FT.	DENS. ALT. $-H_d$ – FT	AIR VECTOR ANG. $-\beta_A$ – DEG.	FAN HT. $-H/D$	PITCH FAN DIR. ANG. $-\delta_{FAN}$ – DEG.	DIFF. STAGGER ANG. $-\Delta\beta_s$ – DEG.	DIFF. VECTOR ANG. $-\Delta\beta_A$ – DEG.
○	7645	7820	5.74 FWD	1	64.02	-.78	-4
□	1955	3570	4.65 FWD	2	77.3	-1.14	-5.5
△	990	2450	5.2 FWD	3	77.7	-.74	-2.9

TECHNIQUE: COLLECTIVE, VECTOR, LONGITUDINAL, LATERAL, AND DIRECTIONAL CONTROLS HELD FIXED WHILE ENGINE SPEED WAS STABILIZED AT EACH POINT.

WIND CONDITIONS

SYM	VEL. – V_w – KTS.	DIR. – DEG. FROM NOSE
○	2	330 L
□	3.5	145 R
△	2	35 R

LANDING GEAR DOWN

COLLECTIVE STICK POSITION – δ_{C_S} – % UP = 100

H/D = 1

H/D = 2

H/D = 3

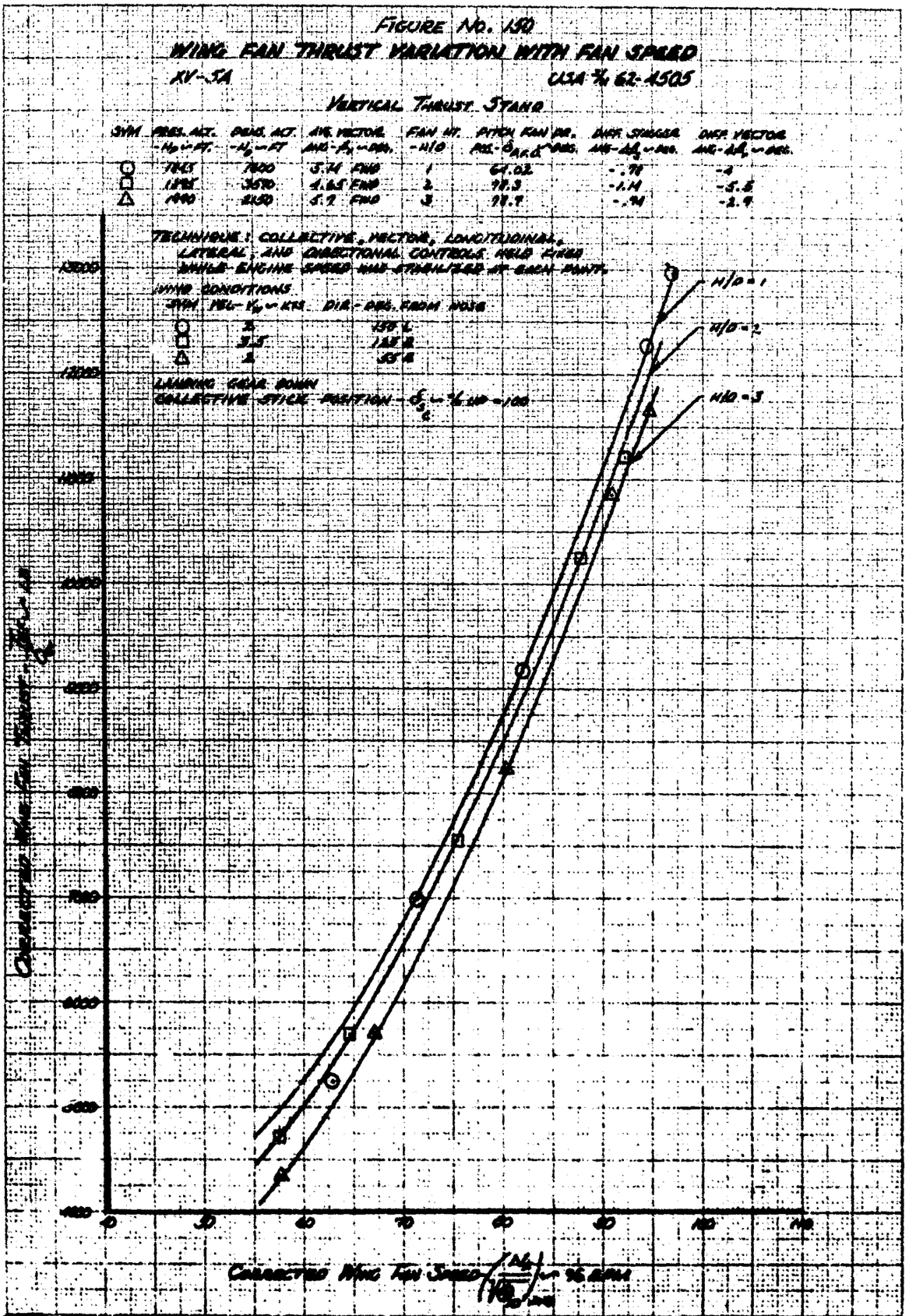

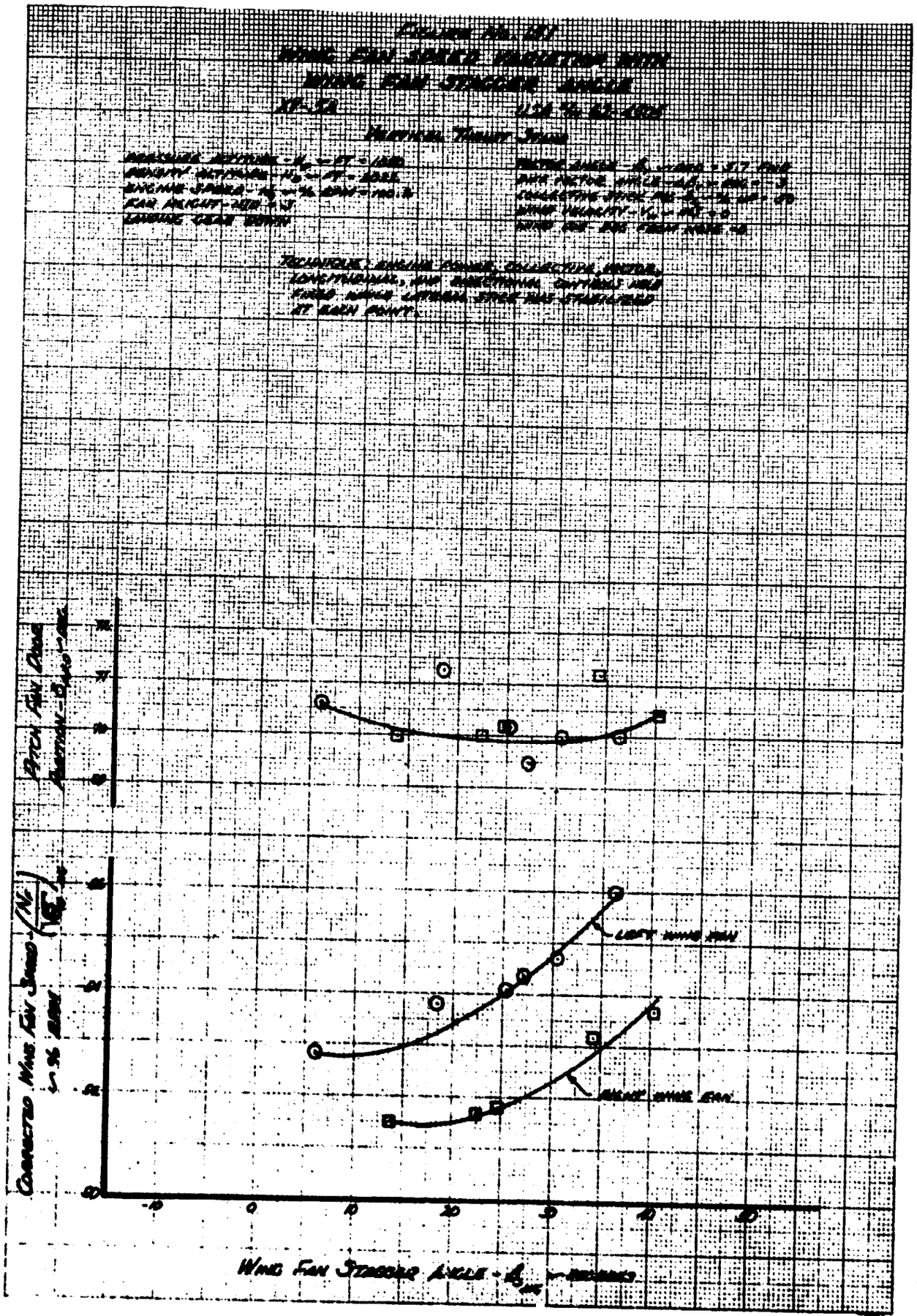
WING FAN SPEED VARIATION WITH
WING FAN STAGGER ANGLE
XF-12
FLIGHT TEST DATA
WING FAN SPEED - (N/√θ)
WING FAN STAGGER ANGLE - i_WF
LIGHT WING FAN
HEAVY WING FAN

FIGURE No. 132

WING FAN SPEED VARIATION WITH WING FAN STAGGER ANGLE

XV-5A USA 3/N 62-4505

VERTICAL THRUST STAND

PRESSURE ALTITUDE - H_p — FT = 1930
DENSITY ALTITUDE - H_D — FT = 2445
ENGINE SPEED - N_E — % RPM = 99.5
FAN HEIGHT - H/D = 3
LANDING GEAR DOWN

VECTOR ANGLE - δ_M — DEG = 4.99 FWD
DIFF. VECTOR ANGLE - $\Delta\delta_M$ — DEG = -2.15
COLLECTIVE STICK POS - δ_C — % UP = 100
WIND VEL - V_W — KTS = 3
WIND DIR - DEG FROM NOSE = 95°R

TECHNIQUE: ENGINE POWER, COLLECTIVE, VECTOR, LONGITUDINAL AND DIRECTIONAL CONTROLS HELD FIXED WHILE LATERAL STICK WAS STABILIZED AT EACH POINT.

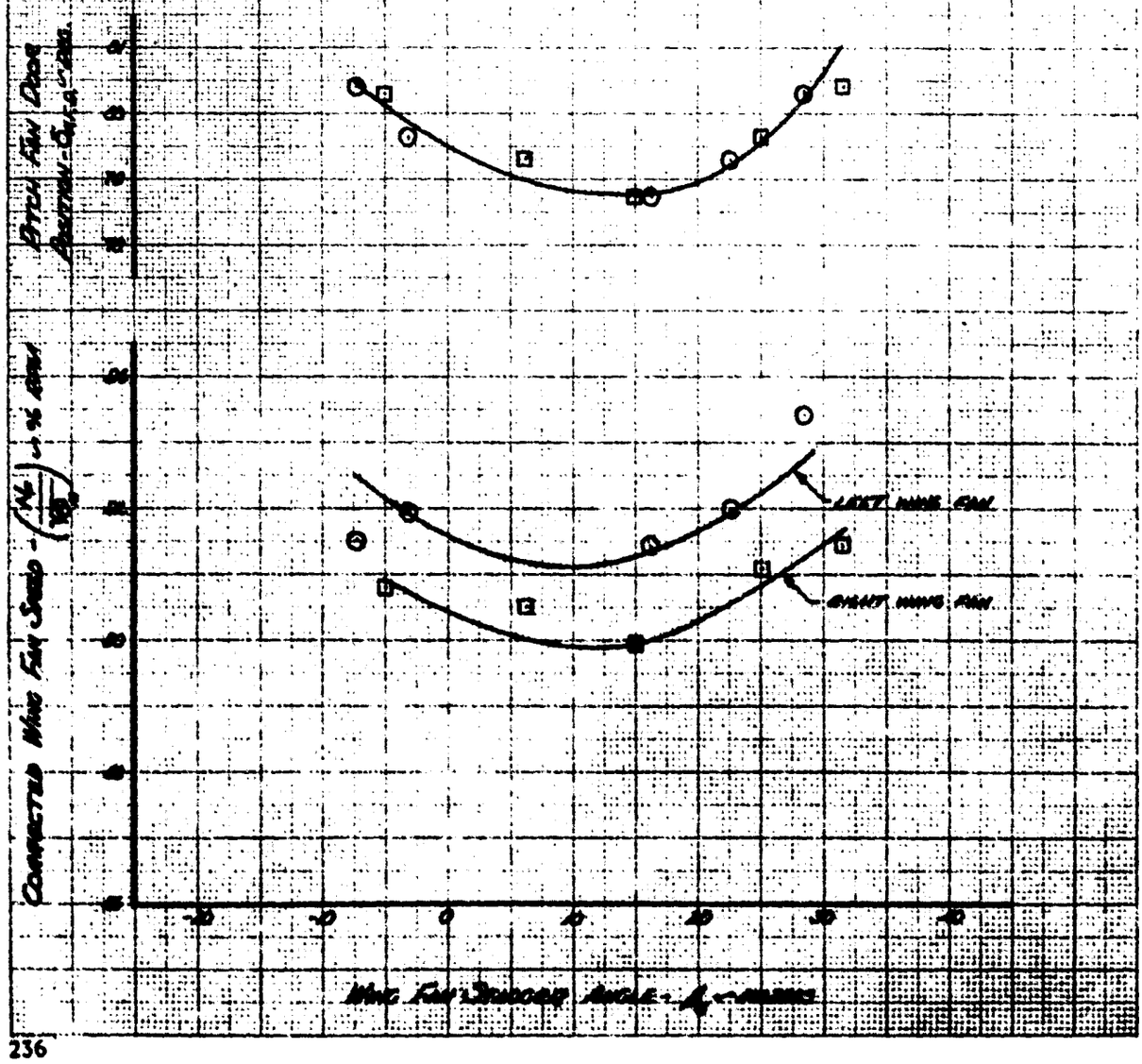

FIGURE A6.1.3.3

PITCH FAN SPEED VARIATION WITH WING FAN STAGGER ANGLE

XV-5A

Vertical Takeoff

PRESSURE ALTITUDE - H_p = 0 FT = SEA LEVEL
DENSITY ALTITUDE - H_D = 0 FT = SEA LEVEL
LANDING GEAR DOWN
FAN HEIGHT - H/D = 3
ENGINE SPEED - N_E = 96.4% RPM = 100

BASIC STAGGER ANGLE - β_{BS} = 0.0 = 1
TORQUE ANGLE β_T = 0.0 = 0 FIXED
LOWER LIMITING ANGLE - β_{LL} = 0.0 = -3.5
WING VELOCITY - V_W = 0 KTAS = 0
WING FAN DIA. TRIM VALVE = 110.0

TECHNIQUE: ENGINE POWER, ADJUSTING LATERAL AND LONGITUDINAL CONTROLS AND FIXED ANGLE COLLECTIVE WAS STABILIZED AT EACH POINT.

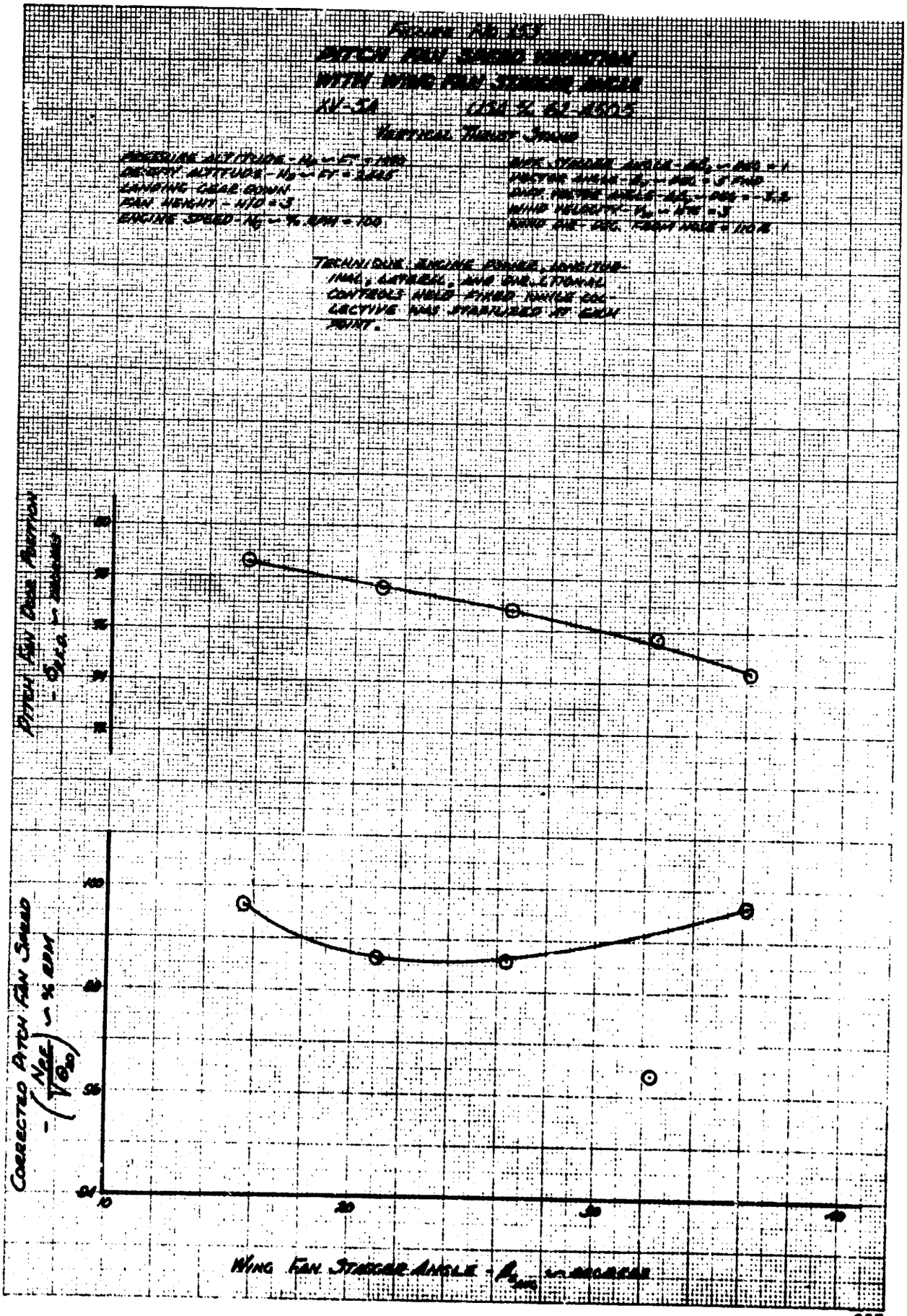

FIGURE No. 154

PITCH FAN SPEED VARIATION WITH WING FAN STAGGER ANGLE

XV-5A USA 3/4 62-4505

VERTICAL TURNOFF STAND

PRESSURE ALTITUDE - H_p = FT = 1890
DENSITY ALTITUDE - H_D = FT = 2445
ENGINE SPEED - N_g = % RPM = 99.5
FAN WEIGHT - MID = 5
LANDING GEAR DOWN

VECTOR ANGLE - β_w = DEG = 4.99 FWD
COLLECTIVE STICK POS - δ_c = % UP = 100
AFT VECTOR ANGLE - $\Delta\beta_w$ = DEG = -2.85
WIND VELOCITY - V_w = KTS = 3
WIND DIR - REL. FROM NOSE = 045R

TECHNIQUE: ENGINE POWER, COLLECTIVE, VECTOR, LONGITUDINAL, AND DIRECTIONAL CONTROLS HELD FIXED WHILE LATERAL STICK WAS STABILIZED AT EACH POINT.

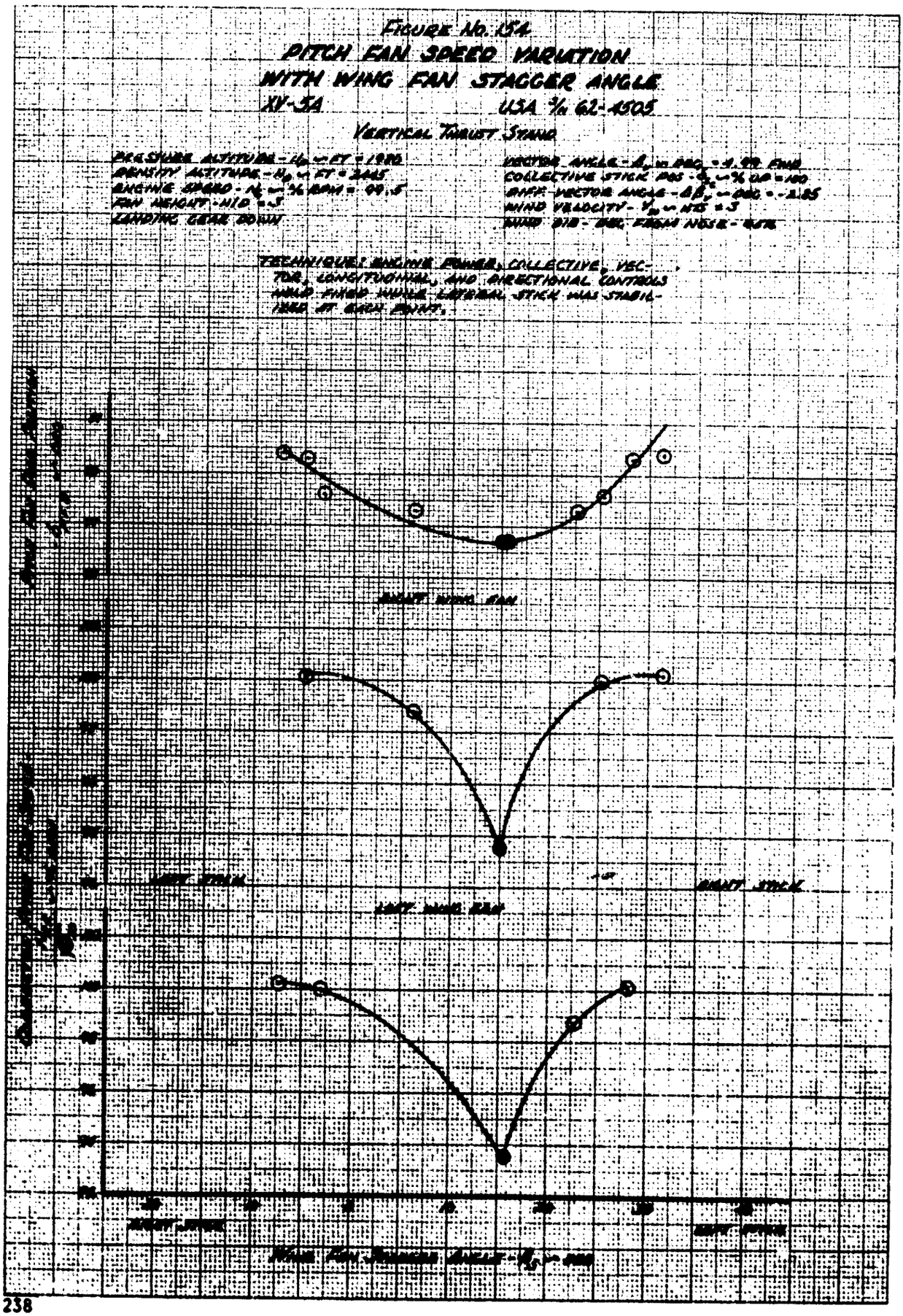

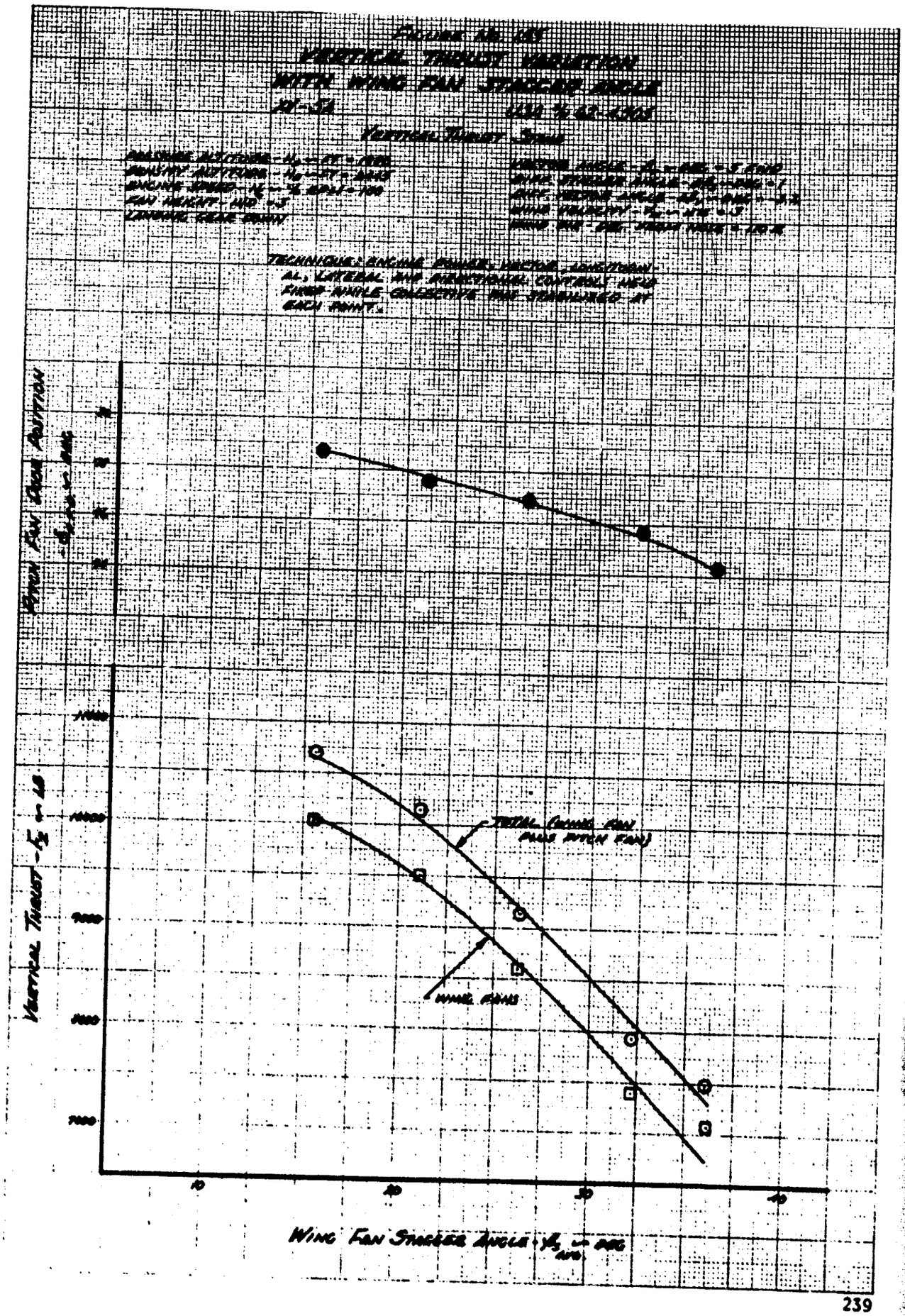
VERTICAL THRUST VARIATION
WITH WING FAN STAGGER ANGLE
XV-5A
Vertical Thrust Stand
TOTAL (CANARD FAN PLUS PITCH FAN)
WING FANS
Wing Fan Stagger Angle - i_{WF} - deg
Vertical Thrust - F_Z - lb
Canard Fan Exit Position

FIGURE NO. 138

PITCHING MOMENT VARIATION WITH WING FAN STAGGER ANGLE

XV-5A USA S/N 62-4505

VERTICAL TAKEOFF STAND

PRESSURE ALTITUDE - H_p = FT = 1930
DENSITY ALTITUDE - H_d = FT = 2445
ENGINE SPEED - N_E = % RPM = 100
FAN HEIGHT - H/D = 3
LANDING GEAR DOWN

VECTOR ANGLE - β_v = DEG. = 5 AND
NOZZLE VECTOR ANGLE - $\Delta\beta_v$ = DEG. = -3.2
PITCH STAGGER ANGLE - $\Delta\beta_f$ = DEG. = 1
WING HEIGHT - H_w = H/D = 3
WING CHORD - REYN. NUMBER = 110 K

TECHNIQUE: ENGINE POWER, VECTOR, AND THRUST AL. LATERAL, AND DIRECTIONAL CONTROLS HELD FIXED WHILE COLLECTIVE WAS STABILIZED AT EACH POINT.

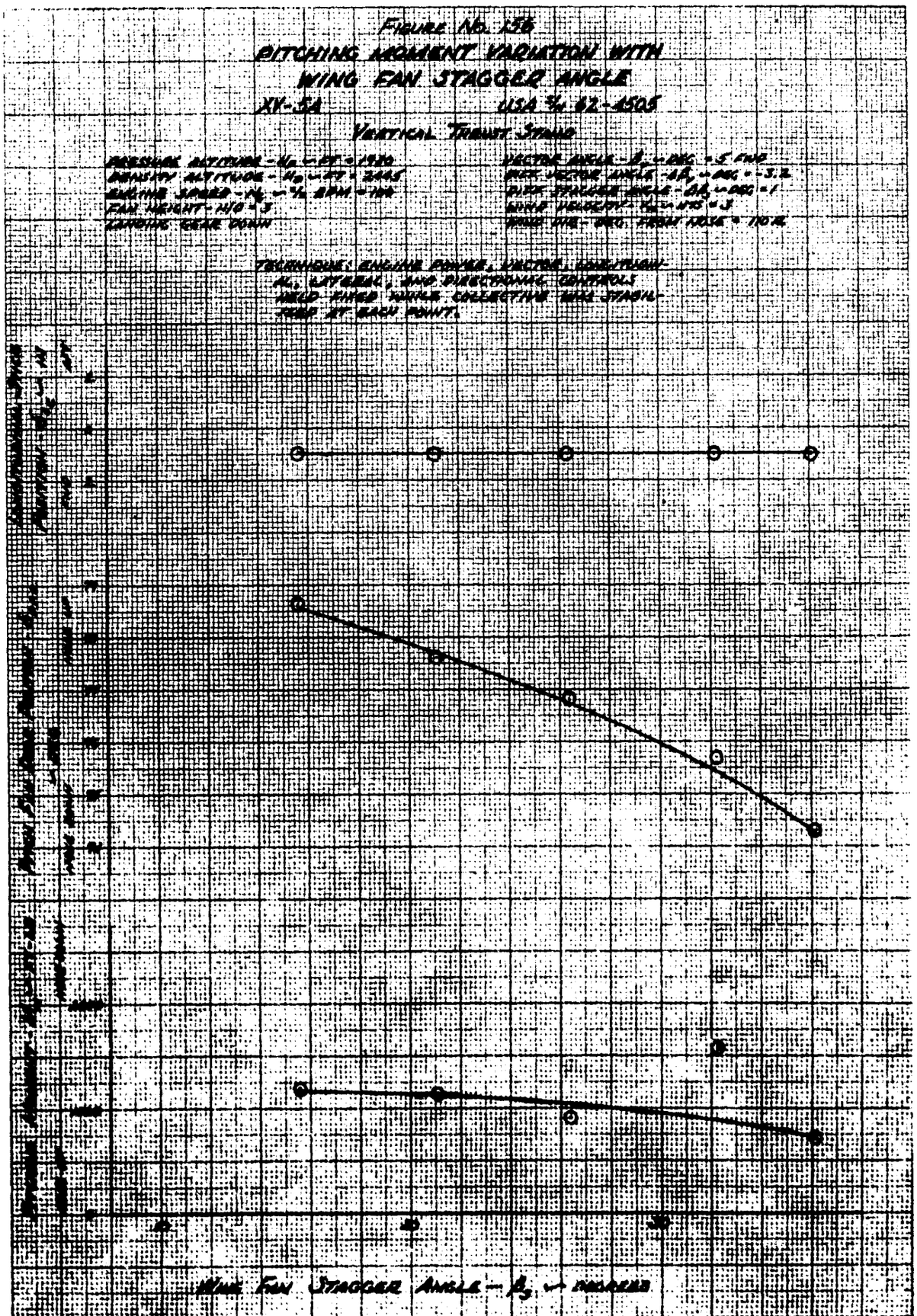

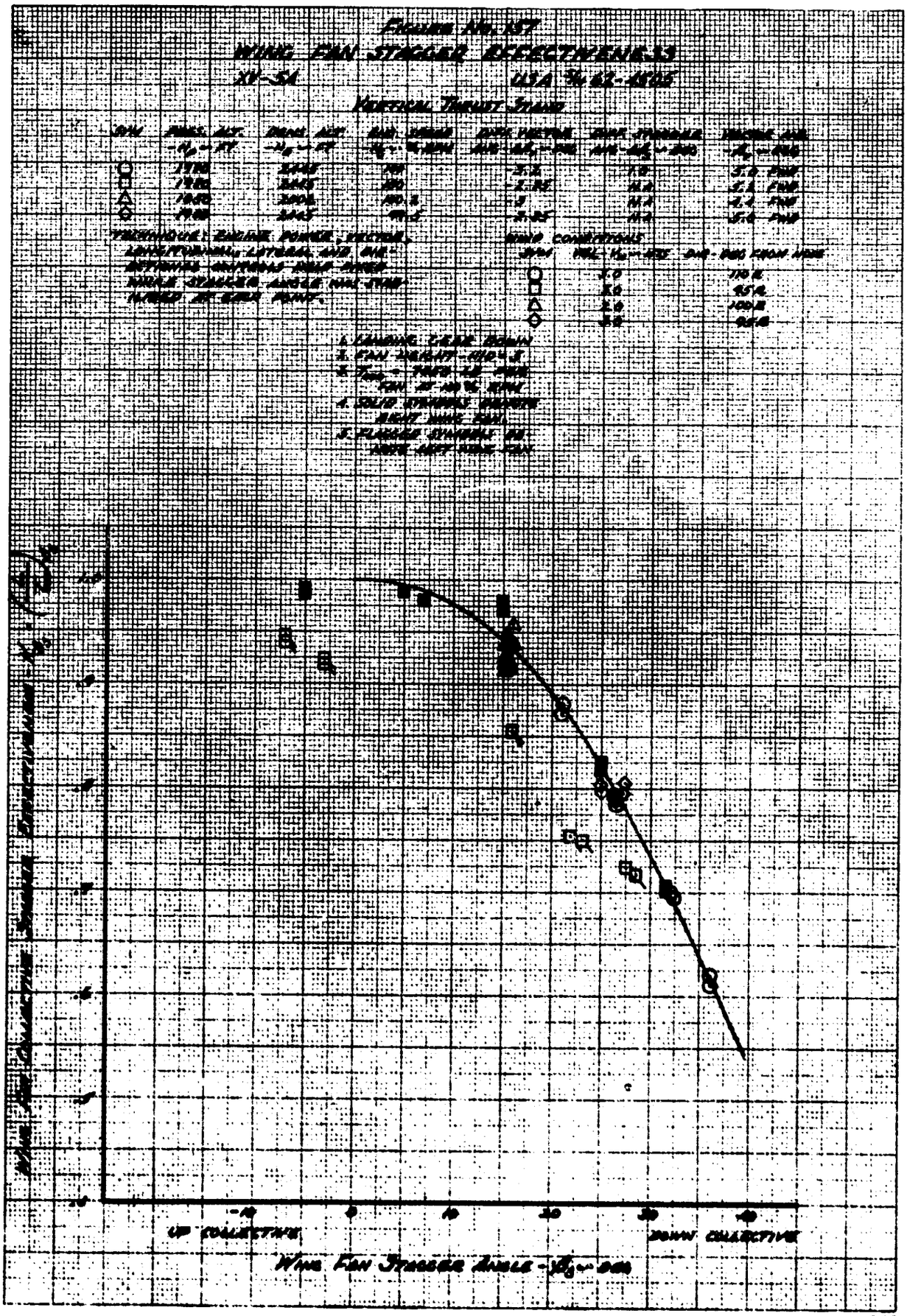
FIGURE NO. 107
WING FAN STAGGER EFFECTIVENESS
XV-5A
USA No 62-4505
VERTICAL THRUST STAND
UP COLLECTIVE
DOWN COLLECTIVE
WING FAN STAGGER ANGLE - i_{W_F} - DEG

FIGURE No. 153

VARIATION OF STAGGER ANGLE WITH COLLECTIVE STICK POSITION

XV-5A USA S/N 62-4505

VERTICAL THRUST STAND

PRESSURE ALTITUDE - H_p = FT = 1980
DENSITY ALTITUDE - H_ρ = FT = 2445
ENGINE SPEED - N_1 = % RPM = 100
FAN HEIGHT - H/D = 3
LANDING GEAR DOWN

VECTOR ANGLE - β_v = DEG = 5 FWD
DIFF. VECTOR ANGLE - $\Delta\beta_v$ = DEG = -3.2
DIFF. STAGGER ANGLE - $\Delta\beta_s$ = DEG = 1
WIND VELOCITY - V_w = KTS = 3
WIND DIR. - DEG. FROM NOSE = 170 R

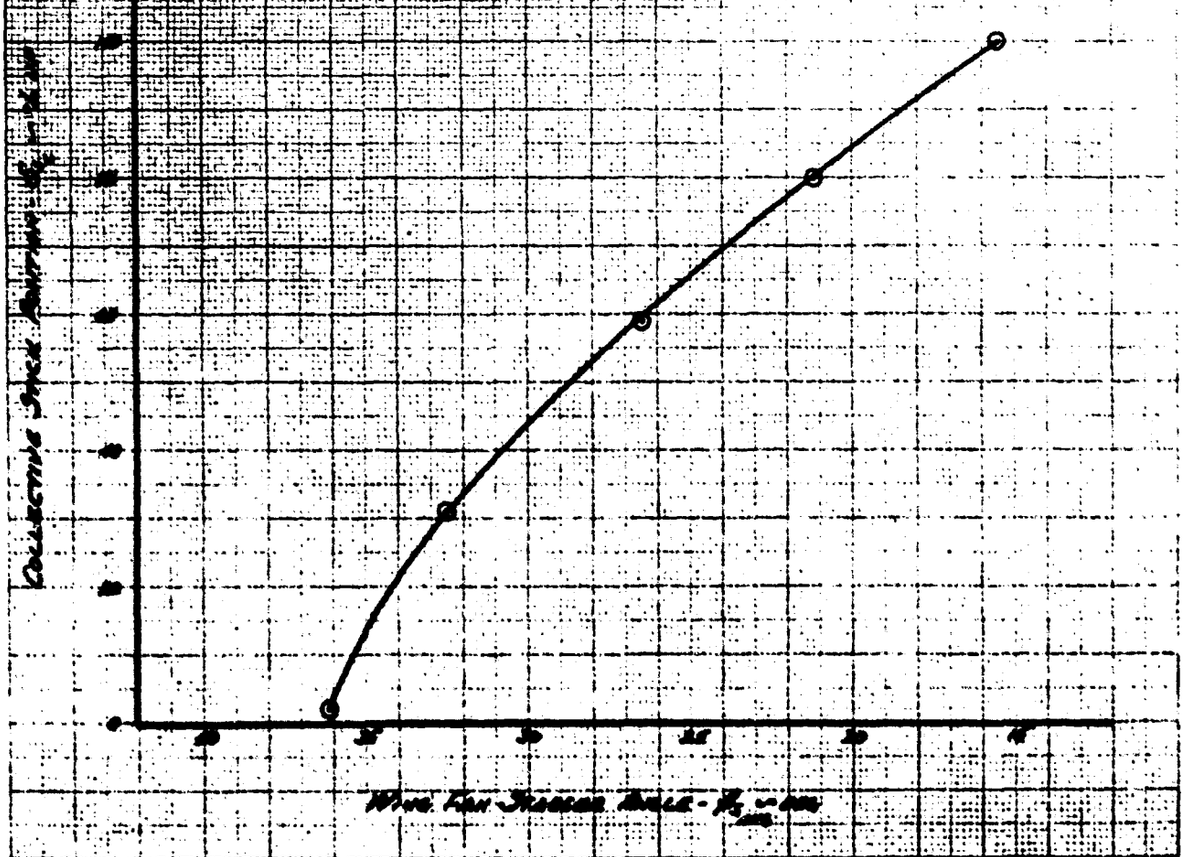

FIGURE NO. [illegible]

PITCH FAN SPEED VARIATION WITH PITCH FAN DOOR POSITION

XV-5A USA S/N 62-4505

VERTICAL THRUST STAND

PRESSURE ALTITUDE - H_p ~ FT = 1890
DENSITY ALTITUDE - H_D ~ FT = 1890
ENGINE SPEED - N_G ~ % RPM = 100.3
FAN SPEED - N_F ~ % RPM = 92
FAN HEIGHT - H/D = 3
LANDING GEAR DOWN

VECTOR ANGLE - β_v ~ DEG = 4.4 FWD
DIFF. VECTOR ANGLE - $\Delta\beta_v$ ~ DEG = -6
COLLECTIVE STICK POS - δ_c ~ % UP = 100
DIFF. STAGGER ANG - $\Delta\beta_s$ ~ DEG = -1.6
WIND VELOCITY - V_w ~ KTS = 2
WIND DIR - DEG. FROM NOSE = 100 R

TECHNIQUE: ENGINE POWER, COLLECTIVE, VECTOR, LATERAL AND DIRECTIONAL CONTROLS HELD FIXED WHILE PITCH FAN RPM WAS STABILIZED AT EACH POINT.

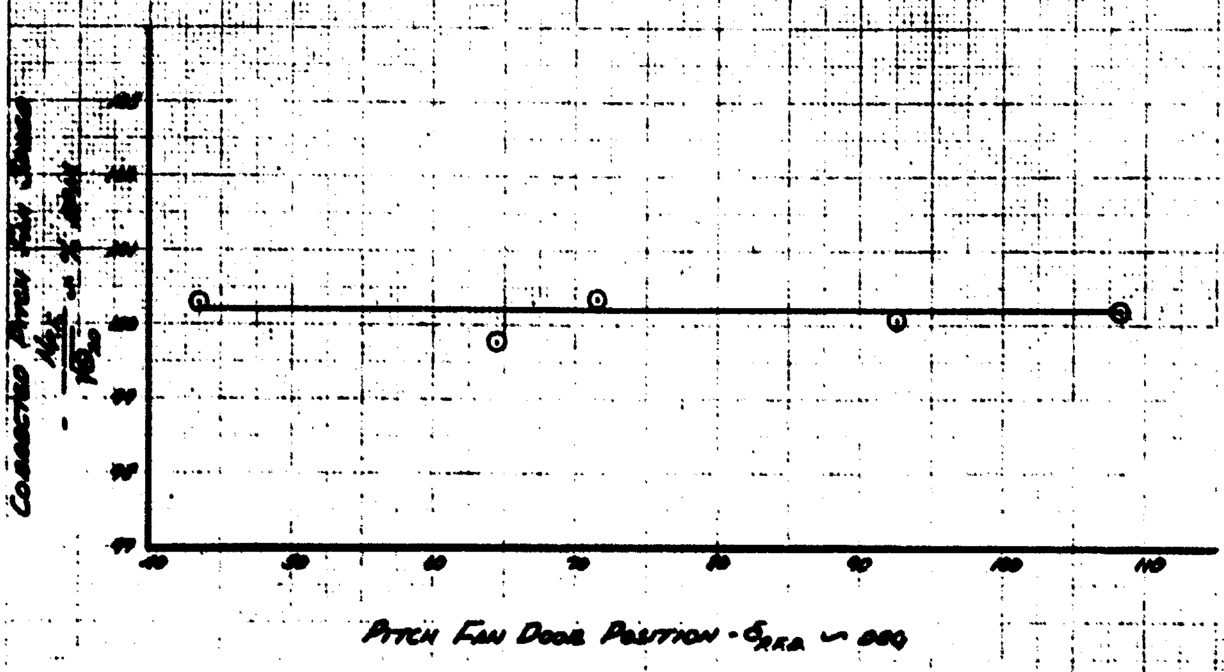

FIGURE NO. 180

WING FAN LIFT VARIATION WITH PITCH FAN DOOR POSITION

XF-5A USA ¾ 62-4505

VERTICAL THRUST STAND

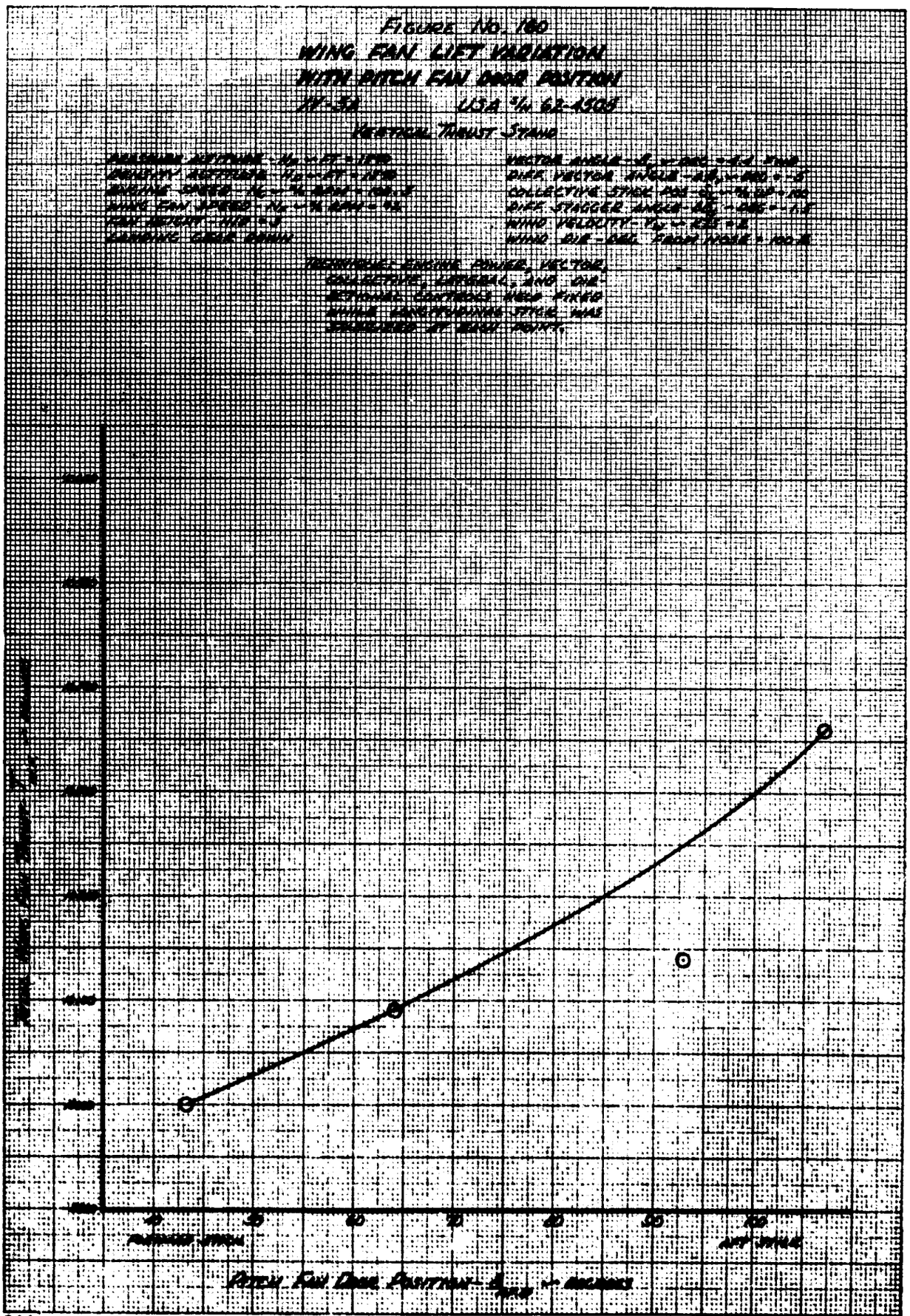

FIGURE NO. 161

PITCH FAN THRUST EVALUATION WITH PITCH FAN DOOR POSITION

XV-5A LTV # 62-4505

VERTICAL THRUST STAND

SYM	H_p — FT	H_c — FT	N_c — % RPM	δ_p — DEG	$\Delta\alpha_c$ — DEG	$\Delta\alpha_s$ — DEG	ΔN_c — % RPM
○	1950	2445	100	5° FWD	-3.2	1	92
□	1950	1150	100.3	44 FWD	-5°	-1.5°	98

TECHNIQUE: ENGINE POWER, VECTOR, LATERAL, AND DIRECTIONAL CONTROLS HELD FIXED. ANGLE OF PITCH FAN EXIT WAS VARIED WITH LONGITUDINAL AIR DEFLECTING STICK.

FAN AIRCRAFT - H/D = 3

LANDING GEAR DOWN

SYM	WHL - V_∞ — KTS	AMB - DOC TEMP °C
○	3	110 IR
□	2	100 IR

CORRECTED PITCH FAN THRUST - $\frac{F_{cp}}{\delta_{amb}}$ - LB

PITCH FAN DOOR POSITION - δ_{FAN} — DEGREES

FIGURE No. 162

PITCHING MOMENT VARIATION WITH PITCH FAN DOOR POSITION

XV-5A USA #1 62-4505

VERTICAL THRUST STAND

PRESSURE ALTITUDE - H_p = FT. = 1890
DENSITY ALTITUDE - H_σ = FT = 1870
ENGINE SPEED - N_E = % RPM = 100.3
FAN AIRCRAFT - N/D = 5
FAN SPEED - N_F = % RPM = 92
LANDING GEAR RETRACTED

VECTOR ANGLE - δ_V = DEG = 4.4 FWD
DIFF. VECTOR ANGLE - $\Delta\delta_V$ = DEG = -5
COLLECTIVE STICK POSITION - δ_c = % UP = 100
DIFF. STAGGER ANG. - Δi_B = DEG = -1.5
WIND VELOCITY - V_w = KTS = 2
WIND DIR - DEG FROM NOSE = 100 R

TECHNIQUE: COLLECTIVE, ENGINE POWER, VECTOR, LATERAL, AND DIRECTIONAL CONTROLS HELD FIXED WHILE LONGITUDINAL STICK WAS STABILIZED AT EACH POINT.

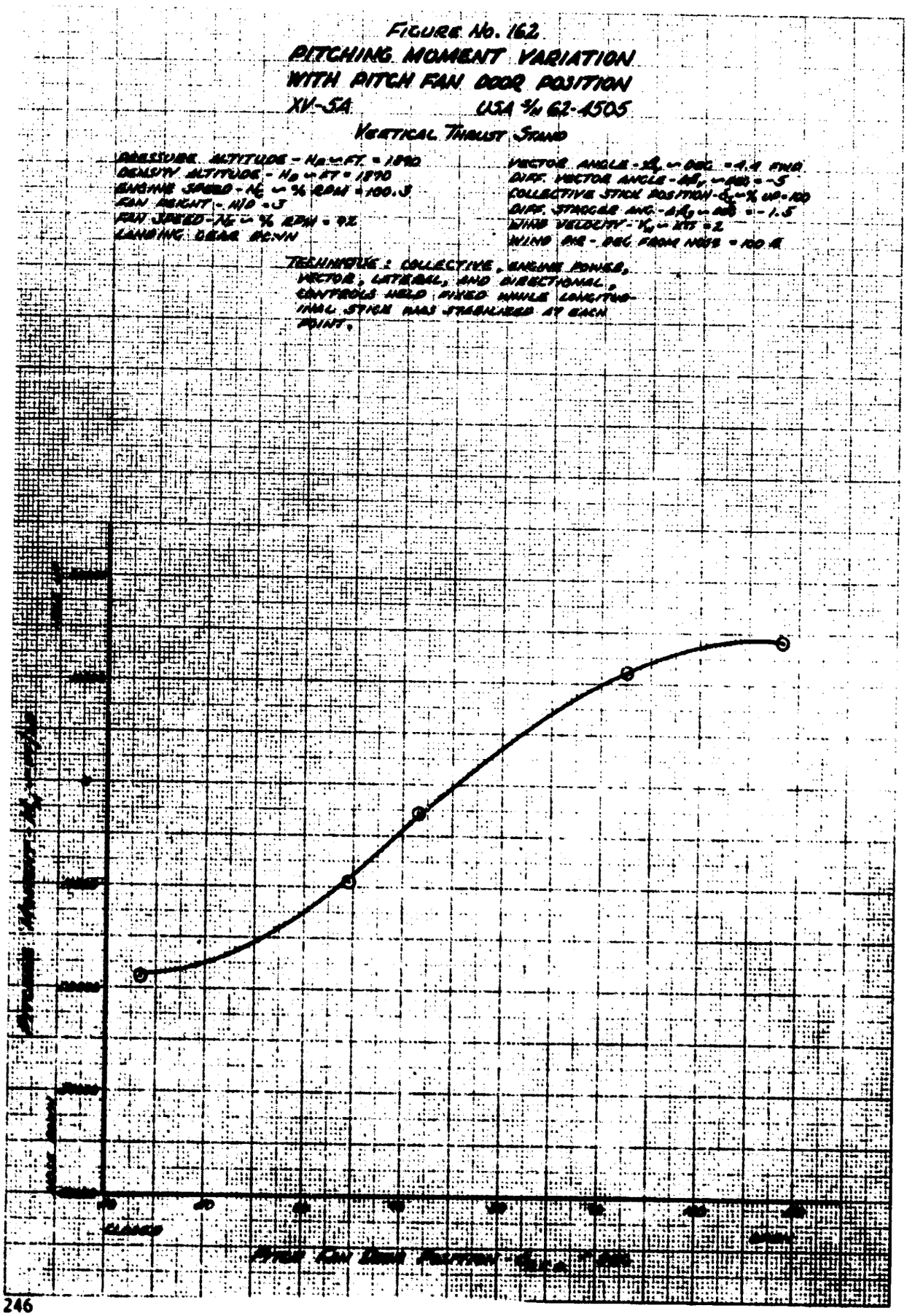

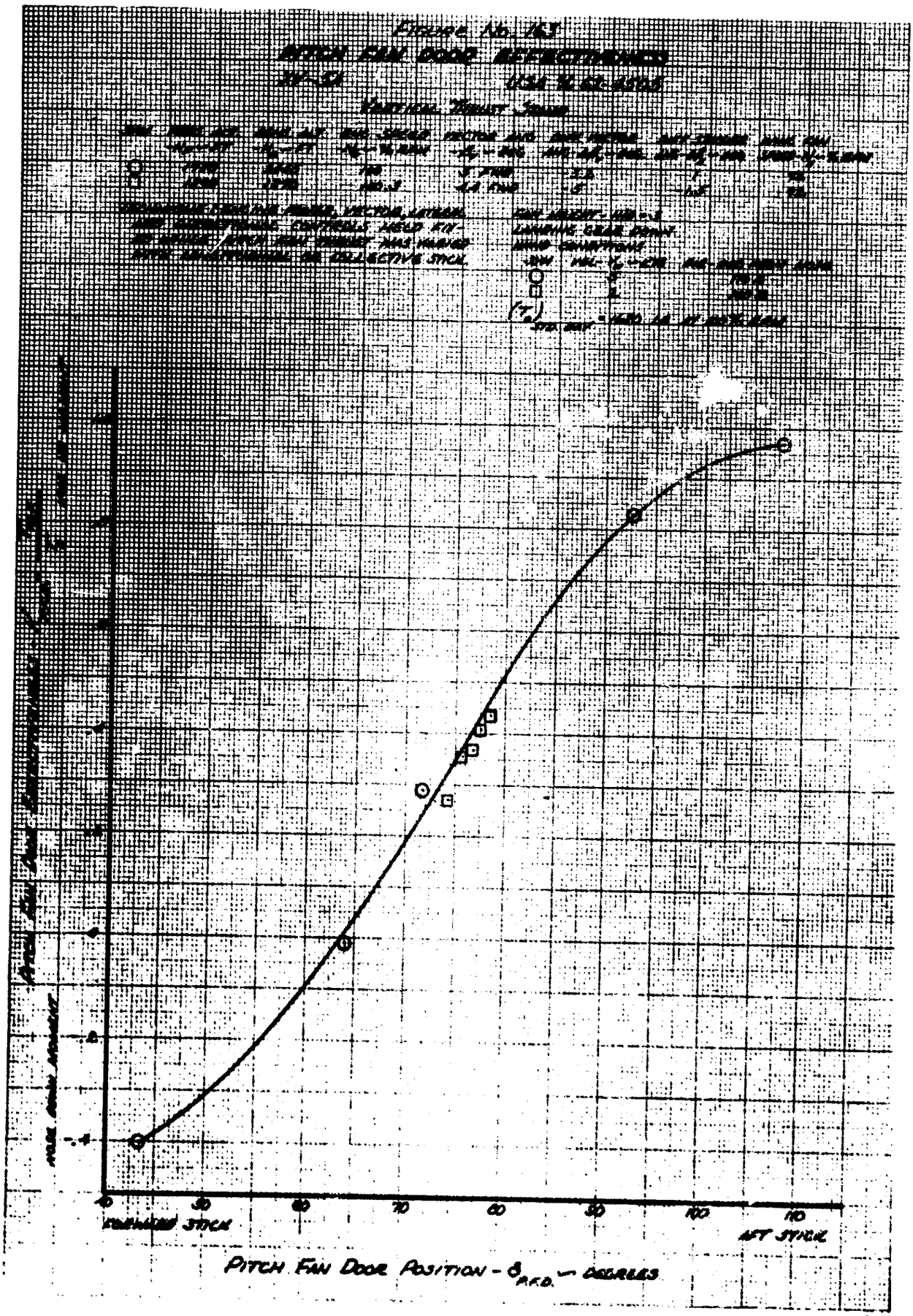
0
10
20
30
40
50
60
70
80
90
100
110
FORWARD STICK
AFT STICK
PITCH FAN DOOR POSITION - $\delta_{P.F.D.}$ — DEGREES

FIGURE No. 164

WING FAN LIFT VARIATION WITH PITCH FAN SPEED

XV-5A USA No. 62-4505

VERTICAL THRUST STAND

PRESSURE ALTITUDE - H_p = FT = 1790
DENSITY ALTITUDE - H_D = FT = 1870
ENGINE SPEED - N_E = % RPM = 100.3
FAN HEIGHT - H/D = 3
WING FAN SPEED - N_{FW} = % RPM = 98
LANDING GEAR DOWN

VECTOR ANGLE - β_V = DEG = 4.1 AFT
OVER VECTOR ANGLE - $\Delta\beta_V$ = DEG = -5
DIFF. STAGGER ANGLE - $\Delta\beta_S$ = DEG = -1.5
COLL. STICK POSITION - δ_C = % UP = 100
WIND VELOCITY - V_W = KTS = 2
WIND DIR - DEG FROM NOSE = 100 R

TECHNIQUE: ENGINE POWER, COLLECTIVE, VECTOR, LATERAL, AND DIRECTIONAL CONTROLS HELD FIXED WHILE LONGITUDINAL STICK WAS STABILIZED AT EACH POINT.

CURVE DERIVED FROM FIGURES NO. 149 AND 152, APPENDIX I.

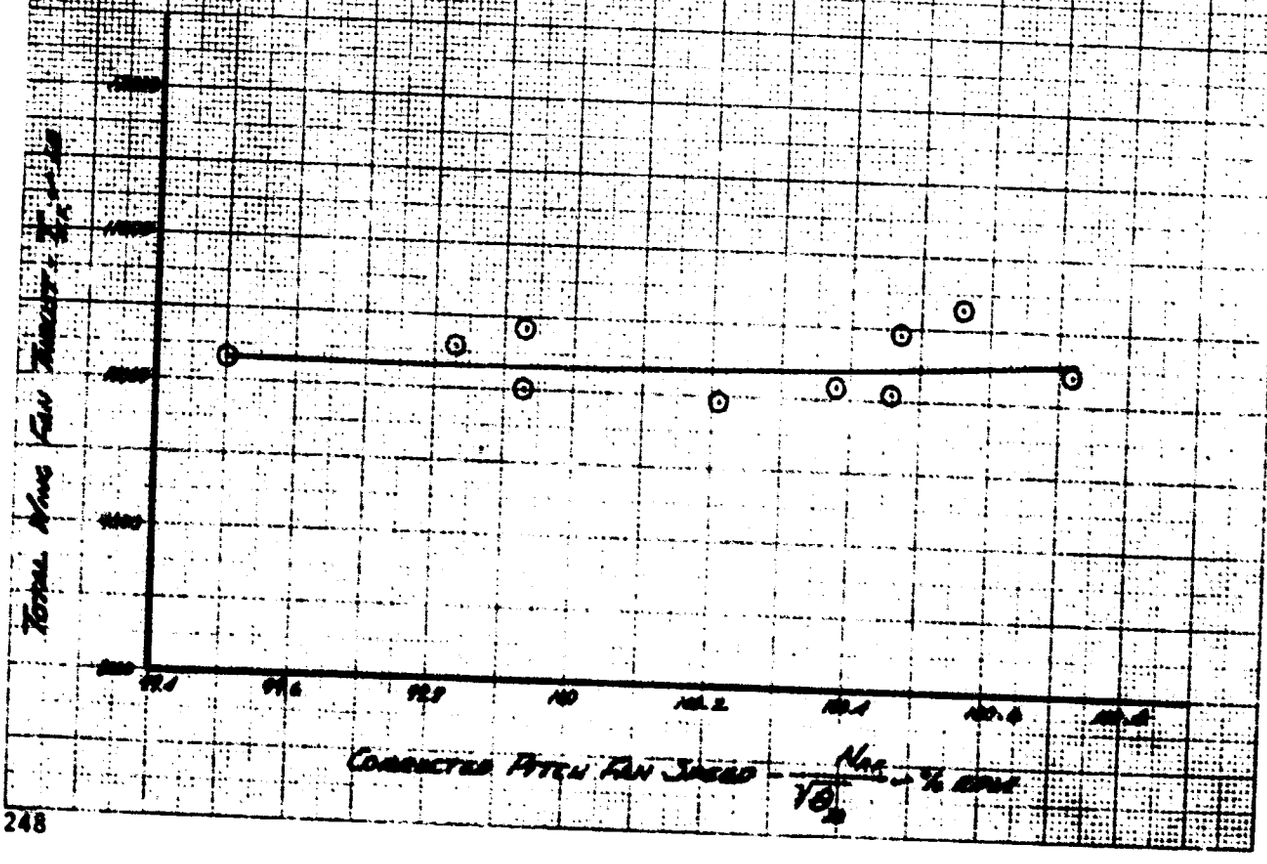

FIGURE No. 165

PITCH FAN THRUST VARIATION WITH PITCH FAN SPEED

XV-5A USA S/N 62-4506

VERTICAL THRUST STAND

SYM.	GROSS WT. $-W_g$ — LB	PRESS. ALT. $-H_p$ — FT.	FAN SEGMENT — NO.	PITCH FAN DIA. POS. — $\delta_{PF.D.}$ DEG.	COLL. STICK POS. — δ_{S_C} — % CHD	FREE AIR TEMP. $-T_{AT}$ — °C
□	1895	3570	2	78.3	100	9.56 ABV
△	1940	4450	3	78.7	100	11.7 ABV
○	1934	1600	1	64.02	100	5.14 ABV

TECHNIQUE: COLLECTIVE, VECTOR, LONGITUDINAL, LATERAL, AND DIRECTIONAL CONTROLS HELD FIXED WHILE ENGINE SPEED WAS STABILIZED AT EACH POINT.

LANDING GEAR DOWN

SYM	WIND VEL. $-V_W$ — KTS	WIND DIR. FROM	NOSE
□	3.5	125	R
△	2	55	R
○	2	150	L

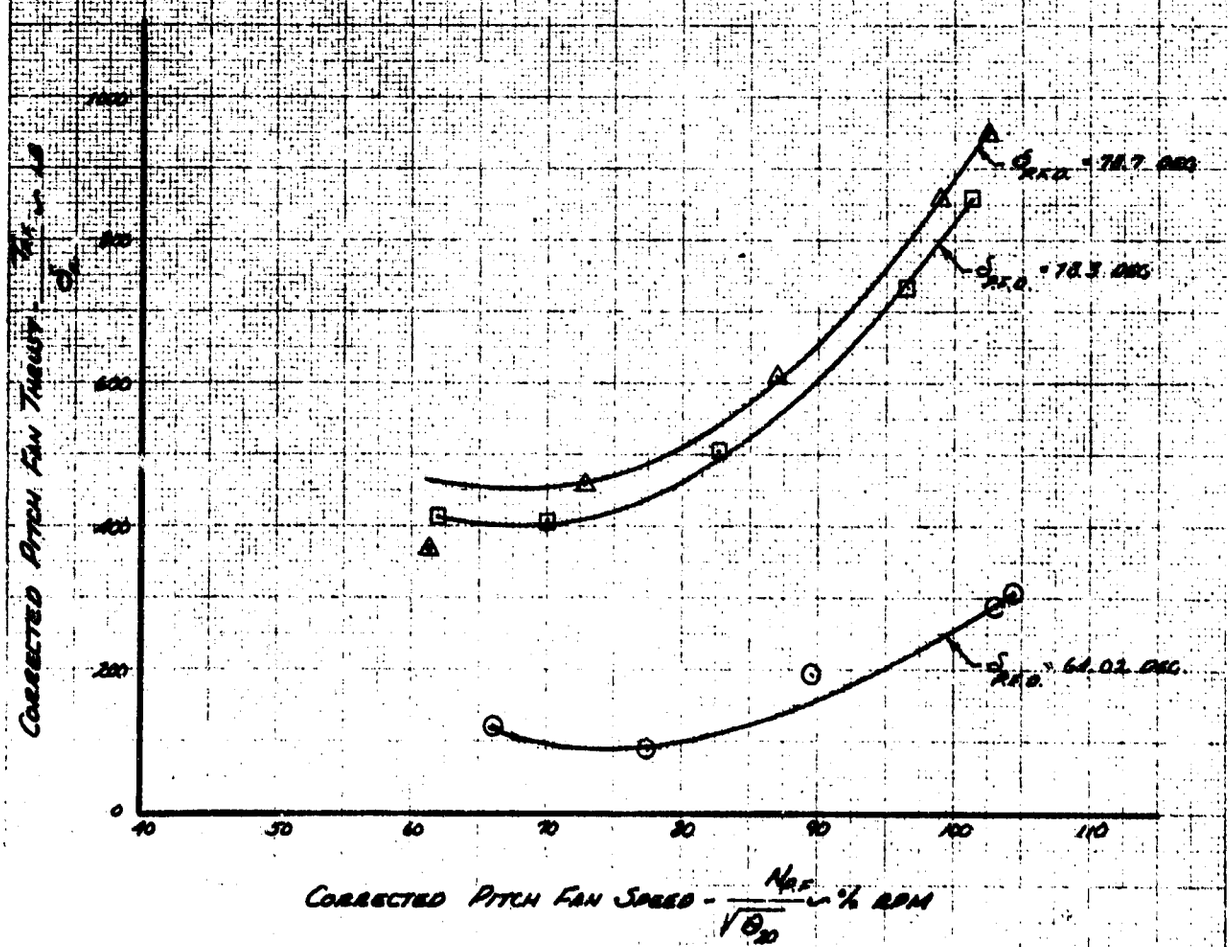

FIGURE No. 166

WING FAN SPEED VARIATION WITH WING FAN VECTOR ANGLE

XV-5A USA S/N 62-4505

VERTICAL THRUST STAND

SYM	BAROM. ALT. $-H_B$ — FT	PRESS. ALT. $-H_D$ — FT	ENGINE SPEED $-N_E$ — % RPM	STAGGER ANG. $-\delta_S$ — DEG	DIFF. STAGGER ANG. $-\Delta\delta_S$ — DEG	RISE VECTOR ANG. $-\Delta\beta_V$ — DEG.
○	2000	2000	100	17	-1	-4
□	1980	2000	100	17	-1	-3
△	1980	2315	100	15	0	-2

LANDING GEAR DOWN

TECHNIQUE: ENGINE POWER, COLLECTIVE, LONGITUDINAL, LATERAL, DIRECTIONAL CONTROLS HELD FIXED WHILE THE VECTOR ANGLE WAS STABILIZED AT EACH POINT.

NOTES
1. FAN WEIGHT - W_{FD} = 1
2. WING INCI. i_W = 4.5° = 2
3. WIND DIRECTION - RWY. HEADING WIND = 150 L

PITCH FAN DOOR POSITION - $\delta_{P.F.D.}$ — DEG.

CORRECTED WING FAN SPEED - $\frac{N_E}{\sqrt{\theta_D}}$ — % RPM

FORWARD ← WING FAN VECTOR ANGLE - $\beta_{V_{AVG.}}$ — DEGREES → AFT

ROLL FAN DOOR POSITION - $\delta_{R.F.D.}$ — DEG

NOTES
1. FAN WEIGHT - W_{FD} = 3
2. WING CONDITIONS

SYM	INCI. - i_W — DEG	WEIGHTING	AVG. WING LOAD
□	1.5		57 #/
△	5		110 #/

CORRECTED WING FAN SPEED - $\frac{N_E}{\sqrt{\theta_D}}$ — % RPM

FORWARD ← WING FAN VECTOR ANGLE - $\beta_{V_{AVG.}}$ — DEGREES → AFT

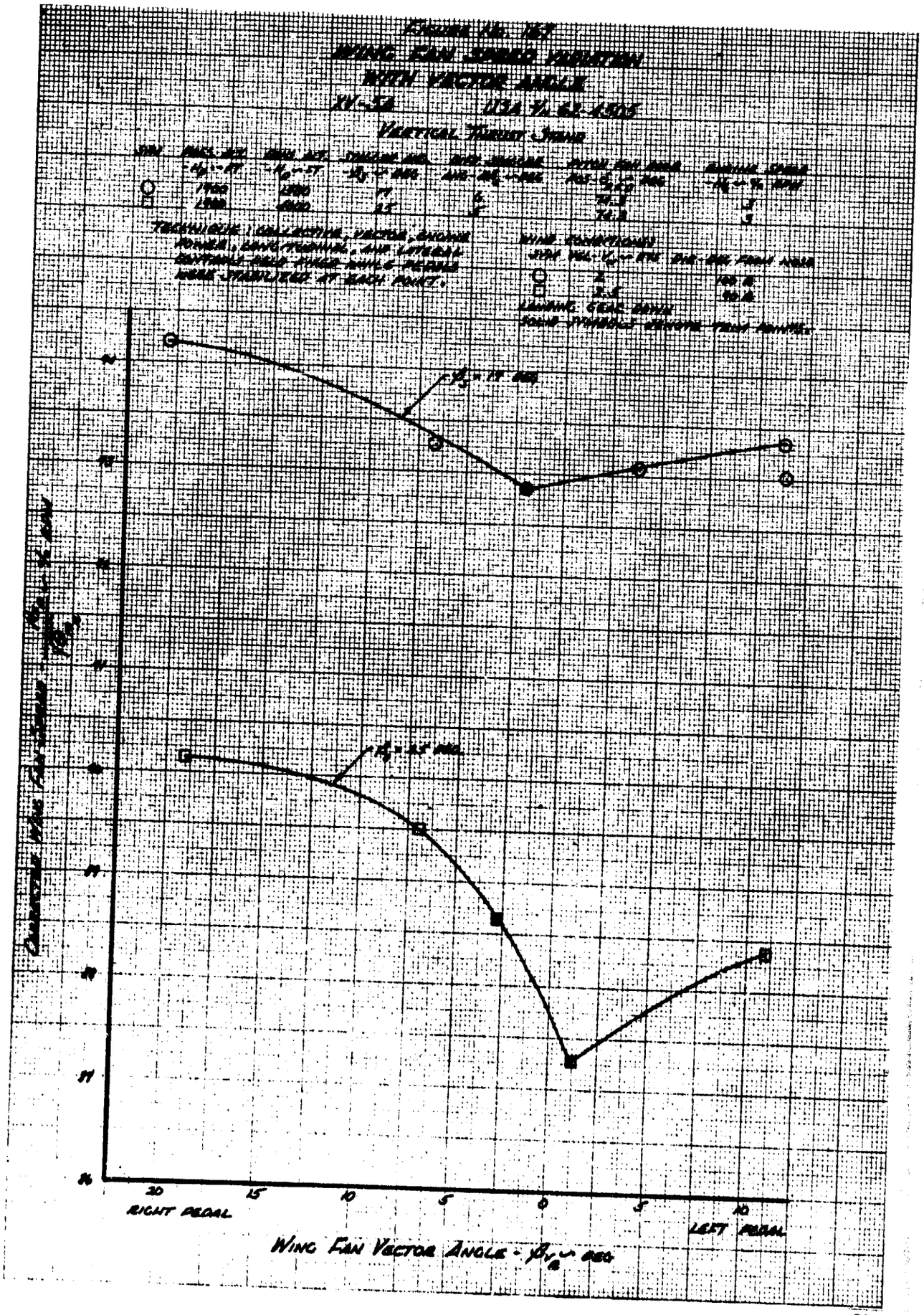
FIGURE NO. 167
WING FAN SURGE MARGIN
WITH VECTOR ANGLE
XV-5A
VERTICAL TAKEOFF STAND
TECHNIQUE: COLLECTIVE, VECTOR, ENGINE POWER, LONG. CONTROL, AND LATERAL CONTROL HELD FIXED AND PEDALS WERE STABILIZED AT EACH POINT.
WING CONDITIONS
LANDING GEAR DOWN
ROUND STABILIZED VERTICAL TAKEOFF ROTATION
Change in Wing Fan Surge Margin, ΔSM, %
RIGHT PEDAL
LEFT PEDAL
Wing Fan Vector Angle - βFan, deg

FIGURE No. 168

WING FAN SPEED VARIATION WITH VECTOR ANGLE

XV-5A USA S/N 62-4505

VERTICAL THRUST STAND

SYM	PRESS. ALT. H_p – FT	PRESS. ALT. H_p – FT	ENGINE SPEED N_E – % RPM	STAGGER ANG. i_{F_S} – DEG.	PITCH FAN BLADE POS. β_{FAN} – DEG	WING STAGGER $i_{WING} - i_{F_S}$ – DEG.
○	1900	1500	100	17	74.3	3
□	1900	4000	100	25	74.3	4

TECHNIQUE: COLLECTIVE, VECTOR, ENGINE POWER, LONGITUDINAL, AND LATERAL CONTROLS HELD FIXED WHILE PEDAL WAS STABILIZED AT EACH POINT.

WIND CONDITIONS SYM	VEL – V_w – KTS	DIR – DEG FROM NOSE
○	2	100 R
□	2.5	90 R

LANDING GEAR DOWN
SOLID SYMBOLS DENOTE TRIM POINTS.
FAN WEIGHT – $W_{FAN} = 3$

$i_{F_S} = 17$ DEG.

$i_{F_S} = 25°$ DEG.

CORRECTED WING FAN SPEED – N_{E_C} – % RPM

WING FAN VECTOR ANGLE – β_{V_L} – DEGREES

FIGURE NO. 160

FAN SPEED RATIO VARIATION WITH WING FAN VECTOR ANGLE

XV-5A USA S/N 62-4505

VERTICAL THRUST STAND

SYM	AVRS. ALT. $-H_p$ — FT	DENS. ALT. $-H_p$ — FT	PITCH FAN BOOM ABS — δ_{FB} DEG.	COLL. STICK ABS — $\frac{1}{2}$ — % CAP	ELEV. STAGGER AND — δE_t — DEG.	RUDD. VECTOR ANG. — δR_f — DEG.
○	2000	2000	76	100	-1	-4
□	1980	2000	76	100	-1	-3
△	1980	2315	74	50	0	-2

TECHNIQUE: COLLECTIVE, ENGINE POWER, LONGITUDINAL, LATERAL, DIRECTIONAL CONTROLS HELD FIXED WHILE VECTOR ANGLE WAS STABILIZED AT EACH POINT.

LANDING GEAR DOWN
ENGINE SPEED - N_g — % RPM - 100
WIND CONDITIONS

SYM	VEL. — V_w — KTS	DIR. — DEG. FROM NOSE
○	2	130 L
□	2.5	35 R
△	5	110 R

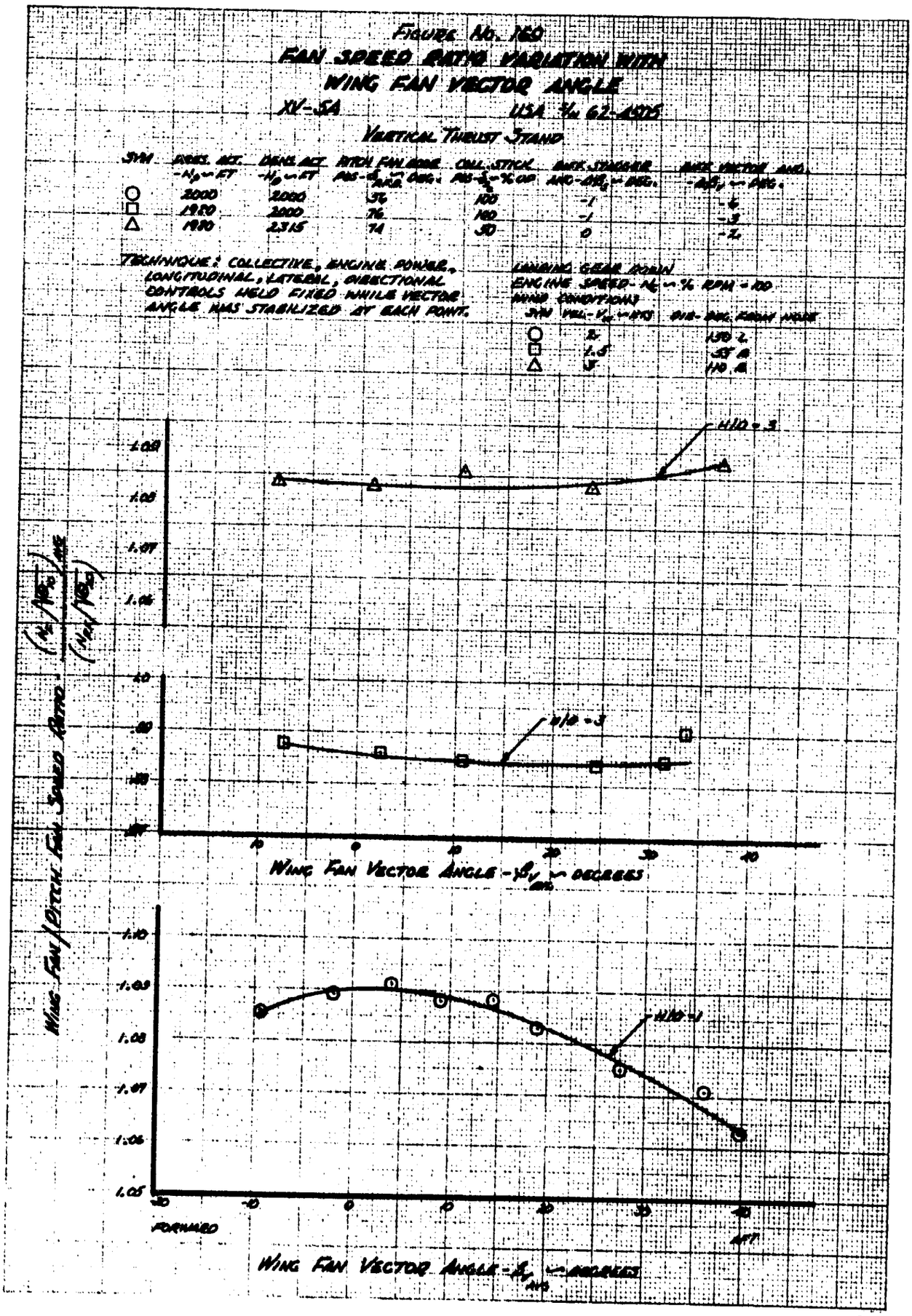

FIGURE No. 170

VARIATION OF VERTICAL THRUST WITH WING FAN VECTOR ANGLE

XV-5A USA S/N 62-1505

VERTICAL THRUST STAND

PRESSURE ALTITUDE - H_p - FT = 1000
DENSITY ALTITUDE - H_ρ - FT = 2000
FAN HEIGHT - H/D = 3
WIND VEL - V_W - KTS = 1.5
LANDING GEAR DOWN

COLLECTIVE STICK POSITION - δ_c - % UP = 100
DIFF. STAGGER ANGLE - $\Delta\theta_c$ - DEG = -1
DIFF. VECTOR ANGLE - $\Delta\beta_y$ - DEG = -3
ENGINE SPEED - N_c - % RPM = 100
WIND DIR - DEG FROM NOSE = 55 R

TECHNIQUE: COLLECTIVE, ENGINE POWER, LONGITUDINAL, LATERAL, AND DIRECTIONAL CONTROLS HELD FIXED WHILE VECTOR ANGLE WAS STABILIZED AT EACH POINT.

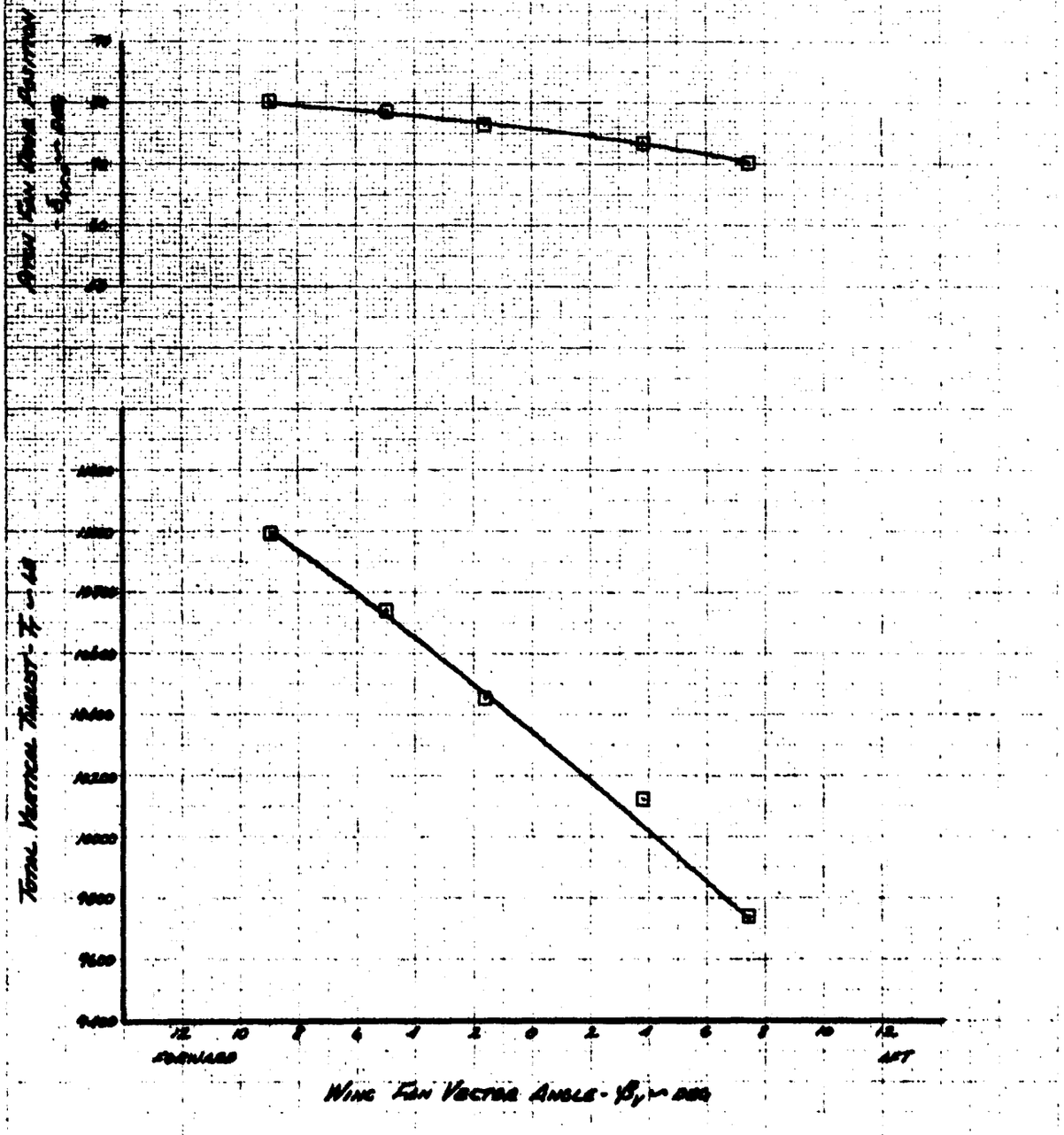

FIGURE NO. 171

PITCHING MOMENT VARIATION WITH WING FAN VECTOR ANGLE

XV-5A LCA # 62-4505

VERTICAL TAKEOFF - STABLE

SYM	ABSL. ALT. $-H_p$ — FT	AMBL. ALT. $-H_{amb}$ — FT.	ENG. SPEED $-N_g$ — % RPM	AIR. ATTITUDE ANG. $-\alpha_B$ — DEG	DUCT VECTOR ANG. $-\delta_{d_{FAN}}$ — DEG	CALC. STABIL. POS. $-\delta_{s_c}$ — % MAC
○	2000	2000	100	-1	-6	100
□	1910	2000	100	+1	-3	100
△	1910	2315	100	0	-2	100

TECHNIQUE - COLLECTIVE, ENGINE POWER, LONGITUDINAL, LATERAL, AND DIRECTIONAL CONTROLS HELD CONSTANT WHILE VECTOR ANGLE WAS STABILIZED AT EACH POINT.

ENGINE SPEED - N_g — % RPM = 100

LANDING GEAR DOWN

SYM	WING CONFIGURATION $-V_{amb}$ — KTS	AMB. - DEG ABOUT AXIS
○	2	170 L
□	1.6	55 R
△	3	110 R

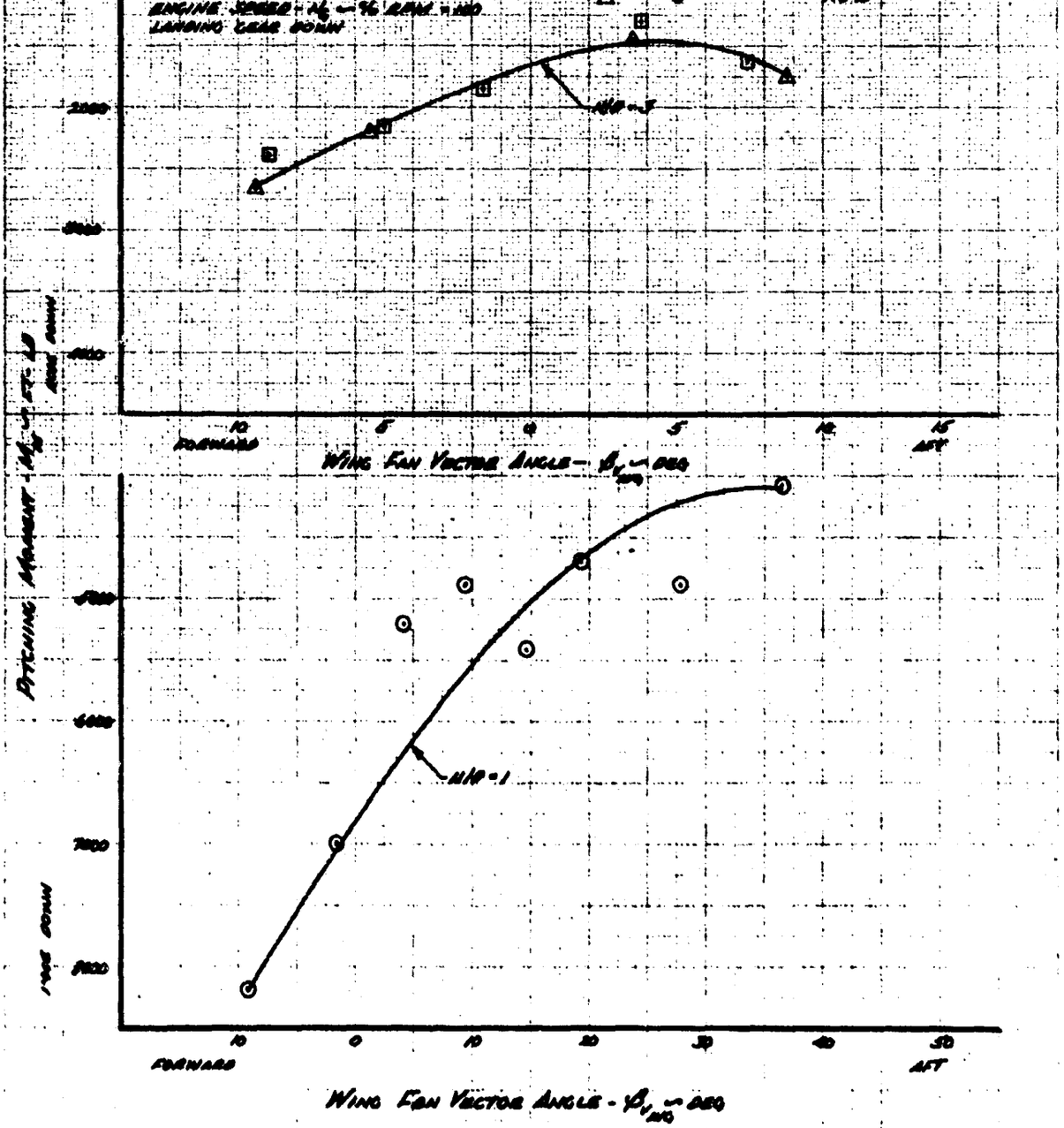

FIGURE No. 172

VARIATION OF HORIZONTAL FORCE WITH WING FAN VECTOR ANGLE

XV-5A

USA 5/4 62-4505

VERTICAL THRUST STAND

SYM	EFFEC. ALT. $-H_e$ — FT	BAR. ALT. $-H_b$ — FT	ENG. SPEED $-N_G$ — % RPM	STAGGER ANG. $-\beta_s$ — DEG	EFFEC. STAGGER $-\beta e_s$ — DEG	ANGL VECTOR $-\Delta\beta_v$ — DEG
○	2000	2000	100	17	-1	-6
□	2000	2000	100	17	-1	-3
△	1980	2315	100	25	0	-2

TECHNIQUE: ENGINE POWER, COLLECTIVE, LONGITUDINAL, LATERAL, AND DIRECTIONAL CONTROLS HELD FIXED WHILE VECTOR ANGLE WAS STABILIZED AT EACH POINT.

NOTES
1. FAN HEIGHT - WL 0
2. WIND VEL - V_w - KTS - 2
3. WIND DIR - DEG. FROM NOSE - 120°L
4. LANDING GEAR DOWN

WING FAN VECTOR ANGLE - β_v — DEG

δ_{LS} - 30% UP

δ_c - 100% UP

NOTES
1. FAN HEIGHT - WL 0
2. WIND CONDITIONS

SYM	WIND VEL - V_w KNOTS	WIND DIR - DEG FROM NOSE
□	15	120°L
△	0	WIND IS CALM

3. LANDING GEAR DOWN

WING FAN VECTOR ANGLE - β_v — DEG

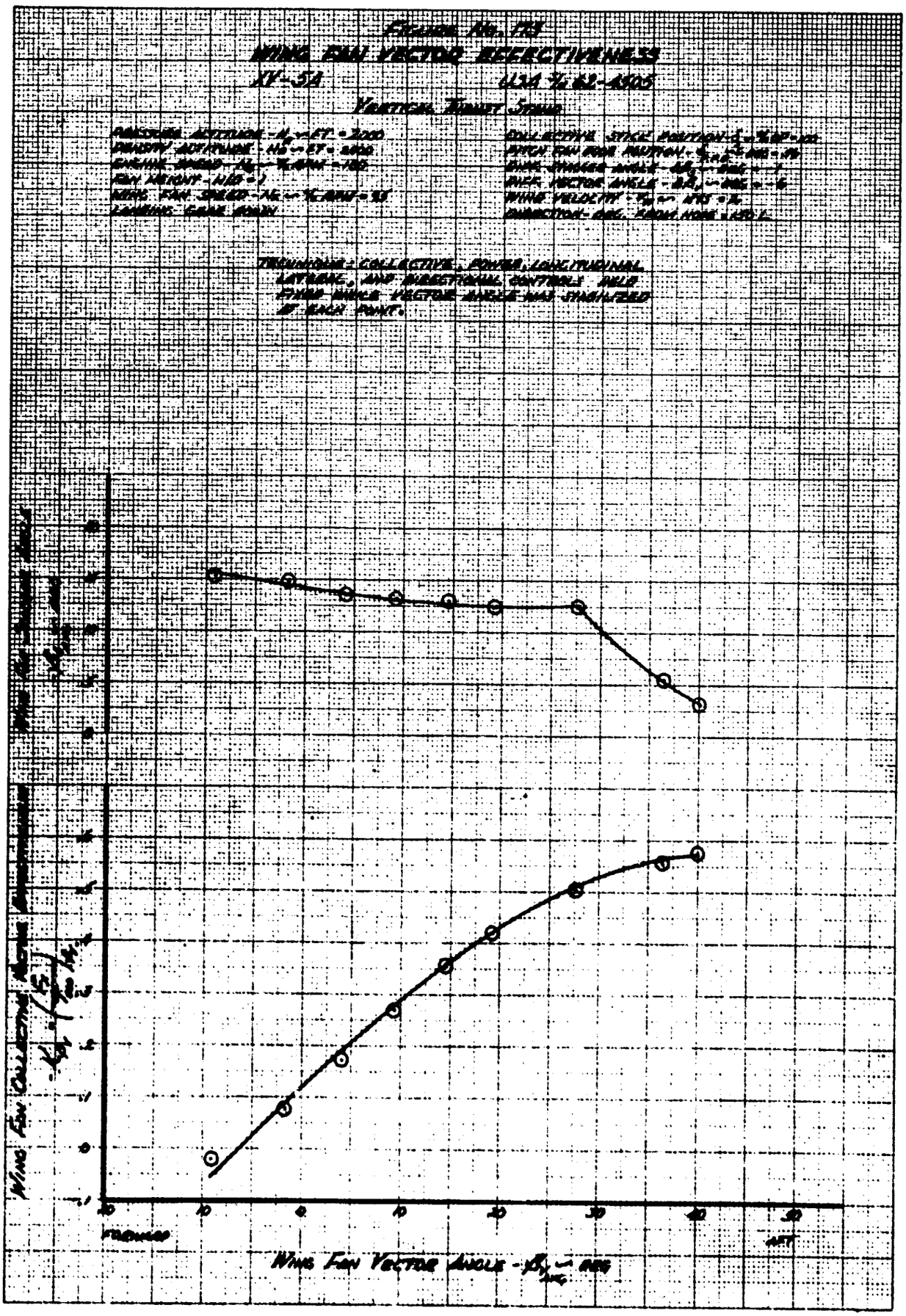
Figure No. 118
WING FAN VECTOR EFFECTIVENESS
XV-5A
Vertical Takeoff
Wing Fan Vector Angle
FORWARD
AFT

FIGURE No. 174

WING FAN VECTOR EFFECTIVENESS

XV-5A USA #62-4505

VERTICAL THRUST STAND

SYM	PRES. ALT. $-H_p$ — FT	DENS. ALT. $-H_D$ — FT	COLL. STICK POS. $-\delta_{s_c}$ — % CAP	WING FAN SPEED $-N_f$ — % RPM	DIFF. STAGGER ANG. $-\Delta\theta_y$ — DEG.	DIFF. VECTOR ANG. $-\Delta\theta_y$ — DEG.
□	1980	2000	100	91	-1	-3
△	1980	2345	50	92	0	-2

TECHNIQUE: COLLECTIVE, POWER, LONGITUDINAL, LATERAL, AND DIRECTIONAL CONTROLS USED. WING FAN VECTOR ANGLE WAS STABILIZED AT EACH POINT.

FAN HEIGHT - $H/D = 3$

LANDING GEAR DOWN

ENGINE SPEED - N_g — % RPM = 100

WING CONDITIONS

SYM	REL. - V_{wf} — KTS	AVE. DIR. FROM MAST
□	1.5	55° R
△	3	110° R

γ_{comb} = 70% AIRFLD PER WING FAN

$\delta_{s_c} = 50\%$ CAP

$\delta_{s_c} = 100\%$ CAP

$-\delta_{s_c} = 50\%$ CAP

$\delta_{s_c} = 100\%$ CAP

WING FAN VECTOR ANGLE - δ_{wf} — DEG

FIGURE No. 125

WING FAN JET INDUCTION WITH WING FAN DIFFERENTIAL STAGGER ANGLE

XV-5A USA # 62-4505

VERTICAL TAKEOFF STAND

SYM.	ENG. ACT. $-N_{g_1}$ — RT	FAN ACT. $-N_{g_2}$ — RT	FAN SPEED $-N_{g_2}$ — % RPM	DIFFERENTIAL ANG. $-\Delta\beta_2$ — DEG	VECTOR ANG. $-\beta_c$ — DEG	FAN FLOW WT. $\frac{W_{a_2}\sqrt{\theta_2}}{\delta_{2_{AS}}}$ — LBS/SEC	JET VECTOR ANG. $-\Delta\beta_j$ — DEG
○	4950	2445	99.5	19°	100% FWD	99.6	-3.0°
□	4910	2025	100.0	35°	50% FWD	69.8	-3.0

TECHNIQUE: POWER, COLLECTIVE, VECTOR, LONGITUDINAL, AND DIRECTIONAL CONTROLS HELD FIXED WHILE LATERAL STICK WAS STAGGERED AT EACH POINT.

LANDING GEAR DOWN
FAN WEIGHT-FLOW = 0
SOLAR STABILIZED OUTSIDE TEMP. RANGE
WIND CONDITIONS

SYM	VEL. — V_o — KTS	DIR. — DEG FROM NOSE
○	0	25 R
□	0	0

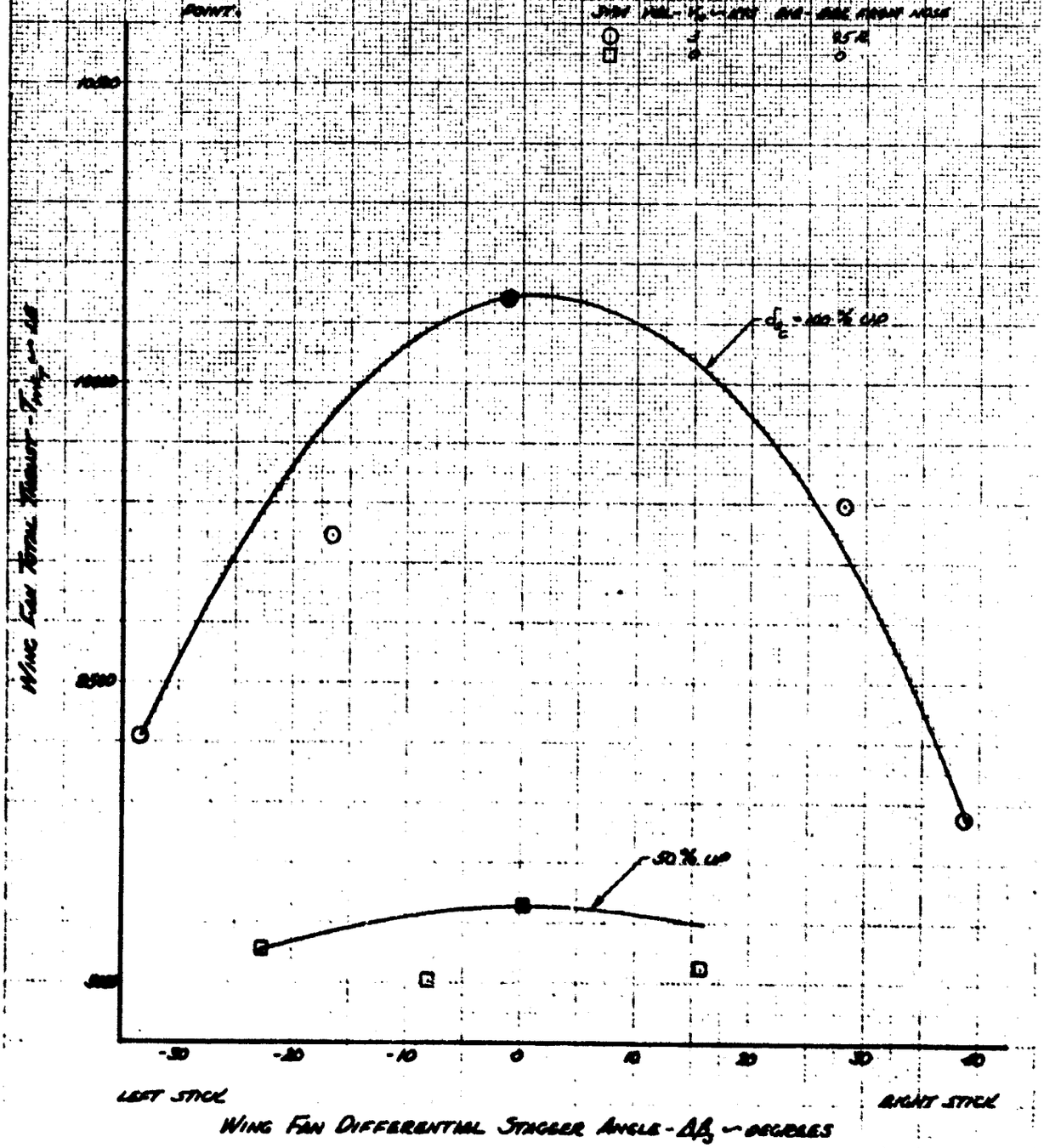

FIGURE No. 176

ROLLING MOMENT VARIATION WITH DIFFERENTIAL WING FAN STAGGER ANGLE

XV-5A USA 62-4505

VERTICAL THRUST STAND

SYM	ABS. ALT. $-H_p$ — FT	REL. ALT. $-H_p$ — FT	ENG. SPEED $-N_c$ — % RPM	COLL. STICK POS. $-\delta_{s_c}$ — % UP	REL. ANGLE $-\Delta\beta_s$ — DEG.	PITCH FAN RT. POS. $-\delta_{p_{RA}}$ — DEG	ANTI. VECTOR ANG. $-\Delta\beta_v$ — DEG.
○	1910	2445	99.5	100	1.99 FWD	79.6	-2.85
□	1710	2035	100.4	50	5.7 FWD	69.2	-3.0

TECHNIQUE: POWER, COLLECTIVE, VECTOR, LONGITUDINAL, AND DIRECTIONAL CONTROLS HELD FIXED WHILE LATERAL STICK WAS STABILIZED AT EACH POINT.

LANDING GEAR DOWN
FAN HEIGHT-H/D = 3
WIND CONDITIONS

SYM	VEL - V_0 — KTS	DIR - DEG FROM NOSE
○	3	45R
□	0	0

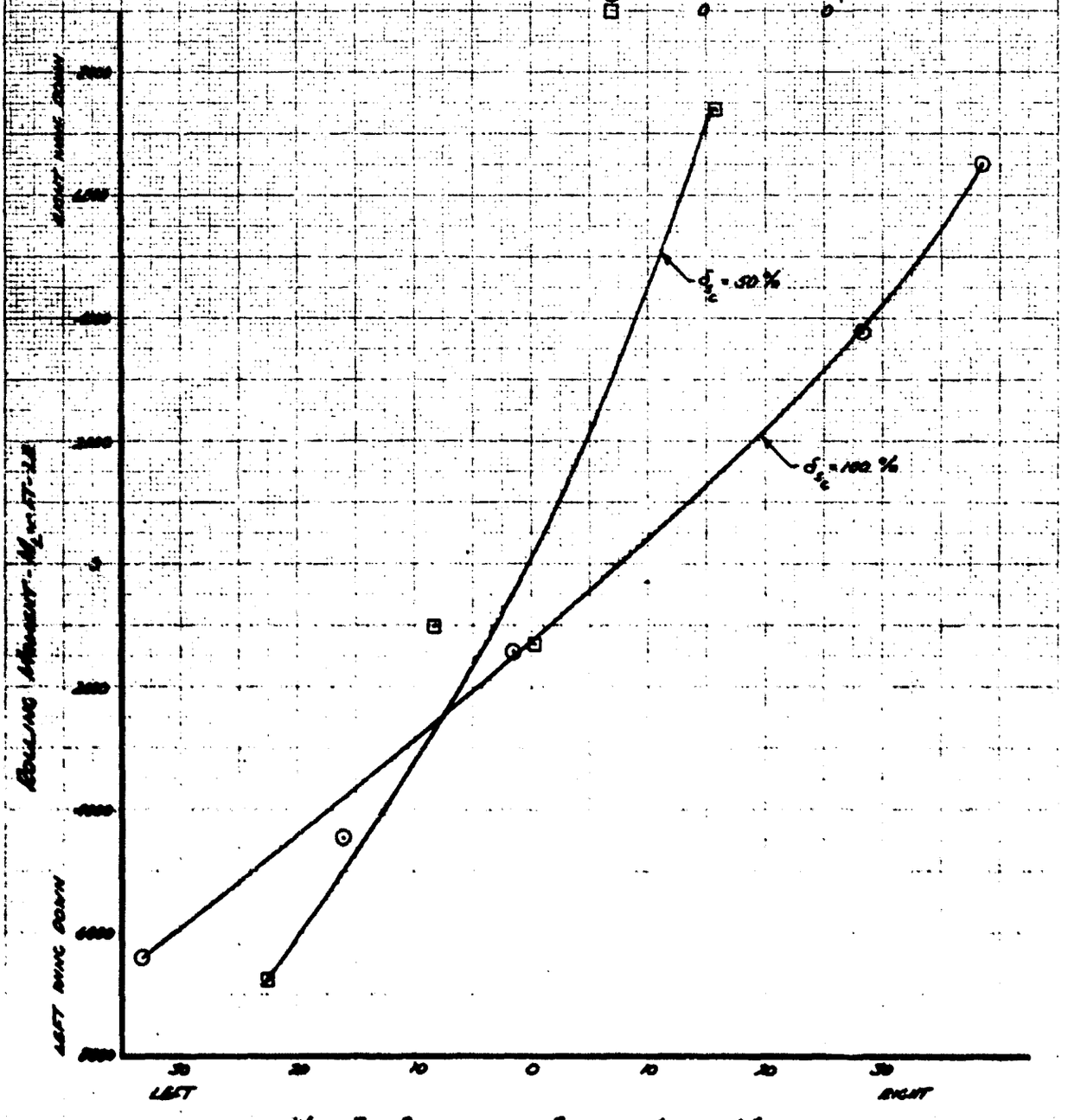

WING FAN DIFFERENTIAL STAGGER ANGLE - $\Delta\beta_s$ — DEG

FIGURE No. 177

VARIATION OF THRUST WITH WING FAN DIFFERENTIAL VECTOR ANGLE

XV-5A USA ½ 62-4905

VERTICAL TAKEOFF SETUP

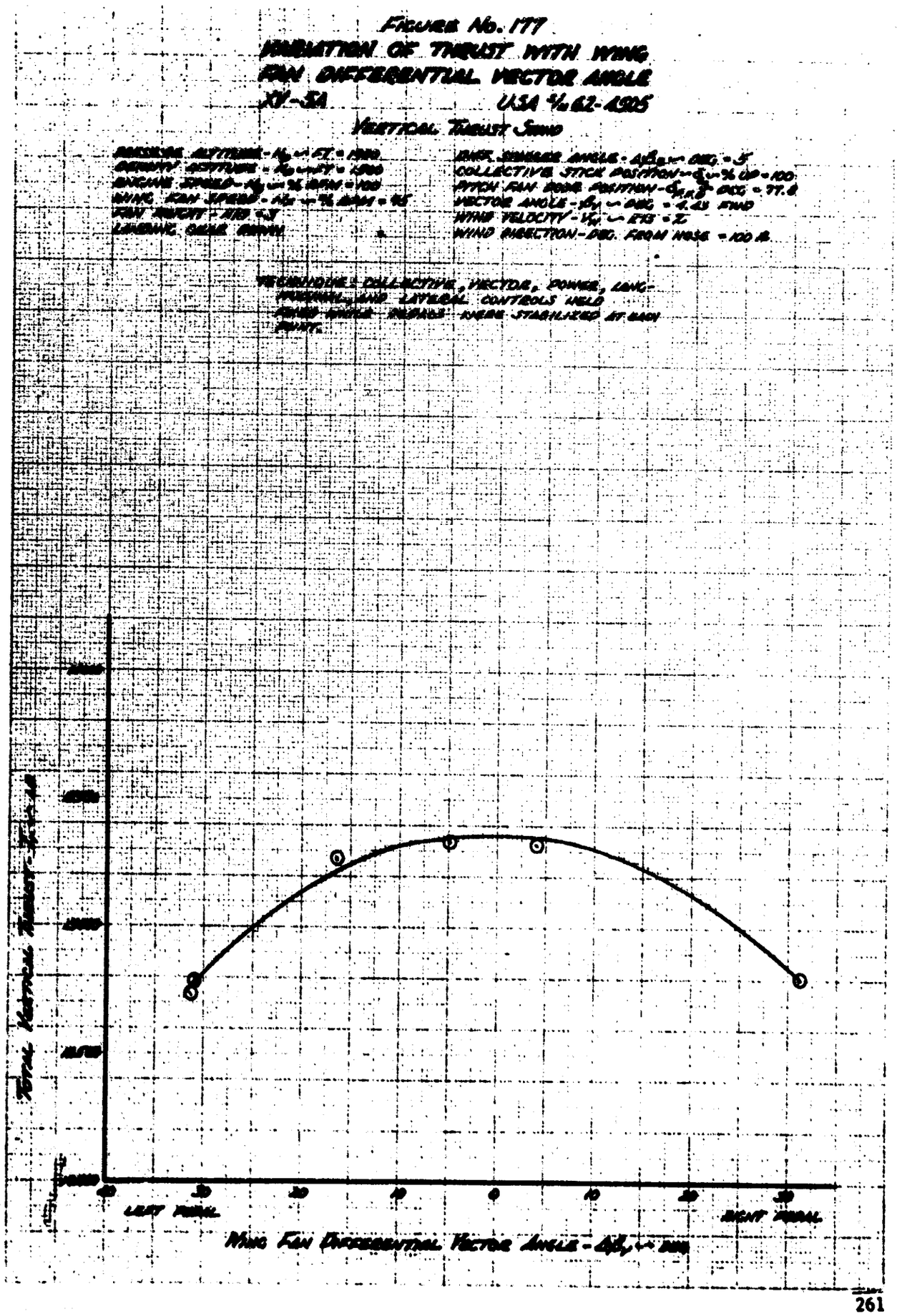

FIGURE No. 128

YAWING MOMENT VARIATION WITH WING FAN DIFFERENTIAL VECTOR ANGLE

XV-5A

USA 3/4 62-4505

VERTICAL TAKEOFF STAND

SYM	FUSEL ALT. H_p — FT	FUSEL ALT. $-H_p$ — FT	COLL. STICK δ_{RC} — % TRAV	DIFF. STICKER $\Delta\delta_{RC}$ — PER	WING FAN DEL. $-\delta_{WF}$ — DEG	WING FAN SPEED $-N_f$ — % RPM	VECTOR ANGLE $-\delta_V$ — DEG.
○	1000	1000	100	5	77.8	95	4.45 FWD
□	1000	1000	80	5	74.3	90	4.21 FWD

TRIM FOR LOW: COLLECTIVE, VECTOR, RUDDER, LONGITUDINAL, AND LATERAL CONTROLS HELD CONSTANTS WHILE AVERAGE STEADY-STATE TRIM AT EACH TEST POINT.

LANDING GEAR DOWN
FAN HEIGHT - H/D = 3
ENGINE SPEED - N_g — % RPM = 100
WIND CONDITIONS

SYM	TRUE - V_w — KTS	DIR. - DEG FROM NOSE
○	2	100° R
□	2.5	90° R

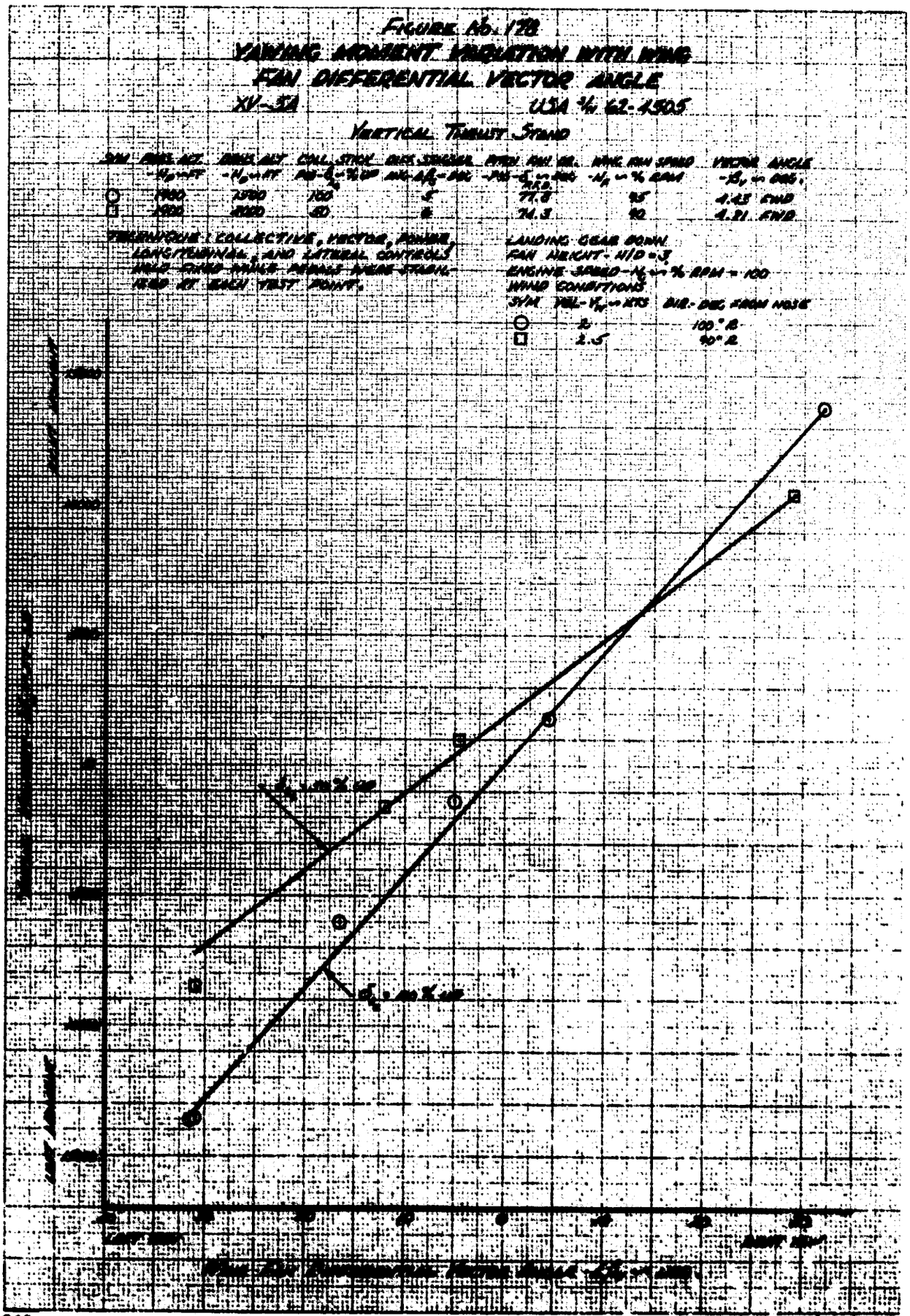

FIGURE NO. 170

THRUST SPOILER EFFECTIVENESS

XV-3A

PRE-CONVERSION CONFIGURATION

VERTICAL THRUST STAND

SYM	ABES. ALT $-H_p$ — FT	FREE AIR TEMP — °C	WHEEL HEIGHT ABOVE GROUND $-H_W$ — FT.	ENGINE SPEED $-N_g$ — % RPM	WIND VEL V_W — KTS	WIND DIRECTION — DEG. FROM NOSE
⊠	1905	10.5	0	IDLE	3	150 L
⊡	1890	18.5	5	IDLE	12	140 R

FULL THRUST SPOILER DEFLECTION = 66 DEG.

THRUST SPOILER EFFECTIVENESS - $\frac{F_z}{F_{z\,\delta_{TS}=0}}$

0 10 20 30 40 50 60 70 80 90 100

CLOSED — OPEN

THRUST SPOILER DEFLECTION - δ_{TS} — % OPEN

293

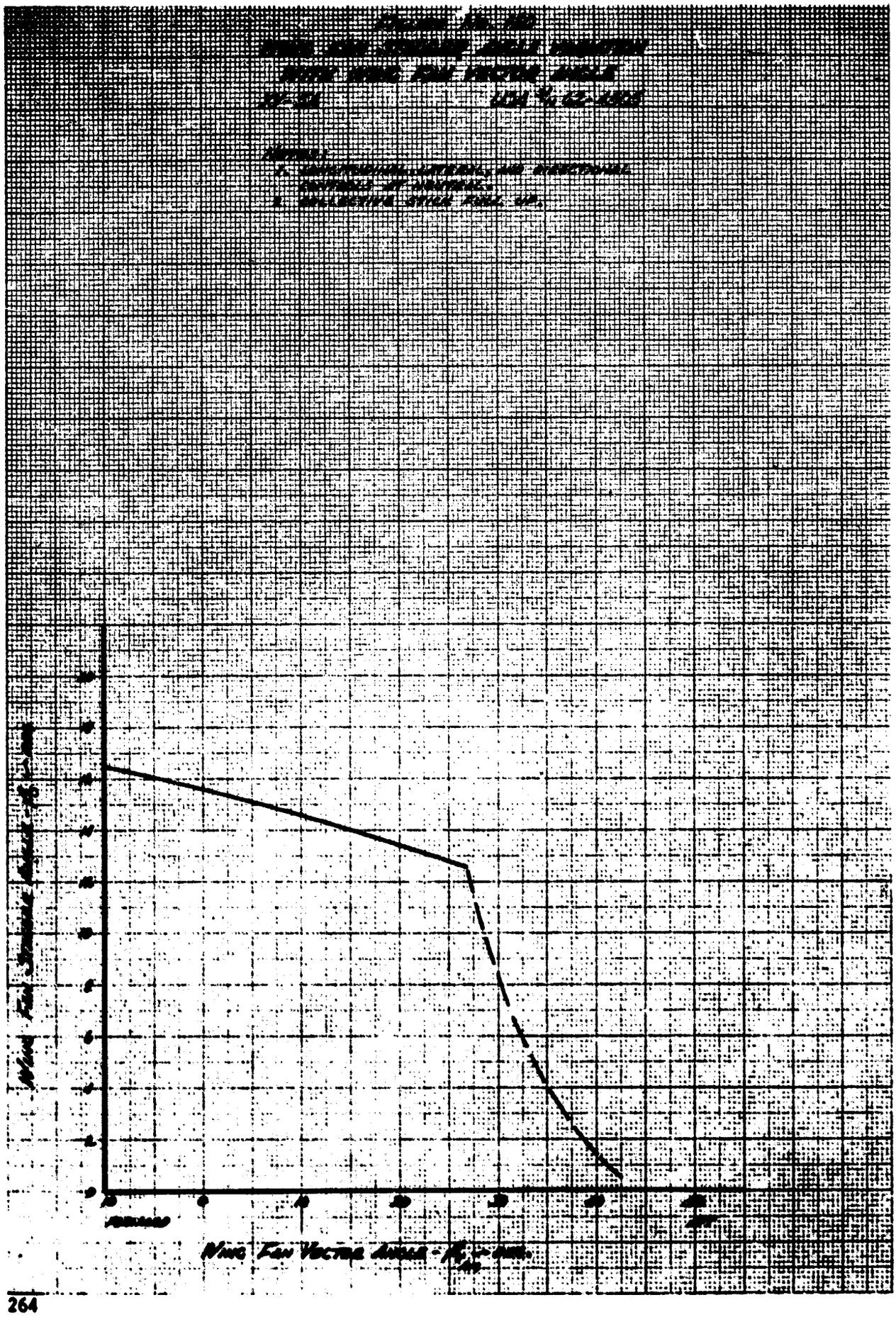
Wind Fan Vector Angle - β_{wf}

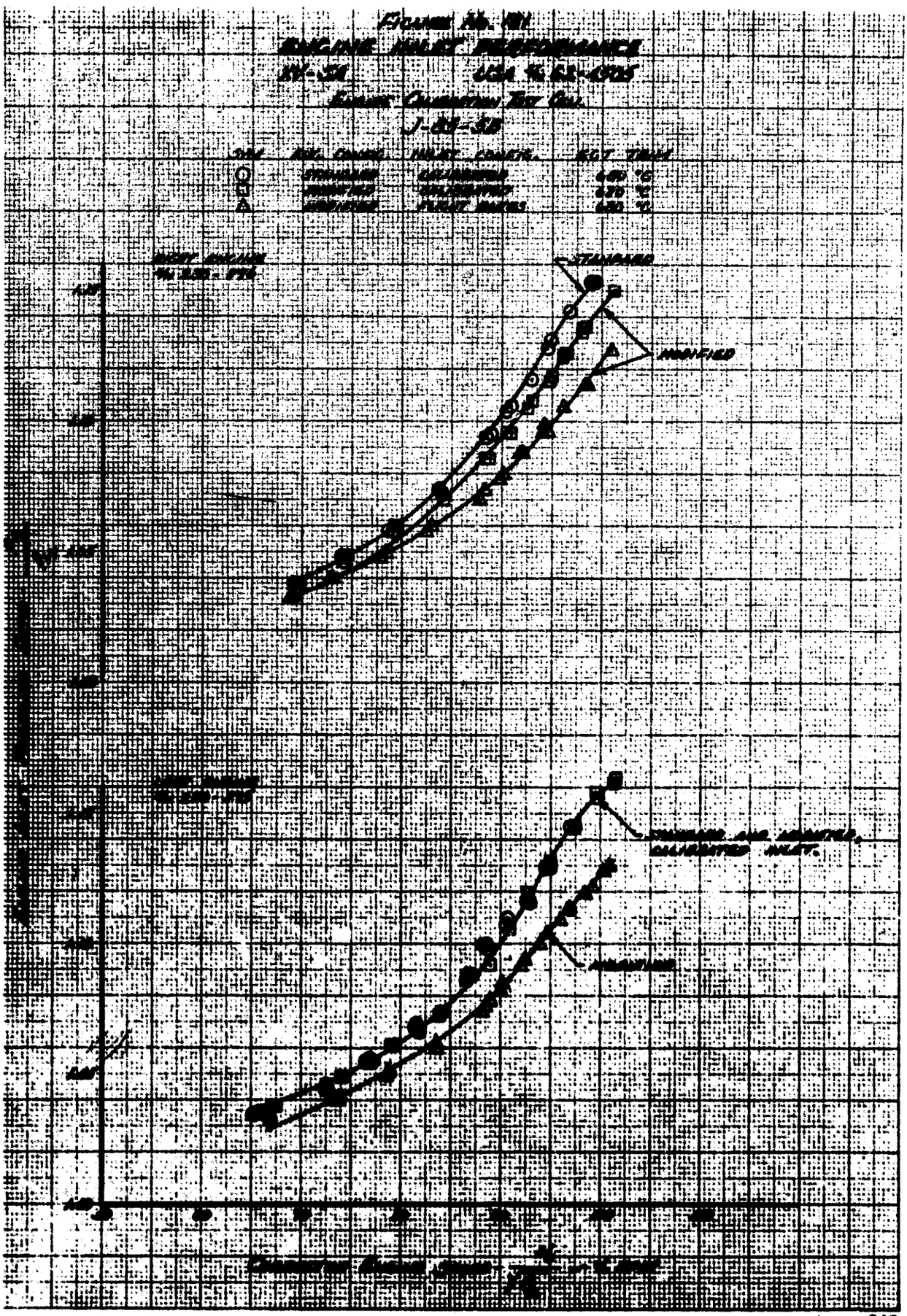
STANDARD
MODIFIED

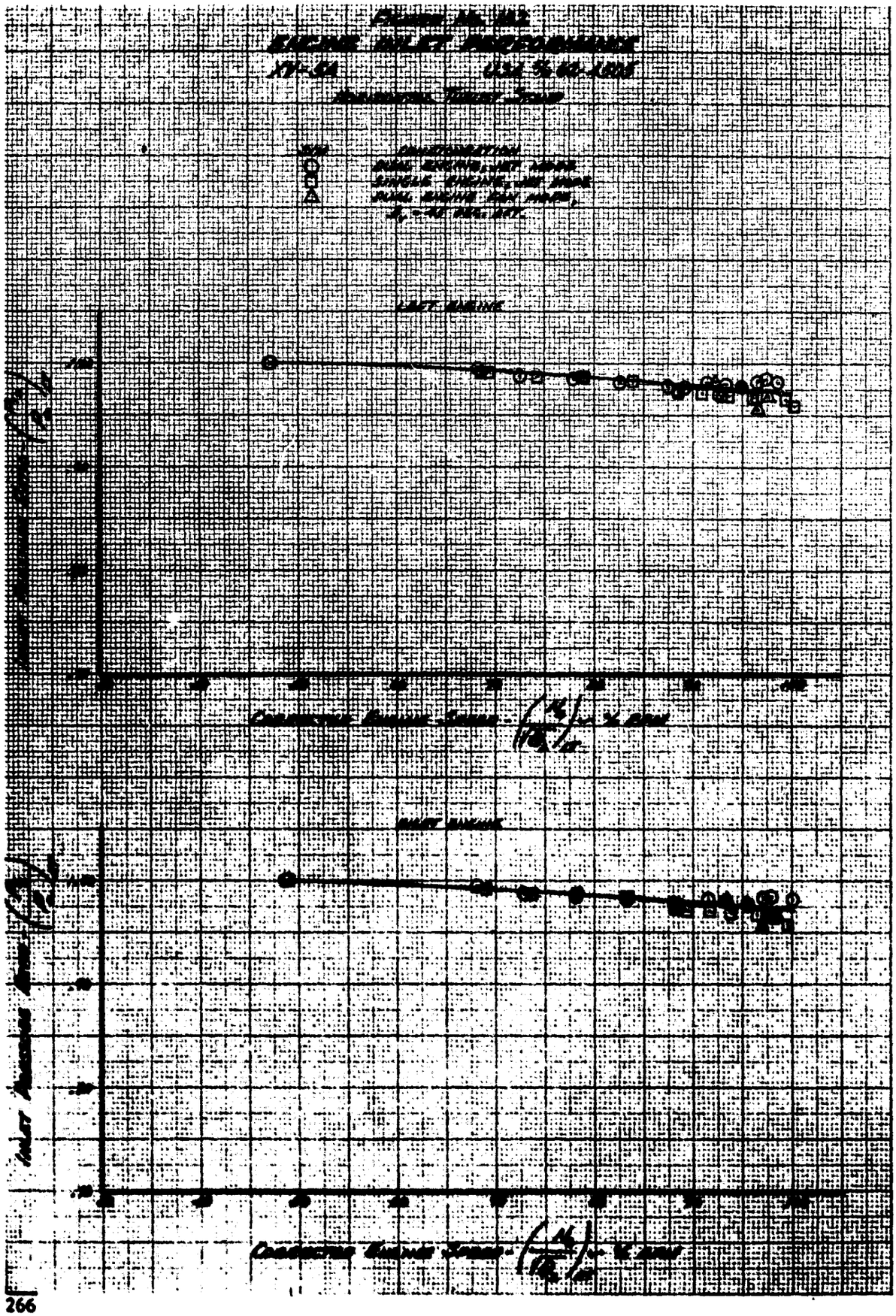
ENGINE INLET PERFORMANCE
LAST ENGINE
Inlet Pressure Ratio

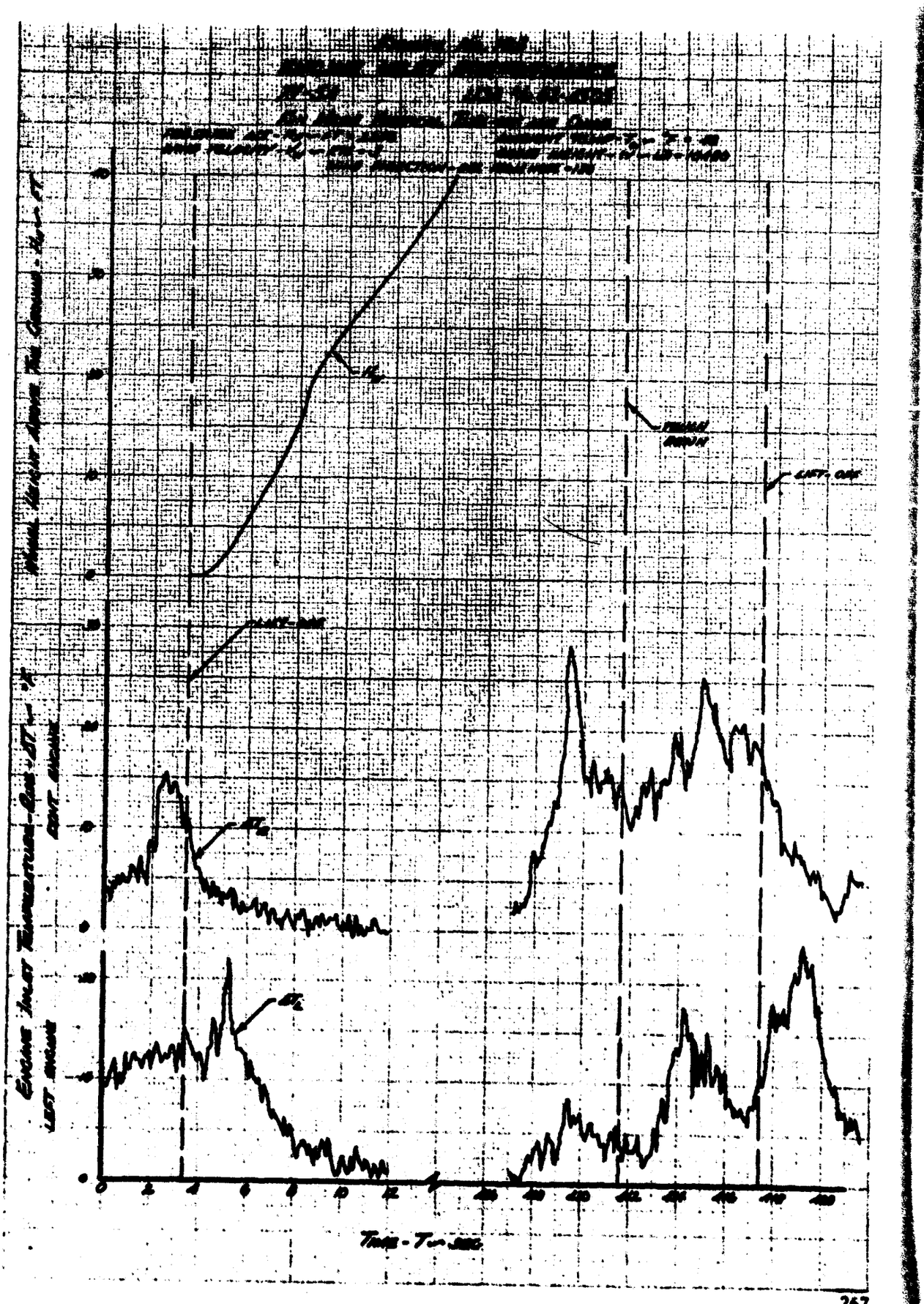

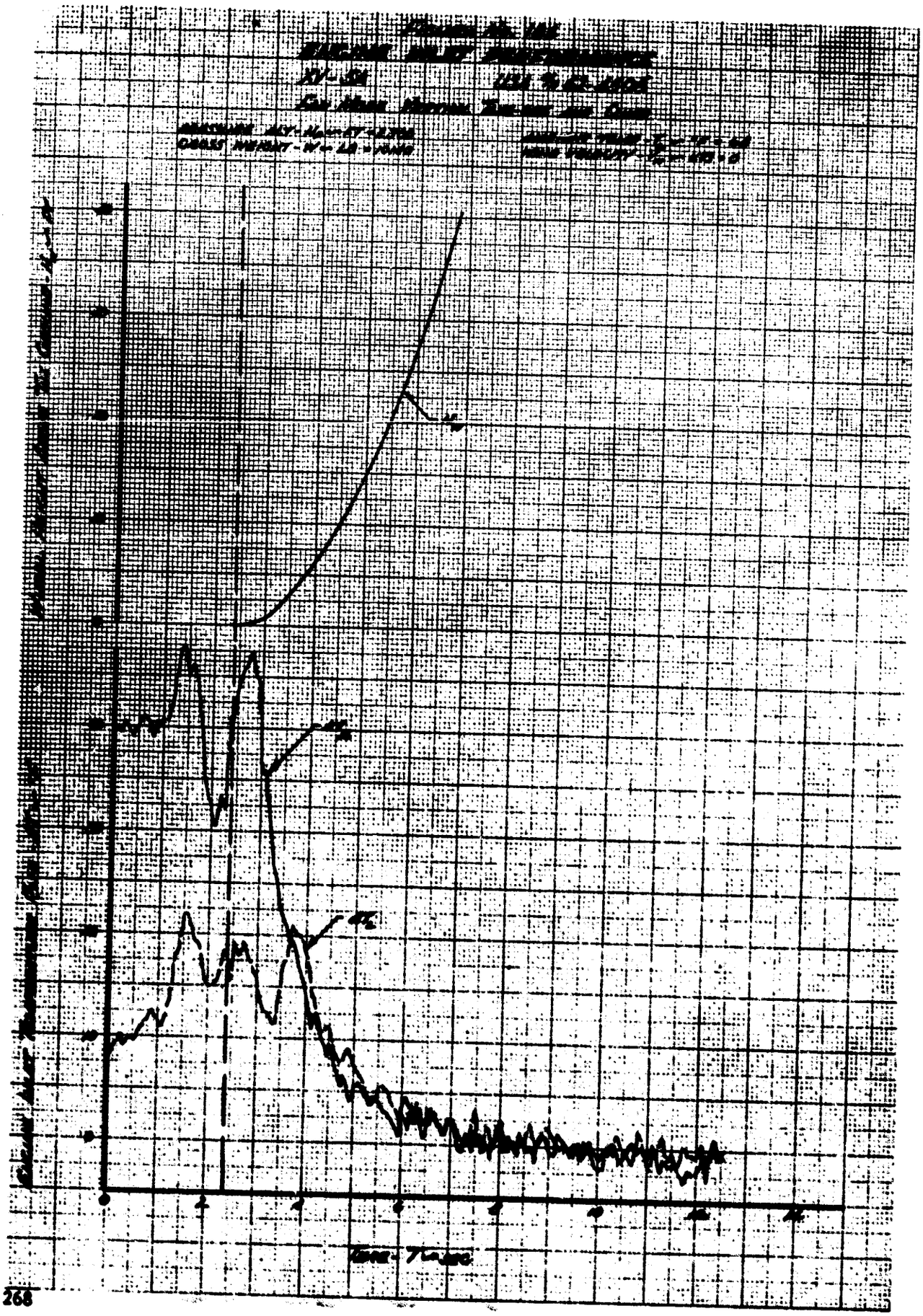

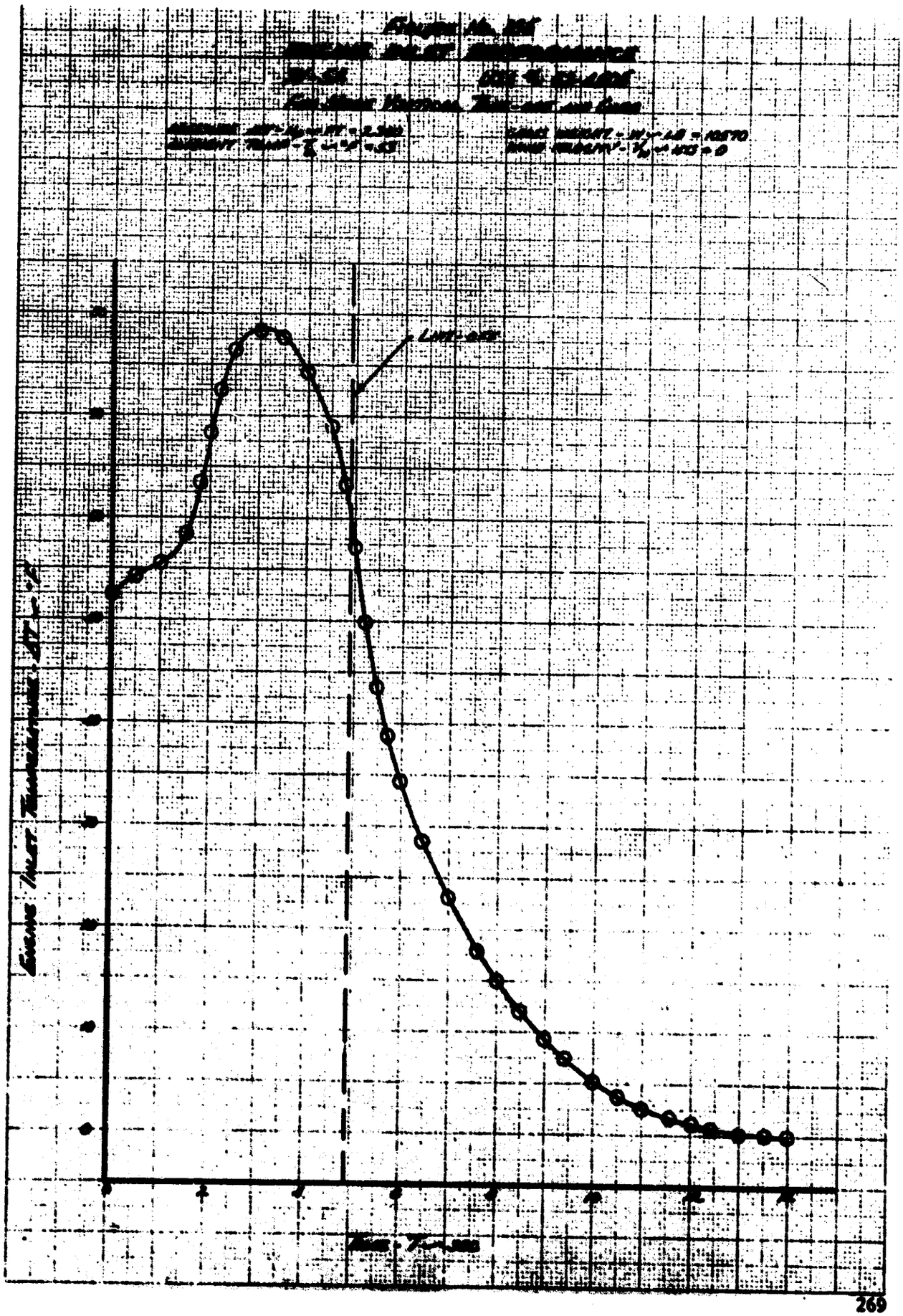

270

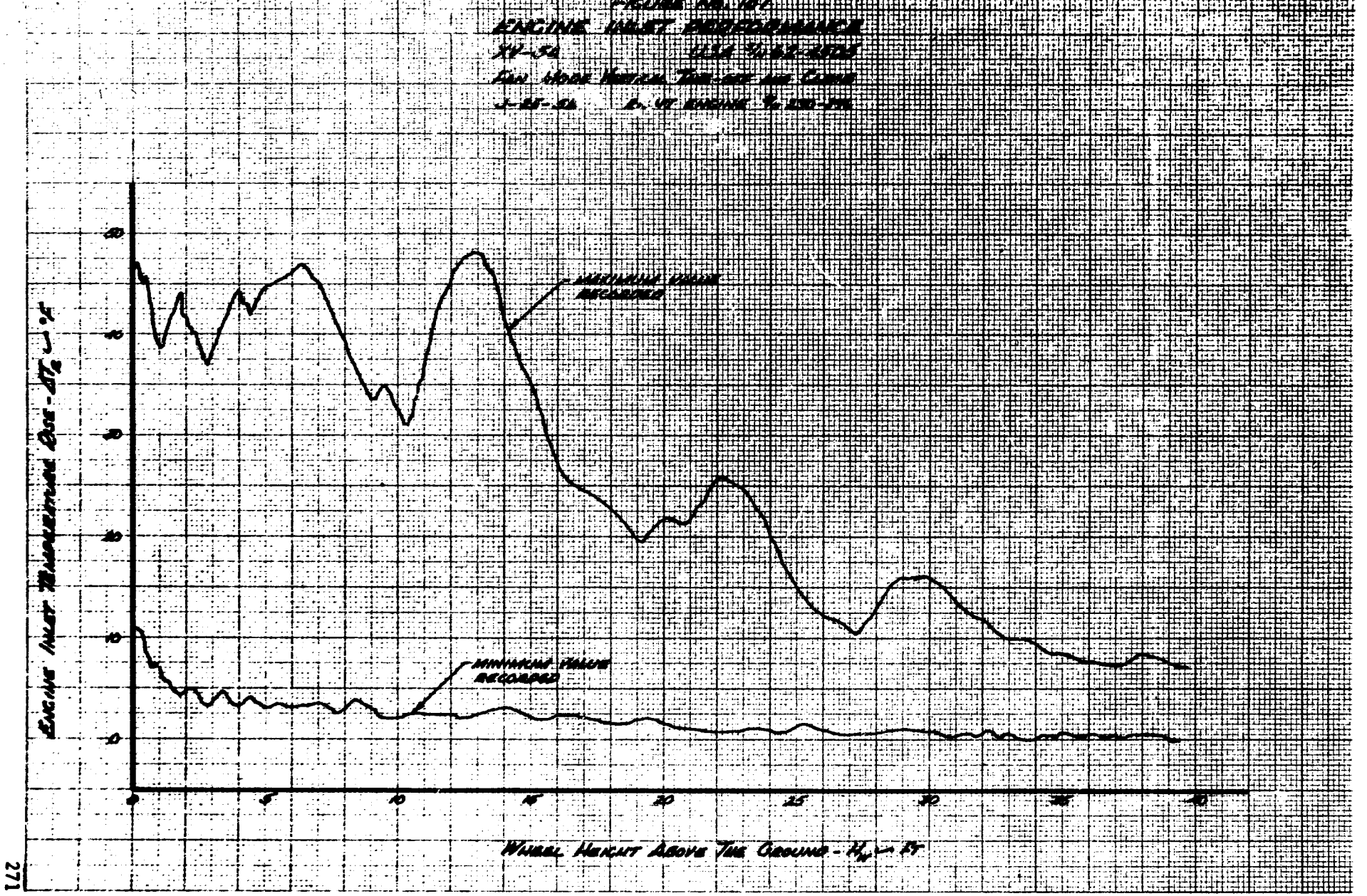
ENGINE INLET PRESSURE RECOVERY
MINIMUM VALUE RECORDED
MINIMUM VALUE RECORDED
Wheel Height Above The Ground - H_w - Ft.

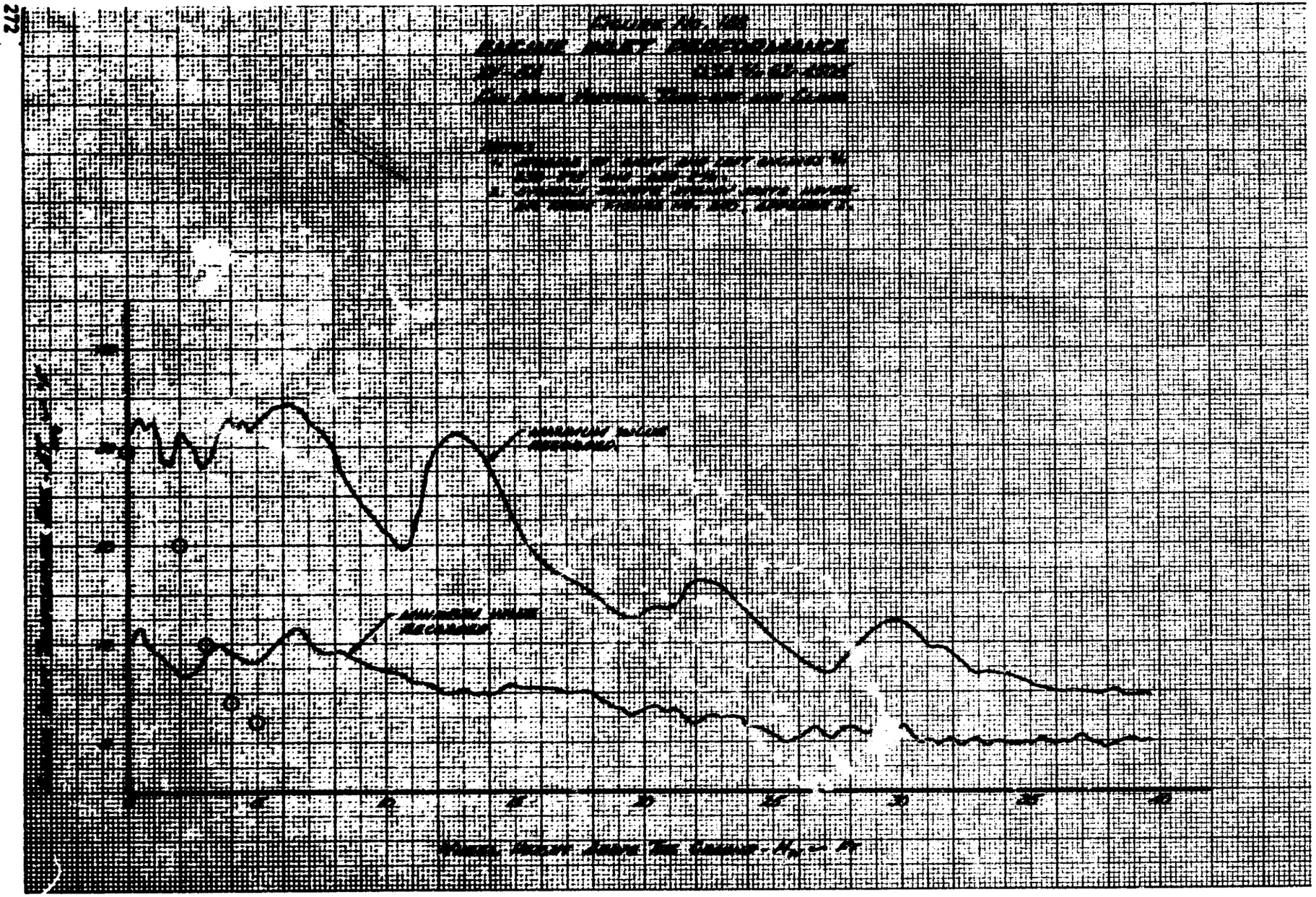

FIGURE No. 180

ENGINE INLET PERFORMANCE

XV-5A

FAN MODE VERTICAL TAKE-OFF AND CLIMB

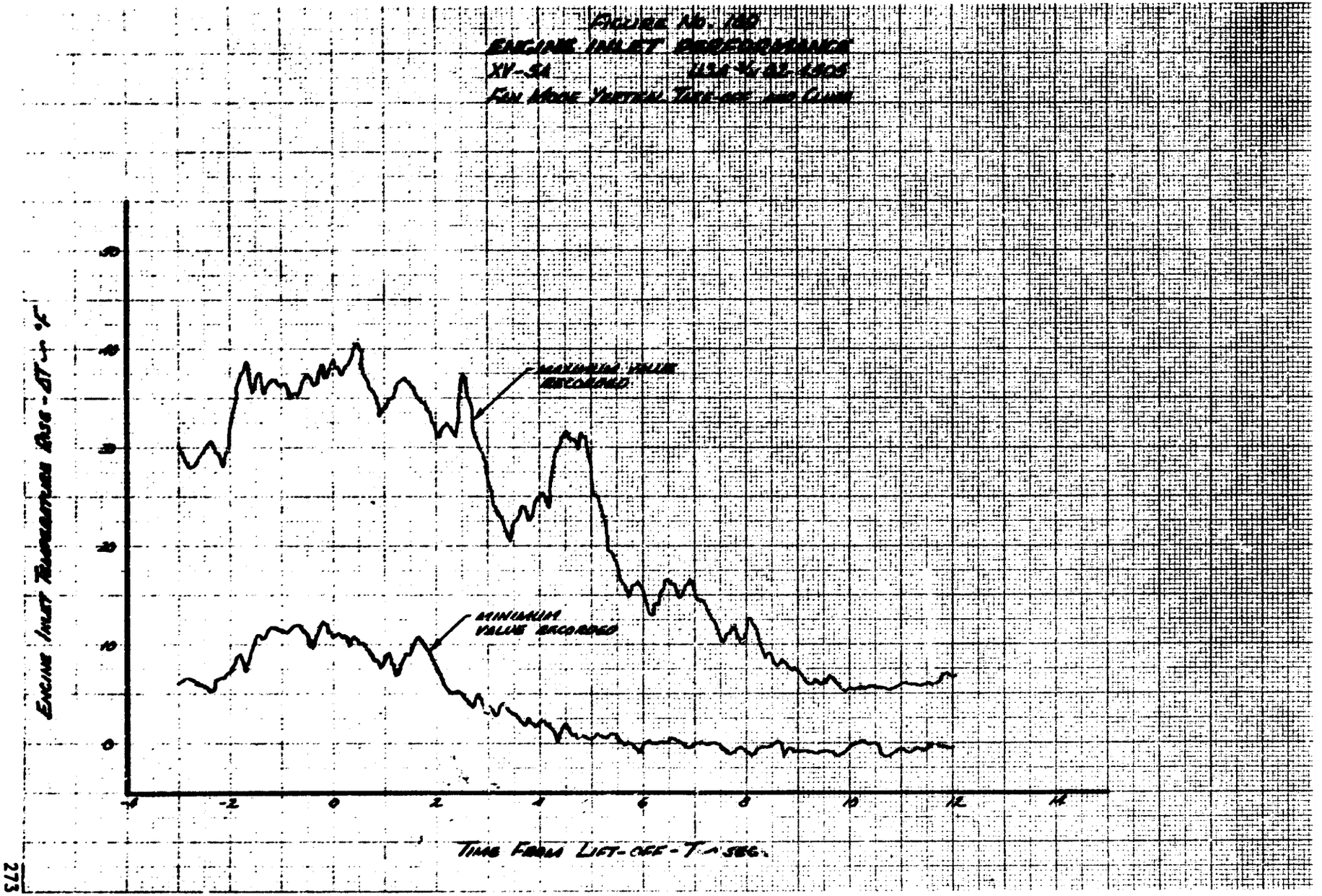

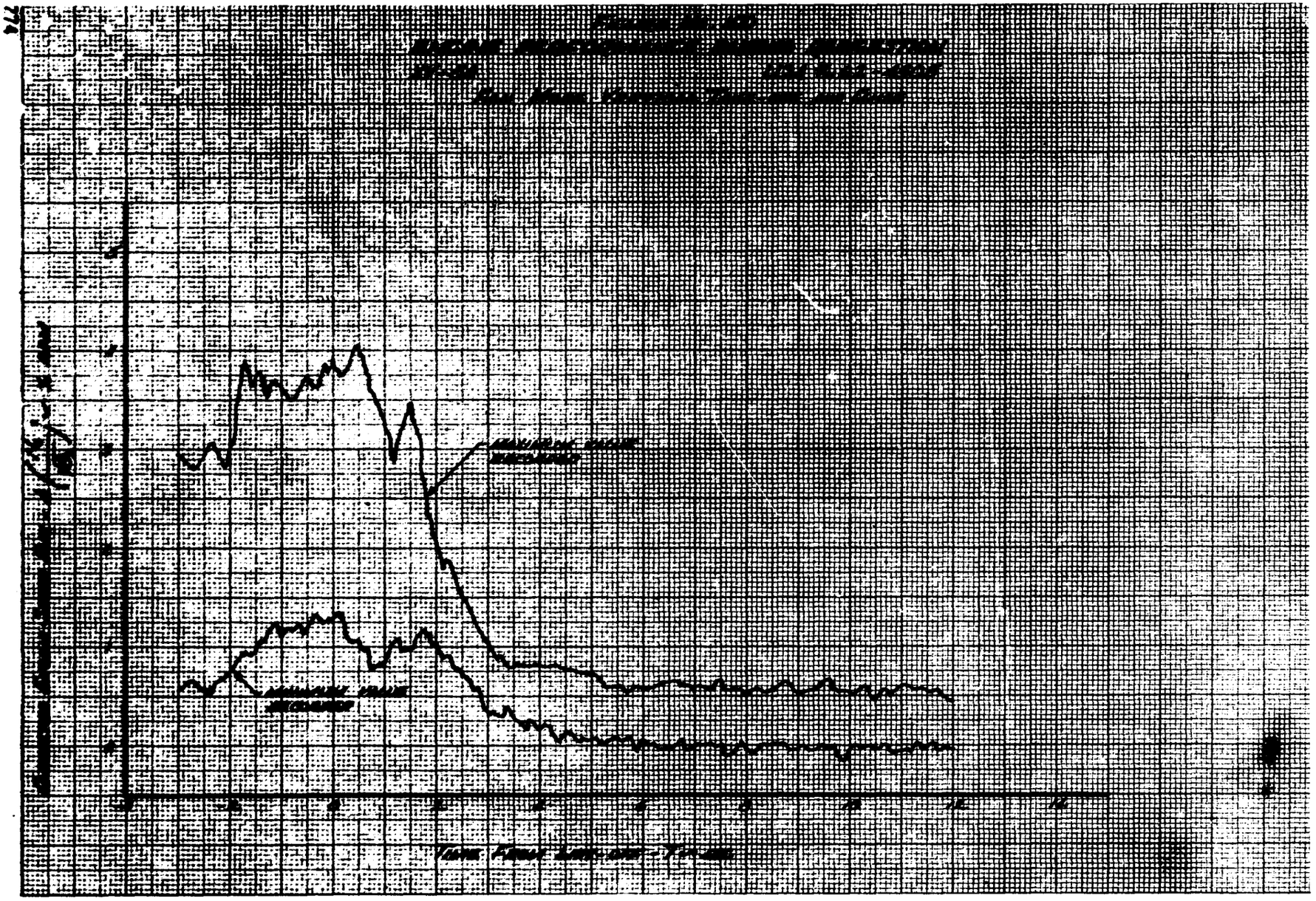

FIGURE NO. 101

VERTICAL THRUST LOSS DURING REINGESTION

XV-5A USA No. 62-4506

FAN MODE VERTICAL TAKE-OFF AND LAND

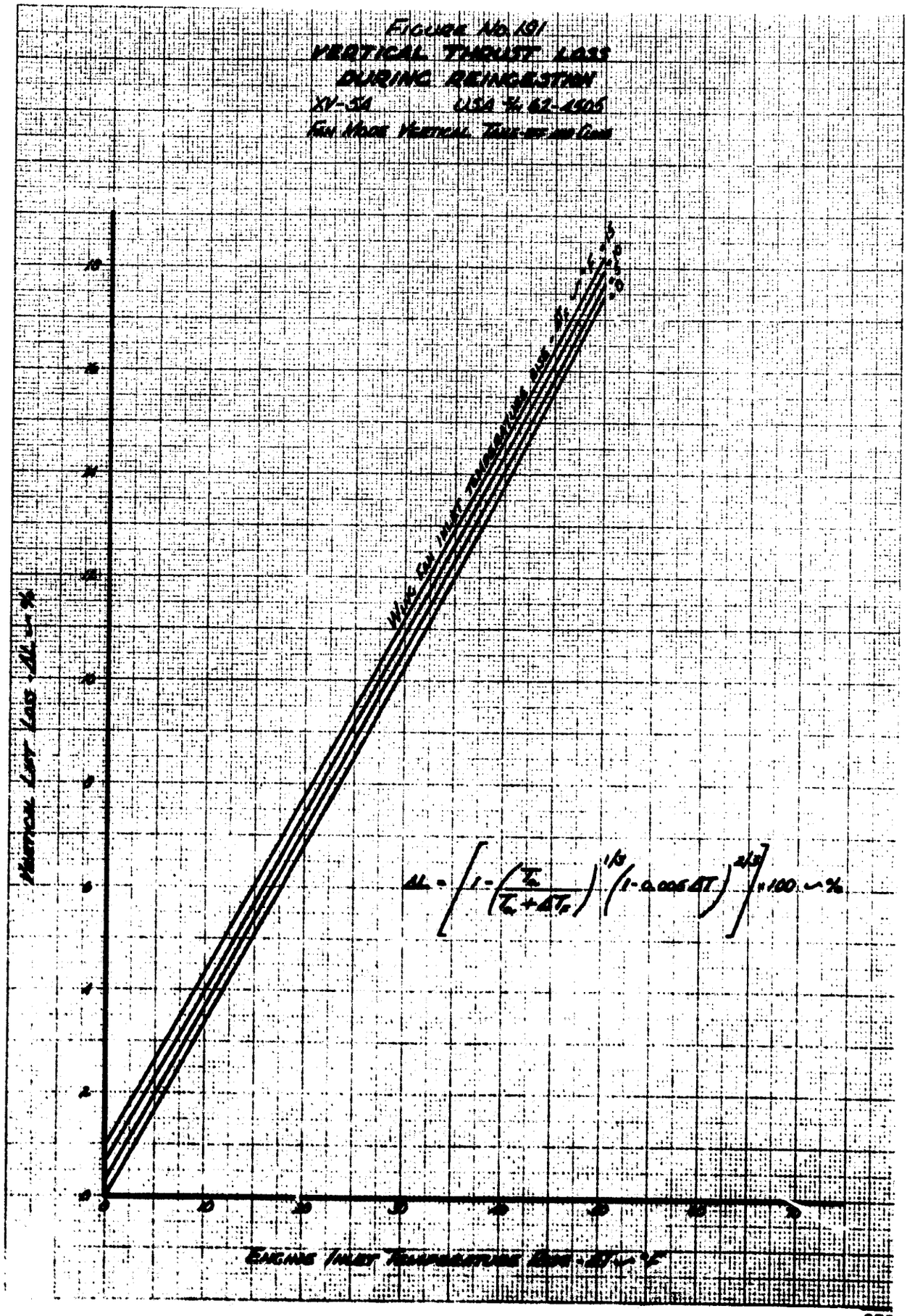

FIGURE NO. 101

ENGINE INLET PERFORMANCE

XV-5A USAF No. 62-4506

FAN MODE HOVERING

J-85-5A

SYM.	ENGINE S/N	ENGINE LOC.
○	230-895	LEFT
□	230-896	RIGHT

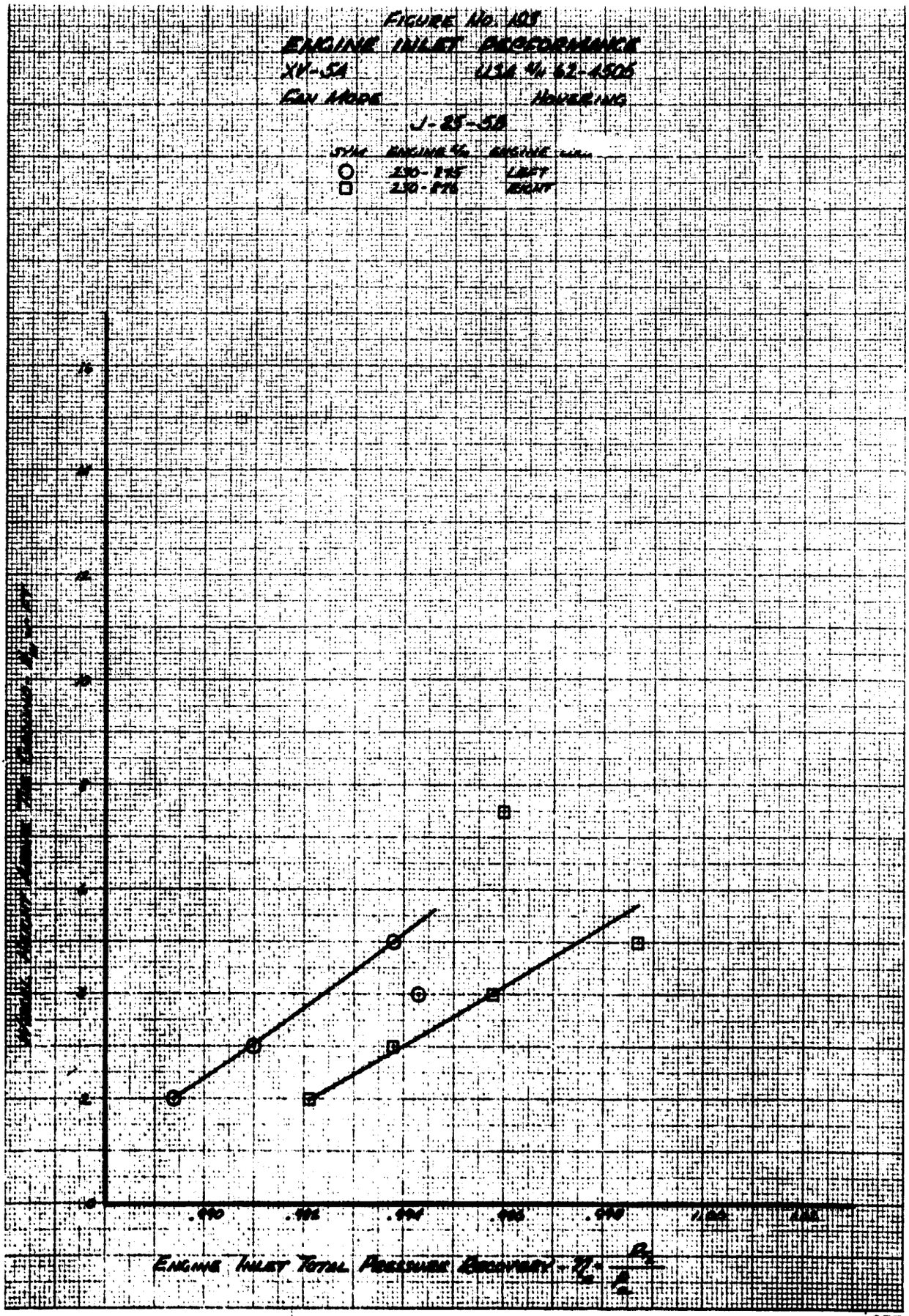

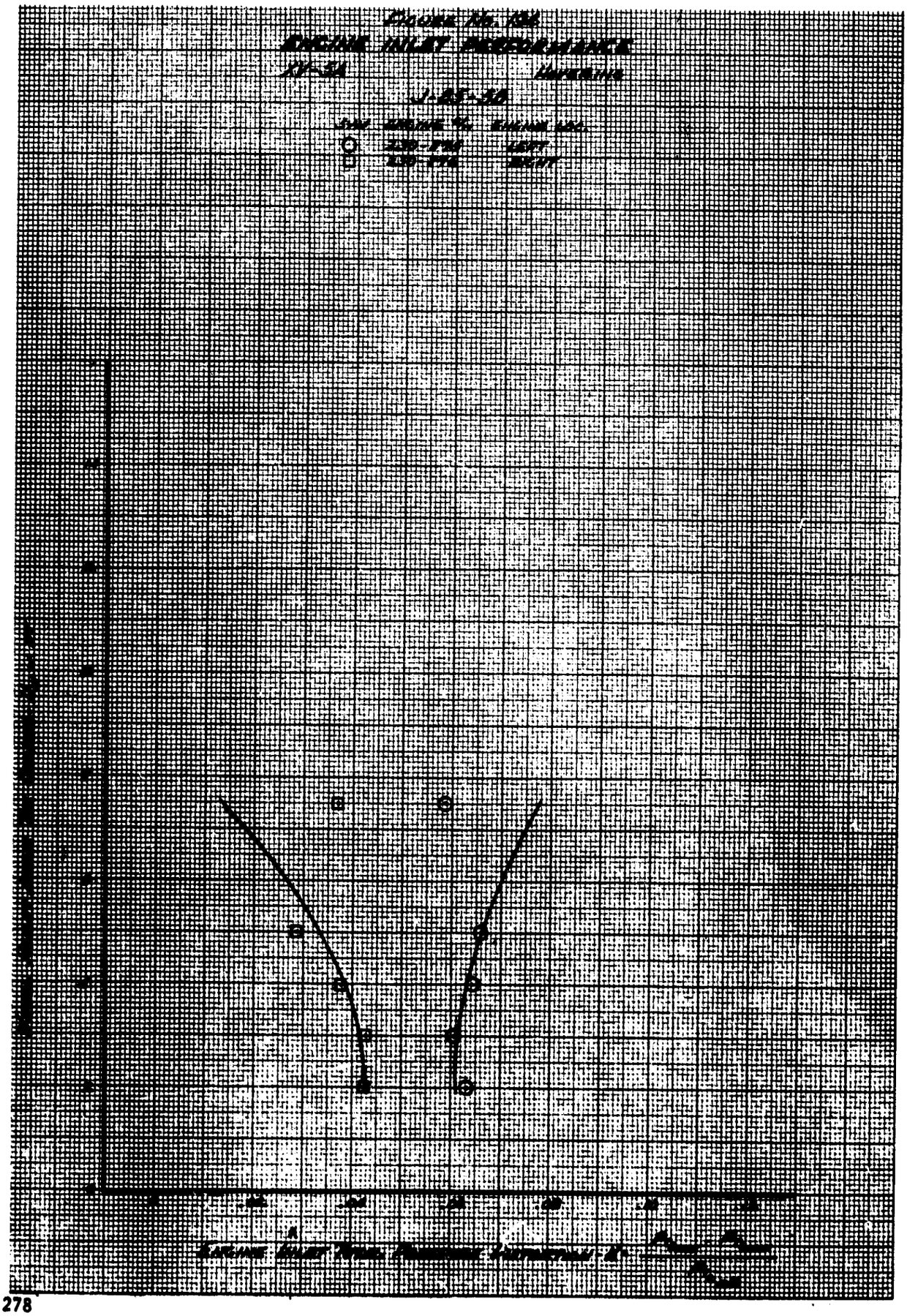
ENGINE INLET PERFORMANCE
XF-84
J-65-B3
SAW ENGINE
ENGINE INLET TOTAL PRESSURE RATIO

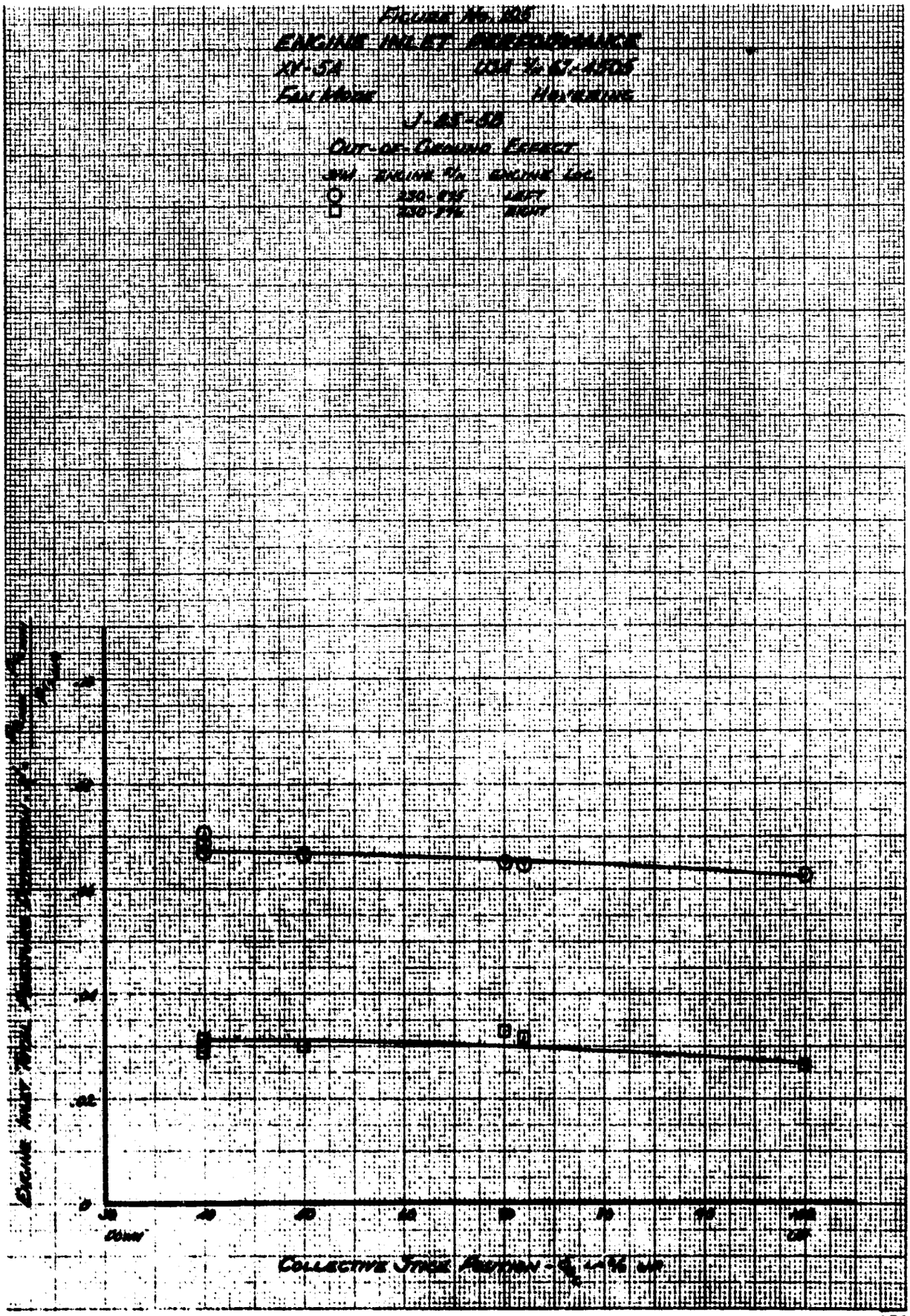
FIGURE NO. 826
ENGINE INLET PERFORMANCE
XH-51A
FULL SCALE
J-85-5A
OUT-OF-GROUND EFFECT
SYM
ENGINE
ENGINE LOC
LEFT
RIGHT
COLLECTIVE STICK POSITION

FIGURE NO. 106

ENGINE INLET PERFORMANCE

XV-5A

FAN MODE

USN 9½ 62-4505

HOVERING

J-85-5A

OUT-OF-GROUND-EFFECT

SYM	ENGINE S/N	ENGINE LOC.
○	130-575	LEFT
□	130-576	RIGHT

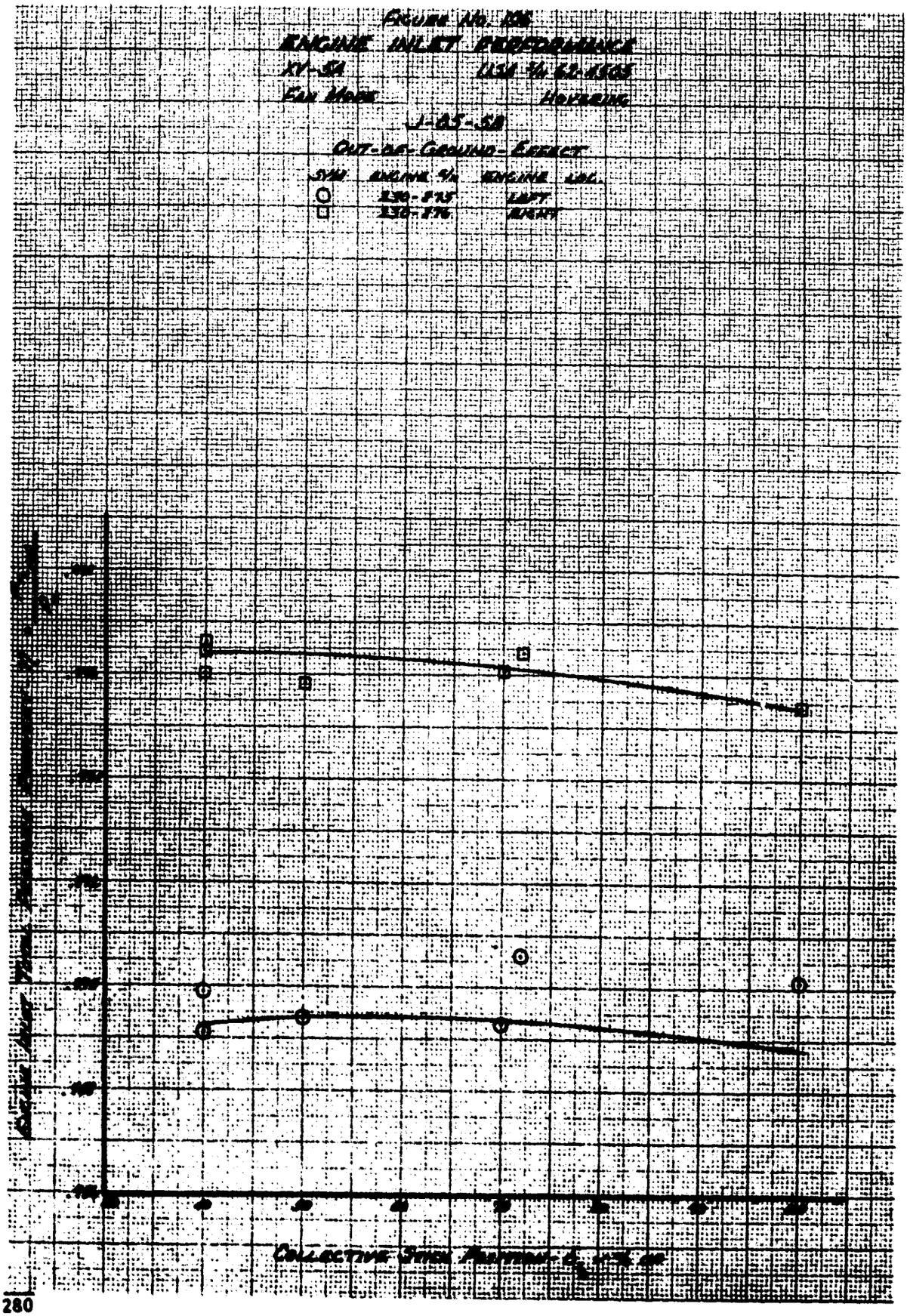

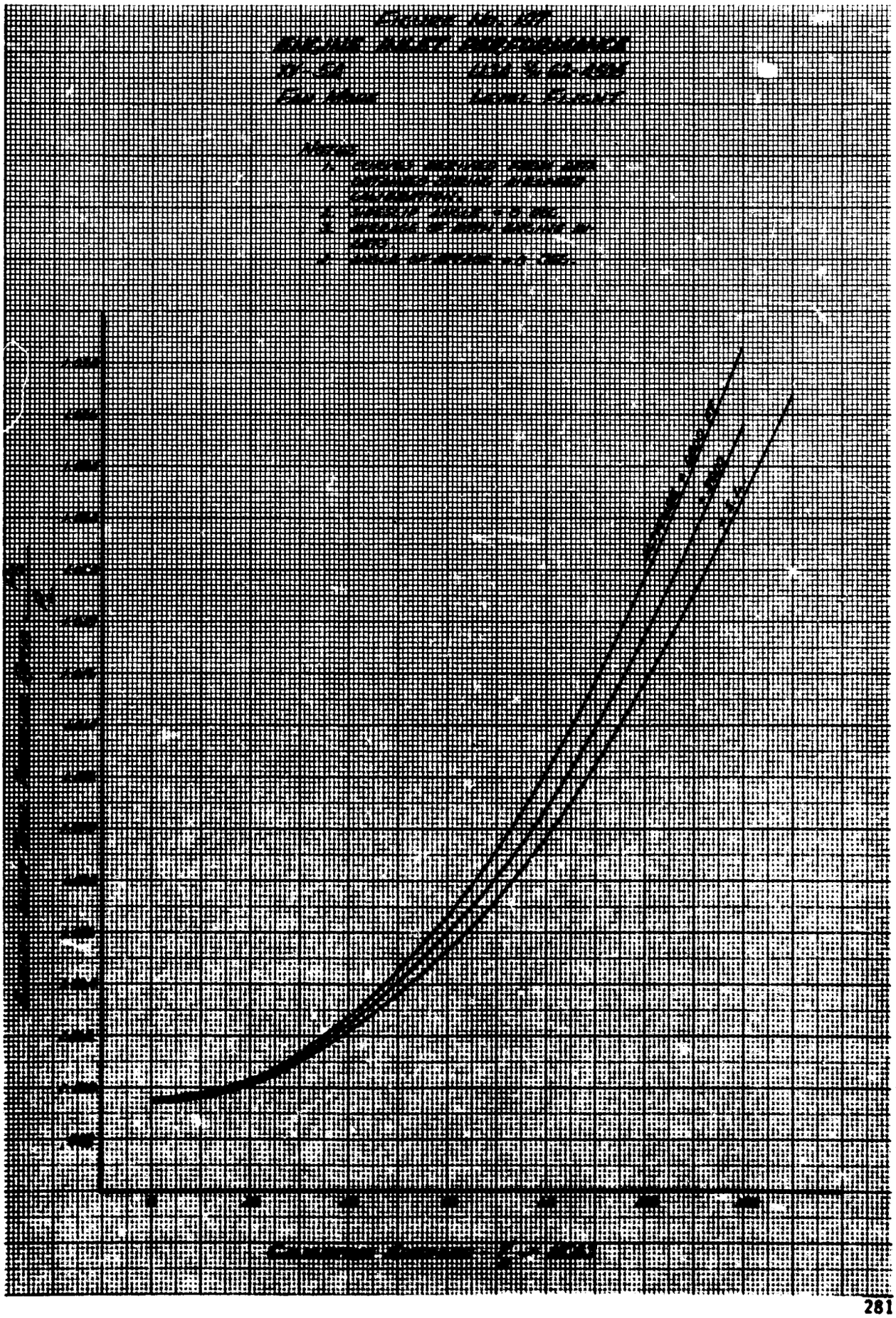

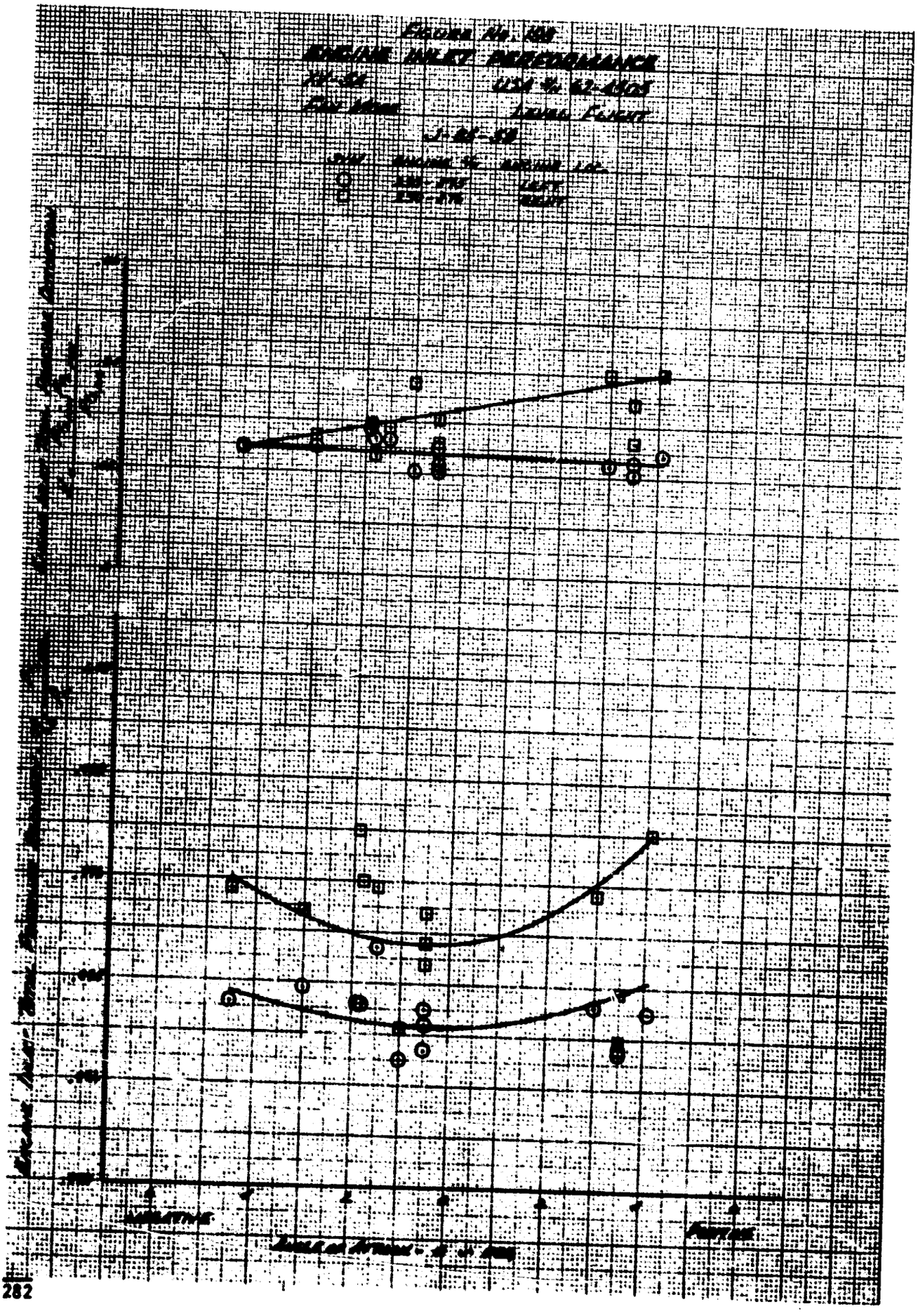
Figure No. 188
ENGINE INLET PERFORMANCE
XF-84
Full Scale
USAF No. 42-5605
Level Flight
M = .84 - .88
Engine % engine rpm
Left
Right
INFLATING
Angle of Attack - α - deg
Positive

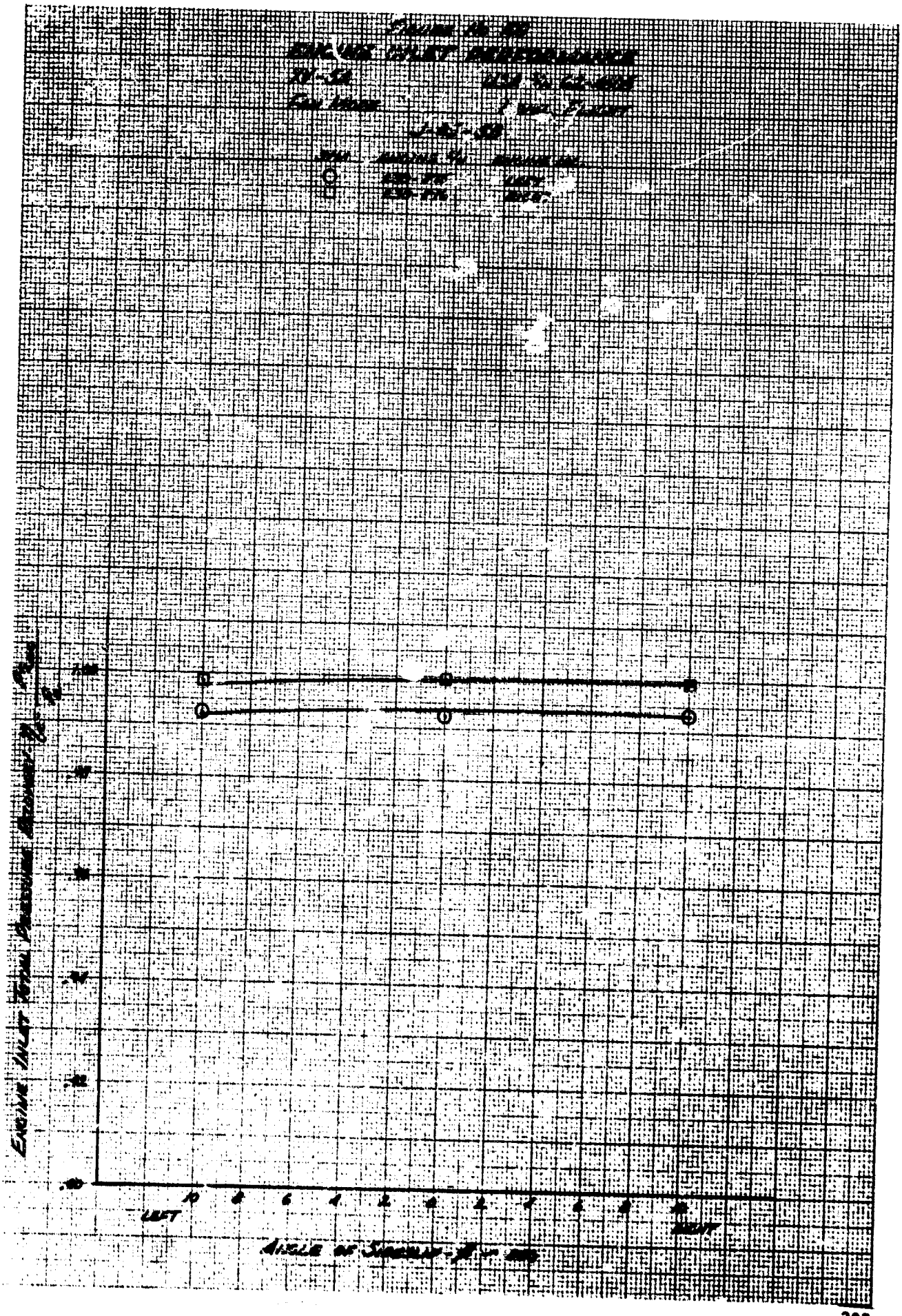
LEFT
RIGHT

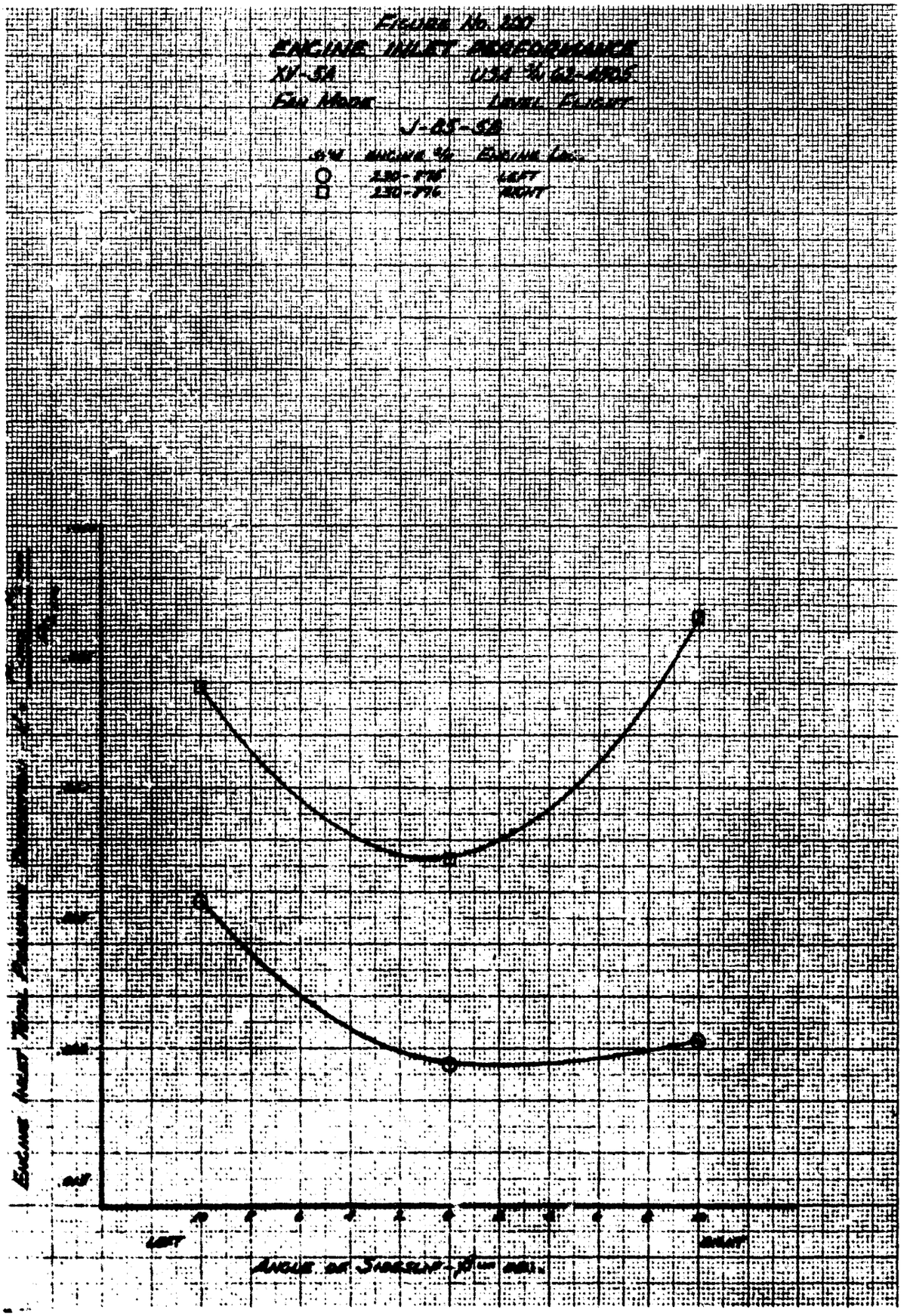
FIGURE No. 220
ENGINE INLET PERFORMANCE
XF-5A
5th Mode
J-85-5A
Engine Inlet Total Pressure Recovery
Angle of Sideslip - β
LEFT
RIGHT

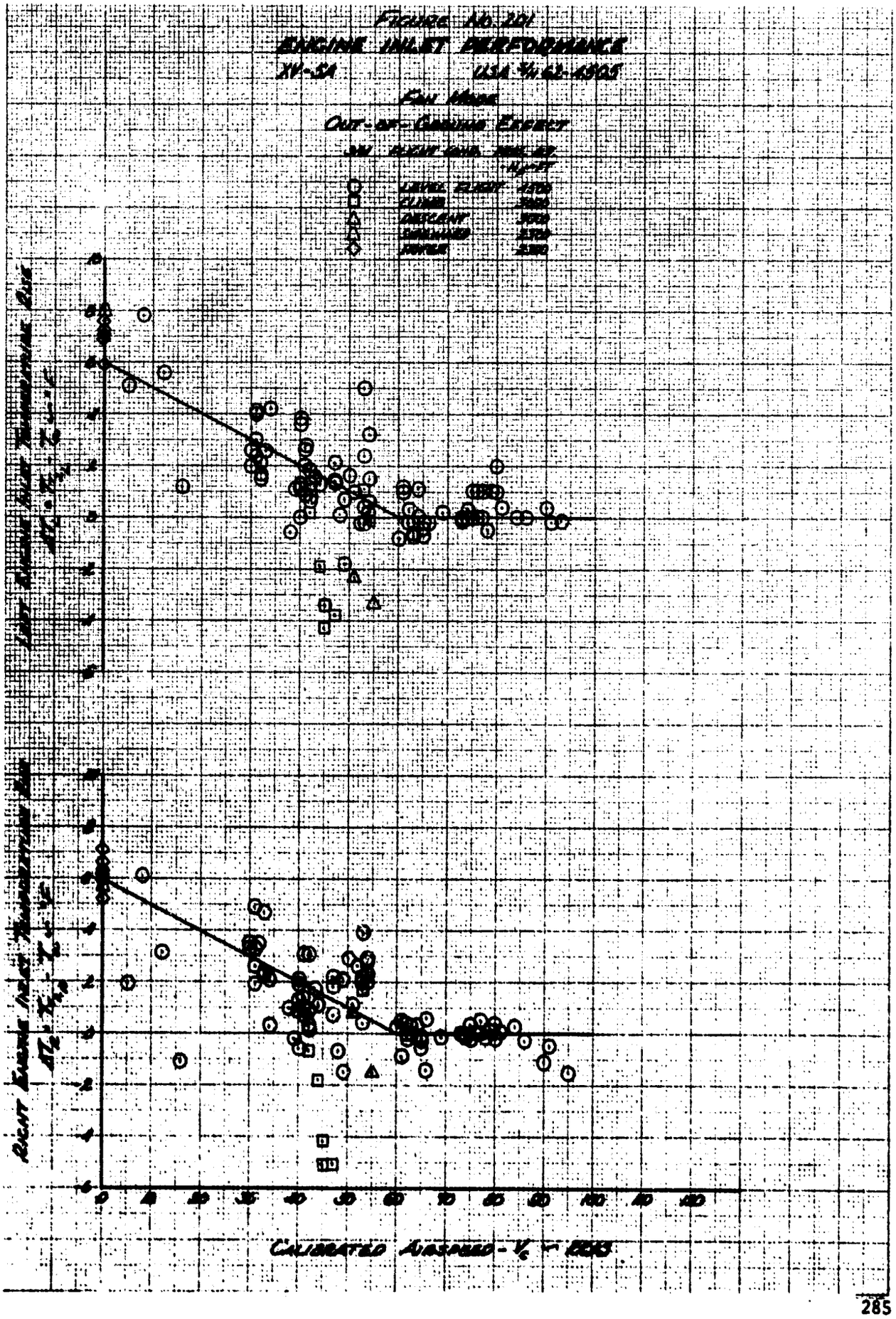
Figure A6.201
ENGINE INLET PERFORMANCE
XV-5A
Fan Mode
Out-of-Ground Effect
Level Flight
Climb
Descent
Landing
Approach
Calibrated Airspeed - V_c - KCAS

FIGURE NO. 202

ENGINE INLET PERFORMANCE

XV-5A USA S/N 62-4505

FAN MODE SIDEWARD FLIGHT

J-85-5B

OUT-OF-GROUND EFFECT

SYM.	ENGINE S/N	ENGINE LOC.
○	230-895	LEFT
□	230-896	RIGHT

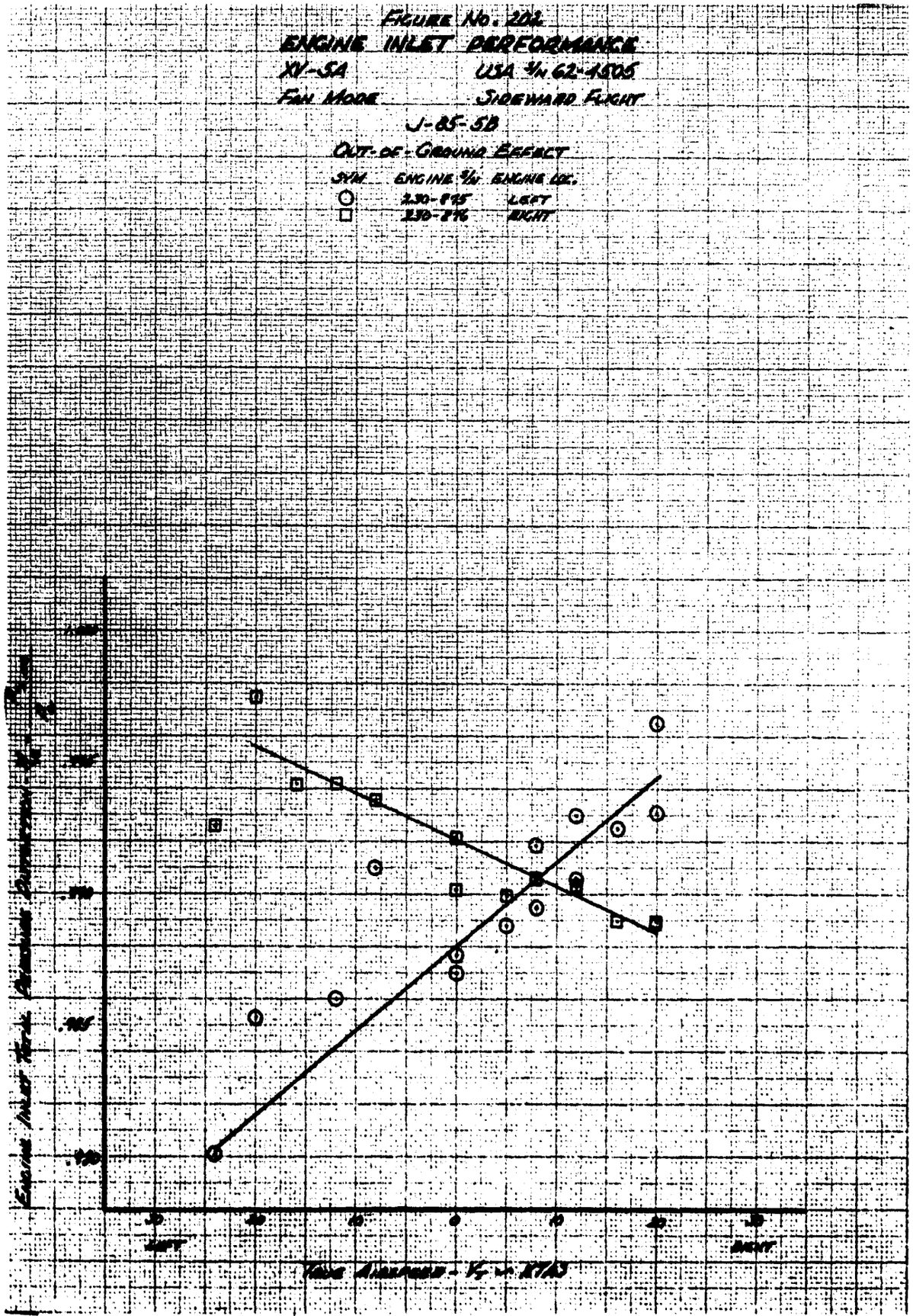

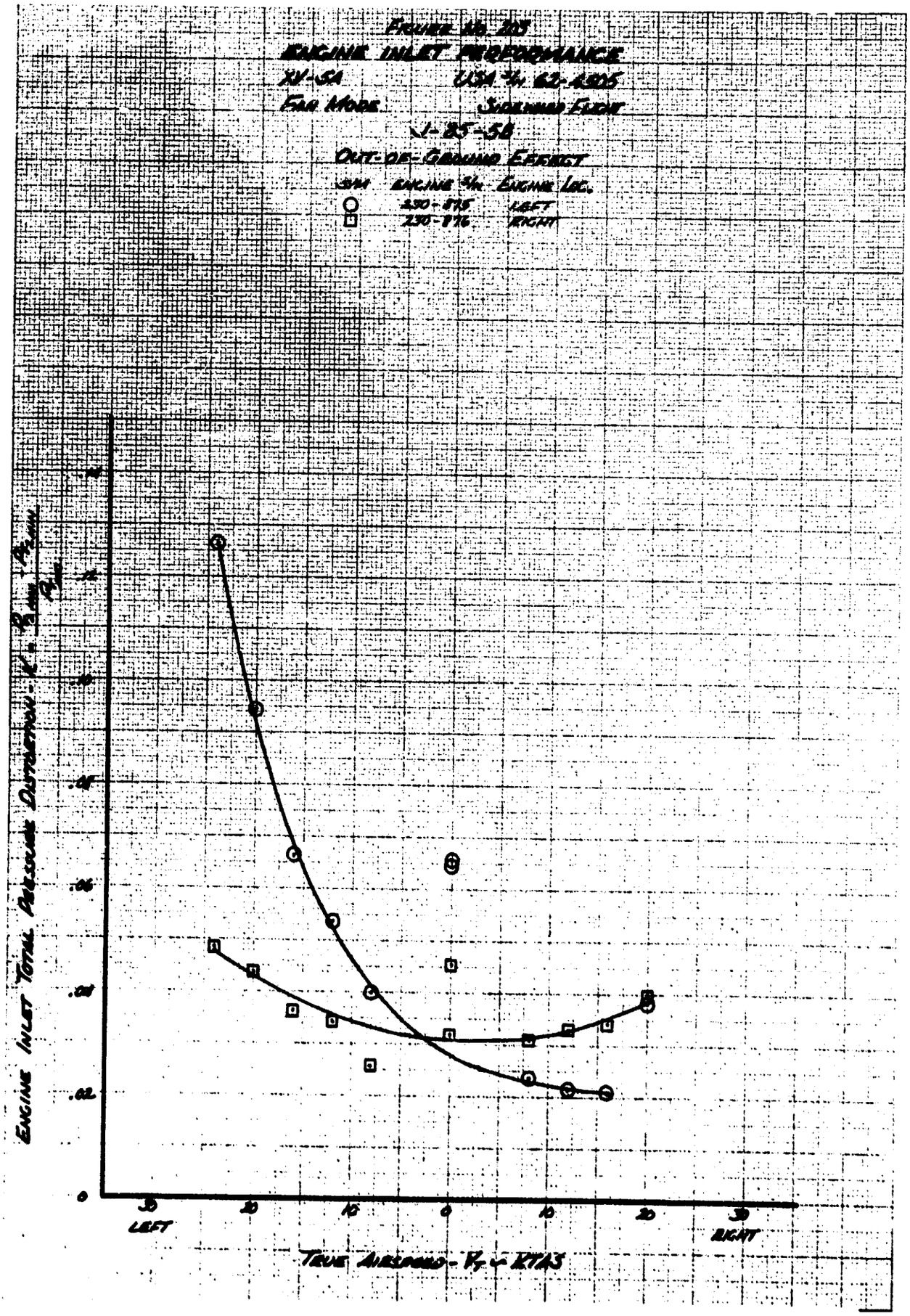
FIGURE NO. 207
ENGINE INLET PERFORMANCE
XV-5A USA No. 62-4505
FAA MODEL SLOWDOWN FLIGHT
V-25-58
OUT-OF-GROUND EFFECT
SYM ENGINE No. ENGINE LOC.
430-875 LEFT
230-876 RIGHT
ENGINE INLET TOTAL PRESSURE DIFFERENCE - $\frac{P_{T_2 \text{ MIN}}}{P_{T_{2\infty}}}$
.16
.12
.08
.04
0
30 LEFT
20
15
0
10
20
30 RIGHT
TRUE AIRSPEED - V_T - KTAS

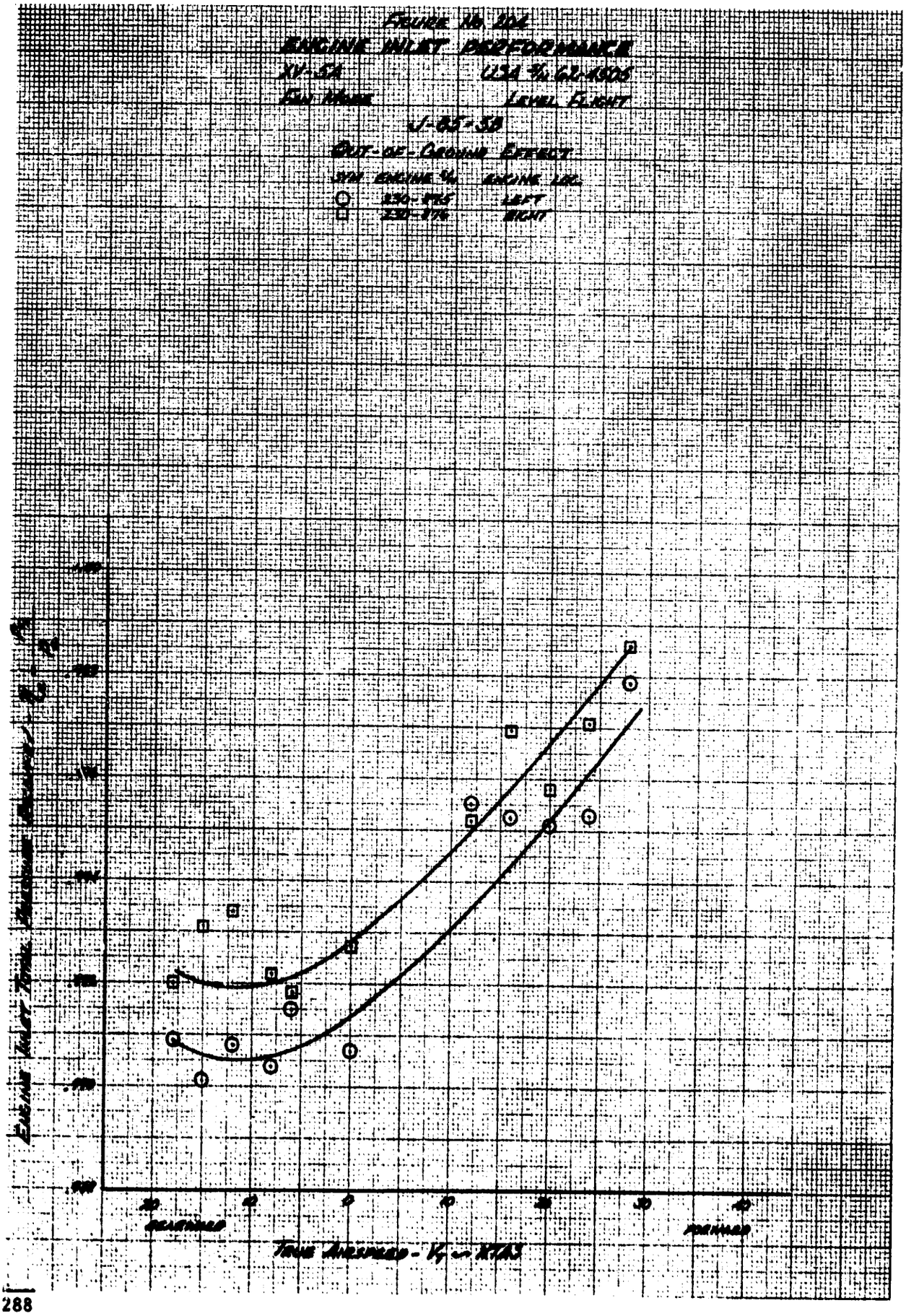
FIGURE No. 204
ENGINE INLET PERFORMANCE
XV-5A
USA 5½ 62-4906
FAN MODE
LEVEL FLIGHT
J-85-5A
OUT-OF-GROUND EFFECT
STAT ENGINE %
ENGINE LOC.
230-PRF
LEFT
230-176
RIGHT
ENGINE INLET TOTAL PRESSURE RECOVERY
TRUE AIRSPEED - KTAS

FIGURE No. 205

ENGINE INLET PERFORMANCE

XV-5A USA #62-4505

Gun Mount LEVEL FLIGHT

J-65-5B

OUT-OF-GROUND EFFECT

SYM	ENGINE %	ENGINE LOC.
○	100 - 97%	INLET
□	100 - 97%	DUCT

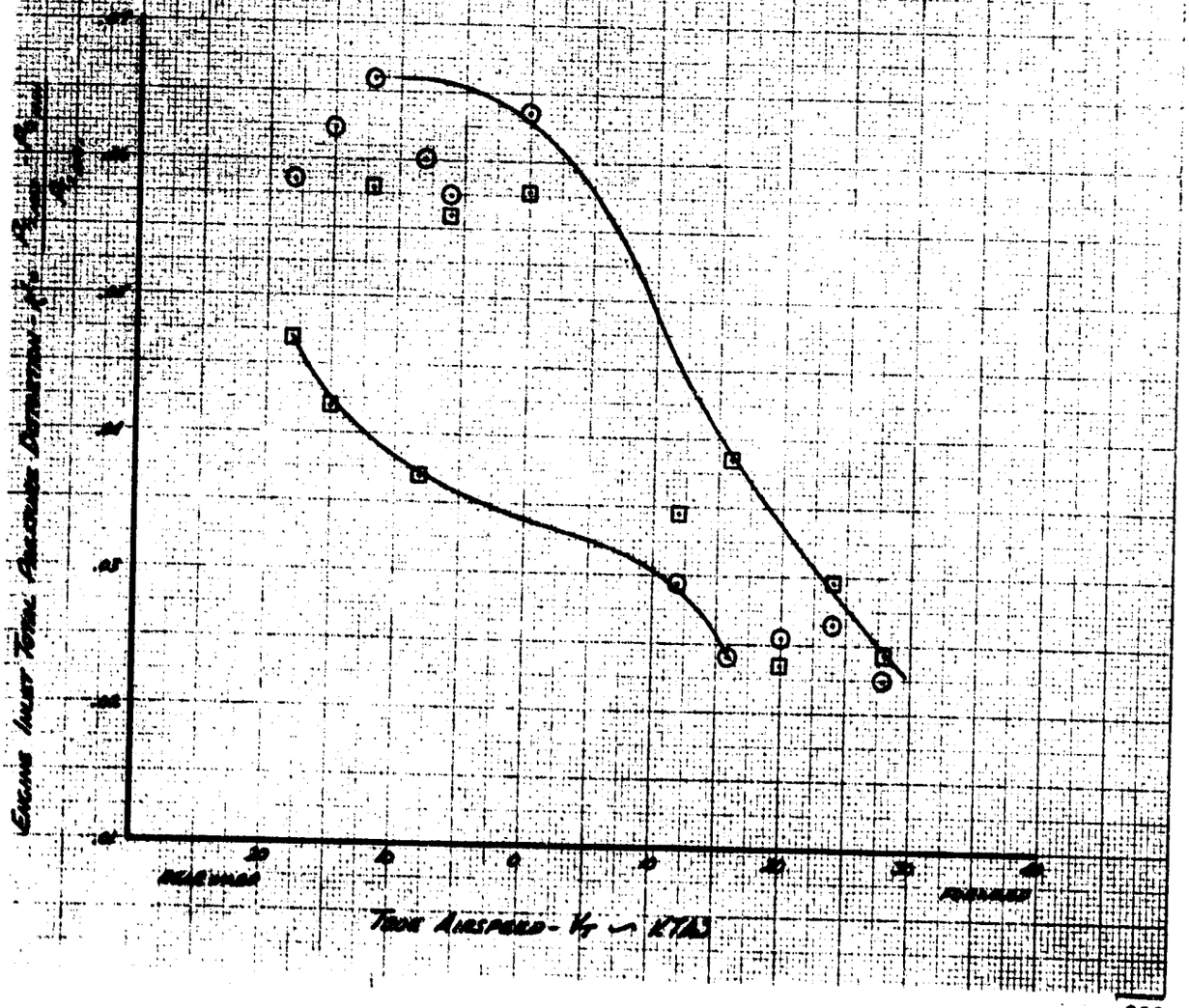

FIGURE No. 206

ENGINE INLET PERFORMANCE

XV-5A USA S/N 62-4505

FAN MODE - HOVER

WHEEL HEIGHT - H_W = 2 FT. PRESSURE ALTITUDE - H_p ~ FT = 2065

LEFT INLET

AVERAGE TOTAL PRESSURE RECOVERY - N_R = 0.9894
AVERAGE TOTAL PRESSURE DISTORTION - K' = 0.0636
AVERAGE STATIC PRESSURE DISTORTION - L = 0.0074
MASS FLOW RATIO - M/M* = 0.665
ENGINE POWER - $HP_{S.L}$ = 5263
ENGINE SPEED - N_G ~ % RPM = 100.4

RIGHT INLET

AVERAGE TOTAL PRESSURE RECOVERY - N_R = 0.9921
AVERAGE TOTAL PRESSURE DISTORTION - K' = 0.0745
AVERAGE STATIC PRESSURE DISTORTION - L = 0.0218
MASS FLOW RATIO - M/M* = 0.665
ENGINE POWER - $HP_{S.L}$ = 4931
ENGINE SPEED - N_G ~ % RPM = 100.2

• TOTAL
⊡ STATIC

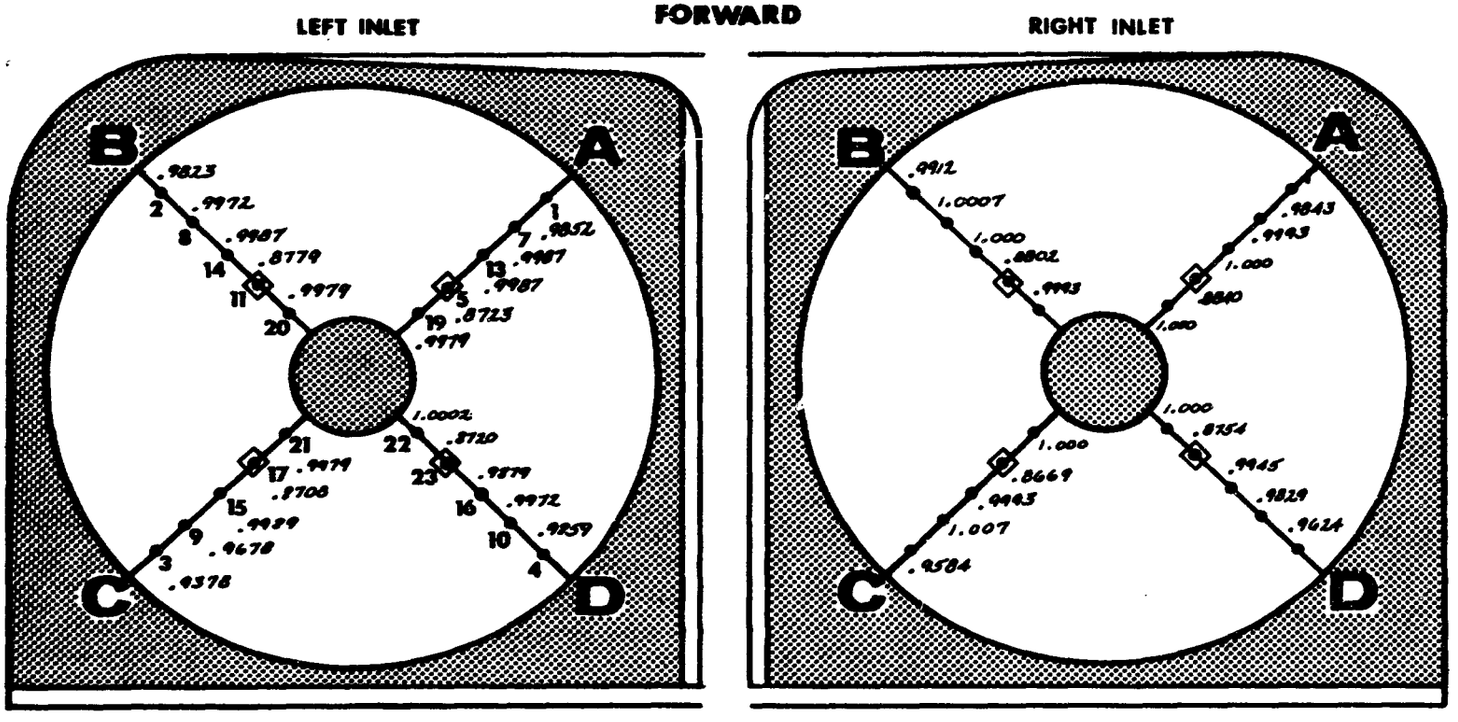

FIGURE No. 207

ENGINE INLET PERFORMANCE

XV-5A USA S/N 62-4505

FAN MODE HOVER

WHEEL HEIGHT - $H_w \backsim$ FT = 5 PRESSURE ALT - $H_p \backsim$ FT = 2029

LEFT INLET

AVERAGE TOTAL PRESSURE RECOVERY - N_R = 0.9894
AVERAGE TOTAL PRESSURE DISTORTION - K = 0.0644
AVERAGE STATIC PRESSURE DISTORTION - L = 0.0092
MASS FLOW RATIO - M/M^* = 0.669
ENGINE POWER - $HP_{S.L}$ = 5322
ENGINE SPEED - $N_G \backsim$ % RPM = 100.8

RIGHT INLET

AVERAGE TOTAL PRESSURE RECOVERY - N_R = 0.9960
AVERAGE TOTAL PRESSURE DISTORTION - K = 0.0371
AVERAGE STATIC PRESSURE DISTORTION - L = 0.0220
MASS FLOW RATIO - M/M^* = 0.675
ENGINE POWER - $HP_{S.L}$ = 5414
ENGINE SPEED - $N_G \backsim$ % RPM = 101.9

• TOTAL
⊡ STATIC

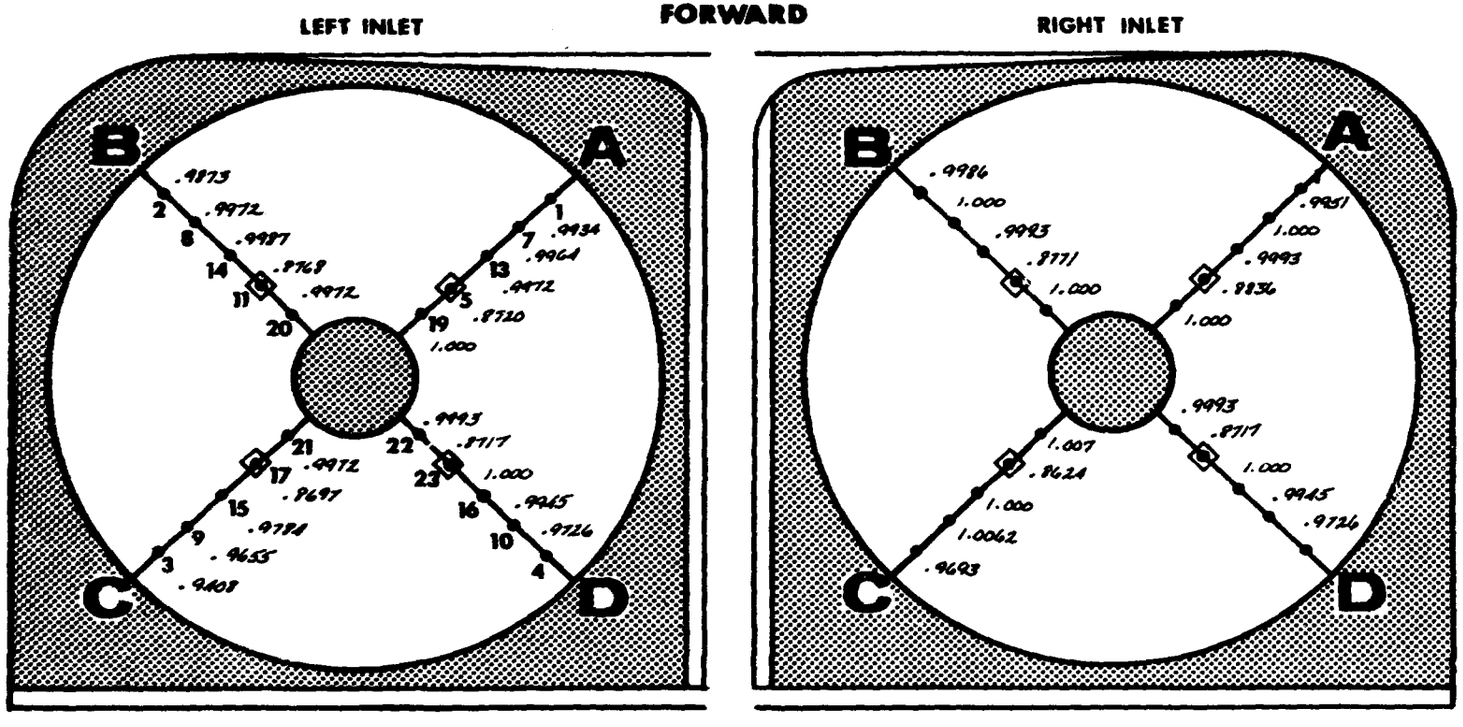

FIGURE No. 208

ENGINE INLET PERFORMANCE

XV-5A USA S/N 62-4505

FAN MODE HOVER

WHEEL HEIGHT - $H_W \backsim$ FT = 15 PRESSURE ALT - $H_p \backsim$ FT = 2141

LEFT INLET
- AVERAGE TOTAL PRESSURE RECOVERY - N_R = 0.9907
- AVERAGE TOTAL PRESSURE DISTORTION - K = 0.0620
- AVERAGE STATIC PRESSURE DISTORTION - L = 0.0077
- MASS FLOW RATIO - M/M^2 = 0.662
- ENGINE POWER - $HP_{S.L}$ = 4214
- ENGINE SPEED - $N_G \backsim$ % RPM = 97.7

RIGHT INLET
- AVERAGE TOTAL PRESSURE RECOVERY - N_R = 0.9907
- AVERAGE TOTAL PRESSURE DISTORTION - K = 0.0678
- AVERAGE STATIC PRESSURE DISTORTION - L = 0.0194
- MASS FLOW RATIO - M/M^2 = 0.658
- ENGINE POWER - $HP_{S.L}$ = 4359
- ENGINE SPEED - $N_G \backsim$ % RPM = 98.6

• TOTAL
⊡ STATIC

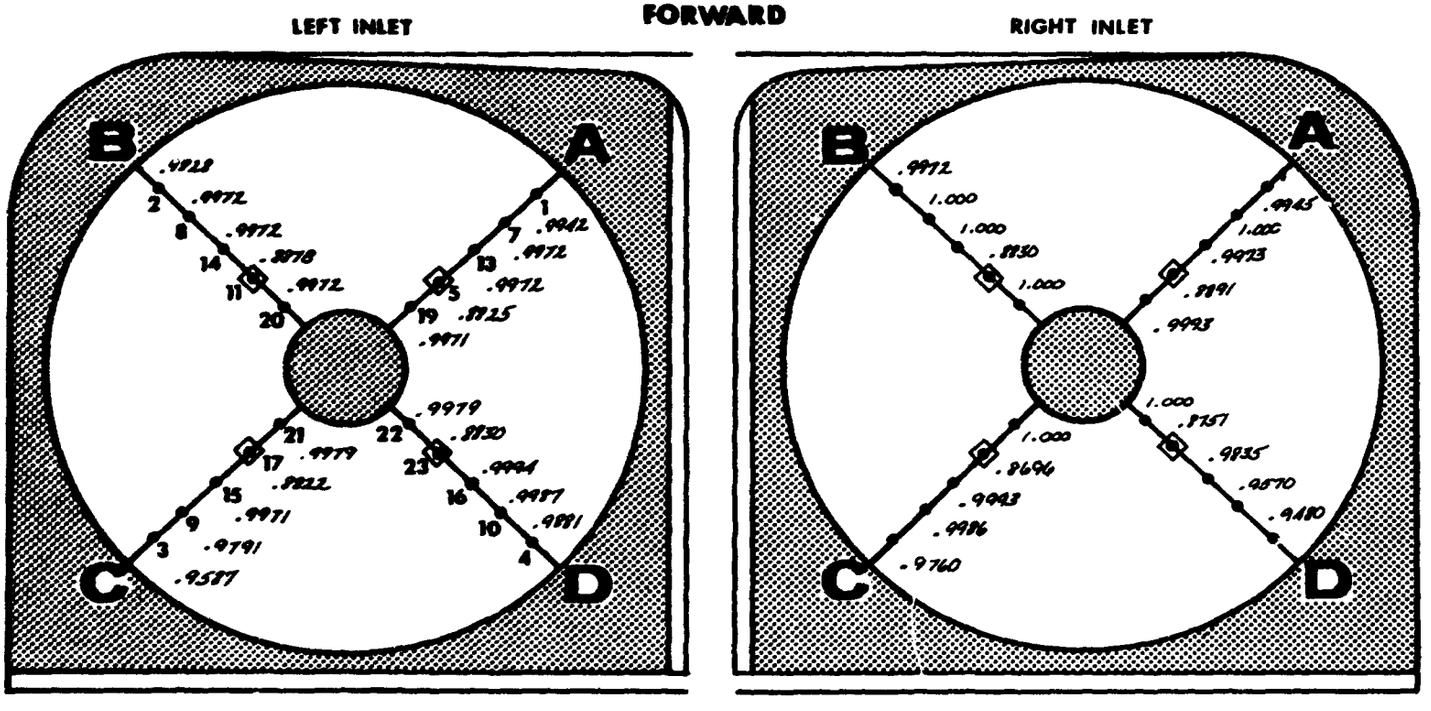

FIGURE No. 209

ENGINE INLET PERFORMANCE

XV-5A USA S/N 62-4505

FAN MODE LEFT SIDEWARD FLIGHT

WHEEL HEIGHT - H_W ~ FT = 15 PRESSURE ALT - H_p ~ FT = 2325

TRUE AIRSPEED - V_t ~ KTAS = 24

LEFT INLET

AVERAGE TOTAL PRESSURE RECOVERY - N_R = 0.9901
AVERAGE TOTAL PRESSURE DISTORTION - K = 0.0799
AVERAGE STATIC PRESSURE DISTORTION - L = 0.0915
MASS FLOW RATIO - M/M^2 = 0.684
ENGINE POWER - $HP_{S.L}$ = 5258
ENGINE SPEED - N_G ~ % RPM = 101.6

RIGHT INLET

AVERAGE TOTAL PRESSURE RECOVERY - N_R = 0.9925
AVERAGE TOTAL PRESSURE DISTORTION - K = 0.0491
AVERAGE STATIC PRESSURE DISTORTION - L = 0.0213
MASS FLOW RATIO - M/M^2 = 0.673
ENGINE POWER - $HP_{S.L}$ = 5429
ENGINE SPEED - N_G ~ % RPM = 102.6

• TOTAL
⊡ STATIC

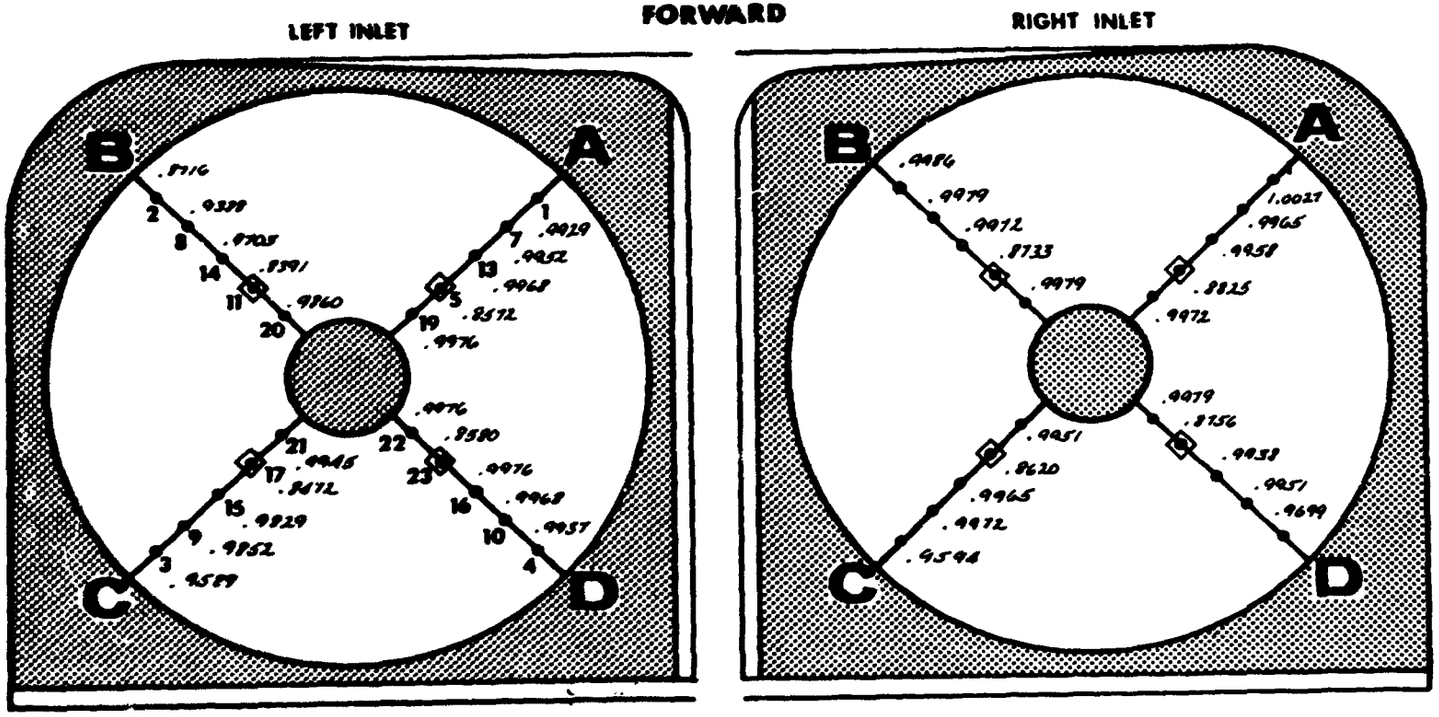

FIGURE No. 210

ENGINE INLET PERFORMANCE

XV-5A USA S/N 62-4505

FAN MODE RIGHT SIDEWARD FLIGHT

WHEEL HEIGHT - H_W ~ FT = 15 PRESSURE ALT - H_p ~ FT = 2325

TRUE AIRSPEED - V_T ~ KTAS = 20

LEFT INLET

AVERAGE TOTAL PRESSURE RECOVERY - N_R = 0.9965
AVERAGE TOTAL PRESSURE DISTORTION - K = 0.0316
AVERAGE STATIC PRESSURE DISTORTION - L = 0.0108
MASS FLOW RATIO - M/M^* = 0.698
ENGINE POWER - $HP_{S.L}$ = 5429
ENGINE SPEED - N_C ~ % RPM = 101.4

RIGHT INLET

AVERAGE TOTAL PRESSURE RECOVERY - N_R = 0.989
AVERAGE TOTAL PRESSURE DISTORTION - K = 0.0603
AVERAGE STATIC PRESSURE DISTORTION - L = 0.0228
MASS FLOW RATIO - M/M^* = 0.691
ENGINE POWER - $HP_{S.L}$ = 5564
ENGINE SPEED - N_C ~ % RPM = 102.2

• TOTAL
⊡ STATIC

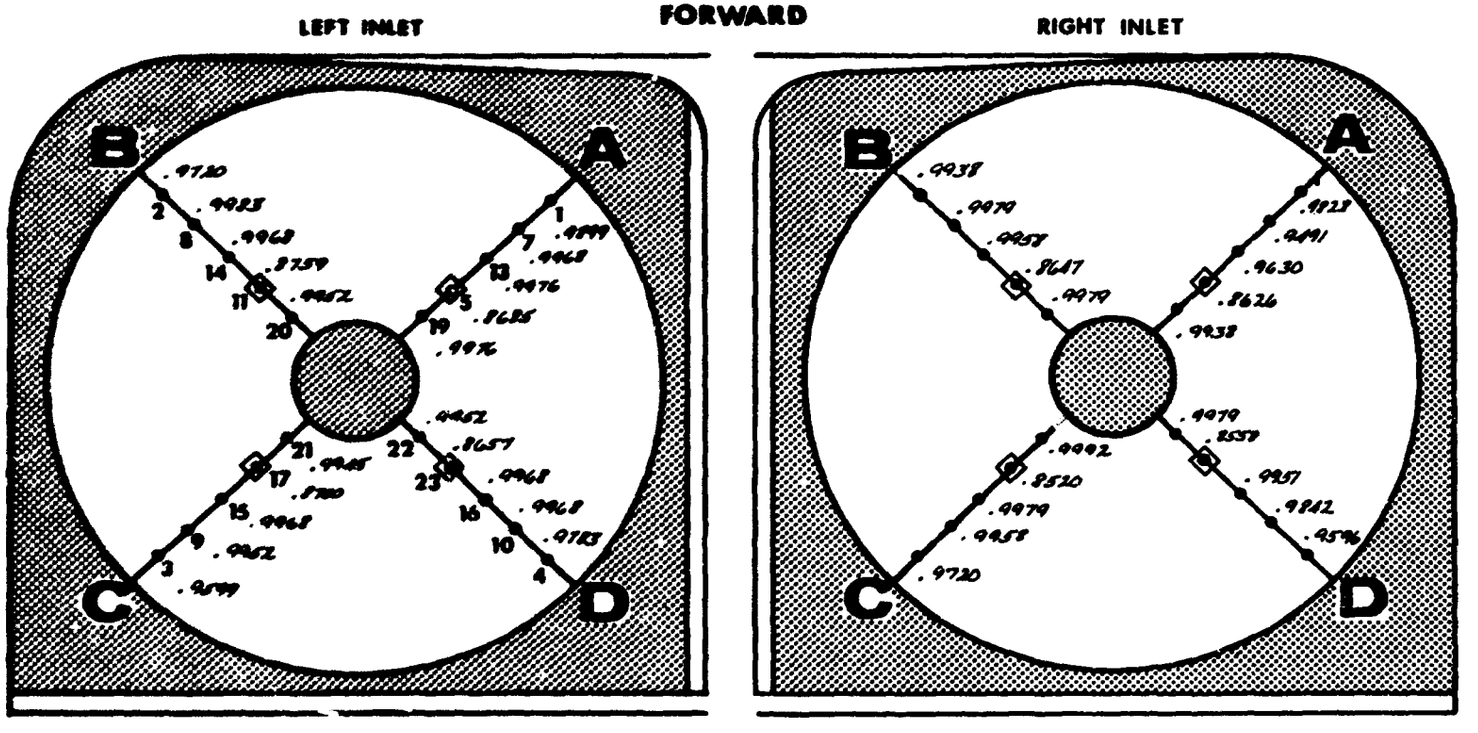

FIGURE No. 211

ENGINE INLET PERFORMANCE

XV-5A USA S/N 62-4505

FAN MODE REARWARD FLIGHT

WHEEL HEIGHT - H_W ∽ FT = 15 PRESSURE ALT - H_p ∽ FT = 2325

TRUE AIRSPEED - V_t ∽ KTAS = 15

LEFT INLET

AVERAGE TOTAL PRESSURE RECOVERY - N_R = 0.9909

AVERAGE TOTAL PRESSURE DISTORTION - K = 0.0585

AVERAGE STATIC PRESSURE DISTORTION - L = 0.0070

MASS FLOW RATIO - M/M* = 0.691

ENGINE POWER - $HP_{S.L}$ = 5368

ENGINE SPEED - N_C ∽ % RPM = 100.5

RIGHT INLET

AVERAGE TOTAL PRESSURE RECOVERY - N_R = 0.9920

AVERAGE TOTAL PRESSURE DISTORTION - K = 0.0471

AVERAGE STATIC PRESSURE DISTORTION - L = 0.0201

MASS FLOW RATIO - M/M* = 0.670

ENGINE POWER - $HP_{S.L}$ = 5444

ENGINE SPEED - N_C ∽ % RPM = 101.9

• TOTAL

⊡ STATIC

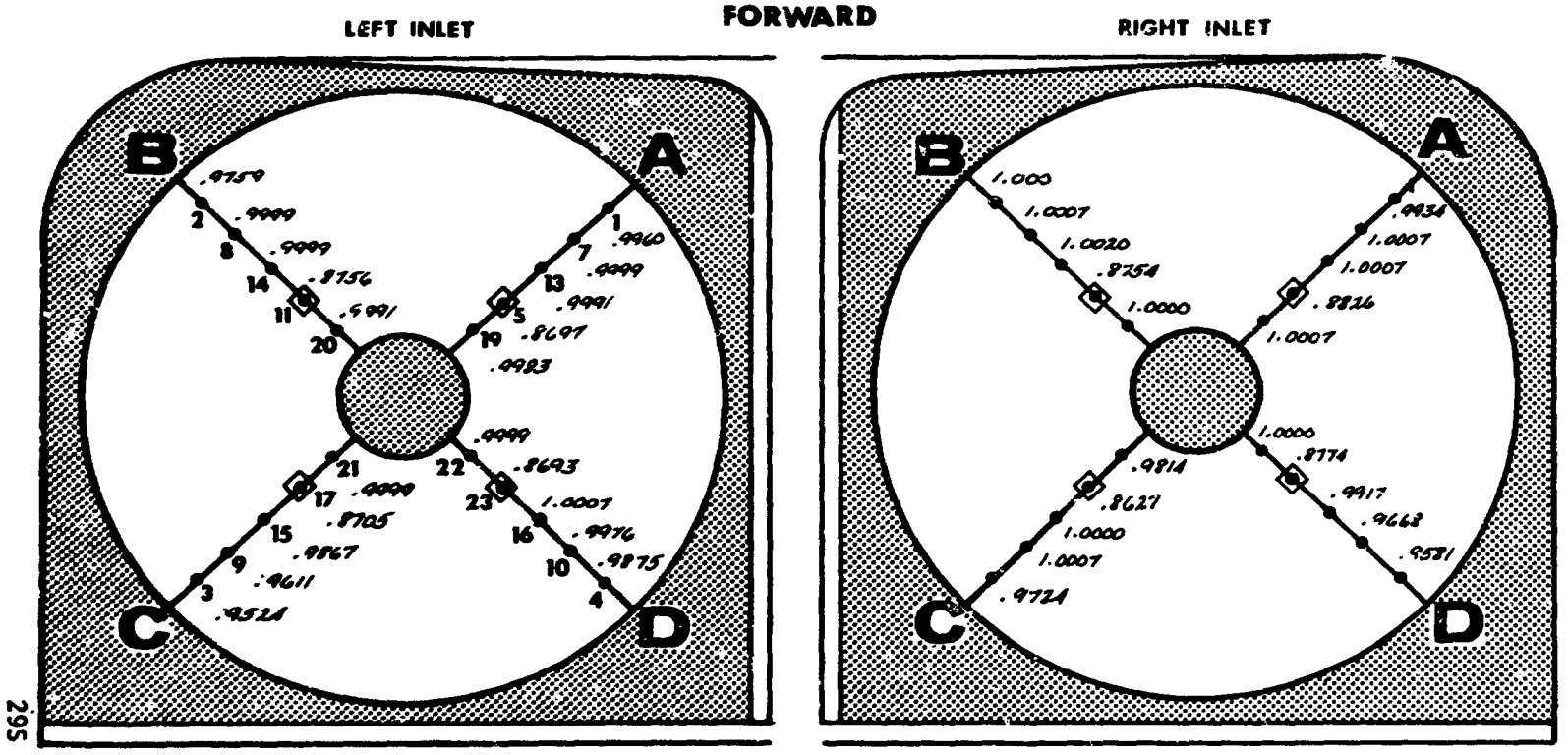

FIGURE No. 212

ENGINE INLET PERFORMANCE

XV-5A USA S/N 62-4505

FAN MODE VERTICAL CLIMB

VERTICAL CLIMB SPEED - V_c ~ FT/MIN = 2100 PRESSURE ALT - H_p ~ FT = 1894

LEFT INLET

AVERAGE TOTAL PRESSURE RECOVERY - N_R = 0.9937
AVERAGE TOTAL PRESSURE DISTORTION - K = 0.0397
AVERAGE STATIC PRESSURE DISTORTION - L = 0.0068
MASS FLOW RATIO - M/M_∞ = 0.673
ENGINE SPEED - N_c ~ % RPM = 100.9
ENGINE POWER - $HP_{S.L}$ = 5099

RIGHT INLET

AVERAGE TOTAL PRESSURE RECOVERY - N_R = 0.9981
AVERAGE TOTAL PRESSURE DISTORTION - K = 0.0239
AVERAGE STATIC PRESSURE DISTORTION - L = 0.0184
MASS FLOW RATIO - M/M_∞ = 0.684
ENGINE POWER - $HP_{S.L}$ = 5284
ENGINE SPEED - N_c ~ % RPM = 101.6

• TOTAL
⊡ STATIC

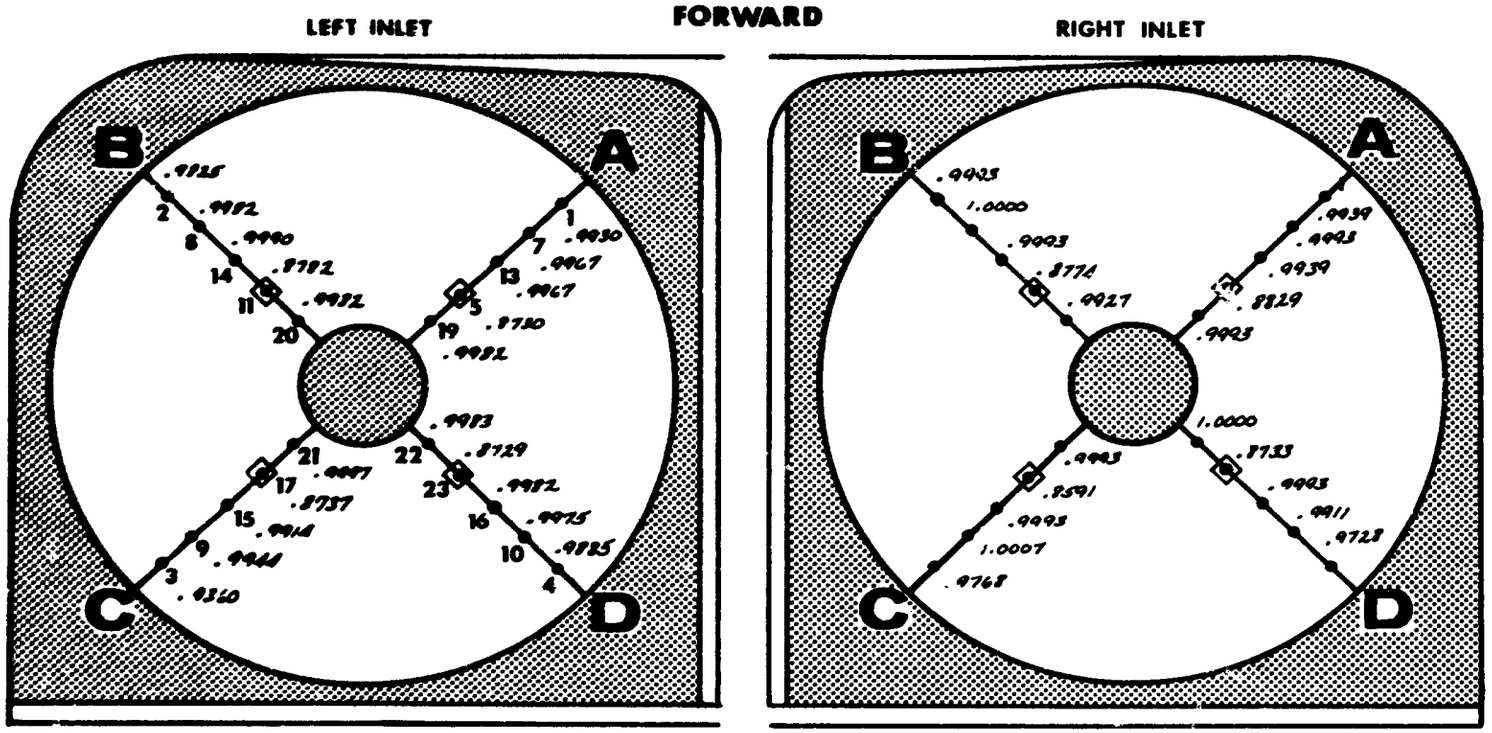

FIGURE No. 213

ENGINE INLET PERFORMANCE

XV-5A USA S/N 62-4505

FAN MODE VERTICAL DESCENT

RATE OF DESCENT - $R/D_y \backsim$ FT/MIN = 500 PRESSURE ALT - $H_p \backsim$ FT = 2200

LEFT INLET

AVERAGE TOTAL PRESSURE RECOVERY - N_R = 0.9936
AVERAGE TOTAL PRESSURE DISTORTION - K = 0.0413
AVERAGE STATIC PRESSURE DISTORTION - L = 0.0153
MASS FLOW RATIO - M/M^* = 0.630
ENGINE POWER - $HP_{S.L}$ = 5330
ENGINE SPEED - $N_c \backsim$ % RPM = 101.1

RIGHT INLET

AVERAGE TOTAL PRESSURE RECOVERY - N_R = 0.990
AVERAGE TOTAL PRESSURE DISTORTION - K = 0.0083
AVERAGE STATIC PRESSURE DISTORTION - L = 0.0144
MASS FLOW RATIO - M/M^* = 0.686
ENGINE POWER - $HP_{S.L}$ = 5392
ENGINE SPEED - $N_c \backsim$ % RPM = 101.7

• TOTAL
⊡ STATIC

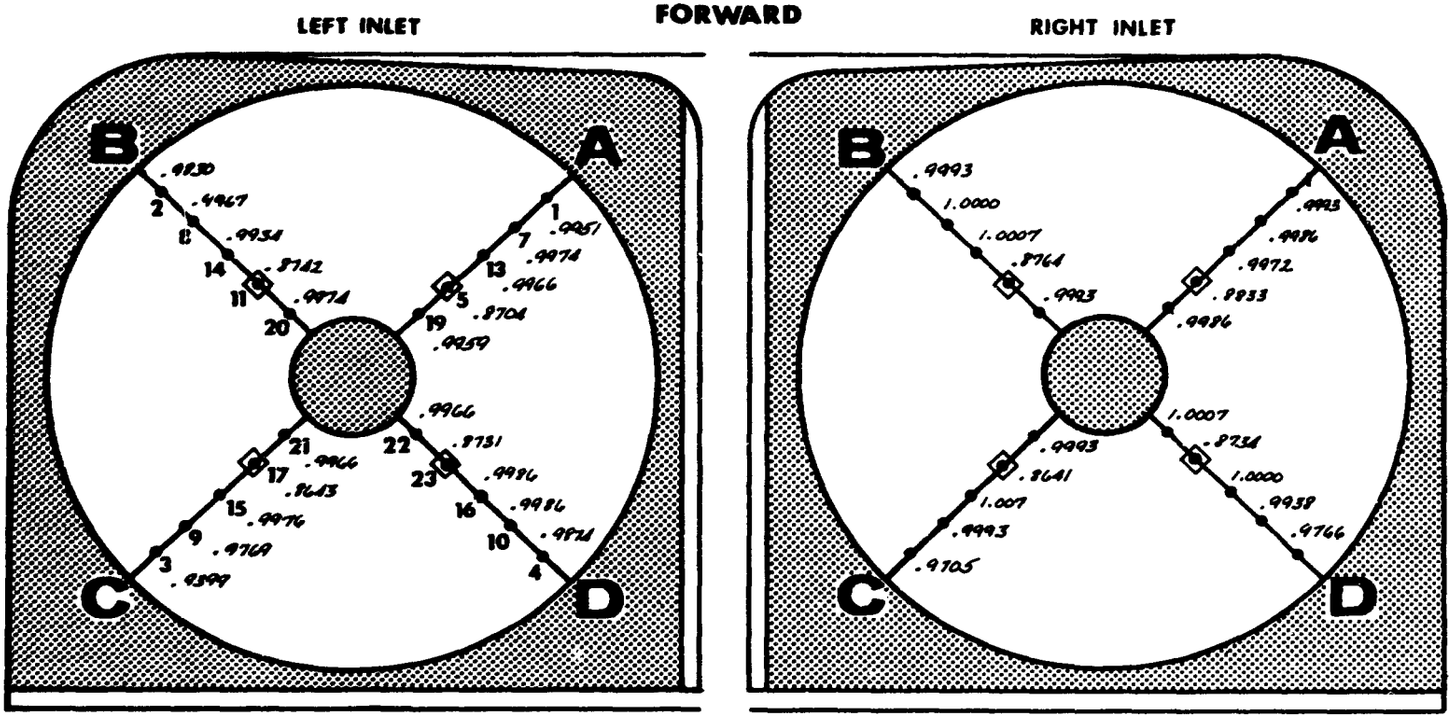

FIGURE No. 214

ENGINE INLET PERFORMANCE

XV-5A USA S/N 62-4505

FAN MODE LEVEL FLIGHT

ANGLE OF ATTACK - $\alpha_T \backsim$ DEG = 4.1
TRUE AIRSPEED - $V_T \backsim$ KTAS = 40

PRESSURE ALT - $H_P \backsim$ FT = 3139
LANDING GEAR DOWN

LEFT INLET
AVERAGE TOTAL PRESSURE RECOVERY - N_R = 0.9935
AVERAGE TOTAL PRESSURE DISTORTION - K = 0.0242
AVERAGE STATIC PRESSURE DISTORTION - L = 0.0097
MASS FLOW RATIO - M/M^* = 0.697
ENGINE POWER - $HP_{S.I}$ = 5103
ENGINE SPEED - $N_L \backsim$ % RPM = 98.9

RIGHT INLET
AVERAGE TOTAL PRESSURE RECOVERY - N_R = 0.9970
AVERAGE TOTAL PRESSURE DISTORTION - K = 0.0107
AVERAGE STATIC PRESSURE DISTORTION - L = 0.0229
MASS FLOW RATIO - M/M^* = 0.677
ENGINE POWER - $HP_{S.I}$ = 5225
ENGINE SPEED - $N_L \backsim$ % RPM = 99.7

• TOTAL
⊡ STATIC

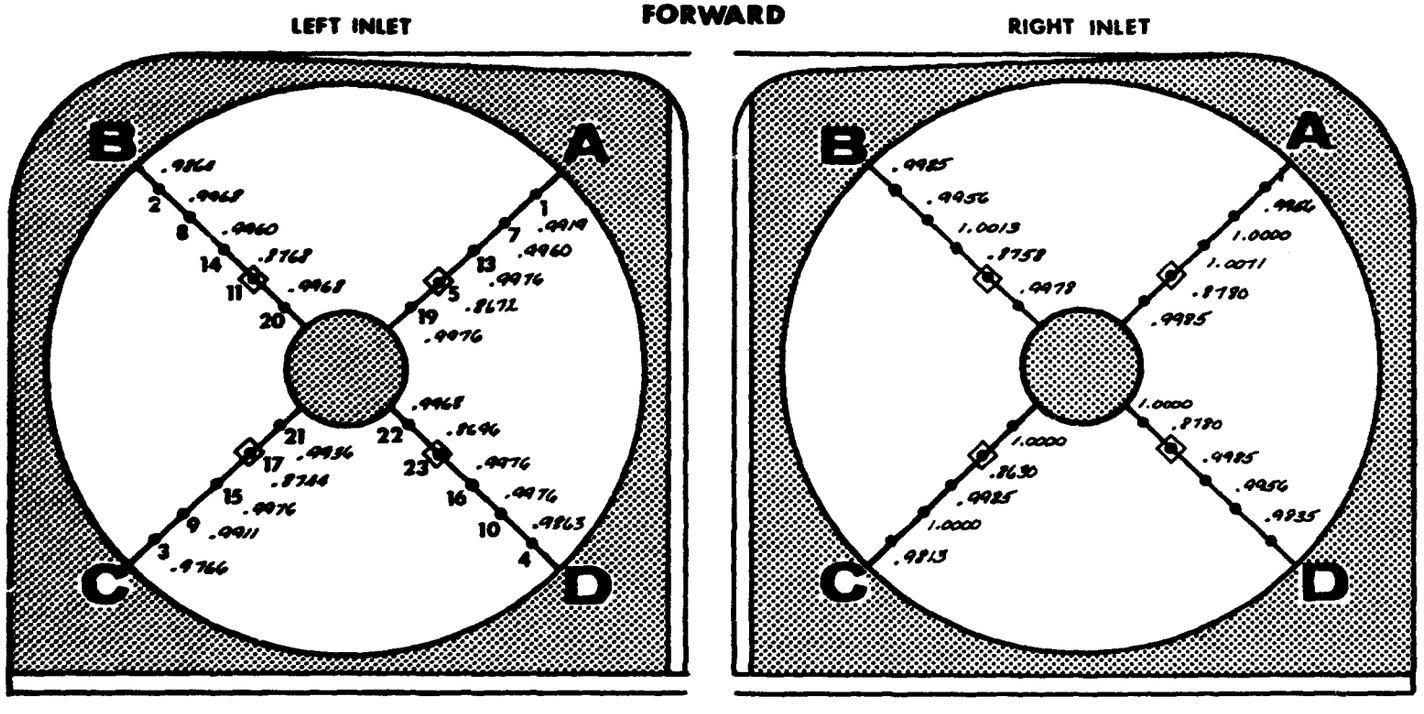

FIGURE No. 215

ENGINE INLET PERFORMANCE

XV-5A USA S/N 62-4505

FAN MODE LEVEL FLIGHT

ANGLE OF ATTACK - α_T = DEG = -.5
TRUE AIRSPEED - V_T ∽ KTAS = 41

PRESSURE ALT - H_p ∽ FT = 2365
LANDING GEAR DOWN

LEFT INLET
AVERAGE TOTAL PRESSURE RECOVERY - N_R = 0.9935
AVERAGE TOTAL PRESSURE DISTORTION - K = 0.0250
AVERAGE STATIC PRESSURE DISTORTION - L = 0.0070
MASS FLOW RATIO - M/M* = 0.681
ENGINE POWER - $HP_{S.L}$ = 4940
ENGINE SPEED - N_C ∽ % RPM = 98.6

RIGHT INLET
AVERAGE TOTAL PRESSURE RECOVERY - N_R = 0.9954
AVERAGE TOTAL PRESSURE DISTORTION - K = 0.0304
AVERAGE STATIC PRESSURE DISTORTION - L = 0.0228
MASS FLOW RATIO - M/M* = 0.676
ENGINE POWER - $HP_{S.L}$ = 5100
ENGINE SPEED - N_C ∽ % RPM = 99.4

• TOTAL
⊡ STATIC

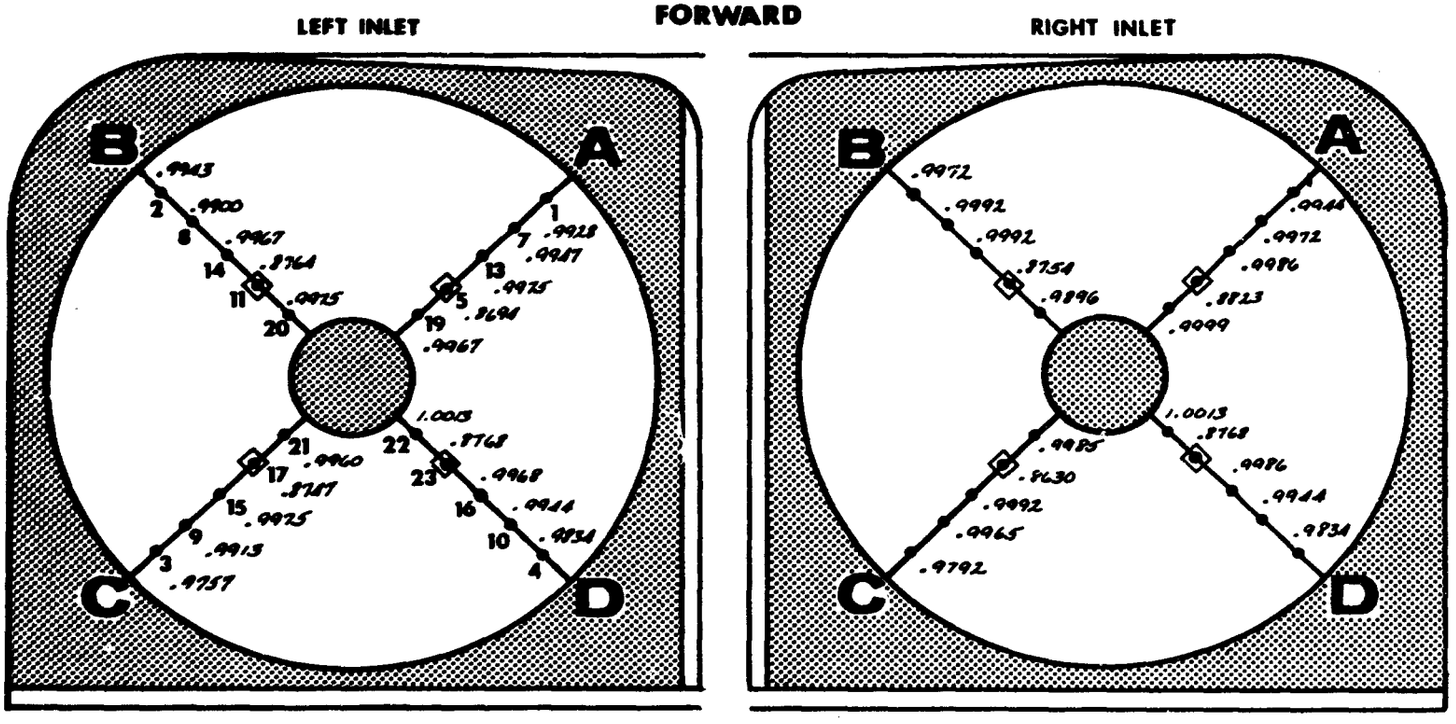

FIGURE No. 216

ENGINE INLET PERFORMANCE

XV-5A USA S/N 62-4505

FAN MODE LEVEL FLIGHT

ANGLE OF ATTACK - d_f ∽ DEG = -4.5
TRUE AIRSPEED - V_t ∽ KTAS = 42

PRESSURE ALT - H_p ∽ FT = 3062
LANDING GEAR DOWN

LEFT INLET
- AVERAGE TOTAL PRESSURE RECOVERY - N_R = 0.9936
- AVERAGE TOTAL PRESSURE DISTORTION - K = 0.0249
- AVERAGE STATIC PRESSURE DISTORTION - L = 0.0976
- MASS FLOW RATIO - M/M^2 = 0.690
- ENGINE POWER - $HP_{S.L}$ = 5032
- ENGINE SPEED - N_C ∽ % RPM = 98.6

RIGHT INLET
- AVERAGE TOTAL PRESSURE RECOVERY - N_R = 0.9958
- AVERAGE TOTAL PRESSURE DISTORTION - K = 0.0242
- AVERAGE STATIC PRESSURE DISTORTION - L = 0.0220
- MASS FLOW RATIO - M/M^2 = 0.674
- ENGINE POWER - $HP_{S.L}$ = 5131
- ENGINE SPEED - N_C ∽ % RPM = 99.3

• TOTAL
⊡ STATIC

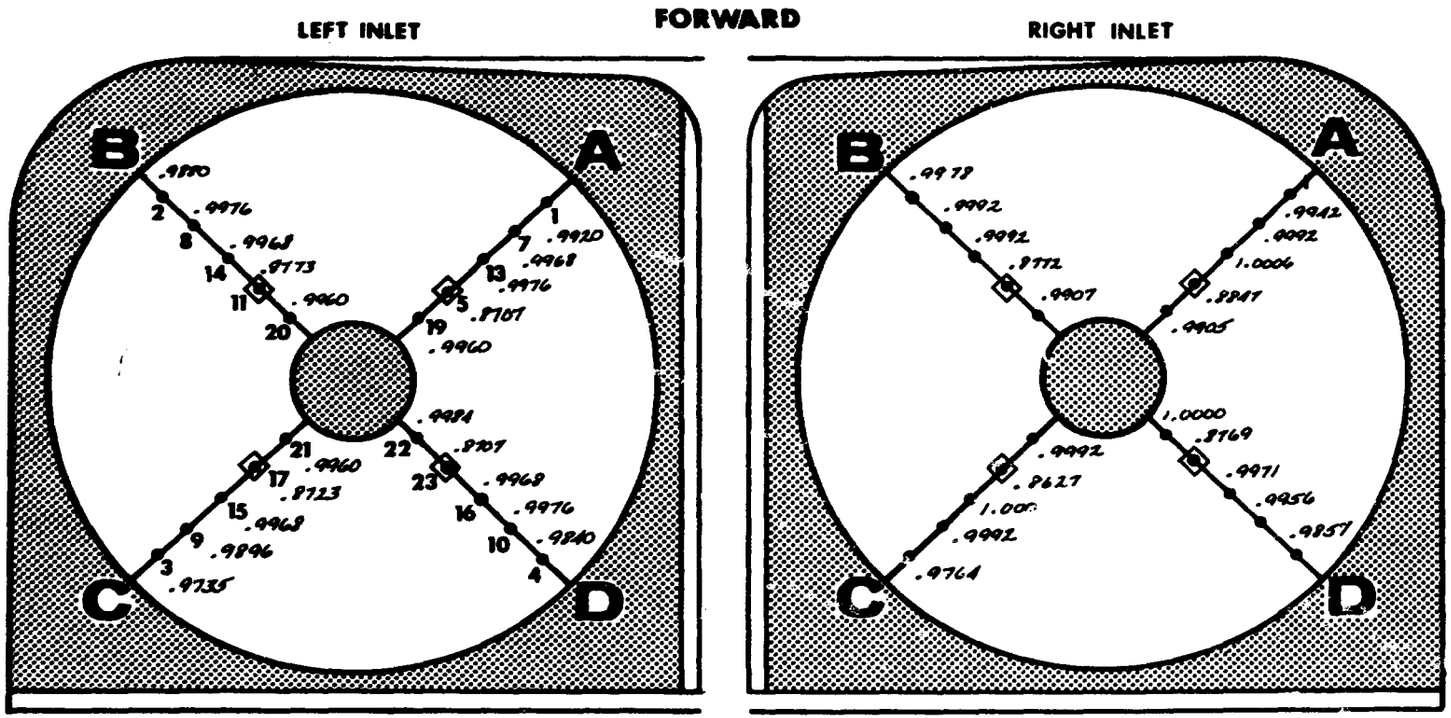

FIGURE No. 217

ENGINE INLET PERFORMANCE

XV-5A USA S/N 62-4505

FAN MODE LEVEL FLIGHT

ANGLE OF SIDESLIP - β ∽ DEG = 0
TRUE AIRSPEED - V_t ∽ KTAS = 60

PRESSURE ALT - H_p ∽ FT = 5026
LANDING GEAR DOWN

LEFT INLET
AVERAGE TOTAL PRESSURE RECOVERY - N_R = 0.9923
AVERAGE TOTAL PRESSURE DISTORTION - K = 0.0194
AVERAGE STATIC PRESSURE DISTORTION - L = 0.0094
MASS FLOW RATIO - M/M^* = 0.670
ENGINE POWER - $HP_{S.I}$ = 5143
ENGINE SPEED - N_c ∽ % RPM = 100.7

RIGHT INLET
AVERAGE TOTAL PRESSURE RECOVERY - N_R = 0.9996
AVERAGE TOTAL PRESSURE DISTORTION - K = 0.0273
AVERAGE STATIC PRESSURE DISTORTION - L = 0.0303
MASS FLOW RATIO - M/M^* = 0.680
ENGINE POWER - $HP_{S.I}$ = 5320
ENGINE SPEED - N_c ∽ % RPM = 101.4

• TOTAL
⊡ STATIC

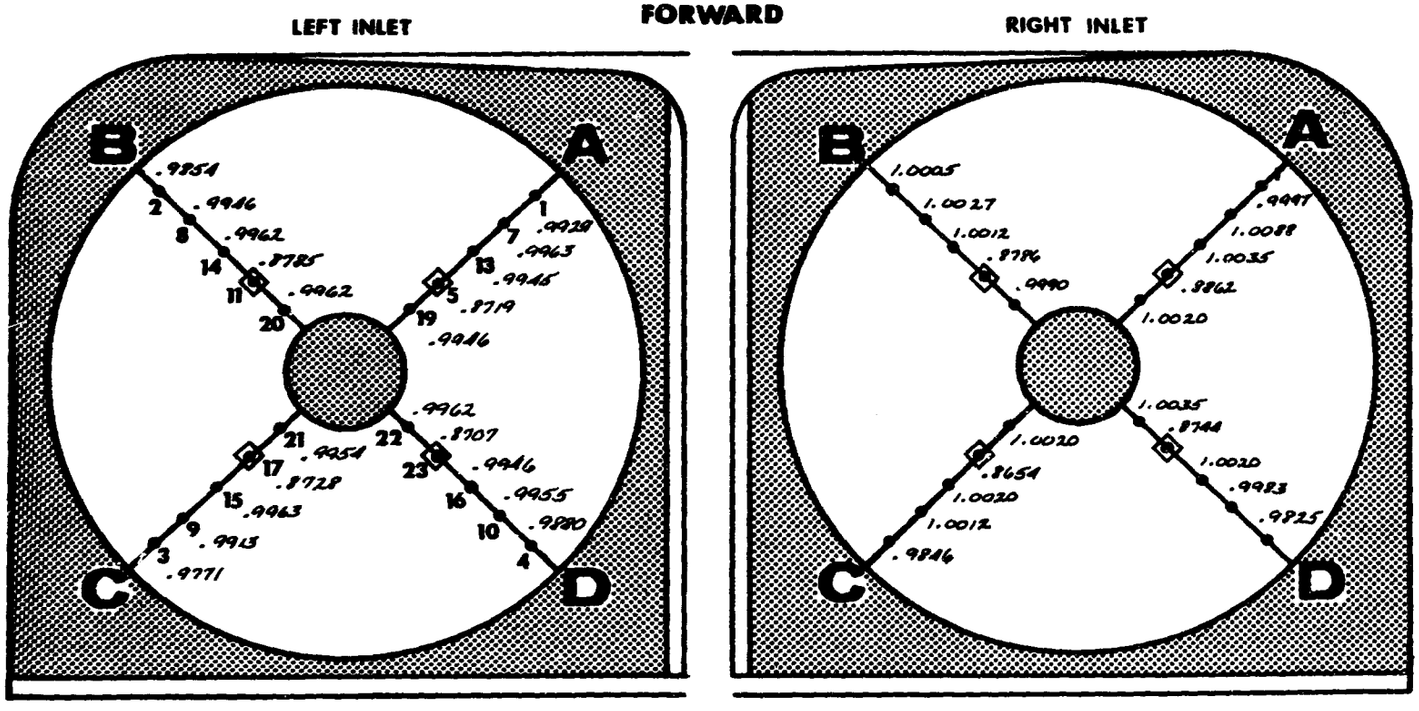

FIGURE No. 218

ENGINE INLET PERFORMANCE

XV-5A USA S/N 62-4505

FAN MODE LEVEL FLIGHT

ANGLE OF SIDESLIP - β ~ DEG = 10 L
TRUE AIRSPEED - V_t ~ KTAS = 59

PRESSURE ALT - H_p ~ FT = 5100
LANDING GEAR DOWN

LEFT INLET
- AVERAGE TOTAL PRESSURE RECOVERY - N_R = 0.9922
- AVERAGE TOTAL PRESSURE DISTORTION - K = 0.0256
- AVERAGE STATIC PRESSURE DISTORTION - L = 0.0060
- MASS FLOW RATIO - M/M^* = 0.677
- ENGINE POWER - $HP_{S:1}$ = 5188
- ENGINE SPEED - N_G ~ % RPM = 100.8

RIGHT INLET
- AVERAGE TOTAL PRESSURE RECOVERY - N_R = 0.9991
- AVERAGE TOTAL PRESSURE DISTORTION - K = 0.0339
- AVERAGE STATIC PRESSURE DISTORTION - L = 0.0385
- MASS FLOW RATIO - M/M^* = 0.676
- ENGINE POWER - $HP_{S:1}$ = 5341
- ENGINE SPEED - N_G ~ % RPM = 101.5

• TOTAL
⊡ STATIC

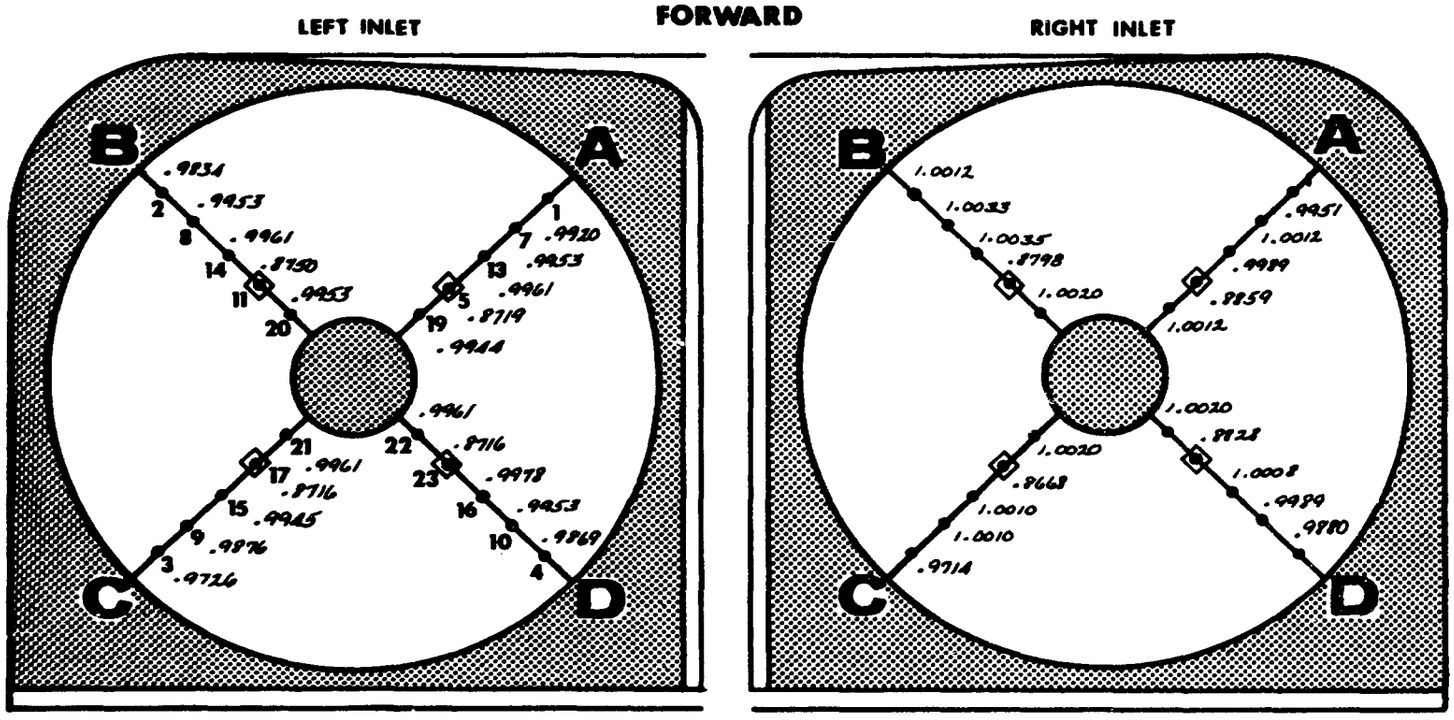

FIGURE No. 219

ENGINE INLET PERFORMANCE

XV-5A USA #'s 62-4505

FAN MODE LEVEL FLIGHT

ANGLE OF SIDESLIP - β ~ DEG = 10 R
TRUE AIRSPEED - V_t ~ KTAS = 55

PRESSURE ALT - H_p ~ FT = 5100
LANDING GEAR DOWN

LEFT INLET

AVERAGE TOTAL PRESSURE RECOVERY - N_R = 0.9952
AVERAGE TOTAL PRESSURE DISTORTION - K = 0.0203
AVERAGE STATIC PRESSURE DISTORTION - L = 0.0085
MASS FLOW RATIO - M/M* = 0.676
ENGINE POWER - $HP_{S.I}$ = 5164
ENGINE SPEED - N_G ~ % RPM = 100.2

RIGHT INLET

AVERAGE TOTAL PRESSURE RECOVERY - N_R = 0.9992
AVERAGE TOTAL PRESSURE DISTORTION - K = 0.0366
AVERAGE STATIC PRESSURE DISTORTION - L = 0.0198
MASS FLOW RATIO - M/M* = 0.680
ENGINE POWER - $HP_{S.I}$ = 5322
ENGINE SPEED - N_G ~ % RPM = 101.3

• TOTAL
⊡ STATIC

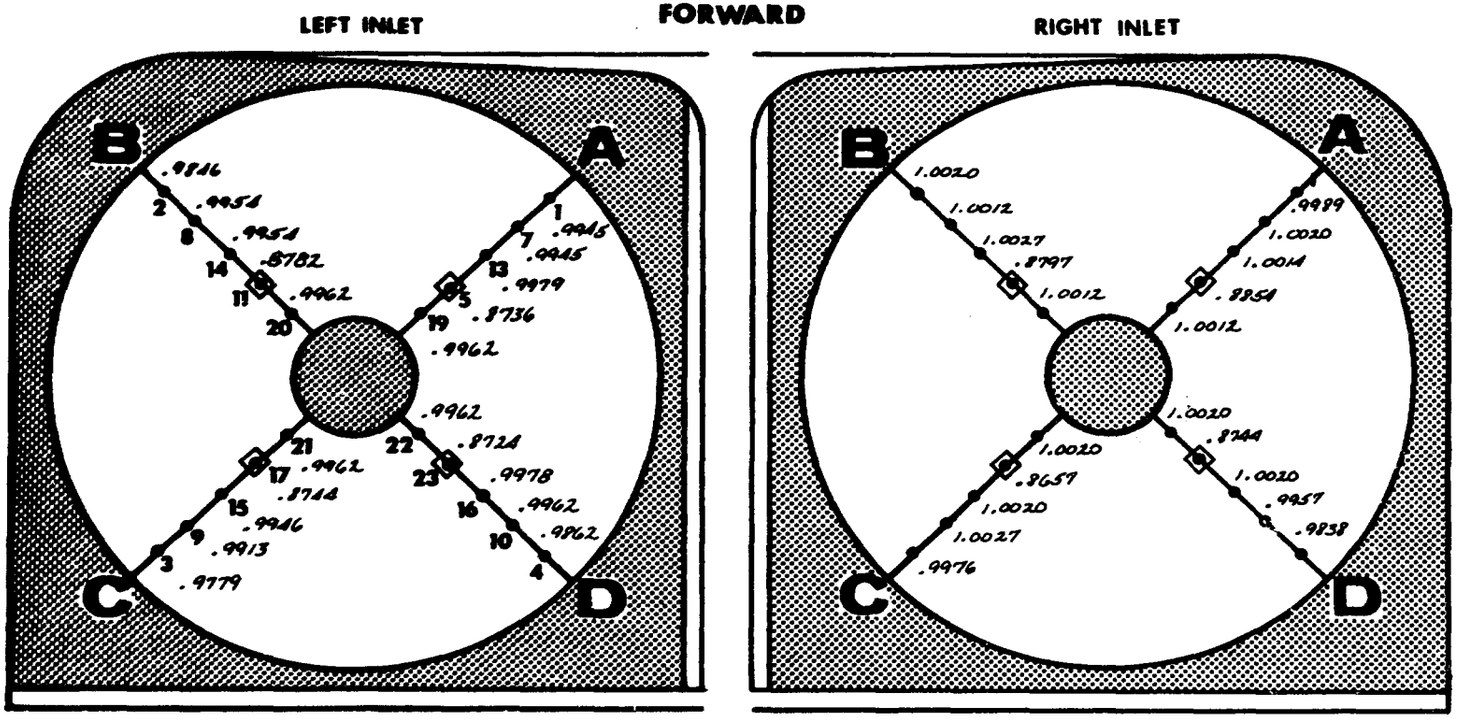

FIGURE No. 220

ENGINE INLET PERFORMANCE

XV-5A USA S/N 62-4505

FAN MODE LEVEL FLIGHT

ANGLE OF ATTACK - α_T ∽ DEG = -2.5
TRUE AIRSPEED - V_T ∽ KTAS = 84

PRESSURE ALT - H_p ∽ FT = 4137
LANDING GEAR DOWN

LEFT INLET
AVERAGE TOTAL PRESSURE RECOVERY - N_R = 0.9944
AVERAGE TOTAL PRESSURE DISTORTION - K = 0.0369
AVERAGE STATIC PRESSURE DISTORTION - L = 0.0098
MASS FLOW RATIO - M/M^* = 0.679
ENGINE POWER - $HP_{S.L}$ = 4856
ENGINE SPEED - N_C ∽ % RPM = 99.1

RIGHT INLET
AVERAGE TOTAL PRESSURE RECOVERY - N_R = 0.9966
AVERAGE TOTAL PRESSURE DISTORTION - K = 0.0346
AVERAGE STATIC PRESSURE DISTORTION - L = 0.0203
MASS FLOW RATIO - M/M^* = 0.680
ENGINE POWER - $HP_{S.L}$ = 4946
ENGINE SPEED - N_C ∽ % RPM = 100.0

• TOTAL
⊡ STATIC

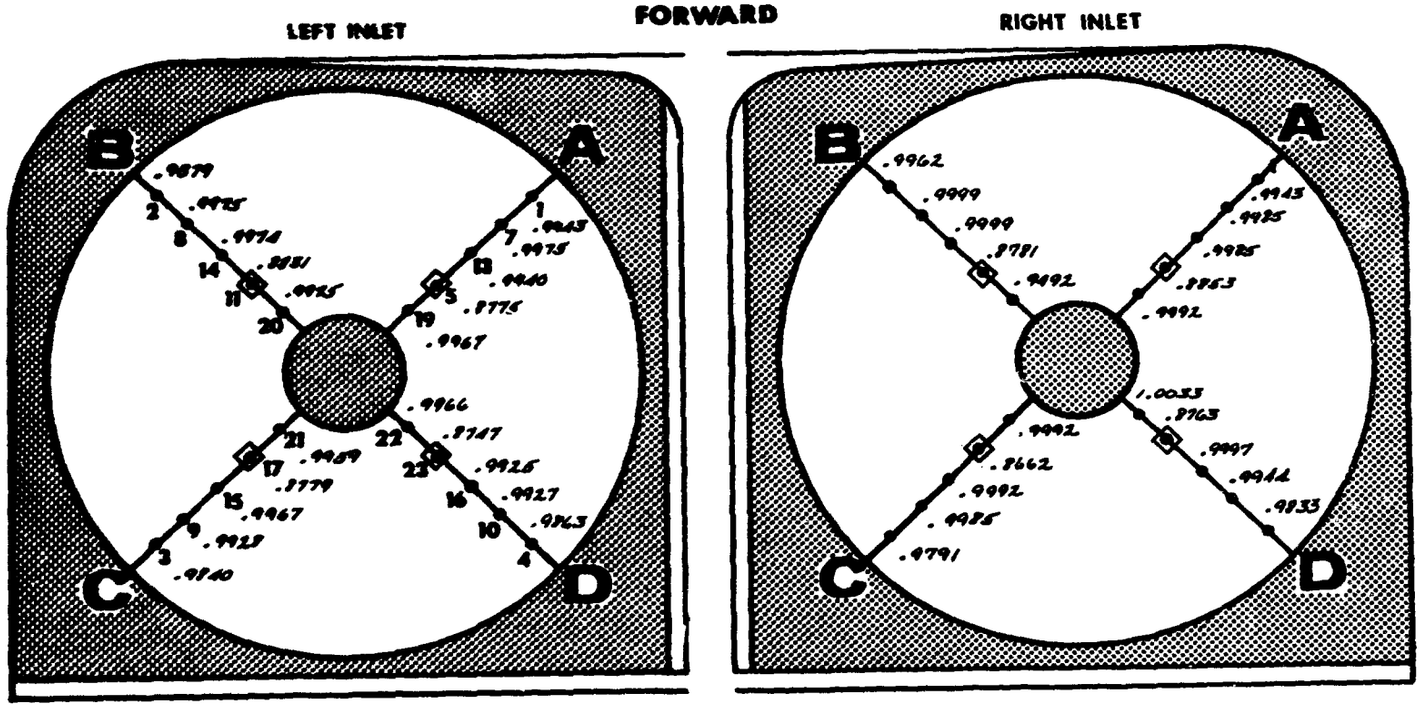

FIGURE No. 221

ENGINE INLET PERFORMANCE

XV-5A USA S/N 62-4505

JET MODE PRE-CONVERSION LEVEL FLIGHT

WING FAN DOORS OPEN

TRUE AIRSPEED - V_T ~ KTAS = 144 PRESSURE ALTITUDE - H_p ~ FT = 10730

LEFT INLET

AVERAGE TOTAL PRESSURE RECOVERY - N_R = 0.9943
AVERAGE TOTAL PRESSURE DISTORTION - K = 0.0179
AVERAGE STATIC PRESSURE DISTORTION - L = 0.0109
MASS FLOW RATIO - M/M^* = 0.684
ENGINE POWER - $HP_{S.L}$ = 5481
ENGINE SPEED - N_G ~ % RPM = 102.0

RIGHT INLET

AVERAGE TOTAL PRESSURE RECOVERY - N_R = 0.9928
AVERAGE TOTAL PRESSURE DISTORTION - K = 0.0467
AVERAGE STATIC PRESSURE DISTORTION - L = 0.0225
MASS FLOW RATIO - M/M^* = 0.683
ENGINE POWER - $HP_{S.L}$ = 5546
ENGINE SPEED - N_G ~ % RPM = 1036

• TOTAL
⊡ STATIC

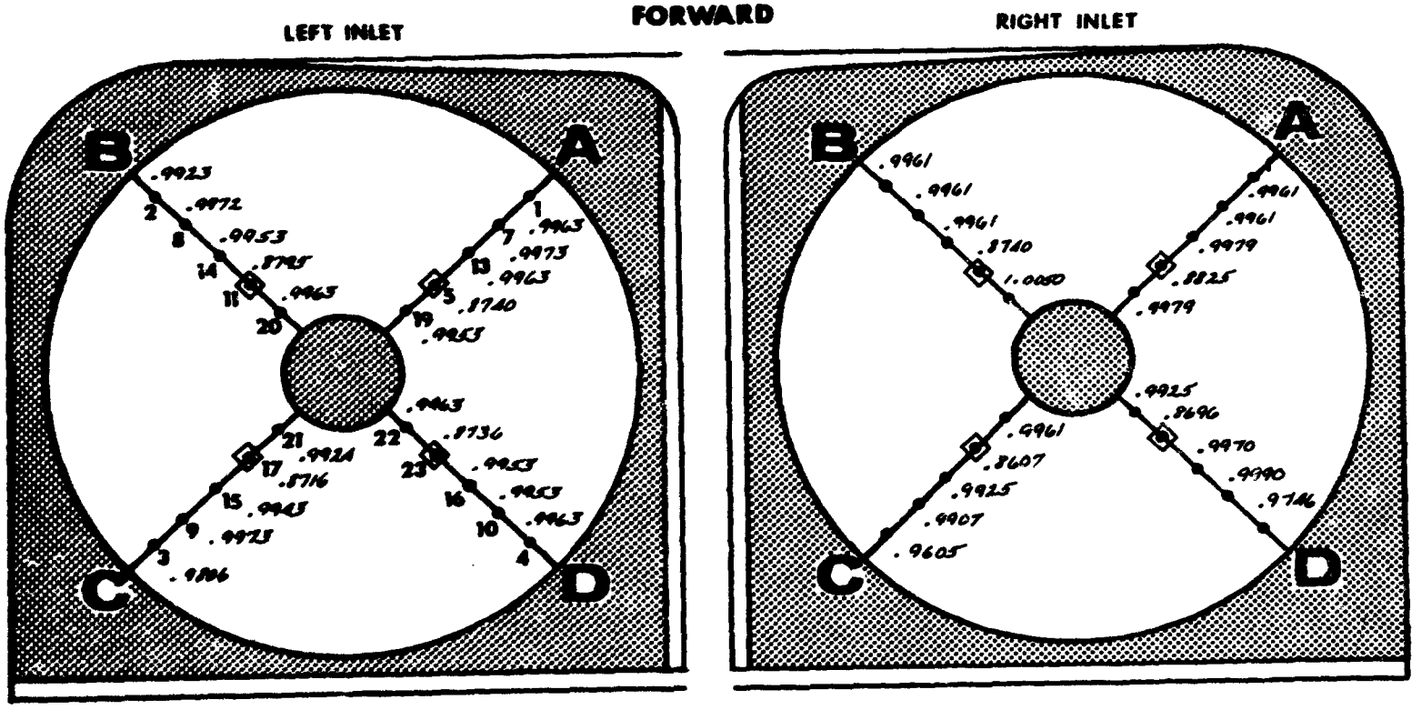

305

FIGURE No. 222

ENGINE INLET PERFORMANCE

XV-5A USA S/N 62-4505

JET MODE PRE-CONVERSION LEVEL FLIGHT

TRUE AIRSPEED - V_t ~ KTAS = 135 PRESSURE ALTITUDE - H_p ~ FT = 10312

LEFT INLET
- AVERAGE TOTAL PRESSURE RECOVERY - N_R = 0.9942
- AVERAGE TOTAL PRESSURE DISTORTION - K = 0.0178
- AVERAGE STATIC PRESSURE DISTORTION - L = 0.0079
- MASS FLOW RATIO - M/M^* = 0.678
- ENGINE POWER - $HP_{S.L}$ = 4844
- ENGINE SPEED - N_G ~ % RPM = 99.7

RIGHT INLET
- AVERAGE TOTAL PRESSURE RECOVERY - N_R = 0.9934
- AVERAGE TOTAL PRESSURE DISTORTION - K = 0.0250
- AVERAGE STATIC PRESSURE DISTORTION - L = 0.0232
- MASS FLOW RATIO - M/M^* = 0.676
- ENGINE POWER - $HP_{S.L}$ = 4736
- ENGINE SPEED - N_G ~ % RPM = 100.6

• TOTAL
⊡ STATIC

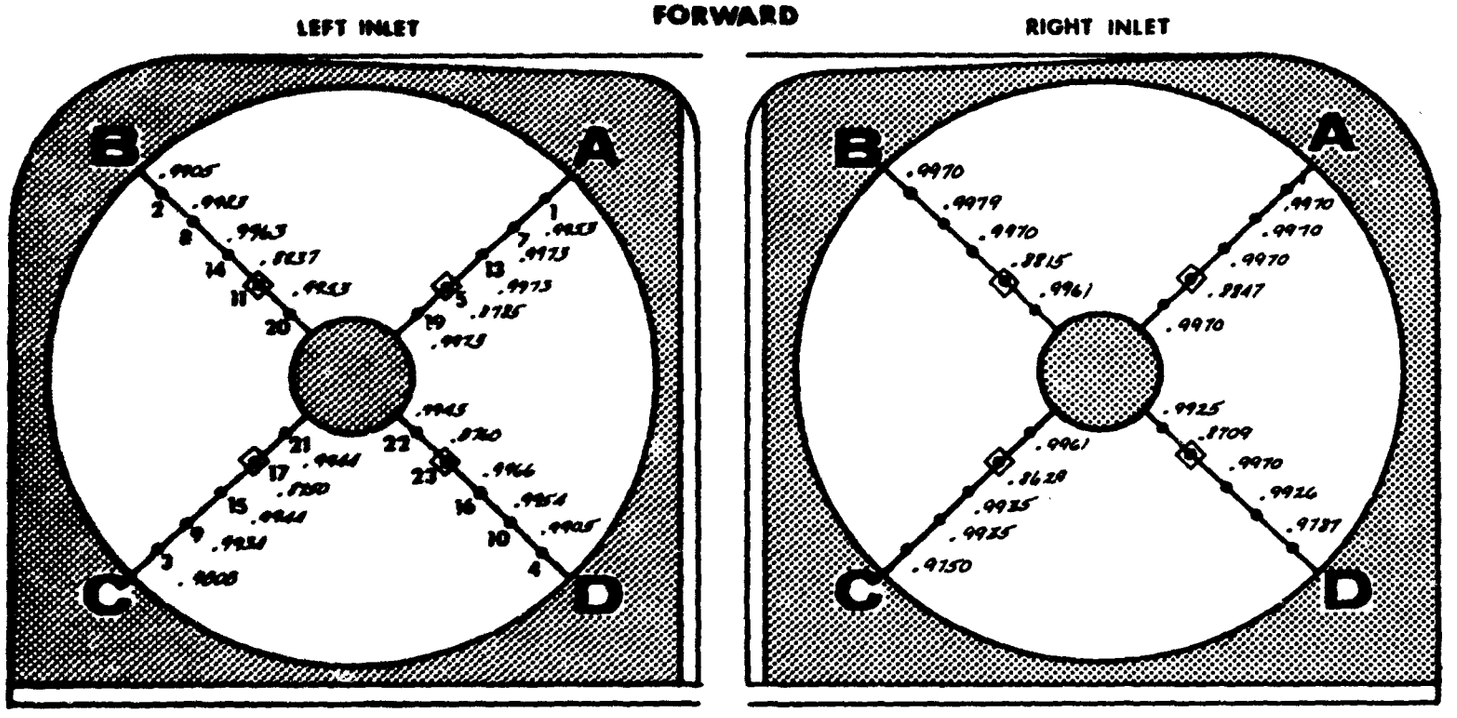

FIGURE No. 223

ENGINE INLET PERFORMANCE

XV-5A USA S/N 62-4505

JET MODE LEVEL FLIGHT

TRUE AIRSPEED - V_t ∽ KTAS = 220 PRESSURE ALTITUDE - H_p ∽ FT = 5000

LEFT INLET

AVERAGE TOTAL PRESSURE RECOVERY - N_R = 0.9972
AVERAGE TOTAL PRESSURE DISTORTION - K = 0.0172
AVERAGE STATIC PRESSURE DISTORTION - L = 0.0062
MASS FLOW RATIO - M/M^* = 0.634
ENGINE POWER - HP S.L = 1937
ENGINE SPEED - N_G ∽ % RPM = 90.2

RIGHT INLET

AVERAGE TOTAL PRESSURE RECOVERY - N_R = 1.0009
AVERAGE TOTAL PRESSURE DISTORTION - K = 0.0127
AVERAGE STATIC PRESSURE DISTORTION - L = 0.0148
MASS FLOW RATIO - M/M^* = 0.627
ENGINE POWER - HP S.L = 1937
ENGINE SPEED - N_G ∽ % RPM = 90.8

• TOTAL
⊡ STATIC

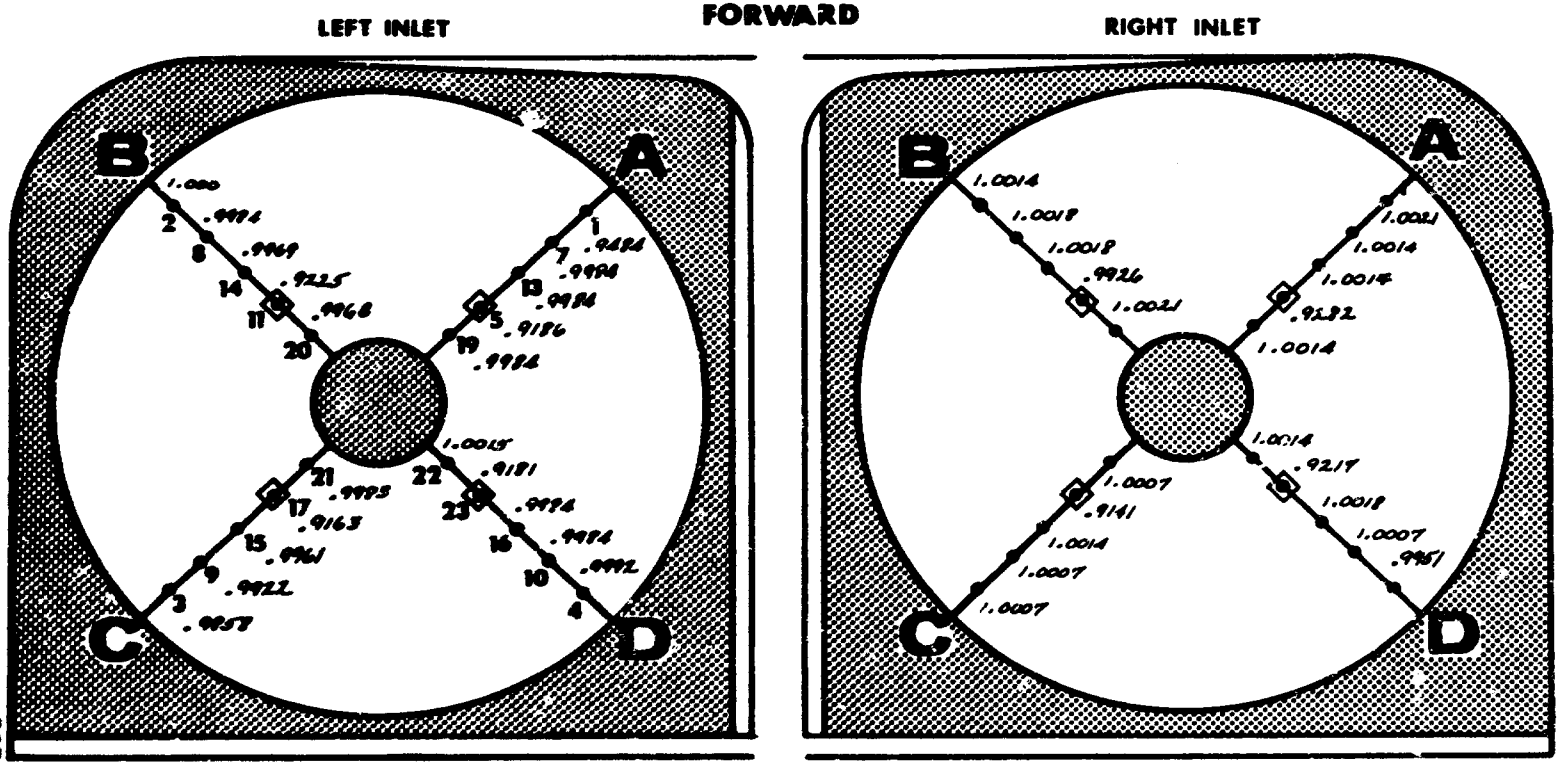

FIGURE No. 224

ENGINE INLET PERFORMANCE

XV-5A USA ¾ 62-4505

JET MODE

LEVEL FLIGHT STANDARD DAY CONDITIONS

DERIVED FROM CONTRACTOR ESTIMATED DATA

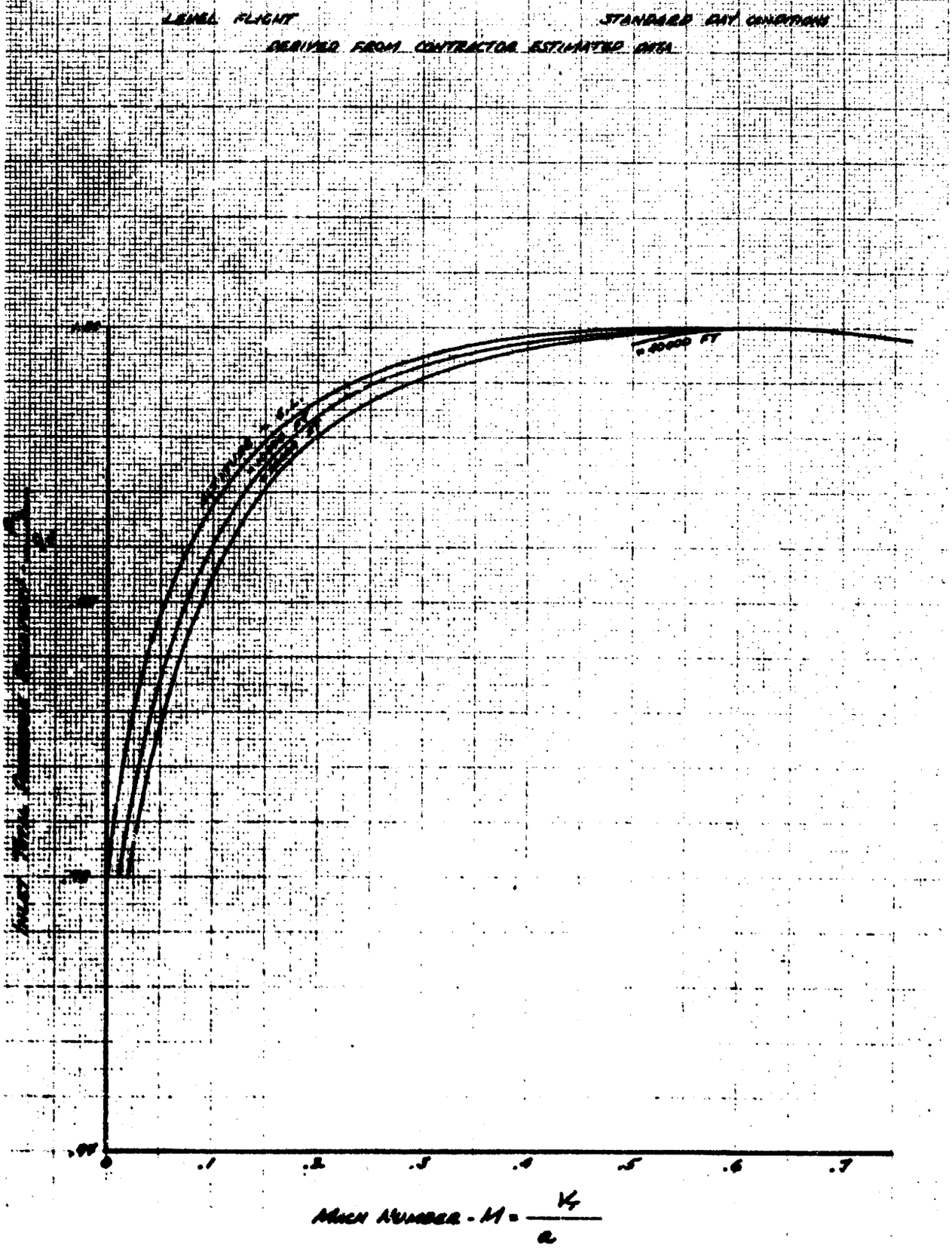

MACH NUMBER - $M = \frac{V_f}{a}$

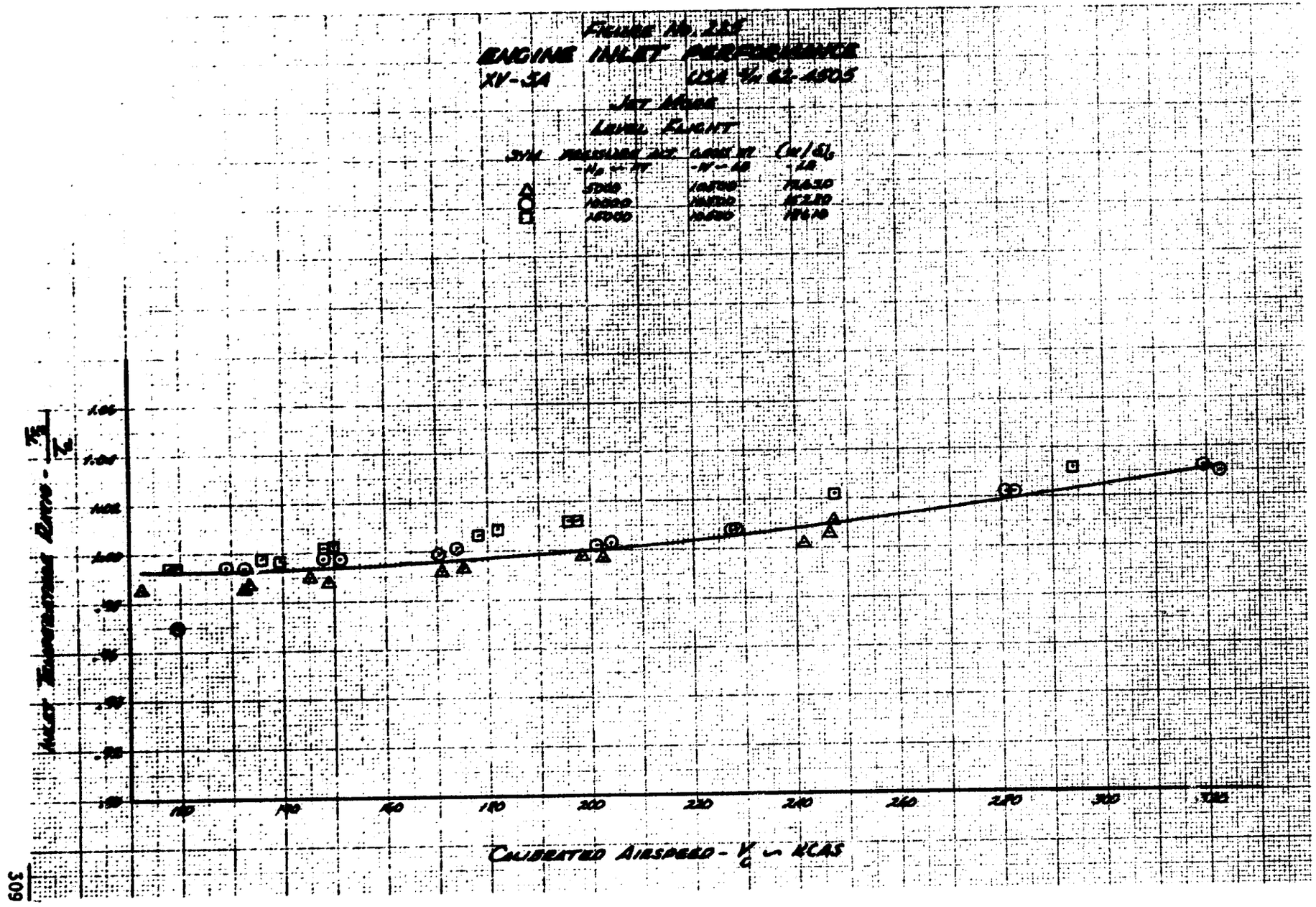
FIGURE NO. 252
ENGINE INLET PERFORMANCE
XV-3A
CCAE TR 62-A905
NOT ADJUSTED
LEVEL FLIGHT
SYM
Inlet Temperature Error - $\frac{T_{T_2}}{T_2}$
Calibrated Airspeed - V_c — KCAS
309

FIGURE NO. 226

ENGINE POWER AVAILABLE

XT-3A USA 41-62-4905

NOTES

1. BASED ON ZERO FORWARD SPEED.
2. ENGINE INLET ARRANGEMENT AND NOZZLE EFFLUX LOSSES ASSUMED ZERO.
3. CORRECTED THRUST ENGINE CHARACTERISTICS SHOWN FIGURES NO. 2.31, 2.32, 2.38 AND 2.39, APPENDIX I.
4. ENGINE LIMITS
   PHYSICAL SPEED = 102 % RPM
   CORRECTED SPEED = 108 % RPM
   EXHAUST GAS TEMPERATURE = 600 °C, MAX °F.

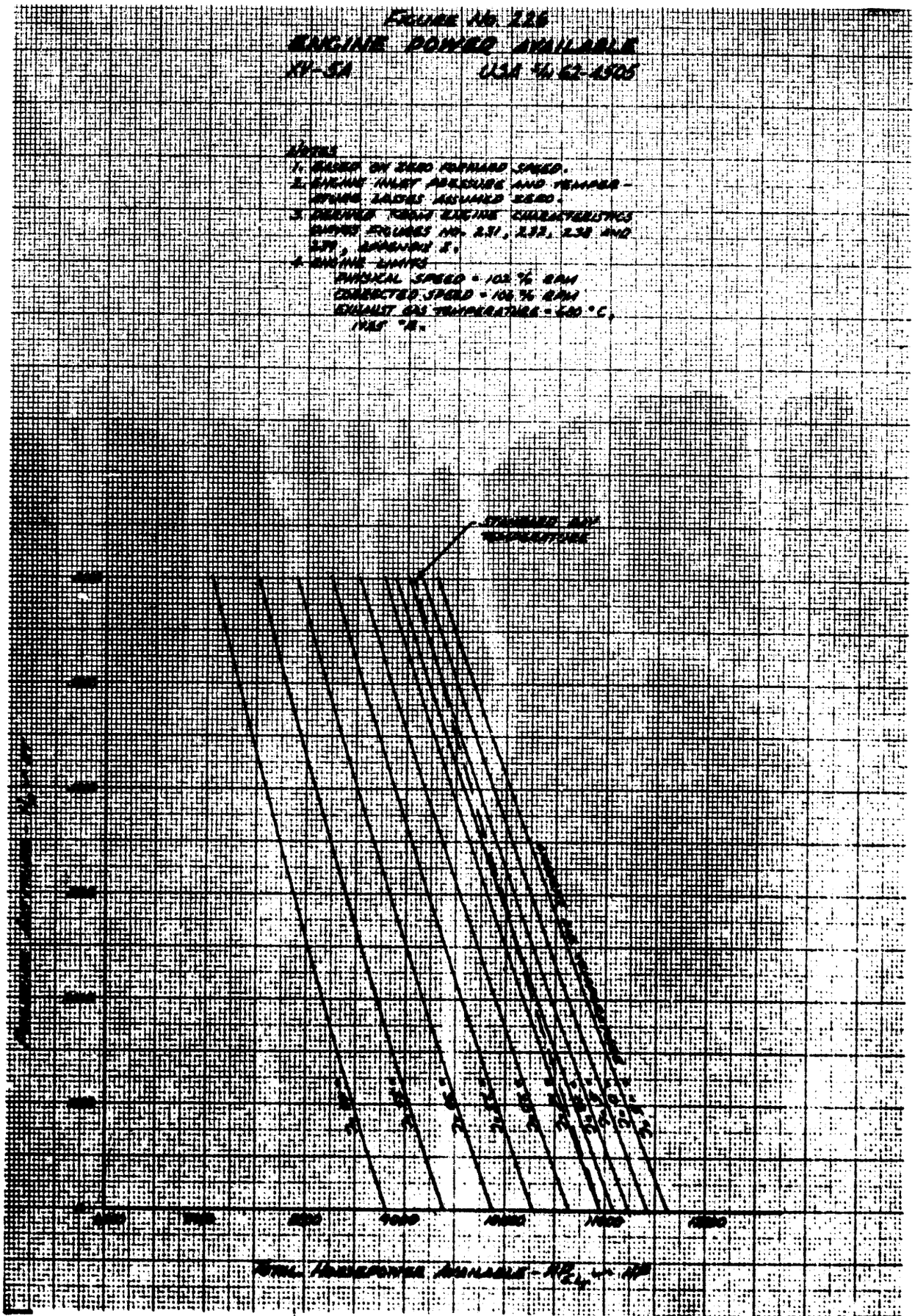

FIGURE No. 2.17

ENGINE CHARACTERISTICS

XF-5A USA No. 42-4505

Fan Model

OUT-OF-GROUND EFFECT

SYM	FLIGHT CONDITION	RPM ACT $-N_1-FT$
◇	GROUND TESTS	2500
◇	UNSTICKING	2500
◇	SIDEWARD	2500
◇	REARWARD	2500
◇	VERTICAL CLIMB	2400
◇	FORWARD CLIMB	3000
◇	LEVEL FLIGHT	4580
◇	FORWARD ACCENT	3000
◇	VERTICAL DESCENT	2400

NOTES

1. SOLID SYMBOLS DENOTE PRE-DOWNWEIGHT CONFIGURATION.
2. J-85-5B, EACT ENGINE S/N 340-275
3. J-1 METHOD, POWER ON 'ELOAD' BASED ON GRAPHICAL ENGINE DATA.

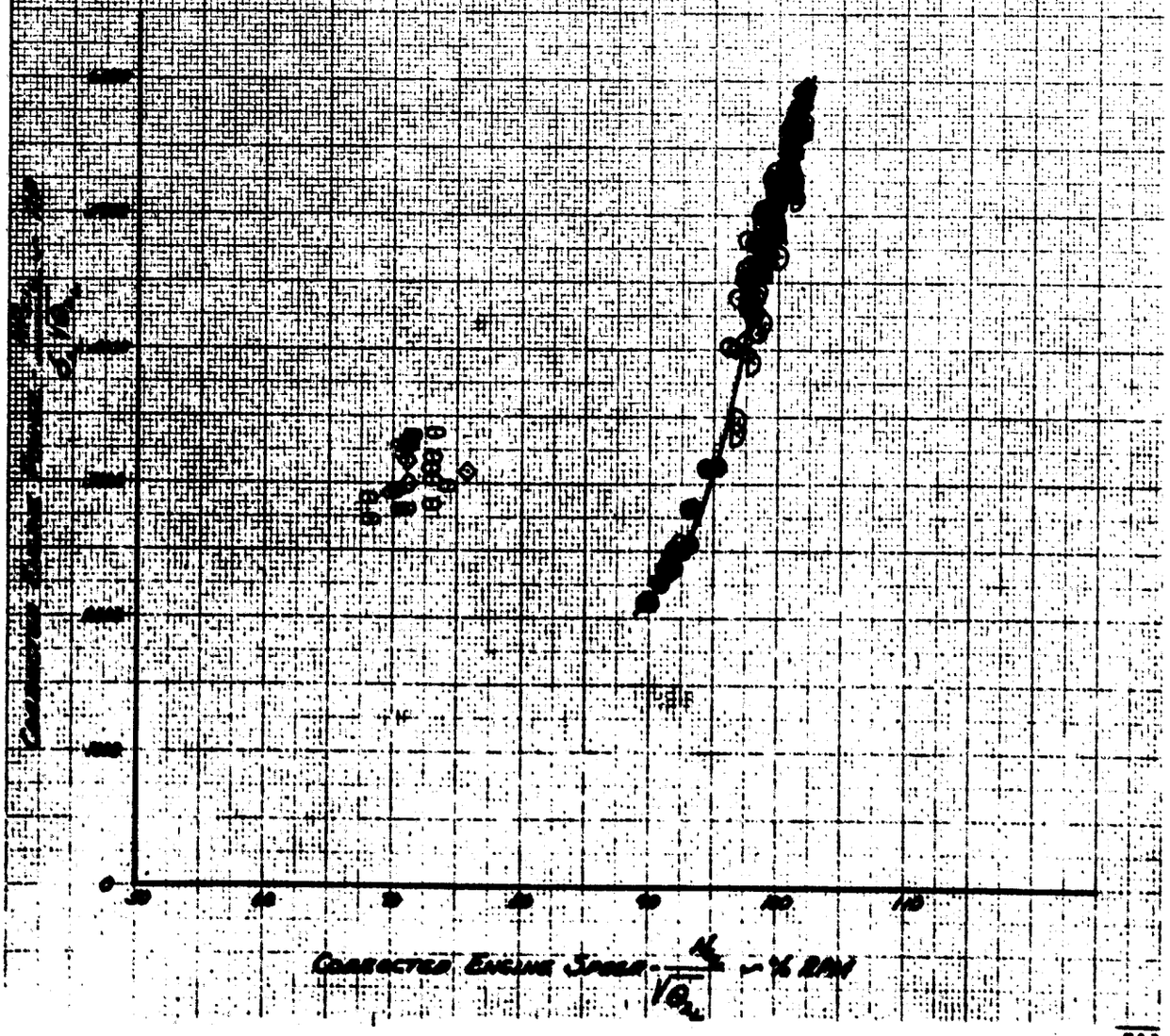

FIGURE NO. 2.18

ENGINE CHARACTERISTICS

XV-5A USA S/N 62-4506

CLEAN NACELLE

OUT-OF-GROUND EFFECT

SYM.	FLIGHT CONDITION	PRESS. ALT. $-h_p$ - FT.
	GROUND TAXI	2300
	TAKEOFF	2300
	STANDARD	2300
	ACCELERATE	2300
	VERTICAL CLIMB	2400
	FORWARD CLIMB	3000
	LEVEL FLIGHT	4500
	FORWARD DESCENT	3000
	VERTICAL DESCENT	2400

NOTES

1. VALUE SYMBOLS DENOTE AIR-CONDITIONER CONFIGURATION.
2. J-85-5D, FLIGHT ENGINE S/N 230-8716.
3. L-1 METHOD, POWER DEVELOPED BASED ON EMPIRICAL ENGINE DATA.

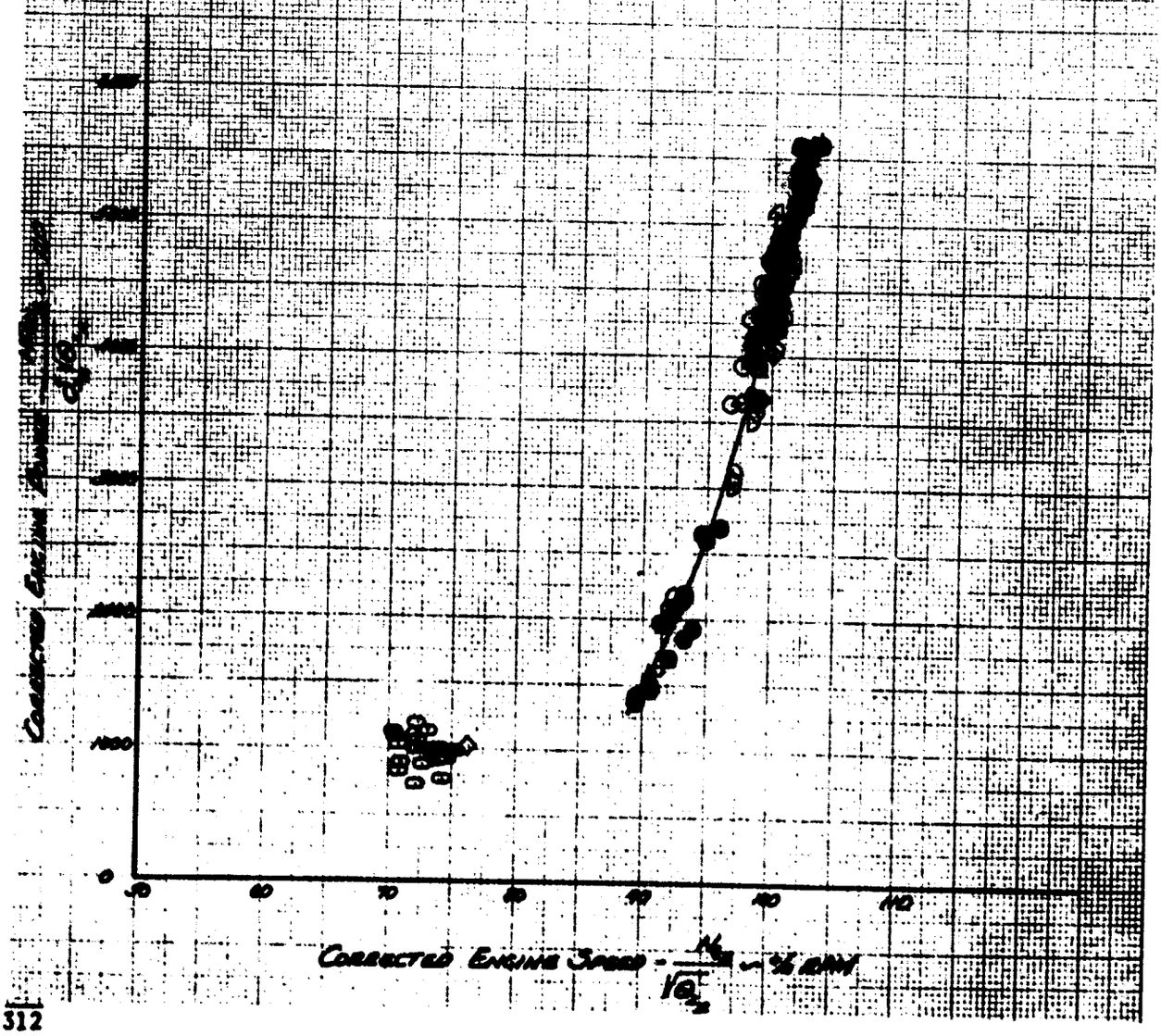

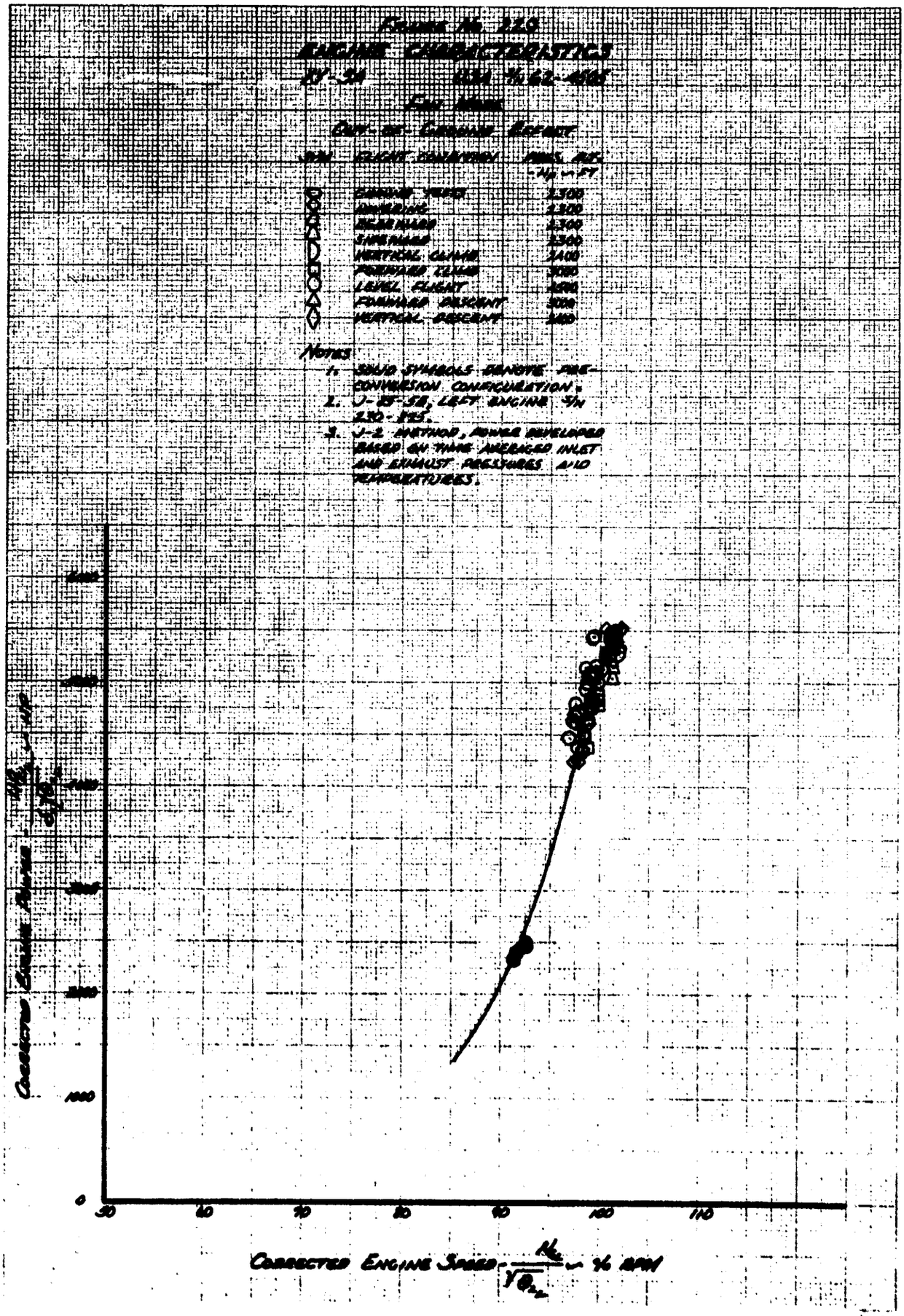
FIGURE No. 2.0
ENGINE CHARACTERISTICS
J2-S2 CSM % 62-4405
Sea Level
Curve and Symbol Legend
Symbol Flight Condition Nozzle Area -Ae in Ft²
Standard Takeoff 3.500
Maximum 3.500
Sea Level 3.500
Sea Level 3.500
Vertical Climb 3.100
Powered Climb 3.050
Level Flight 3.050
Powered Descent 3.050
Vertical Descent 3.100
Notes
1. Solid symbols denote pre-conversion configuration.
2. J-2-S2, Left Engine S/N 2.30-Pts.
3. J-2 Method, Power Envelopes based on time averaged inlet and exhaust pressures and temperatures.
Corrected Engine Thrust - Lbs
0
1000
30
40
50
60
70
80
90
100
110
Corrected Engine Speed - % RPM

FIGURE No. 2.10

ENGINE CHARACTERISTICS

XV-3A USA YM61-4605

FAN RPM

OUT-OF-GROUND EFFECT

SYM	FLIGHT CONDITION	PRESS. ALT. - H_p - FT
◇	GROUND TESTS	2360
◇	APPROACH	2360
◇	TAKEOFF	2360
◇	TAKEOFF	2360
◇	VERTICAL CLIMB	2400
◇	FORWARD CLIMB	3000
◇	LEVEL FLIGHT	4500
◇	FORWARD DESCENT	3000
◇	VERTICAL DESCENT	2400

NOTES:

1. SOLID SYMBOLS DENOTE PRE-CONVERSION CONFIGURATION.
2. J-85-5D, AFTER ENGINE S/N 830-976.
3. POWER DEVELOPED BETWEEN TRUE FREE-AIR INLET AND EXHAUST PRESSURES AND TEMPERATURES, J-2 METHOD.

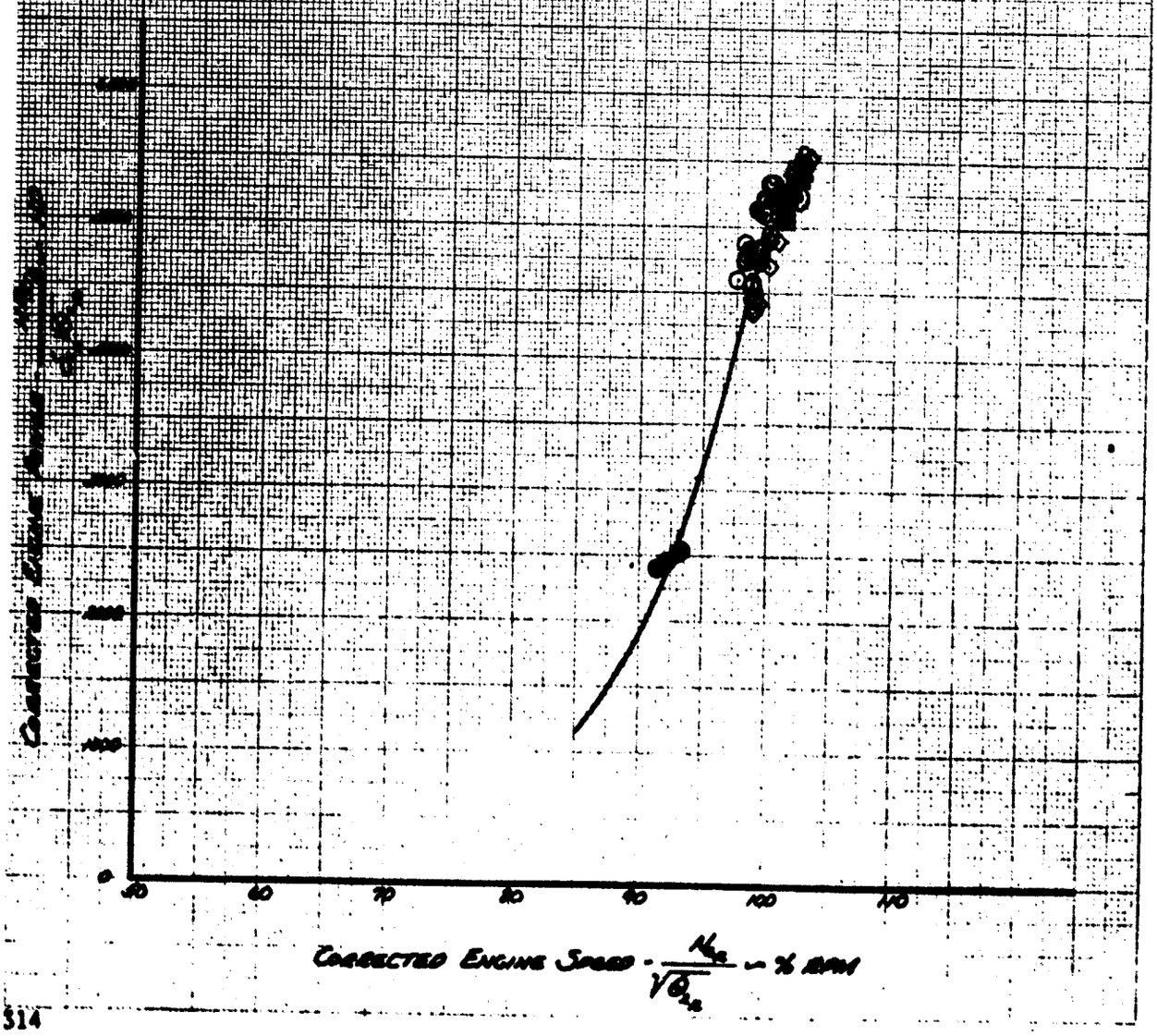

FIGURE No. 231

ENGINE CHARACTERISTICS

XH-5A USA No. 62-4505

EXIT NOZZLE

OUT-OF-CLEARANCE EFFECT

SYM	FLIGHT CONDITION	PRESS ALT. $-H_p$ - FT
◇	CLEARING TESTS	5,300
◇	HOVERING	2,300
◇	SIDEWARD	2,300
◇	REARWARD	2,300
◇	VERTICAL CLIMB	2,100
◇	FORWARD CLIMB	3000
◇	LEVEL FLIGHT	4,500
◇	FORWARD DESCENT	3000
◇	VERTICAL DESCENT	2,400

NOTES:

1. 30,140 STANDARD REMOTE PRE-CONVERSION CONFIGURATION.
2. J-85-5B, LEFT ENGINE S/N 2,30-[illegible]
3. J-3 METHOD, ANNULAR ENVELOPE BASED ON INSTANTANEOUS INLET AND EXHAUST PRESSURES AND TEMPERATURES.

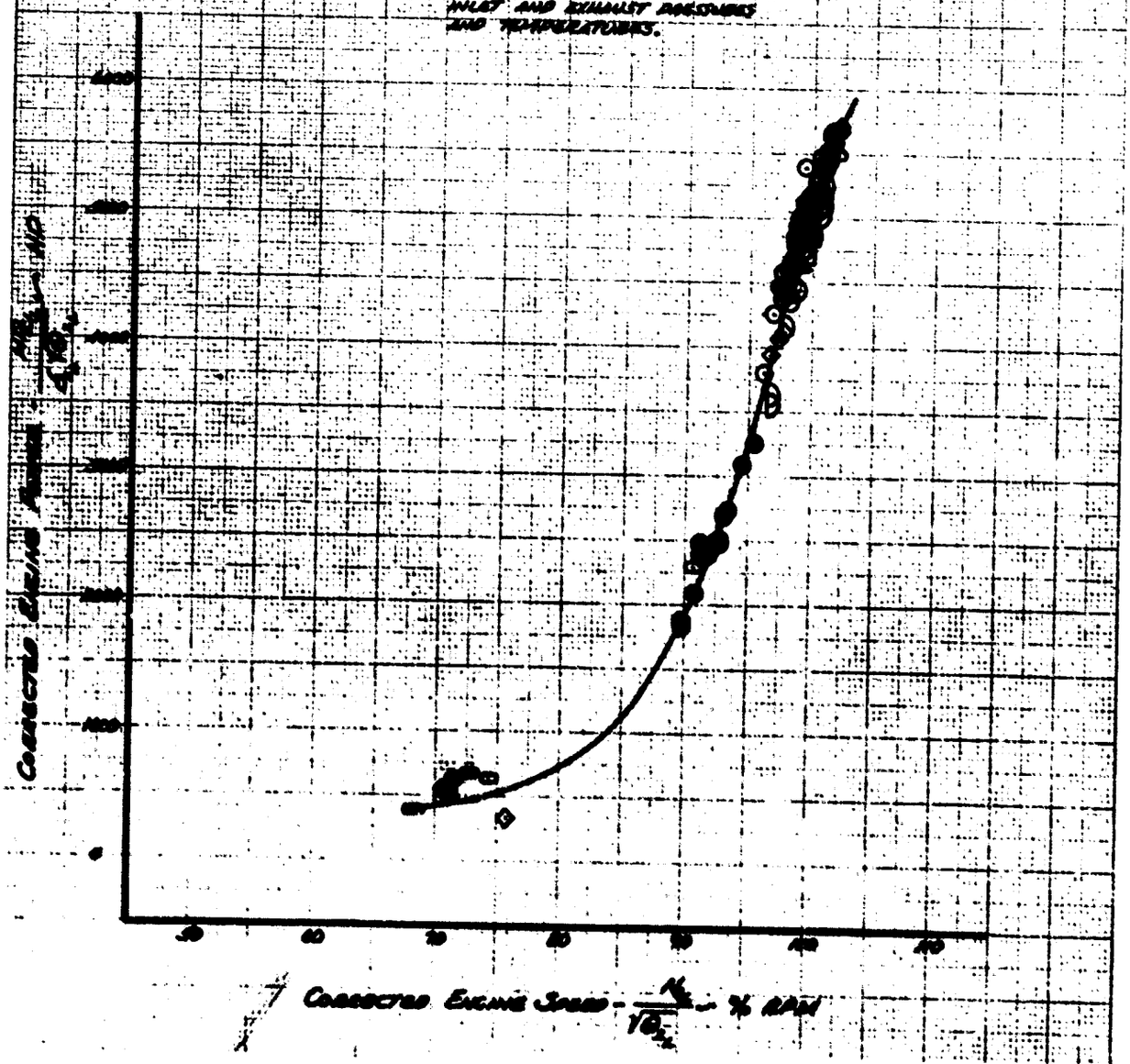

FIGURE 4.6.2.12

ENGINE CHARACTERISTICS

XV-5A USA 62-4505

FAN MODEL

OUT-OF-GROUND EFFECT

SYM	FLIGHT CONDITION	PRESS ALT $-H_p$ - FT
◇	GARRATT RETRO	2300
◇	HOVERING	2500
◇	SUBSONIC	2500
◇	SUBSONIC	2500
◇	VERTICAL CLIMB	2400
◇	FORWARD CLIMB	2400
◇	LEVEL FLIGHT	4700
◇	FORWARD ACCELRAT	2400
◇	VERTICAL ACCELRAT	2400

NOTES

1. SOLID SYMBOLS DENOTE PRE-CONVERSION CONFIGURATION.
2. J-85-5B, RIGHT ENGINE S/N 240-876.
3. J-1 METHOD, POWER SETTING BASED ON ISENTHANICOUS INLET AND EXHAUST PRESSURES AND TEMPERATURES.

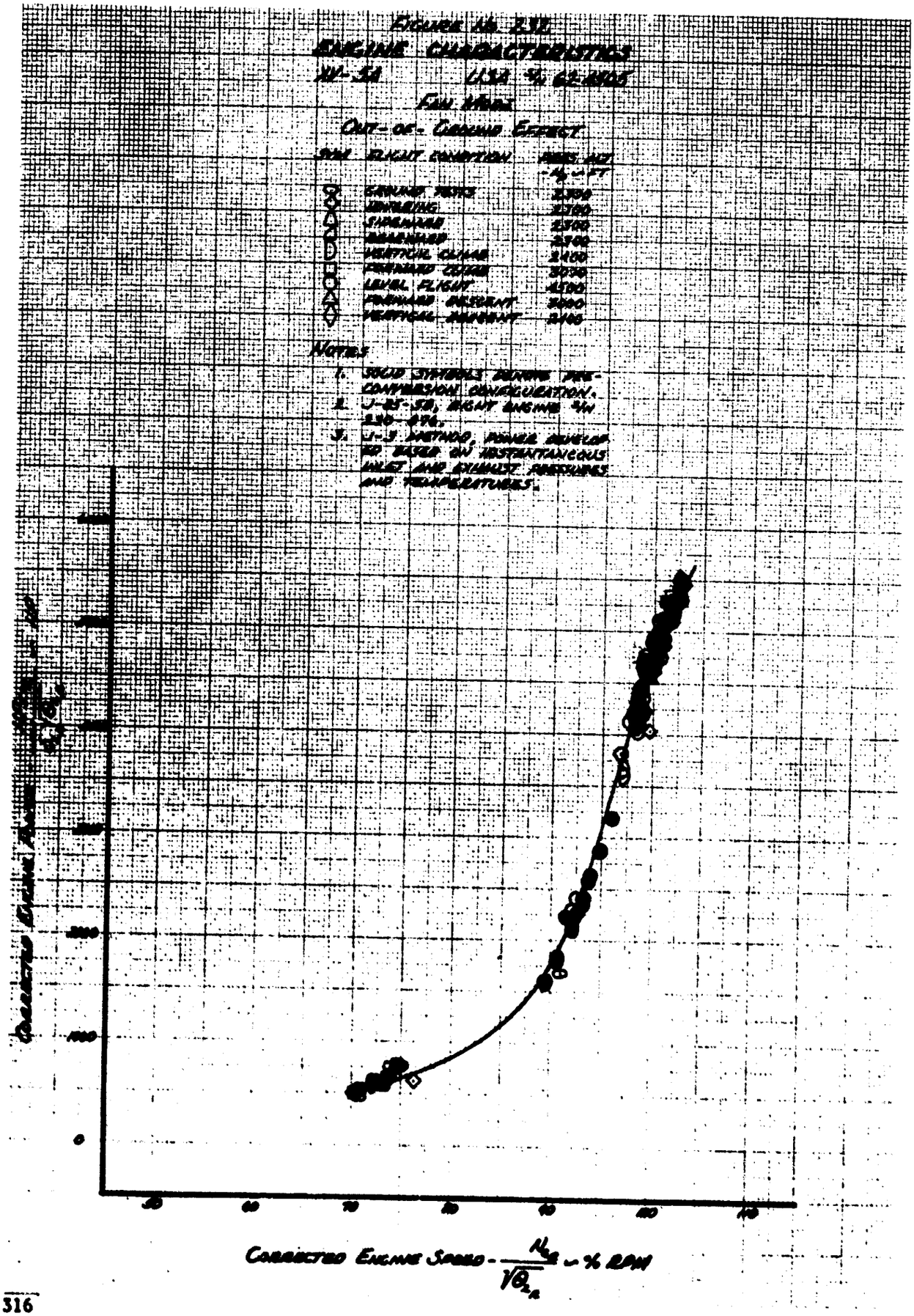

FIGURE NO. 233

ENGINE CHARACTERISTICS

NF-54 USA 7/16-62-4505

GAS MODEL

OFF-OF-CENTER EFFECT

SYM	SLIGHT CONDITION	INST. ACT. $\alpha_p = 17°$
○	ENGINE "RUN"	3360
□	IDLE RPM	3300
△	SURGE UP	3300
◇	ACCEL	3360
⊙	VERTICAL CLIMB	3400
⊡	FORWARD CLIMB	3400
⊞	LEVEL FLIGHT	3400
⊠	FORWARD DESCENT	3400
⊟	VERTICAL DESCENT	3400

NOTES:

1. ENGINE CHARACTERISTICS AND COMPRESSOR CONFIGURATION.
2. J-85-GE-5, LEFT ENGINE S/N 830-385.

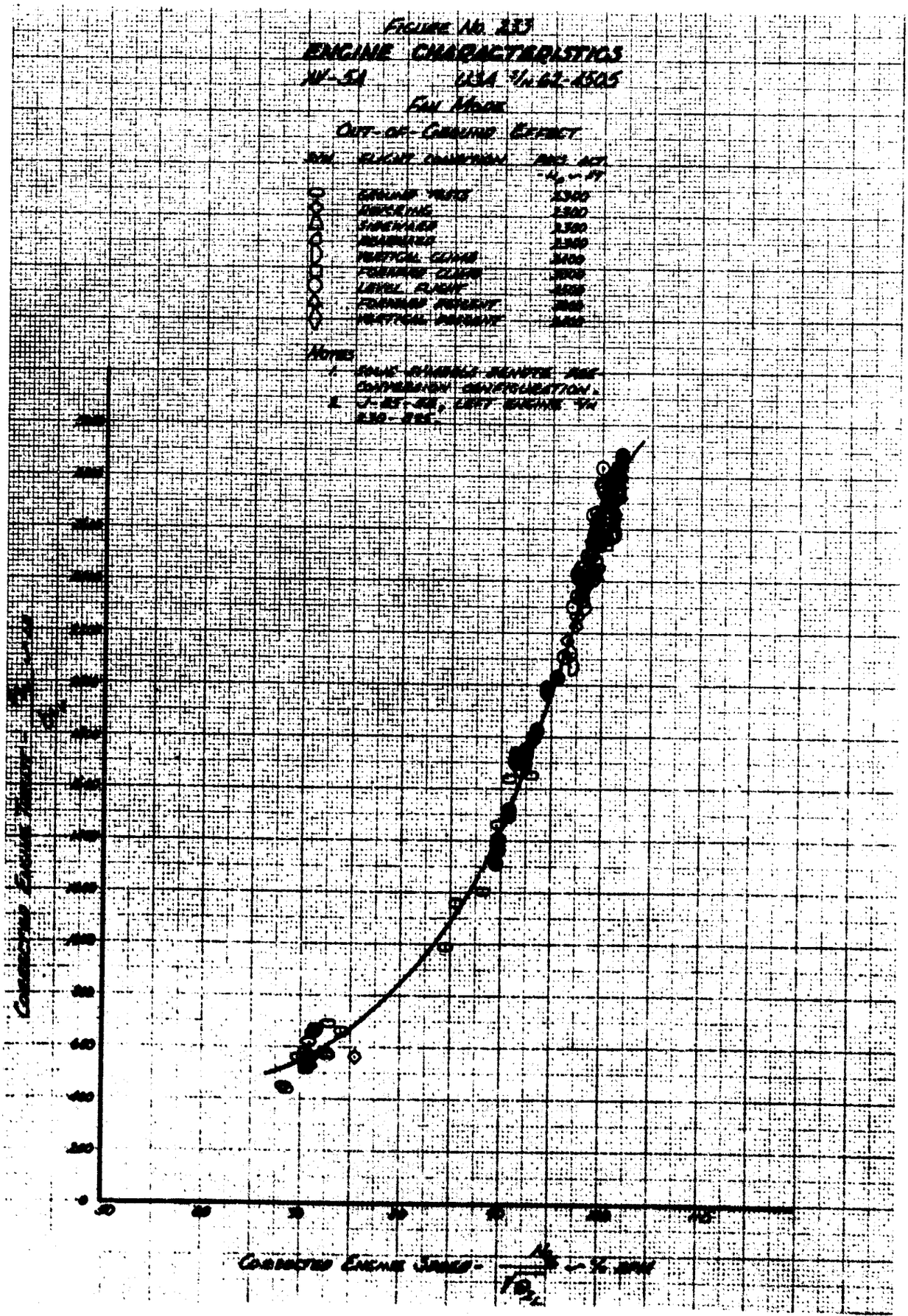

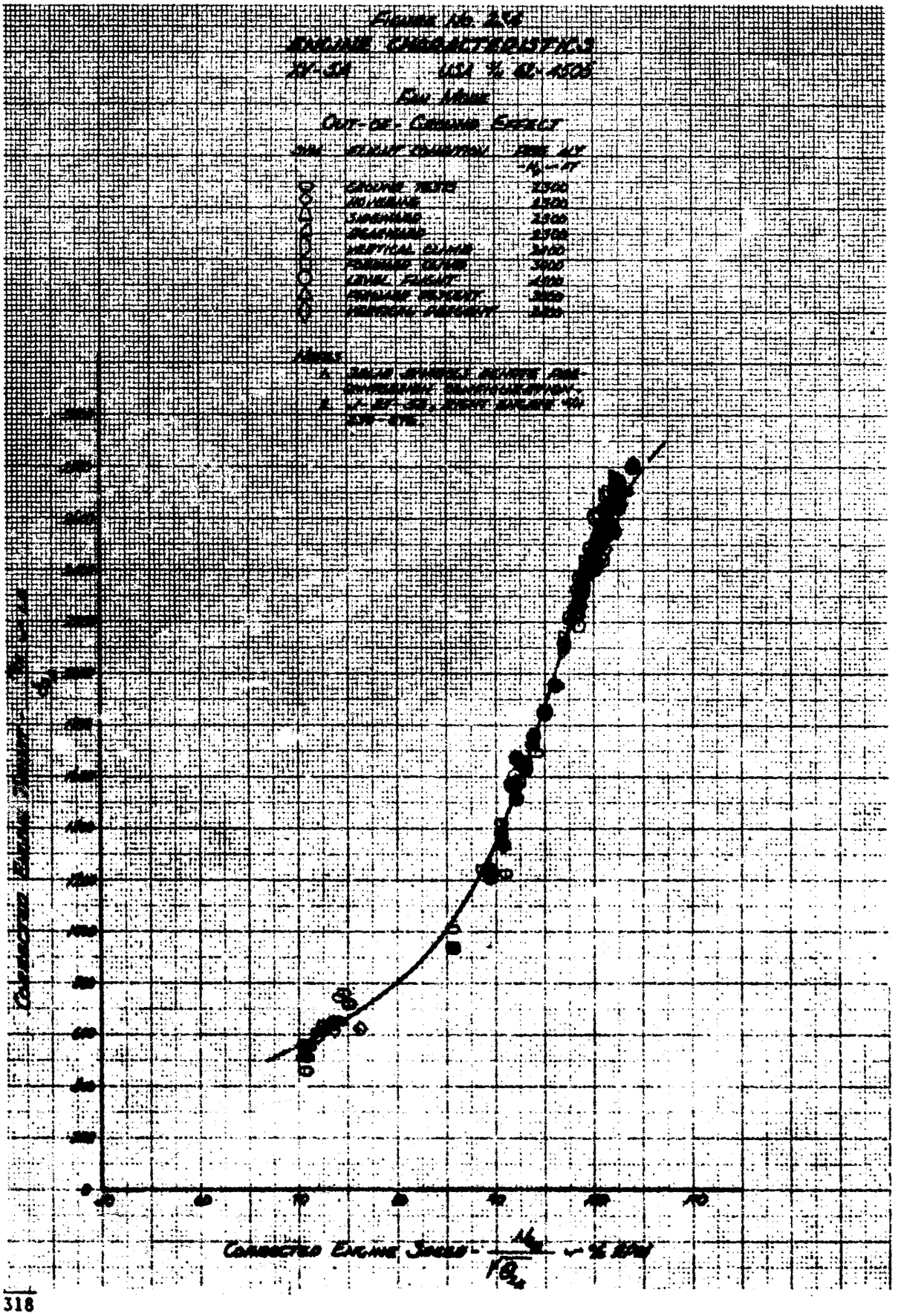
FIGURE NO. 2.4
ENGINE CHARACTERISTICS
XF-84 LOT 1 & 2 AC-4205
SEA LEVEL
OUT-OF-GROUND EFFECT
ENGINE TESTS
AIRFRAME
SUPERVISOR
SEA LEVEL
VERTICAL CLIMB
FORWARD FLIGHT
LEVEL FLIGHT
REMARKS
CORRECTED ENGINE SPEED - $\frac{N_c}{\sqrt{\theta_2}}$ - % RPM

FIGURE No. 335

ENGINE CHARACTERISTICS

XV-5A USA 1962-4505

FAN MODE

OUT-OF-GROUND EFFECT

SYM	FLIGHT CONDITION	PRES ALT. $+H_p$ - FT
○	GROUND TESTS	1300
◇	HOVERING	1300
◇	SIDEWARD	2300
◇	REARWARD	2300
◇	VERTICAL CLIMB	2400
◇	FORWARD CLIMB	3000
◇	LEVEL FLIGHT	4500
◇	FORWARD DESCENT	3000
◇	VERTICAL DESCENT	2400

NOTES

1. SOLID SYMBOLS DENOTE PRE-CONVERSION CONFIGURATION.
2. J-85-5B, LEFT ENGINE S/N 230-824.

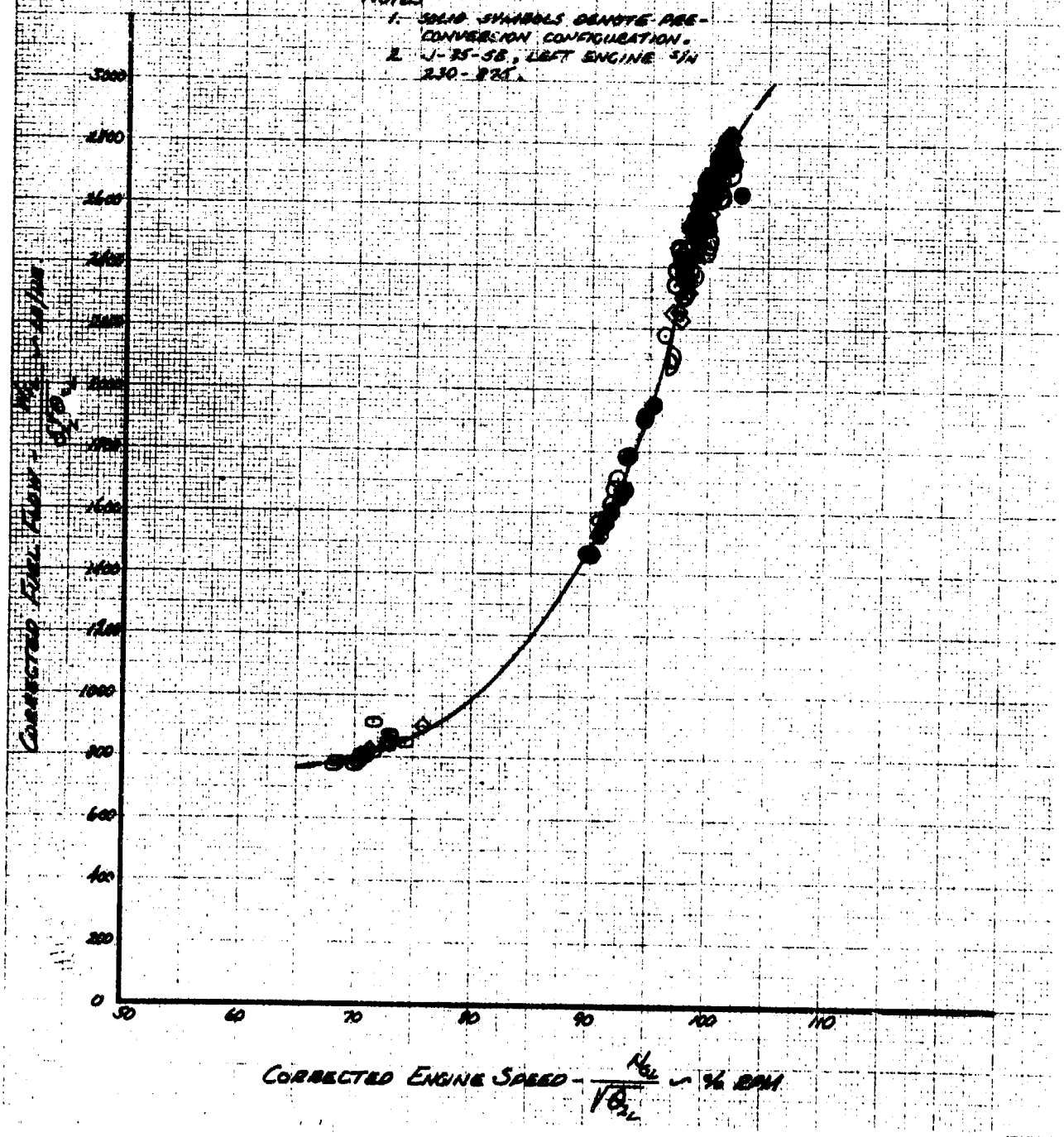

FIGURE No. 236

ENGINE CHARACTERISTICS

XV-3A USA № 62-4505

FAN MODE

OUT-OF-GROUND EFFECT

SYM	FLIGHT CONDITION	PRESS. ALT. $-H_p$ — FT
◇	GROUND TESTS	2500
◇	HOVERING	2500
◇	SIDEWARD	2500
◇	REARWARD	2500
◇	VERTICAL CLIMB	2400
◇	FORWARD CLIMB	3000
◇	LEVEL FLIGHT	4000
◇	FORWARD DESCENT	3000
◇	VERTICAL DESCENT	2400

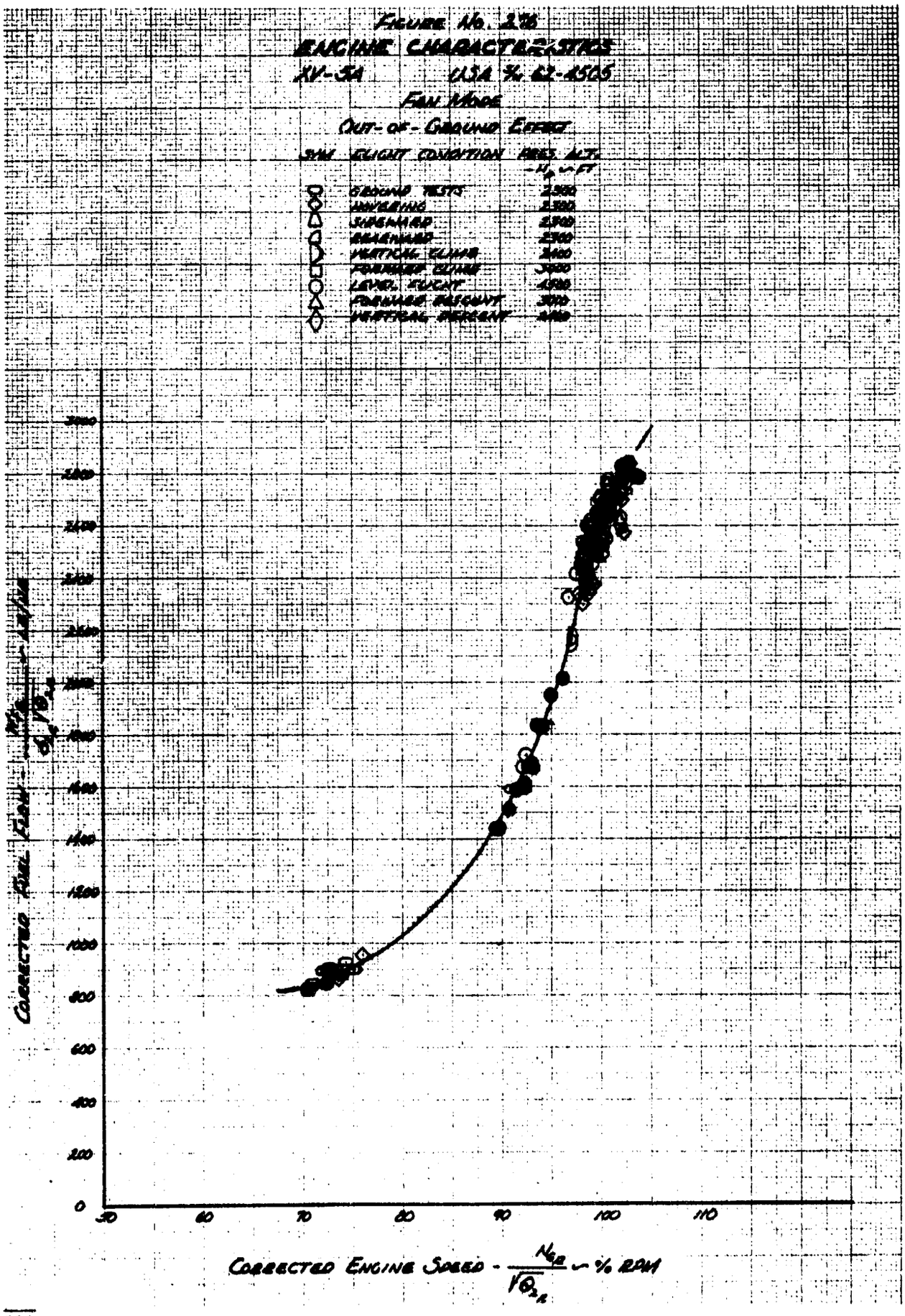

FIGURE No. 2.37

ENGINE CHARACTERISTICS

XV-5A CSA № 62-4505

JET MODE LEVEL FLIGHT

SYM	ALT. H_p FT	THRUST NET F_N LB	$\frac{W_f}{\delta_{t_2}\sqrt{\theta_{t_2}}}$ LB/HR
△	5000	10500	13630
○	10000	10500	13220
□	15000	10500	13010

CORRECTED TOTAL FUEL FLOW - $\frac{W_{f_T}}{\delta_{t_2}\sqrt{\theta_{t_2}}}$ LB/HR

CORRECTED ENGINE SPEED - $\left(\frac{N_1}{\sqrt{\theta_{t_2}}}\right)_{AVG}$ - % RPM

FIGURE No. 238

ENGINE CHARACTERISTICS

XV-5A USA No. 62-4505

FAN MODE

OUT-OF-GROUND EFFECT

SYM	FLIGHT CONDITION	PRESS. ALT. $-H_p$ — FT.
◇	GROUND TESTS	2300
◇	HOVERING	2300
◇	SIDEWARD	2300
◇	REARWARD	2300
◇	VERTICAL CLIMB	2400
◇	FORWARD CLIMB	3000
◇	LEVEL FLIGHT	4500
◇	FORWARD DESCENT	3000
◇	VERTICAL DESCENT	2400

NOTES:

1. SOLID SYMBOLS DENOTE PRE-COMBUSTION CONFIGURATION.
2. J-85-5A, LEFT ENGINE No. 2 - 5TH

CORRECTED ENGINE SPEED - $\left(\frac{N_2}{\sqrt{\theta_2}}\right)_L$ - % RPM

FIGURE NO. 239

ENGINE CHARACTERISTICS

XV-5A LIFT/FAN 62-4505

FAN MODE

OUT-OF-GROUND EFFECT

SYM	FLIGHT CONDITION	ABS. ALT. $-H_p$ - FT
◇	GROUND TESTS	2500
△	HOVERING	2500
◁	SIDEWARD	2500
▷	REARWARD	2500
○	VERTICAL CLIMB	2400
□	FORWARD CLIMB	3000
▽	LEVEL FLIGHT	3500
◇	FORWARD DESCENT	3000
◇	VERTICAL DESCENT	2400

NOTES:
1. SOLID SYMBOLS DENOTE PRE-CONVERSION CONFIGURATION.
2. J-85-5A, RIGHT ENGINE S/N 230-276.

CORRECTED EXHAUST GAS TEMPERATURE - EGT $\div \left(\frac{\theta}{\delta_2}\right)_2$ - °C

1250 1300 1350 1400 1450 1500 1550 1600 1650

CORRECTED ENGINE SPEED - $\left(\frac{N_1}{\sqrt{\theta_2}}\right)_2$ - % RPM

90 92 94 96 98 100 102 104

FIGURE No. 210

PROPULSION SYSTEM PERFORM

XV-5A

PRESSURE ALTITUDE - H_p ~ FT. = 2290
WIND VEL - V_W ~ KTS. = 2
WIND DIR - DEG. FROM NOSE = 10 L

CROSS
AMBI

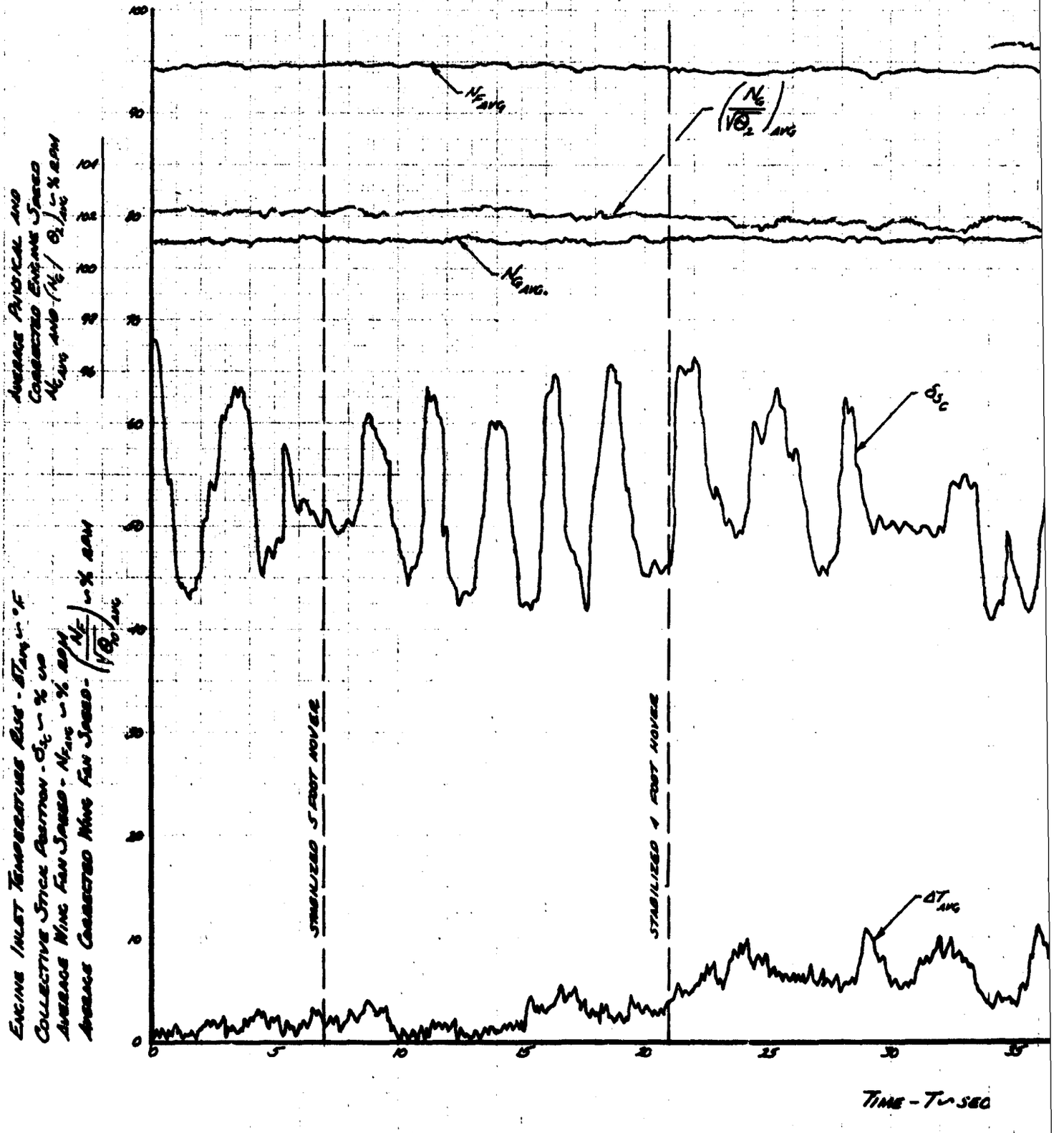

1

FIGURE No. 240

SYSTEM PERFORMANCE DURING HOVER

USA S/N 62-1505

~FT. = 2290

2

VOSE = 10L

GROSS WEIGHT - W ~ LB = 10200

AMBIENT TEMPERATURE - T_a ~ DEG. F = 48

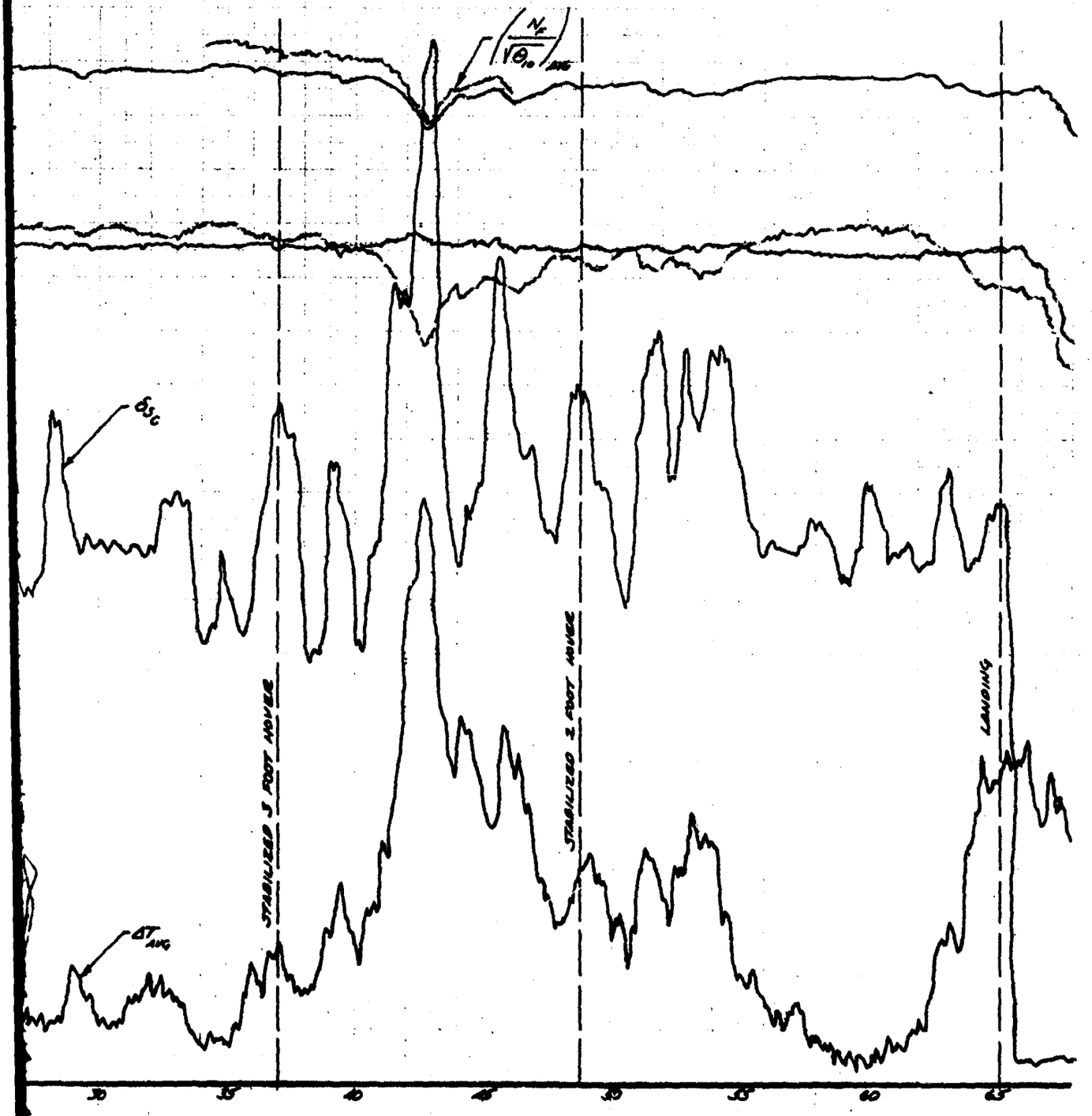

TIME - T ~ SEC

2

FIGURE No.

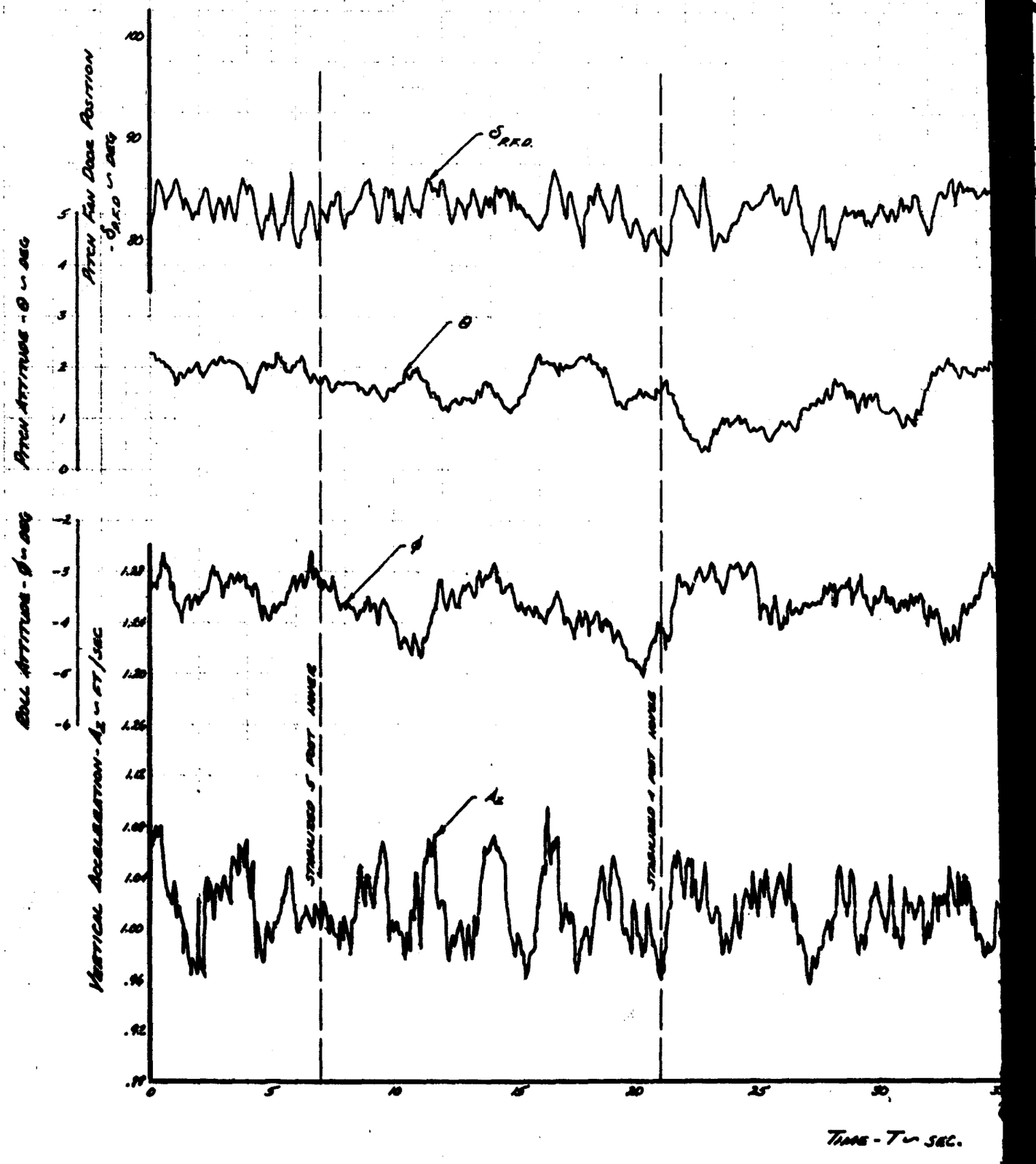
PITCH ATTITUDE - θ ~ DEG
PITCH FIN DOOR POSITION - δ_F.D ~ DEG
δ_F.D.
θ
ROLL ATTITUDE - φ ~ DEG
VERTICAL ACCELERATION - A_Z ~ FT/SEC
φ
A_Z
STABILIZED 5° PITCH ANGLE
STABILIZED 4° PITCH ANGLE
TIME - T ~ SEC.

FIGURE No. 240, CONTINUED

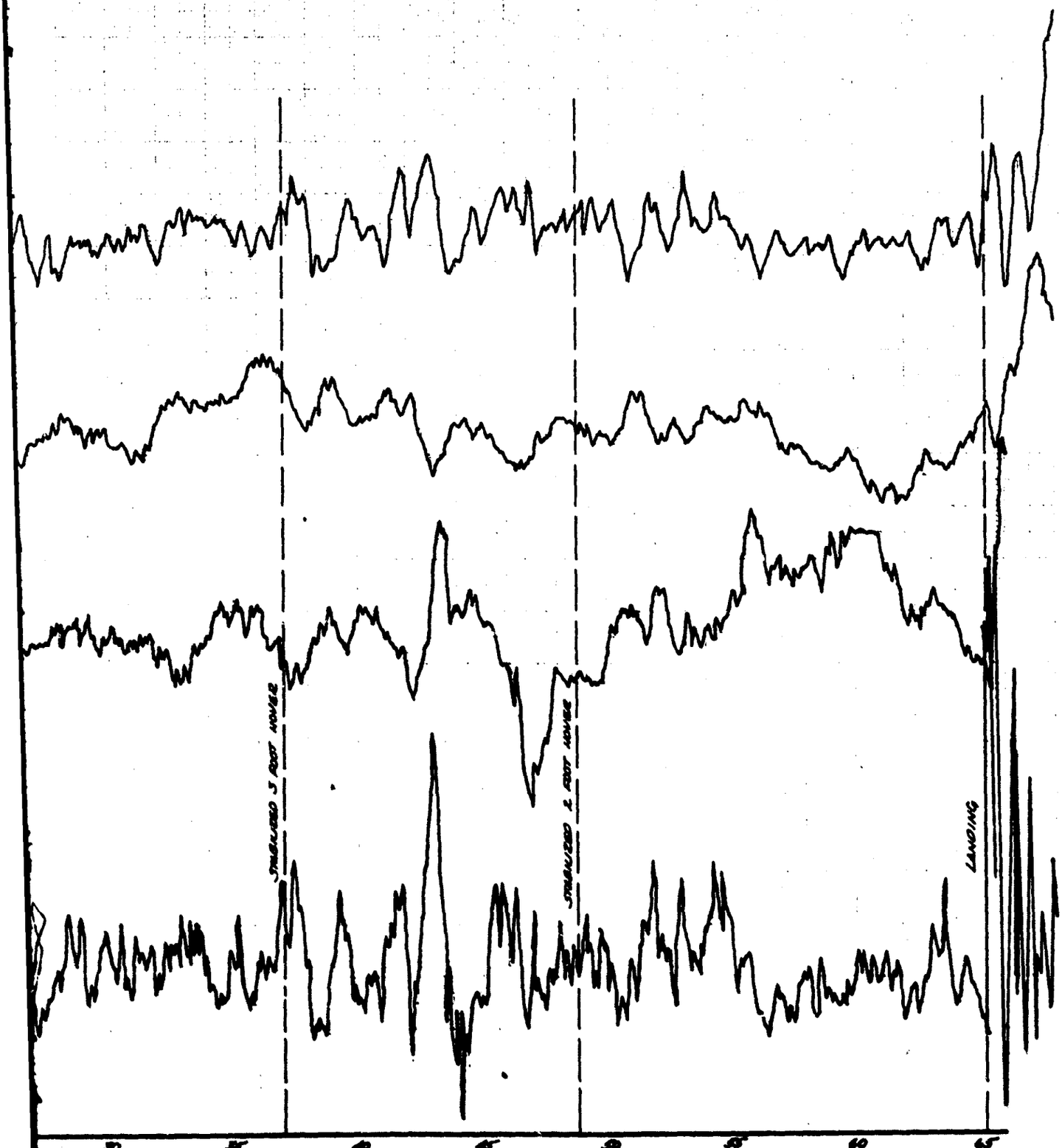

FIGURE No.

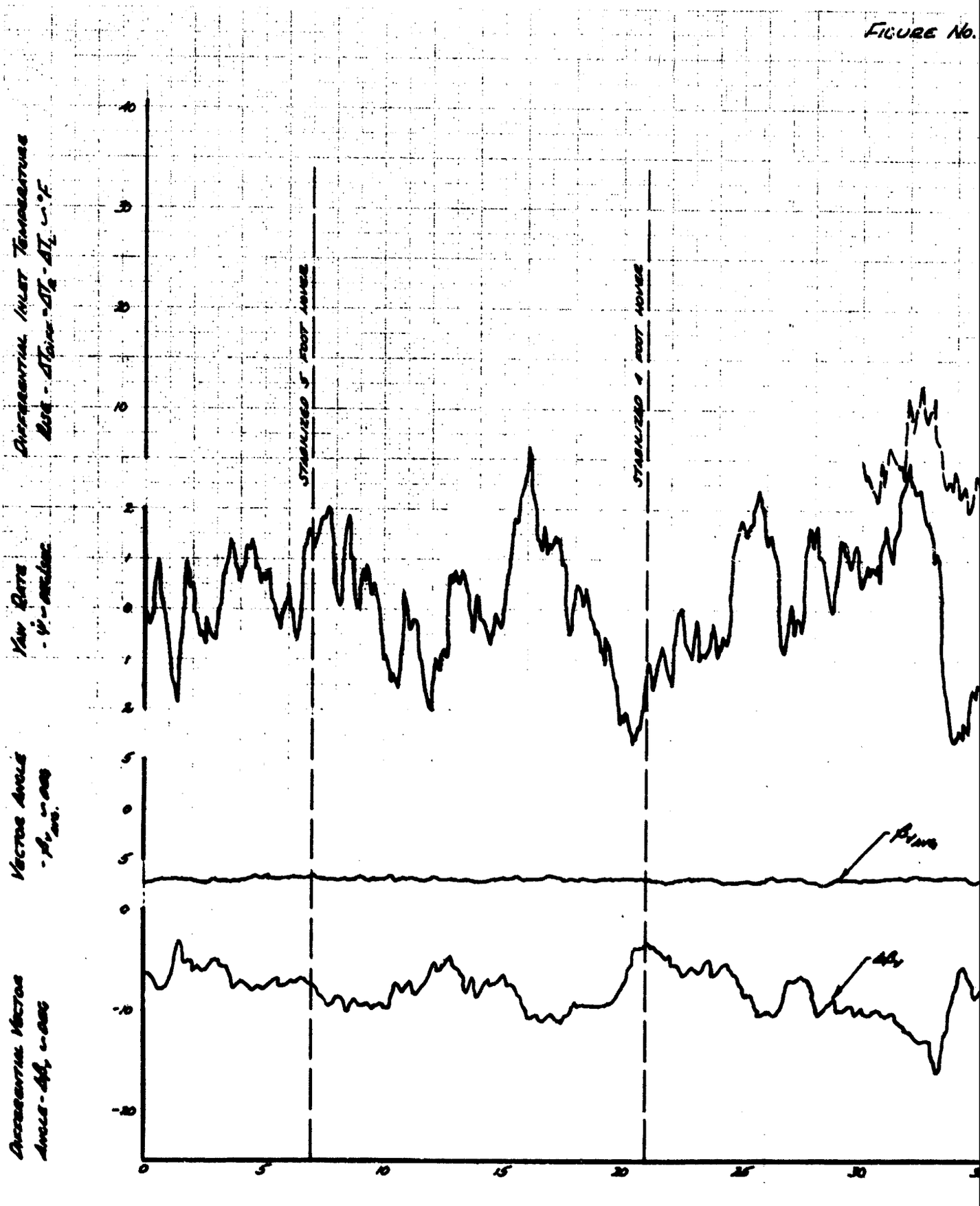
Differential Inlet Temperature
Yaw Rate
Vector Angle
Differential Vector Angle
STABILIZED 5 FOOT HOVER
STABILIZED 4 FOOT HOVER
Time - Tenths sec

FIGURE NO. 210. CONTINUED

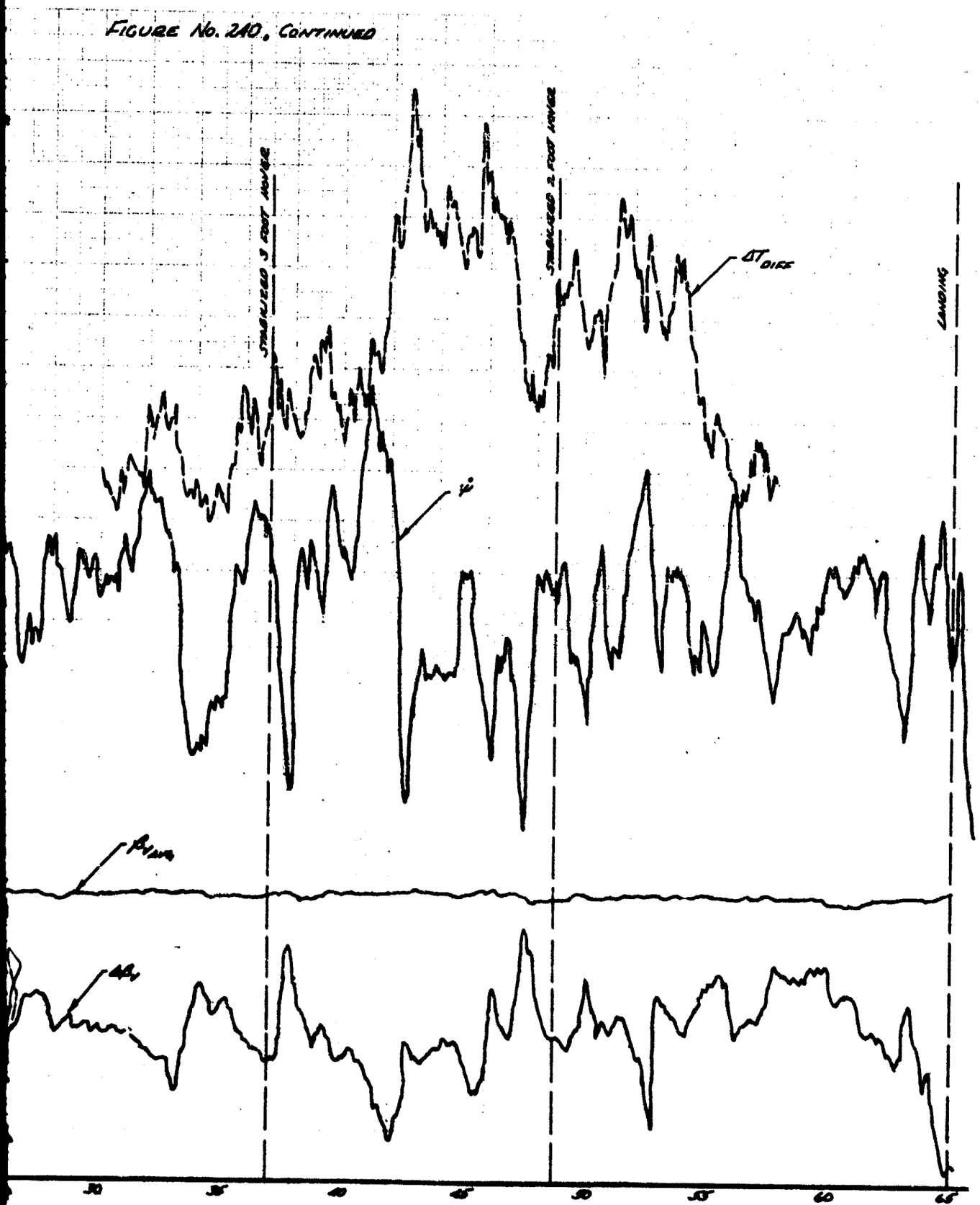

2

APPENDIX II

Definitions, Symbols and Abbreviations

1.0 DEFINITIONS

Fan Mode (FM)	Flight condition in which any part of the vertical lift is provided by the wing fan.
Jet Mode (JM)	Flight condition in which the vertical lift is entirely aerodynamic.
Hover	Fan-Mode flight less than 30 knots in any direction.
STOL	Takeoff or landing which is accomplished with a combination of wing-fan lift and wing aerodynamic lift.
Translation	Flight through all fan-mode configurations to conversion.
Conversion	That portion of the flight that encompasses the action of changing from one flight mode to the other (jet to fan or fan to jet).
Pre-conversion	That portion of the flight in which the lift is purely aerodynamic and the aircraft is preparing to perform a conversion from jet mode to fan mode. The configuration is as follows: Flaps 45 deg, fan doors unlocked but closed, louvers maximum aft (45 deg), pitch-fan doors and [illegible]es open.

Power Approach	That portion of jet mode flight where flaps are down, gear is down and the approach speed is approximately 120 KIAS.
Transition	Flight through all the configurations and regimes from vertical liftoff (fan mode) to jet flight (jet mode) and return.
Louver Stagger Angle (β_s)	The difference in angle between the master even and odd louver for each wing. 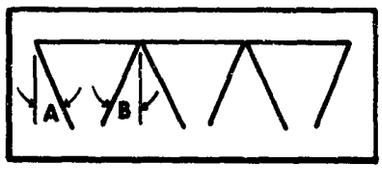 $\beta_s = A - B$
Louver Vector Angle (β_v)	The sum of the 4 master louvers (2 each wing) divided by 4. 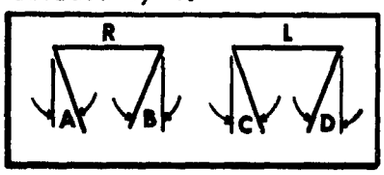 $\beta_v = \frac{A + B + C + D}{4.0}$
Differential Beta Vector ($\Delta\beta_v$)	The sum of the 2 master louvers on the right wing subtracted from the sum of the 2 master louvers on the left wing. 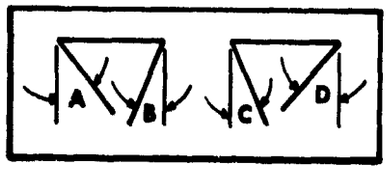 $\Delta\beta_v = (A + B) - (C + D)$

Differential Stagger Vector ($\Delta\beta_s$)

The difference between the 2 master louvers on the right wing subtracted from the difference between the 2 master louvers on the left wing.

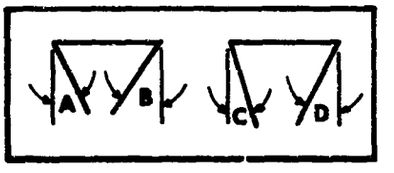

$$\Delta\beta_s = (A - B) - (C - D)$$

2.0 SYMBOLS AND ABBREVIATIONS

Symbols and Abbreviations	Definitions	Equations	Units
a	Speed of Sound	$29.045\ (\sqrt{T_a}\ ^{\circ}R)$	kt
A_F	Wing Fan Reference Area		ft^2
A_Z	Vertical Acceleration		ft/sec^2
AR	Wing Aspect Ratio		
BVP	Engine Bleed Valve Position		%
b	Wing Span		
$C_{D_e}{}^s$	Equivalent Drag Coefficient	$\frac{D_e}{q_s A_F}$	--
C.G.	Center of Gravity		in
$C_{L_e}{}^s$	Equivalent Lift Coefficient	$\frac{L_e}{q_s A_F}$	--

Symbols and Abbreviations	Definitions	Equations	Units
$C_{P_{III}}^{s}$	Engine Power Coefficient	$\frac{550(^{HP}5.1)_{III}\rho_a 1/2}{(T_{000}/A_F{}^{3/2}A_F}$	--
C_N^s	Vertical Thrust Coefficient	$\frac{N}{q_s A_F}$	--
C_T	Nozzle Thrust Coefficient	F_{g_i}/F_g	--
C_W^s	Weight Coefficient	$\frac{W}{q_s A_F}$	--
C_X^s	Longitudinal Force Coefficient	$\frac{X}{q_s A_F}$	--
deg	Degree		
D_e	Stability Axes Equivalent Drag Force		lb
$D_{T\ O}$	Distance Required to Clear a 50-Foot Obstacle		ft
e	Airplane Efficiency Factor		
E	Energy from Gas Generator		horsepower
EGT	Exhaust Gas Temperature-($T_{T_{5.1}}$)		deg
F_g	Engine Gross Thrust		lb
F_{g_i}	Ideal Gross Thrust		lb

Symbols and Abbreviations	Definitions	Equations	Units
fpm	Feet per Minute		
fps	Feet per Second		
F_x	Longitudinal Force		lb
g	Gravitational Acceleration 32.17 ft/sec^2		ft/sec^2
H/D	Wing Fan Height to Wing Fan Diameter Ratio		--
H_D	Density Altitude		ft
H_p	Pressure Altitude		ft
$HP_{5.1}$	Turbine Discharge Horsepower		HP
H_W	Wheel Height		ft
IGE	In Ground Effect		
i_t	Horizontal Stabilizer Incidence Angle		deg
K	Inlet Total Pressure Distortion	$\frac{P_{T_{2_{max}}} - P_{T_{2_{min}}}}{P_{T_{2_{avg}}}}$	--
KIAS	Knots Indicated Airspeed		kt
KEAS	Knots Equivalent Airspeed		kt
KTAS	Knots True Airspeed		kt
K_{β_s}	Wing Fan Collective Stagger Effectiveness	$(\frac{T_{W_f}}{T_{000}})_{\beta_s}$	--

Symbols and Abbreviations	Definitions	Equations	Units
K_{β_v}	Wing Fan Collective Vector Effectiveness	$\left(\frac{F_x}{T_{000}}\right)_{\beta_v}$	--
K_F	Slope of Wing Fan Disc Loading Versus Square of Wing Fan RPM		$331.5\ lb/ft^2$
K_{PFD}	Pitch Fan Effectiveness	$\frac{T_{W_f}}{T_0}$	--
L	Inlet Static Pressure Distortion	$\frac{P_{S_{2_{max}}} - P_{S_{2_{min}}}}{P_{T_{2_{avg}}}}$	
L_e	Stability Axis Equivalent Lift Force		lb
M	Mach Number	V_T/a	--
M_L	Rolling Moment		lb
M_M	Pitching Moment		lb
M_N	Yawing Moment		lb
N	Body Axis Normal Force		lb
N_F	Wing Fan Speed		% RPM
N_G	Engine Speed		% RPM
$N_{P\ F}$	Pitch Fan Speed		% RPM
OGE	Out of Ground Effect		
P_a	Ambient Pressure		psf
P_{S_2}	Inlet Static Pressure		psf

Symbols and Abbreviations	Definitions	Equations	Units
PSF	Pounds Per Square Foot		psf
P_{SL}	Sea Level Standard Day Pressure		29.92 psf
P_{T_a}	Ambient Total Pressure		psf
P_{T_2}	Inlet Total Pressure		psf
$P_{T_{5.1}}$	Turbine Discharge Pressure		psf
q	Free Stream Dynamic Pressure		lb/ft^2
q_s	Slipstream Dynamic Pressure	$\frac{T_{000}}{A_F} + q$	lb/ft^2
R	Universal Gas Constant	55.35 ft-lb/lb/deg	ft-lb/lb/deg
R/C	Rate of Climb		fpm
R/C_v	Vertical Rate of Climb		fpm
R/D_v	Vertical Rate of Descent		fpm
RPM	Revolutions Per Minute		rpm
S	Wing Area		ft^2
SAS	Stability Augmentation System		
SL	Sea Level		
T	Vertical Thrust		lb

Symbols and Abbreviations	Definitions	Equations	Units
T_a	Ambient Temperature (FAT)		deg
T_c^s	Thrust Coefficient	$\frac{T_{000}/A_F}{q_s}$	--
T_L	Diverter Valve Leakage Temperature		deg
To	Total Pitch Fan Static Thrust at Sea Level Standard Day and 100 Percent Pitch Fan Speed		1680 lb
T_{000}	Total Wing Fan Static Thrust at Zero Exit Louver Angle, Given as Curve of Standard Sea Level Thrust as Function of Wing Fan RPM and Corrected by Air Density	$K_F(\frac{\%N_F}{100})(\frac{\delta_a}{\theta_a})$ x AF	lb
T_{PF}	Pitch Fan Thrust		lb
T_s	Standard-Day Temperature		deg
T_{SL}	Sea Level Standard-Day Temperature		59 deg F
T_{T_2}	Inlet Total Temperature		deg
$T_{T_{5.1}}$	Turbine Discharge Temperature		deg
$T_{T_{10}}$	Wing Fan Inlet Temperature		deg

Symbols and Abbreviations	Definitions	Equations	Units
T_{W_f}	Wing Fan Thrust		lb
T/W	Thrust to Weight Ratio		--
V_c	Calibrated Airspeed	$V_{ic} + \Delta V_{pc}$	kt
V_{co}	True Climbout Airspeed		kt
V_e	Equivalent Airspeed	$V_T \sqrt{\sigma_a}$	kt
V_{ic}	Instrument Corrected Airspeed		kt
V_{LO}	Liftoff Airspeed		kt
V_R	Rotation Airspeed		kt
V_T	True Airspeed	$\frac{V_e}{\sqrt{\sigma_a}}$	kt
V_V	Vertical Climb Speed		fps
V_W	Wind Velocity		kt
W	Gross Weight		lb
W_a	Engine Inlet Airflow		lb/sec
W_C	Compressor Customer Bleed		lb/sec
W_f	Fuel Flow		lb/sec
W_{IB}	Interstage Bleed Flow		lb/sec
W_L	Diverter Valve Leakage Airflow		lb/sec
$W_{5.1}$	Turbine Discharge Gas Flow		lb/sec

Symbols and Abbreviations	Definitions	Equations	Units
α	Angle of Attack		deg
α_T	True Angle of Attack		deg
β	Angle of Sideslip		deg
β_s	Wing Fan Collective Stagger Angle		deg
β_v	Wing Fan Collective Vector Angle		deg
$\Delta\beta_s$	Differential Stagger Angle		deg
$\Delta\beta_v$	Differential Vector Angle		deg
ΔP	Differential Pressure		$in.H_2O$
ΔT	Engine Inlet Temperature Rise		deg F
δ_a	Ambient Pressure Ratio	$\frac{P_a}{P_{SL}}$	--
δ_2	Engine Inlet Total Pressure Ratio	$\frac{P_{T_2}}{P_{SL}}$	--
δ_{s_a}	Lateral Stick Position		in
δ_{s_c}	Collective Stick Position		%
δ_{s_e}	Longitudinal Stick Position		in
δ_{s_r}	Rudder Pedal Position		in
δ_T	Throttle Position		

Symbols and Abbreviations	Definitions	Equations	Units
δ_{T_s}	Thrust Spoiler Deflection		%
δ_{PFD}	Pitch Fan Thrust Reverser Door Position		%
$\Delta\alpha_{PE}$	Angle of Attack Position Error Correction		deg
ΔV_{pc}	Airspeed Position Error Correction		kt
η_R	Inlet Total Pressure Recovery	$\frac{P_{T_2}}{P_{T_a}}$	--
θ_a	Ambient Temperature Ratio	$\frac{T_a}{T_{SL}}$	--
θ_2	Engine Inlet Total Temperature Ratio	$\frac{T_{T_2}}{T_{SL}}$	--
θ_{10}	Wing Fan Inlet Total Temperature Ratio	$\frac{T_{T_{10}}}{T_{SL}}$	--
θ_{20}	Pitch Fan Inlet Total Temperature Ratio	$\frac{T_{T_{20}}}{T_{SL}}$	--
ρ_a	Density of Ambient Air		--
ρ_{SL}	Density of Ambient Air at Sea Level Standard Day		.0023769
σ_a	Ambient Air Density Ratio	$\frac{a}{SL}$	--

Subscript	Definitions
a	Ambient
AVG	Average
avail	Available
c	Calibrated
i	Ideal
ic	Instrument Corrected
L	Left
max	Maximum
min	Minimum
R	Right
Req	Required
t	Test
T	Total
2	Engine Inlet
5.1	Turbine Discharge
10	Wing Fan Inlet
20	Pitch Fan Inlet

NOTE: Coefficients with exponents of s denote slipstream notation.

APPENDIX III

General Aircraft Information

1. SOURCE OF INFORMATION

The descriptive and design information in the following paragraphs was obtained from "XV-5A Detail Aircraft Specification" (Reference i).

2. DESCRIPTION OF AIRCRAFT AND SYSTEMS

2.1 DIMENSIONS AND DESIGN DATA

a. Areas

(1) Wing area (including 49 sq ft of fuselage)	260.3 ft^2
(2) Vertical tail area	51.0 ft^2
(3) Flap area	25.4 ft^2
(4) Aileron area (aft of hinge line), total	19.3 ft^2
(5) Horizontal tail area, total	52.9 ft^2
(6) Elevator area (aft of hinge line), total	12.0 ft^2
(7) Vertical tail area, total	51.0 ft^2
(8) Rudder area (aft of hinge line), total	6.4 ft^2
(9) Wing-fan annulus area, total	55.6 ft^2
(10) Wing-fan area (fan tip), total	42.6 ft^2
(11) Pitch-fan annulus area, total	5.64 ft^2

b. Wings

(1) [illegible]	29.83 ft

(2) Chord	
(a) Root	12.08 ft
(b) At break in quarter chord	9.09 ft
(c) Theoretical tip	3.58 ft
(d) Mean aerodynamic (MAC)	9.41%
(3) Sweep at 1/4 chord	
(a) Inboard panel	15.0 deg
(b) Outboard panel	28.3 deg
(4) Airfoil section	
At butt line (BL) 170.05	NACA 0012-24
(5) Aspect ratio	3.42
c. Ailerons	
(1) Span	6.37 ft
(2) Chord	32.7%
(3) Centroid of aileron area	BL-139.6 in
d. Flaps (single slotted)	
(1) Span	43.0%
(2) Chord (average)	19.6%
e. Horizontal tail	
(1) Span	13.18 ft
(2) Chord	
(a) Root	65.64 in
(b) Tip	30.60 in
(3) Sweep of leading edge	19.5 deg

(4) Airfoil section	NACA 64A012
(5) Aspect ratio	3.29
(6) Pivot point	Fuselage Station (FS)-496.7
(7) Distance of 1/4 MAC from wing 1/4 MAC	21.17 ft
f. Elevators	
(1) Span (per side)	5.47 ft
(2) Chord	
(a) Root (BL 4.3)	1.337 ft
(b) Tip (BL 69.9)	.854 ft
(3) Location of 1/4 MAC	FS-521.1 in
g. Vertical tail	
(1) Sweep of leading edge	35.4 deg
(2) Airfoil section	
(a) Waterline (WL) 113.0 in	NACA 64A(012)-016.5
(b) WL 206.0 in (tip)	NACA 64A(012)-013.0
(3) Aspect ratio	1.178
(4) Distance of 1/4 MAC to wing 1/4 MAC	18.25 ft
h. Rudder	
(1) Span	5.20 ft
(2) Chord	
(a) Root	1.47 ft
(b) Tip	.98 ft

(3) Location of 1/4 MAC	FS-507.4 in
(4) Height over highest point of vertical tail (reference line level)	14.75 ft
(5) Length (reference line level)	44.52 ft

2.2 CENTER-OF-GRAVITY LOCATIONS

Aft limit	FS-246 in
Forward limit	FS-240 in

2.3 CONTROL MOVEMENTS

The movements measured during the test program:

a.	Longitudinal control stick	6.5 in. fwd 6.0 in. aft
b.	Lateral control stick	3.90 in. rt 3.20 in. lt
c.	Rudder pedal	3.50 in. lt 3.50 in. rt
d.	Elevator surface (from faired position)	22 deg trailing edge up (TEU) 25 deg trailing edge down (TED)

e. Left aileron surface position

(flaps at zero deg)	18 deg TEU	15.75 deg TED
(flaps at 45 deg)	7.75 deg TEU	26.25 deg TED

f. Right aileron surface position

(flaps at zero deg)	18.9 deg TEU	15.25 deg TED
(flaps at 45 deg)	7.25 deg TEU	25.75 deg TED

g. Rudder surface position

24.5 deg trailing edge right (TER)

24.75 deg trailing edge left (TEL)

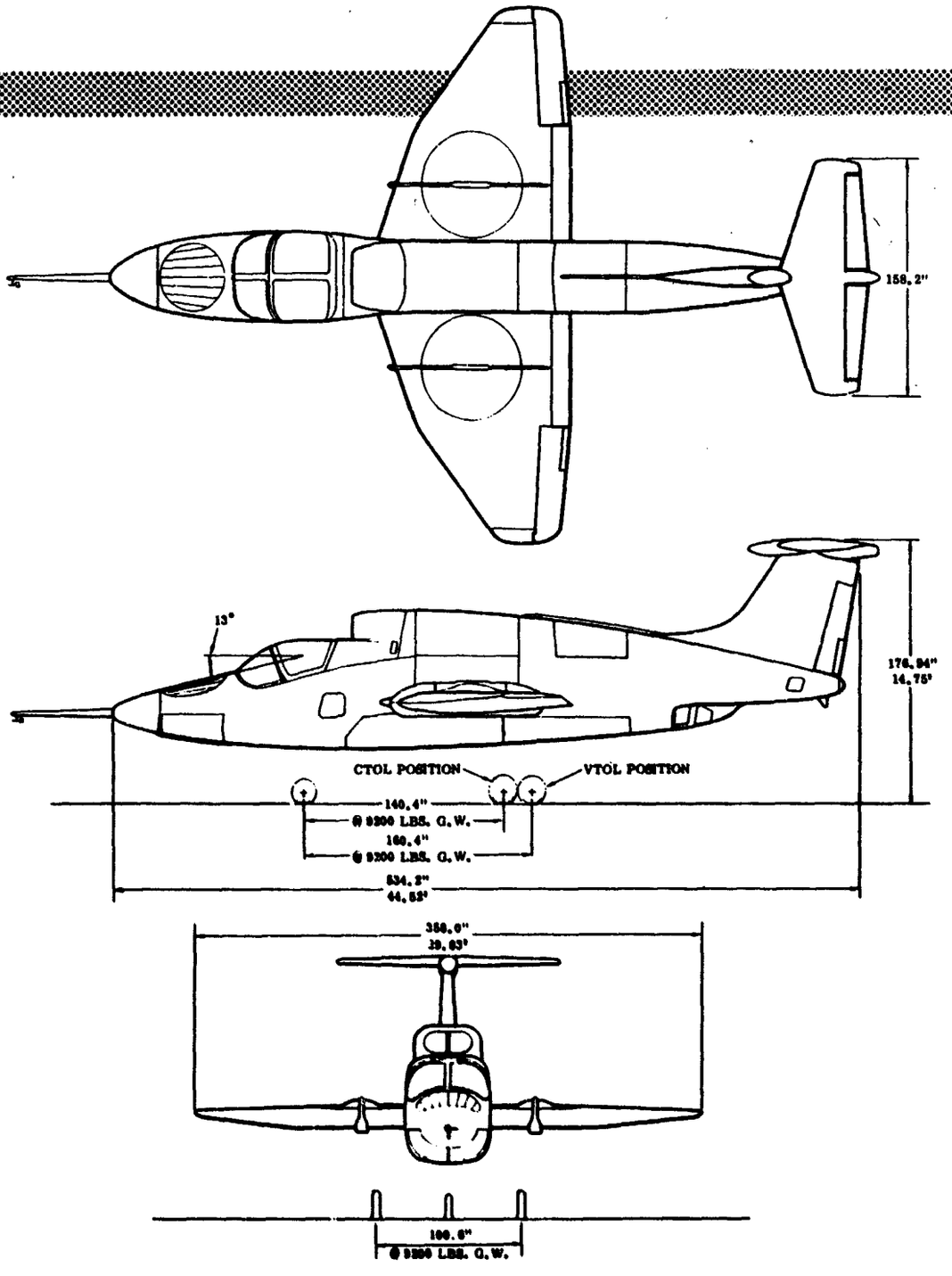

FIGURE 1 - XV-5A Dimensions

h. Horizontal stabilizer

20 deg leading edge up (LEU)

5 deg leading edge down (LED)

i. Flaps (zero %) zero deg

(100%) 45 deg

j. Pitch-fan modulator doors (-10.5 deg beta vector) 65 deg

k. Wing-fan roll control (differential stagger) 32.0 deg lt

(-10.5 deg beta vector) 37.5 deg rt

l. Wing-fan yaw control (differential vector) 31.0 deg lt

(-10.5 deg beta vector) 31.6 deg rt

m. Wing-fan beta vector (with trims and controls centered) -10.5 deg

+38.7 deg

2.4 AIRCRAFT SYSTEMS

2.4.1 FLIGHT CONTROL SYSTEM

The pilot is provided with conventional flight controls, fan-mode (FM) flight controls and control elements required for conversion from one flight mode to another. The primary flight control system consists of a control stick for conventional longitudinal and lateral control, a collective lift stick and rudder pedals for directional control. In addition to necessary instrumentation, the pilot is provided with a power console and an auxiliary console. The auxiliary console is used in conjunction with other controls to accomplish conversion from one flight mode to another.

The control stick is mechanically connected to the aerodynamic flap-type control surfaces, wing-fan exit-louver servo valves, and pitch-fan thrust modulator servo valve. The lift stick is connected to the wing-fan exit-louver servo valves and

is operative only during fan-mode flight. The rudder pedals are mechanically linked to the conventional rudder as well as to the wing-fan exit-louver servo valves. The ailerons, wing-fan exit-louvers and pitch-fan thrust modulators are hydraulically actuated. In addition to being mechanically controlled, the wing-fan exit-louver servo valves and the pitch-fan thrust-modulator servo valve have electrical features which accept input signals from the stability augmentation system (SAS) amplifiers.

The control stick and rudder pedals perform identical attitude control functions in both conventional and FM flight. Longitudinal stick motion controls the elevators and the pitch-fan thrust-modulator doors. Lateral stick motion controls the ailerons as well as the differential stagger of the wing-fan exit louvers. In FM flight, the collective lift stick motion adjusts the wing-fan louver collective stagger and the position of the pitch-fan modulator doors.

A mechanical mixer mechanism is installed between the cockpit controls and the louver actuator valves. This mechanical mixer mechanism interprets pilot commands and positions the wing-fan exit louvers. The mixer also decreases and eventually disengages the wing-fan louver response to pilot commands as a function of louver vector angle (forward speed). This deactivates the wing-fan control system while in the conventional mode. A similar device combines longitudinal control and collective control commands to the pitch-fan thrust-modulator doors and disengages door response to commands as a function of louver vector angle. Another function of the mixer is to compensate for rolling tendencies when yaw commands are given.

In the FM flight, the positions of the wing-fan louvers (see Figure 2) determine beta stagger or vector, either collective or differential, or combinations of both. Thus, the beta stagger angle of the louvers determines the lift of each wing fan for roll, lift control and trim, whereas the vector angle of the louvers determines the horizontal thrust component of the wing. Combinations of these two angles, either collective or differential, results from pilot inputs and/or automatic stabilization of the roll and yaw axes within the limited authority of the SAS system. These control functions are summarized as follows:

a. Collective stagger produces vertical deceleration.

b. Differential stagger produces roll acceleration.

c. Collective vector produces horizontal acceleration.

d. Differential vector produces yaw acceleration.

For the pitch axis, the pitch-fan modulator doors increase or spoil the thrust of the pitch fan. In a manner similar to the roll and yaw-axis control of the wing louvers, the hydraulic actuator for the pitch-fan doors responds to the pilot's input and/or any signal generated by the pitch-rate gyro of the SAS system.

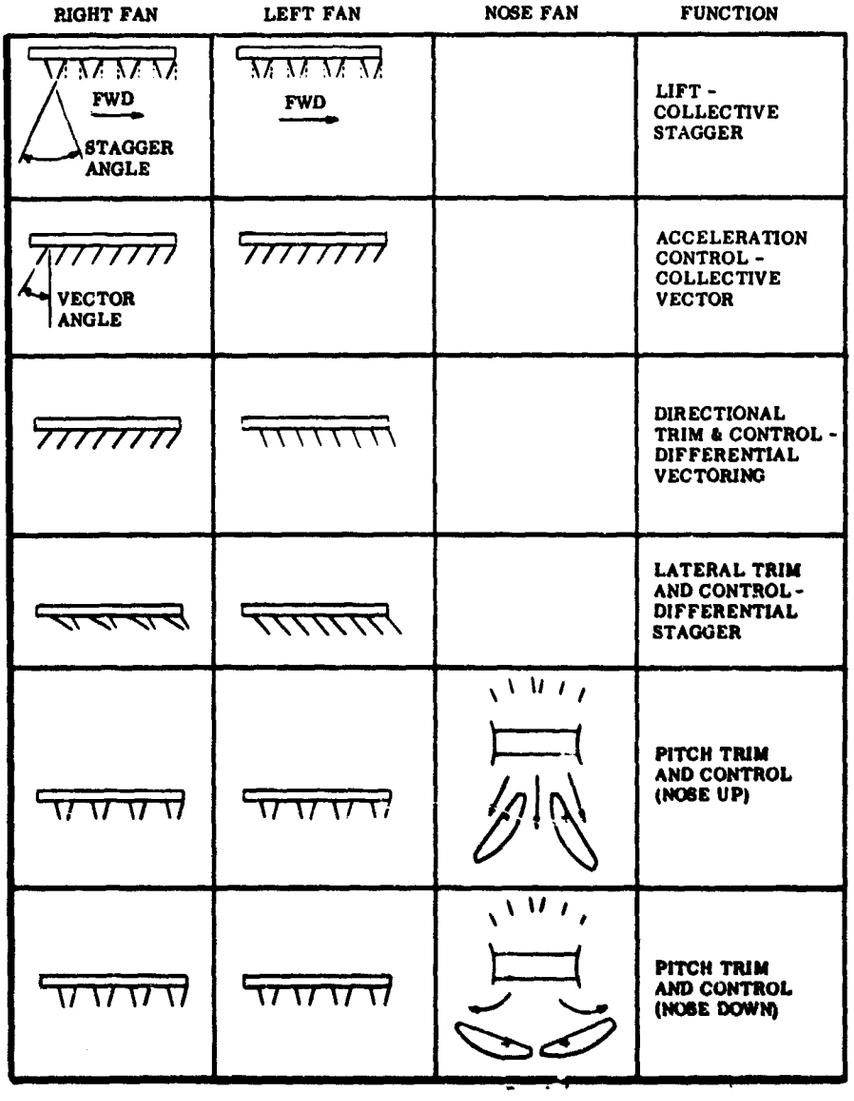

FIGURE 2 - VTOL FLIGHT CONTROL SYSTEM OPERATION

2.4.2 FLIGHT CONTROL ELECTRICAL SYSTEM

Electrical power is supplied by two 28-volt-DC, 165-ampere engine-driven generators and a silver-zinc battery for emergency use. Two inverters supply 115-volt, 440-cycle AC power. If a power loss is realized in one inverter, electrical loads are automatically transferred to the other inverter. Either inverter is capable of supplying normal current loads.

The conversion control and SAS have dual electrical channels for both primary and standby functions. Both primary and standby circuits are energized; however, only one circuit controls at a time. Command signals for conversion and sequencing are always dual except for flaps and ailerons droop commands. All commands are fed to the electrical mixer for conversion control, and the electrical mixer integrates and selects the proper flight control actuator valves. The SAS is inoperative during jet-mode (JM) flight. Special electrical features of the conversion control system include automatic lockout during conventional flight and while the aircraft is hovering in the FM flight.

In JM flight, control functions of the flaps-down switch are selected through the louver selector switch which has two positions, either JM or FM. If the louver selector switch is in the JM position, flaps-down command causes flaps down with aileron droop conditions. If the louver selector switch is in the FM position, the same occurs and, in addition, sequenced preconversion functions of the pitch-fan inlet louvers and wing-fan door locks and vectoring of the wing-fan louvers occur. When these operations are completed, monitoring switches act as an interlock through the mode selector switch and the electrical mixer. The circuitry is arranged so that the mode selector switch cannot command conversion to the FM configuration unless all pre-conversion conditions have been met. If the conditions have not been met on either primary or standby systems, the electrical interlock system causes an interlock "No Go" warning light to illuminate the annunciator panel.

In FM flight in hover, immediate change to JM cannot be made. The pilot's maneuvering to gain a safe airspeed causes a series of sequenced, automatic electrical events to occur. When the fan louver vectoring is sufficient to provide a safe airspeed, the mode selector switch capability is restored to the pilot. At this time, the JM command can be given to the electrical mixer, if desired, and an interlocked sequence of electrical commands is automatically given. These commands include change in angle of attack of the stabilizer, diversion of gases to the tailpipe,

closure of the wing-fan doors and de-activation of the SAS. When these automatic electrical commands to the actuators have been completed, the aircraft is the same pre-conversion configuration as before converting from JM flight to FM flight.

If an actuator failure occurs during any part of pre-conversion or pre-conversion sequence (JM to FM), or if any mechanical interruption occurs in the procedure, the Interlock "No Go" warning light notifies the pilot that he should not change mode. The circuitry is arranged so that a definite sequence has to be followed by the pilot. Similarly, any electrical, hydraulic or mechanical failure causes an interlock channel to be given, thus interrupting the sequence and causing the warning to be displayed on the annunciator panel.

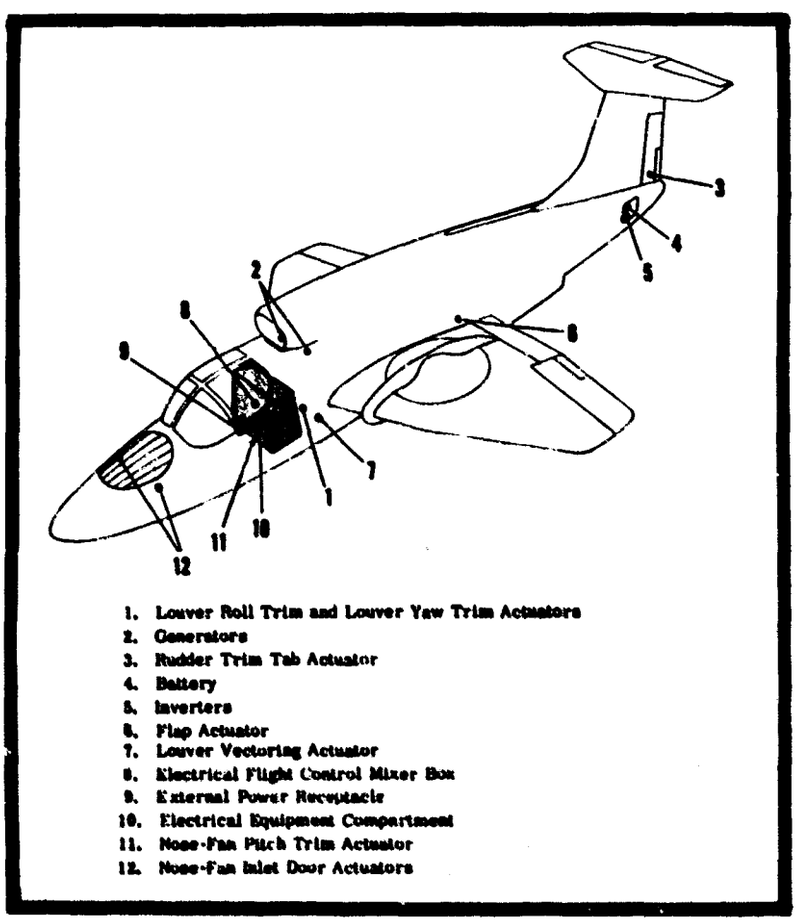

FIGURE 3 - ELECTRICAL SYSTEM COMPONENT LOCATION DIAGRAM

2.4.3 FLIGHT PROPULSION SYSTEM

This system consists of two J85-5B turbojet engines (less afterburners) used as gas generators; diverter valves to direct the gas flow; two X353-5B lift fans equipped with vectorable discharge louvers; one X376 pitch-trim control fan and necessary ducting. The system augments the thrust of the turbojet engines for FM flight.

For vertical flight, the turbojet engines supply hot exhaust gas to the tip turbines of the wing fans. This is accomplished by means of a diverter valve and ducting. During transition from hover to horizontal flight, louvers (located on the lower surface of the fan) vector the fan exhaust rearward to provide horizontal thrust for forward acceleration. Once the aircraft has reached a speed sufficient for wing supported flight, the diverter valve moves to a straight-through position, the exit louvers and the wing-fan doors are closed, and the turbojet operates in the conventional manner. Crossover ducting between the wing fans provides for single-engine operation.

The pitch fan, installed in the nose of the aircraft, provides longitudinal attitude control of the aircraft during FM operation. The pitch fan is coupled to the gas generators in a manner similar to that of the wing fans. Pitch control is obtained by modulation of the pitch-fan control doors, which respond to the pilot's input and/or any SAS signal during FM flight. The doors are closed and locked for JM flight.

In JM flight, the engine compartment is cooled by ram air, which in turn is exhausted by the tailpipe shroud ejector. In the hover mode, cooling air is supplied for four engine-driven fans. The heated air is then exhausted from the forward pitch-fan duct compartment through outlets in the pitch-fan (inlet) struts. The divider-duct and wing-fan compartments are exhausted from the strut fairings of the wing fans.

The aircraft is provided with a conventional throttle quadrant, and in addition a twist grip is incorporated on the collective lift control; this affords joint regulation of engine power when in the FM flight.

2.4.4 FLIGHT CONTROL HYDRAULIC SYSTEM

Two independent hydraulic systems are provided for flight control. Each system operates continuously and consists of separate reservoirs, engine-driven pumps and plumbing. Either system is capable of supplying full load requirements in case of

pressure loss in one system. Hydraulic power is provided to operate the wing-fan inlet door and exit louvers, pitch-fan doors, horizontal stabilizer, thrust spoilers and ailerons.

The wing-fan exit-louver servo valves and the pitch-fan thrust-modulator servo valve are controlled not only by mechanical inputs, but also by an electrical input feature capable of accepting input signals from the SAS amplifiers. Hydraulic actuators also position the thrust spoilers and the ailerons. A hydraulic motor-driven screw jack positions the horizontal stabilizer.

Pressure transmitters for each hydraulic system operate a dual-reading hydraulic pressure gage located in the cockpit. In case of system pressure loss, an annunciator warning panel indicates the affected system to the pilot. Normal hydraulic system pressure is 3000 pounds per square inch. Ground test connections are provided for system checkout and to facilitate filling.

2.4.5 ENGINES

The J85-5B engines, located in the upper fuselage above the wing and aft of the cockpit, are axial-flow trubojets used as gas generators. Uninstalled rating per engine is as follows:

	Jet Thrust lb (min)	Engine Compressor rpm (max)
Sea level rated power	2500	16,500

Major components of each engine include an 8-stage rotor, a matching compressor stator, an annular combustion system, and a 2-stage turbine.

Air enters the inlet duct and is directed into the inlet compressor by the variable inlet guide vanes. As the air is compressed, it is forced back into the combustion chamber. Fuel nozzles, projecting into the combustion chamber, eject a fuel spray which is mixed with the compressed air. Combustion is provided initially by the ignition plug but is self-sustaining thereafter. The combustion gases flow into the 2-stage turbine mounted on a shaft that is splined directly to the compressor rotor. After passing through the turbine section, the exhaust gases flow into the diverter valve ducts, where the gases are diverted either to the wing-fan/pitch-fan propulsion system (for FM flight), or to the engine tailpipe (for JM flight).

Major component details include a 15-strut front frame fabricated of sheet metal, with 15 variable-pitch inlet guide vanes positioned directly downstream of the struts. An anti-icing manifold surrounds the front frame over the hollow struts. The compressor stator casing is split and flanged along the horizontal centerline; this makes it possible to remove the upper or lower half for inspection. The 8-stage axial-flow compressor delivers air to the combustion section at a pressure ratio of approximately 6.8 to 1. The compressor casing is made of chromalloy steel. The external cylindrical part of the main frame is also a chromalloy steel weldment. The frame not only serves as a structural member but houses the power-takeoff drive assembly and provides a mount for the 12 flow-divider fuel nozzles, the fuel manifold, the accessory drive gearbox assembly and the 8-stage compressor stator vanes and exit guide vanes. Six equally-spaced struts provide for extraction of compressor discharge air for auxiliary pressurization use. The outer combustion casing is a one-piece stainless steel weldment that serves as a major structural unit. The inner combustion casing is also a one-piece fabrication. The turbine stator is a sheet metal weldment with a horizontal split line which permits removal of either half for inspection. The air impingement start duct is located on the bottom half of the casing. The turbine rotor is a 2-stage impulse type which was designed to operate at a speed of 16,500 rpm and at a nominal turbine inlet temperature of 1650 degrees F.

Lubrication is provided by a pressurized, closed-circuit system which furnishes oil to the cored and drilled passages of the engine and to a relatively few external oil lines. The lubrication system is pressurized by bleeding compressor air into the oil reservoir. A relief valve prevents excessive pressure.

For engine ignition, a capacitor discharge ignition unit is provided. The engine igniter plug is immersed in the combustor. Alternating current (AC) of 115 volts, 400 cycles is produced by an airframe-mounted inverter. The current passes through a filter which prevents high frequency signals from entering or leaving the unit. The input power is stepped up to approximately 1250 volts by a transformer, then rectified to a pulsating direct current (DC) potential of about 2500 volts, which is stored in the capacitor. A sealed gap allows periodic surges of stored high DC voltage to flow to the igniter. Once ignition has been accomplished, combustion of the engine is self-sustaining.

The overspeed governor is hydro-mechanical isochronous type which senses and governs engine physical speed at one adjustable speed setting by bypassing fuel flow in excess of

engine requirements to the main fuel pump inlet. The overspeed governor system provide a limit steady-state engine speed of 104 percent maximum and a limit transient speed of 108 percent maximum.

2.4.6 FUEL SYSTEM

The fuel system is controlled by the pilot at the fuel management panel. The panel represents the plumbing of the entire fuel system in diagram. For normal operation, the 1710-pound-capacity forward tank supplies fuel to the left engine. The 1720-pound-capacity aft tank supplies fuel to the right engine. The normal setting for the fuel tank valves is to have both tank-to-engine valves open. The fuel level of each tank is shown on the main instrument board by a dual gage in the engine display. Low level in either tank lights the master caution light and a low-level light in the annunciator panel. The tank affected is indicated by low-level amber lights on the fuel management panel and when this occurs approximately 250 pounds of fuel remain.

Each tank is equipped with a boost pump, driven by engine bleed air. The pump is controlled by a switch on the fuel management panel. Caution lights for the boost pumps indicate low pressure or loss of pressure. The boost pumps are used for all engine operations; however, the engine pumps will maintain engine operation below 6000 feet altitude.

2.4.7 STABILITY AUGMENTATION SYSTEM

The stability augmentation system (SAS) operates in the FM flight during transition and conversion and stabilizes the aircraft attitude in all axes. During conventional flight, the SAS system is inoperative. Dual electronic channels provide for both primary and standby systems. The systems consist of the pilot controls, dual 3-axis gyros and dual amplifiers. The 3-axis rate-gyro signals determine the hydraulic actuator positions of the wing-fan louvers and the pitch-fan (modulator) doors. The two systems are identical except for the gain control. The primary system gains are adjustable by the pilot at the instrument panel. In normal flight, the primary system is used and back-up reliability is supplied by the standby system.

The automatic stabilization electrical inputs of the SAS system are summed with the mechanical inputs in both the wing-fan louver and pitch-fan door actuators. The response of these actuators to the electrical signals is such that each actuator has limited authority in case a hardover signal occurs. In the roll axis, the amplifier operates in either a holding or maneuvering mode, depending upon the position of the control stick.

For small motions near the center of the control stick travel, the amplifier operates in the holding mode. In this case, the gyro signal is integrated to produce a quasi-position signal which is combined with the rate signal. For larger excursions (+ 1 inch) of the control stick, switches located on the control linkage cause the integrator in the amplifier to be shorted, and the amplifier operates in the maneuvering mode. In this mode, the quasi-position signal is eliminated and only the rate signal is amplified and sent to the actuators. The pitch and yaw axes operate in the maneuvering mode at all times. There is no integration of the rate signal; however, a change of gain is effected by displacing the controls.

The settings and authority of the optimum SAS configuration used during the tests were:

Collective Stick Position δ_{s_c} - % Up	Vector Angle β_v - deg	Stability Augmentation System Authority - ΔSAS Equivalent Inches of Control		
		Pitch ΔSAS_e - in	Axis Roll ΔSAS_a - in	Yaw ΔSAS_r - in
50	0	2.09	.70	1.55
100	0	1.65	.70	1.58
	15	2.27	1.07	1.61
	30	2.03	2.07	2.05

FIGURE 4 - AUTOMATIC STABILIZATION SYSTEM BLOCK DIAGRAM, page 354

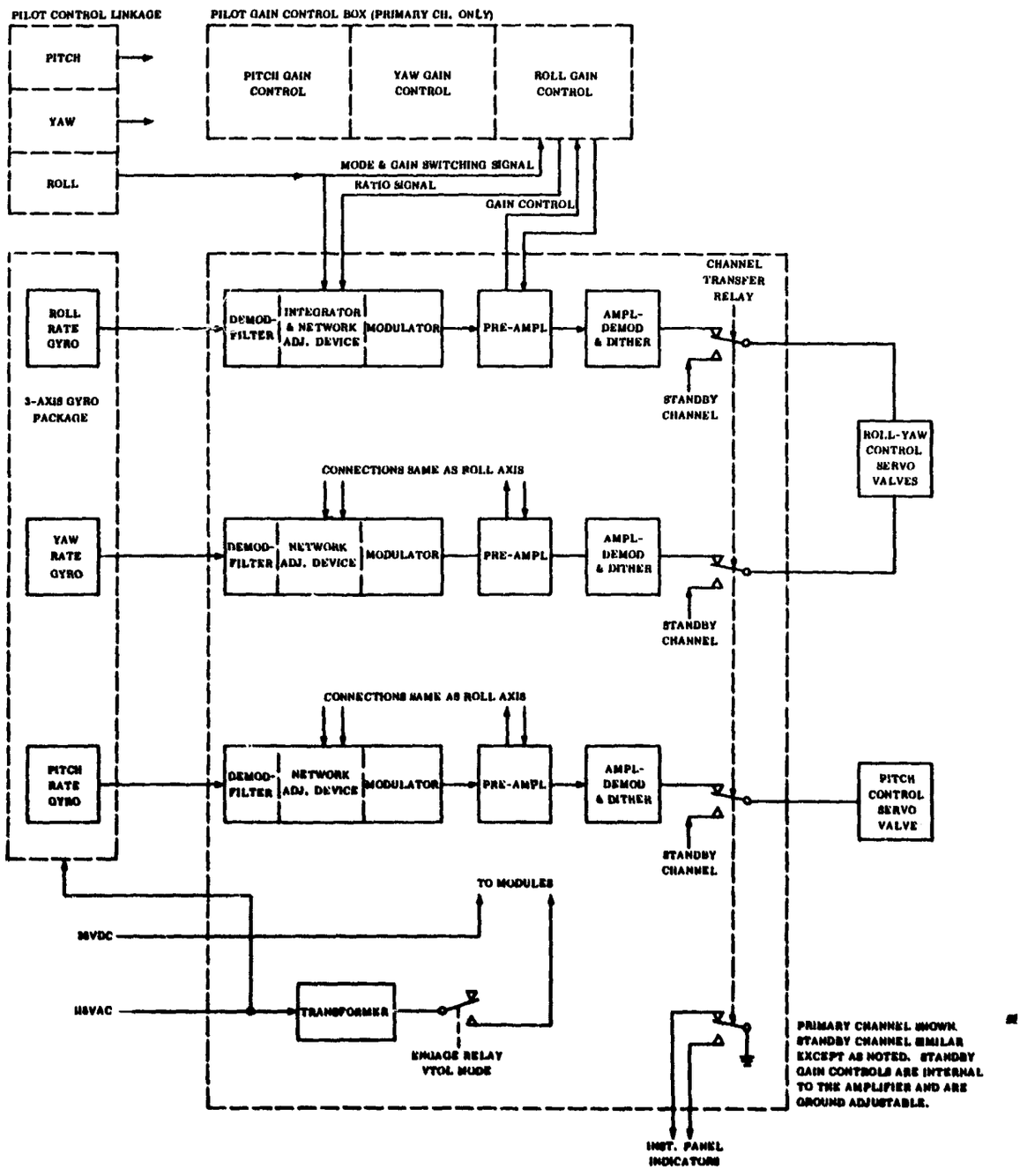

FIGURE 4 - AUTOMATIC STABILIZATION SYSTEM BLOCK DIAGRAM

APPENDIX IV

Flight and Operation Limits

The following flight and operation limits were observed during the Performance evaluation of the XV-5A aircraft:

a. Airspeed Limitations

(1) Jet-Mode Flight

(a) Maximum Flight Speed - Figure 1

The maximum flight speed was 400 knots equivalent airspeed (KEAS) or 0.70 Mach Number based on flutter and stability and control flight tests.

(b) Wing Flap, Landing Gear, Pitch-Fan Inlet Louver, Pitch-Fan Exit Door or Wing-Fan Exit Louver Extension (or Extended).

Maximum structural speed - 180 KEAS

(c) Pre-conversion Configuration

Maximum structural speed	180 KEAS

(d) Low Airspeed System

Maximum design speed, aircraft system	170 KIAS
Maximum design speed, flight test instrumentation system	150 KIAS

(e) Nose Landing Gear Critical Speed (Shimmy Damper Limit)

Maximum - 120 knots ground speed

(f) High Speed Drag Parachute

Maximum design deployment speed	500 KEAS

Minimum design deployment speed 150 KEAS

(g) Landing Deceleration Parachute

Maximum design deployment speed 130 KEAS

Minimum design deployment speed 70 KEAS

(h) Spin Recovery Parachute

Maximum design deployment speed 180 KEAS

(i) Minimum Flight Speed

Minimum speed = that speed at which 15 deg indicated angle of attack occurs

(2) Fan-Mode Flight

(a) Conversion Speed Limits

Turbojets to fans	92 to 110 KIAS
Fans to turbojets	84 to 95 KIAS

(b) Maximum Flight Speed

Maximum design speed	120 knots true airspeed (KTAS)
Maximum demonstrated speed	110 KIAS (approximate)

(c) Minimum Flight Speed at Altitude

Speed below 30 KIAS at altitudes above 500-ft terrain clearance are not recommended due to inadequate pilot visual cues.

(d) Airspeed - Level Flight Angle of Attack Limits Figure 2

(e) Lateral and Rearward Translation Limits

Lateral	26 knots
Rearward	23 knots

b. Conversion Test Limitations

(1) Conventional to Fan-Mode Conversion (Initial Conditions)

Collective lift setting	25% to 100% demonstrated
Gross weight	10,300 lb maximum demonstrated
Altitude	1000 ft minimum terrain clearance
Airspeed	92 - 105 KIAS (demonstrated)
Horizontal tail incidence	10 deg (automatic programming)
	-5 deg (prior to conversion)
Maximum power setting	102% RPM
	700 deg C (10 min) 690 deg C continuous
Minimum power setting	97% RPM (demonstrated)
Thrust spoilers	Retracted
Stability augmentation	On or off
Fan cavity temperature	120 deg C maximum

(2) Fans to Jet-Mode Conversion (Initial Conditions)

Collective lift setting	55% to 100% demonstrated
Angle of attack	+4.5 deg maximum
	-2.0 deg minimum
Bank angle	±30 deg
Sideslip angle	Approximately zero (±2 deg)

Rate of Climb	Zero maximum
	-1000 ft/min minimum
Gross weight	10,300 lb maximum
Altitude	1000 ft minimum terrain clearance
Airspeed	84 - 95 KIAS
Horizontal tail incidence	15 deg maximum
	7 deg minimum
Power setting (J-85-5B)	102% RPM maximum
	94% RPM minimum
	700 deg C(10 min) 690 deg C continuous
Wing fan speed	103% RPM maximum
	88% RPM minimum

c. Flight Time and Temperature Limitations

Certain portions of the airframe were subject to high temperatures requiring time and/or temperature limitations for particular flight conditions and configurations until such time as the thermodynamic properties of the aircraft become more fully defined.

(1) Jet-Mode Flight

No limitations except fan-cavity temperatures, as follows:

Maximum continuous	120 deg C

Maximum for 1 min	120 deg - 150 deg C
Overheat conditions	above 150 deg C

(2) Fan-Mode Flight - Fixed Landing Gear with Heat Shields

(a) Hovering Flight (zero - 30 KIAS)

Total hovering time	10.0 min maximum

(b) Transition Flight (above 30 KIAS, OGE)

Indicated vector angle 35 deg and above	6.0 min maximum
Indicated vector angle less than 35 deg	10.0 min maximum
Total FM flight time	10.0 min maximum

(3) Fan-Mode Flight - Retractable Landing Gear

The landing gear was in the retracted position at airspeeds above 60 KIAS or at indicated vector angles greater than 30 deg. A dash acceleration through conversion, however, was permitted with the gear extended when the extension of the gear was accomplished within a maximum of 15 sec.

(a) Landing Gear Extended, Wheel Well Doors Open

Ground operations at 70% RPM	6.0 min maximum
Hovering IGE	2.0 min maximum
Airspeed less than or equal to 60 KIAS and less than 30 deg vector angle, OGE	same as in Item c(2)

(b) Landing Gear Retracted, Wheel Well Doors Closed

Airspeed above 60 KIAS or greater than 30 deg vector angle	4 min maximum
Airspeed less than or equal to 60 KIAS and less than 30 deg vector angle, OGE	same as in Item c(2)

d. Prohibited Maneuvers

Intentional spins, inverted flight, stalls or aerobatics were prohibited because of unwarranted risk and because no significant contributions would be made to the current evaluation of the aircraft.

e. Maneuvering Limitations and Flight Test Experience

(1) Jet-Mode Flight

(a) Normal Load Factor Envelope - Figure 3

(b) Sideslips - Figure 4

Flight test experience of sideslip maneuvers is presented in Figure 4. No known aircraft restriction as such existed; however, the data shown represented near full rudder input or near maximum pilot effort.

(2) Fan-Mode Flight

(a) Structural Design Envelope - Figure 5

(b) Sideslip - Figure 6

Flight test experience of fan-mode sideslips is presented in Figure 6. It is recommended that these values not be exceeded.

f. Takeoff Limitations

(1) Jet-Mode Flight

Maximum gross weight, Phase II flight test policy	11,600 lb
Maximum forward C.G. location	Fuselage Station 240.0
Maximum wind velocity for flight test operations	15 kt (any direction)
Maximum crosswind component	5 kt
Maximum nosewheel liftoff speed	120 kt ground speed

(2) Fan-Mode - Vertical Liftoff

Maximum gross weight	Figure 7
Maximum forward C.G. location	Fuselage Station 240.0
Maximum wind velocity	5 kt
Maximum crosswind component	zero

The aircraft must be headed into the wind prior to liftoff.

(3) Fan-Mode Flight - Rolling Takeoff (STOL)

Maximum gross weight (Same as FM)	Figure 7
Maximum forward C.G. location	Fuselage Station 240.0
Maximum wind velocity for flight test operations	15 kt

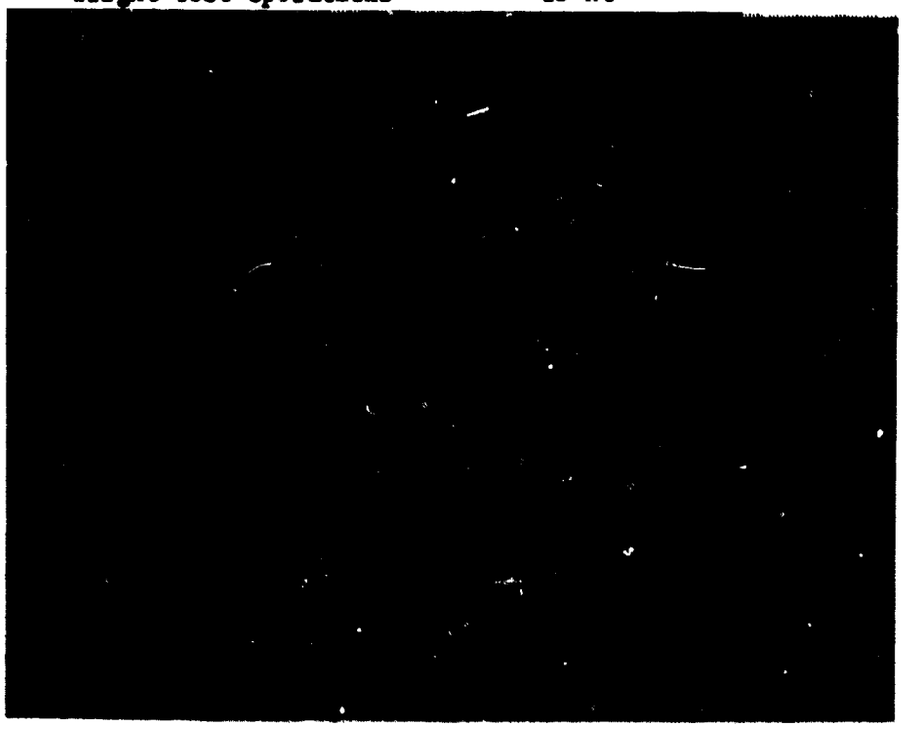

FIGURE NO. 2

FAN MODE AIRSPEED AND ANGLE OF ATTACK ENVELOPE

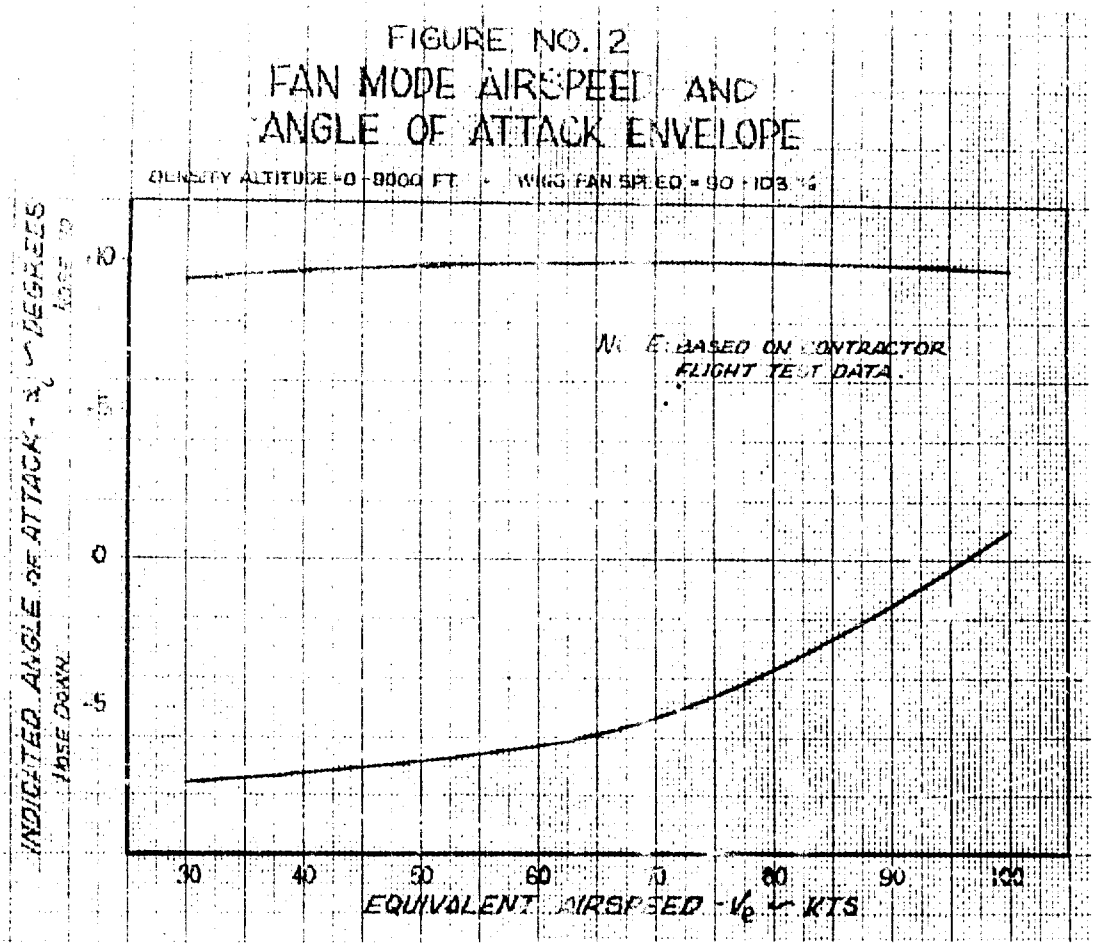

FIGURE NO. 3

JET MODE STRUCTURAL DESIGN ENVELOPE

GROSS WEIGHT = 8200 POUNDS

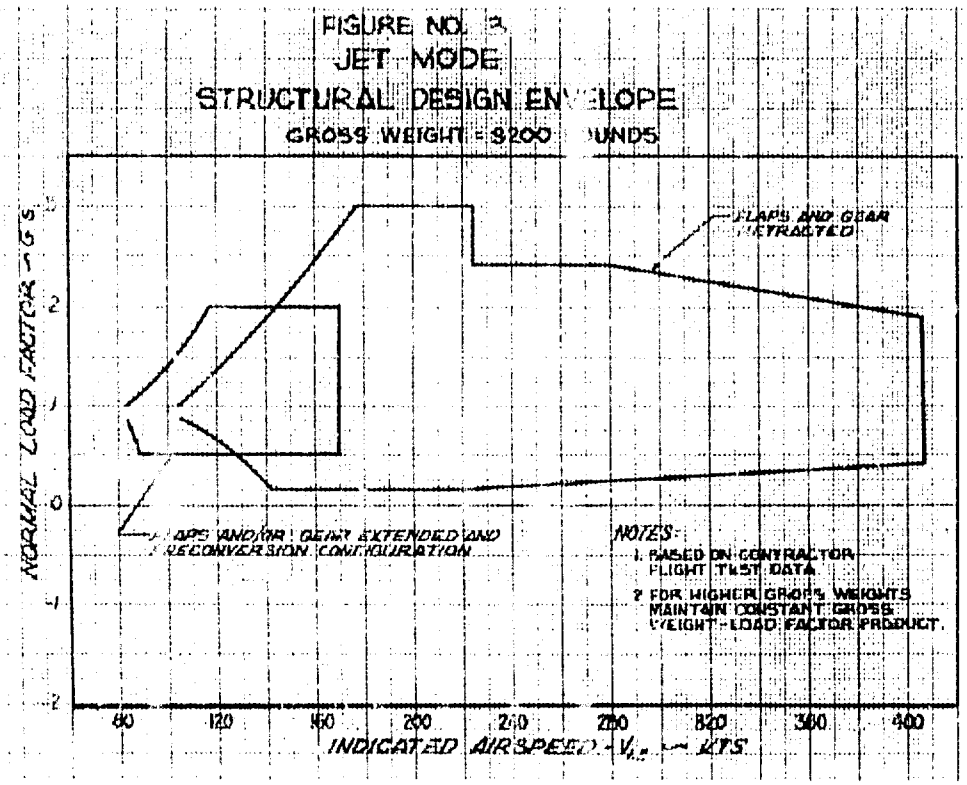

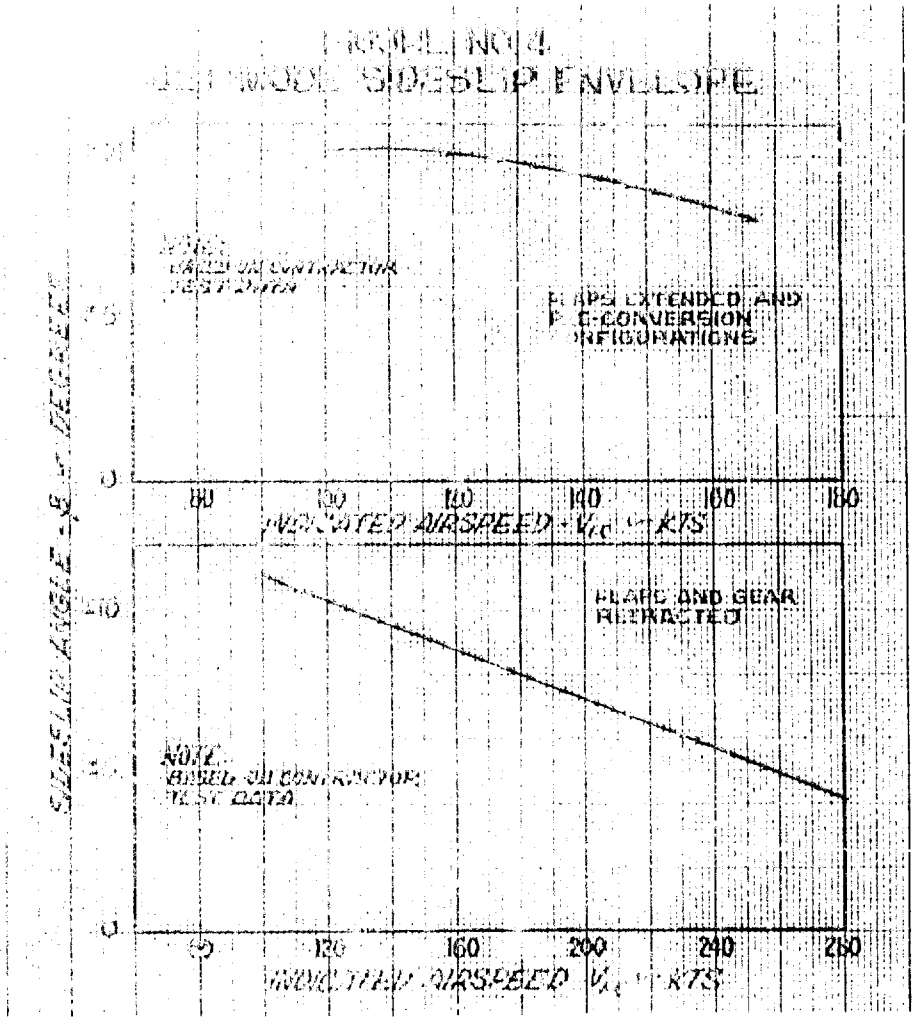

FIGURE NO. 4

FAIL MODE STRUCTURAL DESIGN ENVELOPE

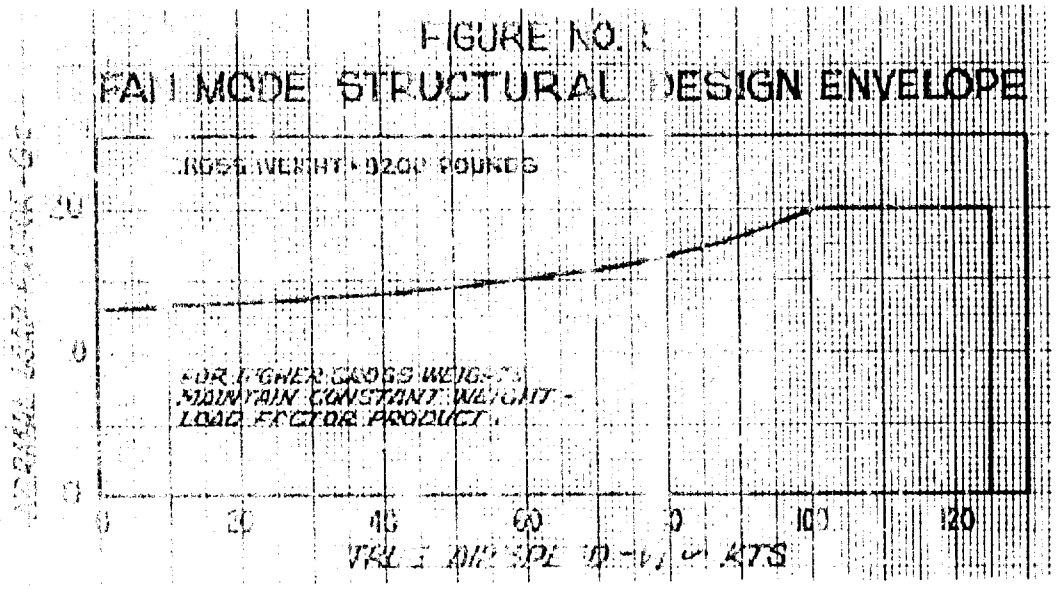

Maximum Design Angular Rate And Acceleration:

	Hover (0 To 30 KTS. TAS)	Transition (30 To 125 KTS TAS)
Pitch Rate-Radians/Sec	±1.0	±1.0
Roll Rate-Radians/Sec	±1.38	±1.38
Yaw Rate-Radians/Sec	±1.31	±1.31
Pitch Accel-Radians/Sec	±1.25	±3.00
Roll Accel-Radians/Sec	±1.75	±2.63
Yaw Accel-Radians/Sec	±1.05	±1.05

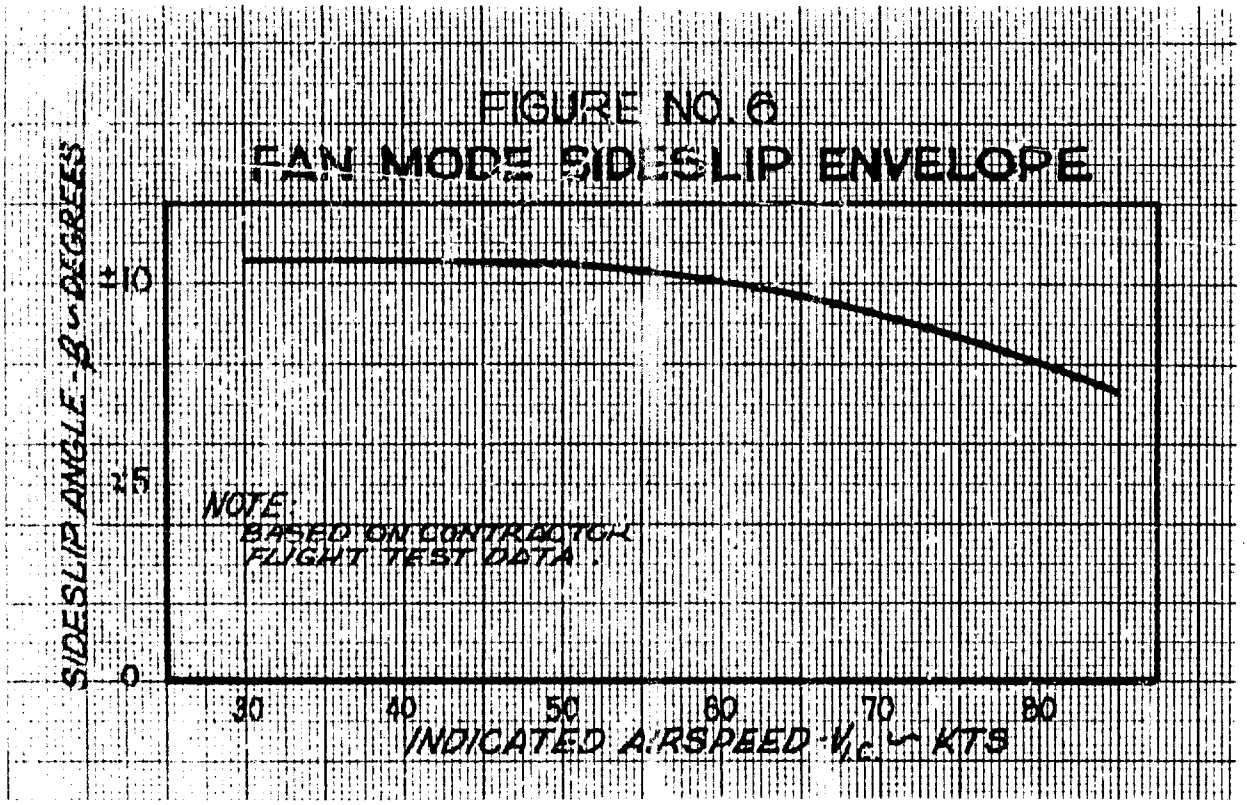

FIGURE NO. 7

FAN MODE TAKE-OFF WEIGHT VS. AMBIENT TEMPERATURE

PRESSURE ALTITUDE = 2500 FEET

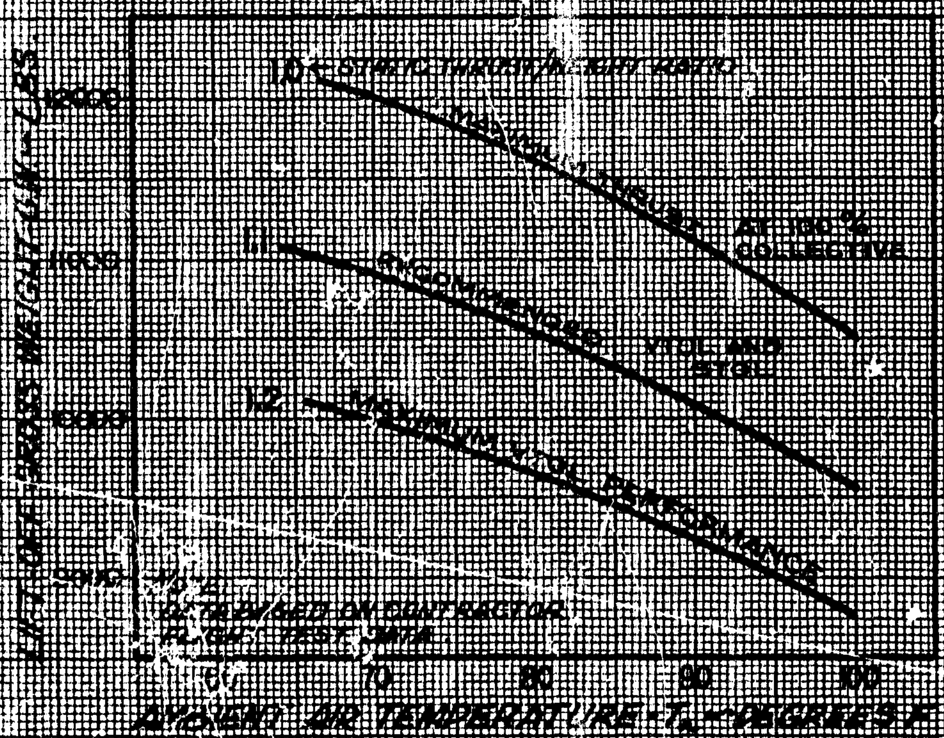

APPENDIX V
Test Instrumentation

1.0 TEST PARAMETERS

The test instrumentation was supplied, installed, calibrated and maintained by the contractor in accordance with reference b.

A General Electric (GE) 300A Airborne Automatic Data Acquisition System was used to record flight data parameters. The following parameters were recorded by this system during the performance testing of the XV-5A:

a. Altitude

b. Airspeed (High and Low)

c. Angle of Attack

d. Angle of Sideslip

e. Fuel Totalizer

f. Engine fuel flow (Left and Right)

g. Diverter Valve Position (Left and Right)

h. Engine Bleed Valve Position (Left and Right)

i. Engine Throttle Position (Left and Right)

j. Engine Speed (Left and Right)

k. Wing Fan Speed (Left and Right)

l. Pitch-Fan Speed

m. Free Air Temperature

n. Engine Inlet Temperature (Left and Right) (5, 8, and 12 o'clock)

o. Engine Exit Gas Temperature (Left and Right)

p. Wing-Fan Inlet Temperature (Left and Right)

q. Pitch-Fan Inlet Temperature

r. Engine Fuel Temperature (Left and Right)

s. Nose Total Pressure

t. Engine Inlet Static Pressure (Left and Right)

u. Engine Inlet Total Pressure (Left and Right)

v. Engine Turbine Discharge Pressure (Left and Right)

w. Longitudinal Stick Position

x. Lateral Stick Position

y. Rudder Pedal Position

z. Collective Stick Position

aa. Pitch-Fan Door Position

bb. Wing-Fan Door Position

cc. Horizontal Tail Incidence Angle

dd. Louver Vector Command

ee. Odd Exit Louver Position (Left and Right)

ff. Even Exit Louver Position (Left and Right)

gg. Differential Vector Angle

hh. Differential Stagger Angle

Other parameters were recorded by the data acquisition system but were not considered mandatory for the performance portion of the test.

2.0 DATA ACQUISITION SYSTEM

The GE 300A Airborne Automatic Data Acquisition System was a high-speed pulse-code-modulation (PCM) system. It was completely transistorized with a self-contained analog-to-digital conversion and packaged for minimum size and weight.

The GE 300A system was capable of recording from 12 to 90 data channels. The recording of both low-and high-level data sources was possible. These analog signals were multiplexed and

converted to a PCM format with parallel output in a form suitable for recording on magnetic tape. The specifications for this system were:

a. Number of Channels	90 channels for data input 10 digital channels
b. Sampling Rate	100 samples/sec/channel
c. Resolution	Ten bits
d. Accuracy	± 0.5% low-level ± 0.2% high-level
e. Recording Time (Maximum)	16 min
f. Tape Speed	30 in/sec
g. Power Requirements	28 volts DC @ 20 amps max
h. Weight	100 lb

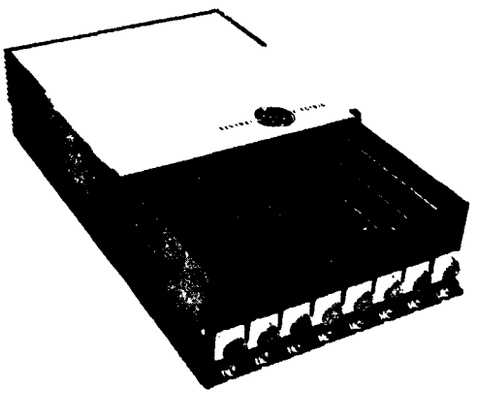

PHOTO 11
PCM SYSTEM WITH
MULTIPLEXER INSTALLED

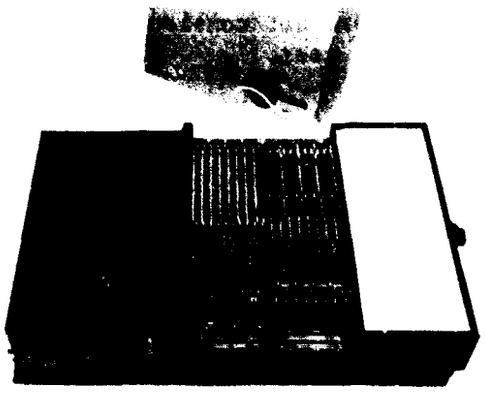

PHOTO 12
PCM SYSTEM WITH ENCODER EXPOSED

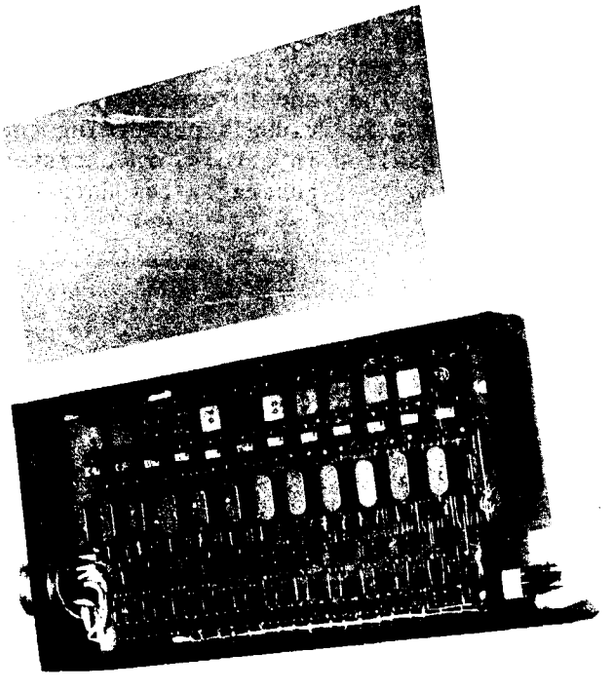

PHOTO 13
MULTIPLEXER UNIT

When operating properly, the data acquisition system had sufficient accuracy for recording stability and control flight data. A continuous check by highly technical personnel, however, was required to verify the validity of the data. The major problems encountered during the test program were overall system noise, shifting of calibrations, and need of a highly complicated ground station to produce the raw data in engineering units.

This type of data acquisition system was not conducive to operating a locations other than the principal test site, where a ground station and the necessary technical personnel were readily available. This ground station required trained and experienced technical personnel for maintenance, operation, and assurance of reproduction of valid data. The data acquisition system was designed, manufactured, and generally serviced and maintained by the contractor.

The preflight time for the PCM system required approximately four hours. When a dawn flight was scheduled this requirement could be successfully accomplished only by providing the necessary personnel to start the preflight procedures at an early hour.

During the initial portion of the program the calibration and preflight procedures were generally outlined in many cases by verbal instructions. This condition required judgment from the individual performing the operation. The same interpretation and judgment were not reached by different individuals performing the same calibration. This situation resulted in errors, inconsistencies and non-repeatability and contributed to a generally low data-accuracy and confidence level.

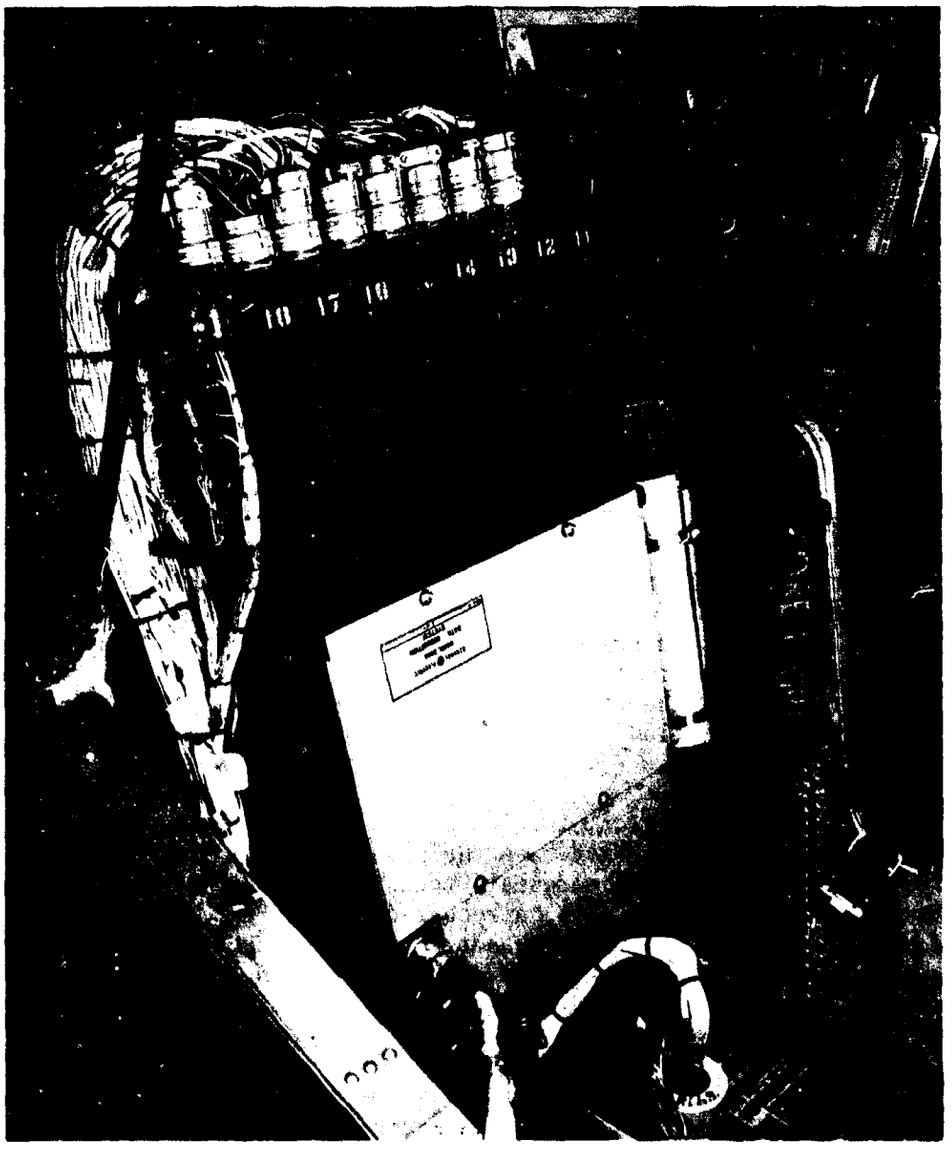

PHOTO 14 • PCM SYSTEM INSTALLED IN AIRCRAFT

PHOTO 15
XV-5A WING BOOM,
AIRSPEED

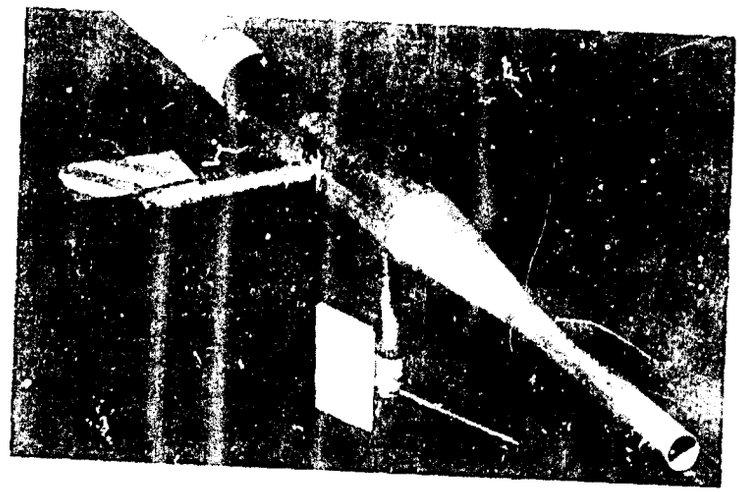

PHOTO 16
XV-5A NOSE BOOM:
AIRSPEED,
ANGLE OF ATTACK,
ANGLE OF SIDESLIP

PHOTO 17
XV-5A WING BOOM
OAT

APPENDIX VI
Weight and Balance

The test aircraft, S/N 62-4505, was weighed prior to the flight. The weighing was accomplished on the weight and balance facilities of the U.S. Air Force Flight Test Center (AFFTC), Edwards Air Force Base. The test instrumentation was installed prior to the weighing. The contractor weight data established the weight of the total instrumentation at approximately 500 pounds. The basic weight (empty weight plus trapped oil and fuel) was 8685 pounds and the C.G. was at Station 243. Changing the gear to the locked-down position and installing the heat shield increased the basic weight by 42 pounds.

The fuel system was also calibrated with the AFFTC facilities. Known fuel quantities were added incrementally to the aircraft. Fuel density and volume were established for each fuel increment added to the system. After the fuel level was allowed to stabilize, the quantity indicators were recorded and the aircraft was re-weighed. These data were then used to calculate C.G. locations for various fuel loadings. Weight and balance data were also obtained in a similar manner to determine the C.G. change with aircraft attitude and fuel loading.

APPENDIX VII Description of Test Responsibilities

XV-5A TEST PROGRAM RESPONSIBILITIES

1.0 XV-5A PROGRAM MANAGER'S REPRESENTATIVE AT EDWARDS AIR FORCE BASE (PROVIDED BY USAAVLABS)

a. Be responsible to the Lift-Fan Program Manager for conduct of the XV-5A Government Flight Evaluation at Edwards Air Force Base.

b. Provide necessary technical and contractual support to, and coordination with, the XV-5A Test Director.

c. Assure necessary coordination with the contractor and other Government agencies.

d. Recommend contract program changes to the Lift-Fan Program Manager, USAAVLABS, for execution.

e. Provide Contracting Officer's Representative (COR) services at the XV-5A test site.

f. Provide briefing on the XV-5A program to certain visitors at the direction of CO, USAAVLABS, or at the request of CO, USAAVNTA, or CG, AFFTC.

2.0 XV-5A TEST DIRECTOR AT EDWARDS AIR FORCE BASE (PROVIDED BY USAAVNTA)

a. Provide technical and administrative direction for the research flight test of the XV-5A.

b. Be responsible to the XV-5A Program Manager's Representative for conduct of the approved XV-5A flight test program.

c. Establish and/or approve flight test operational procedures and monitor their compliance by contractor and Government personnel.

d. Supervise daily flight test activities:

(1) Approve each scheduled flight, including aircraft configuration, pilot selection, flight test card to be flown, alternate test card to be flown, instrumentation, aircraft maintenance, etc.

(2) Supervise instrumentation of the test aircraft; e.g., modification and calibration.

(3) Supervise the collection, reduction, plotting and analysis of flight test data.

e. Recommend aircraft and instrumentation modifications to the XV-5A Program Manager's Representative.

f. Provide the COR information by which to validate charges against the Government under terms of the support contract.

g. Supervise pilot proficiency, general qualification and proficiency in the XV-5A.

3.0 XV-5A TECHNICAL CONSULTANTS AT EDWARDS AIR FORCE BASE (GOVERNMENT AND NON-GOVERNMENT)

a. Be selected on the basis of their ability to contribute to the successful attainment of the established program objectives.

b. Be supplied to the program for varying periods, depending upon their assignment and the type of testing and/or problems encountered, in many cases for the duration of the program.

c. Be assigned as follows: (1) Staff consultants, as assistants to the Test Director to contribute to the assigned phase of the overall test program and (2) Other consultants, as engineering support to one of the two project engineers.

d. Report administratively and technically to the Test Director, if Government consultants.

4.0 CONTRACTOR SUPPORT PROGRAM MANAGER AT EDWARDS AIR FORCE BASE

a. Be responsible to the Test Director for all contractor support supplied to the program.

b. Manage the approved program, including modifications, under the direction of the Test Director.

c. Provide administrative and technical control over non-Government support personnel.

d. Plan, schedule and conduct program planning meetings, review meetings, briefing and debriefing of each test flight.

e. Be responsible to the Test Director for off-site design, test and/or fabrication of aircraft/propulsion system hardware in support of the flight test program.

f. Establish priorities for facilities, equipment, special support shops and personnel.

g. Provide for flight test support, e.g., chase-pace aircraft, emergency equipment, radio frequencies, airspace allocations, tracking and camera facilities, etc.

5.0 LIFT-FAN PROGRAM MANAGER AT USAAVLABS, FORT EUSTIS

a. Be responsible to CO, USAAVLABS , for the conduct of all Lift-Fan research.

b. Provide technical guidance and contractual support to the XV-5A Government Flight Evaluation.

c. Provide public information services through the Public Information Officer, USAAVLABS .

APPENDIX VIII
References

a. Contract No. DA 44-177-TC-715, "Lift-Fan Flight Research Aircraft Program," U.S. Army Aviation Materiel Laboratories (USAAVLABS), 10 November 1961.

b. Contract No. DA 44-177-AMC-54 (T), "Support for Army Flight Tests of XV-5A Aircraft," USAAVLABS, 28 June 1963.

c. Modification No. 3, Contract No. DA 44-177-AMC-54 (T), "Support for Army Flight Tests of XV-5A Aircraft," USAAVLABS, 10 February 1965.

d. Modification No. 8, Contract No. DA 44-177-AMC-54 (T), "Support for Army Flight Tests of XV-5A Aircraft," USAAVLABS, 26 July 1965.

e. Unclassified Message 10-2131, AMCRD, Hq, U.S. Army Materiel Command (USAMC), 20 October 1964, subject: "XV-5A Aircraft 100-Hour Flight Research Program."

f. Plan of Test, USATECOM Project No. 4-5-1220-01, "Engineering Research and Evaluation Test of the XV-5A Lift-Fan Aircraft," U.S. Army Aviation Test Activity (USAAVNTA), December 1964.

g. Letter Report of Preliminary Pilot Qualitative Evaluation of the XV-5A Research Aircraft, USAAVNTA, 28 October 1965. (AD623514)

h. Report, "Engineering Flight Research Evaluation of the XV-5A Lift-Fan Aircraft, Part 1-Stability and Control," USAAVNTA, August 1966. (AD800973L)

i. Report No. 153, "XV-5A Full-Scale Wind Tunnel Test Report," General Electric Company, December 1964.

j. Report No. 29466-2, Volumes I, II, III, "Phase I Flight Test Results U.S. Army XV-5A Lift Fan Research Aircraft," Ryan Aeronautical Company, December 1965.

k. Specification No. 118, "XV-5A Detail Specification," General Electric Company, 17 August 1962.

1. Report No. 62B125A, "XV-5A Detail Aircraft Specification," Ryan Aeronautical Company, 30 December 1964.

m. General Electric XV-5A Datum No. 4, "Some Comments on Reingestion-Ames Wind Tunnel Results," General Electric Company, 1 September 1964.

n. Report No. 29475-3, "XV-5A Flight Test Data Reduction Procedures," Ryan Aeronautical Company, 30 June 1966.

o. Report, AFFTC-R-59-47, "Flight Test Handbook," U.S. Air Force, January 1960.

p. Report, AFFTC-FTC-64-2007, "Aerodynamic Theory," U.S. Air Force Aerospace Research Pilot School."

q. Air Force-Navy Aeronautical Bulletin No. 421, "Atmospheric Properties - Extreme Cold and Hot; Standard for Aeronautical Design," 26 February 1953.

Legible page

AD-821123

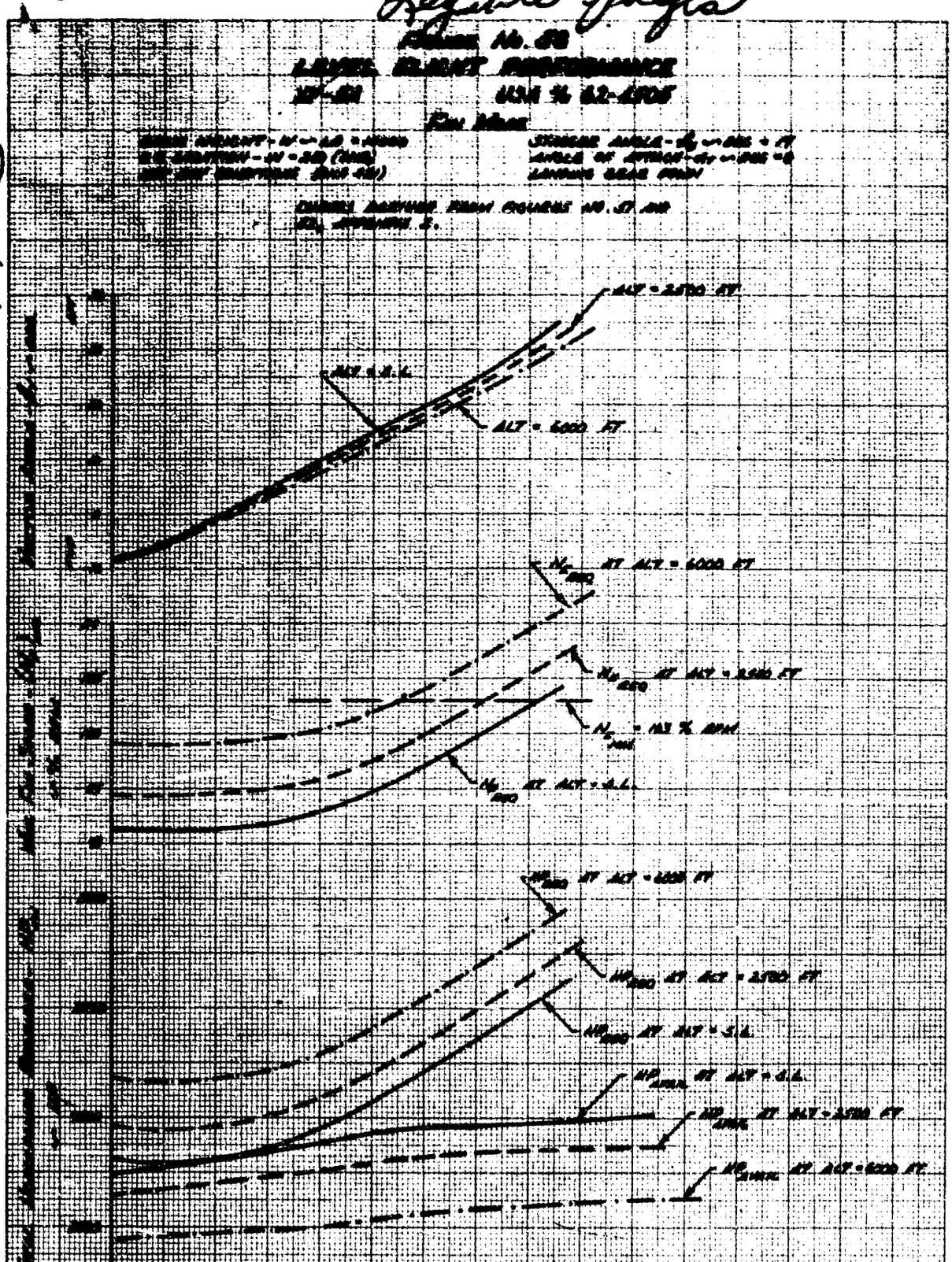

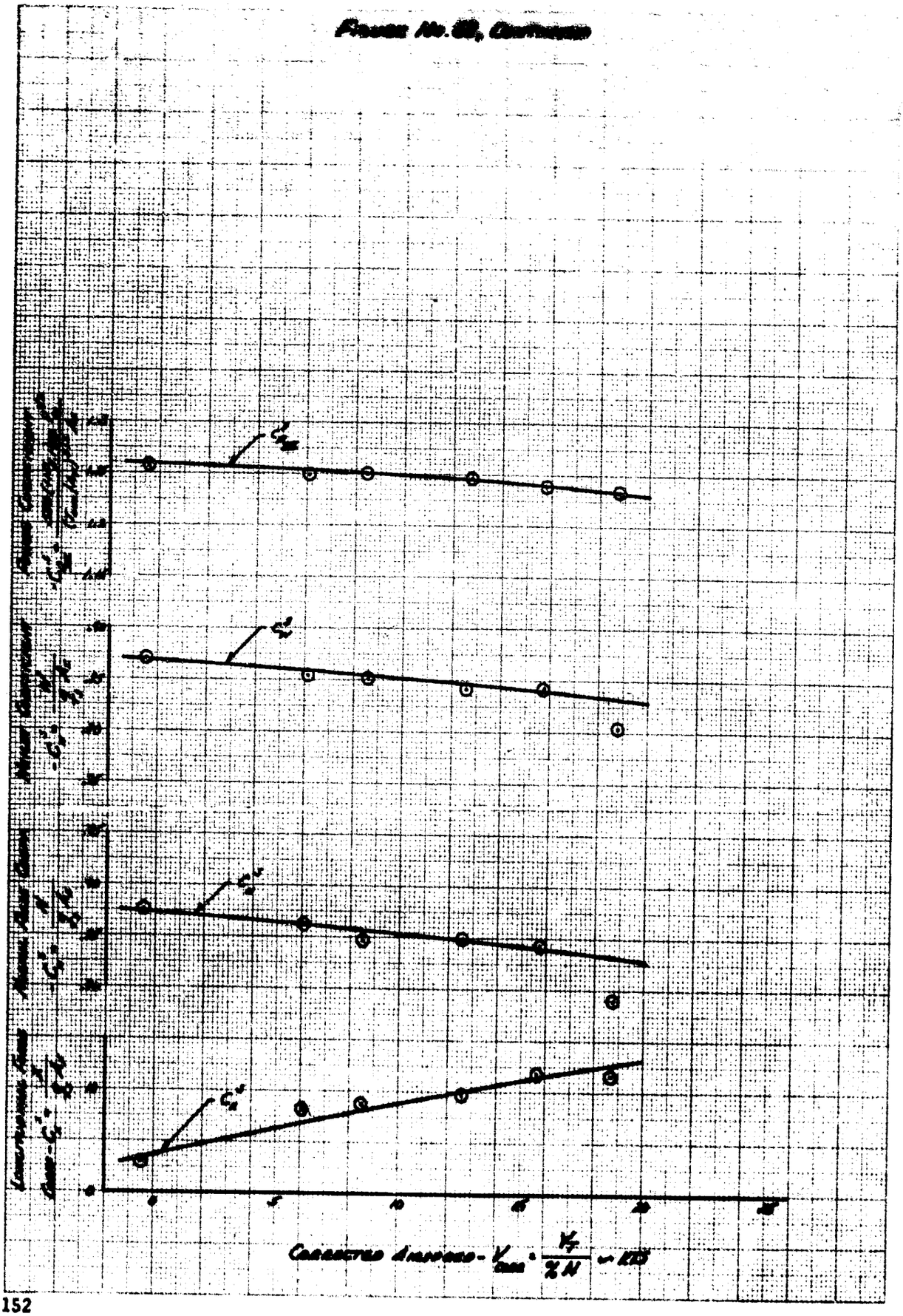

152

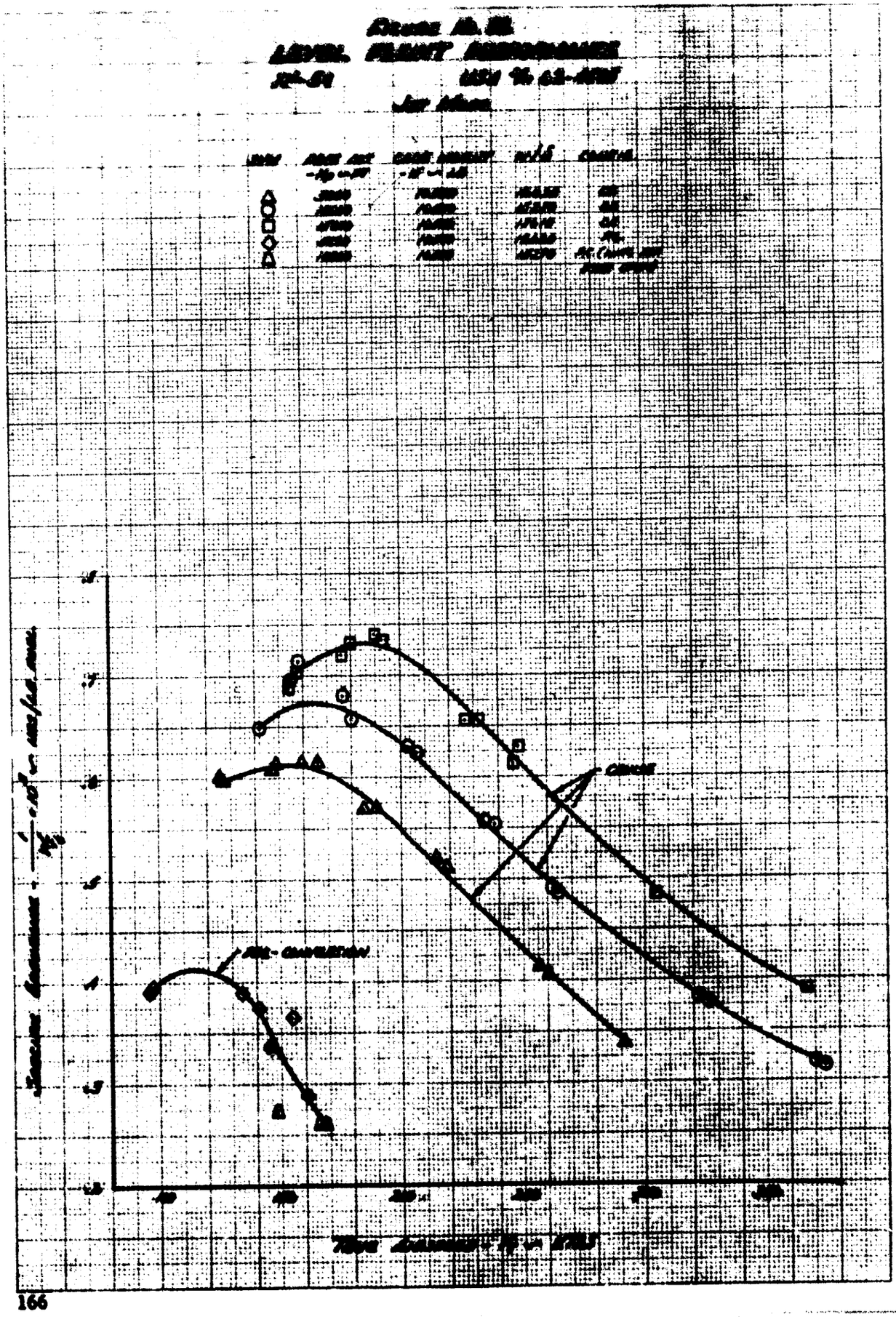

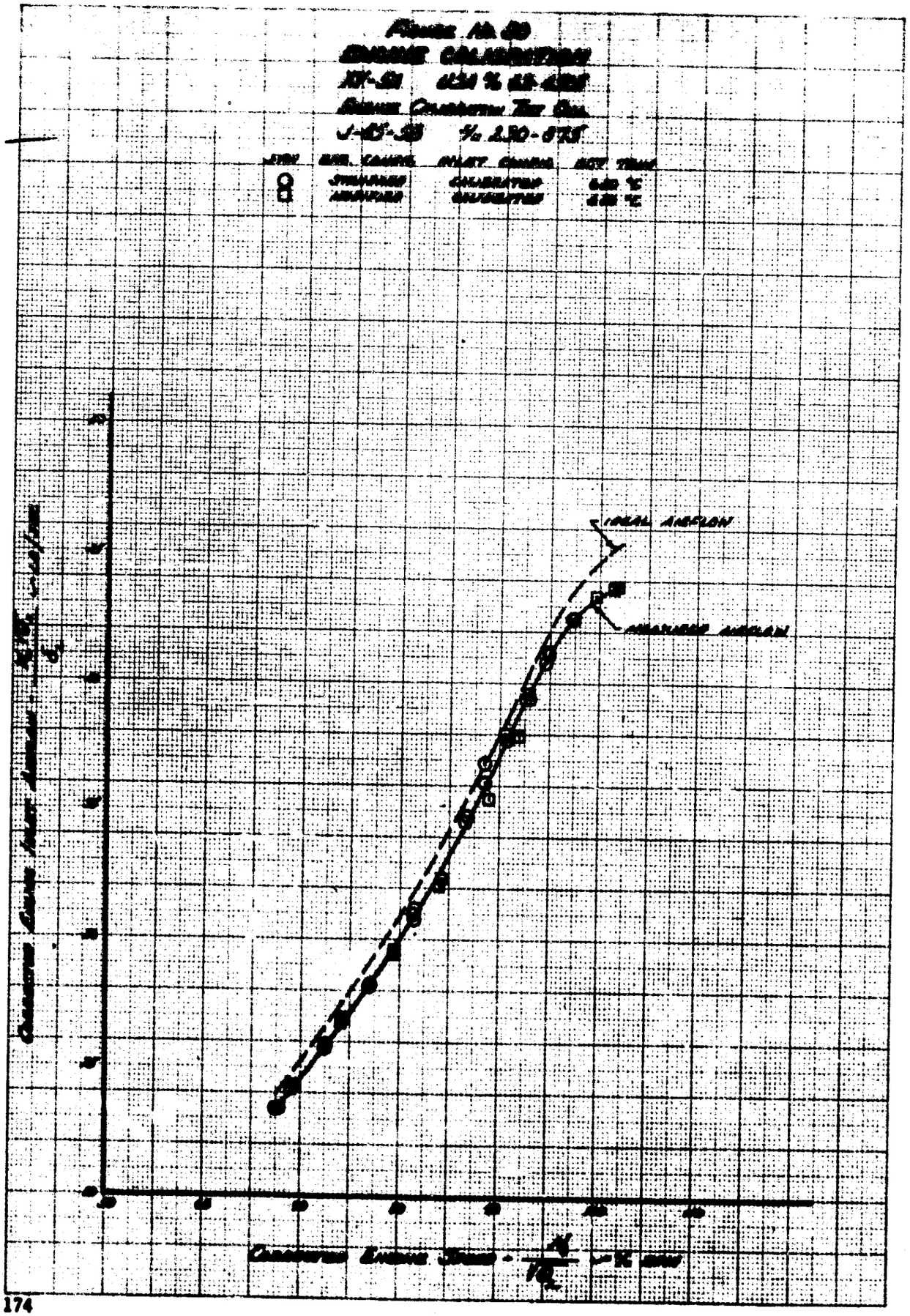
IDEAL AIRFLOW
MEASURED AIRFLOW

Report No. 190

ENGINE CALIBRATION

XP-51 USA No. 43-6006

Engine Calibration Test Cell

J-65-3B

Run	Engine No.	Engine Config.	Inlet Conditions	Jet Temp.
8	230-176	Airframe	Flight Ramjet	700 °C
8	230-176	Airframe	Flight Ramjet	640 °C

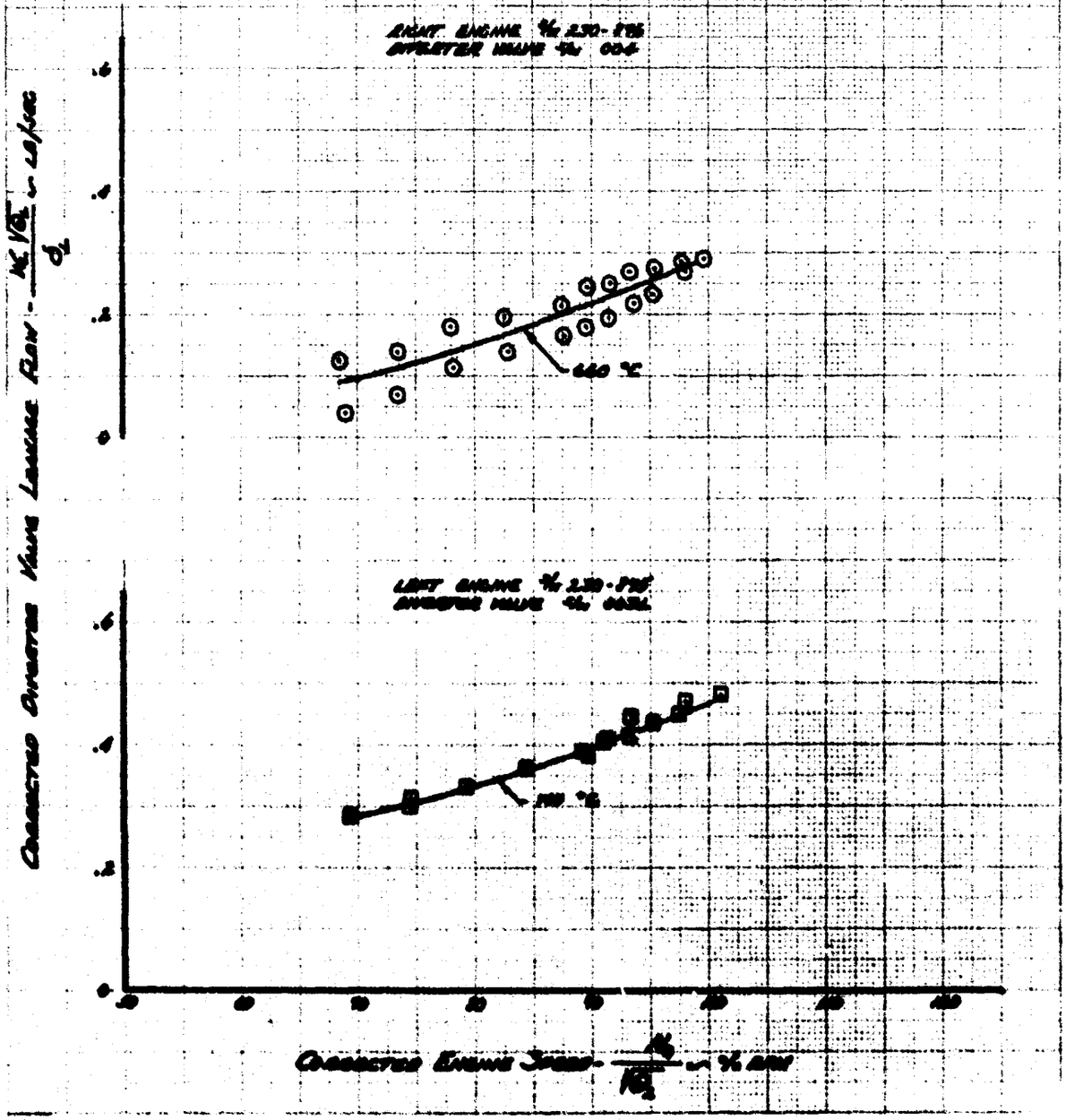

PROGRAM NO. 110
ENGINE CALIBRATION
J57-59 USN No. 43-4086
ENGINE CALIBRATION TEST CELL
J-65-58 No 230-230

SYM BLEED VALVE RIGGING
○ HIGH
□ NOMINAL
◇ LOW

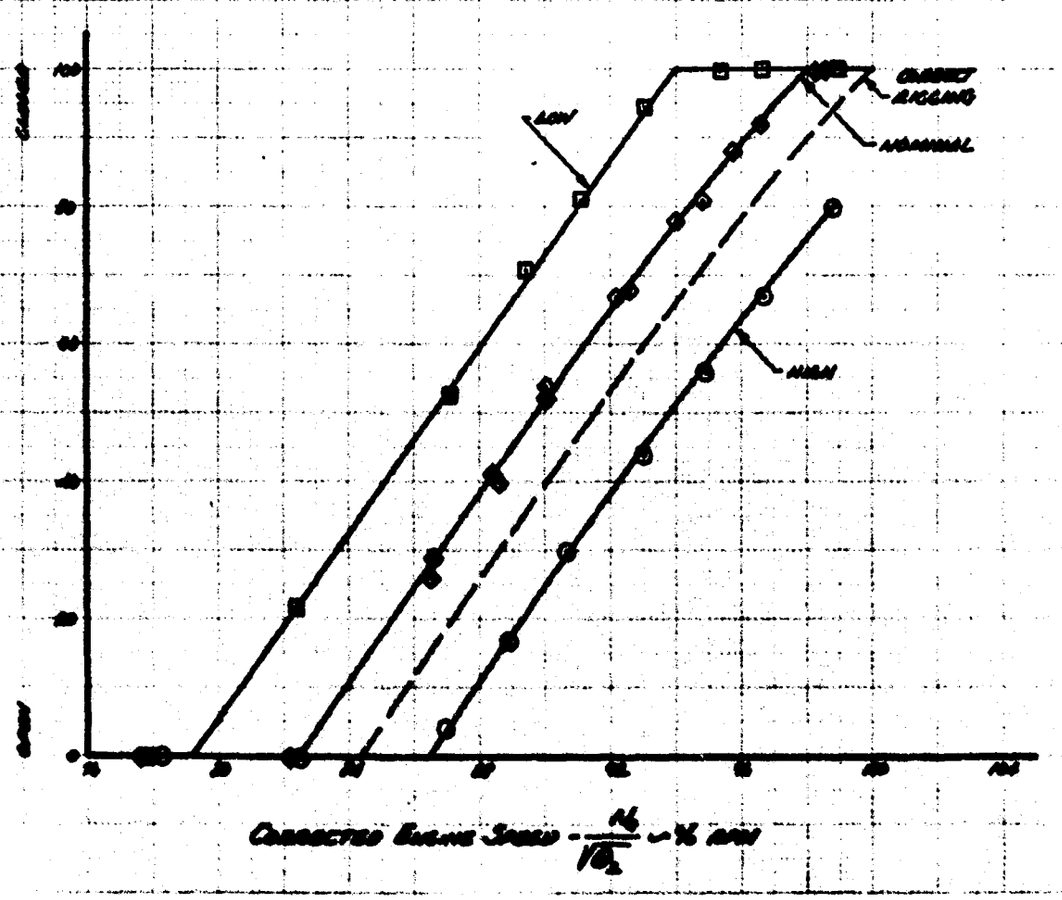

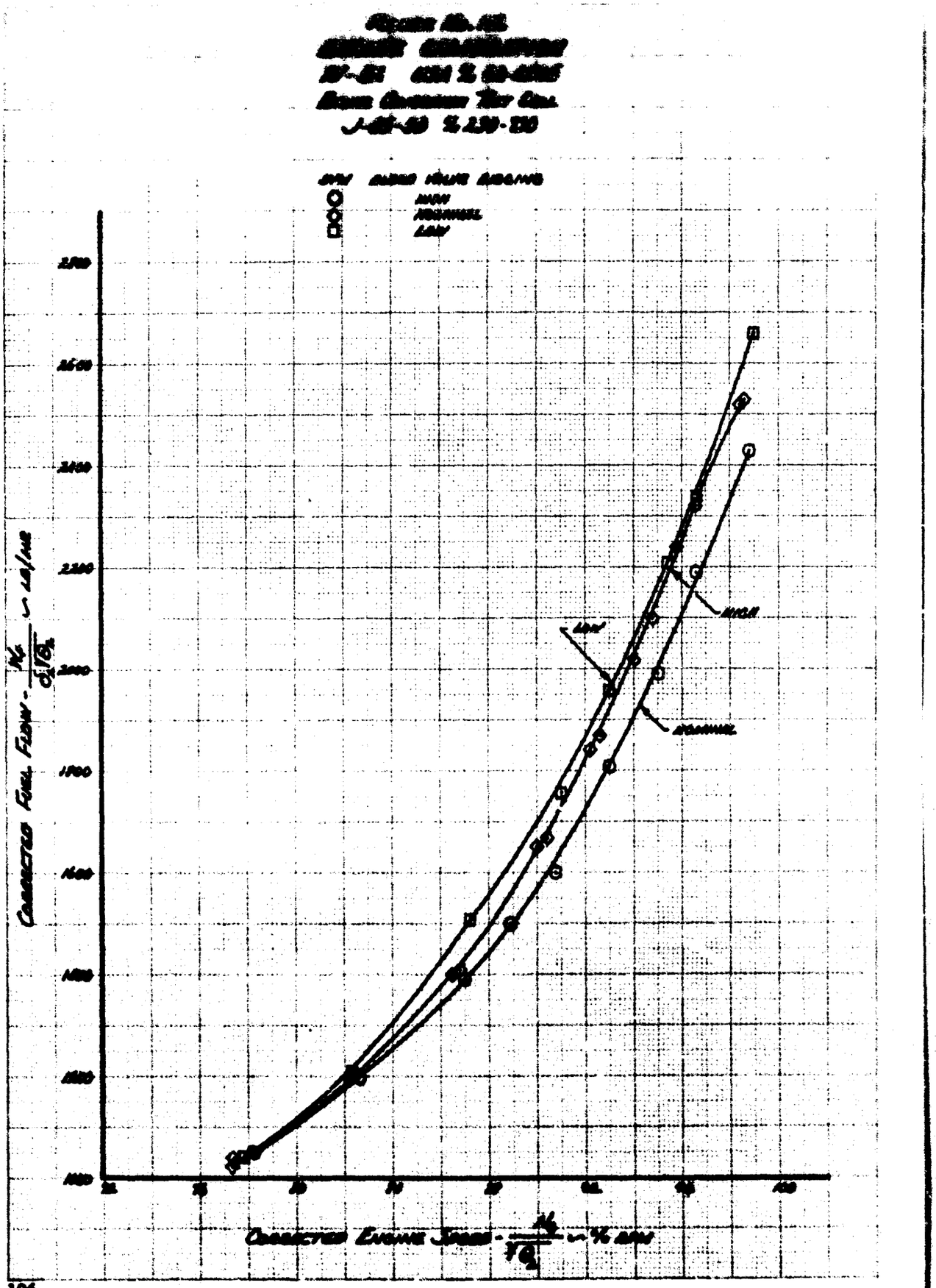

[redacted]

SYM	[redacted]	[redacted]	[redacted]	[redacted]	[redacted]	[redacted]	[redacted]
○	[redacted]	[redacted]	1	[redacted]	-.10	-4	[redacted]
□	[redacted]	[redacted]	2	70.3	-1.41	-5.5	[redacted]
△	[redacted]	[redacted]	3	70.7	-.74	-2.9	[redacted]

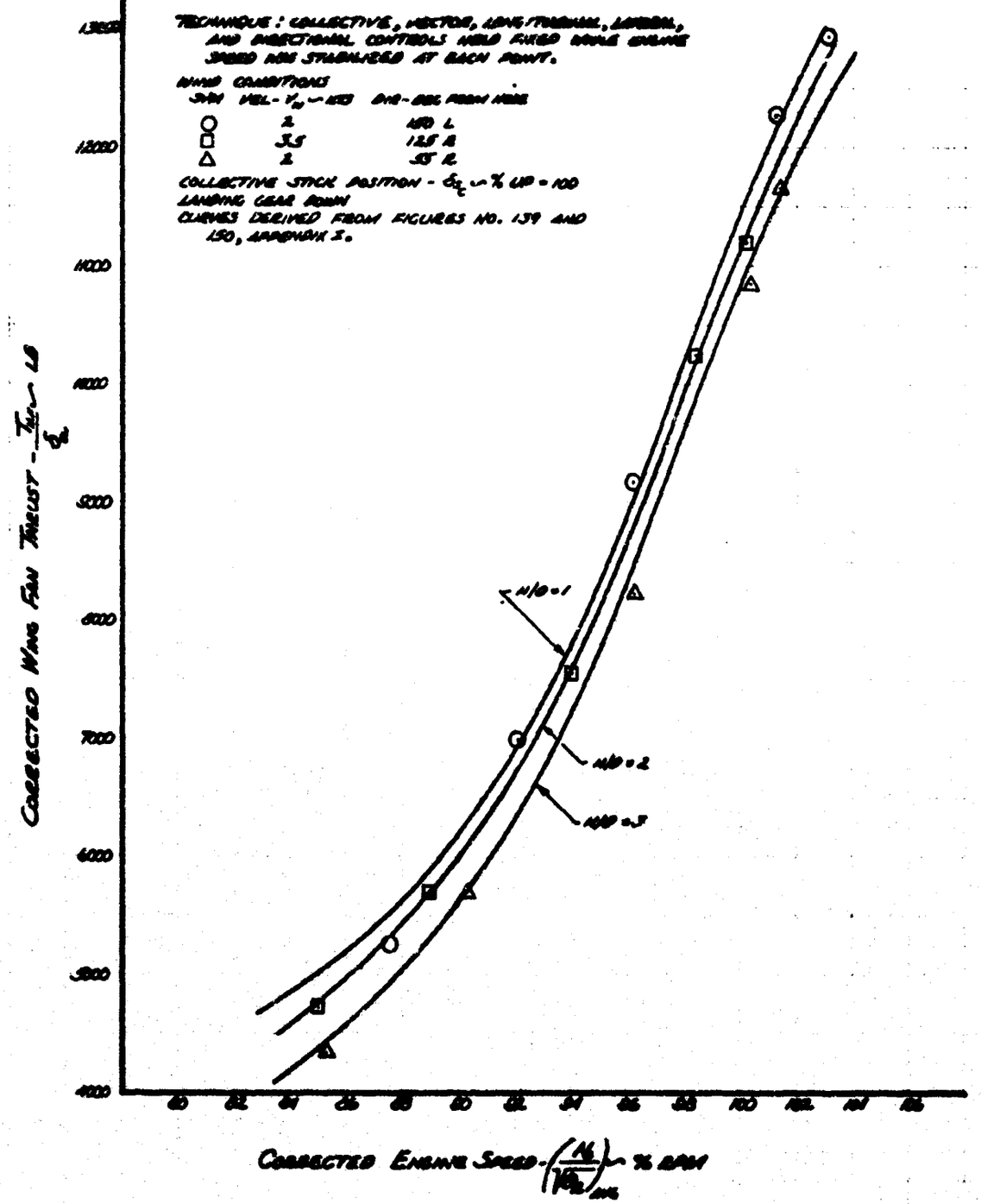

FIGURE [illegible]

ENGINE INLET PERFORMANCE

[illegible] USA [illegible]

Mach Number Level Flight

J-85-GE

Symbol	Engine No.	Engine Loc.
○	[illegible]	Left
□	[illegible]	Right

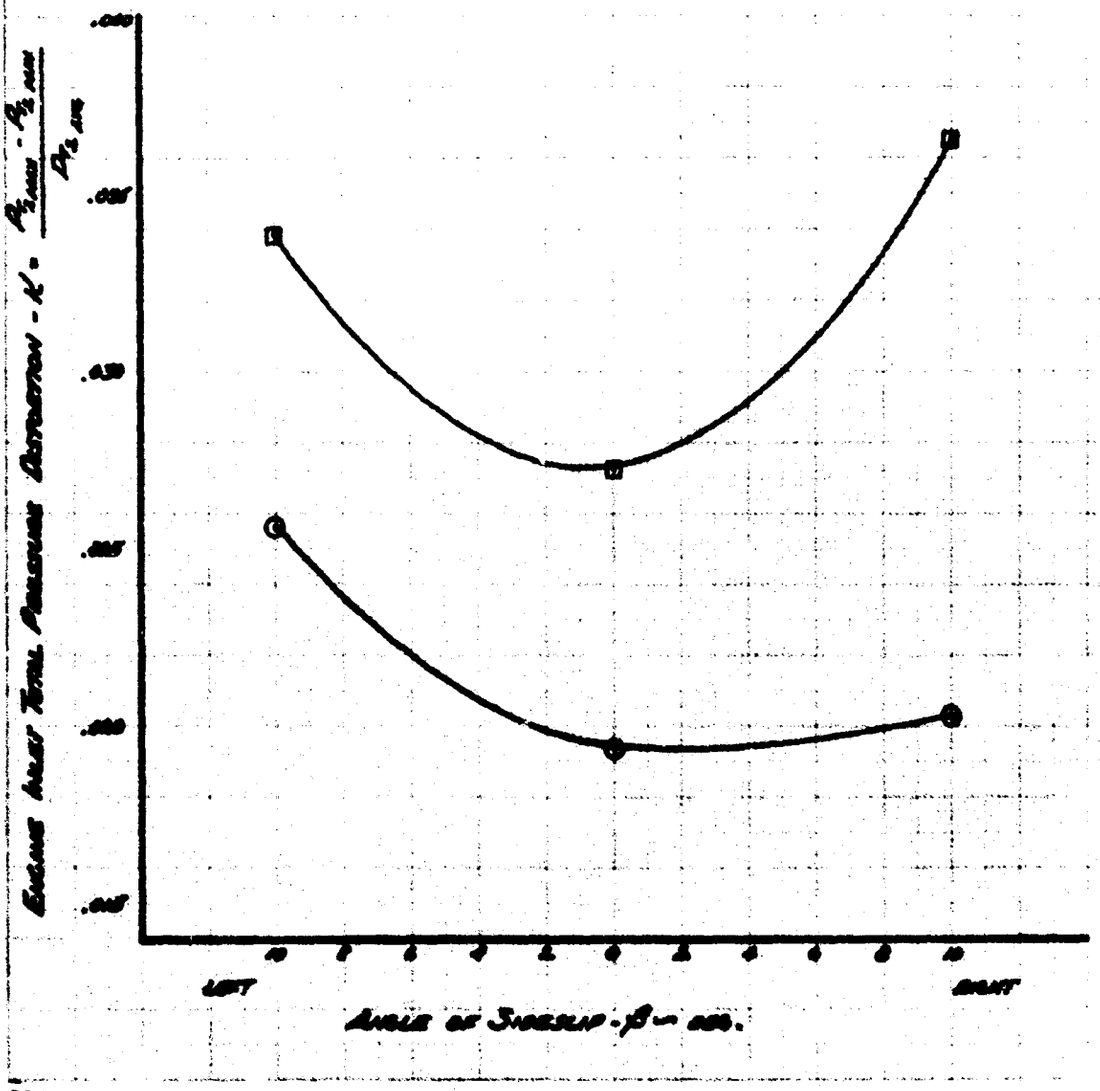

FIGURE NO. 234

ENGINE CHARACTERISTICS

XV-5A USA S/N 62-4505

FAN MODE

OUT-OF-GROUND EFFECT

SYM	FLIGHT CONDITION	PRES. ALT. $-H_p$ – FT
○	GROUND TESTS	2300
◇	HOVERING	2300
◁	SIDEWARD	2300
▷	REARWARD	2300
□	VERTICAL CLIMB	2400
○	FORWARD CLIMB	3000
◇	LEVEL FLIGHT	4500
△	FORWARD DESCENT	3000
◇	VERTICAL DESCENT	2400

NOTES

1. SOLID SYMBOLS DENOTE PRE-CONVERSION CONFIGURATION.
2. J-85-5B, RIGHT ENGINE S/N 230-876.

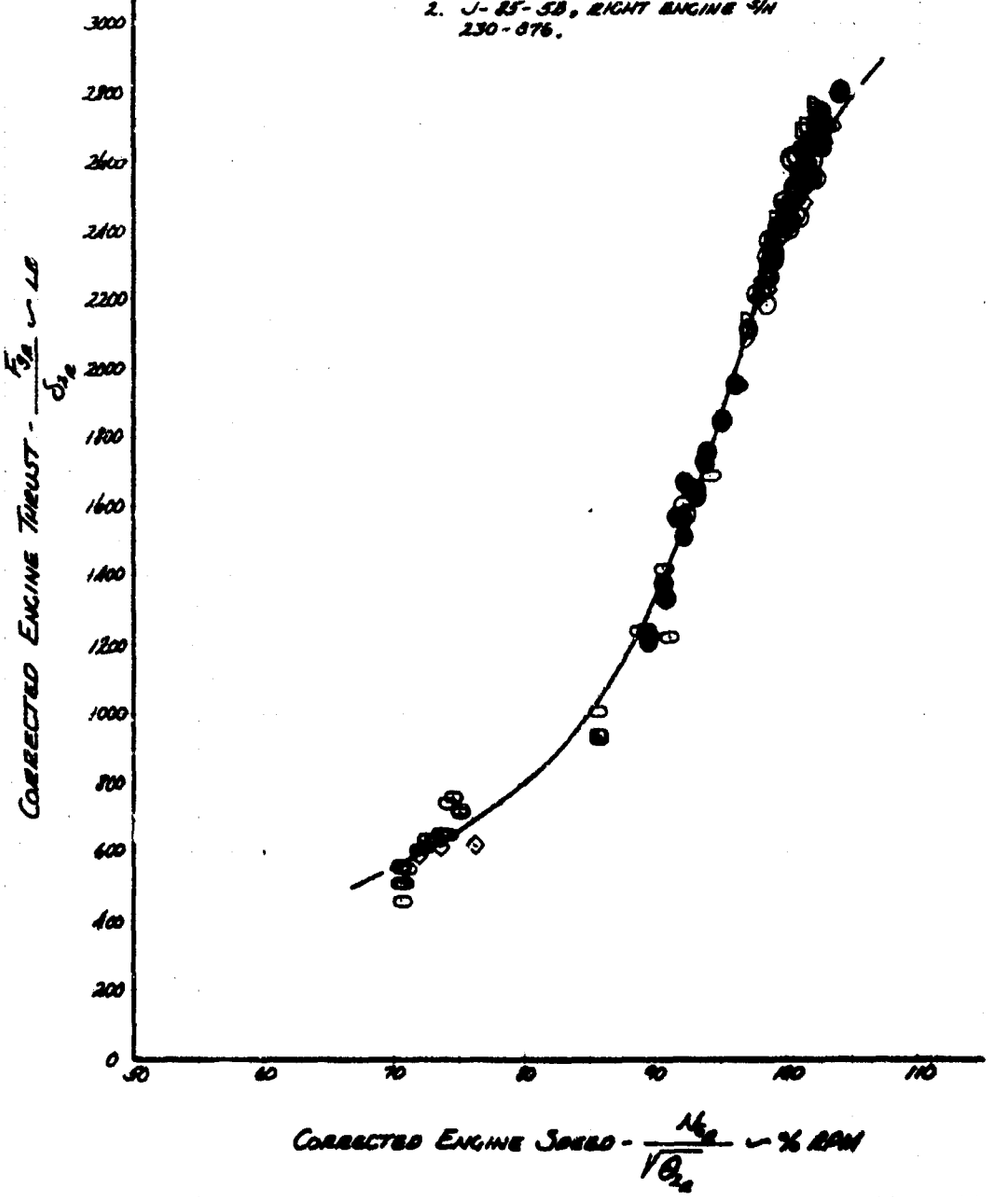

Figure No. 2

PROPULSION SYSTEM PERFOR

XV-5A

PRESSURE ALTITUDE - H_p = FT. = 3210
WIND VEL - V_W = KTS. = 2
WIND DIR - DEG FROM NOSE = 10 L

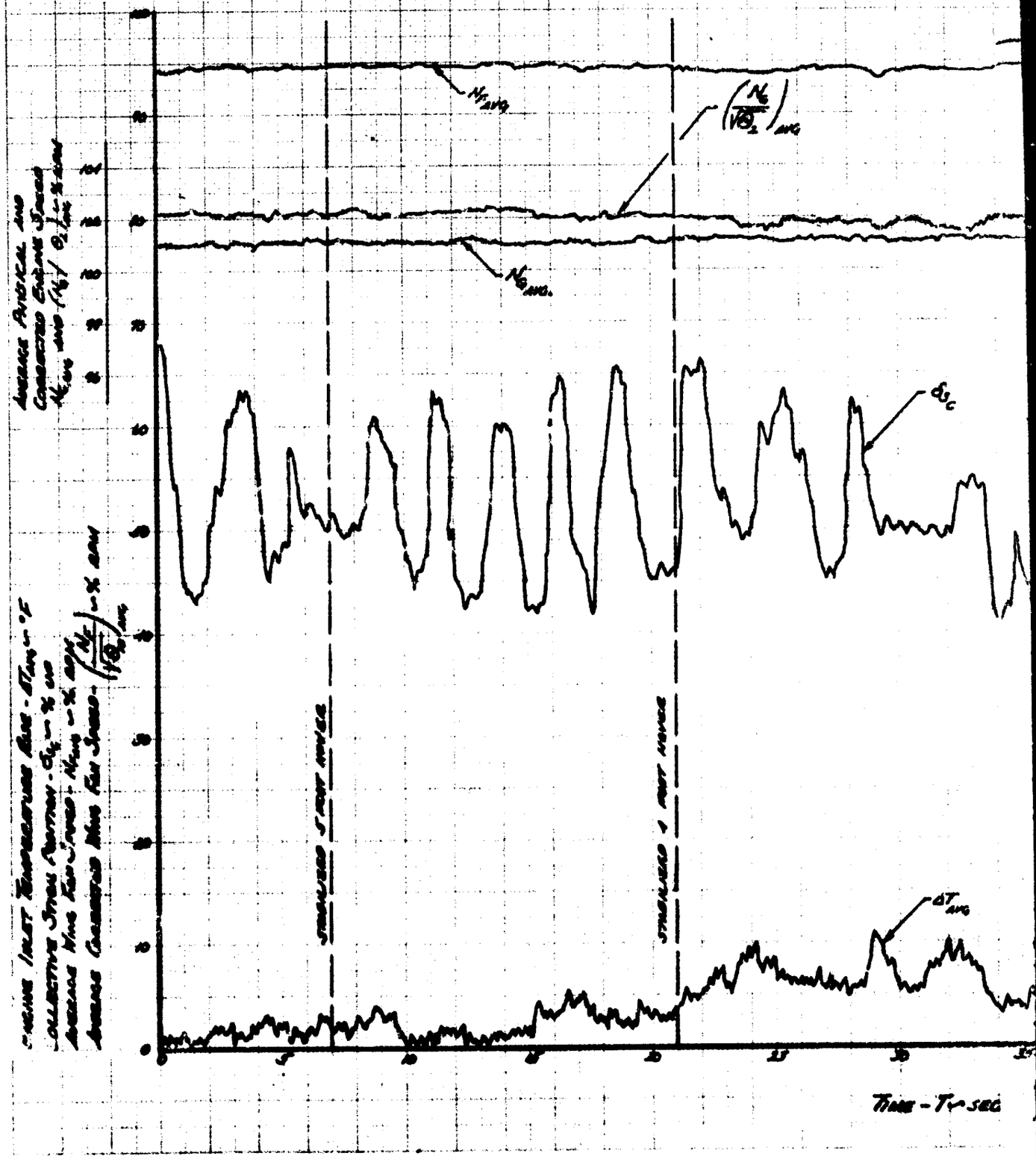

Figure No. 210

STEM PERFORMANCE DURING HOVER

USA 3/4 62-1505

= 2290

= 10 L

GROSS WEIGHT - W - LB = 10,200

AMBIENT TEMPERATURE - T_a - DEG F = 48

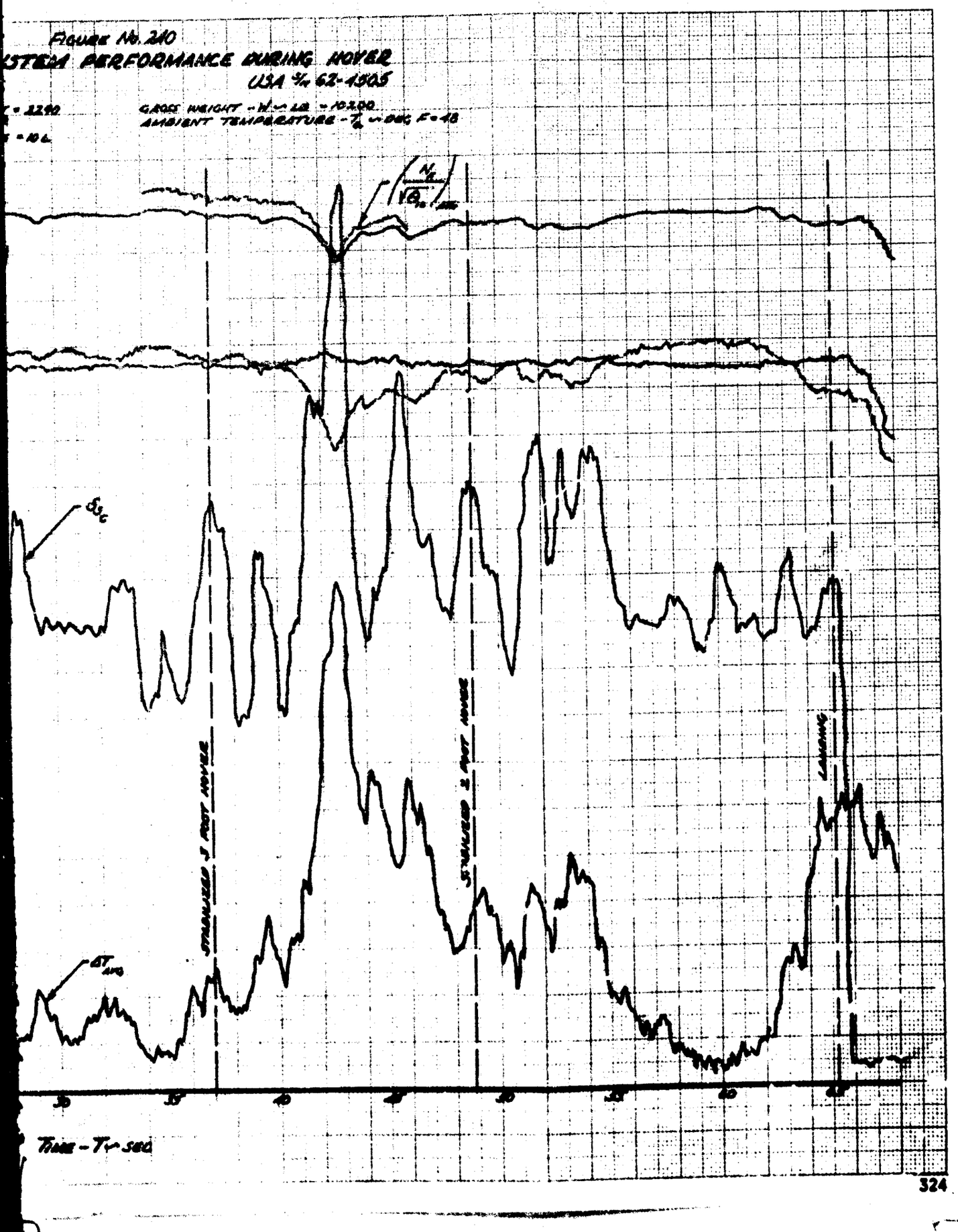

324

2

FIGURE No.

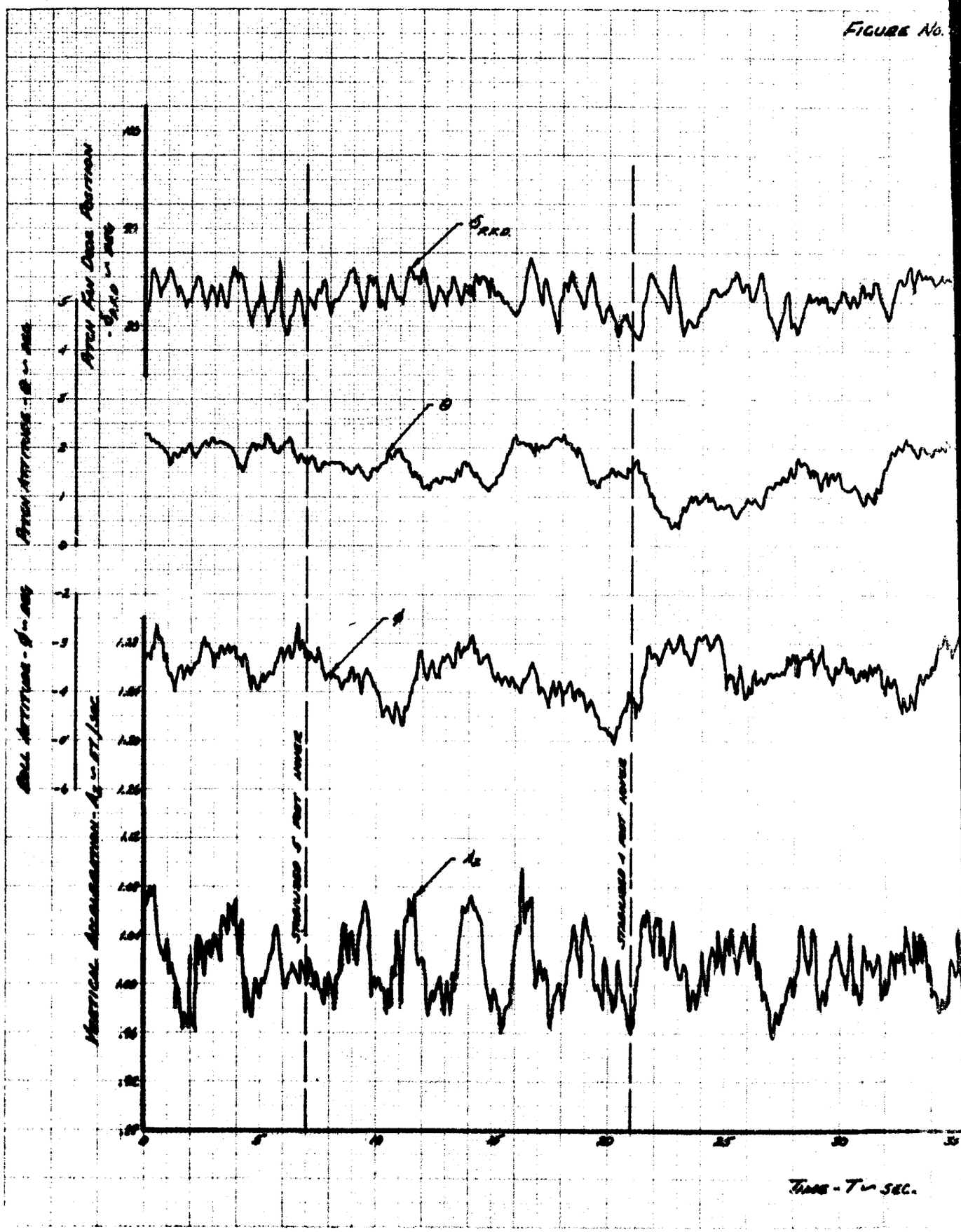
δ_{RRO}
θ
ϕ
h_2
STANDARD 5 FOOT WAVE
STANDARD 1 FOOT WAVE
TIME - T — SEC.

FIGURE No. 240, CONTINUED

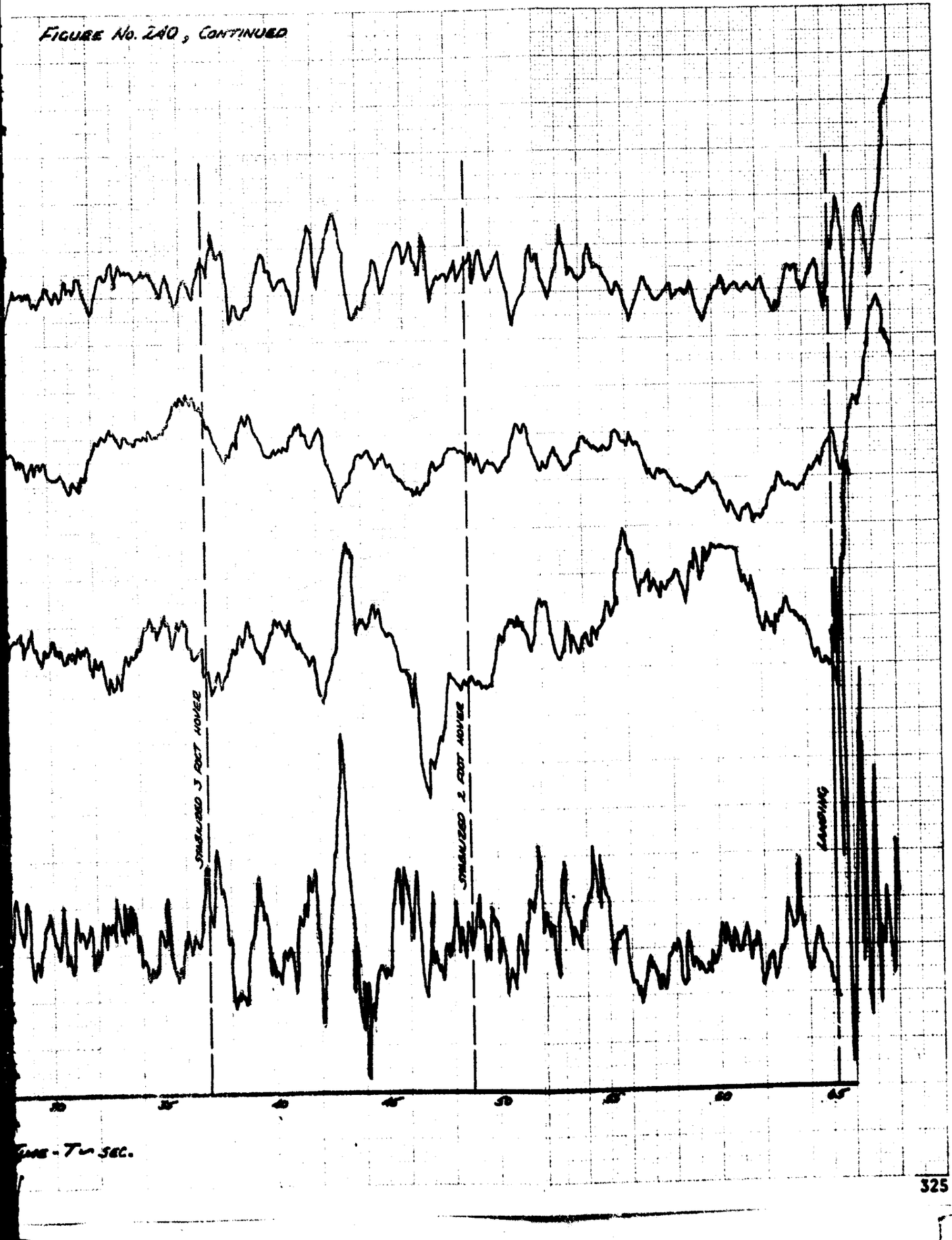

TIME - TENTHS SEC.

2

FIGURE No. 2

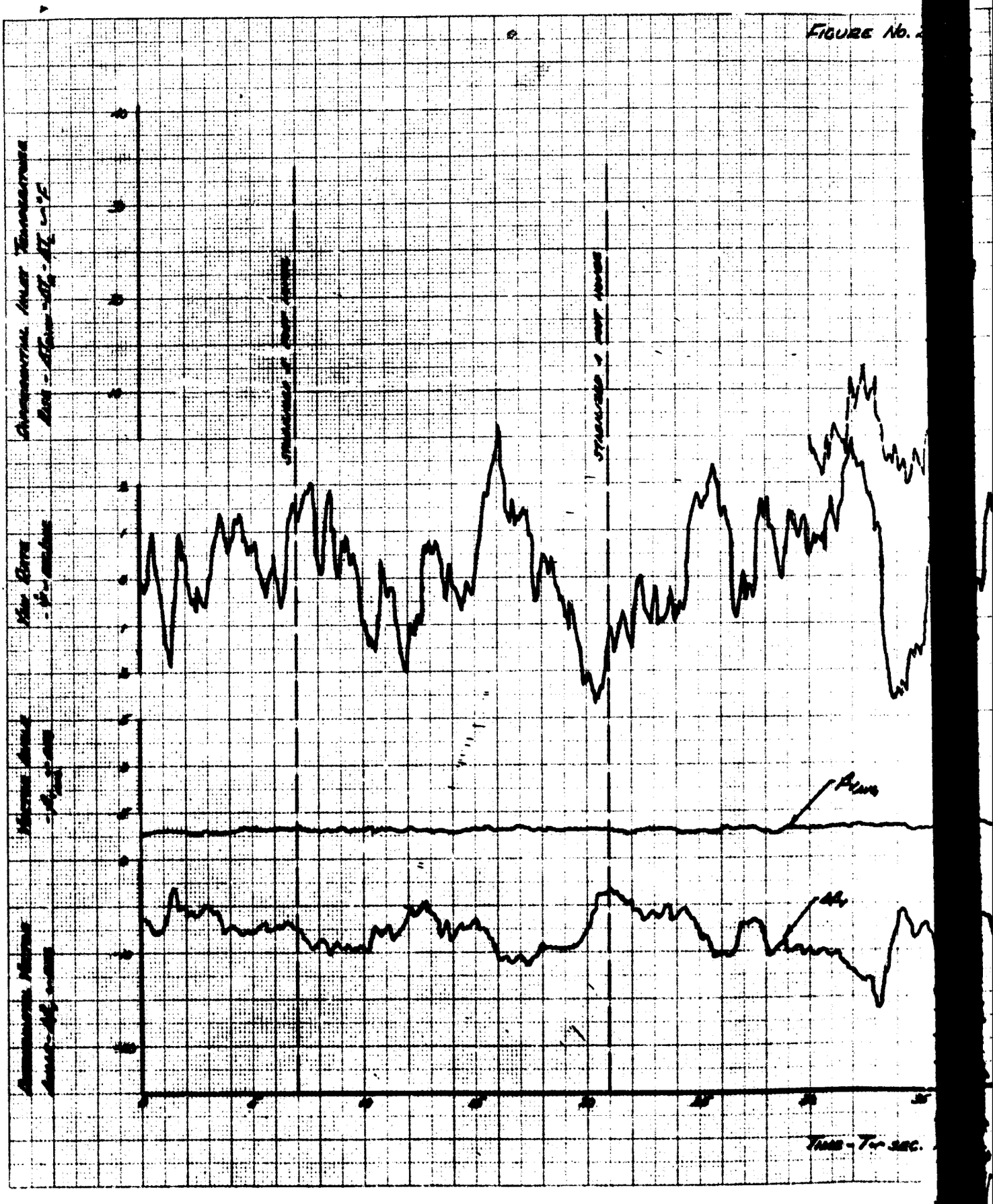

FIGURE No. 240, CONTINUED

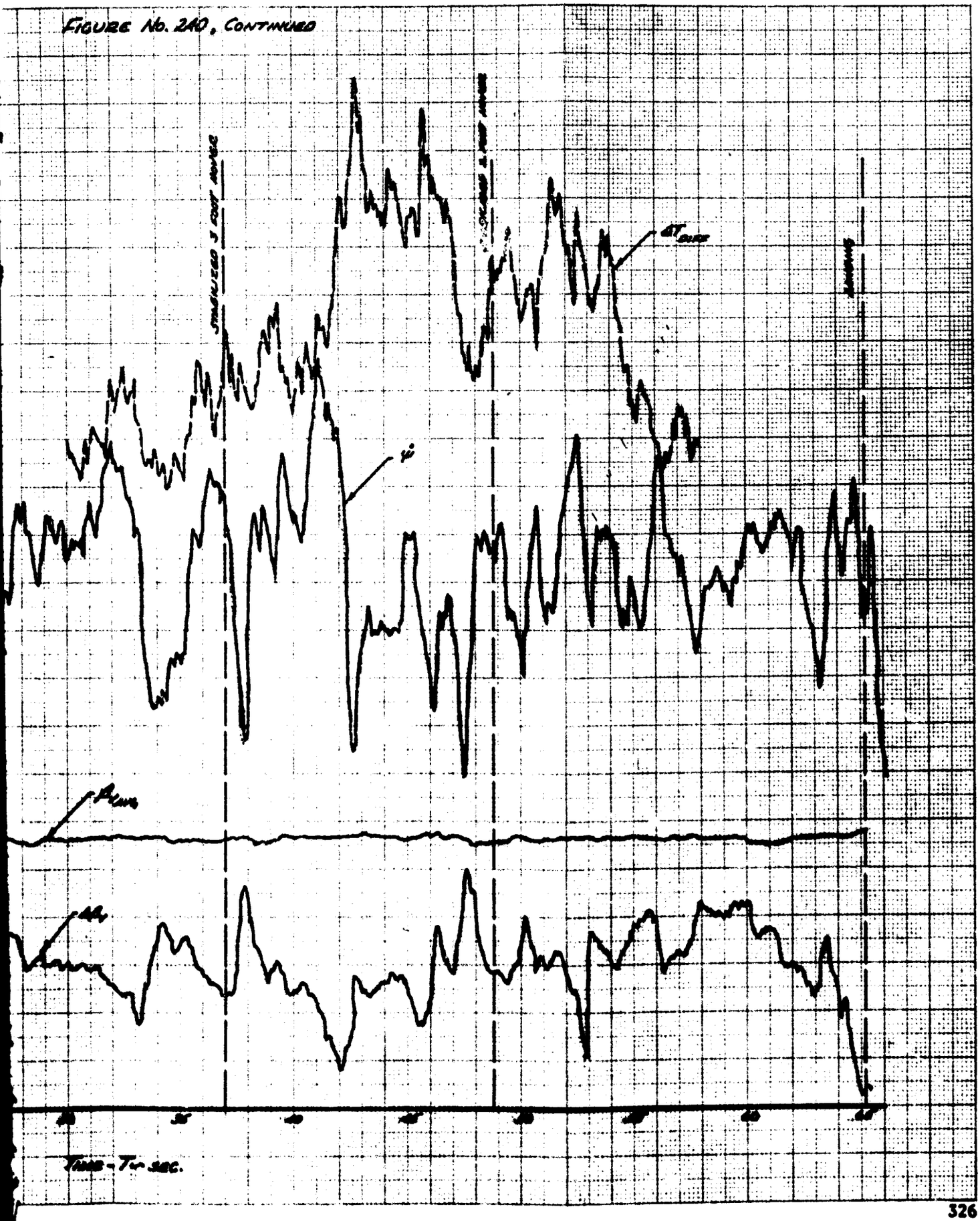

2